ALKYL–TRANSFER (TRANSALKYLATION) REACTIONS OF ALKYLAROMATICS ON SOLID ACID CATALYSTS

Kgutso Mokoena

A thesis submitted to the faculty of Science, University of the Witwatersrand, Johannesburg, in the fulfillment of the requirements for the degree of Doctor of Philosophy

Johannesburg 2005

ALKYL–TRANSFER (TRANSALKYLATION) REACTIONS OF ALKYLAROMATICS ON SOLID ACID CATALYSTS

Kgutso Mokoena

DECLARATION

I declare that this thesis is my own, unaided work. It is being submitted for the Degree of Doctor of Philosophy in the University of the Witwatersrand, Johannesburg. It has not been submitted before for any degree or examination in any other University.

_____

(Signature of candidate)

_____ day of _____ (year) _____

ABSTRACT

Alkyl-transfer (transalkylation, disproportionation) reactions of alkylaromatics were studied for the purpose of finding out the principles that governs them. Alkyl-transfer of simpler alkylaromatics ranging from mono to polyalkyl-benzenes and alkylnaphthalenes were studied in a fixed bed reactor system on solid acid catalysts (zeolites) at temperatures up to 400 °C. Results showed that alkyl-transfer reactions are reversible reactions with disproportionation favoured at lower temperatures while transalkylation seemed to be dominant at higher temperatures. The outlined mechanism showed that the catalyst pore sizes and the type of pores as well as the feed composition of binary mixtures play important roles in the transfer of alkyl groups between aromatic molecules. In alkyl-transfer reactions, the ease of conversion depends on the number of alkyl groups on the aromatic ring/s, the chain length, the type of alkyl substituent/s and the ring conjugation of the aromatic moiety.

Zeolitic catalysts are rapidly deactivated by carbonaceous material deposition during alkyl-transfer reactions especially at higher temperatures while deactivation through molecular retention is dominant at lower temperatures. Nevertheless, zeolites can be regenerated by high temperatures in oxidizing atmospheres. Bulkier alkylaromatics (those found in coal and petroleum liquids) can be transformed through alkyl-transfer reactions if a suitable catalyst with the required strength and appropriate pore sizes can be developed, preferably a *tri*-dimensional arrangement as shown by the results of this study. Thus the alkyl-transfer process has promising future applications in petrochemical and related industries; especially those interested in the transformation of coal to chemicals.

DEDICATION

This thesis is dedicated to my family: my wife Nthati Mokoena, our two sons Qenehelo and his younger brother Thoriso; my parents, Napo and Thokozile Mokoena, my brother Kutlwisiso and my sister Mmasello. My extended families are never forgotten……

ACKNOWLEDGEMENTS

I would like to thank first and foremost my supervisor Professor Mike S. Scurrell who has been my light and my guide, without him this work wouldn't have been possible. Thanks also to my loving family who've patiently supported me through hard times that came with this work; this family has been the pillar of my strength. Thanks also to Sasol limited for the financial support they've given me and the University of the Witwatersrand for giving me the opportunity to fulfill my dreams.

Great thanks goes to the most High GOD our LORD for LOVING and saving me through his son JESUS CHRIST the LORD of my life by the POWER of the HOLY SPIRIT.

CONTENTS PAGE

LIST OF FIGURES PAGE

NOMENCLATURE

1,2,3	1,2,3-trimethylbenzene
1,2,3,4	1,2,3,4-tetramethylbenzene
1,2,3,5	1,2,3,,5-tetramethylbenzene
1,2,4	1,2,4-trimethylbewnzene
ArH	Aromatic hydrocarbon
As	Active site
B	Benzene
BA	Brönsted acid
BAS	Brönsted acid site
BBS	Brönsted base site
BET	Brenauer, Emmet and Teller
BNZ	Benzene
BTX	Benzene, Toluene and Xylene
CAA	Clean Air Act
Ceq	Conversion at equilibrium
DEALK	Dealkylation products
DEB	Diethylbenzene
DIALK	Dialkylbenzenes
DI-MN	Dimethylnaphthalene
DIPB	Diisopropylbenzene
DIPBP	Diisopropylbiphenyl
DISPR	Disproportionation
DISPROP	Disproportionation
DMN	Dimethylnaphthalene
DMQ	Dimethylquinoline
DUR	Durene
EFAl	Extra framework Aluminium

FAl	Framework Aluminium
ISOMER	Isomerization
LA	Lewis acid
LAS	Lewis acid site
LBS	Lewis base site
LHSV	Liquid Hourly Space Velocity
LZY-82	Zeolite-Y, Y-zeolite, HLZY-82
MES	Mesitylene
MN	methylnaphthalene
N	Naphthalene
NAPH	Naphthalene
OTHERS	Bulky poly-alkylated aromatic species and/or dealkylation products
p- + m-	para- + meta-xylene
PentMB	Pentamethylbenzene
PROD	The sum total of products in the outlet stream
TetMB	Tetramethylbenzene
TMB	Trimethylbenzene
TMN	Trimethylnaphthalene
TOL	Toluene
TRANS	Transalkylation
TRANSAL	Transalkylation
WHSV	Weight Hourly Space Velocity
XYL	Xylene

1 INTRODUCTION

1.1 Background

Aromatics have a wide variety of applications in the petrochemical and chemical industries. They are an important raw material for many intermediates of commodity petrochemicals and valuable fine chemicals such as monomers for polyesters, engineering plastics, and intermediates for detergents, pharmaceuticals, agricultural-products and explosives. Among them are benzene, toluene and xylene (BTX), the three basic materials for most intermediates of aromatic derivatives. Tseng-Chang *et al.*[1] demonstrated this in a flow chart as shown in figure 1.1.

Dialkylbenzenes, a subcategory of aromatics, includes xylenes, diethylbenzene (DEB) and diisopropylbenzene (DIPB), all of which may be converted to valuable performance chemicals. For example, xylene is the key raw materials for polyester, plasticizers and engineering plastics; *p*-DEB is a high valued product used in *p*-xylene adsorptive separation process. Increasing applications of diisopropylbenzene (DIPB) have been found, ranging from photo-developers, antioxidants to engineering plastics. Process development in aromatic interconversion to produce valuable chemicals is therefore an important research task with great industrial demands.

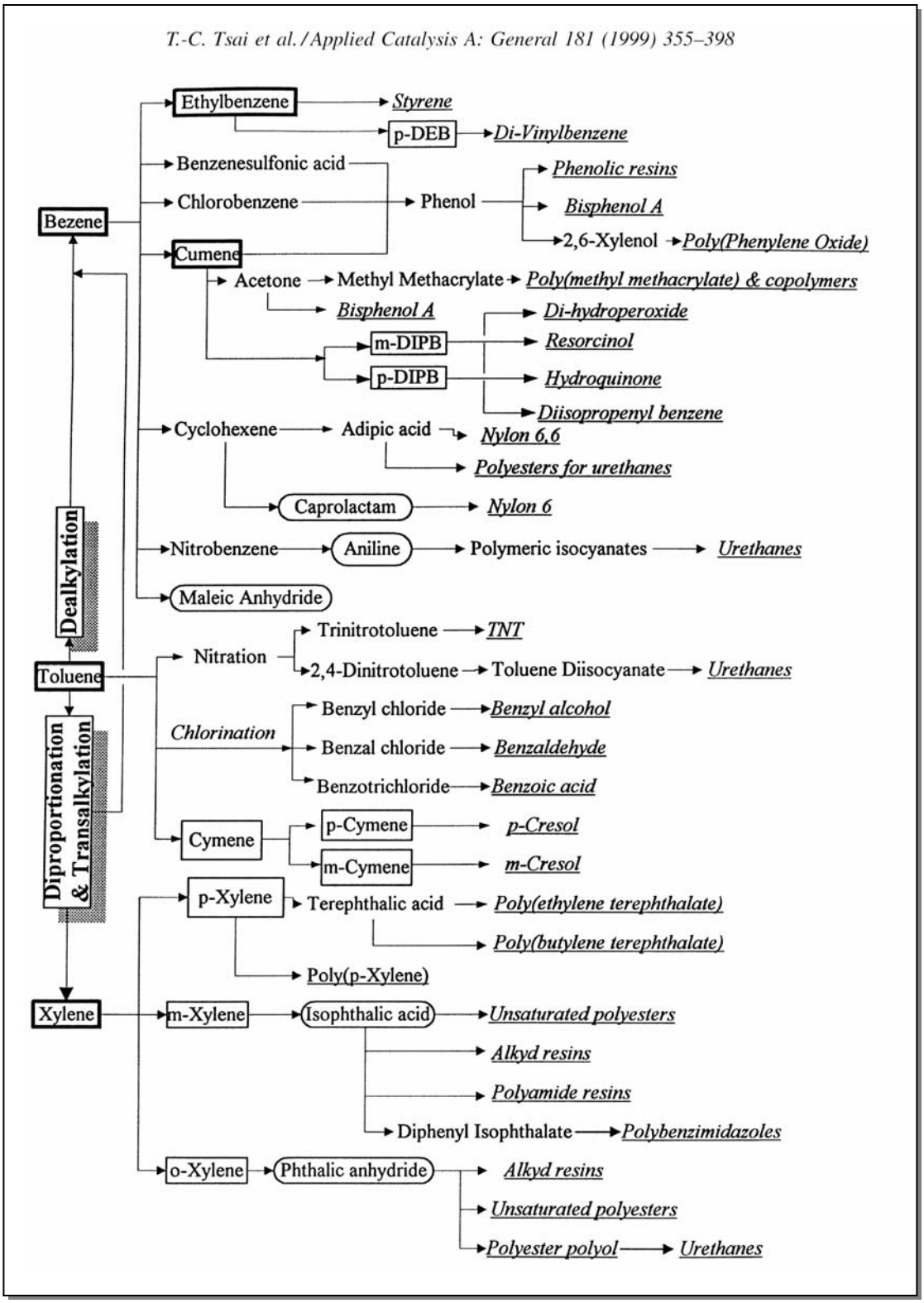

Figure 1.1: Derivatives of benzene, toluene and xylene[1]

There are many driving forces for the development of a new process. In addition to the economically relevant variables such as market demands, feedstock availability and cost, operational cost, legislative aspects such as environmental laws and new reformulated gasoline specifications, etc. also come into play.

Another environmental factor that concerns the 1990 clean air act (CAA) had re-defined the gasoline specifications to enforce the so-called "reformulated gasoline" (RFG) act. The initial stage of the enforcement applied the simple model regulation, by which the maximum benzene content in gasoline is limited to less than 1 vol %. The benzene content in the reformate can be lowered by alkylation to form toluene and xylene or by extraction and subsequent sale into the petrochemical market. The allowable benzene content of gasoline is being lowered to below 1 % to secure environmental safety.[2]

Benzene is obtained from the products of the distillation of coal gasification/pyrolysis products and from the cracking of certain light-oils. It is an excellent solvent for resins and fats and in crude form (benzol) is extensively used as a fuel for motors. Its toxicity as a powerful destroyer of blood corpuscles is a factor that should always be borne in mind by users[3] and it is a well known carcinogen, causing lung cancer.[4]

The process of catalytic reforming and naphtha pyrolysis are the main sources of benzene, toluene and xylene (BTX) production. The product yield of those processes is normally controlled by thermodynamics and hence results in a substantial mismatch between the supply and the actual market demands. The conversion of dispensable aromatics into more valuable aromatics therefore has an economic incentive.

In response to market situations and legislation changes, the main areas of new aromatic process innovations were:

1 conversion of surplus toluene

2 upgrading of heavy aromatics, which are benzene and xylene oriented

3 selective production of *p*-dialkylbenzene isomers against thermodynamic equilibrium, such as *p*-xylene and *p*-diethylbenzene, and

4 the production of dialkylbenzenes with carbon number of alkyl group larger than 3.

Disproportionation and Transalkylation are the two major practical processes for the interconversion of alkylaromatics, especially for the production of dialkylbenzenes (scheme 1.1).

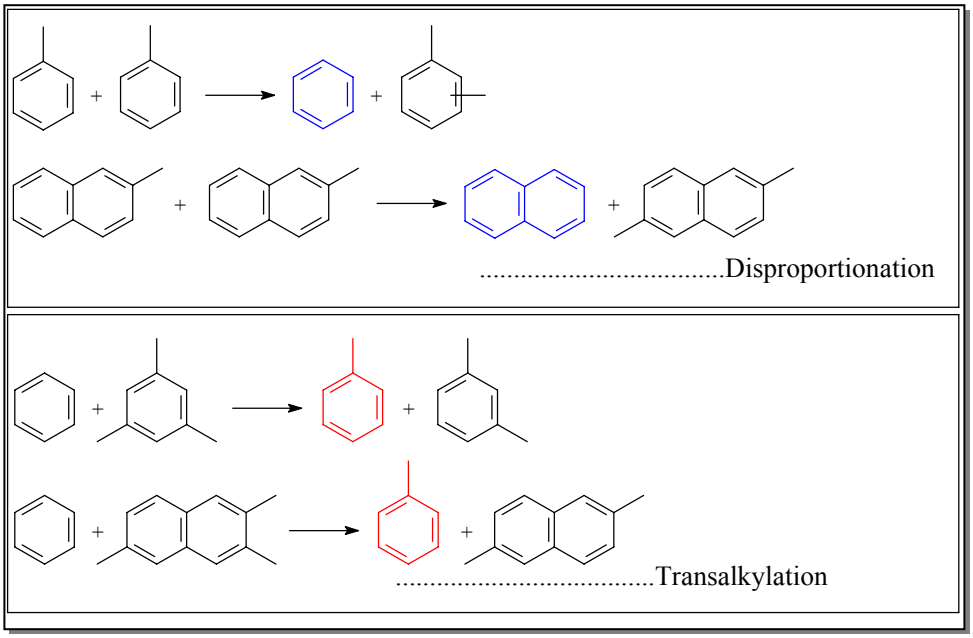

Scheme 1.1: Major routes for alkyl-transfer reactions

The two processes are coined as “alkyl group transfer reactions” or “alkyl-transfer reactions”, which deal mainly with the alkyl group transfer among different aromatic rings.

Owing to the recent development in catalytic chemistry of zeolites, a drastic improvement in aromatic conversion process technology has been found. There has been a growing research interest in both academic and industry. The results obtained

from the fundamental research in turn promote more innovation and development and hence stimulate fine tuning of zeolite catalysts from the approach of molecular engineering level. Improving and finding cost effective disproportionation and transalkylation catalytic processes are interesting and challenging tasks in industrial research.

In response to the world wide environmental awareness, there are active programs to search for cleaner processes. Solid acid catalysts have long been demonstrated as the keys to the success of the historical efforts. Zeolites were used to replace the traditional Friedel-Crafts acid catalysts (BF_3, $AlCl_3$), making the process cleaner, less corrosive and more economic. By using Friedel-Crafts catalysts, solid and liquid wastes in ethylbenzene production of 390 000 tons/year were 500 and 800 tons/year respectively. By using ZSM-5 catalysts, the wastes were significantly reduced to 35 and 264 tons/year respectively.[1]

1.2 Coal tar-pitch

Most organic substances (e.g. coal or wood) other than those of simple structure and low boiling point, when pyrolized (heated in absence of air or oxygen), they yield a dark-coloured, generally viscous liquids termed tar and/or pitch.[5] When the by-product is a liquid of fairly low viscosity at ordinary temperature, it is regarded as tar; if of very viscous, semi-solid, or of solid constancy, it is designated as pitch. Thus in preparative organic chemistry, a tar or pitch is frequently the distillation residue. The distillation of crude petroleum yields a pitch-like residue termed bitumen or asphalt.

By far the largest source of tar and pitch is the pyrolysis or carbonization of coal. Generally, crude tar was subjected to a simple flash distillation in pot stills to yield a solvent naphtha, creosote for timber preservation, and a residue of pitch that found an outlet as a binder for coal briquettes. Later coal was the main source of aromatic hydrocarbons, phenols and pyridine based chemicals needed by the rapidly expanding

dyestuffs, pharmaceuticals and explosives industries. Further developments led to the recovery of tar chemicals, i.e. benzene, toluene, xylenes, phenols, naphthalene and anthracene, in addition to the so-called bulky products, e.g. creosote, tar paints, road tars and pitch binders.

Pitch contains, from a whole lot of other heavier chemicals, the following high molecular weight constituents: aromatic hydrocarbons with four rings, e.g. chrysene, fluoranthene, pyrene, triphenylene and benzanthracene; five membered ring systems are represented by picene, benzopyrene (BaP & BeP), benzofluoranthene and perylene (figure 1.2).

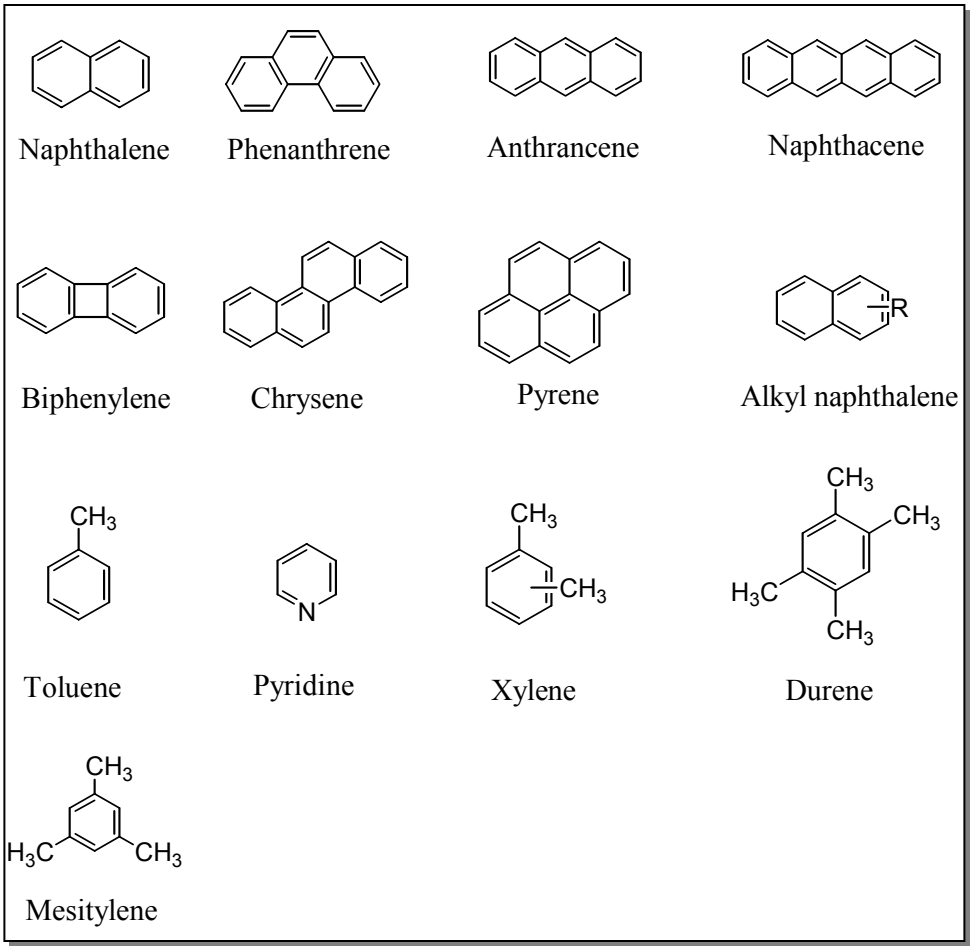

Figure 1.2: Representatives of coal tar-pitch molecules (simpler molecules)[5]

Most petrochemical industries around the world use highly aromatic coals (high rank), which are processed in coke ovens at 1200 °C in the absence of oxygen in order to obtain metallurgical coke and volatile material (tar) (figure 1.3). The volatile material is then separated by distillation into different tar chemicals. The pitch that comes from this process is highly aromatic (good quality) and has important uses as a binder in the aluminum industry in the making of electrodes. In South Africa, coal is processed in gasifiers in the presence of oxygen to produce volatile gasses which condense into light and heavy oils and other products. Unlike any other counties these oils are mixed together as "Tar" which is then further processed in a distillation chamber.

During the distillation of tar, at temperatures lower than 160 °C, light naphtha fractions are separated; at higher temperatures (160-200 °C) heavy naphtha is produced. Medium creosote is distilled at the temperature range of 200-280 °C and heavy creosote at 280-350 °C. Heating the residue oils at the temperature range of 350-420 °C (distillation) leaves pitch as the residue product. In South Africa this pitch contains about 2.5 % of unsubstituted aromatics and about 4 % of alkylated aromatics, while other countries obtain 10 % of the unsubstituted aromatics and about 2 % of alkylated aromatics; these are represented below in figure 1.4 as naphthalene and alkylnaphthalene for simplicity since pitch contains much bulkier and complex aromatics than the naphthalene organic moiety.

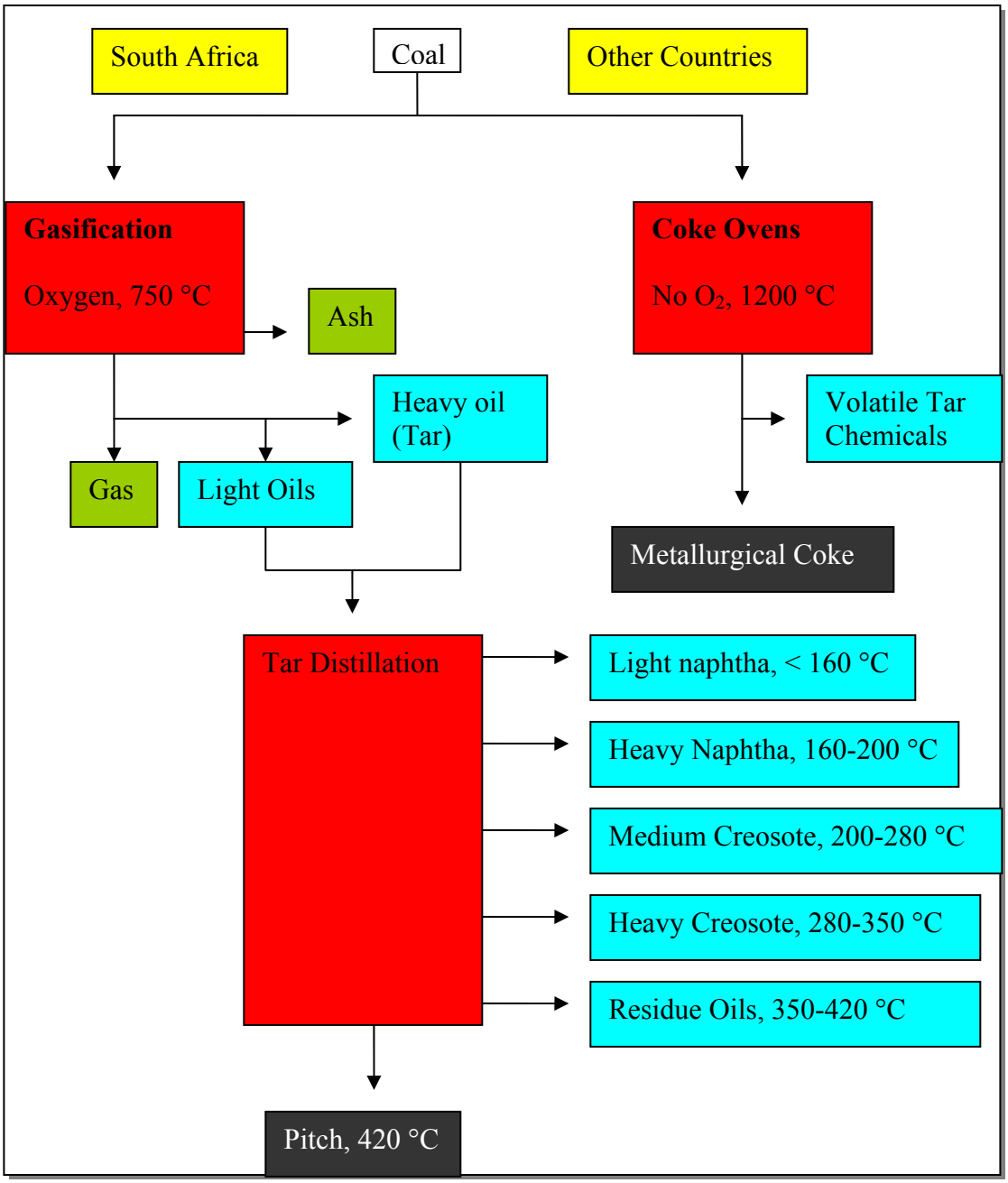

Figure 1.3: Coal processing schemes

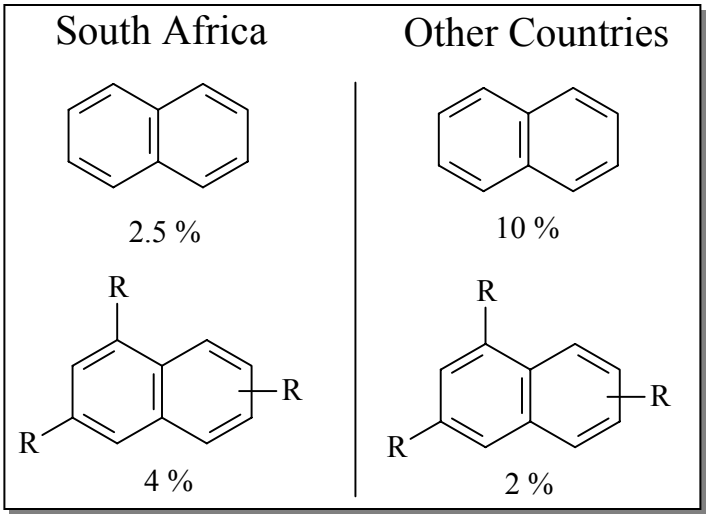

Figure 1.4: Aromatic compounds in Coal tar-pitch (representatives)

A binder pitch used in the manufacture of electrodes and other carbon and graphite products have specific requirements such as a minimum specific gravity or density, a narrow softening point range, a minimum C/H ratio, a minimum cocking value, maximum for the permissible ash content, moisture content and amount of volatile matter at 300 °C, and a minimum of ca 20 % for the amount of toluene-isoluble/quinoline soluble β-resin content.[6] The principal binder material, coal-tar pitch, is produced by the distillation of coal tar. Coal-tar pitches are composed primarily of unsubstituted polynuclear aromatic hydrocarbons and heterocyclics; this is quite normal with countries that uses high rank coals but opposite for lower rank bituminous coals used in South Africa.

1.3 Objectives and motivations for this study

The objective of this project (study) was to explore the chemistry of the removal of alkyl substituents from aromatic complexes found in pitch (naphthalene derivatives will be used as model compounds because compounds found in pitch or tar are extremely complex and difficult to work with) via alkyl-transfer reactions to a suitable alkyl-acceptor such as benzene and/or toluene. This process is of potential importance since it will provide a suitable means (information/knowledge) of

improving and manipulating the quality of coal tar-pitch (scheme 1.2). By alkylating to benzene, valuable alkylbenzenes used as raw materials in chemical industries will be produced and considerable amounts of benzene in the reformate and hopefully in gasoline will be reduced; this will help comply with the Clean Air Act (CAA) gasoline specifications and also reduced the toxicity levels and cancer risks of the final product. The advantage of using benzene and toluene as alkyl-acceptors other than that of producing fine chemicals and reducing amounts of the toxic benzene is that they are good solvents for heavy aromatics (represented below by the naphthalene framework) found in coal tar-pitch. Hopefully more chemicals can be extracted from coal tar-pitch by similar methodologies.

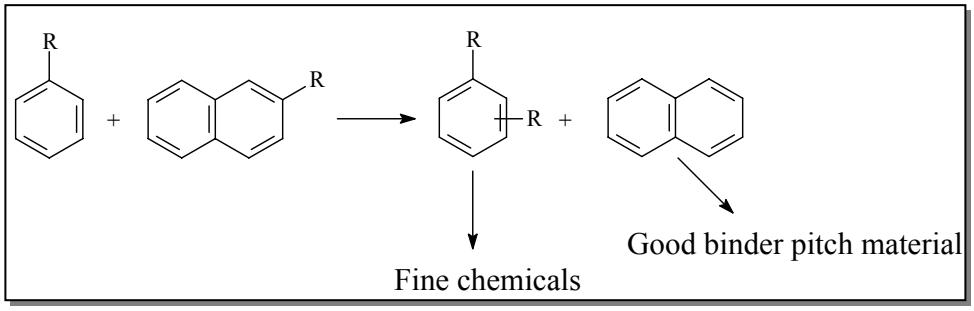

Scheme 1.2: Transalkylation (alkyl-transfer) objectives

For environmental awareness reasons, solid acid catalysts (zeolites) will be used in the study and suitable catalysts for such reactions should be identified. The intention was also to extend the study of acid catalysts to include wider pore materials such as mesoporous silica suitably activated for acid catalysis by aluminium; the reasons being that coal tar-pitch contains large polynuclear aromatic molecular complexes which might not be accommodated in the pores of known microporous zeolite catalysts.

1.4 Thesis Overview

The style used in this thesis is such that each chapter is in the form of a publication. Hence, some duplication (e.g. repetition of experimental set-up and reaction

conditions, coverage of some of the literature, etc) will be encountered in almost every chapter.

The following two chapters are mainly concerned with the literature findings and the experimental part respectively. Chapter 2 covers mostly work reported on solid acid catalysts using alkylaromatics, focusing mostly on alkyl-transfer and alkyl-shift (isomerization) reactions. Most of the work in the open literature only focused on alkyl-aromatics and not on benzene interconversions on zeolites. Toluene disproportionation to benzene and xylene and further xylene isomerization to *p*-xylene are well studied reactions and very well documented. Work involving trimethylbenzene, naphthalene, alkylnaphthalenes and polynuclear alkylaromatics is still under ongoing research and publications are usually only in patent forms. Chapter 3 focuses mainly on the reaction setup for alkyl-transfer reactions, procedures followed in the pretreatment of the catalysts, reaction conditions and analysis techniques used in this particular study. Activation of MCM-41 materials for acid catalysis and the room temperature synthesis of MCM-48 and its grafting methods are also discussed; this also includes their characterization methods.

Chapter 4 deals with the identification of suitable solid acid catalysts for alkyl-transfer reactions of alkyl-aromatics and ethylbenzene disproportionation was used as a test reaction to evaluate the potentiality of the three chosen catalysts, i.e. ZSM-5, mordenite and LZY-82 which were used in the open literature as solid acid catalysts. This method of characterization by ethylbenzene disproportionation was introduced by Karge *et al*.[7] for characterizing Brönsted acidity of large pore zeolites and was later published by the International Zeolite Association[8] (IZA) as a standard test reaction for acidity characterization.

Preliminary studies on simple alkyl-aromatics including the two chosen alkyl-acceptors (benzene and toluene) are documented in chapters 5, 6, 7, and 8. The study was carried out mainly to evaluate the product behaviour of transalkylation/disproportionation reactions on solid acid catalysts. Benzene and

toluene transalkylation reactions on zeolites are discussed in chapter 5 and 6 respectively; these particular compounds were very special in this study since they were used both as solvents and alkyl-acceptor molecules and thus their effects on the catalyst under reaction conditions are discussed. Chapter 7 and 8 discuses the interconversions of xylene and mesitylene on zeolites respectively; levels of conversion and the temperature effects are parameters which are discussed and these are compared to the results found with benzene and toluene.

Transalkylation studies commence with alkyl-transfer reactions between benzene and trimethylbenzene (mesitylene) in chapter 9; here the preferential adsorption between the two compounds (binary systems) is highlighted. The effects of temperature and that of feed composition on transalkylation reactions are briefly evaluated and discussed.

Increasing the size of alkyl-aromatics by a ring resulted in bulkier reactant molecules. Chapter 10 deals with the transalkylation reactions between benzene and methylnaphthalene and the observed low conversions are discussed. Logically, chapter 11 discuses attempts made to improve on the conversion levels of transalkylation reactions between benzene and alkylnaphthalene by increasing the number of alkyl groups on the naphthalene moiety. Selectivities induced by temperature are also elaborated upon to some extent. Further attempts to improve on the alkyl-transfer conversions are discussed in chapter 12 where alkylbenzenes such as toluene and ethylbenzene were used as alkyl-acceptors of the alkyl groups from methylnaphthalene.

The effects of transalkylation/disproportionation product on transalkylation binary systems are documented in chapter 13. Toluene and *o*-xylene were used to 'back-transalkylate' to naphthalenes. The effects of the number of alkyl groups on the benzene ring on this kind of alkyl-transfer reactions are discussed and this covers also the feed composition effects on the systems. Studies on microporous catalytic materials are concluded by studying their thermal stabilities which are discussed in

chapter 14. The feed type, reaction temperature (fouling temperature) and to a less extent the regeneration temperature are parameters on which this chapter focuses. TGA was the main analytical technique in this case in conjunction with the online G.C for regeneration effects on selectivities.

Focus was then turned to mesoporous catalytic materials such as the recently discovered MCM-41 and MCM-48 materials. Chapter 15 discuses the activation of the as-synthesized Al-MCM-41 materials using metal exchange methods and the conversion of the resulting materials to acid catalysts for alkyl-transfer reactions. These were characterized by XRD and TPD techniques which were followed by the important test reactions (alkyl-transfer reactions). Chapter 16 compares and contrasts results of alkyl-transfer reactions on microporous materials to that of mesoporous (MCM-41) materials; these are then discussed against thermodynamic calculated values from SASOL where the effect of the number of alkyl groups and their type, and also the effect of the type of aromatic conjugation on transalkylation reactions are discussed.

Attention was then shifted from the uni-dimensional MCM-41 to the tri-dimensional MCM 48 materials in chapter 17. The chapter focuses on the room temperature synthesis of the purely siliceous MCM-48 and its subsequent post alumination via incipient wetness method using different solvents. The study was conducted in an attempt to improve on the thermal stabilities of these mesoporous materials. XRD is one of the analytical techniques used in addition to alkyl-transfer test reaction with simple alkylaromatics of the formula C_9H_{12}. Results of this study are discussed and compared to those of MCM-41 materials. The study is further pursued in chapter 18 where the effects on transalkylation systems of the amounts of grafted alumina (through incipient wetness method) on the framework of siliceous materials are evaluated and discussed. To a less extent, the feed composition of the transalkylation binary mixtures and their effects on the reactions are discussed, the study also covers briefly the binuclear systems. The study on mesoporous material is also concluded by studying the thermal stabilities of these grafted materials using cumene as a foulant.

Each chapter has its own conclusions but the overall conclusions on alkyl-transfer reactions of alkylaromatics on solid acid zeolites are found in chapter 19; while chapter 20 gives a list of references used in the study.

2 LITERATURE REVIEW

2.1 Introduction

The oil refinery industry is currently facing a number of important challenges. A major drive exist world wide towards high-quality transport fuels, which for gasoline includes a need for high-octane components.[9] For automotive gasoils, sulphur specification and, in some countries, aromatic specifications are becoming very severe. On the other hand the refinery margins are generally low, forcing refineries to choose the most effective technologies. Finally, environmental considerations also apply to the refinery operation itself and the search for a cleaner technology is continuous.

Zeolitic catalysts can address many of the issues outlined above and have been used commercially in the process industry for several decades. In oil refining the impact of zeolitic catalysts, notably in fluid catalytic cracking (FCC), is substantial. In the chemical industry the application of zeolitic catalysts is clearly smaller, but in aromatic processing for example, they are used extensively. In industry R&D, the major challenges are to effectively match the opportunities offered by new catalytic materials or insights with the current and future needs of the refiner and the transport fuel consumer.

In recent years the emphasis has been on increasing the pore size of the crystalline molecular sieves, aiming at structures with pores greater than 10Å in diameter.[10] This trend reflects the need to selectively convert heavier oil molecules or bulky chemical compounds which do not fit in the pores of current zeolites and related sieves. A

diversity of factors can be identified which have stimulated the development in zeolite catalysis, i.e.:

1) Intense business competition in oil refinery and petrochemicals.
2) Changes in product quality and environmental demands.
3) Technology push through innovative catalyst research which has led to the development of new processes.

In general, zeolite catalysts exhibit superior activity, stability and selectivity compared to their amorphous equivalents in major refinery conversion and upgrading processes. Thus they allow higher throughputs, deeper conversion, more stable operation, higher yields and better product quality. In other words zeolite catalysts contribute significantly to the margin of refinery processes. The development of new zeolites to full commercial scale is a time-consuming and expensive process, the cost of which must be balanced against the potential benefits in using the new zeolite instead of an earlier one.[11] On the other hand, once a zeolite is commercial, new commercial applications may readily develop.

Zeolites have been used in the production of petrochemicals, as well as in the numerous reactions that they undergo (cracking, hydrocracking, hydration, dehydration, alkylation, isomerization, oxidative addition and dehydrocyclization) in Industrial scale catalysis world wide.[12]

The detailed characterization of a zeolite is a prerequisite to establishing property/performance relationship in zeolite catalysis. An obvious example is the characterization of zeolite acidity.[13] The number of Brönsted acid sites can be counted fairly easily either spectroscopically or by titration. However, the determination of their exact distribution over the zeolite lattice is quite a challenge to the analyst.[14] This holds even more for Lewis acid sites. Methods have been sought to properly characterize the exact distribution of acid sites in the zeolite. In-situ FTIR adsorption studies with a suitable basic probe molecule (e.g. quinoline) provides essential information. By monitoring the reaction of the intensity of the acid OH-

vibration peak at 3610 cm^{-1} with FTIR during exposure to the external surface could be quantitatively determined. A definite attribution will require further study, including the use of probe molecules of different size and basicity.

Catalyst testing is a crucial step in the exploration of new applications, the optimization of process conditions, the unraveling of feedstock effects in a new process, the scrutiny of concepts as well as in guiding catalyst commercialization.[12] Further application of zeolites can be envisaged in higher-stability catalysts (e.g. through reduced coke formation) and as supported and as supports for non acid catalysis. At present the major applications of zeolites are in acid catalysis, using the about 1000 fold higher activity compared to the older amorphous silica alumina ratio, but this can be controlled quite well.[12]

2.2 Zeolites

Microporous aluminosilicate catalysts possessing structure of well-known minerals (such as faujasite, ferrierite, mordenite and erionite) as well as many more that have no known naturally occurring analogues (for example, ZSM-5, Theta-1, ZSM-23, zeolite RHO) are particularly well suited for the conversion of hydrocarbons, certain oxygenates and other species into useful products.[15] They are in effect, replete with cages and channels made of Si and Al atoms linked by an oxygen atom (see figure 2.1). They are solids possessing tri-dimensional (3-D) surfaces, which may or may not intersect, linking the pores and distributed in a more or less spatially uniform fashion, throughout their bulk are the active sites which are bridging hydroxyl groups; these are shown in figure 2.2.

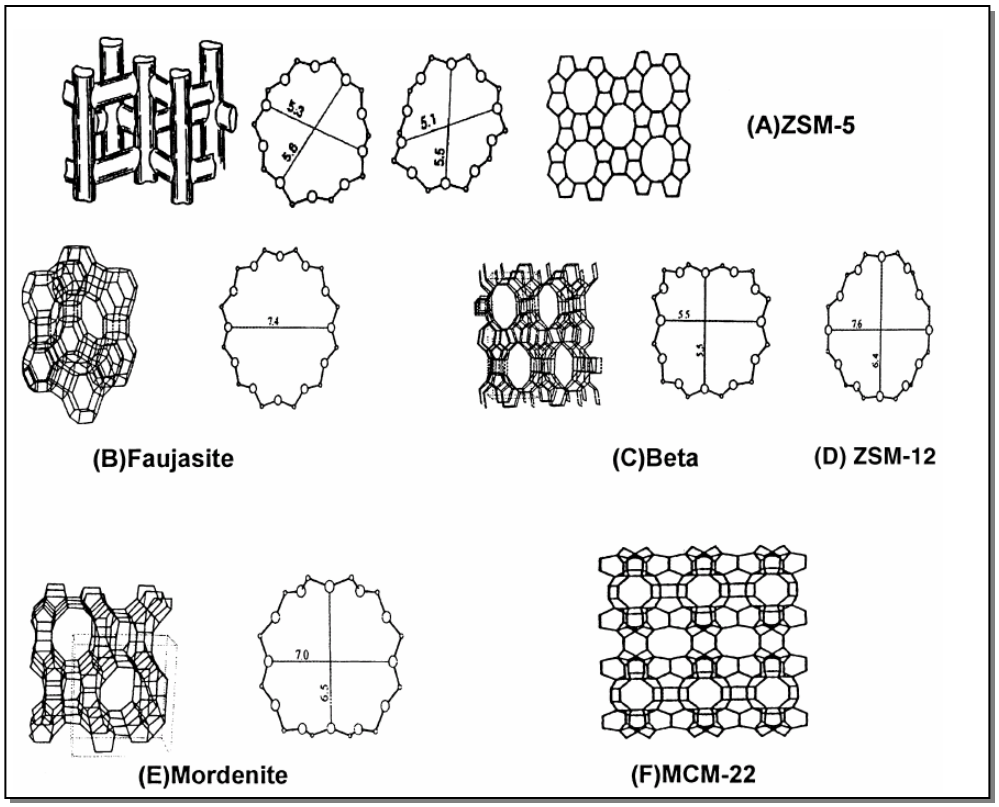

Figure 2.1: Zeolite structures[15]: Small pore zeolites: 8 atom (Si and/or Al) rings, 3-5 Å; Medium pore zeolites: 10 atom (Si and/or Al) rings, 4-6 Å; Large pore zeolites: 12 atom (Si and/or Al) rings, 6-8 Å)

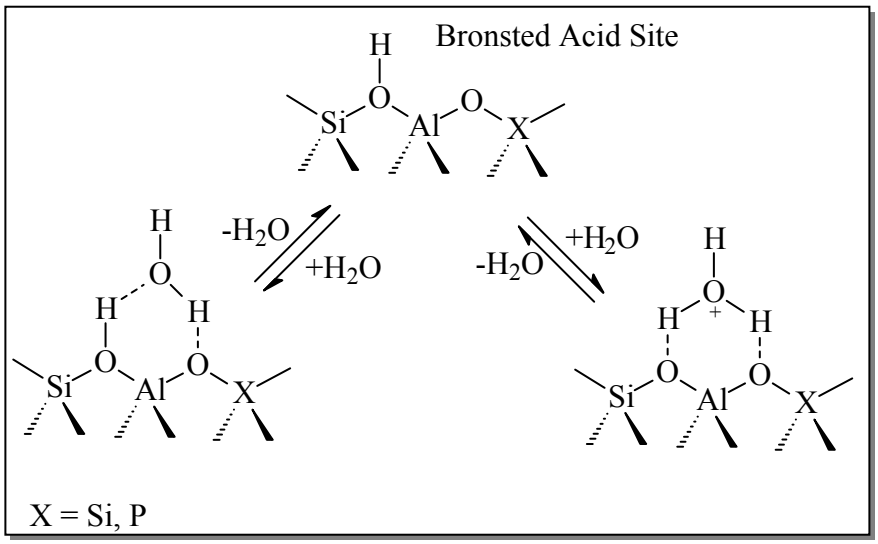

Figure 2.2: These are the classic Brönsted acid sites/centers[15]

The acid strength is a function of both the particular local environment of the aluminosilicate structure in which they occur and also the Si/Al ratio. Other heteroatoms other than Al may be substituted for Si into the framework structure, e.g. Fe-ZSM-5, trivalent iron, also the trivalent Gallium and Boron, the Phosphate type $AlPO_4$. Replacing the Al with Co, Zn and Mg results in a metal aluminum phosphate (MeAlPO); replacing a pentavalent phosphorous with Si results in a silicon-aluminium phosphate (SAPO).[15]

Zeolites are crystalline aluminosilicates whose general formula is:

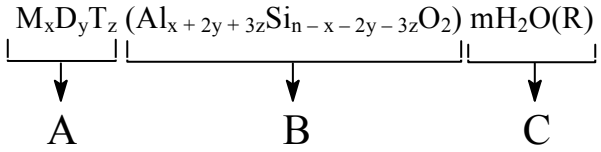

where A represents mono- (M), di- (D), or tri- (T) valent exchangeable cations, B represents the tri-dimensional framework with an intercrystalline void space consisting of channels and cages that may sometime be interconverted; and C represents molecules sorbed in their crystalline volume which are either water (Zeolite, from the Greek, means “boiling stone”), organic templates used during their synthesis, or sorbed species which can also be reactants, intermediates, and product for a certain catalytic reaction.[16] Water molecules exist in zeolites as clusters hydrogen bonded to the zeolite wall and definitely are not a gas or a liquid. Water in zeolites has a higher density than liquid water and the motion of water molecules in the intracrystalline volume is most different from that of liquid water. Although the second observation is trivial the first one underpins the proposal that a higher virtual pressure exists in the intercrystalline volume of zeolites. A higher “virtual pressure” of reactants thus exists inside the zeolite which results in an increase of the reaction rate.[16]

The molecular shape-selective properties of zeolites during catalytic reactions result from constraints, in other words "negative" interactions, imposed by the limited size of their channels and cages. Reactant selectivity is observed when some reactants only can access their intracrystalline volume. Product selectivity occurs when reaction products have very different diffusional behaviour in the zeolite pores; the formation of products with high diffusivity favoured. Restricted transition state selectivity results from constraints which prevent the formation of reaction transition state, thus preventing the occurrence of certain reactions. In contrast, confinement effects are favourable, "positive" interaction of supramolecular nature which leads the reactant(s) to recognize the active site(s), and stabilize the reactant(s) and the reaction transition state in an environment promoting the desired catalytic transformations, in a manner resembling strikingly the action of enzymes.[16]

Indeed, zeolite frameworks have some flexibility (as well recognized today, e.g. MFI, RHO, MOR….), and have receptor sites (pockets, cages, curved channel walls) which accommodate guest molecules. They are the locus of supramolecular effects and steric constraints, e.g. those restricting reaction transition states, which affect catalytic activity and selectivity.

Restricted transition state molecular shape selectivity states that the size and shape of transition state along the path of chemical transformation in zeolites may be restricted by their available void volume (defined by the size of the channels and/or cages), thus affecting the specificity of the catalyst and the selectivity of the transformation. Bimolecular transition state with at maximum about nine carbon atoms only can be formed at the intersection of zeolite channels in zeolite ZSM-5.

The fact that constraints on the transition state limit or prevent the occurrence of bimolecular reactions is critical for the understanding and rationalization of zeolite deactivation by coking (coke should be regarded, in this context, as carbonaceous residues with typical H/C ratio in the range 0.6 – 1.5). Deactivation of small pore zeolites occurs by deposition of "oligo/polymers" which cannot desorb easily and

cause pore blockage unless the temperature is high enough, e.g. greater than about 300 °C, for them to crack into smaller fragments which can desorb more easily.[16] For large pore materials the residue may be di- or poly-aromatic in nature and block the cages and the pore mouths. Such carbonaceous residues are removed by oxidative ("burning") regeneration treatments. Intermediate pore size zeolites are highly resistant to deactivation by coke as (i) poly-aromatics cannot be formed because of restricted transition state selectivity constraints and (ii) "oligo/polymers" can be desorbed easily either following cracking or their conversion to mono-aromatic compounds with a limited number of methyl or ethyl side chains. Intermediate pore size zeolites can be regenerated by oxidative or reductive "selectoforming" by treatment in hydrogen.

The concept of molecular traffic control predicts that when a zeolite has a pore network consisting of differentiated (by size or shape) channels, reactants and/or products having distinct steric requirements can diffuse along different paths in its intercrystalline void volume. Small and large molecules diffuse preferentially in the small and large pores, respectively. Thus competitive and/or counter diffusion are minimized and catalytic activity (sometime selectivity) may thereby be enhanced when otherwise governed by diffusion limitations because of the operating conditions.

The Nest effect concept proposes that some of the remarkable properties of zeolites originate from their (somewhat flexible) open framework which offers channels and/or cages, acting as "pockets" where the activation and the conversion of the substrate occur. The three ideas underpinning this proposal are that:

- There will be situations where the selectivity of zeolites will be dominated by positive (attractive) interactions, in contrast to the negative (repulsive) constraints which govern molecular shape selective catalysis;

- in such cases, the substrate molecules and the zeolite framework will reciprocally optimize their respective structures to maximize their van der Waals interaction;
- nesting can occur both in the intracrystalline volume of the zeolite and at the external surface which is made of "craters" and "hills" (the zeolite surface cuts through cages and pore walls).

The action of zeolites as molecular traps becomes obvious as a result of confinement effects. Their trapping efficiency increases as the sorbate size tends towards the size of the channels or cages, i.e. as confinement increases.

Zeolite catalysis in liquid phase distinguishes itself from zeolite catalysis in vapour phase in several ways:

- the high concentration of reactants resulting in a high utilization of the intracrystalline volume of the zeolite,
- the competition of the reactants for the zeolite intracrystalline volume, governed by molecular shape selectivity, confinement, and polarity effects,
- the competitive adsorption of the solvent,
- the accumulation of product(s) in the solvent when operating in batch conditions, resulting in a progressively slower egression of the products from the zeolite and a decrease in catalyst productivity as the reaction proceeds (mass transfer effects).

Maximum efficiency is achieved when the reactants are stoichiometrically adsorbed in the zeolite,[16] when the products are easily desorbed, and when the solvent does not compete with the reactants. A solvent which is poor for the reactants and good for the product(s) will prevent accumulation of the product(s) inside the zeolite.

2.2.1 Nomenclature

All zeolitic and AlPO (MeAlPO) structure types consists of three capital letters. Structure types do not depend on composition, distribution of the various possible T-atoms (B, Be, Al, P, Si, Ge, Zn, Sn, Co, Fe, V, etc) unit cell dimensions or symmetry. In general,[11] the codes (AEI, ATS, CHA, FAU, etc) are derived from the names of the type species and not include numbers and characters other than capital roman letters, e.g.:

AEI [$AlPO_4$-18, AlPO eighteen]
AEL [$AlPO_4$-11, AlPO eleven]
CHA [Chabazite, $Ca_6[Al_{12}Si_{24}O_{72}]\cdot 40H_2O$]
FER [Ferrierite, $Na_2Mg[Al_6Si_{30}O_{72}]\cdot 18H_2O$]
TON [Theta-one, $Na_n[Al_nSi_{24-n}O_{48}]4H_2O$]

For Linde type L zeolite (LTL) the secondary building units (SBUs) are single 6-rings.

2.2.2 Microporous solids as catalysts

The key role of the acid catalyst is to function as a rich source of protons, thereby facilitating the formation of carbocations.[11] These in turn greatly accelerates the process of polymerization, isomerization, alkylation and cracking. The most novel feature of this class of catalysts (zeolites) is their shape selectivity because the dimensions of the cages and channels, and more importantly the diameters of the aperture are comparable to the cross-sections of the reactant and product molecules. Clean technology nowadays provides the stimulus for many new developmental concerns about the use of corrosive liquid acids such as hydrofluoric acid (HF) and 96 % sulfuric acid (H_2SO_4) as catalysts for the alkylation or isomerization of hydrocarbons.

2.2.3 Mesoporous solids as catalysts

Even for the largest pore openings of ~ 7.4 Å present in zeolitic (aluminosilicates) solids such as FAU, LTL and DFO, there are severe limitations for the size of molecules that can be subjected to shape-selective catalytic conversion.[11] With the so-called MCM-41/48 larger-pore mesoporous structure, with the dimensions varying from 20 to 100 Å in a regular fashion, large hydrocarbons can be catalyzed. This type of catalysts will be discussed in more details later in the chapter.

2.2.4 Acidity and Basicity in zeolites

Abbreviations: Brönsted acid site = BA; Brönsted base site = BBS,
Lewis acid site = LA; Lewis base site = LBS.

Lewis acids, such as incompletely coordinated Al ions, have a very close similarity with Brönsted acids in their reactions with electron donors, and partly because both types of acids are present on aluminium silicates surface.[17] Ammonium ions completely decompose at 600 °C in mordenite and 500 °C in Y-zeolites. The fact that higher temperatures are required to remove ammonia in the case of mordenite indicates that this zeolite is more strongly acidic than Y-zeolites. From observations, it was clear that Brönsted acid sites rather than Lewis are the seats of activity in zeolites.

The complete characterization of the acidic-basic properties of a zeolite comprises several aspects, such as the determination of the:[11]

i) nature of the acid and base sites (Brönsted versus Lewis sites);
ii) concentration of the acid and base sites in the solid;
iii) distribution of the acid and base site strengths.

2.2.4.1 Quantification of acid sites

2.2.4.1.1 Direct methods

There exist two techniques that enable direct observation of protons in an acid zeolite sample, namely proton magic angle spinning nuclear magnetic resonance (^{1}H MAS NMR) and infrared (IR) spectroscopy.[11] The major advantage of ^{1}H MAS NMR over IR spectroscopy is that the relative signal intensities are directly proportional to the relative concentrations of the different types of hydrogen atoms in the sample. Provided a reference sample is available, the ^{1}H MAS NMR measurements allows determination of absolute proton concentrations. All protons in acid zeolites are bound to oxygen atoms, and the O-H stretching vibrations investigated with IR constitute a second direct way to observe the Brönsted acid sites.

2.2.4.1.2 Indirect methods

i) Determination of total acid sites (BAS + LAS)

A common, indirect approach to the determination of the total concentration of acid sites irrespective of their Brönsted or Lewis nature is possible by chemisorptions of basic probe molecules and quantification of the number of adsorbed molecules.[11] In temperature programmed desorption (TPD) experiments, a zeolite sample is saturated with a strong basic molecule, and after evacuation of the chemisorbed probe molecules, the chemisorbed molecules are swept from the sample in a flow of inert carrier gas during a temperature programmed desorption profile.

ii) Discrimination among BAS and LAS sites

Pyridine is favoured as a probe molecule for quantification of Brönsted and Lewis acid sites separately, since its adsorption on these sites gives discrete IR bands.[11] Pyridine is a strong base probing the whole spectrum of Brönsted and Lewis acid strengths. Because of the size of the pyridine molecules, pyridine cannot be used for quantification of zeolites containing a large concentration of Brönsted sites. In FAU zeolites, two pyridinium ions per supercage can be generated at the maximum, limiting the applicability of the IR-pyridine technique to aluminosilicate zeolites with Si/Al larger than 4.

X-ray photoelectron spectroscopy (XPS) and probe adsorption is sometimes handled to characterize the acidity on the external surface of the zeolite crystals. The N_{1s} signal of adsorbed pyridine can be decomposed into two components arising from pyridinium ions and coordinative adsorbed pyridine. It has to be stressed that the XPS data reflects the [BAS]/[LAS] ratio on the external surface of the zeolite crystals and are not representative for overall bulk acidity.

2.2.4.2 Determination of distribution of sites strengths

2.2.4.2.1 Direct methods

In principle, the NMR ^1H chemical shift is correlated with the proton donor ability of the BAS and provides information on the Brönsted acid strength.[11] Similarly, the O-H stretching frequency reflects the strength of the O-H bond and the proton donating ability of a BA site. Many acid zeolites have BAS involving framework oxygen at crystallographically different positions, i.e. bridging hydroxyls freely vibrating in large cages or channels next to bridging hydroxyls in small cavities surrounded by 6- or 8-rings of T-atoms. Since the proton of a bridging hydroxyl may interact with several framework oxygen atoms, these interactions may give rise to different

bathochromic shift in the IR spectra, to different shift (downfield) in ^{1}H MAS NMR, not necessarily reflecting an increase in acid strength.

2.2.4.2.2 Indirect methods

i) Non-selective method: Calorimetry of base adsorption

Access to the acid strength spectrum of BA and LA sites in a zeolite can be obtained from calorimetric measurements that determine the heat of adsorption of basic probe molecules at increasing amounts of sorbate.[11] A major difficulty of this technique when using strong adsorbing molecules are the long times needed to reach the adsorption equilibrium.

ii) Selective methods: TPD combined with selective spectroscopy detection

The distribution of BA and LA strength can be obtained simultaneously when the TPD method uses a spectroscopic detection technique to determine the nature of the acid sites the probe molecule is interacting with.[11] Pyridine is typically used as spectroscopic probe in such experiments and IR spectroscopy as the detection technique.

iii) Selective methods: IR spectroscopy of interactions with a weak base

Strong bases such as ammonia and pyridine reacts unspecifically with weak and strong acid sites and therefore TPD has to be applied in order to discriminate among the site strength.[11] Alternatively, weaker bases (benzene, carbon monoxide, ethylene, deuterated acetonitrile, etc) may be used as spectroscopic probes for acid strength. Upon interaction of a hydroxyl group with the π-electrons of benzene, ethylene, carbon monoxide or other unsaturated probe molecules, the O-H stretching frequency undergoes a bathochromic shift, the extent of which increases with the acid strength.

Carbon monoxide with its small kinetic diameter and molecular size can reach all BA sites in many zeolites and can be used to probe zeolites. Frequency in carbon monoxides is sensitive to interactions with LAS and is suitable for determination of the LAS strength.

2.2.5 Acid properties of aluminosilicates (zeolites)

The tri-dimensional microporous framework of a zeolite is made up by corner sharing of SiO_4 and AlO_4 tetrahedra.[18] They can be considered as originating from an all-silica lattice, in which some of the Si atoms have been replaced with Al by isomorphic substitution. The substitution generates an excess negative charge in the silicate lattice, which is compensated for by cations. A general formula for an aluminosilicate zeolite is

$$M^{z+}_{x/z}[(AlO^{-}_{2})_x(SiO_2)_y]\cdot nH_2O$$

in which the framework composition is shown within square brackets. Here, *z* is the valence of the charge compensating cations M and the ratio *x/y* is smaller than or equal to 1 because there is no linking of alumina tetrahedral in aluminosilicate frameworks (Löwenstein rule).[18] To variable degree, the charge compensating cations can be exchanged for other cations including protons.

Many large scale catalytic application of zeolites are based on their Brönsted acidity, which is provided either by one of the following processes[18]:

i) ion exchange with protons in a liquid Brönsted acidic medium;
ii) exchange of ammonium ions, followed by an activation step whereby ammonia vapour is expelled;
iii) calcinations whereby organic structuring cations are thermally decomposed;

iv) hydrolysis of hydration water by polyvalent (e.g. di- and trivalent) cations;

v) reduction of cations to a lower valence state.

Theoretically, one bridging hydroxyl or BAS can be generated for each Al in the framework. The larger the aluminium content or the lower the Si/Al ratio of the sample, the larger is the potential number of BASs. Recent developments in theoretical modeling of acid catalysis with zeolites have revealed the existence of synergism between BASs and LASs. According to this model active sites are of a bifunctional nature, and consequently the properties of a molecule adsorbed in a zeolite cavity are influenced not only by the interaction with a proton having BA properties, but also with the oxygen atom of the cavity surrounding the proton and having Lewis basic properties (LBS). The BAS protonates the adsorbed molecule, while interaction with the neighboring LBS converts the protonated intermediate into a species covalently bounds to the framework. Since the size of the adsorbed molecules and that of the zeolite cage is close, the stabilization of the protonated species through interaction with LBSs will also depend on the zeolite topology. The Lewis acidity in protonic zeolites is associated with aluminium species dislodged from the framework. The exact nature of these extraframework aluminium species and of the role of the Lewis acid sites in catalysis remains an unsettled issue.

The system with high affinity for electrons will have lower deprotonation energies or higher intrinsic acid site strength.[18] Lowest acid sites strengths are on the terminal hydroxyls (on the surface) and highest strengths are of the bridging hydroxyls. In comparison, the bridged hydroxy Si/Al unit is proportional to the acid strength of H_2SO_4, and the terminal hydroxyl is proportional to CH_3COOH and the Si/B, Si/Ga and Ge/Al are lesser in acidity than the Si/Al.

2.2.6 Compositional Gap

The early work on zeolite synthesis (1950-1965) dealt with crystallization from inorganic gels and culminated in the synthesis of the so-called first generation of high-aluminium zeolites, including zeolite A (LTA topology) X and Y (FAU topology), L (LTL topology), and so on.[11] These high-aluminium zeolites have Si/Al ranging typically from 1 to 6. One of the more recent developments in zeolite synthesis has been the use of organic structuring agents. Dozens of new topologies with Si/Al ratios generally higher than 10 and belonging to the second generation of high silica zeolites have been obtained using this approach, showing improved activity in acid catalyzed reactions. Examples are the ZSM-5 (MFI topology) Theta-1 (TON topology), and zeolite-Beta (BEA topology). Theory commonly predicts a continuous increase of the acid strength per site with decreasing Al content until a significant degree of dealumination has been reached. Al-rich first generation material can be dealuminated chemically with steam, silicon tetrachloride, di-ammonium hexaflourosilicate, etc. These methods often partially destroy the micropore structure of the zeolite, and generate mesopores and extraframework aluminium (and silicon) species. These extraframework species can modify the acid-base properties considerably.[11]

2.2.7 BASs and LASs in hydrogen zeolite containing extraframework aluminium and silicon species

The dealumination of zeolite-Y is an essential step in the manufacturing of catalysts for fluid cracking catalysis (FCC) and hydrocracking.[11] Dealumination of the parent Na-Y zeolite with a Si/Al ratio of ca 2.5 leads to an enhanced acidity as the BAS strength is increased by degreasing the concentration of bridging hydroxyls (Al atoms) and to enhanced (hydro) thermal stability of the material.

With steaming temperatures in excess of 500 °C, framework Al-O-Si bonds are hydrolyzed and aluminium is dislodged from the framework as a monomeric cationic species.[11] The dealumination is the most pronounced in the core of those catalysts where the highest temperatures are reached. The dislodged aluminium may then migrate to the crystal surface and depending on the conditions accumulate as oligomeric and polymeric species of aluminium oxyhydroxide or oxide. The later are sometimes removed during an additional leaching with diluted mineral acids. In hydrothermal dealumination processes lattice defects left after aluminium removal can be healed either by the formation of new oxygen bridges between adjacent silicon atoms, or by substitution with Si atoms coming from the amorphous parts of the crystal. As a result, the framework becomes more siliceous and through removal of the least stable parts of the lattice adjacent cages become interconnected. This generates a network of secondary pores with substantially larger pore diameters, usually situated in the mesopores range. In parallel, multivalent rare earth metal cations, if present migrate to the hexagonal cages or after hydrolysis are trapped in the β–cages where they stabilize the structure.

The extraframework aluminium atoms may be present in a variety of chemical species, depending on the specific dealumination conditions used:

i) Monomeric, partially hydrolyzed cationic aluminium species such as Al^{3+}, $Al(OH)^{2+}$, or $Al(OH)^{+}_{2}$, fully dislodged from the framework, neutralizing framework charges and acting as strong LASs;
ii) Monomeric aluminium species, coordinated to less than four framework oxygen;
iii) Oligomeric aluminium oxyhydroxides or oxides;
iv) An amorphous, silica-alumina phase occluded in the zeolite.

According to one of the proposed model, a super-BAS is formed through interaction of a bridging hydroxyl (regular BAS) and neighboring LAS. Provoked by the presence of extraframework aluminium species, the HF (high field) and the LF (low

field) hydroxyl vibration undergo a bathochromic shift, confirming that electron withdrawal from the bridging hydroxyl by neighboring extraframework Al species leads to weakening of the O-H bond and an increase in acid strength.[11] A similar role of LAS is ascribed to partially hydrolyzed polyvalent cations such as La^{3+} in the form of $[La_2(OH)_2]^{4+}$ or $La(OH)^{2+}$, located in the β–cages of FAU-type zeolite.

The acidity of strongly dealuminated zeolites is reduced due to a process of partial charge balancing with cationic extraframework aluminium species rather than with protons or by simple pore blocking.

2.2.8 Dealumination of Silica-rich zeolites

When mild steaming is applied, a dramatic increase in the catalytic acidity is observed in zeolites including H-ZSM-5, H-mordenite and H-ZSM-20 in demanding hydrocarbon reactions such as toluene disproportionation, aromatics and alkane isomerization and cracking.[19] It was postulated that paired Al framework atoms act as Lewis acid site withdrawing electrons density from the neighboring intact BAS, thus increasing its BAS strength. Materials dealuminated by steaming showed to be considerably more active than those dealuminated by chemicals.[20] Steamed zeolite differs from chemically dealuminated zeolite mainly in that they contain considerable amount of non-framework Al. Non-framework Al can affect activity by[20]:

i) being a catalytic site
ii) interacting with framework Al sites to stabilize the negative charge on the lattice following the removal of acidic protons, thus increasing the Brönsted acid strength
iii) working in symbiotic manner with nearby Brönsted acid sites, increasing the rate at which a protonated molecule reacts to form product. Thus it can promote bond session of carbenium ions formed at the Brönsted site without affecting the strength of the Brönsted site

Dealumination at temperatures higher than 500 °C and 100 % steam and reaction pressure of 1 atm, cause significant changes in the catalyst activity.[21] Mild conditions, i.e. 440 °C and 1 % steam, did not lead to any loss of the platinum dispersion on Pt containing catalysts or to gross morphological changes with respect to the catalytic components. Steaming the H-mordenite at 440 °C for 3 - 5 hours leads to an increase in acidic site strengths. The mild steaming conditions have no significant effect on the platinum dispersion. Prolonged heating at temperatures above 500 °C is required to sinter platinum particles supported on alumina.

It is the low concentration of steam that is produced in situ within the zeolite micropores that can then cause dealumination of the zeolite structure during regeneration of the catalyst (thermally).[21] Prolonged steaming leads to the formation of less active catalysts but to high selectivity to disproportionation products.

2.2.9 Grafting of siliceous materials

The idea of grafting Al atoms on silica frameworks was stimulated by the need to improve acidic strengths of the already synthesized crystalline aluminosilicates (zeolites).[22] It was then realized that Al in the framework was the cause of thermal instabilities and thus grafting was going to incorporate Al atoms on the thermally stable siliceous framework without Al in the bulk; this then resulted in zeolites which were thermally stable but with reduced acid strength compared wit that of the as-synthesized aluminosilicates.

In grafting the mordenite framework Wu *et al*.[22] diverted the helium stream through a bed of anhydrous $AlCl_3$ powder in a quartz container placed over the reactor. The container was heated to achieve a vapour pressure of 11 kPa. The helium carrier containing $AlCl_3$ vapour was passed through the zeolite bed at the reaction

temperature to bring about alumination (873 K). The alumination temperature of 873 K was optimum for the incorporation of the maximum amount of framework alumina (FAL). Alumination temperature lower than the optimum temperature of 873 K was favourable for the introduction of Al atoms as extra framework alumina (EFAL).

Mordenites aluminated[22] at 873 K and higher had the larger amount of FAL than that of lower temperatures than 873 K. The latter had larger amount of EFAL. Alumination with $AlCl_3$ generates not only the Brönsted acid sites but also Lewis acid sites. They suggested that EFAL species generated by the alumination are not Brönsted acid sites; and Lewis acid sites in the aluminated mordenite are so-called 'true' Lewis acid sites which arise from the EFAL species.

Chen *et al*.[23] used the strong basic $NaAlO_2$ solution which facilitated the insertion of Al into the framework of the Si-MCM-41. However, at a higher concentration of $NaAlO_2$ or a higher reaction temperature the mesoporous phase was not stable. Even under optimal conditions the mesoporous structure was destroyed to a great extent. This confirmed earlier observations that MCM-41 materials were not very stable in alkaline solutions, and tend to become amorphous or form other zeolite phases (zeolite A or faujasite). In contrast, $Al(NO_3)_3$ aqueous solution is strongly acidic and had no harmful effect to the mesoporous structure. However, only a small amount of Al was incorporated with this reagent.

With increasing Al content, the BET surface area and pore size decreased. A further increase of the Al content in the synthesis gel resulted in a material (Si/Al = 1.9) which was no longer mesoporous and had a surface area of only 336 m^2g^{-1}. In contrast, the materials prepared by post-alumination of Si-MCM-41 (siliceous framework) remained mesoporous even after the incorporation of a large amount of Al.[24] Post-synthesis grafting with $AlCl_3$ was successful in incorporating four-fold Al into the framework of the lattice. Four-, five- and six-coordinated Al were observed in the samples with a higher proportion of octahedrally-bound Al at low Si/Al content.

The Al-MCM-41 samples prepared by using aluminium isopropoxide and pseudo boehmite had better crystallinity compared to the one with aluminium sulphate probably due to the lower pH of the resulting gel.[24]

2.2.10 Mesoporous materials

Recently a new family of mesoporous molecular sieves denoted as M41S was invented by Mobil researchers.[24] One member of this series, MCM-41, possesses a regular array of uniform and one-dimension mesopores that can be tuned to the desired pore diameter in a range of 15 to 100 Å.

The narrow pore size distribution adjustable in a wide range (15 – 100 Å) and the extremely high surface area of ca. 1000 m^2g^{-1} makes these materials promising candidates as catalysts or as catalysts support.[24] Purely siliceous MCM-41 has no Brönsted acidity. With Al incorporated in the framework, it was apparent that these materials had lower acidity and poorer thermal stability than the widely used catalysts such as the zeolite-Y and the ZSM-5. Al-containing MCM-41 tends to dealuminate during the removal of the surfactant (during their synthesis) by calcination processes.[23] This has been attributed to hydrolysis of the framework Al by steam generated form the combustion of the surfactant. The higher temperature during calcinations or under process conditions lead to disruptions in the framework and to the subsequent collapse of pores or channels in the molecular sieve especially when too much Al is incorporated (thermal instability).

The mesoporous structure of Si/Al = 5.0 collapsed totally when heated at 800 °C for 24 hours, whereas samples with Si/Al = 15.3 and 7.3 disintegrated partially with some retention of mesoporosity.[23]

Incorporation of aluminium into the structure leads to aluminosilicate MCM-41 with much shorter channels, than in the purely siliceous material.[25] The decrease in mesopore surface area and volume can be explained by the increase of the wall thickness of Al-MCM-41 materials and/or by the dealumination of framework during calcinations.[26]

MCM-41 material with higher thermal stability and therefore higher residual acidity could be prepared using amines during the synthesis [as-synthesized].[27] It was also found that in samples with low bulk Si/Al ratios (below 10) most of the aluminium was part of a separate dense phase. The use of primary amines as surfactant resulted in an aluminosilicate material with higher acidity than the material synthesized with quaternary salts such as CTMA-Br; this was attributed to the type of decomposition reactions, products formed and their effect on the framework dealumination process.

The source of Al controls the environment and location of Al atoms within the wall, and hence, the acidity of Al-MCM-41 mesostructures.[28] Materials synthesized with $NaAlO_2$ contained the strongest Brönsted acid sites. The small aluminate species are believed capable of binding to the bulky surfactant cation head groups present in the synthesis mixture. In contrast, materials synthesized with $Al(OH)_3$ presented a heterogeneous distribution of acid site strengths indicating that, in this case, there is no preferential location of Al.

When $Al(iPrO)_3$ is used, hydrolysis and condensation reactions of the alkoxide with the silicate species in the hydrogel form aluminosilicate units that, when incorporated within the mesoporous structure generates a distribution of acid sites strengths similar to those in amorphous aluminosilicate gels of the type used in hydrotreating catalysts preparation. Al-MCM-41 is believed to contain at least three types of acid sites[28]:

1) acid sites from Al(iv)-species located within the mesostructure channels yielding strong L-sites;

2) acid sites at the surface of the pores with strengths comparable with that of bridging hydroxyls in zeolites, and
3) Al(vi) sites sandwiched between silica layers with strengths similar to those of smectite.

The type and strength of these acids sites is controlled by the nature of the precursor and by the synthesis conditions used. Cracking of cumene is often used as a test for strong acid sites for Al-MCM-41 materials.[29]

The higher the Al content in the sample, the lesser the mesopores surface area and pore volume.[26] The percentage of mesopore surface area in total surface area increases with the increase in Si/Al ratio, suggesting that the size of mesopores of the sample with less Al content is more uniform than that for the sample with high Al-content. From these results it could be conclude that adding Al in the synthesis system will result in scattering of the mesopore distribution. With increase of Al content of the samples, the amount of Brönsted and Lewis acid sites both increase while their acid strengths decrease.

2.3 Alkylation of aromatics

The alkylation of aromatics is widely used in the large scale synthesis of petrochemicals, and a great variety of fine chemicals and intermediates.[30] The essential feature of the reaction consists of the replacement of a hydrogen atom of an aromatic compound by an alkylating agent. If the replaced hydrogen is on the aromatic ring, the reaction is an electrophilic substitution and is carried out in the presence of an acid catalyst; if hydrogen on the side chain of an aromatic is replaced, base catalysts or radical conditions are required. The nature of alkylation product thus depends on the catalyst used (scheme 2.1).

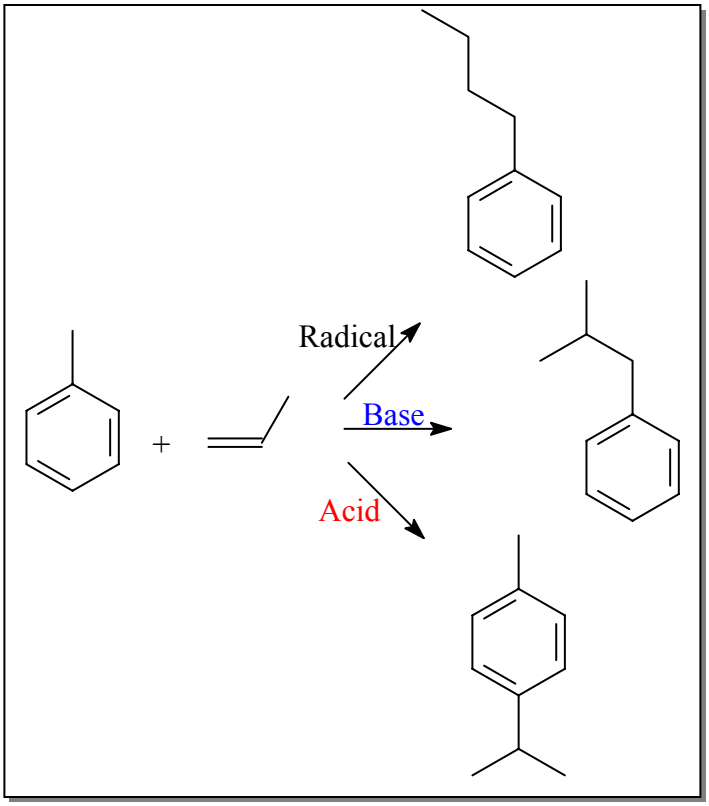

Scheme 2.1: The effect of the type of catalyst on aromatic alkylation[30]

Acid catalysts used for alkylation of aromatic hydrocarbons are Brönsted acids containing acidic protons. These include acidic halides such as aluminium chlorides and boron fluoride, acidic oxides and zeolites, protonic acids especially sulfuric acid, hydrofluoric acid and phosphoric acid, and organic cation exchange resins.

Metal halides usually called Friedel-Crafts catalysts, have been used extensively for aromatic alkylation in the past, they are highly active and allow the reaction to be carried out in liquid phase at low temperatures. However, for large scale applications they are being rapidly replaced by solid alkylation catalysts especially by crystalline aluminosilicates, i.e. zeolites. These are much more desirable for environmental reasons; they are non-corrosive and offer additional advantages for controlling the selectivities via their shape-selective properties. They are less active than the typical Friedel-Crafts catalysts and are therefore applied at higher temperatures and mostly in the gas phase. This is however not necessarily a disadvantage since alkylations are usually exothermic reactions.

i) General aspects

The net reactions in the alkylation of an aromatic hydrocarbon, ArH, with alkyl halides, alcohols and alkenes are:

$$RCl + ArH \longrightarrow RAr + HCl$$
$$ROH + ArH \longrightarrow RAr + H_2O$$
$$R\text{-}CH{=}CH_2 + ArH \longrightarrow R(CH_3)CHAr$$

The activated species, i.e. the intermediate, $CH_3\text{-}CH_2^+$ $(catalyst)^-$, is often written for simplicity's sake as a free carbenium ion, $CH_3\text{-}CH_2^+$ in the representation of such reactions.

Base catalyzed hydrocarbon reactions occur formally via carbanion intermediates. Modes of reaction, relative rates and product selectivity,[30] are governed by the relative stability of the carbanions involved, which follows the order:

Benzylic ~ allylic < primary < secondary < tertiary

ii) Kinetic consideration

Protonation/Proton affinities:

Ethylene	681 $kJmol^{-1}$
Propylene	747 $kJmol^{-1}$
i-Butene	803 $kJmol^{-1}$

They reflect the greater rate of formation and reactivity of the corresponding carbenium ions, which follows the sequence:

Primary < Secondary < Tertiary

iii) substrate selectivity

Substrate selectivity, i.e. the relative activity of various aromatics, is governed by their nucleophilicity and their ability to delocalize the positive charge in the Wheland intermediate by inductive and resonance effects.[30] For instance, a phenol react many orders of magnitude faster than benzene. The aromatic should not, or only weakly compete with the alkene for the sites. Although true for benzene, this is not always true for the much more basic phenol. Strong chemisorption of phenol almost completely inhibits the activation of the weakly basic ethylene, but not that of more basic propylene and isobutylene.

iv) Positional selectivity

Positional selectivity, such as the distribution of ortho, meta and para isomers obtained in the alkylation of toluene, depends on reactivity of the electrophile and on steric factors.

v) Mono- and poly-alkylation

However, the mechanistic considerations indicate that, for benzene alkylation, consecutive alkylation of the primary product should occur with a greater rate than the first alkylation step.[30] Thus there is a kinetic bias in favour of poly-alkylation. For example, in methanol conversion with ZSM-5 zeolite catalyst, tri- and tetra-methylbenzenes are predominantly primary products at moderate temperatures; conversions resulting from increasingly rapid methylation in the sequence benzene < toluene < xylene.

2.3.1 Alkylaromatics

i) Ethylbenzene

Ethylbenzene is predominantly produced by the alkylation of benzene with ethylene. The reaction is highly exothermic with a reaction enthalpy of -113 $kJmol^{-1}$. Earlier attempts to use zeolites such as HY, REY and Mordenite failed because of rapid coke deactivation and poor yields.[30] This is a result of the high hydride transfer activity occurring in the large pores of these catalysts. In the medium pore ZSM-5, bimolecular hydride transfer is greatly retarded for steric reasons. High yields of ethylbenzene (over 99 %) can be obtained. Catalyst deactivation is slow, the catalyst can be regenerated by coke burning and has a long ultimate life.

The alkylation process operates in the gas phase at 380 – 450 °C, 20 – 30 bar pressure and high mass of feed per mass of catalyst per hour (WHSV > 100), byproducts poly-ethylbenzenes can be recycled together with recycled benzene to the synthesis reactor for transalkylation.

ii) Isopropylbenzene

Consequently, the zeolite must contain pore of sufficient dimensions to effect the formation of cumene, and also allow any poly-alkylated species to pass through so that they may eventually be transalkylated.[30] Associated problems include increased formation of diisopropylbenzenes, and very rapid deactivation since large polyalkylated species are not easily desorbed.

In the Dow technology, two highly dealuminated mordenite catalysts are used for alkylation and transalkylation steps. The alkylation catalyst is silica bound and has a Si/Al = 156 and the transalkylation catalyst has a Si/Al = 108. Alkylation is done at 130 °C since the catalyst is less selective towards the desired product; the products

are then handled in the subsequent transalkylation step over the more active mordenite catalyst (Si/Al = 108).

iii) Alkylation of Naphthalene

Alkylnaphthalenes are important monomers for the production of advanced aromatic polymer materials and are used in fine chemical synthesis as intermediates for commercially produced vitamin K via 2-methylnaphthalene,[31] and the 2,6-dialkylnaphthalene is an important precursor for the production of polyethylene-naphthalene (PEN).

Naphthalene is a white solid crystalline material and needs to be dissolved in a certain solvent. A good solvent should dissolve large amounts of both methanol and naphthalene and remain unreacted under alkylation conditions. It also should not inhibit catalyst activity (e.g. by poisoning Brönsted acid sites) and not interfere in the G.C analysis. Mesitylene appeared to generally obey these criteria but not on H-mordenite and HLZY-82 and wider-pore catalytic materials.[32] Tetralin and nitrobenzene were reactive and inhibited naphthalene alkylation. In the alkylation of 2-methylnaphthalene carried out by Kutz *et al*.[32] on H-mordenite showed high initial reactivity with poor selectivity and rapid deactivation. The main products were 1-methylnaphthalene from isomerization of 2-methylnaphthalene, and naphthalene a dealkylation product was formed. The advantage of mesitylene as a solvent in the alkylation of naphthalene and the 2-methylnaphthalene was attributed to its relatively large size preventing them from easily reaching ZSM-5 cavity sites. They however, diffused rapidly and therefore readily react in the large channels of H-mordenite and HLZY-82.

It is well known that in the channel system of ZSM-5 zeolites the coke formation is hindered. Popova *et al*.[33] assumed that naphthalene alkylation proceeded in the channels of ZSM-5, where steric factors determine the formation of the less bulky 2-

methylnephthalene. The stability of the reaction with the experimental duration was also in favoured of the suggestion.

Fraenkel *et al*.[34] carried out the alkylation of naphthalene in a continuous flow reactor in the temperature range of 400 – 500 °C at LHSV between 0.5 and 2.0 h^{-1}. The optimal alkylation conditions established experimentally were 400 °C and 1 h^{-1}, the naphthalene to methanol ratio 1:1. The introduction of metal cations in H- and Na-forms of mordenite resulted in appreciable enhancement of the activity. This was related to the higher acidity of the metal cation containing samples.

It was initially reported that 2-methylnaphthalene could not diffuse into the pores of ZSM-5, it was later reported that the mixture of 2,6- and 2,7-dimethylnaphthalene was selectively formed over ZSM-5 catalysts. It was proposed that ZSM-5 has half cavities on the external surface which were responsible for the selective formation of 2,6- and 2,7-dimethylnaphthalene. Matsuda *et al*.[35] dealuminated ZSM-5 zeolite with $(NH_4)_2SiF_6$ to eliminate the external acid sites and this resulted in a decrease in isomerization of 2-methylnaphthalene to 1-methylnaphthalene. Disproportionation of the 2-methylnaphthalene was stable against dealumination as compared to 1-methylnaphthalene. Naphthalene was the abundant product showing that demethylation occurred. They then concluded that isomerization to 1-methylnaphthalene occurred on the external surface and the smaller molecular dimension (0.58 nm) 2-methylnaphthalene was the only one that could penetrate the ZSM-5 pores rather than the bigger (0.62 nm) 1-methylnaphthalene.

Loktev *et al*.[36] supposed that alkylation reactions mainly proceeded on the outer zeolite surface, but it was not correlated with the observed ZSM-5 selectivity in 2,6- and 2,7-dimethylnaphthalene formation. On H-mordenite the external acid sites were deactivated by cerium modification[37] to achieve high performance in the alkylation of naphthalene with propylene at 250 – 300 °C.

H-mordenite catalysts displayed unacceptable catalyst life, presumably due to excessive cocking. Improvements in catalyst life were achieved using dealuminated H-mordenite. Horsley *et al*.[38] achieved maximum catalyst life using a mild dealumination techniques such as gentle catalyst steaming followed by dilute acid wash and calcinations.

2.4 Isomerization (xylene)

The intramolecular isomerization and the transfer of alkyl groups between aromatic molecules are both acid catalyzed reactions.[39] Disproportionation is a special case of transalkylation and is used when alkyl groups are transferred between identical molecules and is one of the isomerization mechanisms.

2.4.1 Aspect of isomerization

Two mechanisms of acid catalyzed xylene isomerization have been identified. In liquid phase at low temperatures with a large pore zeolite-Y catalyst, isomerization occurs in a bimolecular mechanism by consecutive transalkylation/disproportionation steps, apparently through a low activation energy path-way.[31] With a medium pore zeolite or at high temperatures in the gas phase isomerization occurs uni-molecularly by 1,2-shifts of a protonated intermediate.

Tanabe *et al*.[31] proposed the two mechanisms below; one on large pore materials at low temperatures (scheme 2.2), the other one on medium pore materials at high temperatures (scheme 2.3):

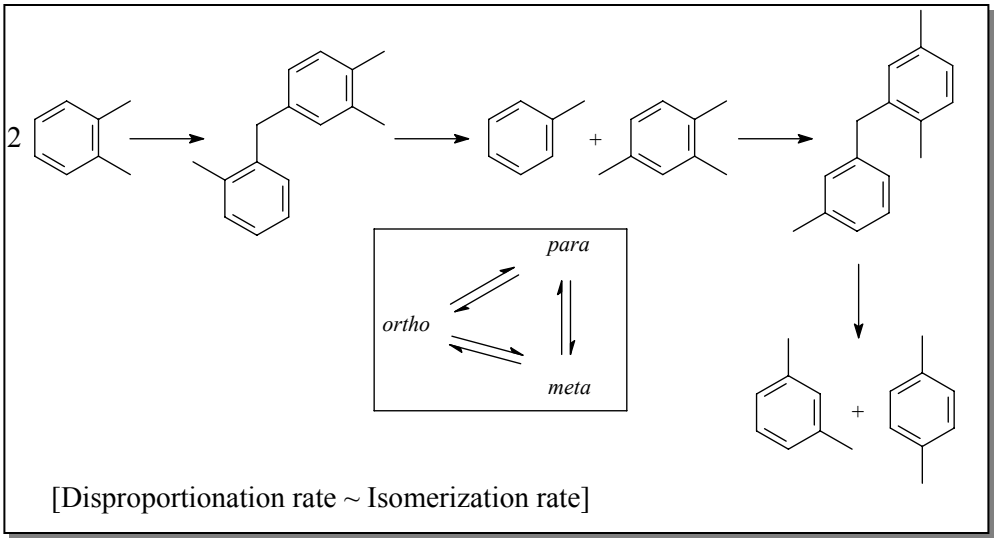

Scheme 2.2: Isomerization of xylene on large pore materials at low temperatures[31]

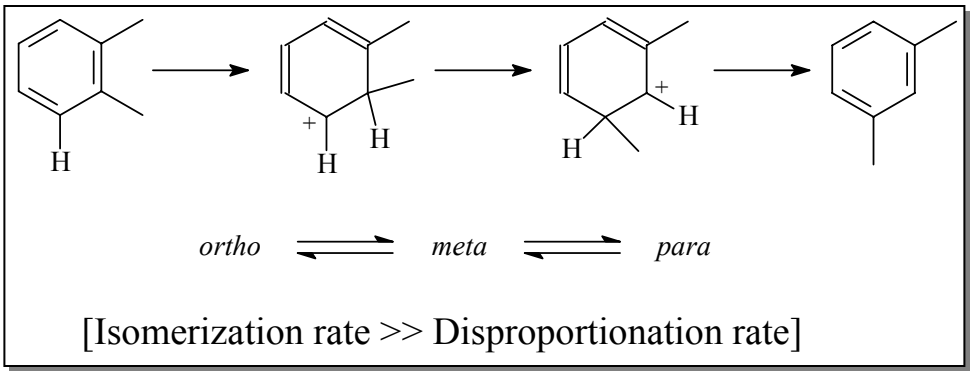

Scheme 2.3: Isomerization of xylene on medium pore materials at high temperatures[31]

Magnoux *et al*.[40] on the other hand proposed the mechanism of xylene isomerization to ethylbenzene (scheme 2.4):

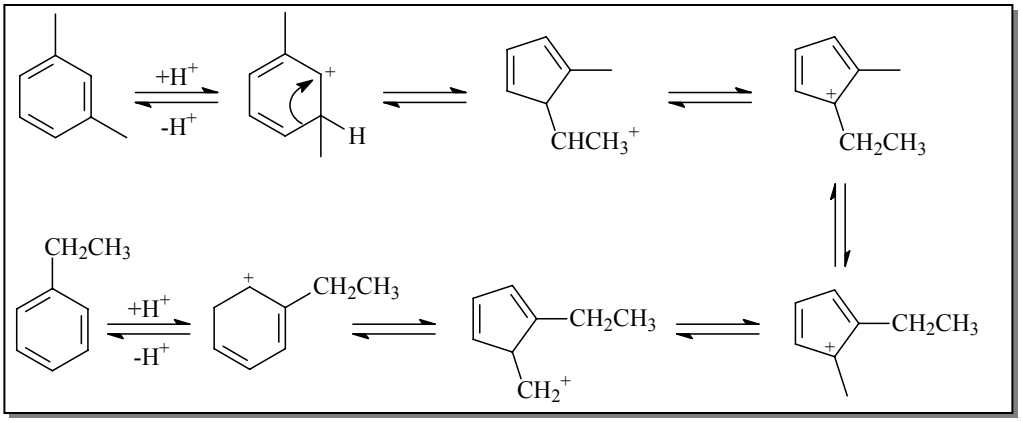

Scheme 2.4: Isomerization of xylene to ethylbenzene[40]

Xylene isomerization may be accompanied by an undesirable side reaction, xylene disproportionation which leads to loss of xylene to less valuable toluene and trimethylbenzene.[31] It has been found that the rate ratio of disproportionation to isomerization increases with size of intracrystalline zeolite cavity.

ZSM-5 = 5/0.6; ZSM-4 = 10/0.8; Mordenite = 15/0.7; HLZY-82 = 50/1.1

The 1,2 shifts on the aromatic ring of alkyl groups can only compete with transalkylation/disproportionation reactions and the product isomers derived from the isomerization of alkyl-aromatics can be due to both intra- and intermolecular reactions; the individual contribution being a function of the structure of the alkylaromatic. Lanewala *et al*.[41] have shown that the isomerization of the xylenes over a zeolite catalyst is accompanied by a transalkylation/disproportionation reaction. The principal transalkylation/disproportionation products obtained from the isomerization of *o*- and *m*-xylene at 300 °C are toluene and the trimethylbenzenes. Both the extent of transalkylation/disproportionation and the percentage approach to equilibrium in xylene fraction increases with conversion.

Trimethylbenzene was transalkylated with benzene,[41] and benzene was chosen in preference to toluene in order to differentiate between the xylene isomers formed by the removal of the methyl group form the trimethylbenzene and the one formed by

transalkylation to toluene. With zeolite catalysts the xylene isomerization does not occur in the absence of transalkylation/disproportionation and that the more extensive the transalkylation/disproportionation the greater the degree of isomerization. Since trimethylbenzenes are present during xylene isomerization and since it has been demonstrated that under the same reaction conditions they reconvert to the xylene isomers, at least part of the isomerization must be intermolecular over zeolite catalyst.

Using the limitations imposed on the transalkylated products the following reaction scheme (scheme 2.5) was derived by Lanewala and co-workers.[41]

In order to achieve a 95 % approach to equilibrium in the xylene fractions it was necessary to have over 50 % transalkylation. From the equilibrium scheme, the *para* isomer would thus require a relatively higher concentration of transalkylate than the other isomers before its formation. The transfer of a methyl group from the trimethylbenzene to toluene occurs in a kinetic and not in an equilibrium distribution. The principal evidence for the intramolecular isomerization of the xylenes is the apparent absence of direct conversion of the *para* isomer to the *ortho* or visa versa.[41]

Csicsery *et al*.[42] suggested that at low temperatures (< 200 °C) isomerization proceeded through transalkylated intermediates, above 300 °C isomerization primarily occurs by intramolecular 1,2-shifts. Under these conditions transalkylation and isomerization occur in parallel and are independent of each other. Isomerization has significantly higher activation energy than transalkylation. The isomerization/transalkylation ratio increase with increasing temperature.

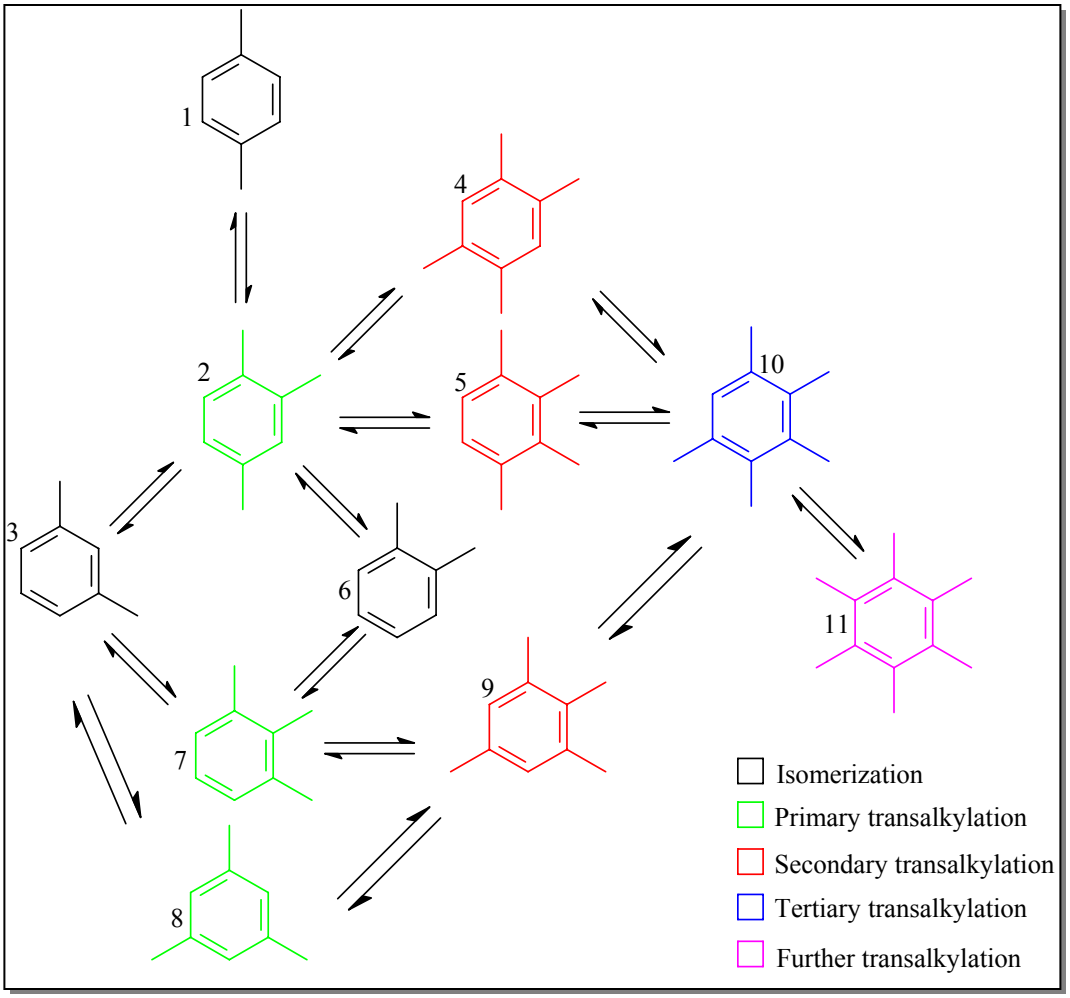

Scheme 2.5: Benzene-trimethylbenzene transalkylation products: 1 = *p*-xylene; 2 = 1,2,4-trimethylbenzene; 3 = *m*-xylene; 4 = 1,2,4,5-tetramethylbenzene (durene); 5 = 1,2,3,4-tetramethylbenzene; 6 = *o*-xylene; 7 = 1,2,3-trimethylbenzene; 8 = 1,3,5-trimethylbenzene (mesitylene); 9 = 1,2,3,5-tetramethylbenzene; 10 = pentamethylbenzene; 11 = hexamethylbenzene[41]

Young *et al.*[43] suggested that xylene isomerization was about 1000 times faster than toluene disproportionation in ZSM-5 catalysts. The transalkylation reaction to form benzene and xylenes within the pores is relatively slow; benzene diffuses out of the pores rapidly, as such, Wang *et al.*[44] suggested that benzene yield is a good indicator of toluene disproportionation. The xylene isomerize rapidly within the pores, para-xylene diffuses out moderately fast while ortho- and meta-xylenes diffuse relatively slow and further convert to para-isomer before escaping form the channel system.

Zeolite-mediated steric effects in the xylene-forming transition state may also enhance the amount of para isomer formed initially within the pores; this is illustrated schematically in scheme 2.6 below:

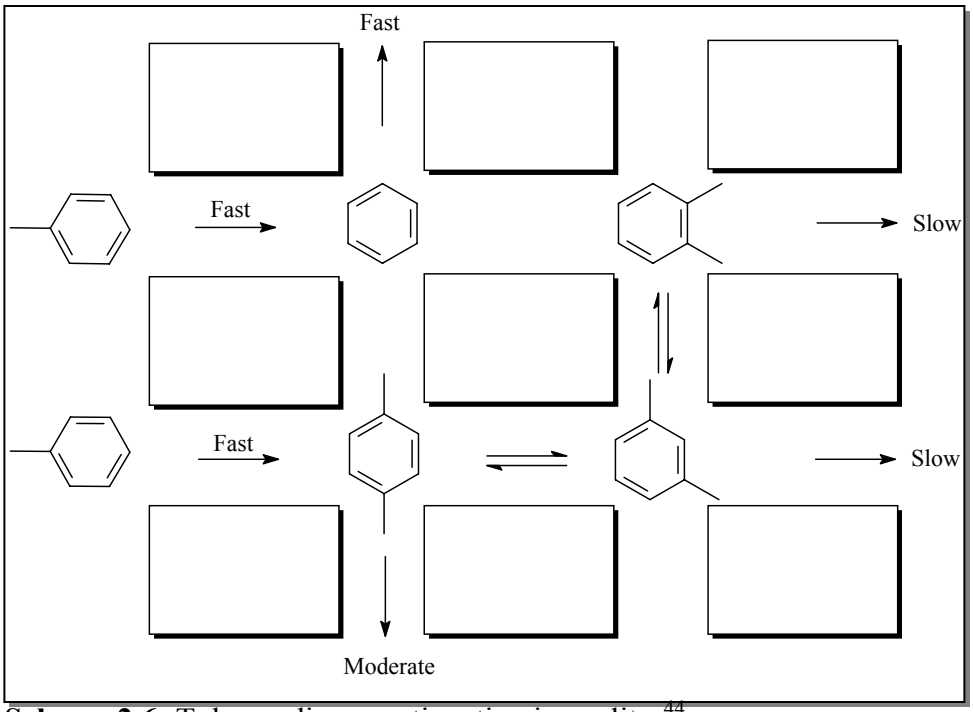

Scheme 2.6: Toluene disproportionation in zeolites[44]

2.5 Disproportionation

i) Toluene disproportionation

It was proposed that strong sites promote dealkylation of toluene, while the medium sites promote the disproportionation reaction. Bhaskar and Do[45] reported that toluene in the presence of hydrogen not only disproportionates but also undergoes a dealkylation reaction. During toluene disproportionation the dealkylation reaction should be inhibited hence they suggested that changing the carrier gas from hydrogen to nitrogen will give good disproportionation results.

In the study of transalkylation over zeolite-Y and mordenite it was apparent that among various types of cation in the zeolites the hydrogen form exhibited the greatest activity.

The thermal hydrodealkylation of toluene to benzene and methane has been practiced as a means to upgrade toluene to the more valuable benzene.[31] Toluene can also be blended with C_9 aromatics where transalkylation occurs to form xylene.

Tanabe *et al*.[31] came up with this product (table 2.1) distribution at thermodynamic equilibrium (mol %) for toluene disproportionation:

Table 2.1: Equilibrium (mol %) for toluene disproportionation[31]

Temperature (K)	Benzene	Toluene	Xylene	Tri-methylbenzene	Tetra-methylbenzene
600	31.5	41.7	22.7	3.8	0.3
800	32.0	40.6	23.1	3.9	0.4

ii) Ethylbenzene disproportionation

It was noted that mostly very strong Brönsted acid sites are capable of catalyzing the reaction.[31] Disproportionation of ethylbenzene was carried out over a variety of catalysts and Karge *et al*.[46] concluded that this reaction is a valuable test reaction for the characterization of zeolites of unknown structure. Useful criteria are the presence of an induction period or its absence, rate of deactivation, yield ratio of diethylbenzene to benzene isomers.

Tanabe *et al*.[31] also proposed the mechanism of ethylbenzene on large pore materials at low temperatures (scheme 2.7) and on medium pore materials at high temperatures (scheme 2.8) as shown below:

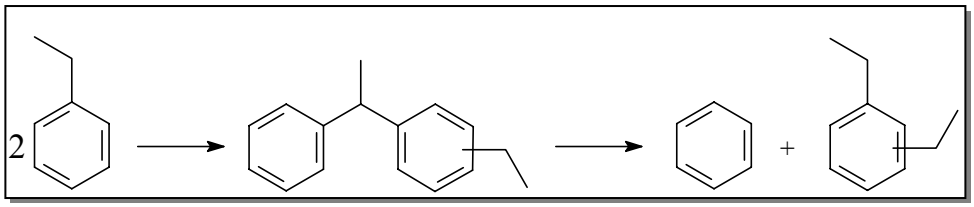

Scheme 2.7: Ethylbenzene disproportionation mechanism on large pore materials at low temperatures[31]

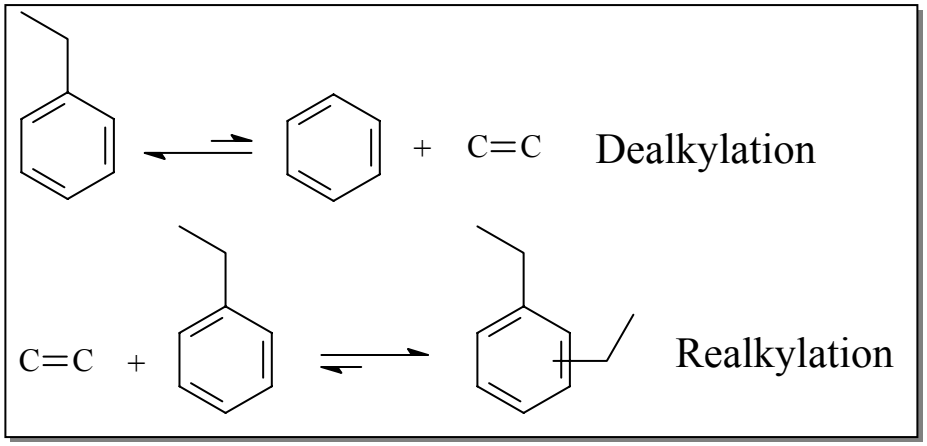

Scheme 2.8: Ethylbenzene disproportionation mechanism on medium pore materials at high temperatures[31]

Medium pore zeolites such as the ZSM-5 cannot accommodate bulky intermediates (diphenyl, scheme 2.7), and ethylbenzene disproportionation proceeds via dealkylation-realkylation path shown in scheme 2.8.

Thus the "restricted transition state-type selectivity" was proposed in which certain reactions are prevented because the transition state is too large for the cavities of the zeolite. However neither reactants nor products are prevented from diffusion through the pores, only the formation of the transition state is hindered.[31] A typical example can be found in acid-catalyzed transalkylation of dialkyl-benzenes. This is a

bimolecular reaction involving a diphenylmethane transition state. It was found that in the reaction of 1-methyl-2-ethylbenzene over mordenite, 1,3,5,- substituted products were observed in the products.[31] This fact was explained as following: the formation of diarylmethane-type transition state, which might lead to their formation, is hindered by the special restriction of the mordenite pores. It should be noted that the 1,3,5-isomers undergo no steric hindrance for their diffusion through pores of mordenite.

Pradhan *et al*.[47] found that benzene was the major product (40 - 60wt %) which formed during the dealkylation reaction of ethylbenzene. Other minor products were toluene (5 - 10wt %), xylenes (2 - 4wt %), C9 – C11 aromatics (1 – 2wt %), diethylbenzenes (1 – 5wt %) and C12+ aromatics (4 – 6wt %), and ethylene was the major gas product.

Melson and Schiith[48] stated that for the disproportionation of ethylbenzene over ZSM-5 sample with large crystal size, a high concentration of para-diethylbenzene was formed than over small crystals. They attributed this effect to the lower amounts of external surface sites which are responsible for the non-selective reactions on the larger crystals as compared to the small size samples.

iii) Methylnaphthalene Disproportionation

The synthesis of 2-methylnaphthalene and 2,6-dimethlnaphthalene is of great practical interest.[49] Thus for instance, 2-methylnaphthalene is a starting material to vitamin K synthesis, while 2,6-dimethylnaphthalene is used in the production of polyester fibers and plastics. These hydrocarbons can be obtained by isomerization and disproportionation of mono-methylnaphthalenes; a similar reaction to toluene disproportionation.

2.6 Transalkylation

Unlike disproportionation, in transalkylation one of the alkyl groups is transferred from one alkylaromatic molecule to another aromatic molecule of a different kind. The following mechanism (scheme 2.9) was proposed for disproportionation of toluene over zeolites by Csicsery[50] but it applies both for transalkylation:

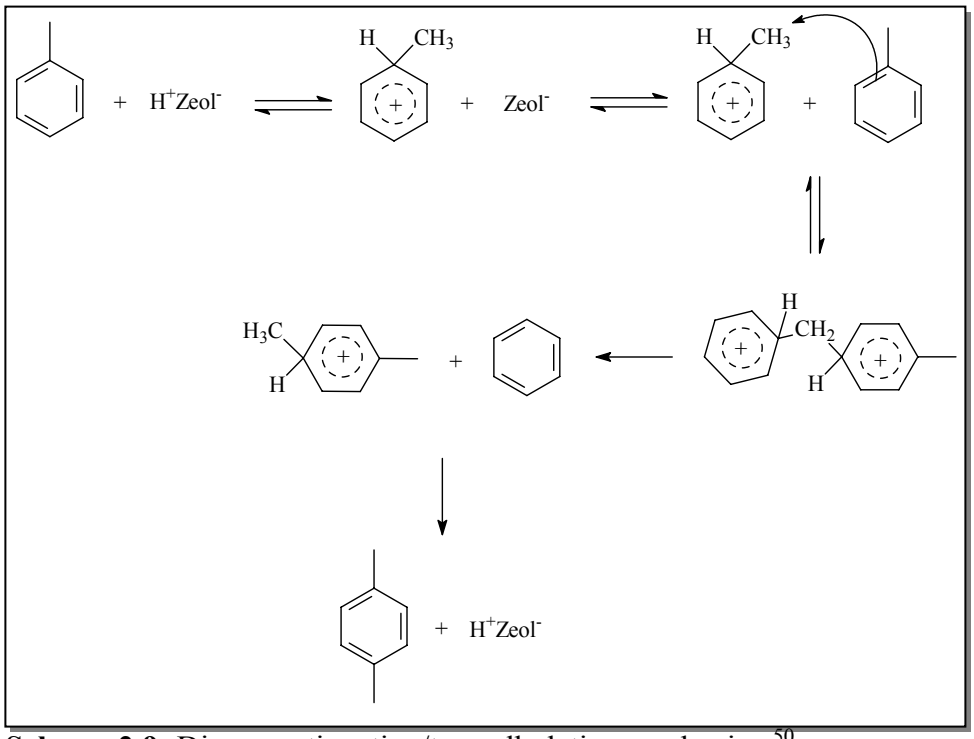

Scheme 2.9: Disproportionation/transalkylation mechanism[50]

The protonation of an alkylaromatic molecule occurs at its *ipso* position. This weakens the carbon-methyl bond and initiates transfer to a second aromatic molecule.

It was also reported that mordenite was about 8 times more active than the zeolite-Y and that the active centers were Brönsted acid sites; ZSM-5 zeolite is also active for transalkylation reactions.[50] Transalkylation (alkyl-transfer) and isomerization are the principal acid catalyzed reactions of poly-alkylbenzenes. Effective channels aperture in mordenite would be between the diameters of the symmetrical and unsymmetrical

tri-alkylbenzenes (i.e. between 8.2 and 8.6 Å). Symmetrical tri-alkylbenzenes cannot form in the pores of mordenite because diphenylmethane type intermediates or transition states leading to symmetrical isomers require more space than available. But they can diffuse out of the pores, i.e. transalkylation is inhibited.

Forni *et al*.[51] have shown that in the transalkylation reactions between benzene (B) and diethylbenzene (DEB) the equilibrium mol-% conversion (C_{eq}) of DEB is practically independent of temperature. However, a strong dependence of C_{eq} on the B/DEB feed ratio (R) was noticed. From a practical point of view, reasonable values of C_{eq} may be attained only for $R \geq 95$ %. Based on this, a value of R = 17.7 correspond to 10 vol/vol and the expected value of C_{eq} is 97 %.

To resolve the problem of catalyst aging during benzene-trimethylbenzene transalkylation, Tsai *et al*.[52] used metal incorporated catalysts, however, as the consequence of hydrogenation reactions, the formation of saturates jeopardized the purity of benzene products. They found that the hydrogen activities of transalkylation metal catalysts were closely related to the physical property (location and particle size) of the metal and acidity of the catalyst. A more active hydrogenation activity and thus lower purity of benzene products was observed for Pt/mordenite.

Nafion-H (an organic resin, scheme 2.10) is a very useful catalyst for transalkylation reactions,[31] e.g. used in the transfer of a *t*-butyl group at temperatures of 330 K.

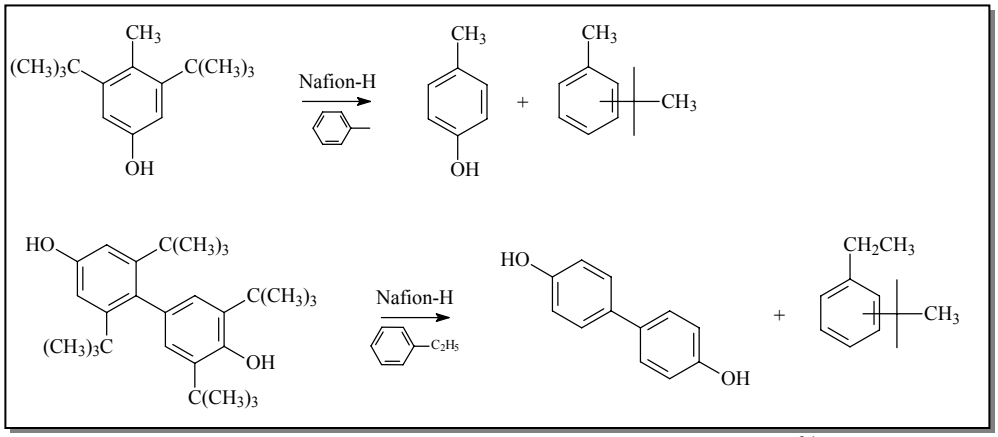

Scheme 2.10: Alkyl-transfer reactions catalyzed by Nafion-H[31]

2.7 Catalyst deactivation

i) External surface sites

The decrease of the selectivity of 4,4'-diisopropylbiphenyl (4,4'-DIPBP) was observed with the increase of reaction temperature, or with the decrease of propylene pressure.[53] These phenomena were explained by the isomerization of the 4,4'-DIPBP to 3,4'DIPBP at the external acid sites. Therefore, the deactivation of the external acid sites was essential for the prevention of isomerization and other non-selective catalysis. The Ceria modification was a potential method for the deactivation of external acid sites of H-mordenite.

Komatsu *et al*.[54] reported that 2,4-dimethylquinoline (DMQ) selectively poisons the acid sites on the external surface of HZSM-5 crystallites. The cracking of 1,3,5-triisopropylbenzene, which can not enter the ZSM-5 pores, was almost inhibited by co-feeding 2,4-DMQ, that is, conversion decreased from 68 % to 1 %. On the other hand, the yield of dimethylnaphthalene (DMN) did not decrease greatly by co-feeding with 2,4-DMQ (conversion changed from 9.9 to 8.6 mol %), suggesting that alkylation of 2-methylnaphthalene takes place mainly inside the crystallites.

ii) Deactivation of acid sites

Deactivation of acid zeolite catalysts is caused by mainly the retention of carbonaceous compounds; mainly (coke) inside the pores or on the outer surface of the crystallite.[40] This depends on the characteristic of the active sites and on the operating conditions: reaction time, temperature, pressure and the nature of the reactants. Coke formation is slow when transformation of an alkylaromatic is by disproportionation/transalkylation and fast with dealkylation. Coke formation occurs from the olefins produced by dealkylation and not directly from aromatic rings. At

low temperatures carbonaceous deposits are mainly consisting of unconverted reactants and at high temperatures one finds condensed ring aromatics.[40] Whatever the reaction temperature there is retention of heavy compounds (coke) in the zeolite, and the rate of coke formation increases with temperature.

During toluene disproportionation, after 6 hours at 120 °C, Manoux *et al*.[40] observed that the zeolite was beige, at 200 °C yellow, brown at 350 °C and black at 400 – 450 °C. The H/C ratio decreased (i.e. aromaticity increases) when the reaction temperature increased. The highly condensed polyaromatic compounds were insoluble in CH_2Cl_2. The coke compound can be classified into families with C_nH_{2n-z} as the general formula, i.e. the constituent of a family have molecular weights differing by 14 units, which can correspond to substitution of a methyl group for a hydrogen. The compounds of the soluble coke were identified by G.C-M.S coupling.

Products, even when they are not bulky, remain blocked in the zeolite, (not steric blockage), they are retained in the zeolite because of their low volatility (boiling points higher than the reaction temperature) and also because of their chemical or physical adsorption when working at low temperatures. At high temperatures, the coke that forms is insoluble in methyl chloride, this coke is black and constitutes highly aromatic molecules and it can be assumed that these compounds are sterically blocked in the zeolite.

Magnoux *et al*.[40] proposed the following transformations (scheme 2.11) during toluene disproportionation with respect to reaction temperature.

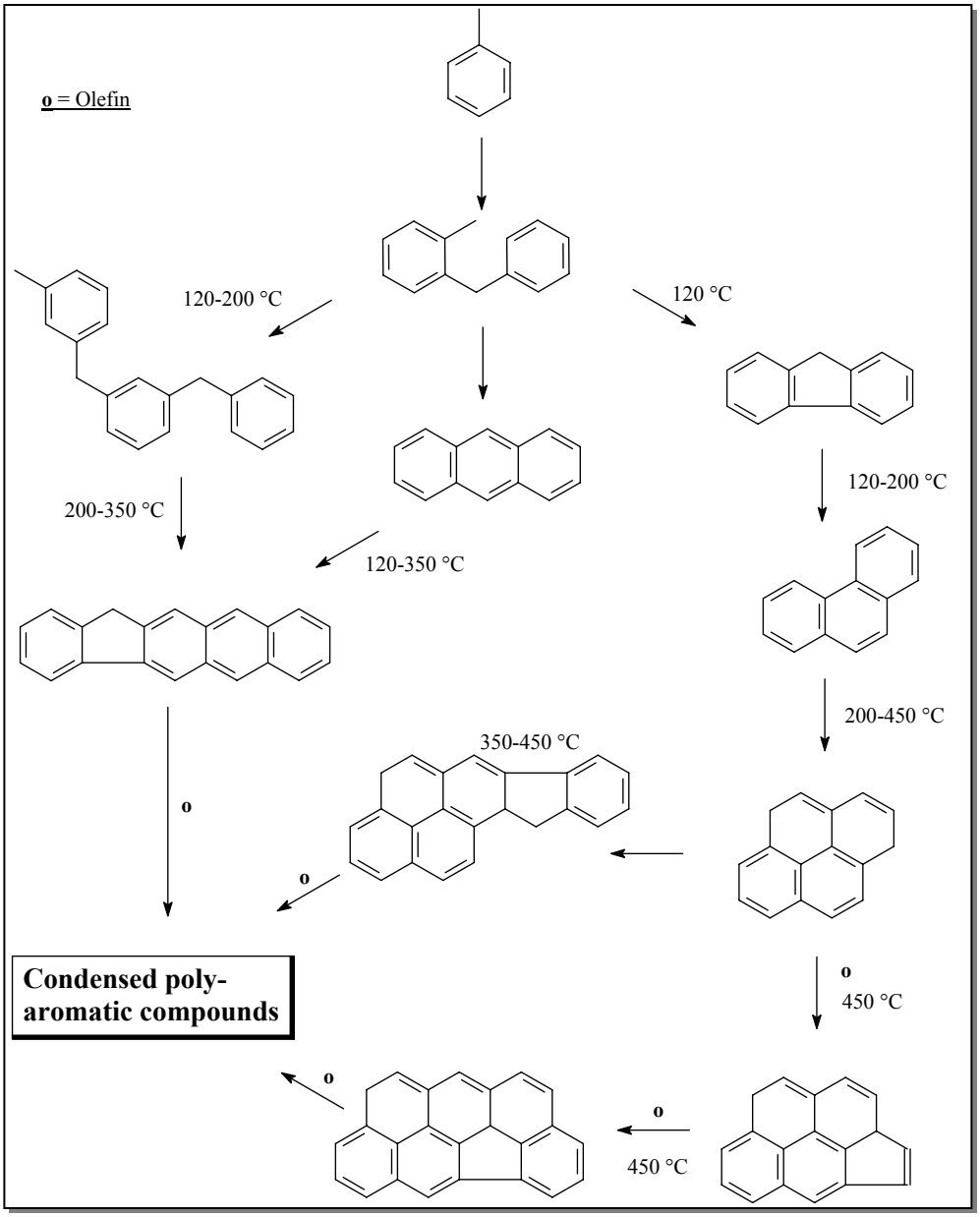

Scheme 2.11: The effect of temperature on the type of aromatic carbonaceous material that formed[40]

The coke molecules not only limit the diffusion of reactants and products, but block it. The mode of catalytic deactivation depends on the reaction temperature. At low temperatures deactivation is due to a limitation of the access to the acid sites and at high temperatures to a blockage of these sites. Products formed have long contact time, enough to allow condensation reaction to occur. As the bulky and poorly volatile products are formed, the diffusion becomes slow and various transformations

take place leading to coke formation. This is schematically (scheme 2.12) represented below[40]:

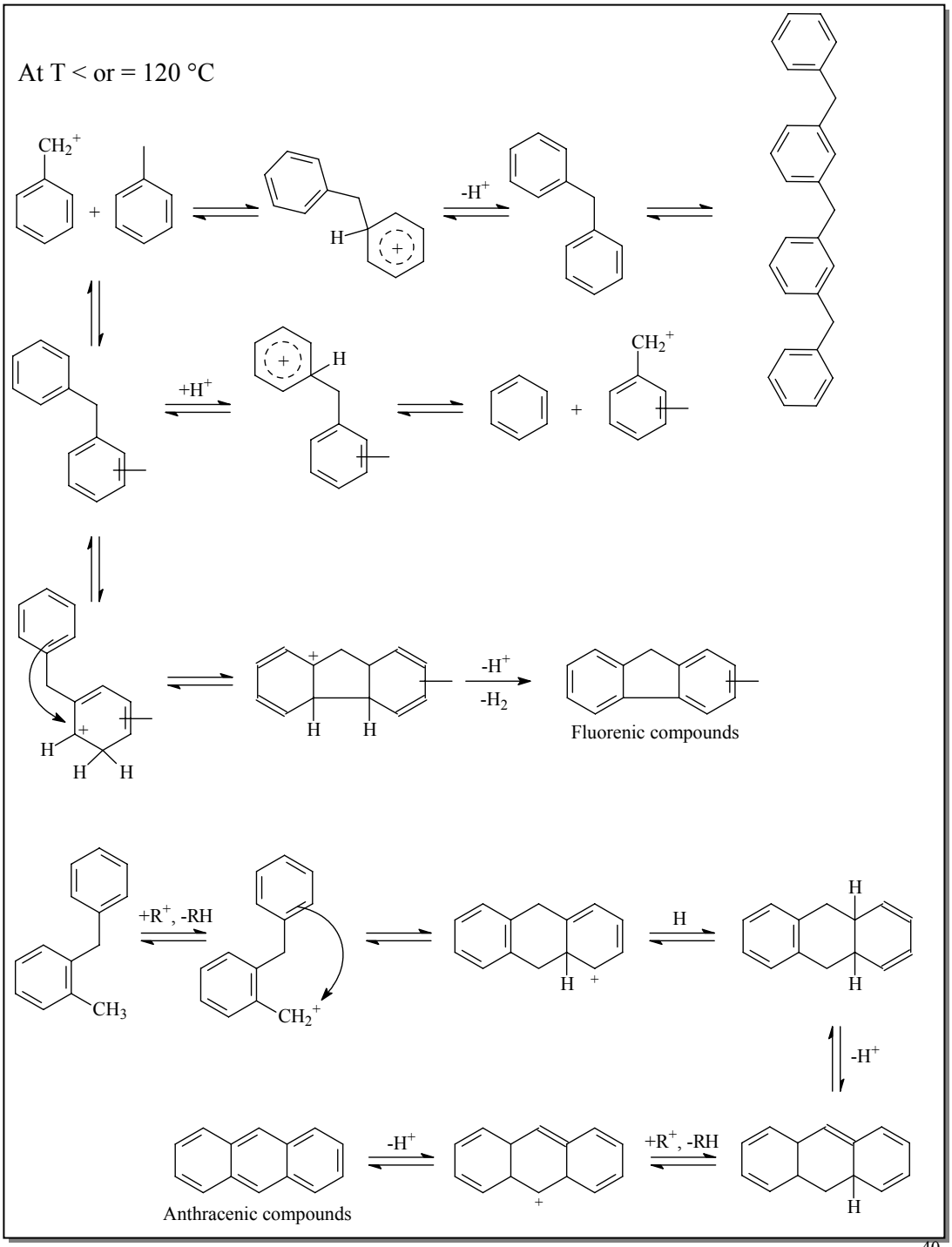

Scheme 2.12: Carbonaceous material formation during toluene disproportionation[40]

Alkylation of aromatic molecules with olefins followed by cyclization then aromatization through hydrogen transfer reaction allow the explanation of the formation of highly aromatic compounds that constitute the non-soluble coke; temperature ≥ 350 °C. This is also shown schematically (scheme 2.13) below[40]:

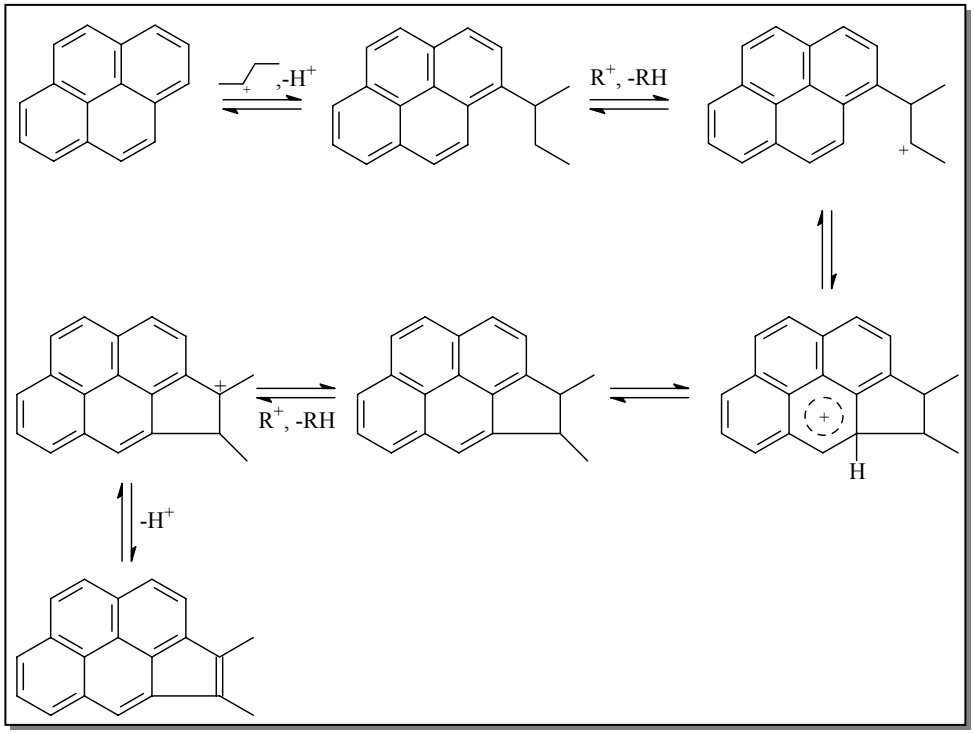

Scheme 2.13: Formation of aromatic carbonaceous material at elevated temperatures[40]

Walsh and Rollmann[55] reported that at low temperatures or with catalysts of higher framework aluminium content, aromatics dominated probably due to selective adsorption effects but when these effects were eliminated, a nearly equal paraffin-aromatic participation in coke formation was found suggesting aromatics alkylation as the key step in the eventual formation of coke. There is preferential adsorption of aromatics at low temperatures (360 °C).

Solid acid catalysts, particularly zeolites, exhibit redox properties. Therefore, they are expected to generate radicals from adsorbed unsaturated hydrocarbons. Lange *et al*.[56] have shown that mordenite nearly always possess the so-called Lewis acid sites (e.g.

only three-fold coordinated Al). Such Lewis sites may well function as electron acceptors which may accommodate hydrogen radicals. Similarly they might be involved in formation and/or stabilization of radicals during coke formation. It was reported by Ajit *et al*.[47] that cocking in zeolites leads to the formation of free radicals.

As far as zeolites are concerned, coke could be located either in the microporous lattice or on the external surface depending upon the zeolite type and operating conditions. Gallezot *et al*.[57] treated the coked zeolite with 40 % hydrofluoric acid (HF) solution to dissolve the aluminosilicate lattice and then methylenechloride (CH_2Cl_2) at room temperature to dissolve the soluble coke. They suggested that coke is produced inside the zeolite micropores and then emerges from the zeolite like an extrudate from a nozzle (figure 2.3) as shown below:

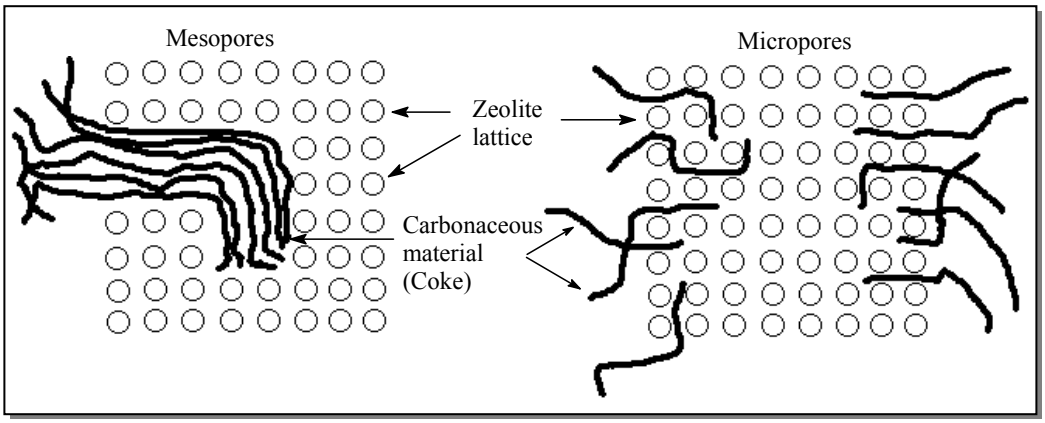

Figure 2.3: Coke formation in zeolite pores[57]

It has been shown that a conventional TEM study conducted on coked zeolites can give detailed information on the coke morphology and its relation with the zeolite crystal.

Walsh and Rollmann[58] reported that the C/H ratio in coke formation depended on the specific condition of their formation. Coke formation is an intrinsic property of zeolite pore structure, the spatial restriction in small-pore zeolite often severely inhibits formation of coke and of its precursors. They applied hydrogen pressure to retard coke deposition rates and to thereby provide an opportunity for selectivity in

that deposition. Coking tendency is strong in large-pore structures such as zeolite-Y and mordenite. Coke yields generally increased with increasing aluminium content. They also suggested that direct reactions such as disproportionation were not strong coke producers.

Magnoux *et al*.[59] observed that the activity of H-mordenite decreases rapidly with the time *t* and becomes almost equal to zero after 30 min; the activity of H-zeolite-Y decreases more slowly and that of HZSM-5 extremely slow. Coke formation, initially very rapid on H-zeolite-Y and H-mordenite, is very slow on HZSM-5. Initially on H-mordenite the rate of coke formation is close to that of cracking, on H-zeolite-Y, it is 4 times slower and on HZSM-5 nearly 1000 times slower. The above is also shown in a table (table 2.2) below:

Table 2.2: Activity and rates of deactivation of zeolites: a_o = Initial activity; n = Deactivation Coefficient[59]

Zeolite	H-zeolite-Y	H-mordenite	HZSM-5
Cracking			
a_o	110	165	55
n	0.6	1.4	0.05
Coke formation			
a_o	30	160	0.065
n	1.1	2.5	0.4

With H-zeolite-Y and H-mordenite the coke deposition prevents NH_3 from reaching the strongest acid sites[59]: thus for H-zeolite-Y a 10 % coke deposition eliminates all those sites (1.2 - 1.5×10^{20} g^{-1}) on which the adsorption heat is greater than 115 $kJmol^{-1}$, the weaker sites being particularly unaffected. On H-mordenite, 3 % coke prevents NH_3 adsorption on 3×10^{20} of very strong sites g^{-1} (adsorption heat about 140 $kJmol^{-1}$) and 4.5 % coke eliminates all those sites on which the adsorption heat is greater than 130 $kJmol^{-1}$ (4 - 6×10^{20} sites per gram). In HZSM-5 coke seemed to have little effect up to 2.5 % coke; for 4.5 % coke a greater part of the strong sites is eliminated:

0.6×10^{20} out of the 0.9×10^{20} sites per gram on which the adsorption heat is greater than 100 $kJmol^{-1}$.

Magnoux *et al*.[59] also suggested that initially the cracking activity of H-mordenite is 15 times greater than that of H-zeolite-Y and 3 times than that of HZSM-5. The same order is found for the formation of coke but the differences are more pronounced: H-mordenite is 5 times more active than H-zeolite-Y and 2500 than HZSM-5. The differences in the cracking activity: H-mordenite has 4.5×10^{20} site g^{-1} (adsorption heat is greater than 100 $kJmol^{-1}$), H-zeolite-Y about twice less and HZSM-5 about 6 times less. On average these sites are stronger on HZSM-5 (adsorption heat 145 $kJmol^{-1}$) than on H-mordenite (135 $kJmol^{-1}$) and H-zeolite-Y (120 $kJmol^{-1}$). As far as the formation of coke is concerned, the greater strength and the high number of H-mordenite acid sites can probably explain why it is more active than H-zeolite-Y. On the other hand, the very low activity of HZSM-5 cannot be due entirely to its acidity. Indeed while the lower density of its acid sites is partly responsible for its reduced coke activity, the steric constraints exerted by its porous network on the formation of bulky intermediates of coking also play a significant role: The coking activity of a strongly dealuminated H-zeolite-Y zeolite which present a site density even lower is 10 times greater than that of HZSM-5.

Magnoux *et al*.[59] concluded that for H-zeolite-Y deactivation was due to a total obstruction of the access to part of the pores and a partial obstruction to the remainder; the coke molecules are formed rapidly on the very strong acid sites.

Two situations of coke formation in zeolites are outlined below:

a) Initially polyaromatics with alkyl substituents are very rapidly formed on the strongest acid sites, as soon as they attain a certain size (more than 3 aromatic rings) their migration becomes very slow and these molecules obstruct the pore entry (~ 8 Å, diameter) of the super-cages, limiting or preventing the penetration of *n*-

heptane (4.3 Å). The degree of obstruction depends not only on the size of the molecules but also on their location in the super-cages.

b) Then the coke content increases very slowly. This increase is due to (not only) the formation of new coke molecules but also to the growth in size of the molecules already formed. Certain molecules can occupy several super-cages and even spread over the outer surface, they obstruct access to a great part of the pore volume not only of *n*-heptane but also of smaller molecules such as a nitrogen or ammonia.

For HZSM-5 deactivation is initially due to the coverage of acid sites located at channel intersections by alkylaromatics with 1 or 2 rings, later on, bulkier molecules (insoluble poly-aromatics) formed extremely slow either on the external acid sites or more likely by growth of the coke molecules[59] located on the acid sites near the external surface (not only there) can obstruct the porosity (pore blockage). By the first mode (site coverage) about 16 % coke would be necessary to suppress the activity and the adsorption capacity, whereas by pore blockage (which becomes significant above 4 % coke) 8 % would be enough for all the volume to become in-accessible to *n*-hexane.

With H-mordenite deactivation, as already noted by other authors, the decrease of the adsorption capacity is very pronounced: 3.5 % coke is sufficient to eliminate 90 % of the volume accessible to *n*-hexane and to suppress almost all the activity.

Eisenbach *et al*.[60] reported that the external O-H groups possess a lower affinity towards olefins than those in super-cages, and this can be explained by their different surroundings, in comparison with OH groups inside the zeolitic faujasite framework. During the formation of internal groups, a three-fold coordinated aluminium atom is produced (scheme 2.14) according to the following reaction:

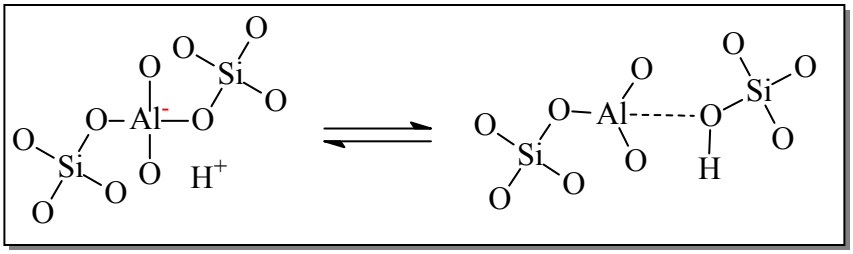

Formation of Brönsted acid sites[60]

This electron deficient aluminium atom interacts with the *p*-electrons of the oxygen atom of the new formed O-H groups and consequently increases its affinity towards olefins. The external O-H groups terminating the zeolite crystals are not produced by a proton attack as shown above. Their nearest neighbours do not include low-coordinated aluminium atoms which are due to delocalization as in the case of internal O-H groups.

The O-H groups react with adsorbed hydrocarbons species producing coke and thereby are consumed irreversibly. The rate of coke production is strongly depended on the concentration of the acidic O-H groups and the coke formation will stop first, when all the reachable O-H groups have reacted. There is no equilibrium concentration of coke for a given temperature, but the rate the maximum coke concentration will be reached is a function of temperature.

The hydrocarbon molecules are hydrogenated on the zeolite surface and gradually transformed to the energetically favorable turbostatic carbon structure.[60] The dehydrogenation of hydrocarbons to coke passes through polycyclic aromatic intermediates, which already contain a preformed graphitic structure. The external Brönsted sites are not consumed during coke formation, and are still available as active sites on a coked catalyst but this do not mean that external O-H groups are not consumed at all during coking.

It has been proved that coking is a shape selective process: indeed, the rate and selectivity are essentially determined by the zeolite pore structure. Magnoux *et al*.[59] reported that the coke formation rate is from 50 to 1000 times slower on the small or

intermediate pore-size zeolites than on those with large pores: the coke composition depends mainly on the space available for its formation. Coke will be poly-aromatic and very heavy if the reaction leading to its formation is not limited by steric constraints (e.g. in super-cages, zeolite-Y). The selectivity of a reaction to cocking is greater with mono-dimensional than with three-dimensional circulation. Coke deposition reduces the number and strength of the adsorption sites.

Fang *et al*.[61] also reported that in the presence of nitrogen as a carrier gas, light volatile soft coke and/or coke precursors prefer to deposit inhomogeneously within the intercrystalline channels of the zeolite. This internal coke may be effectively removed when hydrogen is used as a carrier gas. Coke that deposit on the external surface of the zeolite is mostly bulky hard coke. This coke is more difficult to remove by simple hydrogen treatment. As a result this external coke effectively modifies the surface acid properties of the zeolite crystallites.

In the analysis of coke materials Colón *et al*.[62] used HF to dissolves the zeolitic matrix and CH_2Cl_2 to extracts (dissolve) coke. They suggested that coke formation occurs suddenly to a remarkable extant when time on stream is still low, and increases slowly. Up to 80 % of the coke formed is soluble in CH_2Cl_2, and it is mainly composed of poly-alkylated naphthalene and pyrenic and indenopyrenic compounds. After 6 hours the coke seems to become completely aromatic, as only 33 % of it can be extracted by CH_2Cl_2 (poly-nuclear aromatics).

iii) Regeneration

Zeolite-containing catalysts, when used for hydrocarbon transformations, are also deactivated by coke, a carbonaceous material that contains mainly carbon and some hydrogen. This is usually removed by controlled oxidation so that the catalyst activity is restored.[21]

Eisenbach *et al*.[60] reported that in hydrocarbon conversion reactions over zeolitic catalysts, carbonaceous materials gradually deposits on the catalyst surface. These deposits tend to lower the catalytic activity due to poisoning of the catalytically active centers and due to a change in the macro- and micropore structure of the zeolite (specific surface area, specific pore volume and mean pore radius). From time to time these "coke deposits" have to be removed from the catalyst surface by burning.

Jong *et al*.[63] reported that the activity of the fouled zeolite catalyst can be regenerated by the combustion of coke at an elevated temperature. Such oxidative treatment which is normally carried out under the flow of air or diluted oxygen depends on the characteristics of the coke and the thermal stability of the zeolite catalyst. It was concluded that three types of reactions may take place during coke oxidation:

i) Condensation of poly-aromatic molecules,
ii) oxidation of poly-aromatics into aldehydes, ketones, acids and anhydrides,
iii) Decarboxylation or decarbonylation of the oxygenated compounds.

They also suggested that during the initial coke regeneration in air or dilute oxygen, coke present in the intracrystalline channels is removed preferentially to that present on the external surface. The rate of regeneration is much higher in the initial stages. Reactivating gases used during regeneration have a great influence on selective removal of the coke. During oxidative removal of the coke in the presence of air or dilute oxygen, alkyl poly-aromatic carbonaceous compounds become converted into more condensed structure during coke oxidation.

The activity of the catalyst can only be partly recovered while the coked catalyst is reactivated in the presence of hydrogen, although a lesser amount of coke is removed in this case. The same applies with oxygen treatment but the coke is effectively removed in this case.

3 EXPERIMENTAL

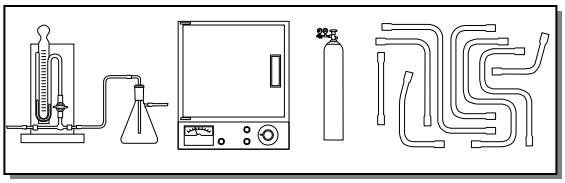

3.1 Introduction

This is one of the most important parts of any research study, and here the reactants/chemicals used, how they were used and their manufacturers are presented. The chapter also discuses the reactor set-up in detail including reaction conditions and methods followed in alkyl-transfer studies from the pre-treatment of the catalysts to the analysis of alkyl-transfer products. Characterization techniques used like the gas chromatography (G.C), gas chromatography-mass spectroscopy (G.C.M.S), temperature programmed desorption (TPD), X-ray diffraction (XRD), thermogravimetric analysis (TGA) and Inductively Coupled Plasma-Optical emission spectroscopy (ICP-OES) are discussed to some extent, this also includes the conditions of the catalyst regeneration studies.

3.2 Reagents, Chemicals and Catalysts

Aluminium nitrate ($Al(NO_3)_3 \cdot 9H_2O$, 98.5 %), N-hexadecyltrimethylammonium bromide (HTMABr), ethanol (C_2H_5OH, 98 %) and toluene (C_7H_8, 99.5 %) were obtained from MERCK; ammonia solution containing about 25 % NH_3 was obtained from (BDH) Analar. Tetraethoxysilane ($Si(OC_2H_5)_4$, 98 %), 2,7-dimethylnaphthalene ($C_{12}H_{12}$), 2,3,6-trimethylnaphthalene ($C_{13}H_{14}$), 2-methylnaphthalene ($C_{11}H_{10}$) and mesitylene (C_9H_{12}, 99 %) were obtained from Fluka A.G Chemische Fabrik Buchs/SG. Naphthalene ($C_{10}H_8$) was purchased from Schering-Kahlbaum A.G Berlin, while propylbenzene (C_9H_{12}, 99 %) was obtained from MERCK-SCHUCHARDT. *o*-Xylene (C_8H_{10}, 98 %, HPLC grade) and ethylbenzene (C_8H_{10}, 99

%) were both from Aldrich. Anthracene (technical) was from BDH Chemicals Ltd and benzene was from Associated Chemical Enterprises, Pty Ltd. Ammonium nitrate (NH_4NO_3, 99 %) was obtained from UnivAR. All of the above chemicals were used without further purification or any other treatments.

The mordenite catalyst (H-Zeolon) was purchased from Norton and the Linde Zeolite-Y (LZY-82) catalyst was from Union Carbide Molecular Sieves. The ZSM-5 used here was prepared by Prudence Sincadu at the University of the Witwatersrand (RSA) in fulfillment of her PhD studies.

3.3 Catalyst Preparation

3.3.1 H-mordenite

This catalytic material was purchased in the H-form (acid form) with H^+ as the cation, and it was used without any further treatment except the pre-treatment in the reactor just before the reaction to remove adsorbed species and mainly water.

3.3.2 HLZY-82

The Linde Zeolite-Y (LZY-82) was in the sodium form, i.e. Na^+ was the cation and it had to be converted to the acidic form for catalysis. This was achieved by ion exchange methods using ammonium nitrate (NH_4NO_3) 1M solutions. Na-LZY-82 samples were stirred overnight at room temperature in 1M ammonium nitrate solutions for 3 days, and each time a fresh NH_4NO_3 solution was used. After each exchange (Na^+ for NH_4^+) the resulting material was washed with plenty of distilled water. The NH_3 exchanged LZY-82 materials were filtered and dried in air overnight then calcined in air at 600 °C for 8 hours during which NH_3 decomposed and the protonic form of LZY-82 (HLZY-82) was formed.

3.3.3 Al-MCM-41

MCM-41 materials were synthesized by Peter Mokhonoana in fulfillment of his PhD degree at the University of the Witwatersrand (RSA); this was carried out by adding 26.4 g of sodium silicate (SiO_2 source) drop-wisely to a stirred (clear) solution of 2430 g distilled water and cetyltrimethylammonium bromide (CTMA, template solution). The mixture was then stirred for further 10 minutes and the pH was adjusted to 10 with 1M HNO_3. The resulting solution was further stirred for 30 minutes then transferred to a polypropylene (PP) bottle and autoclaved for 48 hours at 100 °C. The solid product was then recovered by suction filtration and washed free of the Br^- ions with distilled water, then calcined at 560 °C in air for 6 hours.

A total of 5 samples was prepared and they contained Al from Al $(NO_3)_3$ source, and these were designated as *1, *2, *3, *4 and *5 according to their synthesis methods. These samples had a ratio of Si/Al = 30 except for *5 which had a ratio of 9.9 (analysis by ICP-OES), and were all as-synthesized materials. Both Al and Si sources were introduced at the same time in the synthesis of *1, but $Al(NO_3)_3$ was introduced before acid treatment for *2 and after acid treatment for *3; *4 was prepared similarly to *1 but only aged for 2 days at room temperature. The last sample, *5 was synthesized in an oil-bath instead of an autoclave.

The resulting Al-MCM-41's were then cation exchanged with 1M NH_4NO_3 at 80 °C overnight for 2-3 days and each time a fresh solution was used. In between the exchange procedures the samples were repeatedly washed with distilled water. The exchanged samples were then dried in air overnight and calcined at 550 °C overnight to get the H-Al-MCM-41 materials

3.3.4 MCM-48

A 2.6 aliquot of N-hexadecyltrimethylammonium bromide (HTMABr) was dissolved in 120 ml of distilled water and 50 ml of ethanol (EtOH) and 15 ml of aqueous ammonia were added to the surfactant solution. The solution was stirred for 10 min and 3.4 g of tetraethoxysilane (TEOS) was added at one time. The molar composition of the gel was 1M TEOS: 12.5M NH_3: 54M EtOH: 0.4M HTMABr: 417M H_2O. This method of preparation which was quite different from the hydrothermal (autoclave) synthesis was introduced by Schumacher *et al*.[64] The mixture was stirred for 6 hours (A) and 3 days (B) at room temperature, and the resulting solids were recovered by filtration, washed with distilled water to remove Br^-, and dried in air at ambient temperatures. The template was then removed by calcination at 550 °C for 6 hours at ramping of 1 °C per minute.

3.3.5 Post alumination of MCM-48

Arbitrary mixtures of $Al(NO_3)_3$ close to saturation in distilled water (at room temperature) or ethanol (at 25-60 °C) were prepared, and siliceous MCM-48 material was aluminated by incipient wetness method using the prepared $AlNO_3$ mixtures. The dried (at room temperature) material was calcined at 550 °C for 6 hours at ramping of 1 °C per minute. The resulting zeolite materials were designated as A-H_2O (aluminated by the water solution) and A-OH (aluminated by the ethanol solution). Solutions of 0.5 and 1.0 M $Al(NO_3)_3$ were also used for post-alumination and this will be discussed in the chapter concerned. The A in A-H_2O/A-OH refers to the preparation method as discussed in section 3.3.4, and the subsequent –H_2O or –OH indicates the $AlNO_3$ mixture used for alumination.

3.4 Reactor set-up

3.4.1 The rig:

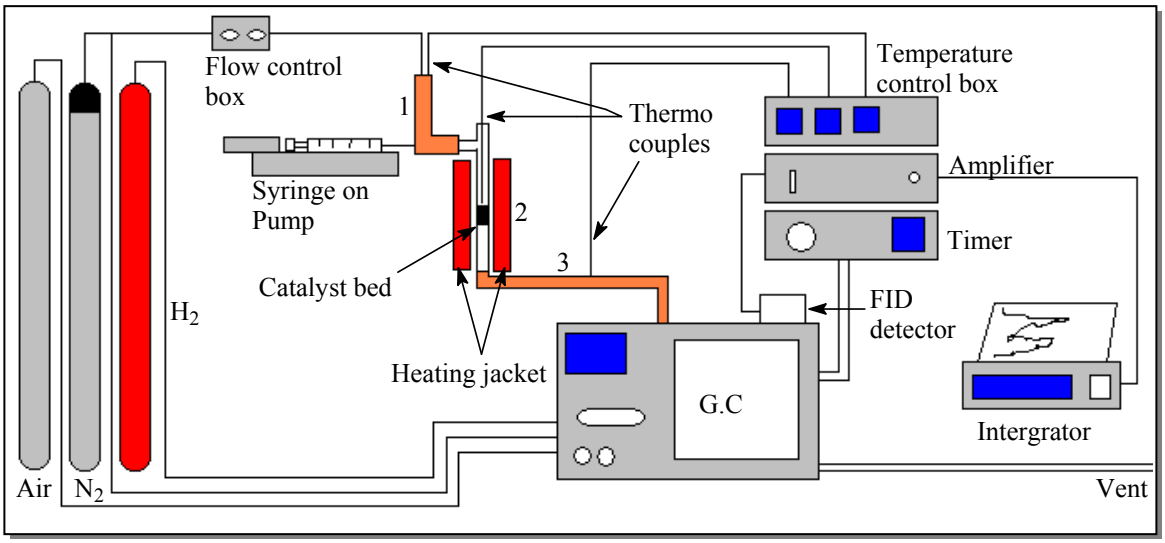

Reactants were introduced into the pre-heated section (1) of the reactor which contained heated N_2 gas (carrier gas) by an automatic syringe pump, the temperature of the section was constantly set at 150 °C by a heating tape and these conditions aided the vapourization of reactants for gas phase reactions. The N_2-reactant gas mixture was then passed on to the reactor which was set at a constant temperature of choice ranging from 180 to 600 °C. The reactions took place in the reactor (2) in the presence of a catalyst and the resulting gas mixture was maintained in the gas phase by using heated tubing (by heating tapes) at 150 °C (3) and the outlet stream led to the online G.C for immediate and direct analysis.

The G.C was equipped with a flame ionisation detector (FID) where H_2 and air were used to produce and maintain the flame (flow rates (pressures) of the 'flame-gases' were variant depending on the humidity, temperature and atmospheric pressure on that day).

Two types of reactors were used and these are shown below. Reactor A was used when online analysis was desired and reactor B was used when other kinds of analysis were required like the G.C.M.S. Reactor B was equipped with a collector maintained at low temperatures using an ice-bath to condense and collect products.

Reactor apparatus:

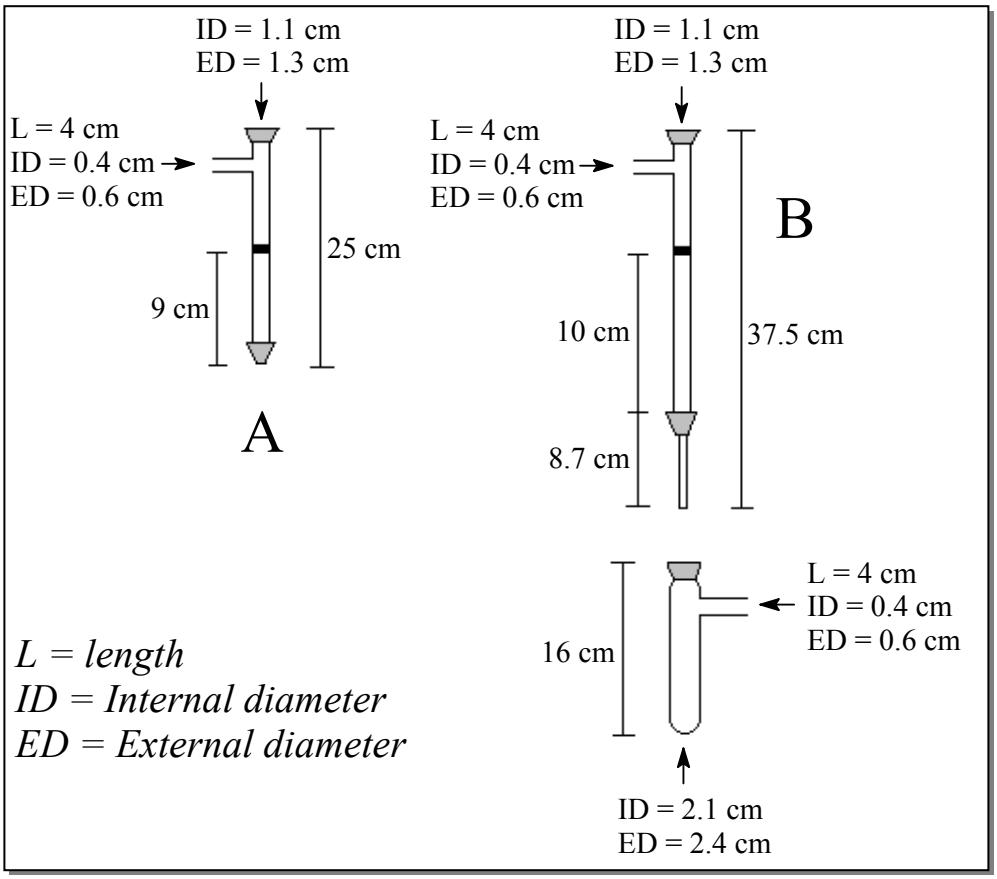

3.4.2 Reaction Conditions

The nitrogen carrier gas was set to flow at desired rates from 1 to 7 ml/min depending on the desired dilution. Weight Hourly Space Velocities (WHSV) were mainly determined by the ease of product/reactant separation, i.e. lower velocities if separation was poor and higher velocities when separation was good or when

regeneration of the catalyst was studied. The mass of the catalyst which was always in the powder form was 0.24 g for all the reactions studied. As mentioned before the reaction temperatures were set as desired from 180 to 600 °C.

3.4.3 Catalyst Pre-treatment

All catalysts used were pre-treated in the reactor prior to catalysis. This was carried out under nitrogen flowing at desired rates (1-7 ml/min) to flush the catalyst. The temperature for this process was always 400 °C and this was ideal to remove both physisorbed and chemisorbed water molecules; this process activated the catalysts. The pre-treatment procedure lasted for approximately 2 to 3 hours.

3.5 Other Conditions

3.5.1 G.C conditions

Nitrogen gas was also used as a carrier gas through the separation columns and this was at 400 kPa of pressure. During automated sampling, the temperature of the G.C was automatically controlled, i.e. it was kept at 40 °C for 10 min then ramped to 150 °C in 10 min, from there the temperature would shoot to 250 °C in no time (program setting) and maintained there for approximately 10 min to flush and clean the column for the next analysis. These conditions were also used for the G.C.M.S technique.

The G.C was equipped with two columns connected together in series for better separations. The one column was a Hewlet Packard HP-5 crosslinked 5 % PHME Silicone with a length of 25 m, an internal diameter of 0.32 mm and the film thickness of 0.52 μm; the one joined to it was a Quadrex Corporation column with a Methyl Silicone phase, a length of 30 m, an internal diameter of 0.25 mm and a film thickness of about 0.5 μm. The FID detector set at 250 °C was connected to the

amplifier which fed the integrator for analysis traces. Sampling was carried out automatically at hourly intervals

3.5.2 Fouling and Regeneration conditions

During regeneration studies, catalysts were fouled with a desired alkyl-aromatic or benzene at high velocities (WHSV) for 4 hours at high temperatures. Carbonaceous materials would form on the catalyst as it deactivates; then spent catalysts were heated to high temperatures (400 – 600 °C) in the calcination ovens in an oxidizing atmosphere (air) for ca. 8 hours. Regenerated catalysts were free of coke (carbonaceous materials) judging by their colour and depending on the regeneration temperature (the higher the regeneration temperature the whiter the catalyst). Similar conditions were used also for calcinations.

3.6 Analytical Techniques

3.6.1 Gas chromatography

The main analysis technique for alkyl-transfer reactions was with the on-line G.C as discussed earlier in section 3.4.1 and 3.5.1. The technique was calibrated by running pure compounds and noting their retention times. Then, mixtures of known compounds whose individual retention times were also known were prepared and consistency of their retention times was evaluated (retention time depended to a small extent on the analysis mixture). Finally a known mixture made up of anticipated products from the intended reaction was prepared and a G.C trace was taken and evaluated. Before every reaction, a blank run was conducted, i.e. the reactant or a mixture of reactants intended for the reaction would be passed through the reactor set at an intended reaction temperature and desired condition but without the catalyst. This was important since it also confirmed the calibration results before the reactions.

The G.C temperature profiles and conditions set for a desired separation as indicated by the equipment calibration before hand, obviously changed with the reactant type and importantly the separation of the products to effect good separation; this will be indicated in a small experimental section of each chapter.

The integrator gave a plot with peaks according to the separation of individual compounds from the reactor as they came out of the G.C column; the data was fed into the integrator by the amplifier which was connected to the flame ionization detector (FID). The integrator automatically integrated the area below the curves given out as a plot on hourly basis. The area in percentages, divided by the number of carbon atoms of the particular compound which gave rise to a relative peak, was equivalent (proportional) to the amount in moles of that compound in the outlet or product stream. Hence conversion and product distribution were all calculated in mole percentages (mol %) as shown below:

$$\text{Conversion (\%)} = \frac{\text{Sum of } n_{\text{products}}}{\text{Sum of } n_{\text{products}} + n_{\text{reactants}}} \times 100$$

$$\text{Product Distribution (\%)} = \frac{n_{(\text{product})i}}{\text{Sum } n_{(\text{product})i}} \times 100$$

where conversion = disproportionation or transalkylation or both (alkyl-transfer)
n_{products} = proportion of the amount of a particular compound or products in moles
$n_{\text{reactants}}$ = proportion of the amount of reactants (starting material) in moles

Due to the fact that reactants, products and intermediates are retained, adsorbed, trapped and they actually participate in carbonaceous material deposition (formation) and deactivation in the zeolite pores and cavities, the conversion calculations were based only on the outlet stream and not on the amount of feed and its relation to the outlet stream like its normally done. Thus mass balances, though important parameters in the current study, were impossible to determine due to the lack of

relevant analytical equipments. For the sake of alkyl-transfer reaction study, this determination was overlooked but chapter 14 gives a slight idea of the rates of carbon deposition and the effects of reactant molecules as studied by TGA. The knowledge of the modes of deactivation (molecular retention/absorption or carbonaceous material formation) was also an anticipated factor that could hinder good understanding and correct results to be achieved with limited uncertainties.

3.6.2 X-Ray Diffraction

Powder X-ray diffraction has been used for structural characterization of zeolite catalysts (large pore MCM's) and to follow changes accompanying grafting with Al. Samples were crushed to a fine powder, ~ <45 μm and pressed in the form of thin layer on a silicon disk. A Phillips PW 1710 Difractometer was used and it was equipped with monochromator and Cu cathode ray tube, a generator at a voltage of 40 kV and a current of 20 mA. An automatic divergence slit, a receiving slit of ~ 0.1 and irradiation length of 12 mm was used for all the samples. Samples were also run in a continuous scan mode in the range 1-10 (in scale of 2θ) using a step size of 0.020 (in scale of 2θ) with time per step of ~ 1.0 seconds.

3.6.3 Temperature Programmed Desorption

The temperature programmed desorption (TPD) apparatus consisted of a U-shaped quartz reactor housed in a temperature-controlled heating jacket (this was an in-house technique). In this technique, a base is adsorbed onto the acid sites of an acid catalyst and the physically adsorbed molecules are first removed (the method is outlined below); the sample is then subjected to a temperature gradient to remove the chemically adsorbed (chemisorbed) base. The temperature at which desorption takes place is taken as an indication of the strength of the acid sites from which the base

desorbed. Ammonia is often used as a base for the investigation since it does not decompose on the acid as or before it desorbs. The signal was measured by a low-temperature dual filament temperature conductivity detector (TCD) and recorded by a PC equipped with an I/O card.

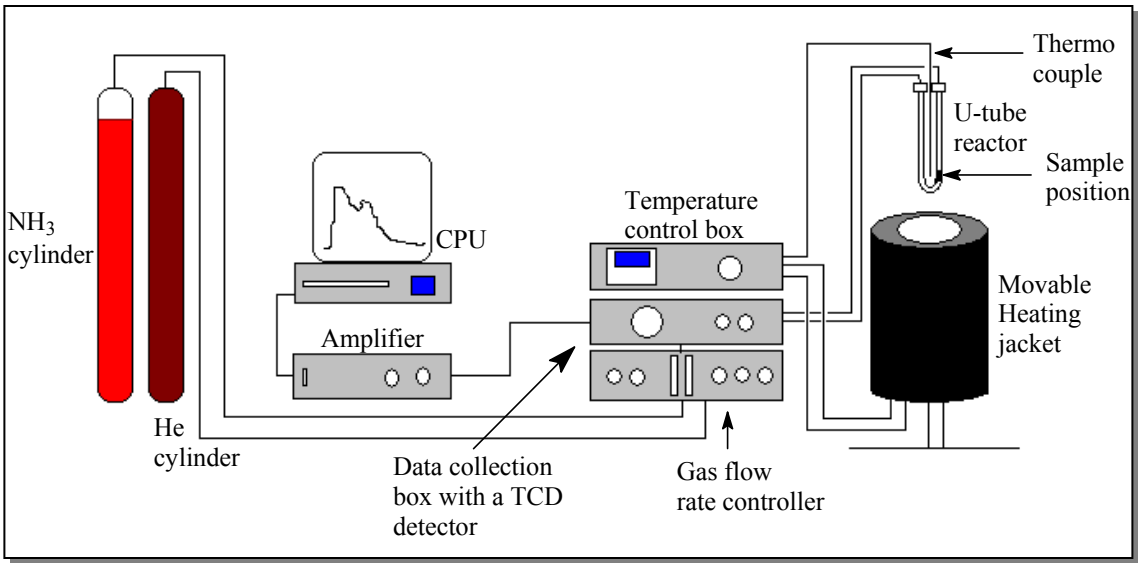

TPD Apparatus

The sample placed in its position in the U-tube reactor was pre-treated at 400 °C with helium gas flowing at 4 ml/min to remove adsorbed water and other molecular species. The pre-treatment took about 2 to 3 hours before the temperature was cooled down to 100 °C and kept there for 1 hour during which the He was cut off and NH_3 gas was allowed to flow through and adsorb on the sites of the catalysts. After ammonia adsorption, the temperature was cooled further down to around 50 °C then ramped to 800 °C at 7 °C/min and the desorbing ammonia molecules were detected by the TCD detector and the computer gave a plot of the amount desorbed (intensity (a.u)) against temperature.

3.6.4 Thermogravimetric analysis

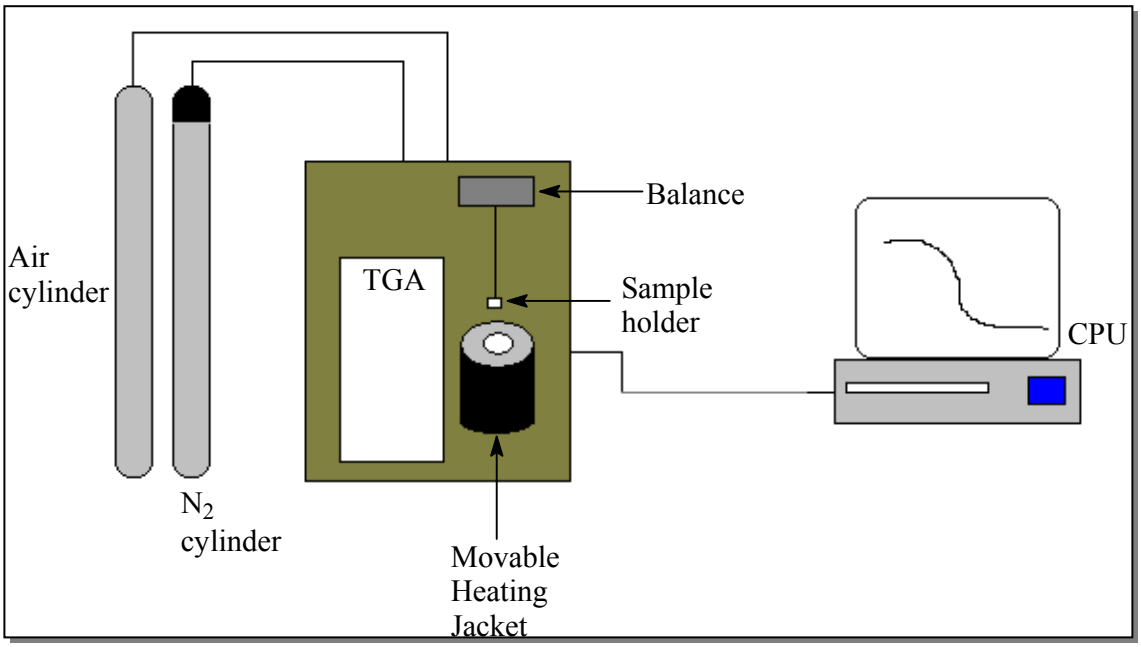

TGA Apparatus

PerkinElmer Thermogravimetric analyzer (Pyris 1) was used for TGA analysis and it used a Pyris Series program. This set-up functioned more like the calcination ovens only that the sample weight was constantly monitored with an on-board balance. In this technique, a given reaction can be followed by keeping a record of mass change as a function of temperature and time. For analysis, a known amount of a sample is placed in a furnace in a controlled gaseous atmosphere at the desired temperature or, dynamically (a common way), where a continuous recording of the weight change of the sample in a flowing gas atmosphere is made as a function of time or temperature at a fixed heating rate and plotted against temperature.

For this study, a certain amount of a sample whose mass was determined automatically by the equipment (it matters not what the initial mass of a sample is) was placed in the sample holder and lowered into the furnace. The temperature was then ramped at 3 °/min to 800 °C and the balance (connected to the computer) fed in data which was then plotted as weight loss (%) against temperature. The gaseous

atmosphere was determined by the type of analysis desired and this will be indicated in the experimental section where the technique was used.

3.6.5 Gas Chromatographic-mass spectrometer

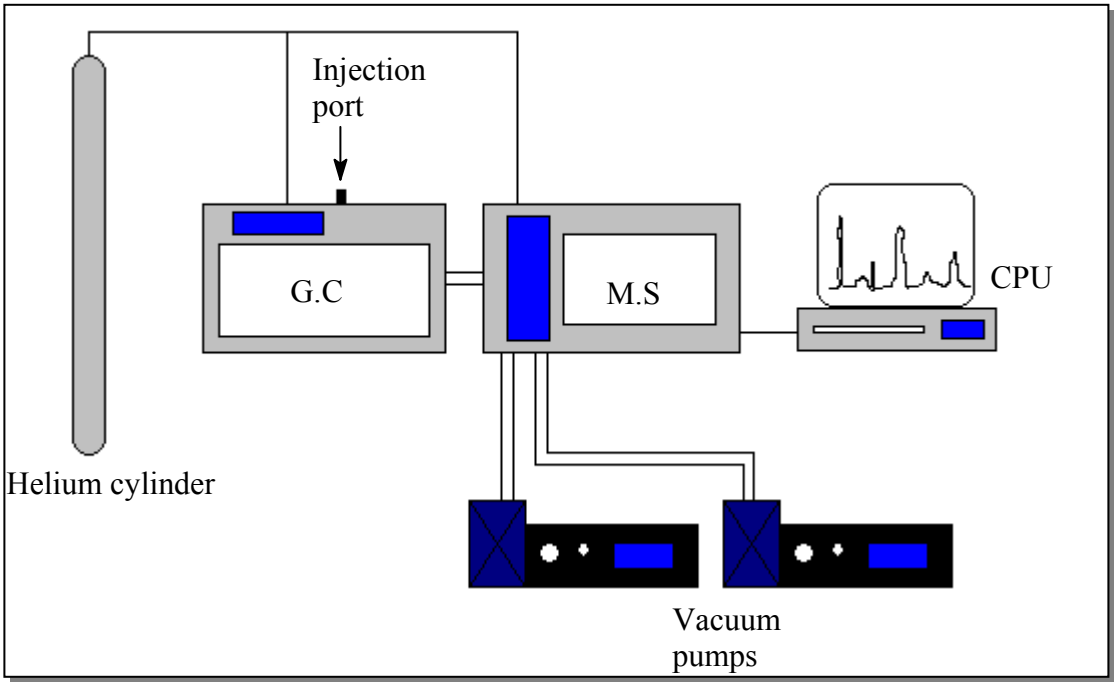

GCMS Apparatus

One of the attributes of the mass spectrometer is the ability to identify and measure minute quantities of material; one of its limitations is the difficulty in resolving a multi-component mixture where ions of normally the same mass-to-charge ratio occur in the composite spectrum. To counter the above, the most widely used application is gas-liquid chromatographic presentation followed by mass analysis. The analysis gas (analyte) pass through a column, which is usually a small diameter tube installed in an oven (G.C equipment, see section 3.5.1 and 3.6.1) and a normal separation takes place. The part of the effluent from the column is diverted to the connected mass spectrometer, and then a mass spectrum of the chromatographic peaks is obtained. Finnigan Mat, GCQ was the name of the machine used and separated compounds from the G.C were passed on to the mass spectrometer where

the atomic make-up of the molecules was determined. The results from such an analysis were normally that of a typical G.C trace but with the possible identification of the formulae of the compounds separated. This technique was mainly used to confirmed the (already known from the calibration) normal G.C analysis results. The G.C part of this was equipped with the column from Restek Corporation with a RTX-5ms stationary phase, of a length of 30 m and an internal diameter of 0.25 mm.

3.6.6 Inductively Coupled Plasma-Optical Emission Spectroscopy (ICP-OES)

This analysis was carried out at the Wits-analytical laboratory (School of Chemistry) by Ruphat Morena. Calibration standards for ICP were prepared as follows: In addition to the blank solution, for aluminium and sodium calibration curves, 5 ppm and 10 ppm standards were prepared. For the 10 ppm solution, 1 ml each of aluminium and sodium (from 1000 ppm standards) were transferred, followed by 1 ml hydrofluoric acid solution (HF) (49%), 2 ml hydrochloric acid solution (HCl) (33%) and de-ionized water to make up a 100 ml solution. For the 5 ppm solution, 1 ml each of aluminium and sodium standard solutions were added to a 100 ml flask, followed by 2 ml HF, 4 ml HCl and water up to the 100 ml mark. A 50 ml portion of the solution was diluted to 100 ml to obtain a 5 ppm solution. The blank contained 1 ml HF, 2 ml HCl and water up to the 100 ml mark. For the silicon calibration curve, 10 and 30 ppm calibration standards were prepared by transferring 1 ml and 3 ml, respectively, of 1000 ppm standards into volumetric flasks, then adding 1 ml HF and 2 ml HCl to each, followed by de-ionized water to 100 ml mark.

For the sample solutions, approximately 0.04 g sample was dissolved in a 100 ml volumetric flask by adding 1 ml HF, 2 ml HCl followed by water to make up a 100 ml solution. The solutions were then used for aluminium and sodium analysis. For silicon, 5 ml of the above solution (containing ~182 ppm silicon) was diluted to 100 ml with de-ionized water after addition of 1 ml HF and 2 ml HCl.

A 2:1 mixture of concentrated hydrochloric acid and nitric acid heated to some desired temperature was used to dissolve the zeolitic framework structures.

3.6.7 Thermodynamic determinations

Thermodynamic calculations of alkyl-transfer reactions were carried out at SASOL using the DMol^3 Density Functional Theory (DFT) code from Accelrys, Inc.

4 ETHYLBENZENE DISPROPORTIONATION

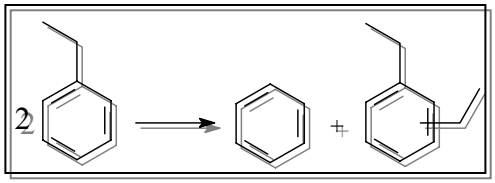

4.1 Introduction

The disproportionation of ethylbenzene was introduced by Karge *et al*.[7] as a test reaction for characterizing the Brönsted acidity of large pore zeolites; e.g. the mordenite and faujasites. After a sufficiently long time on stream, the rate of this acid catalysed reaction is virtually constant and can be correlated to the number of strong Brönsted acid sites. It was also found that the higher the rate of ethylbenzene disproportionation the shorter the induction period. They also suggested that the rate of ethylbenzene disproportionation seemed to be a suitable parameter for characterizing the acidity of monofunctional catalysts.[46] Karge *et al*.[7] have also shown that under appropriate conditions, acidic zeolites catalyze disproportionation reaction of ethylbenzene in a completely selective manner; yielding benzene and diethylbenzene as the only products.

During the disproportionation of ethylbenzene on large pore zeolites, Cardoso *et al*.[65] observed:

1) an induction period, where conversion increased with time on stream until a maximum was reached,
2) during the induction period, the yield of benzene was sufficiently higher than that of diethylbenzene, although under these reaction conditions since no dealkylation occurred they should be equal on the basis of reaction stoichiometry (1:1) and
3) during the induction period the distribution of the diethylbenzene isomers changed considerably and no shape selectivity was observed.

During the same reaction with medium pore zeolites the same authors observed:

1) no induction period
2) a net deactivation of the catalyst
3) and the shape selectivity effect of the diethylbenzene isomers.

Critical factors were identified which lead to the following precautions[66] to be taken in studying this reaction:

1) Granulated catalysts should be diluted with quartz chips so to avoid a fast deactivation.
2) Oxygenated aromatics in the impure feed are a further cause of deactivation. Therefore a highly purified feed is advisable.
3) The saturator design is crucial (if used): the residence time of the gas flow must be sufficient to ensure the complete saturation of the flow by the vapour of ethylbenzene feed.
4) Reaction temperature control within 1 °C seems critical. High initial conversions may help to achieve a homogeneous temperature profile.
5) A delay of 2 hours between pre-treatment and reaction start up is advisable.
6) Quantitative determination of product distribution is largely related to a correct G.C. analysis procedure: the response factors must be carefully controlled as they can vary with a few percent for different FID detectors

This test reaction was later published as a standard reaction for acidity characterization by the International Zeolite Association (IZA).[66]

In the current transalkylation study, ethylbenzene test was used mainly to evaluate the potentiality of the three chosen catalysts, i.e. mordenite, LZY-82 and ZSM-5 for catalyzing alkyl-transfer reactions since they were well known acidic zeolites (containing Brönsted acid sites).

4.2 Experimental

The study was carried out at 180 °C. Nitrogen was used as a carrier gas at a flow rate of 1 ml/min. Mordenite, HZSM-5 and LZY-82 zeolites were used as acid catalysts and the mass used was 240 mg at WHSV = 1 h^{-1}. Analysis was carried out by an online G.C. at hourly intervals.

4.3 Results and Discussion

4.3.1 Ethylbenzene disproportionation on HZSM-5

The ZSM-5 material did not show any activity for ethylbenzene disproportionation probably due to its smaller pores and cavities; the method of preparation might be another reason why it did not work since it was not a commercial catalyst. This lack of activity and the fact that the study aimed at involving bulkier molecules which are bigger than the narrower pore sizes and ethylbenzene, the alkyl-transfer study on this material was discontinued.

4.3.2 Ethylbenzene disproportionation on H-mordenite

A conversion of more than 50 % (figure 4.1) at 180 °C was achieved on mordenite, and the main products were benzene and the diethylbenzenes as expected.

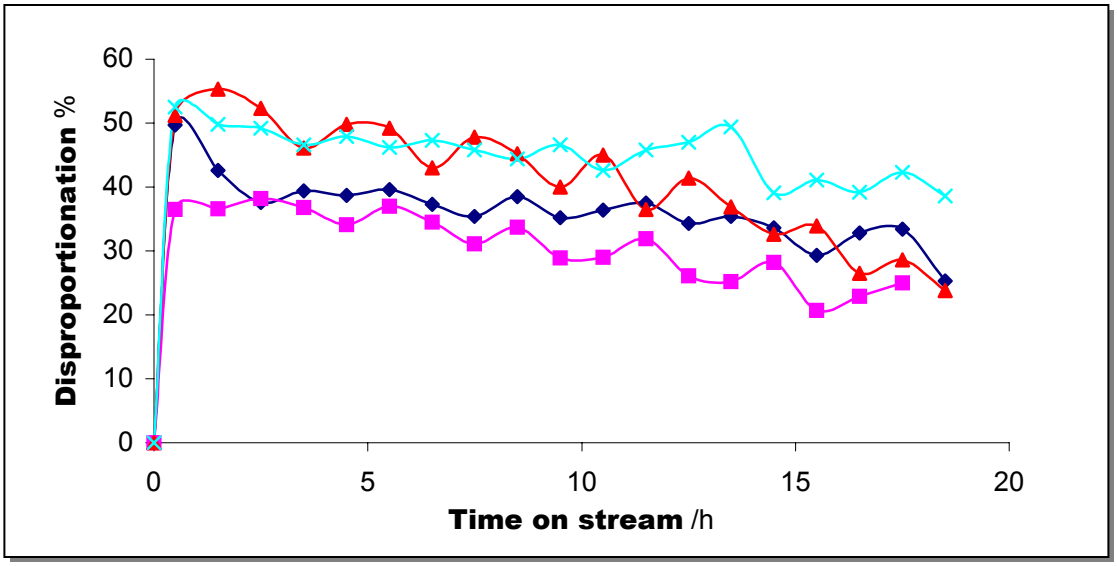

Figure 4.1: Ethylbenzene disproportionation (mol %) on mordenite at 180 °C

The test showed that this catalyst was active for such reactions and had a reasonable lifetime. The fact that the induction period was not observed, strongly suggested that the catalyst had strong acid sites which were capable of inducing disproportionation/transalkylation (or alkyl-transfer) reactions in the transformation of alkyl-aromatics. Figure 4.1 also shows repetition of the same reaction under same conditions each time with a fresh catalyst. This was carried out with the aim of evaluating the reproducibility as well as the reliability of the analytical technique and methods used. All spent catalysts were black in colour (white before the reaction) due to carbonaceous material deposition (deactivation) during the reaction.

Benzene deficit was observed in the product stream (figure 4.2). Benzene could be undergoing some further conversion into unknown products referred to as others (OTHERS), or its consumption may be favoured in carbon deposition. The catalyst could again be strongly adsorbing benzene preferentially despite its expected high diffusion rate due to its smaller molecular size. Confirmation of the above speculations would be dealt with in the following chapters.

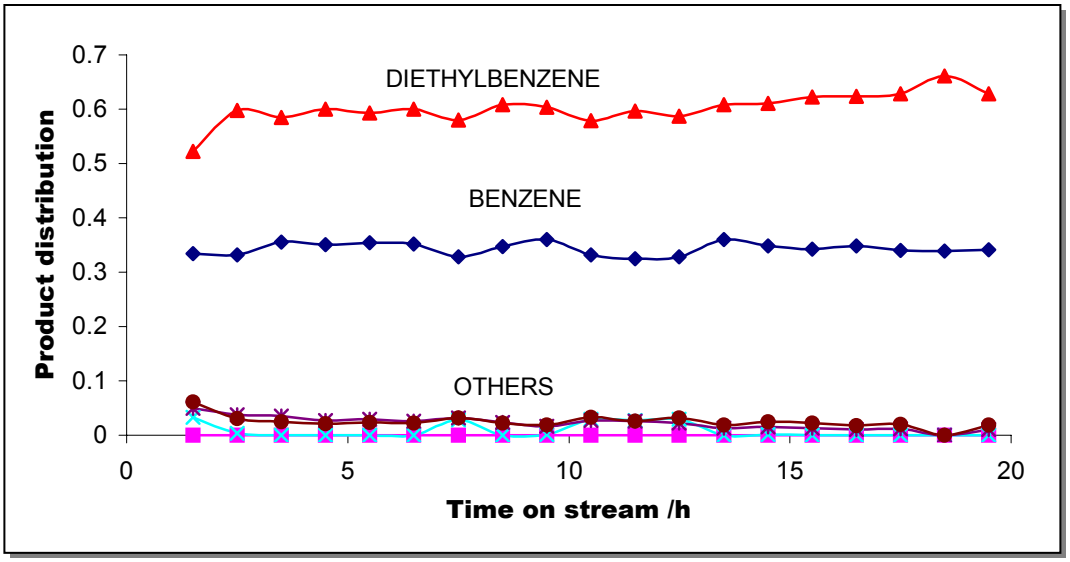

Figure 4.2: Product distribution (mol %, fractional units) of the ethylbenzene disproportionation on mordenite at 180 °C

4.3.3 Ethylbenzene disproportionation on HLZY-82

LZY-82 (zeolite-Y) showed similar behaviour except during the early stages of the reaction. Benzene was in high concentrations in the product stream mainly due to its rapid diffusion out of the pores of the 3-D zeolite as expected. This was hence interpreted as high conversion by the G.C's conversion calculations in the outlet stream; and this is shown as a 'peak' just after an hour during the reaction (figure 4.3).

The initial high amounts of benzene in the product stream was not the case with mordenite mainly due to its one-dimensional channel structure; whereby molecules queued up in the same channel and any strong adsorption of molecules would result in the blockage of the entire channel, including the passage of the smaller benzene molecules. The bulky polyalkylated diphenylethanes (scheme 4.1) were the kind of transition state molecules through which the alkyl-transfer reactions took place in both zeolites. The slow diffusion of other products other than benzene and

diethylbenzene, was due to their bulkier sizes (poly-alkylates), and presumably they did not form on mordenite due to limitations posed on the transition state by the pore structure.

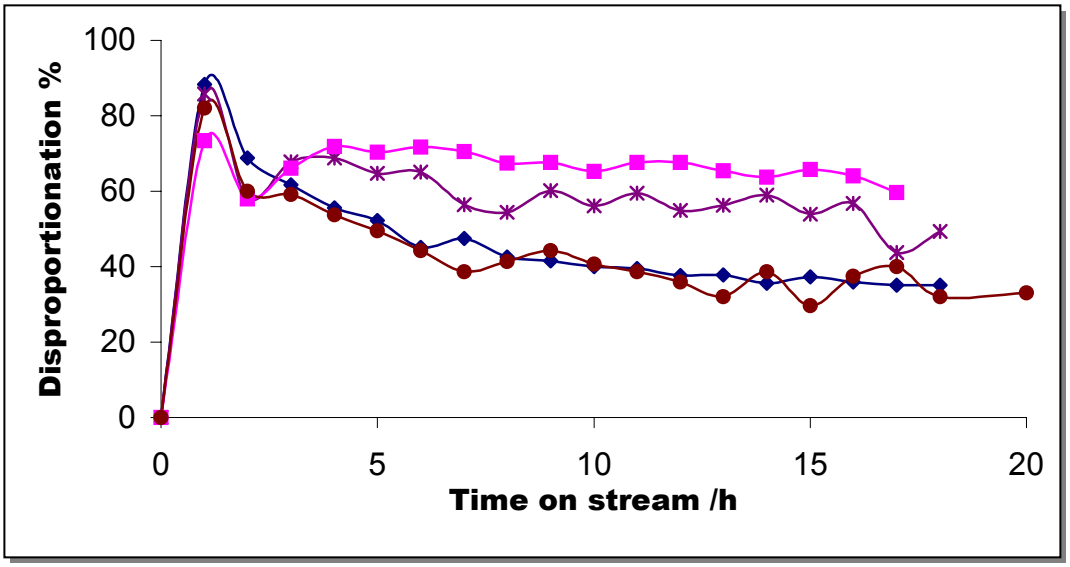

Figure 4.3: Ethylbenzene disproportionation (mol %) on LZY-82 at 180 °C

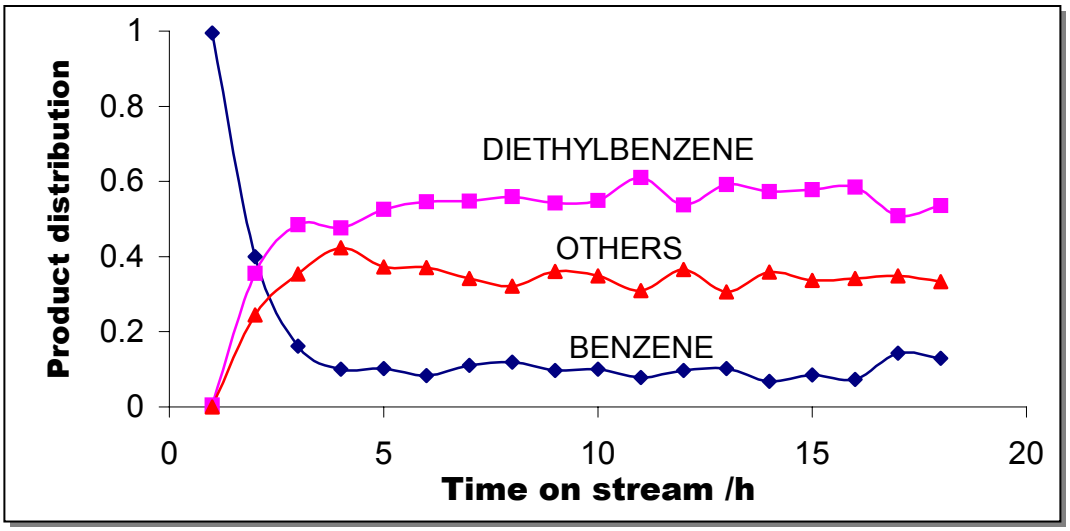

Figure 4.4: Product distribution (mol %, fractional units) of the disproportionation reaction of ethylbenzene on LZY-82 at 180 °C

Ethylbenzene deficit during the early stages of the reaction is clearly depicted in figure 4.4, which shows the product distribution during the reaction at 180 °C. During the first three hours of the reaction benzene was the major product, after which some sort of an equilibrium was attained and a similar trend to that on mordenite was observed, i.e. benzene deficit in the product stream. The concentration of the 'others' (dealkylation and heavy aromatic products) was higher than in the case of H-mordenite. This was mainly due to the spacious cavities of the zeolite-Y allowing bulkier intermediate molecules to be formed, and the products of which were obviously bulky. This supported the earlier suggestion that there were limitations on mordenite.

Camiloti *et al*.[67] also observed the ethylbenzene deficit during the induction period on H-Beta zeolite; consequently, they suggested that polyalkylated diphenylethanes (scheme 4.1) were species that built up in the zeolite during the early stages of the reaction. The scheme shows that benzene and diethylbenzene were the main products of the reaction, and thus differences in molecular sizes and simpler diffusions allowed benzene to be the main product species in the outlet stream mainly during the early stages. This resulted in high benzene concentrations in the product stream. Arsenova *et al*.[68] reported on the inhibiting effect of diethylbenzene produced in the reaction, which was mainly due to preferential adsorption of the diethylbenzenes by the zeolite, blocking the active sites.

Looking at the disproportionation reaction on scheme 4.2, it is apparent that benzene and diethylbenzene are stoichiometrically produced in a 1:1 relation, and that further (secondary) reactions would lead to the consumption of mostly the diethylbenzenes.

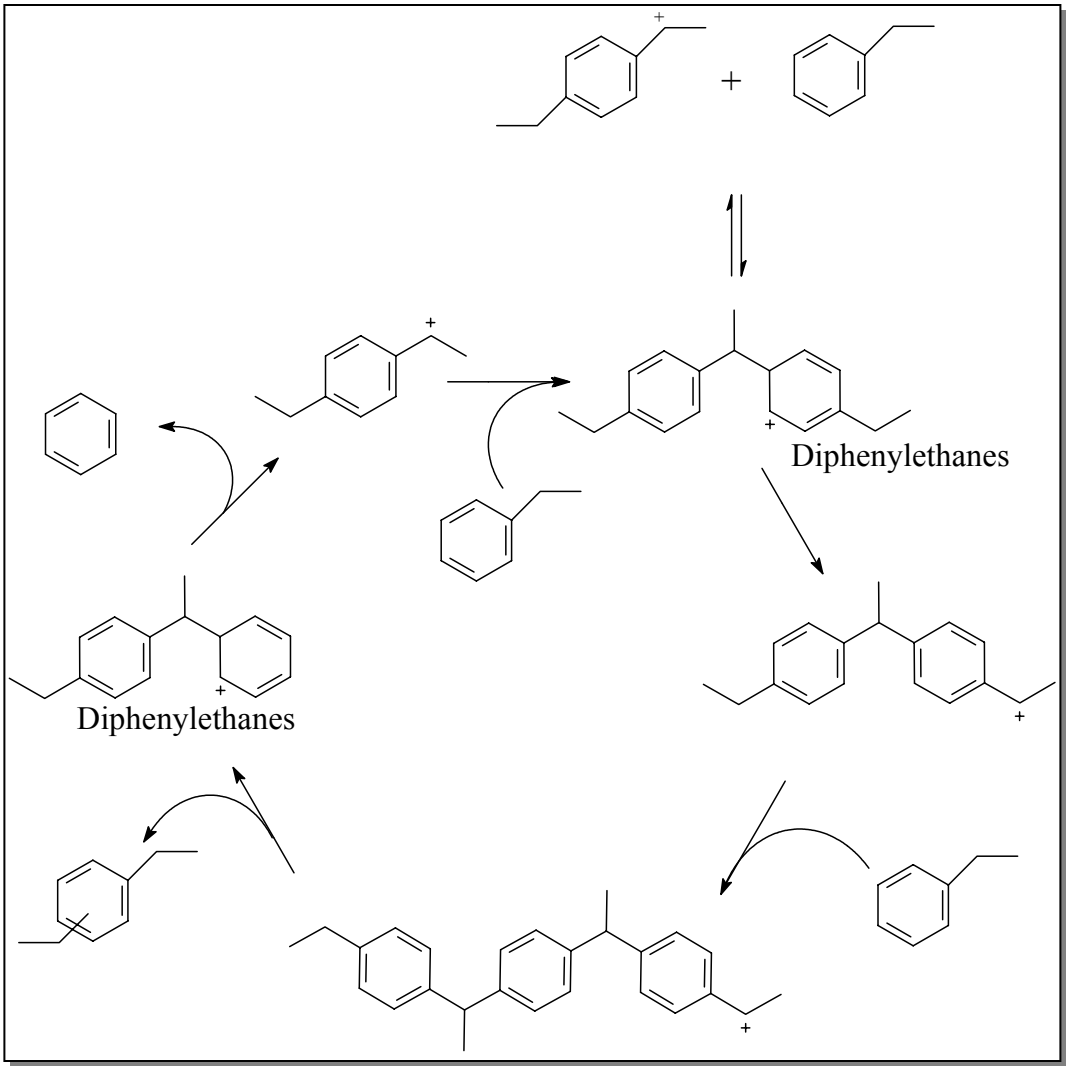

Scheme 4.1: Polymeric and polyalkylated species that formed during ethylbenzene disproportionation in zeolites[67]

These further reactions would be favoured during the early stages of the reaction while the reaction space occupied by deposition (formation) of carbonaceous materials is minimal. This somehow explains the diethylbenzene deficit observed during the very early stages of the reaction, i.e. alkylated species were further involved in secondary reactions mainly due to their preferential adsorption and thus their delayed diffusions. The preferential adsorption of alkylated species will be dealt with in the following chapters.

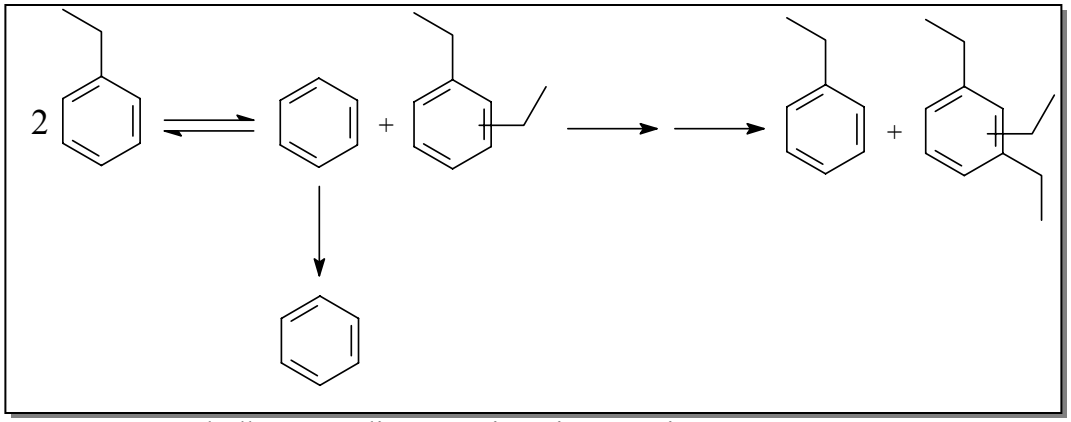

Scheme 4.2: Ethylbenzene disproportionation reaction

Other authors reported on the diethylbenzene deficit during the early stages of the reaction and later on steady states were reached and they observed a 1:1 relation benzene:diethylbenzene) in the product stream. Pradhan *et al*.[47] observed benzene as the major product in an 80 % of ethylbenzene conversion on HZSM-5, and he attributed this to the dealkylation reactions (due to smaller pores) and this was supported by minor products being toluene, xylene and diethylbenzene. Similar results were observed by Rhodes and Rudham[69] while disproportionating ethylbenzene on zeolite-Y without the production of toluene and xylene.

Whether the reaction results in a benzene or diethylbenzene deficit during the early stages of the reaction seem, as other authors suggests, to depend on the way reactants are fed into the reactor. Feed injection by a syringe (liquid form) mostly results in the diethylbenzene deficit while inert carrier gas saturation with ethylbenzene led to benzene deficits.

4.4 Conclusion

The ethylbenzene test thus showed that both mordenite and LZY-82 were potential catalysts for the disproportionation/transalkylation (alkyl-transfer) reactions in the

conversions of alkyl-aromatics; they both showed presence of strong Brönsted acid sites (lack of observable induction period). Catalyst deactivation was more severe on the mordenite than on the zeolite-Y mainly due to the catalyst structure. The ethylbenzene test can also be used to assess structural types of zeolitic materials by following the benzene patterns during the early stages of the reaction, as shown by the differences on mordenite and zeolite-Y which themselves have different structures.

5 BENZENE CONVERSION

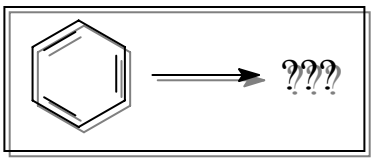

5.1 Introduction

Primary products of simple alkyl-aromatics like toluene and ethylbenzene disproportionation reactions are mainly benzene and the respective dialkyl-benzenes. To fully understand and to be able to interpret results form such reactions, the product behaviour on acidic solid catalysts had to be evaluated. Benzene and toluene were very special in this particular alkyl-transfer study since they were used both as solvents for poly-aromatic species and importantly as alkyl-acceptors; thus their effect on the catalyst or the effect of the catalyst on them had to be known. The anticipation with benzene was that it would be a good solvent for poly-aromatics and most importantly it probably would be very inert (benzene is known to be a very stable compound) on contacting the catalyst; but it would not be as effective as toluene in accepting alkyl groups. There was no awareness at the moment of any literature information regarding benzene conversions on solid acid catalysts except benzene hydrogenation which normally occurs on bifunctional catalysts containing a noble metal like platinum. In absence of a hydrogenating environment and a metal, benzene was expected to be very inert on H-zeolites.

5.2 Experimental

The study was conducted at temperatures ranging from 200 to 400 °C. Nitrogen was used as a carrier gas at flow rates of 1 ml/min. Mordenite and LZY-82 zeolites were used as acid catalysts at WHSV = 1 h^{-1}.

5.3 Results and discussion

5.3.1 Benzene conversion on Mordenite

As expected, benzene was almost inactive on mordenite and this was expressed by the very low conversions observed. During benzene conversions three products were formed all of which were unknown. Since the reaction was carried out in a non-hydrogenating environment one could only think of cracking of the benzene ring. Cracking also required, to some extent, a hydrogenating environment but less hydrogen was needed in this regard and could have been provided by protonic sites in the zeolite which would defy the meaning of a catalyst. The only logical explanation would be that H_2 was produced during carbonaceous material deposition. Judging by their retention times in the G.C column one of the products was lighter than benzene while others proved to be heavier or just bulkier or branched alkyl-chains. Figure 5.1 below depicts patterns followed by these unknowns which could not be condensed in an ice-bath for further analysis.

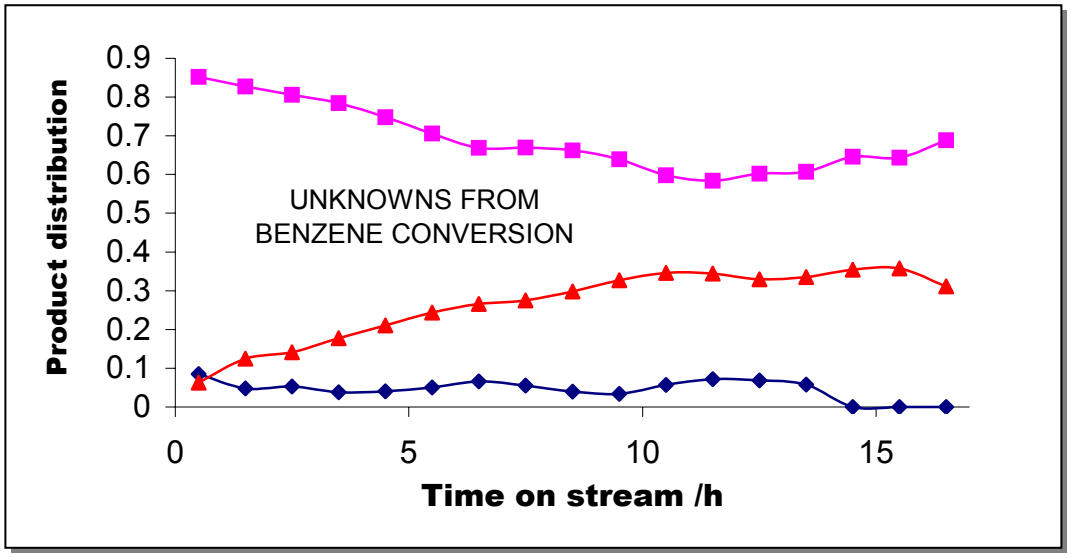

Figure 5.1: Unknown product distribution (mol %, fractional units) from benzene conversion at 300 °C on mordenite

The highest conversion was achieved at 400 °C as conversion increased with temperature (figure 5.2).

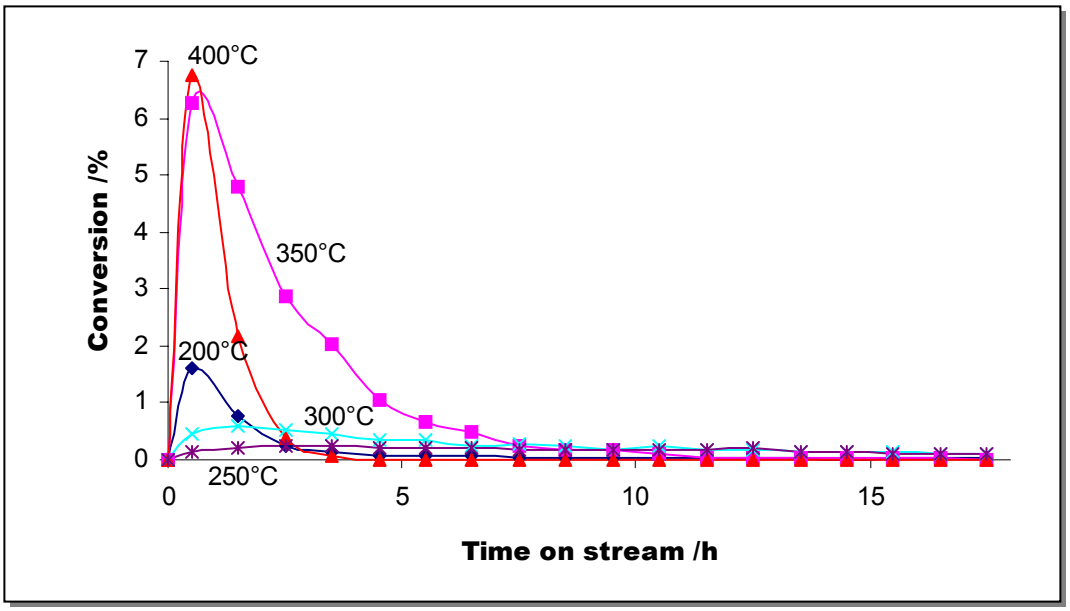

Figure 5.2: Benzene conversion (mol %) on mordenite

The high conversion at 200 °C observed was probably due to preferential adsorption of benzene at this low temperature allowing product concentration to build up in the product stream; this was not the case with higher temperatures (250 and 300 °C) which suggested that benzene adsorption (retention) was somehow inhibited at these temperatures. Another feature about the reaction at 200 °C was that of high rate of deactivation of the catalyst with time on stream. This supported adsorption of the benzene molecules which mainly blocked access towards active sites rendering the catalyst inactive without poisoning active sites. All spent catalysts were black in colour after the reactions, which also suggested that carbonaceous material deposited on the catalyst even at temperature as low as 200 °C. Several reactions were carried out at 300 °C, under the same conditions, and results were reproducible to some reasonable extent (figure 5.3).

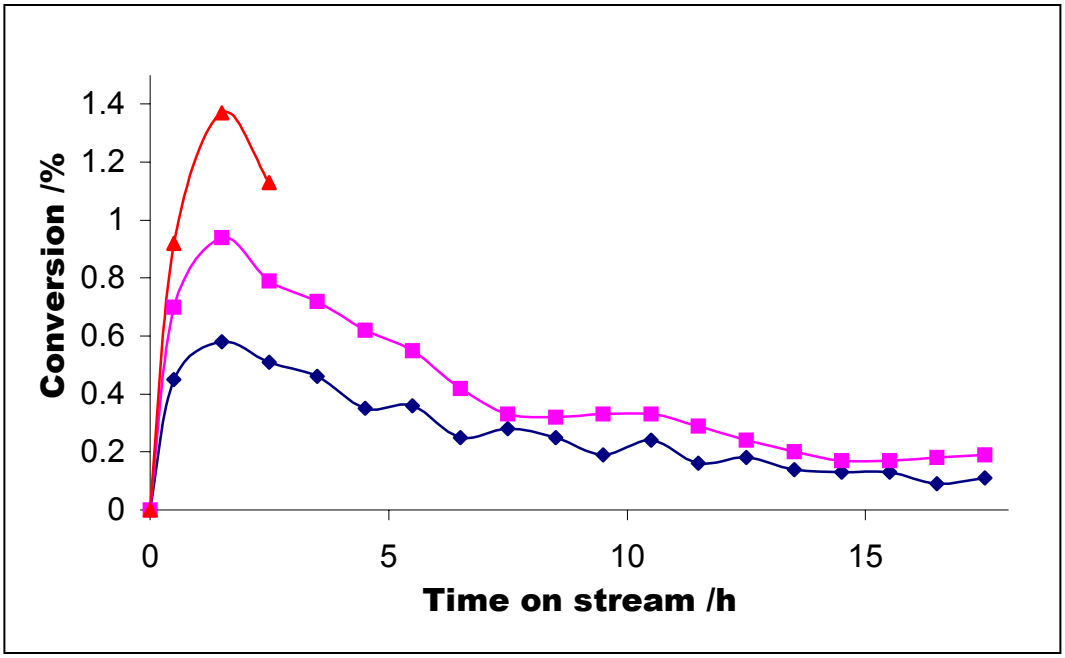

Figure 5.3: Reproducibility of benzene conversion (mol %) on mordenite at 300 °C

5.3.2 Benzene conversion on HLZY-82

This catalyst showed little (0.3 % conversion) or no activity for benzene conversion in the temperature range of 200-350 °C, but an activity of up to 15 % was achieved at 400 °C (Figure 5.4), and the product distribution of which all were unknown is depicted in figure 5.5. The low or no activity on the zeolite-Y was attributed to weaker acid sites as compared to those on mordenite, though it contained many sites (higher density) than the later. The high activity at 400 °C even though there was non at temperatures lower than that was thus due to activation of the numerous active sites of this catalyst by higher temperatures which then started to behave like the mordenite; and presumably further increase in temperature would have resulted in similar patterns to those of mordenite. The concentration of the products in the product stream was more pronounced on the zeolite-Y than on mordenite mainly due to differences in structures; i.e. simple diffusions on the three-dimensional zeolite-Y.

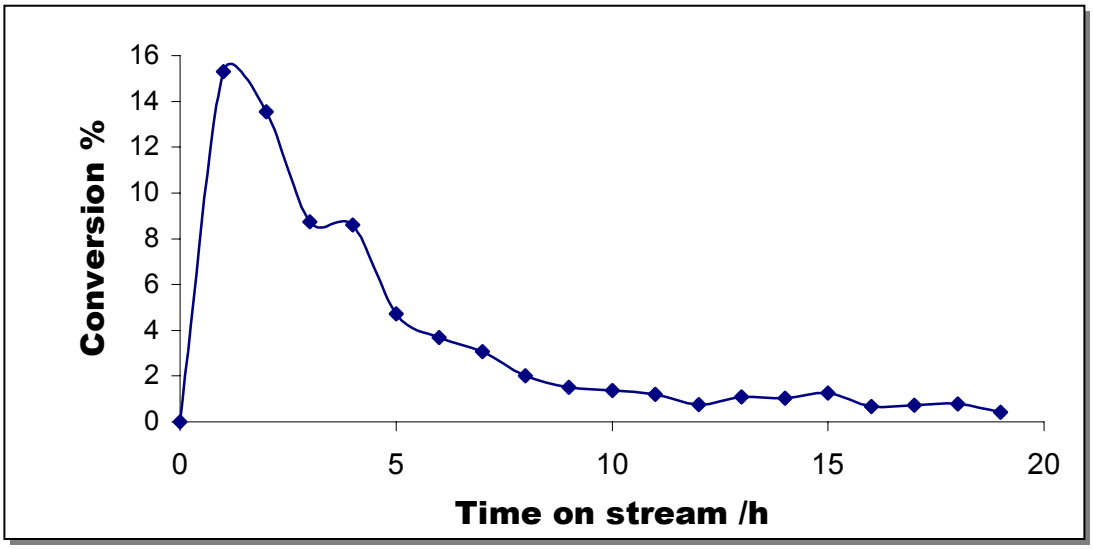

Figure 5.4: Benzene conversion (mol %) on LZY-82 at 400 °C

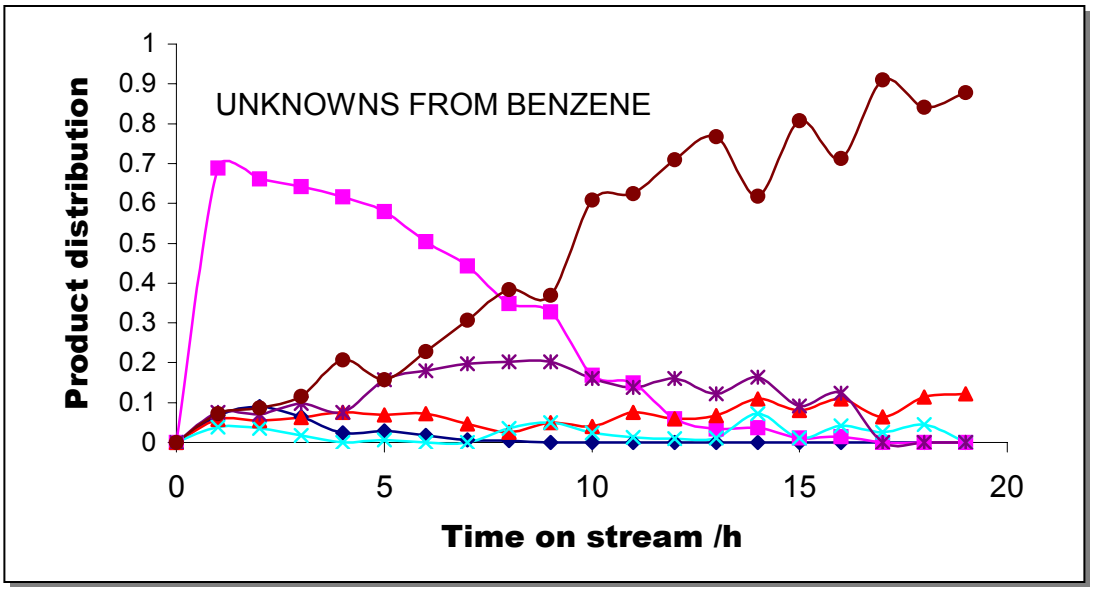

Figure 5.5: Unknown product distribution (mol %, fractional units) from benzene conversion on LZY-82 at
400 °C

The higher number of products formed in this case was mainly due to the more open structure of the zeolite-Y catalyst which provided more room for the formation of bulkier molecules, most importantly the transition state molecules (intermediates) which led to their formation..

5.4 Carbonaceous deposits

Instead of analysing online, the outlet stream was condensed using a collector (reactor B) which was cooled down in an ice-bath during the collections. Further analysis of the collected samples by the G.C.M.S did not show some of the products which were observed online, this then suggested that those products were very volatile substances (gasses) which could not be condensed in the ice-bath. Surprising enough, the G.C.M.S analysis showed presence of toluene and the expected diphenylenes (scheme 5.2). As difficult as it was to conceive the formation of toluene in this reaction, much of it was attributed to the actual carbon formation (deposition) in the catalyst rather than secondary reactions from benzene cracking.

Magnoux *et al*.[40] suggested that the main reaction in carbon formation was the alkylation of poly-aromatics that formed in the zeolite by olefins (scheme 5.1), followed by cyclisation then aromatisation through hydrogen transfer forming highly aromatic compounds (carbonaceous material).

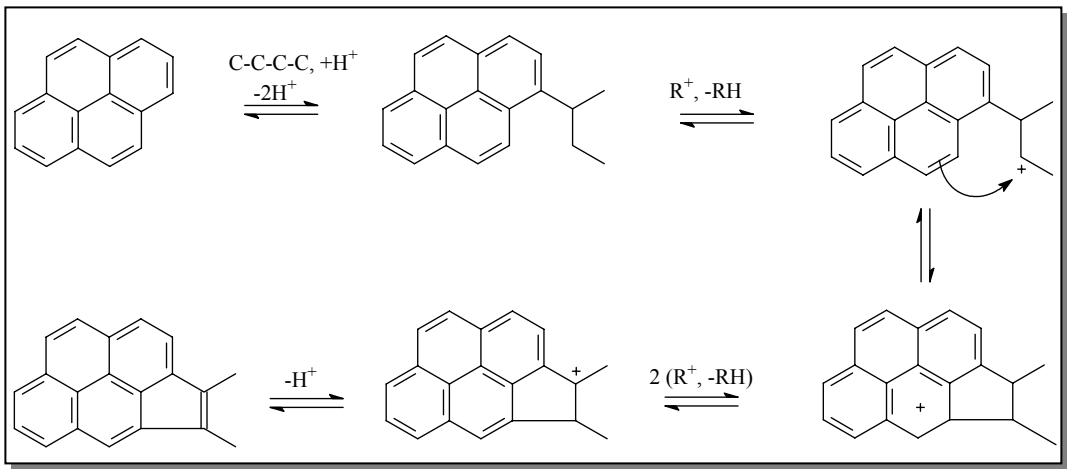

Scheme 5.1: Carbon formation through alkylation of aromatics by olefins[40]

Based on scheme 5.1, carbon deposition during benzene conversion on zeolites was then suggested to go through a series of reactions (scheme 5.2) which also showed and explained the formation of diphenylenes. From this it can be seen that the process

produced hydrogen as poly-aromatic substances were formed. These poly-aromatic products had a very long contact time and high boiling temperatures due to their molecular sizes resulting in low diffusion rates. These substances were subsequently trapped in the catalyst resulting in its deactivation.

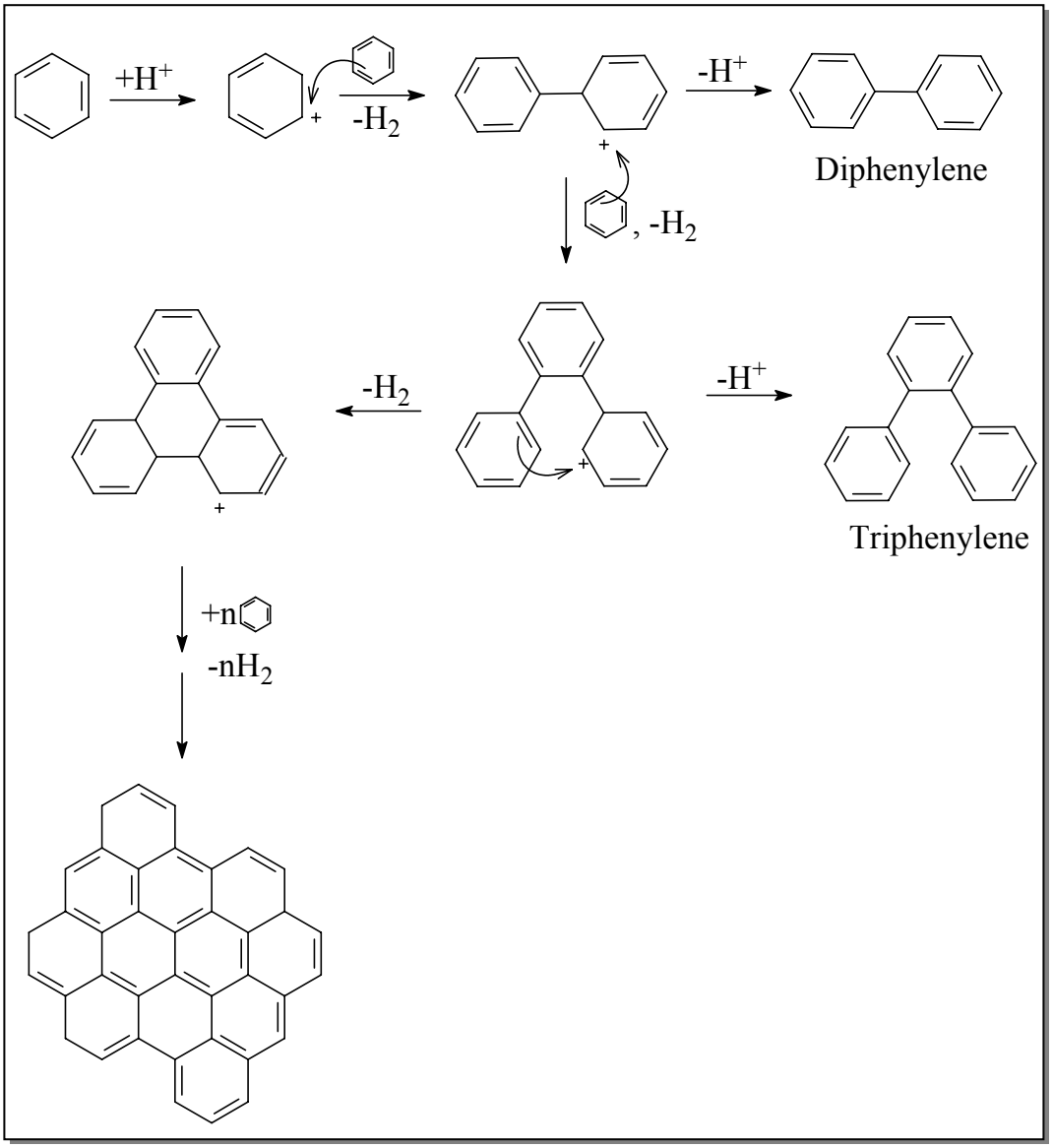

Scheme 5.2: Carbon formation during benzene conversion in zeolites

The production of hydrogen by the carbonaceous material formation process probably led to cracking of benzene producing mostly olefins. Thus deactivation might have also gone through reactions shown on scheme 5.1 and toluene production through transalkylation between poly-aromatics and benzene (scheme 5.3).

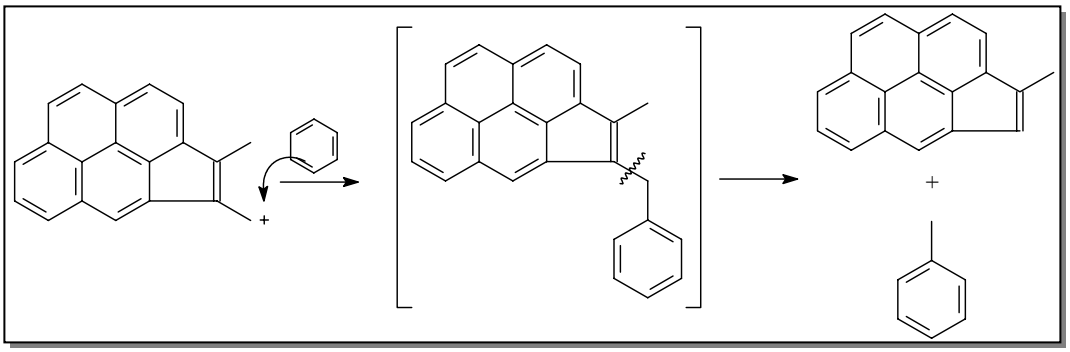

Scheme 5.3: The formation of toluene during benzene conversion

The type and size of the transalkylation intermediate would be determined by the size of the catalyst pores and cavities. Unfortunately there was no further evidence for the processes outline above even though toluene was actually detected in the product stream.

5.5 Conclusion

Spent catalysts of both mordenite and LZY-82 were black in colour signifying the formation of carbonaceous material, and proving that benzene had undergone some transformations. The formation of toluene from benzene reactions further supported cracking reactions proving even further that benzene was not actually an inert solvent as expected.

6 TOLUENE DISPROPORTIONATION

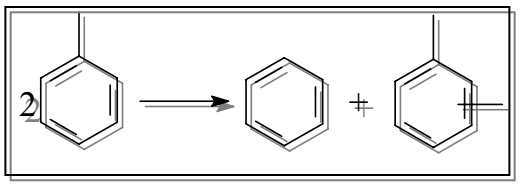

6.1 Introduction

Many variations of process schemes for transformation of relatively low cost aromatic mixtures to desirable high value products such as *p*-xylene are becoming available;[70] and these are usually based on solid catalysts which disproportionates, alkylate, transalkylate, isomerize or dealkylate various aromatic feed stocks. Increased global demand for xylenes and intentions to upgrade low value C_7 (toluene) and C_9 aromatics to valuable C_8 aromatics have led to the development of processes like toluene disproportionation by the Mobil Oil Corporation which uses the ZSM-5 based catalysts.[71] Although toluene disproportionation is well reported in the open literature most of the information on transalkylation and disproportionation are patented.

In the presence of hydrogen on HZSM-5 not only disproportionation but also dealkylation of toluene occurred, and this was inhibited[45] by using N_2 as a carrier gas instead. Dealkylation was promoted by strong sites while medium sites promoted disproportionation reaction. The disproportionation reaction to form benzene and xylene within the pores is relatively slow and benzene diffuses out the pores rapidly.[43] As observed by Kaeding *et al*.[70] toluene conversion on HZSM-5 increased in direct proportion to the temperature from 8 to over 50 % in the range of 450-600 °C. At the lowest temperature, the mole ratio of benzene/xylene was 1.07, close to the theoretical 1.00 value. The observed ratio increased with increase in temperature to a value of 1.77 at 600 °C. This was due primarily to a demethylation reaction as indicated by the corresponding increase in the yield of methane.

Das *et al*.[71] observed that mordenite was more active than Y-faujasite[17] for toluene disproportionation at all stages of zeolite composition.

6.2 Experimental

Toluene disproportionation was carried out at temperatures ranging from 200 to 400 °C. N_2 was used as a carrier gas at 1 ml/min.

Analysis by the on-line G.C. was getting complicated due to poor column separation which was cause by too much hydrocarbon injection (feed); the situation was resolved by decreasing the amount of the feed per hour injected into the reactor system from 0.24 ml/h to 0.07 ml/h. This decreased the hydrocarbon/nitrogen ratio from 1:1 to 1:27. This also reduced the WHSV from 1 to 0.3 h^{-1}.

6.3 Toluene disproportionation mechanism

The proton from the acid form of the zeolite, H^+zeol^-, attacks a toluene molecule at the *ipso* position (scheme 6.1 and 6.2). This weakens the carbon methyl bond and initiates transfer to a second molecule.[72]

But majority of opinion seemed inclined towards mechanism M_2 which was plausible in view of the Streitweiser's results,[73] and the well recognized instability of the methyl cation. The disproportionation results on ZSM-5 (<3 % conversion) appeared in general to support the M_2 mechanism, based on similarity to the calculated M_2 deuterium distribution.

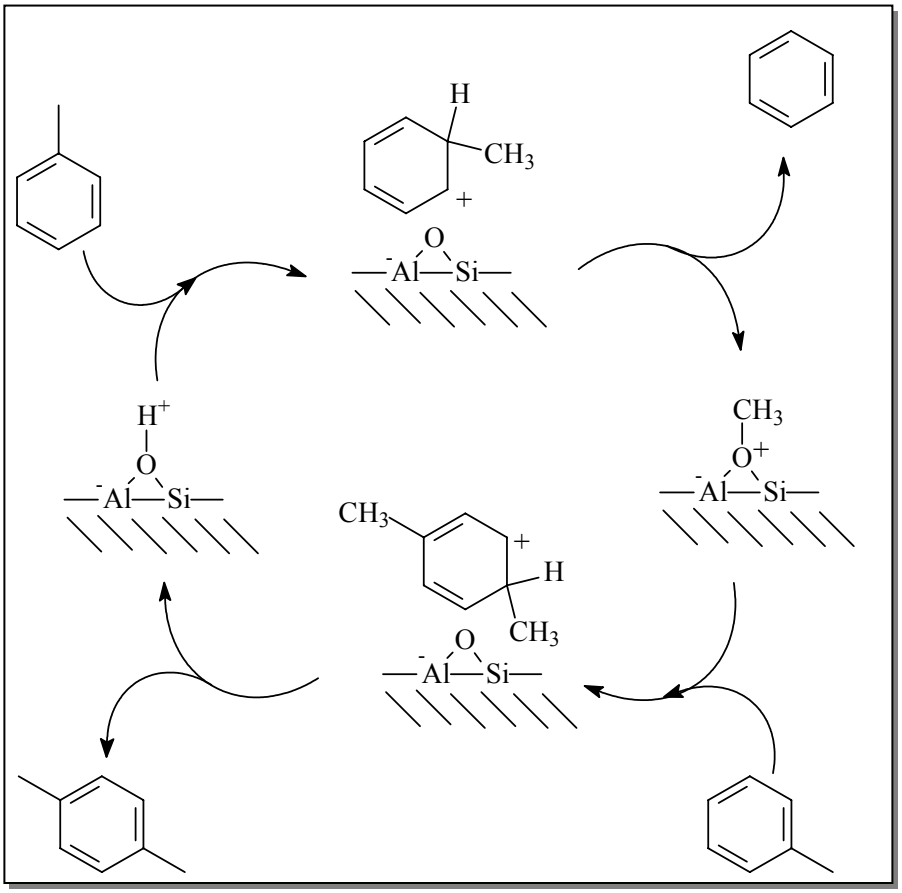

Scheme 6.1: Toluene disproportionation mechanism, M_1[73]

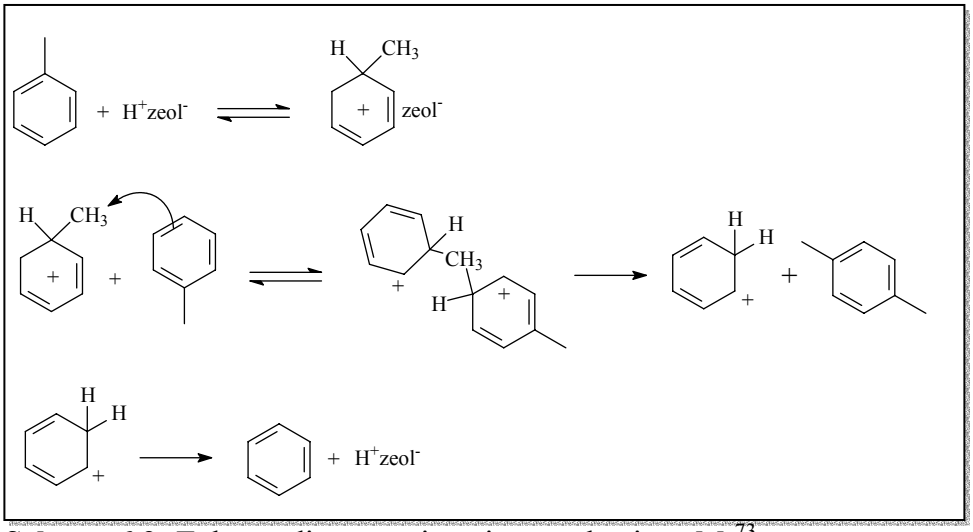

Scheme 6.2: Toluene disproportionation mechanism; M_2[73]

Though the disproportionation of toluene was investigated to some extent in the current study, the main objective was to evaluate the patterns followed by this reaction. Toluene disproportionation is catalysed by acid catalysts which also catalyses transalkylation; for this reason the disproportionation studies were conducted and again as mentioned in the previous chapter, toluene was intended to be used as a solvent and also as an alkyl-acceptor of alkyl groups from bulkier molecules in alkyl-transfer reactions.

6.4 Results and discussions

6.4.1 Toluene disproportionation on H-mordenite

More than 50 % conversion of toluene to benzene, xylenes and other heavier products was achieved on H-mordenite at the temperature range of 300–400 °C (figure 6.1). The figure shows the increase in conversions with increase in temperature, this was also accompanied by an increase in the deactivation rate. The observed better conversions as compared to benzene (figure 5.2) were expected since the methyl group on the benzene ring activated the toluene molecule. The presence of benzene in the system was probably the reason why disproportionation patterns resembled that of benzene conversions on the same catalyst. As shown earlier, benzene contributed to some extent on carbonaceous material deposition and hence catalyst deactivation; in this case probably toluene and to a lesser extent xylene contributed to carbonaceous material deposition as well.

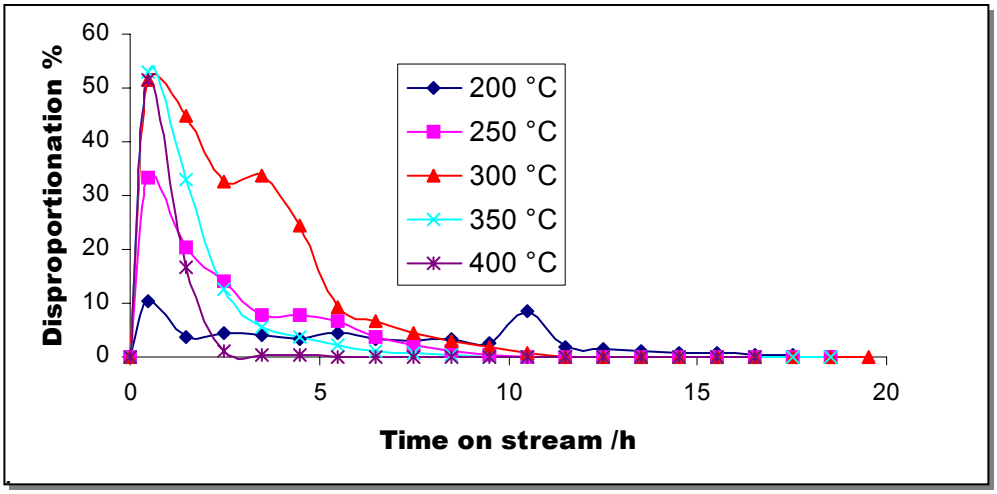

Figure 6.1: Toluene disproportionation (mol %) on mordenite

The expected 1:1 relation between benzene and the xylenes was achieved at 300 °C and this is shown in figure 6.2. With other temperatures the ratio of benzene to xylenes was fluctuating between 0.9 and 1.1. The cause of these fluctuations was mainly attributed to the effects of temperature on the reaction patterns.

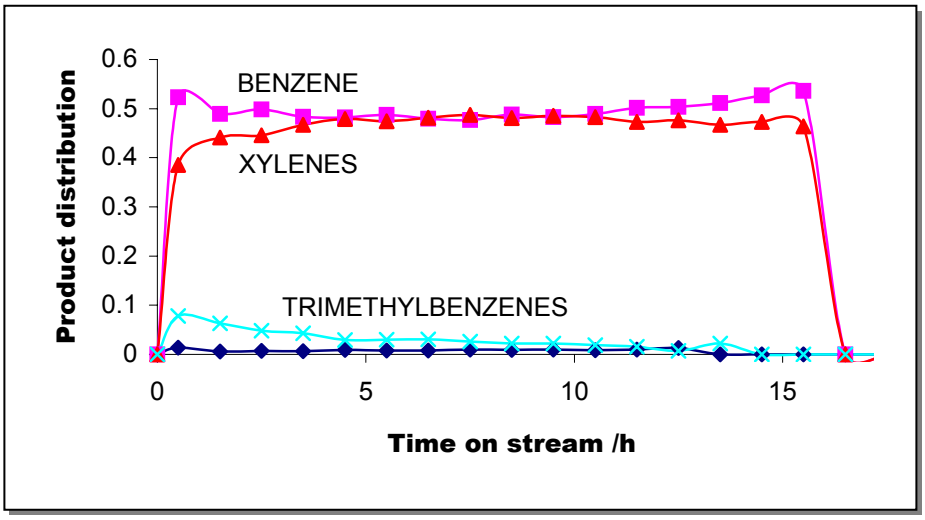

Figure 6.2: Product distribution (mol %, fractional units) of the toluene disproportionation reaction on H-mordenite at 300 °C

During the early stages of the reaction in figure 6.2, i.e. the first three hours, there was a xylene deficit caused by secondary disproportionation of xylene to toluene and the trimethylbenzenes, and also to the diffusion rate through the catalyst which favoured the smaller benzene. The same behaviour was observed after 10 hours during the reaction but then this was due to restricted diffusion by carbon deposition in the catalyst, which reduced the pore volumes and thus allowed the smaller benzene to diffuse quickly or preferentially out of the zeolite catalyst.

The reproducibility of the results was conducted at 300 °C under same conditions and this is shown in figure 6.3 below. Such reproducibility showed also the reliability of the analytical technique and methods used.

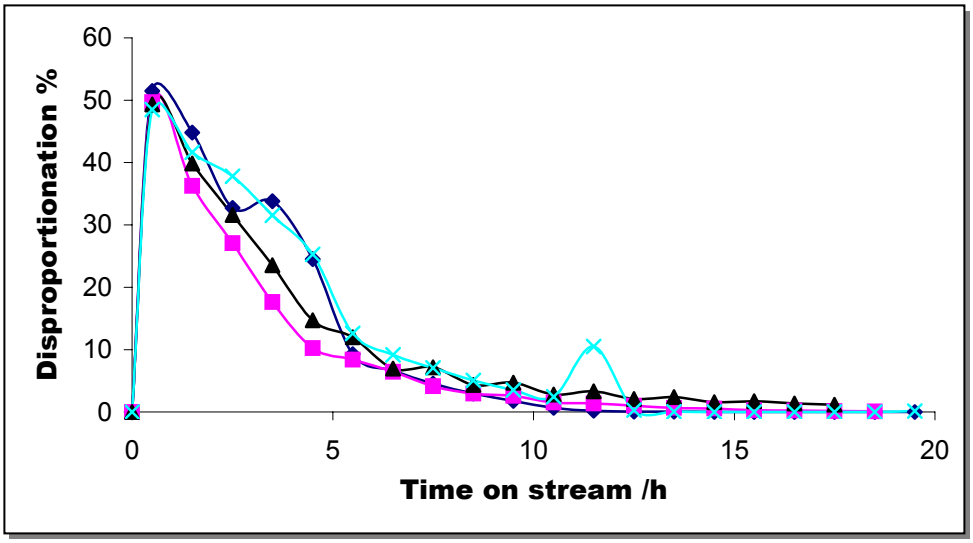

Figure 6.3: Reproducibility of the toluene disproportionation (mol %) reaction on H-mordenite at 300 °C

6.4.2 Toluene disproportionation on HLZY-82

Conversions of up to 50 % were also achieved on HLZY-82, but overall results were different from those observed on H-mordenite. In contrast to H-mordenite, there was an increase in catalyst lifetime with an increase in temperature (figure 6.4). This

behaviour was attributed to the fact that HLZY-82 contained larger (*tri*-dimensional) cavities and many active sites (higher density) than mordenite, this slowed down the rate of site deactivation (poisoning) and pore narrowing by carbon deposition. This catalyst contained acid sites which were not as strong as those on mordenite and strong molecular adsorption of the reactants and/or products which might have resulted in the blockage of the pores and the active sites was minimal. The high activity at 400 °C suggested that high temperatures had something to do with the activity/strength of the active sites in zeolites. Similar behaviour was observed during benzene conversions (figure 5.4). This temperature effect may have been on all or some of the acid sites.

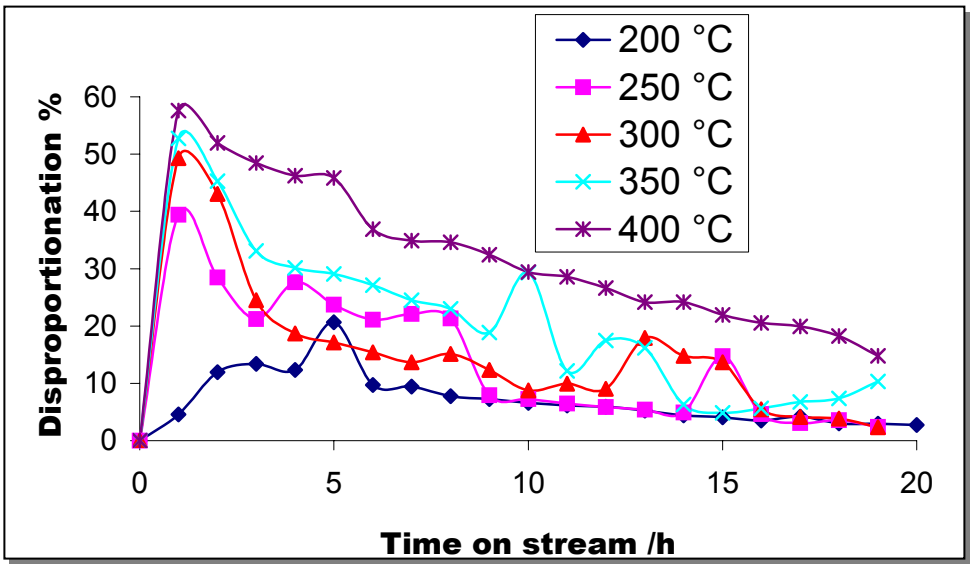

Figure 6.4: Toluene disproportionation (mol %) on HLZY-82

From the results of the study on ethylbenzene disproportionation on both zeolites where benzene deficit was observed, and form the study of benzene transformation on these catalysts where it was shown that benzene fouled the catalysts, and from the current study where increase in temperature resulted in higher deactivation rate on mordenite but improved lifetimes on zeolite-Y, it was apparent that the structure of the catalyst had a huge impact on transalkylation and the overall behaviour of

reactions. At this moment though, a lot was still to be confirmed and supported, this will be brought forth again in subsequent chapters.

A 1:1 relation between benzene and the xylenes was achieved at 400 °C (figure 6.5). The deficit in the xylenes during the early stages of the reaction was observed, and this was due to quick diffusion of the smaller benzene out of the zeolite pores as it was the case on mordenite and during ethylbenzene disproportionation on the same catalyst. The deficit was also due to secondary disproportionation of the xylenes to toluene and the trimethylbenzenes (TMB).

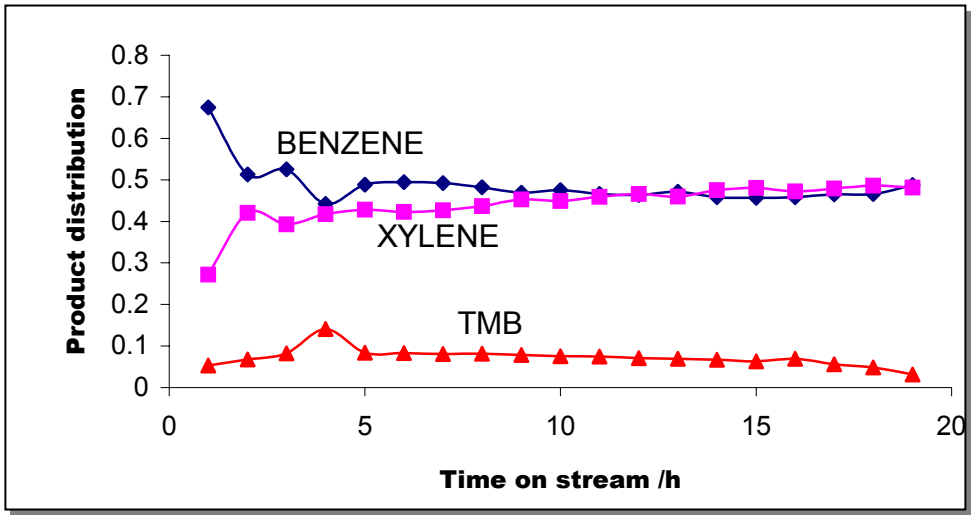

Figure 6.5: Product distribution (mol %, fractional units) of the toluene disproportionation on HLZY-82 at 400 °C

The perfect 1:1 benzene/xylene ratio after 9 hours on stream, and the fact that there was still some trimethylbenzenes (TMB) observed in the product stream, suggested that xylene disproportionation to form trimethylbenzene occurred during the very early stages of the reaction as shown by the lower amounts of xylene during the first few hours; and the gradual narrowing of pore by carbon deposition inhibited this reaction with time on stream to allow only the formation of benzene and xylene. Thus the continued observation of trimethylbenzene in the product stream long after its

formation has been inhibited was mainly due to its slow diffusion out of the zeolite pores because of its bulkier sizes.

6.5 Conclusion

Toluene disproportionation proved to be more difficult than ethylbenzene disproportionation due to the fact that, the higher number of carbon atoms on the alkyl substituent made it easier for the alkyl group to be cleave off from ethylbenzene as an alkene rather than as a radical like from toluene. Benzene studies earlier showed some conversions but in the presence of toluene in the system benzene (produced in the system) did not show any conversion evidence even at high temperatures on both catalysts, the same was the case during ethylbenzene disproportion though the later was performed at lower temperatures.

Toluene proved to be active in the system and might interfere strongly during transalkylation reactions, but then the presence of the methyl group on the ring facilitates also the addition of other alkyl groups on the ring; thus toluene may presumably be the alkyl-acceptor of choice depending on the type of reaction involved and reaction conditions.

7 *o*-XYLENE DISPROPORTIONATION

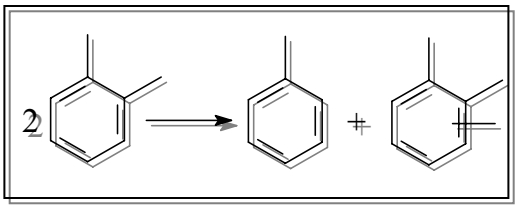

7.1 Introduction

Xylene isomerization reactions, for example, to produce higher amounts of *para*-xylene, are well studied reactions mainly due to the applications of the particular isomer in process chemistry. With the shape-selective zeolites the *para-/meta-/ortho*-xylene selectivity depends mainly on the diffusion path of xylene (size of the pores, crystallite size, etc).[74] The transalkylation step is faster than xylene disproportionation (primary products of disproportionation are potential transalkylation reactants) which explains why xylenes resulting from transalkylation can appear as primary products mimicking isomerization.[74] *para*-Xylene which is the precursor of major commercial fibers is mainly produced from the isomerisation of the C_8 aromatics.[75] Thus, the *meta*- and *ortho*-xylenes are isomerised into the thermodynamic equilibrium mixtures of xylenes if no selectivity induced mainly by the catalyst is experienced.

In transalkylation reactions between aromatics there will be xylene production/formation through both transalkylation to toluene especially if the accepted alkyl group is a methyl group and/or through toluene disproportionation. The increased number of alkyl groups on the benzene ring will surely increase the reactivity of the resulting xylenes, and thus there was a need to evaluate the reaction patterns followed by xylene on solid acid catalysts since its formation during transalkylation reactions involving mainly toluene (solvent and alkyl-acceptor) is inevitable.

7.2 Experimental

For analytical reasons, the flow rate of the carrier gas (nitrogen) was increased from 1 to 2 ml/min; this further decreased the hydrocarbon/nitrogen ratio from 1:27 to 1:54, further diluting the feed while keeping WHSV at 0.3 h^{-1}.

7.3 Results and Discussions

7.3.1 *o*-Xylene disproportionation on H-mordenite

This reaction proved to be very simple on mordenite with about 90 % of overall conversion (isomerisation + disproportionation) being achieved at temperatures as low as 200 °C (figure 7.1). The slow deactivation observed at 200 °C was mainly due to preferential adsorption (and polymerisation) of reactants and/or products; and this was inhibited by higher temperatures. And hence, molecular adsorption was favoured as the main deactivation route in this case because increasing the temperature to 300 °C resulted in an increase in life-time rather than deactivation. The reaction seemed to be very unstable at 300 °C (figure 7.2) and higher temperatures: it showed an increase in deactivation with increase in temperature, i.e. the rate of carbon deposition increased with increase in temperature. The suggestion here was that at temperatures below 300 °C deactivation was predominantly through molecular retention (adsorption, polymerization and trapping), and above 300 °C the mode of deactivation was by carbonaceous material deposition. This was somehow manifested when results at 300 °C could not be reproduced as shown in figure 7.2. Further suggestion was that 300 °C was the transition temperature where both modes of deactivation (molecular retention and carbonaceous material deposition) were highly competitive resulting in the observed instability.

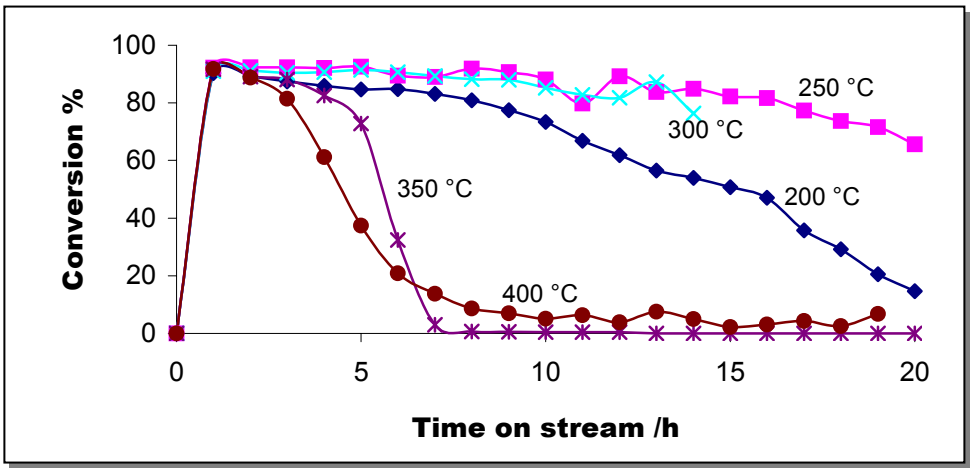

Figure 7.1: *o*-Xylene conversion (mol %) on H-mordenite

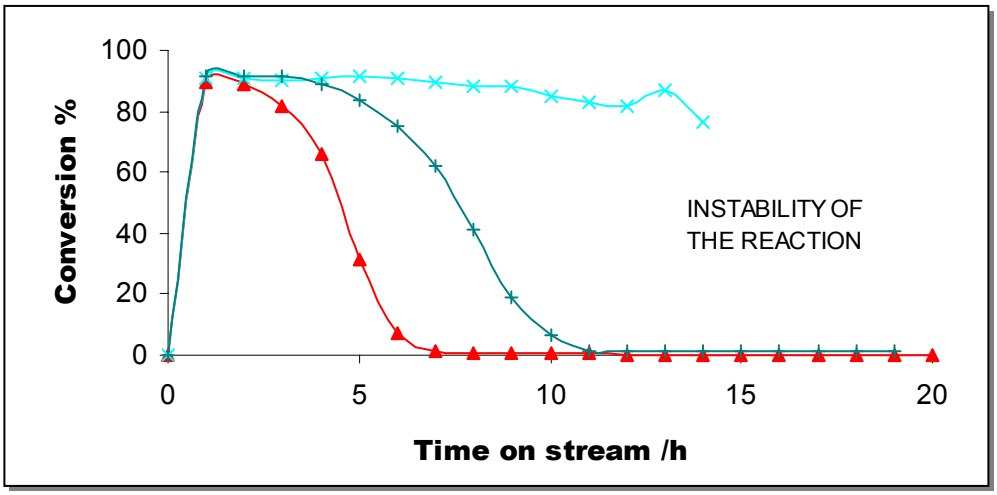

Figure 7.2: *o*-Xylene conversion (mol %) on H-mordenite at 300 °C

Disproportionation (without isomerization) patterns of the same reaction shown in figure 7.3 showed that disproportionation was actually the major reaction especially during the early stages of the reaction when compared to figure 7.1. What could be suggested from both figure 7.1 and 7.3 was that deactivation by molecular build-up (polymerization) through strong adsorption and molecular trapping in the zeolite channels did not directly target the active sites but restricted the formation of bulkier intermediates and prohibited alkyl-transfer reactions at 300 °C and lower temperatures; but deactivation through carbon formation which was dominant at

higher temperatures occurred directly on the active sites deactivating the catalyst and inhibiting both alkyl-transfer and alkyl-shift (isomerization) reactions. The conversion (isomerisation + disproportionation) and the disproportionation patterns were similar at 350 and 400 °C (figure 7.1 v/s 7.3). Colour changes of the catalyst after the reactions suggested that both modes of deactivation were occurring in the zeolites at any given temperature, with carbon deposition mainly dominating at high temperatures and molecular retention at lower temperatures.

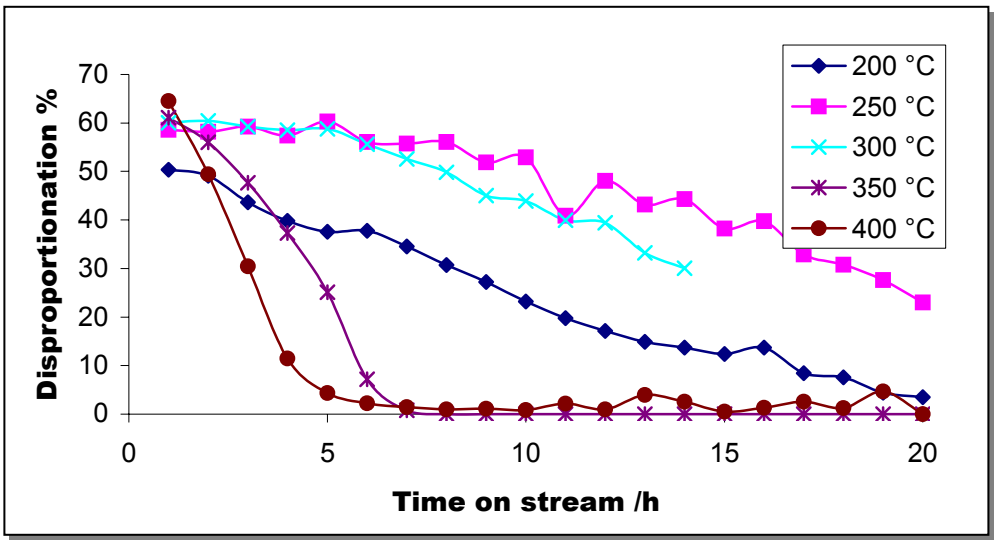

Figure 7.3: *o*-Xylene disproportionation (mol %) on H-mordenite

The major (primary) reactions were isomerization (ISOMER) of 1) *o*-xylene to 2) *p*-xylene and 3) *m*-xylene; and the disproportionation (DISPR) of *o*-xylene to 4) toluene, 5) 1,2,3-trimethylbenzene (mesitylene), 6) 1,2,4-trimethylbenzene and 7) 1,2,3-trimethylbenzene (scheme 7.1).

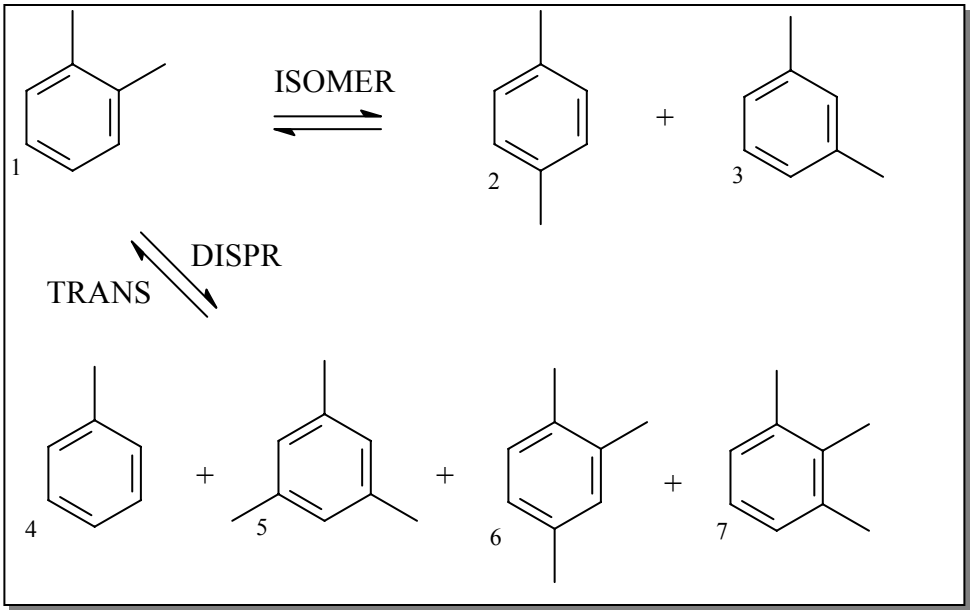

Scheme 7.1: Primary reactions of *o*-xylene in the zeolite pores

The product stream also contained secondary reaction products from alkyl-transfer reactions between toluene, xylene and the trimethylbenzenes (scheme 7.2), which further resulted in the production of *tetra*-methylbenzenes (durene; 1,2,3,5- and 1,2,3,4-tetramethylbenzenes) (1, scheme 7.2), the disproportionation of toluene to benzene and the xylenes (2, scheme 7.2), the transalkylation between benzene and *tri*-methylbenzene to form toluene and xylene (3, scheme 7.2), and also the *tri*-methylbenzene disproportionation to xylene and the *tetra*-methylbenzene (4, scheme 7.2).

The above just shows how complex the reaction was and in such reactions the selectivity towards the desired products can be difficult to achieve. In the production of the valuable *p*-xylene by toluene alkylation or xylene isomerization, small pore zeolites such as the familiar HZSM-5 are used. Because of the narrow pores of the ZSM-5 the bimolecular intermediate which might lead to the formation of undesired products is inhibited. Thus no transalkylation and disproportionation occurs but monomolecular isomerization (alkyl-shift) and the toluene alkylation reactions occur. The preferential isomerization to *p*-xylene occurs during the diffusion of the bulkier *o*- and *m*-xylene to the dimensionally smaller *p*-xylene through the zeolite pores.

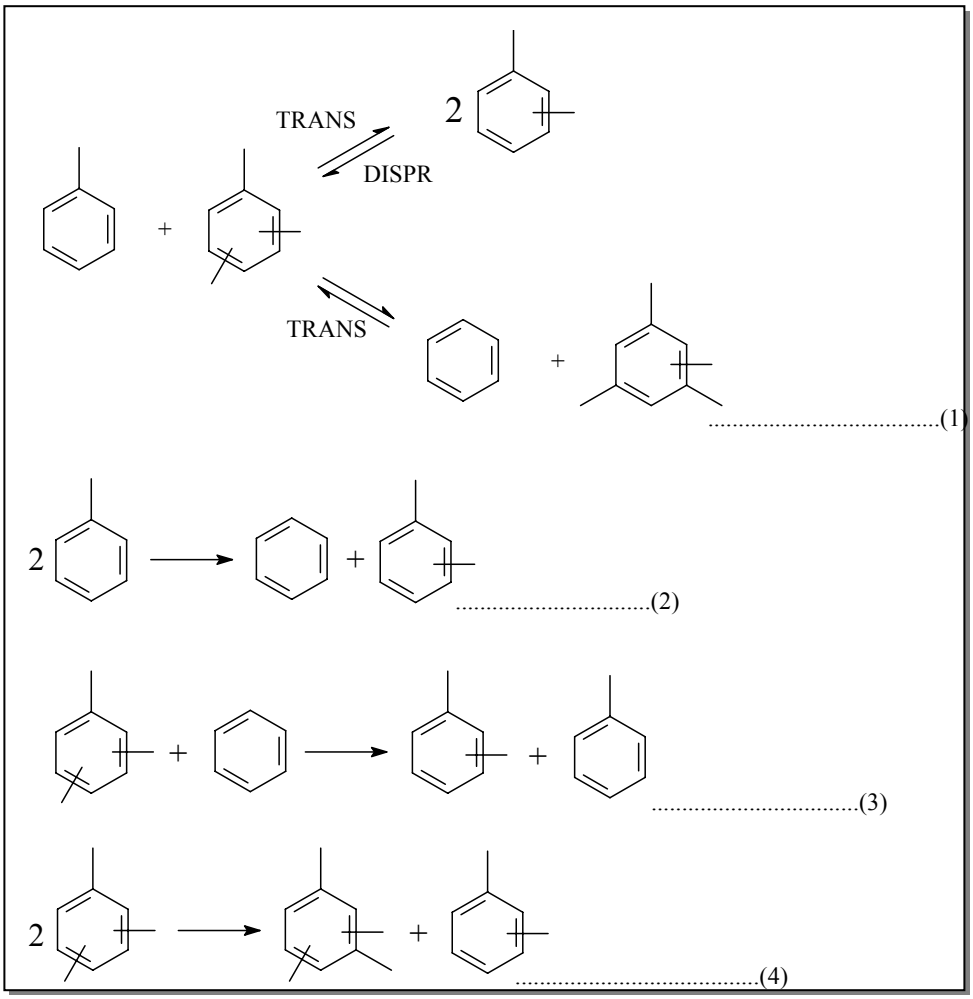

Scheme 7.2: Secondary reactions of *o*-xylene's primary products in the zeolite

An example of the product distribution from these reactions is shown in figure 7.4 for the 250 °C reaction, and it might look like major products were from isomerization (p- + m-xylene isomers), but as shown by the comparison of figure 7.1 and 7.3 the major reactions were alkyl-transfer (just above 60 %) reactions during the early hours. Unknowns and bulkier products are represented as 'others' (OTHERS).

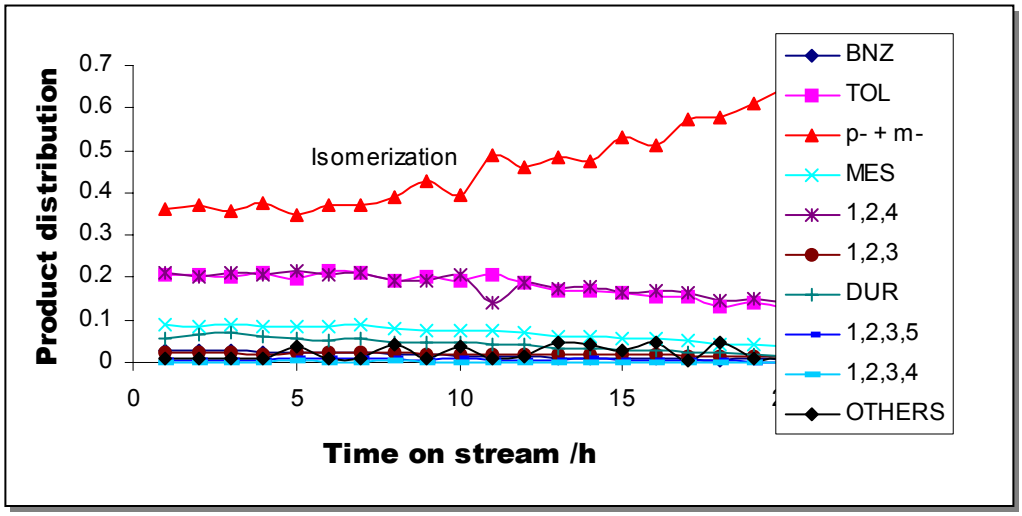

Figure 7.4: The distribution of products (mol %, fractional units) from the disproportionation of *o*-xylene on H-mordenite at 250 °C

The main feature of figure 7.4 is that of the isomerization trace which showed an increase in isomerization products with time on stream. The increase was accompanied by the decrease in alkyl-transfer reaction products. The suggestion that carbon deposition with time narrows the catalyst pores and cavities and as a result bimolecular intermediates which lead to alkyl-transfer reactions are minimized is greatly justified with time on stream. In other words, isomerization reactions are favoured as the reaction space is limited; that is why commercial xylene isomerization reactions to selectively produce *para*-xylene are carried out with partially deactivated zeolites.

Since the main focus of the study was on alkyl-transfer reactions, a more simplified product distribution was necessary as shown in figure 7.5 where the tri-methylbenzenes (TMB) comprised of mesitylene, 1,2,4- and 1,2,3-tri-methylbenzenes; and tetra-methylbenzenes (TetMB) consisted of durene, 1,2,3,5- and 1,2,3,4-tetra-methylbenzene.

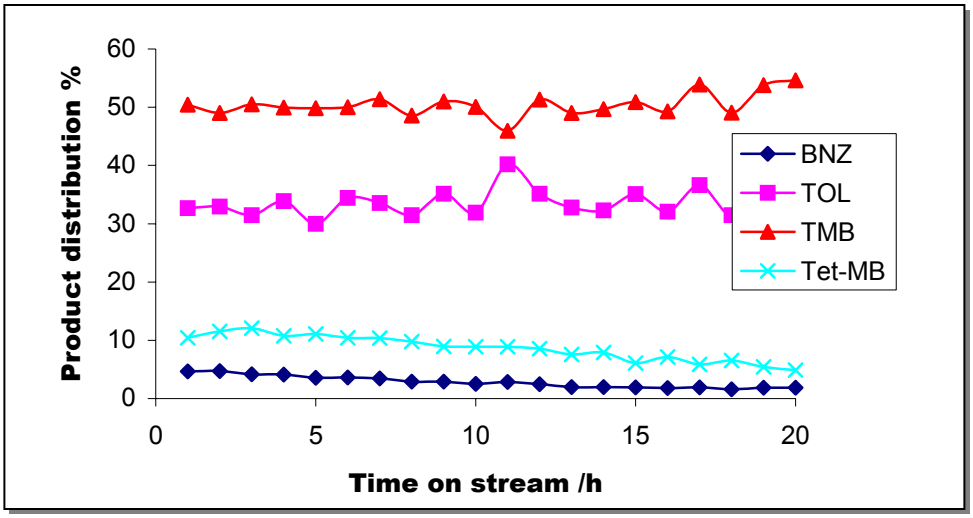

Figure 7.5: Product distribution (mol %) from alkyl-transfer reactions of *o*-xylene on H-mordenite at 250 °C

The 1:1 ratio between toluene (TOL) and the trimethylbenzenes (TMB) (products of primary disproportionation reaction) was not observed. As discussed before this was due to secondary reactions in the system.

Though the disproportionation intermediate (transition state) was bulky (figure 7.6) what was known for sure was that it was the only intermediate which had led to alkyl-transfer reactions; and its formation had dominated during the early stages of the reaction. It is the intermediate that led to the production of transalkylation reagents in the zeolites, and without it only isomerization would have existed for this particular system. With steric restrictions in the zeolite, intermediates involving bulky molecules like *tetra*methylbenzene and higher alkylated benzenes (i.e. transalkylation) would be less favoured. The smaller the transition state molecule, the more favourable the reaction. Since products from a bimolecular system consists of bulkier and smaller molecules than the starting material, bulky molecules would not participate much in further reactions but smaller ones would and this always leads to their consumption. The deficit in the smaller molecules (toluene and benzene in figure 7.5) somehow supported the suggestion that carbonaceous material deposition (pore narrowing) led to their consumption.

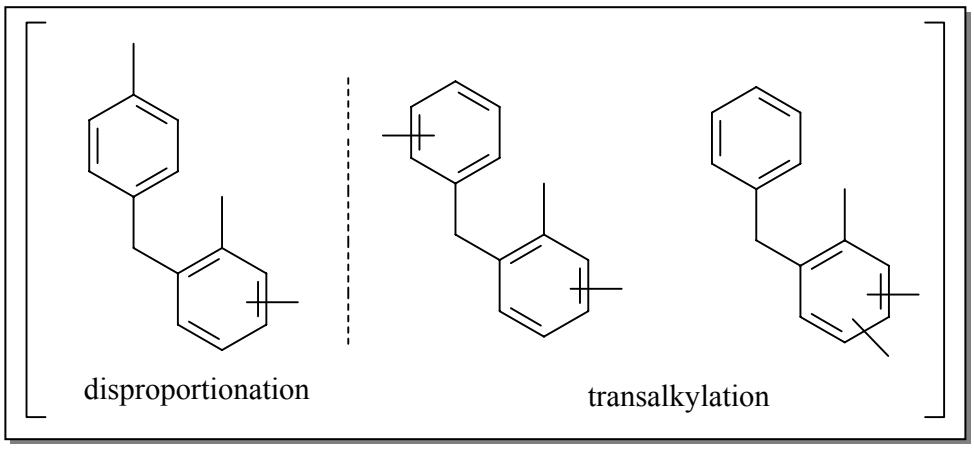

Figure 7.6: Alkyl-transfer intermediates during *o*-xylene disproportionation on zeolites

It is apparent from scheme 7.1 and 7.2 that one cannot achieve equilibrium molar distributions in the product stream; because reactants did not follow one type of reaction but rather several routes. In addition, transition state selectivity also resulted in a very complicated system. This presented some problems for analysis and interpretations. For simplicity, it was further assumed that *p*- and *m*-xylenes were only formed by isomerization of the *o*-xylene; and toluene and trimethylbenzenes were disproportionation products; finally, the benzene and the *tetra*methylbenzenes were products from transalkylation, while the "others" referred to poly-alkylaromatics and bulky molecules. The results of this assumption are depicted in figure 7.7 as catalytic routes against time on stream for the reaction at 250 °C.

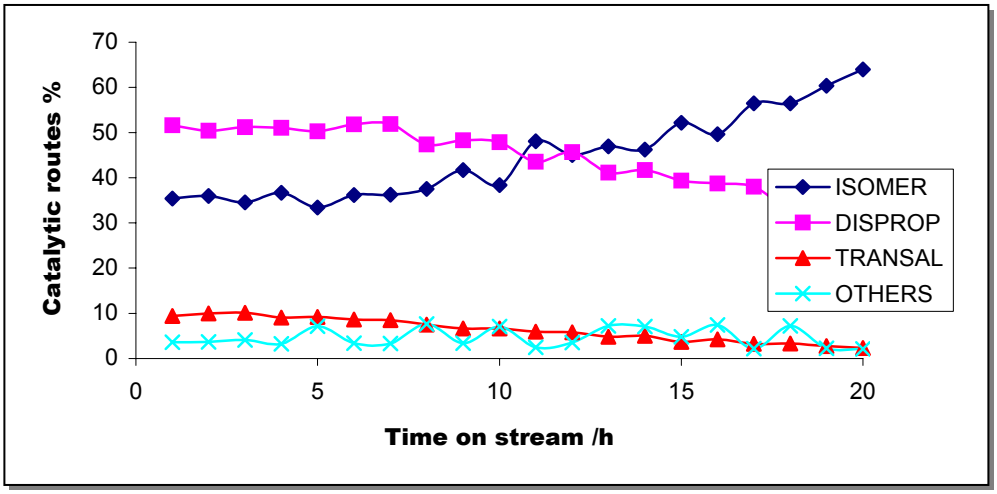

Figure 7.7: Catalytic routes (mol %, activities) followed by *o*-xylene on H-mordenite at 250 °C

This figure further emphasized that the disproportionation and isomerization reactions (primary reactions) were the major reactions while transalkylation was the minor secondary reaction. The effects of carbon deposition (deactivation) with time on stream are also shown in figure 7.7 which indicated the crossing over of the disproportionation/isomerization traces caused by narrowing of pores which then favoured the uni-molecular isomerization rather than the bulky bimolecular disproportionation pathways. The point at which the two lines crossed was expectedly shortened with increase in temperature (300 °C), as the rate of deactivation (carbonaceous material deposition) increased accordingly (figure 7.8).

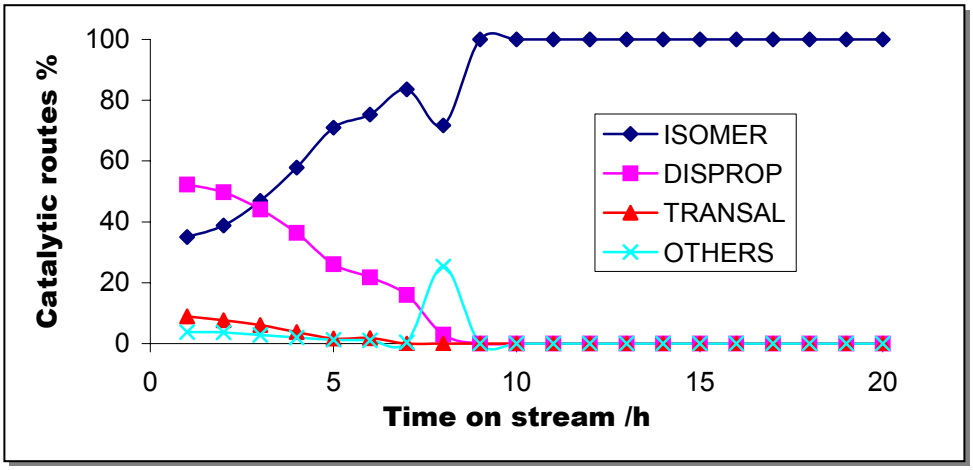

Figure 7.8: Catalytic routes (mol %, activities) followed by *o*-xylene conversion on H-mordenite at 300 °C

7.3.2 *o*-Xylene disproportionation on HLZY-82

Like toluene disproportionation (figure 6.4) *o*-xylene showed an increase in conversion (isomerization + disproportionation) and catalyst lifetime with the increase in temperature on this particular catalyst (Figure 7.9); with the exception of the reaction at 400 °C which showed some degree of deactivation with time on stream. The deactivation was mainly due to carbonaceous material deposition at these high temperatures. HLZY-82 showed a reasonable activity in the temperature range 300-350 °C. The fact that the reaction was more stable at high temperatures (300-350 °C) as compared to the situation found with mordenite (stable between 200 and 250 °C, figure 7.1), showed not only the difference in catalyst pore channels but also the strength of the acid sites favouring the mordenite catalyst since the stronger the sites the faster the deactivation rate.

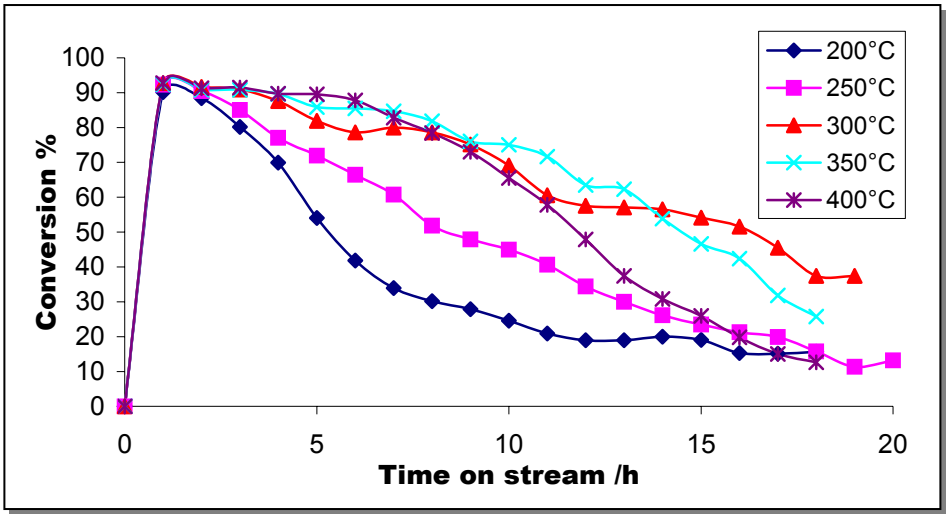

Figure 7.9: *o*-Xylene conversion (mol %) on HLZY-82

Figure 7.9 shows that the conversion (disproportionation + isomerization) of *o*-xylene, in contrast to the situation found with mordenite, started at ca 90 % for all reaction temperatures studied. This then suggested that if it were not for catalyst deactivation through either mode, all traces would have followed exactly the same pattern; and this would mean that xylene conversion have little or no dependency on the reaction temperature. The disproportionation (without isomerization) patterns are shown in figure 7.10; and looking at the very first hour of the reactions there was almost a 10 % (between the 200 and 400 °C reactions) range depending on the reaction temperature. The very first hour in figure 7.9 did not show such differences meaning that the rate of reactions was somehow similar irrespective of the routes taken; but what figure 7.10 showed is that the reaction routes were influenced by the reaction temperature. The important thing from these two figures is that it is shown that alkyl-transfer (disproportionation) was favoured at high temperatures, i.e. there was an equilibrium shift in the reaction routes. For the 200 °C reaction 58% of the conversion was due to alkyl-transfer reactions and 31% was isomerization; increase in temperature caused a shift and at 400 °C 68% was alkyl-transfer and about 11% was isomerization (comparing figures 7.9 and 7.10).

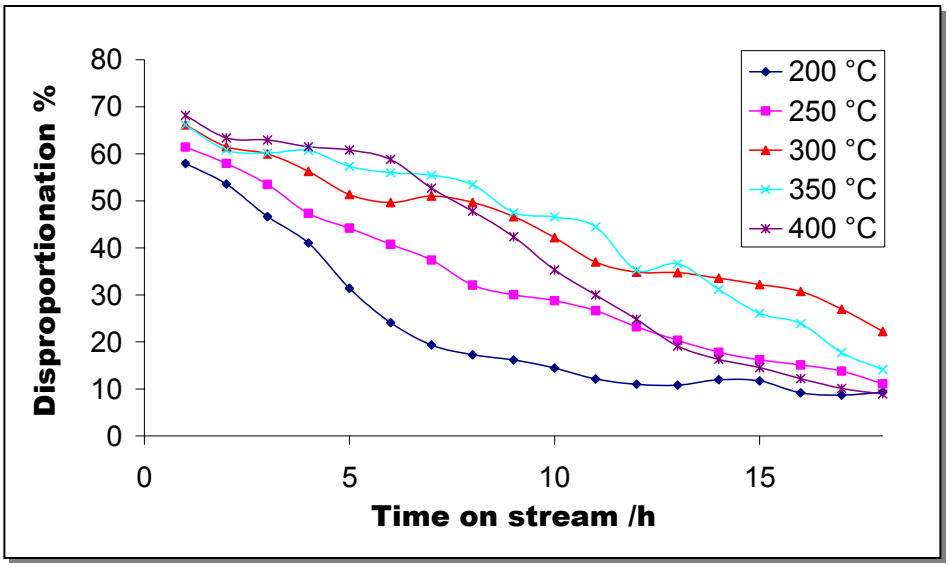

Figure 7.10: *o*-Xylene disproportionation (mol %) on HLZY-82

The product distribution on figure 7.11 showed that the toluene and benzene concentrations were initially considerable in the product stream but decreased with time on stream. These initial concentrations were most probably due to their rapid diffusion out of the zeolite pores due to their smaller molecular sizes as was the case during ethylbenzene disproportionation (figure 4.4).

The product distribution and the 'catalytic routes' at 300 °C are shown in figures 7.11 and 7.12 respectively. In contrast to the reactions on H-mordenite, figure 7.12 showed no crossing over of the disproportionation/isomerization lines. This was mainly due to the three-dimensional pore structure of the zeolite-Y where carbon deposition or molecular adsorption did not lead to the blockage of the entire pore channel, as was the case with mordenite and the results of which promoted deactivation. Due to larger cavities/pores in the zeolite-Y, deactivation had a larger effect on the active sites rather than on the space available for the formation of the transition state, and carbon deposition was less likely to lead to transition state selectivity as observed on mordenite. Figure 7.12 also showed that the disproportionation reaction was the major reaction route throughout the reaction at 300 °C.

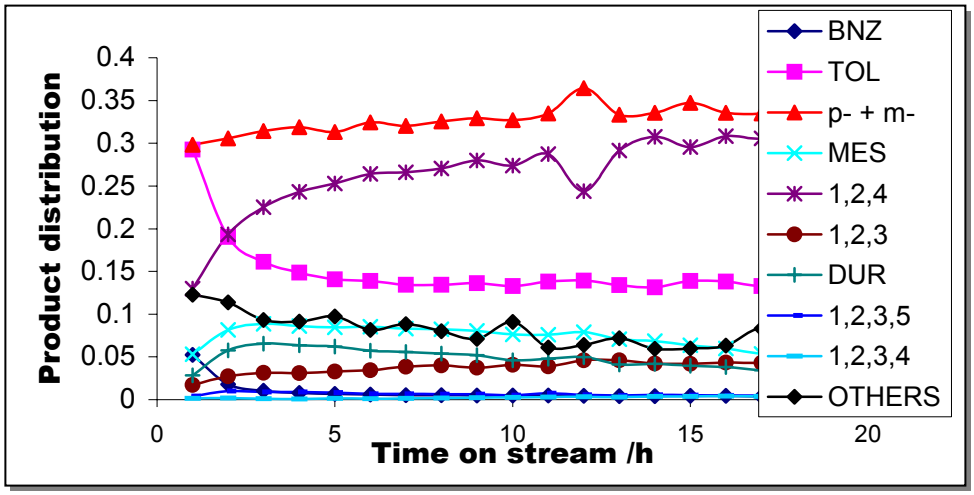

Figure 7.11: Product distribution (mol %, fractional units) of *o*-xylene disproportionation on HLZY-82 at 300 °C

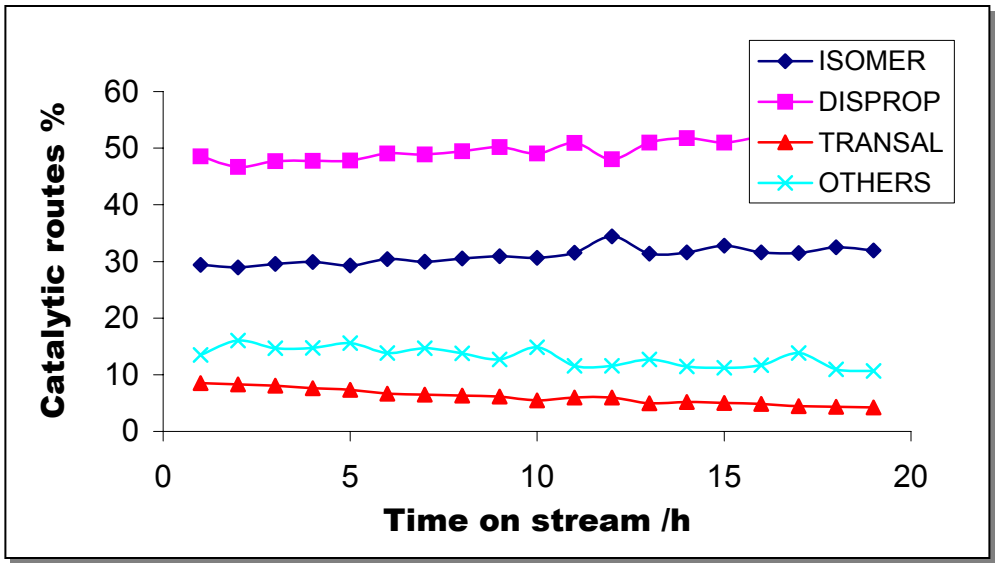

Figure 7.12: Catalytic routes followed by *o*-xylene conversion (mol %) on HLZY82 at 300 °C

Figure 7.13 showed an unusual catalytic behaviour at 400 °C where the isomerization reaction route initially showed an increased and then decreased with time on stream, and the disproportionation reaction initially decreased and then increased. Figure 7.9 showed that there was an increase in conversion and in catalyst lifetime with increase in temperature, but at high temperatures (400 °C) the catalyst showed some degree of deactivation. Due to the observed deactivation, the

isomerization/disproportionation lines were expected to cross as was seen for the reactions on H-mordenite. The observed crossing in figure 7.13 was also attributed to carbonaceous material deposition which narrowed the pores and also targeted active sites. The transition state selectivity induced by material build-up in the zeolite was not evident from this graph but the fact that deactivation was due to poisoning of active sites was shown by the decrease in isomerization products, and the observed increase in disproportionation products was mainly attributed to the slow molecular diffusion out of the zeolite pores by the bulky molecules and not catalytic routes. In other words, if deactivation was dominated by carbon deposition with the end result of pore and cavity narrowing, isomerization (monomolecular) would have significantly dominated the product stream; but in this case active site were fouled hence there were no reactions even though there was enough room for reactions to take place.

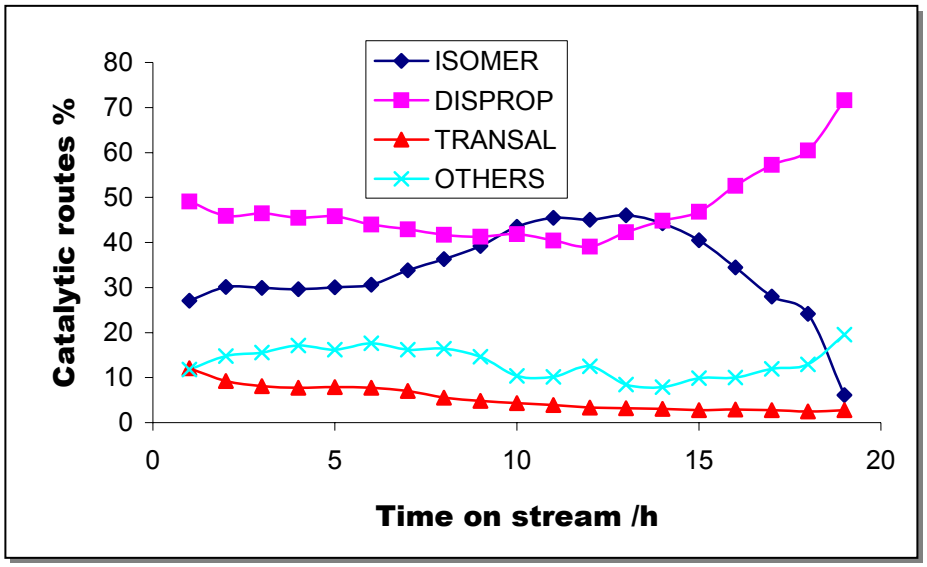

Figure 7.13: Catalytic routes (mol %) followed by *o*-xylene conversion on HLZY-82 at 400 °C

7.4 Conclusion

Xylene has shown much higher catalytic conversions than toluene on zeolites and greater potential to compete for active sites in transalkylation systems, thus it should not be used in transalkylation reactions as an alkyl acceptor, and this conclusion then crowns toluene and benzene as preferred candidate. The xylene disproportionation system has also shown slow deactivation rates suggesting that the more difficult it is to convert a molecule/s, the higher the rate of catalyst deactivation. This was based on the fact that stronger sites would be required for the conversion of stubborn molecules and those are normally the first ones to be deactivated; i.e. the simpler the conversion of a molecule/s the longer is the catalyst lifetime. As also shown by the toluene disproportionation reaction the three-dimensional zeolite proved to be a more favourable catalyst than the uni-dimensional one due to its resistance to deactivation, more room for the reactions and more active sites (higher density).

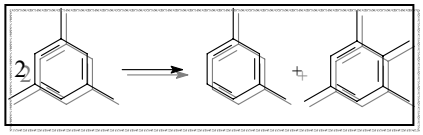

8 MESITYLENE DISPROPORTIONATION

8.1 Introduction

Mesitylene disproportionation is not a well researched topic and if work has been done it is almost always patented. Better researched is the transalkylation reaction between toluene and trimethylbenzenes to form the valuable xylenes. Present studies focused on mesitylene (1,3,5-trimethylbenzene) solely because trimethylbenzenes are some of the disproportionation products of toluene (which will be used as an alkyl acceptor). The additional methyl groups on the benzene ring was expected to improve the reactivity of the mesitylene molecule as was the case with xylene but the anticipation was that it would suffer steric constraints which might make it difficult for it to access active sites.

8.2 Experimental

Same conditions as the xylene disproportionation reactions were used for these reactions.

8.3 Results and discussions

8.3.1 Mesitylene disproportionation on H-mordenite

This reaction on H-mordenite showed a different reaction pattern from that of toluene and *o*-xylene disproportionation. During toluene disproportionation there was a

significant increase in conversion with increase in temperature (figure 6.1) accompanied by a decrease in the catalyst lifetime with time on stream, and the highest conversion achieved was about 50 %. The introduction of the second methyl group in the *o*-xylene disproportionation reactions seemed to facilitate the conversions (figure 7.1). But the increased conversion was also attributed to the occurrence of isomerization rather than alkyl transfer reactions alone. The initial conversions (during the first hour) for mesitylene disproportionation reaction (figure 8.1) were almost identical to those of *o*-xylene disproportionation in the temperature range of 200-400 °C with reasonable stability at 200 °C and significant deactivation rates at higher temperatures compared to xylene disproportionations.

There was a change in the reaction pattern with the introduction of a third methyl group on the benzene ring. Mesitylene, like xylene, showed some stability at 200 °C but there was a strong/rapid deactivation on going from 200 to 250 °C. The deactivation appeared to be less rapid at 300 and 350 °C. Higher temperatures (400 °C) saw a strong deactivation. This pattern was never observed on toluene or xylene disproportionation reactions.

The behaviour shown in figure 8.1 supports the suggestion that there might have been different modes of deactivation which were temperature dependent; the possible explanation for this kind of behaviour was that some transition state was initiated at 250°C but it did not lead to the formation of products. Thus deactivation at this stage was much attributed to molecular adsorption (trapped transition state) which in turn blocked the access to the active sites, and negatively affected desorption of the products and molecular diffusion through the catalyst and access to active sites.

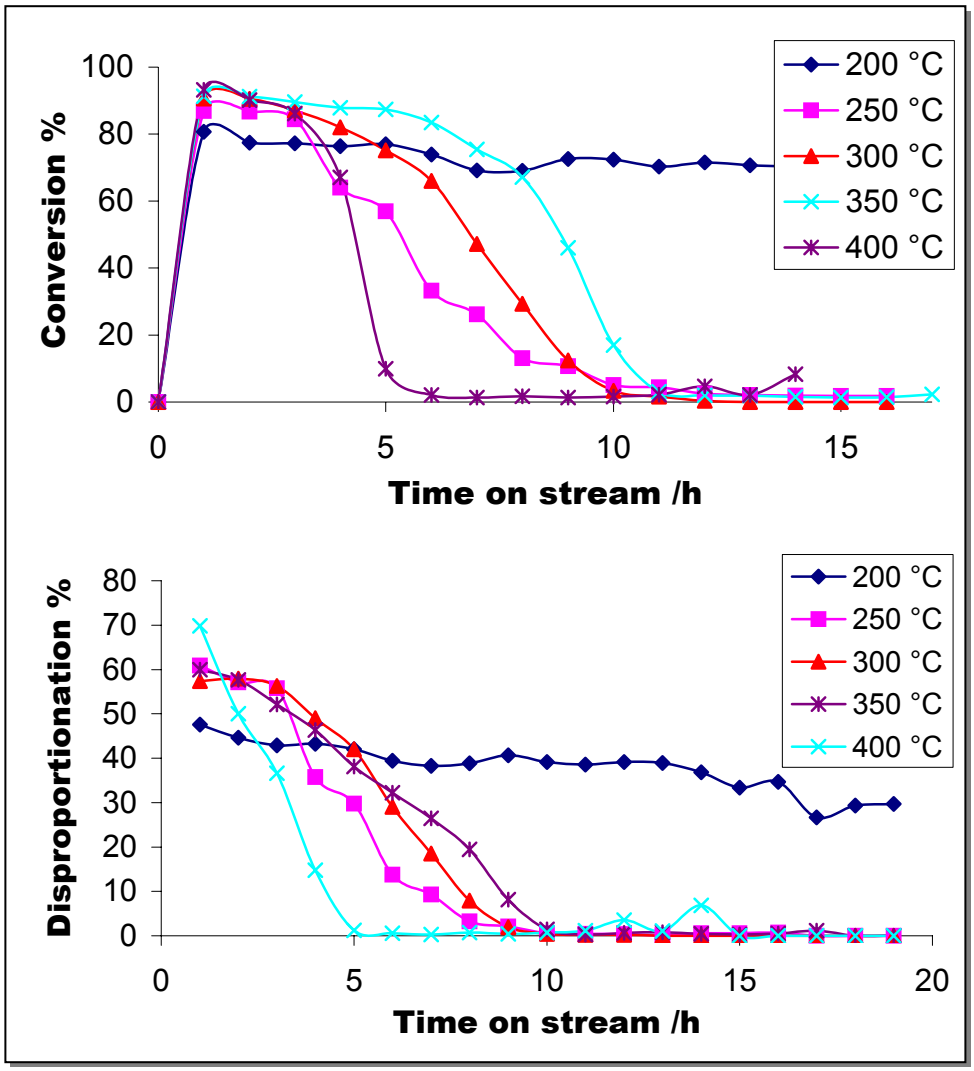

Figure 8.1: Mesitylene disproportionation (mol %) on H-mordenite

Higher temperatures promoted the formation of products form this transition state intermediate and this increased with temperature up to 350 °C. At high temperatures (400 °C) the observed strong deactivation was mainly attributed to carbon deposition (active site poisoning). The above suggested that the formation of a certain intermediate complex was dependent on the reaction temperature, and so was the alkyl transfer process (reaction routes). In trying to reproduce the results, a reaction at 250 °C was carried out under the same conditions as before, still rapid deactivation behaviour was observed (figure 8.2).

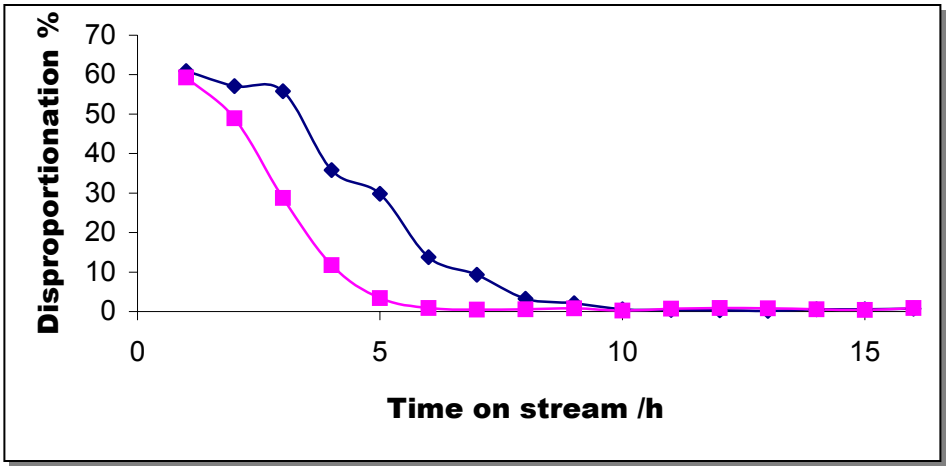

Figure 8.2: Mesitylene disproportionation (mol %) on H-mordenite; reproducibility at 250 °C. ◊ run 1, □ run 2

The reactions in the temperature range of 250 - 400 °C showed a very chaotic catalytic behaviour with the disproportionation reaction decreasing indefinitely while the isomerization reaction increased with time on stream accompanied by the increase in the 'others' (figure 8.3). Due to the one-dimensional structure of the catalyst and the bulkiness of the reactant molecule, the low value of the 'time on stream' at which the disproportionation (DISPROP) and isomerization (ISOMER) lines crossed was expected; but the production (desorption) of the 'others' (OTHERS) which was believed to involve even bulkier products (and stable transition states) was not expected. This appearance of bulky molecules at later stages of the reaction was probably due to the growth of carbonaceous materials which ultimately pushed and squeezed out trapped molecules out of the zeolite pores and cavities; or it could be just slow diffusions and these molecules were probably polyalkylated benzenes or stable bimolecular intermediate molecules such as biphenyl methanes.

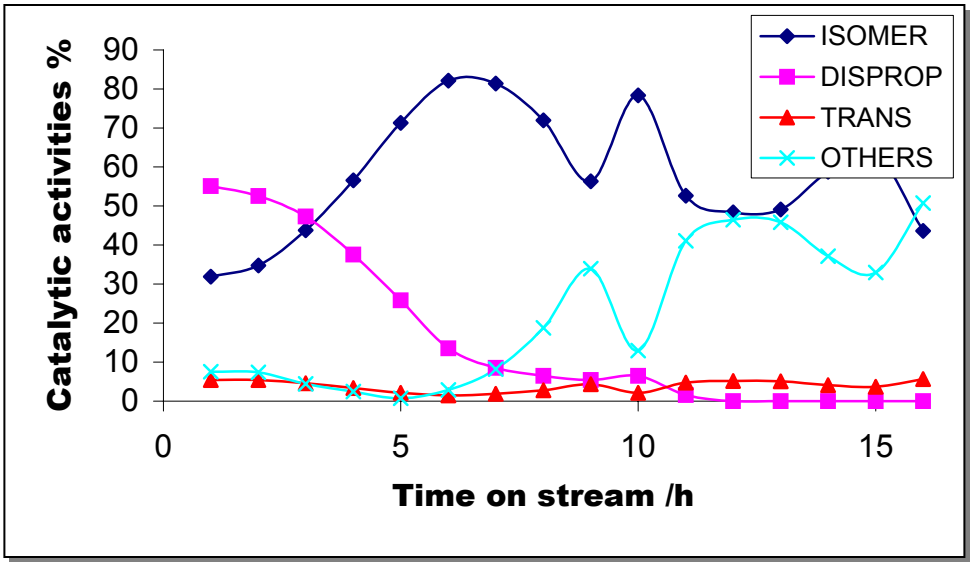

Figure 8.3: Catalytic routes (mol %, activities) followed by mesitylene disproportionation on H-mordenite at 250 °C

By following the disproportionation trace (see figure 8.3) it was clear that alkyl-transfer reactions lasted for almost 10 hours, and the trace for the 'others' became significant only after 7 hours. Considering the fact that the catalyst that was used possessed a one-dimensional pore structure and that carbonaceous material deposition and possibly molecular build-up would have a considerable effect on deactivation by narrowing the pores and cavities; it is apparent that the bulky 'others' should have formed during the very early stages of the reaction. Their late appearance was surely due to slow diffusion (or forced out) rather than their formation at late stages. Thus the suggestion that growth of carbonaceous material pushes retained molecules out of the catalyst seems plausible but needed to be confirmed.

A comparison of figure 7.7 and 8.3 showed that with the *o*-xylene disproportionation reaction the isomerization/disproportionation lines crossed after 10 hours at 250 °C and the 'others' were not as significant; with the mesitylene disproportionation reaction the traces crossed after 3 hours. It was then apparent that not only smaller molecules are responsible for rapid deactivation as suggested before, but even bulkier molecules showed similar characteristics in a sense that little of carbonaceous material deposition is necessary to inhibit the reactions because of the bulkiness of

the transition state molecule as compared to smaller molecules like toluene or xylene. Therefore, it could be safely concluded that the catalytic lifetime of the zeolite depends also on the molecular sizes of the reactants and their types.

If somehow the rate and amount of carbonaceous material depositions could be controlled in such a way that everything is the same in terms of the deactivation rate and the extent of pore narrowing, then obviously mesitylene would severely suffer molecular size exclusion compared to xylene and this is consistent with the faster deactivation observed in the current study.

The decrease in the disproportionation products with increasing time on stream implied that there would be selectivity effects induced by the narrowing of pores by carbonaceous material, and this would obviously allow for smaller monomolecular isomerization. The late appearance of the 'others' does not mean they formed only after 6 hours of time on stream, but showed the effect of carbon growth on the contents of the intrazeolitic pore aperture. Thus the observed chaotic behaviour after six hours was caused by an irregular growth of carbonaceous material. A much simpler behaviour was shown by the reaction at 200 °C where the disproportionation reaction was the major reaction (figure 8.4), and the crossing over point occurring after 15 hours on stream showing that the effect of deactivation was not that significant. In some way the temperature seemed to affect the rate at which molecular build-up (trapped molecules), carbonaceous material deposition and the type of carbon that forms occurred. Further more, these modes of deactivation seemed also to be competitive at certain temperatures while at other temperatures there was that tendency for one deactivation route (mode) to dominate.

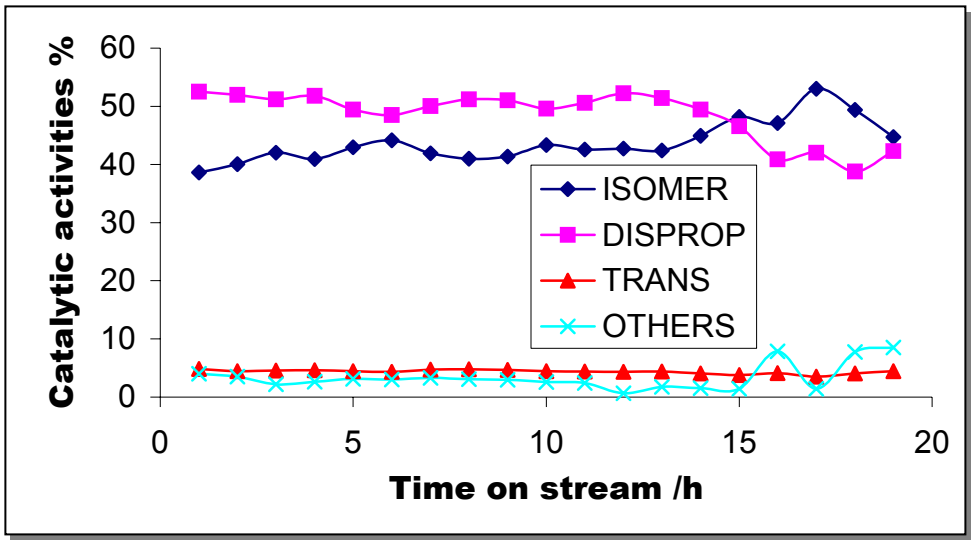

Figure 8.4: Catalytic routes (mol %, activities) followed by mesitylene disproportionation on H-mordenite at 200 °C

NB: The amount of products formed (conversion) decreased with time on stream and with the rate of deactivation. Thus the observed increase in the 'others' products were of very little amounts in the product stream at later stages of the reactions and this applies to all alkyl-transfer reactions studied. This is illustrated in figure 8.5 below.

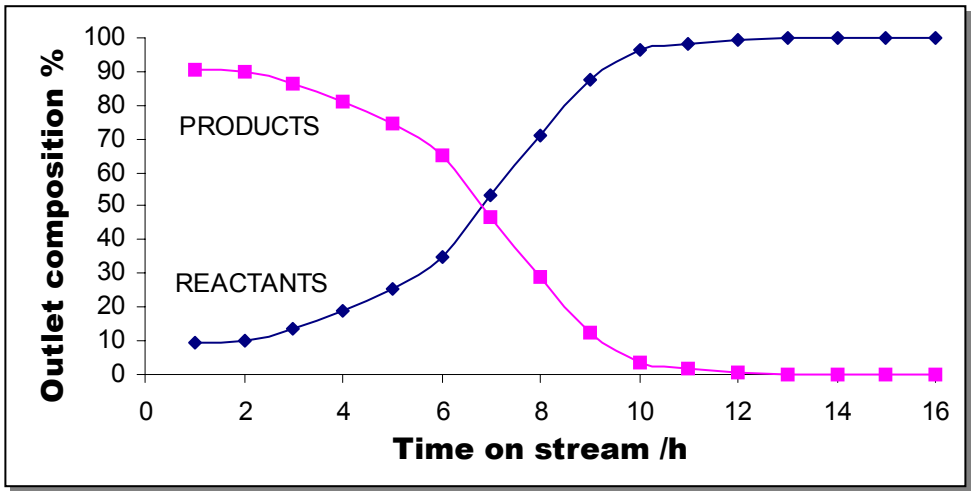

Figure 8.5: Outlet stream (mol %) of the mesitylene disproportionation reaction on H-mordenite at 300 °C

The product stream contained mostly the 1,2,4-trimethylbenzene (1,2,4) and durene (DUR), and no benzene or toluene was observed during the reaction at 200 °C (figure 8.6). The figures also showed the presence of heavier alkylaromatics referred to as others (OTHERS).

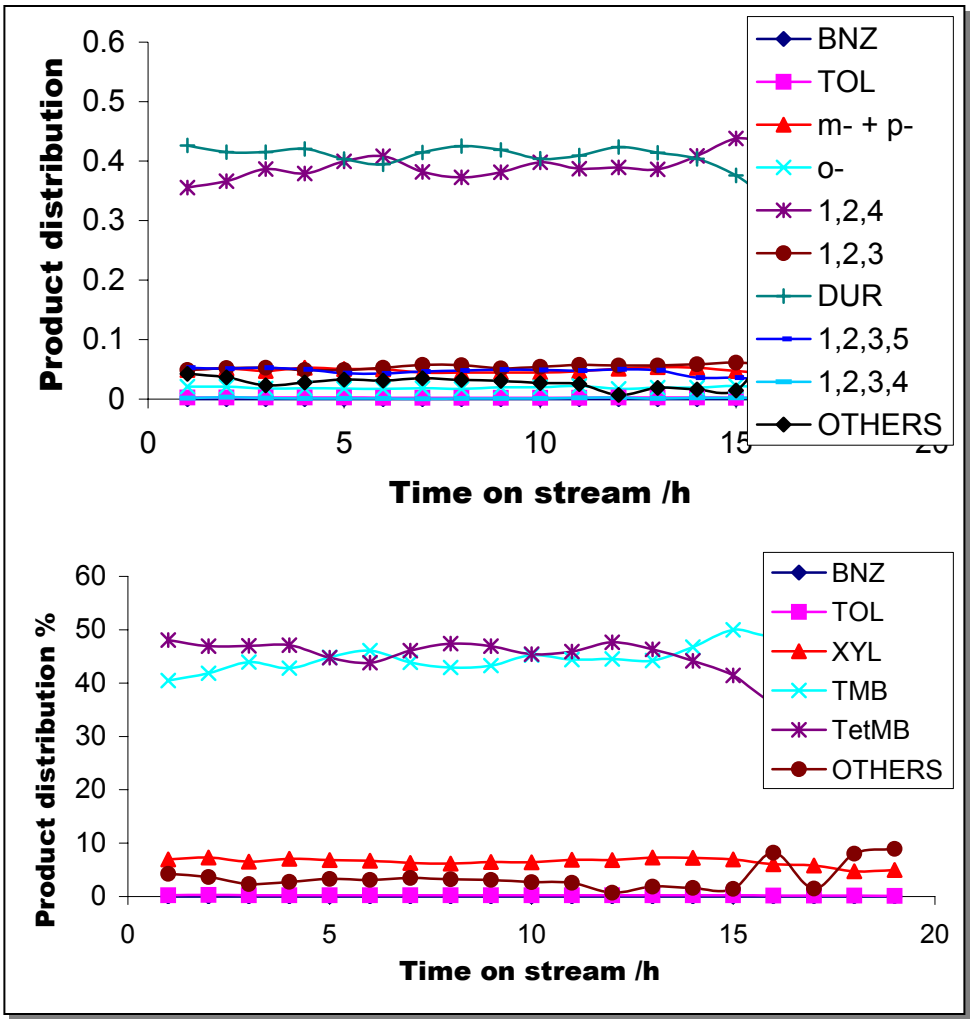

Figure 8.6: Mesitylene disproportionation (mol %) on H-mordenite at 200 °C; Product distribution (fractional units); (TMB = isomerization products, TetMB = *tetra*methylbenzenes)

Interestingly, the bulkier products seemed to be diffusing out in larger quantities than the less bulky ones. This was due to secondary and tertiary reactions undergone by smaller molecules, and preferential adsorption due to their smaller molecular

dimensions and most probably their participation in carbonaceous material deposition.

Scheme 8.1 depicts the main reactions, i.e. alkyl-transfer and the monomolecular isomerization. The disproportionation scheme 8.2 and 8.3 suggested that bulky tetramethylbenzenes most probably did not disproportionate or transalkylate further due to the bulkier transition state (its formation is sterically hindered), and the other product (xylenes) disproportionated further to reform the trimethylbenzenes and toluene. Since toluene was not that significant in the product stream, it should have disproportionated to reform the xylenes and benzene, and again it appeared that smaller molecules preferentially took part in the formation of carbonaceous materials.

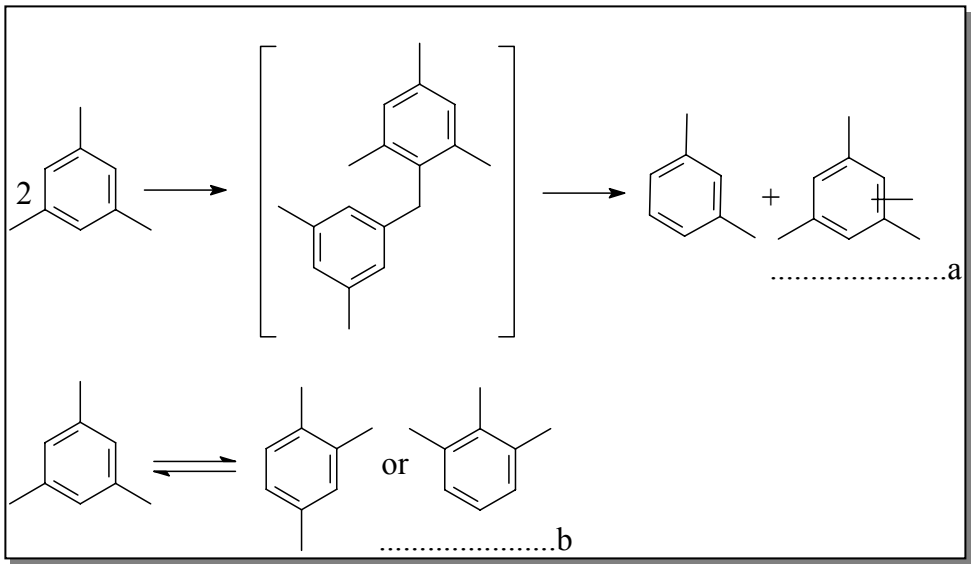

Scheme 8.1: Primary reaction of mesitylene disproportionation; a = disproportionation, b = isomerization

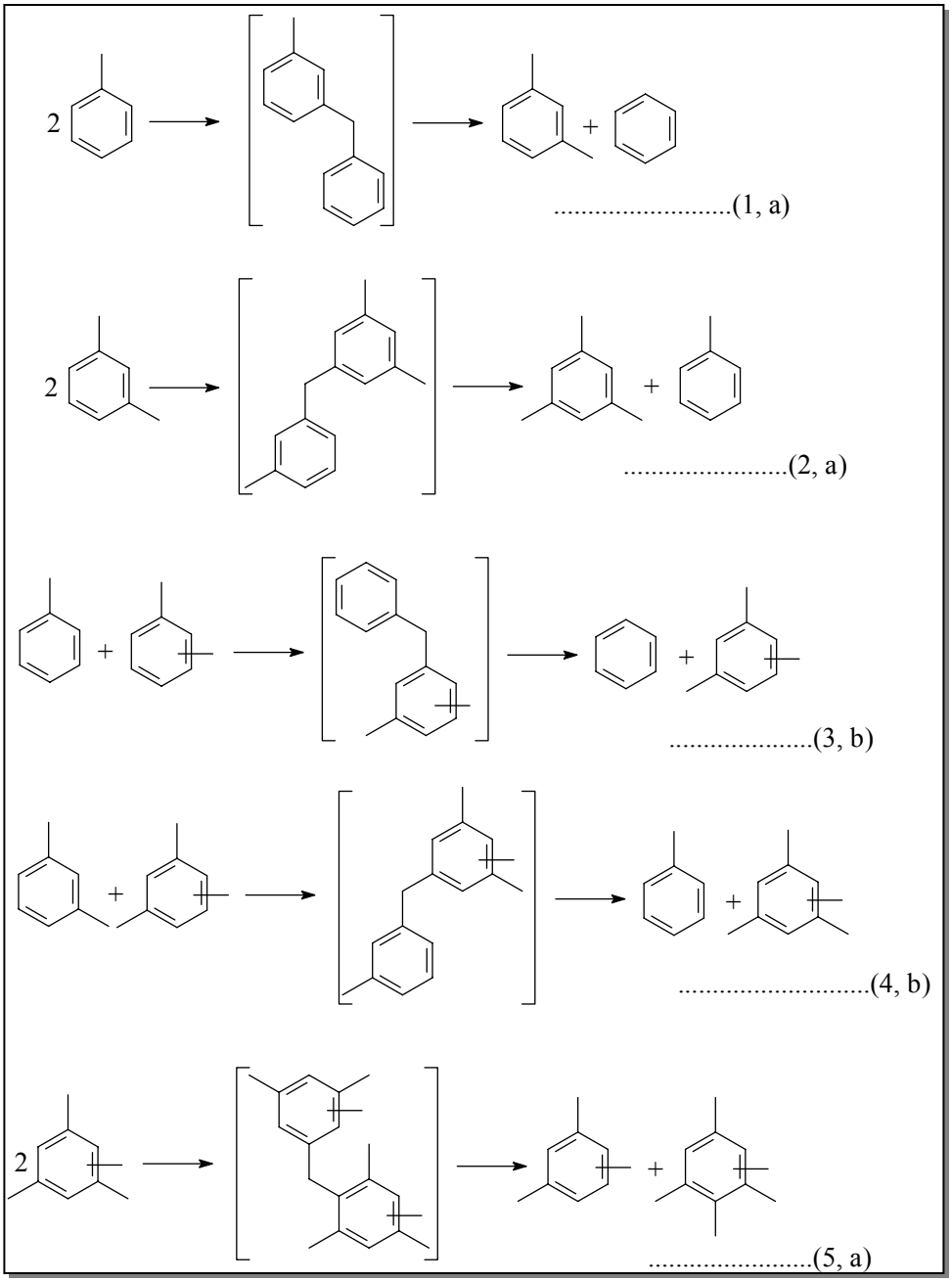

Scheme 8.2: Secondary and tertiary reactions during mesitylene disproportionation; a = disproportionation, b = transalkylation

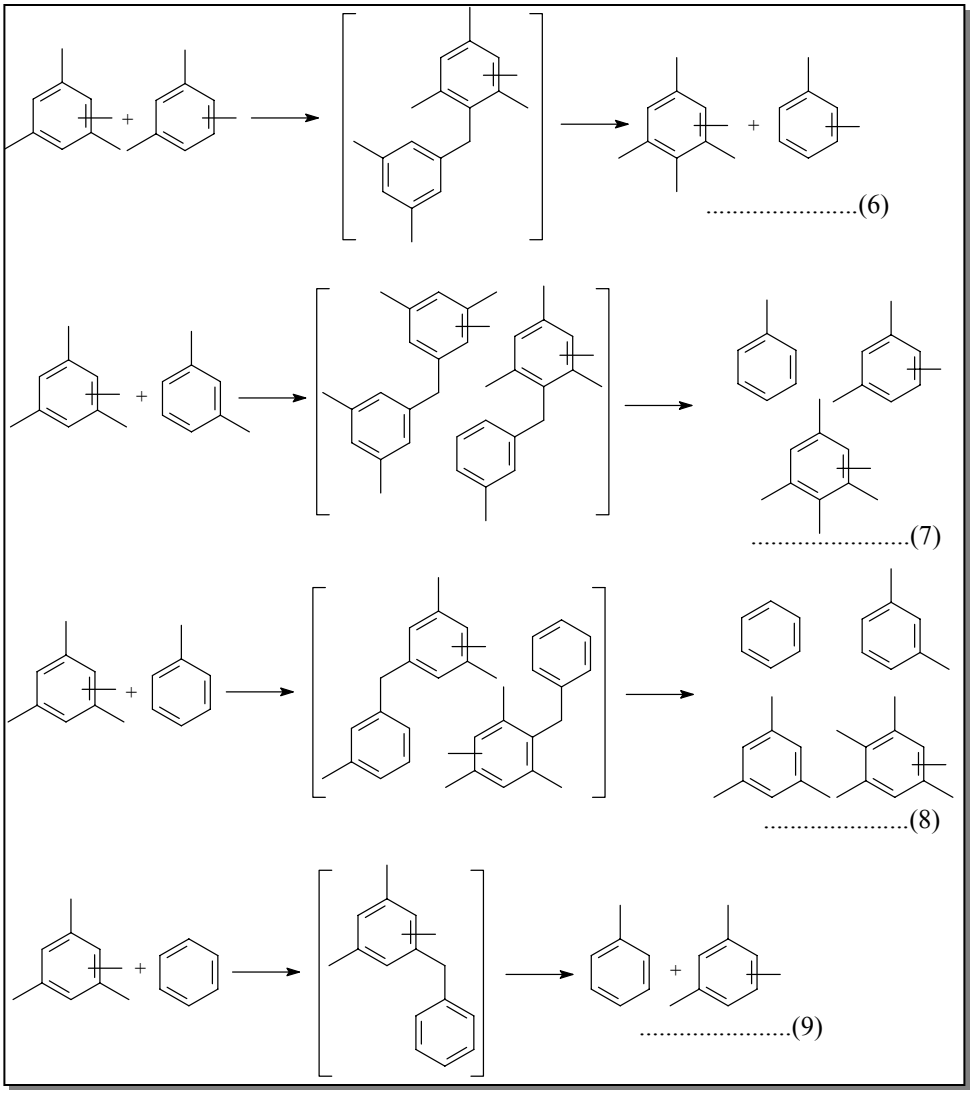

Scheme 8.3: Transalkylation reactions involving tetramethylbenzenes during mesitylene disproportionation

A careful inspection of the transition states involved in these reactions and the product distribution in figure 8.6 suggested that there was a strong possibility that reactions 5 and 6 were not favoured in the catalyst due to the bulky transition state required. In principle, the mesitylene disproportionation reaction should produce equal amounts of molecules larger and smaller than itself; figure 8.7 shows the differences in molecular size and the amounts observed in the product stream.

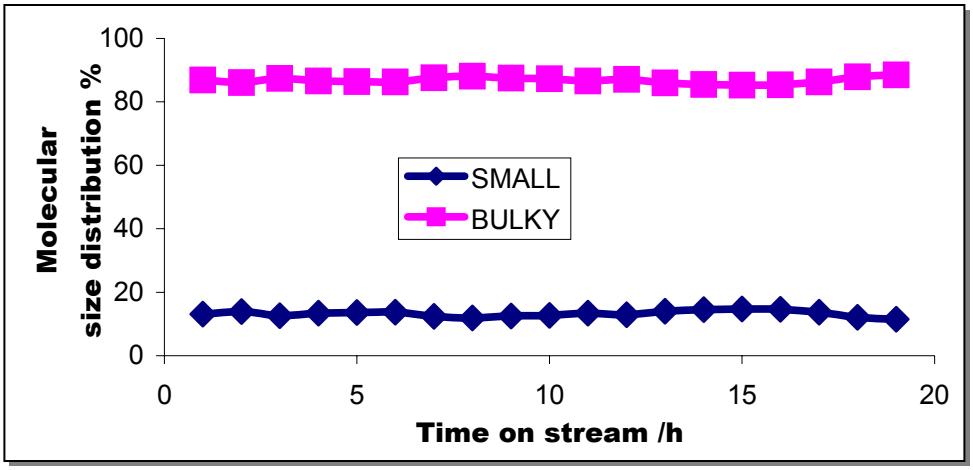

Figure 8.7: Mesitylene disproportionation (mol %) reaction on H-mordenite; Molecular size distribution in the product stream

Small = molecules smaller than the trimethylbenzene molecule

Bulky = molecules larger than the trimethylbenzene molecule

Considering the fact that the diffusion of the smaller molecules was not that sterically affected in the zeolite as compared to bulky molecules, it should be expected that the opposite of what is shown in figure 8.7 would be the outcome. Reactions like 1 (scheme 8.2) occurred in the catalyst but they did not have any effect on the amount of smaller or bulky molecules formed. Reactions 2 and 3 would implicitly consume smaller molecules but this should be minimal. Thus formation of coke was probably the major consumer of smaller molecules.

8.3.2 Mesitylene disproportionation on HLZY-82

Very interesting results were observed on the zeolite-Y (figure 8.8) which showed some remarkable stability and almost similar conversion behaviour at the temperature

range of 200-400 °C, and some similarity to the o-xylene disproportionation reaction (figure 7.9). Though not that apparent, reaction traces in figure 8.8 showed that temperatures 250 and 350 °C were less efficient compared to 200 and 300 °C respectively.

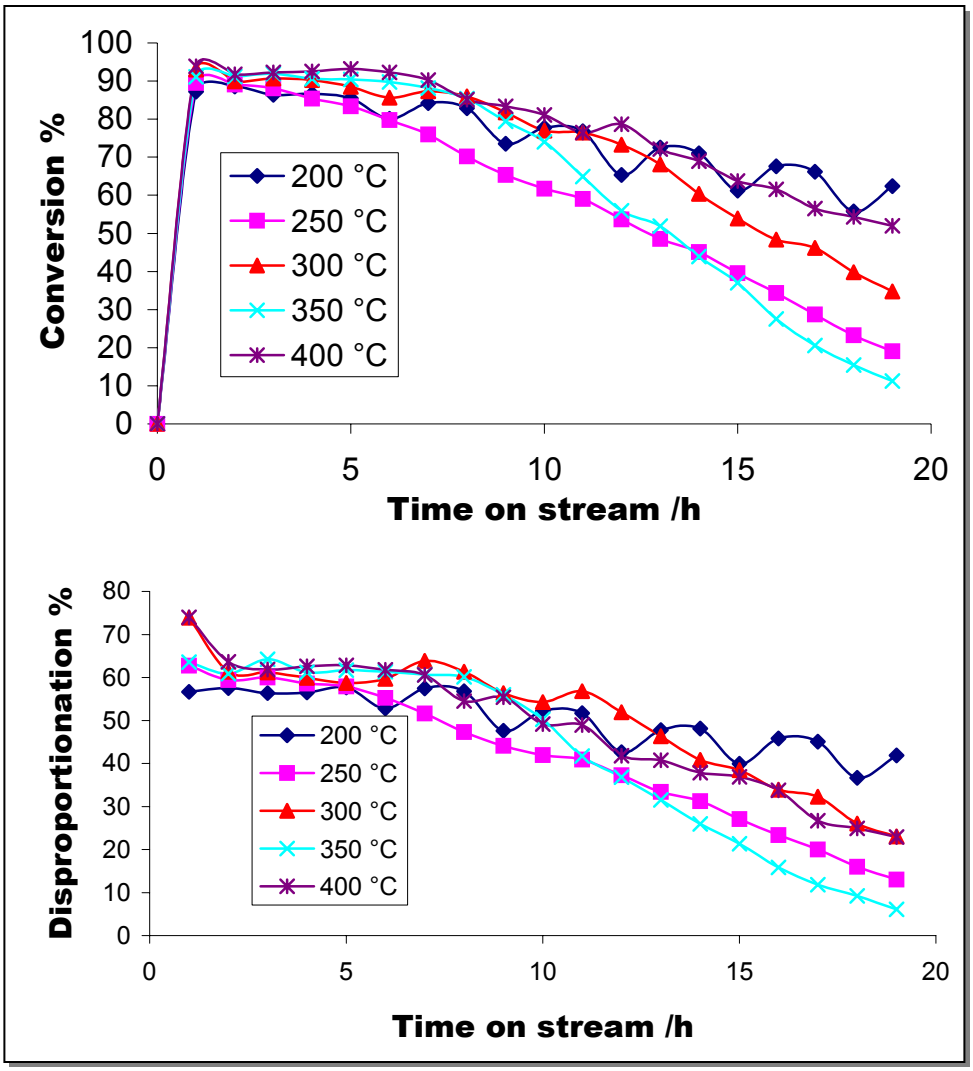

Figure 8.8: Mesitylene disproportionation (mol %) on H-LZY-82

A possible explanation for this kind of behaviour was that, as found on mordenite, there was a transition state formed but trapped in the pore of the zeolite, and thus less effectively deactivated the catalyst at 250 °C; a different transition state molecule

may also have been formed at 350 °C and got trapped as well and the two transition states here rather than like on mordenite showed that the second one came about because of the more room offered by the zeolite. Increase in the temperature from 250 to 300 °C and from 350 to 400 °C may be promoting the formation of the necessary products from such intermediates. This explanation supports the earlier suggestion that temperature had an influence on the reaction mechanism of either the alkyl transfer reaction or catalyst deactivation.

The product stream, as in the case of mordenite, contained durene (DUR) and 1,2,4-trimethylbenzene (1,2,4) in large amounts as compared to other products (figure 8.9), but on LZY-82 the amount of durene produced exceeded that of the 1,2,4-trimethylbenzene (they were formed in an approximately 1:1 proportion on mordenite (figure 8.6) at the same temperature). This was possibly due to the more spacious cavities allowing also the transition state formed by the bulkier 1,2,4-trimethylbenzene intermediates leading to its consumption and the production of tetramethylbenzenes (probably the 1,2,4,5-tetramethylbenzene, durene) and the xylenes. This then suggested that there were certain transition states in the zeolites the formation of which was temperature dependent. The possible intermediates (transition states) are shown in figure 8.10. There was also a slight increase in the concentration of benzene and toluene on zeolite-Y in the product stream but again only small quantities (~5 %) were produced during the early stages. As concluded in the previous chapter that the stronger the sites the higher the rate of deactivation and that smaller molecules were actively involved in carbonaceous material formation; the observed smaller molecules on LZY-82 further supported the fact that mordenite contained stronger sites than the former, but again due to the 3-D structure of the catalyst the presence of smaller molecules in the product stream could be due to a rapid diffusion out of the catalyst pores as observed with ethylbenzene. Contrary to the situation found on H-mordenite, there were significant amounts of the xylenes and the ‘others’ in the product stream; nevertheless, their amounts were considerably small in the product stream and only concentrated during the initial stages of the reaction.

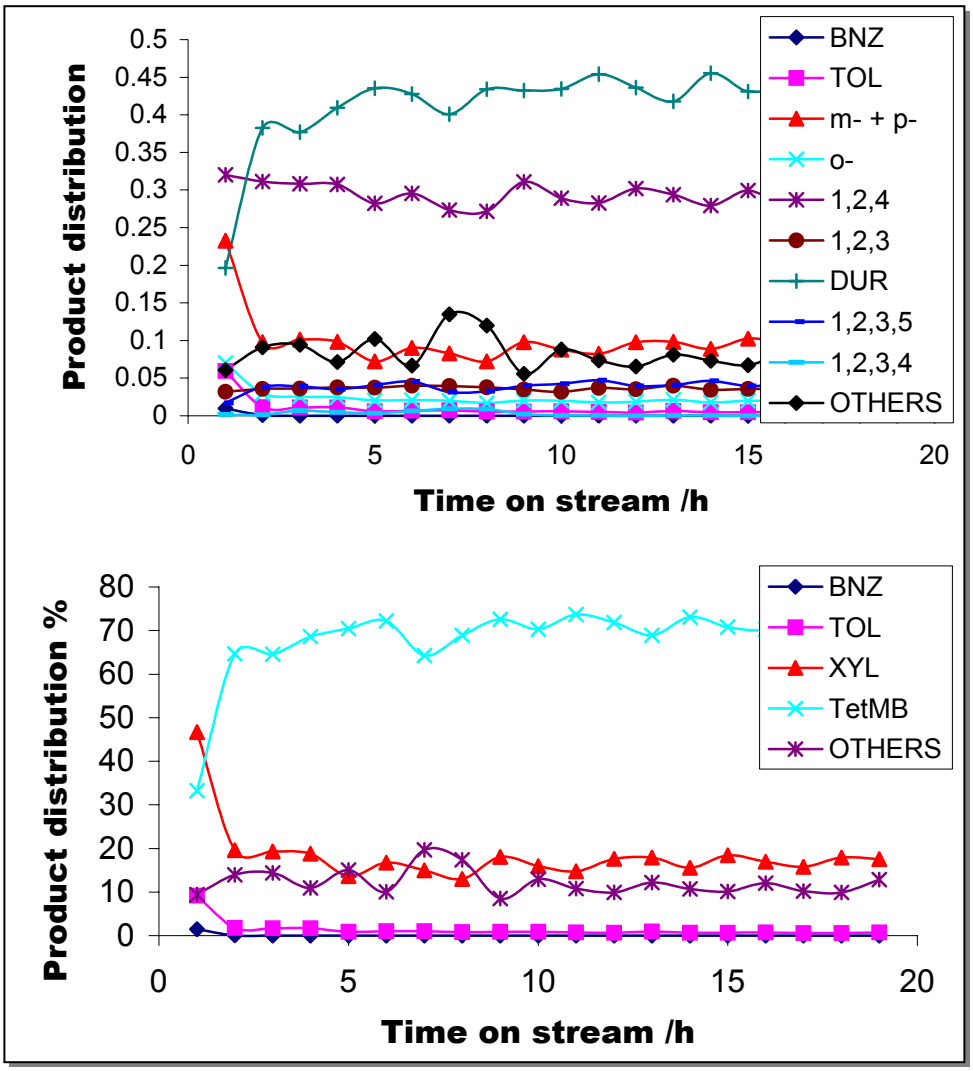

Figure 8.9: Product distribution (mol %, fractional units) of the mesitylene disproportionation reaction on HLZY-82 at 200 °C

The catalyst behaviour with increase in temperature was more stable than found with mordenite (figure 8.3); at lower temperatures (200 °C) the activity was very stable with respect to the reaction mechanisms followed (no crossing over of the different reaction routes) and this is shown as figure 8.11(a). The crossing over was observed at higher temperatures (400 °C); this is shown in figure 8.11(b). The deactivation

resistance which was characteristic of the zeolite-Y in alkyl-transfer reactions is also reflected in these plots.

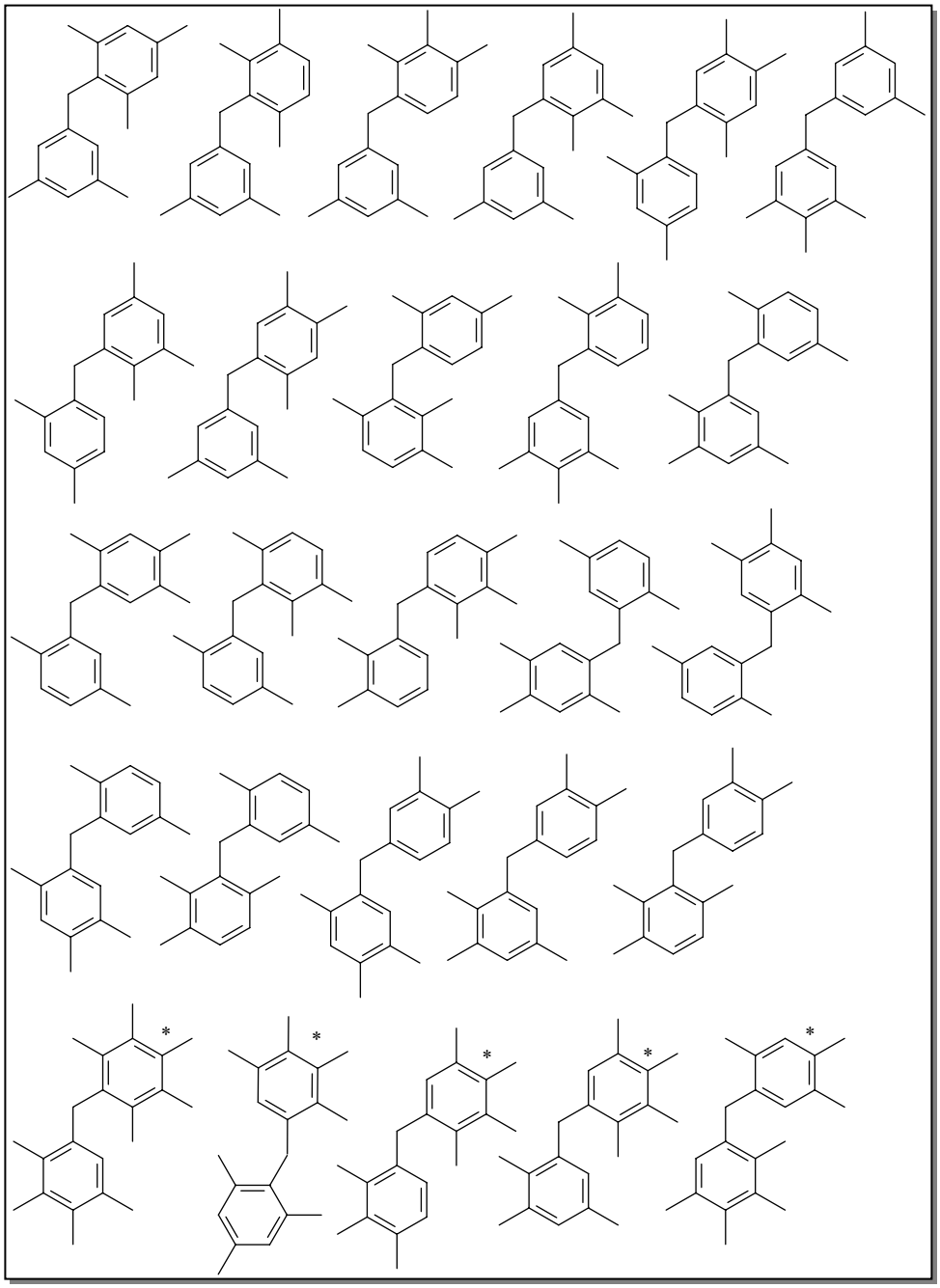

Figure 8.10: Possible reaction intermediate during mesitylene disproportionation on zeolites, * = intermediates involving tetramethylbenzene

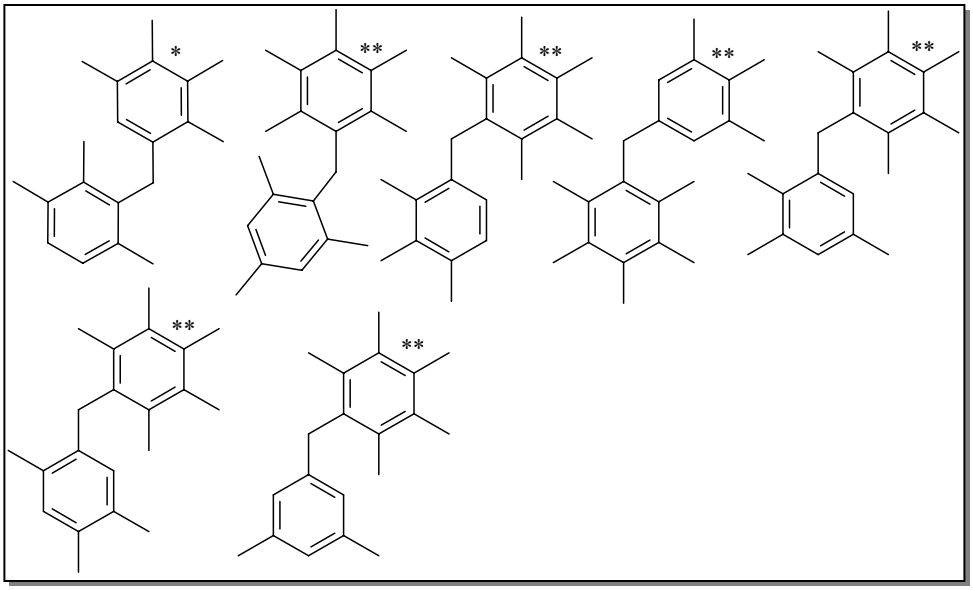

Figure 8.10 continued: ** = intermediates involving pentamethylbenzene

A comparison of the conversions of toluene, xylene and mesitylene on mordenite at different temperatures is shown in figure 8.12. The figure greatly supported the conclusion made earlier that the rate of deactivation is dependent on the ease with which the compound is converted. If one considers the deactivation rate being somehow related to the size of the molecule involved then the bigger the molecule the higher the deactivation rate should be, but the opposite trend is shown by figure 8.12 implying that the bigger the molecule the simpler (easier) the conversion.

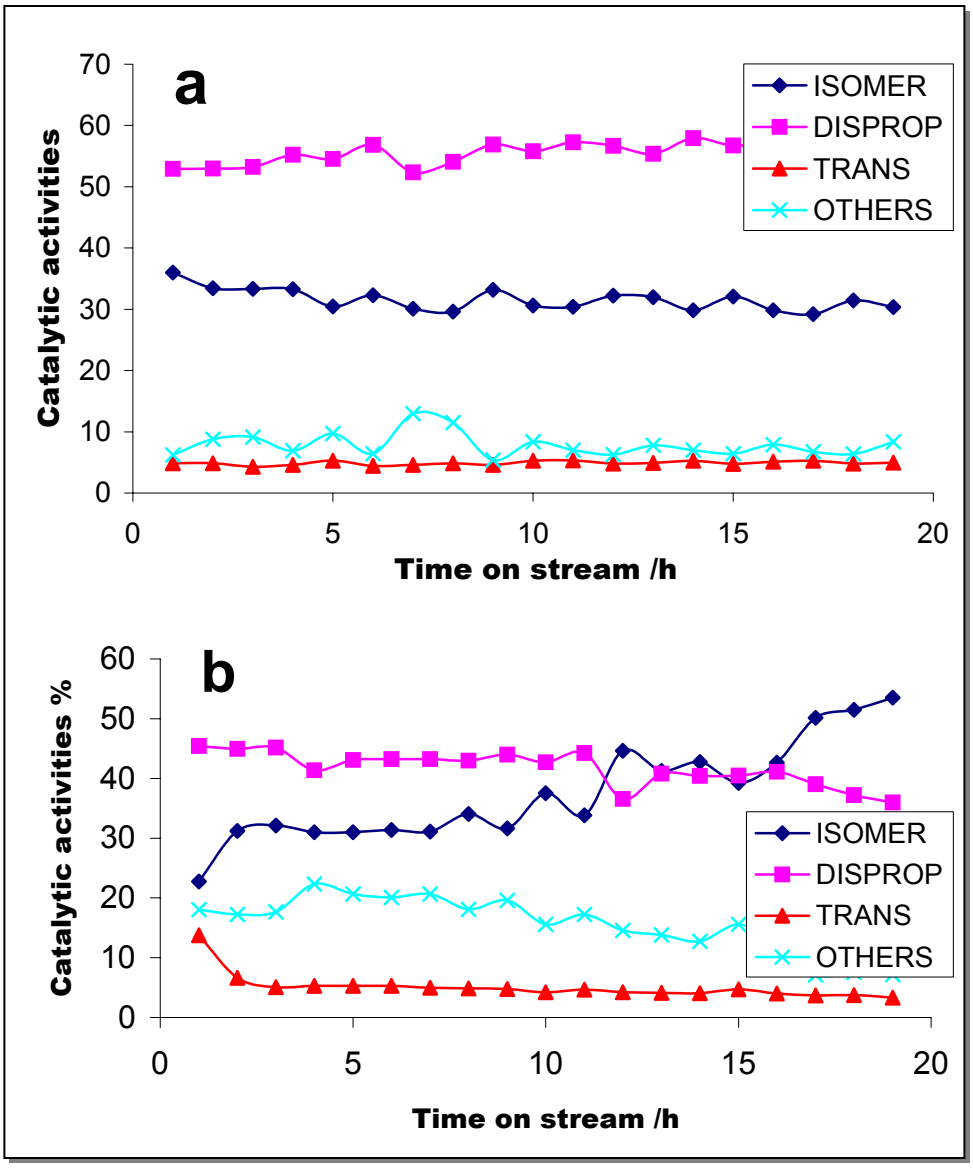

Figure 8.11: Mesitylene disproportionation (mol %) on HLZY-82; Catalytic activities (routes) at a) = 200 °C, b) = 400 °C

The figure also highlights the fact that toluene was the least reactive of the three and for this reason low conversions and fast deactivations were observed. The increase in the number of alkyl groups present on the ring in xylene made it more reactive than toluene and thus its conversion did not rely on the presence of only strong sites in the catalyst, those with intermediate strengths also catalyzed the reaction.

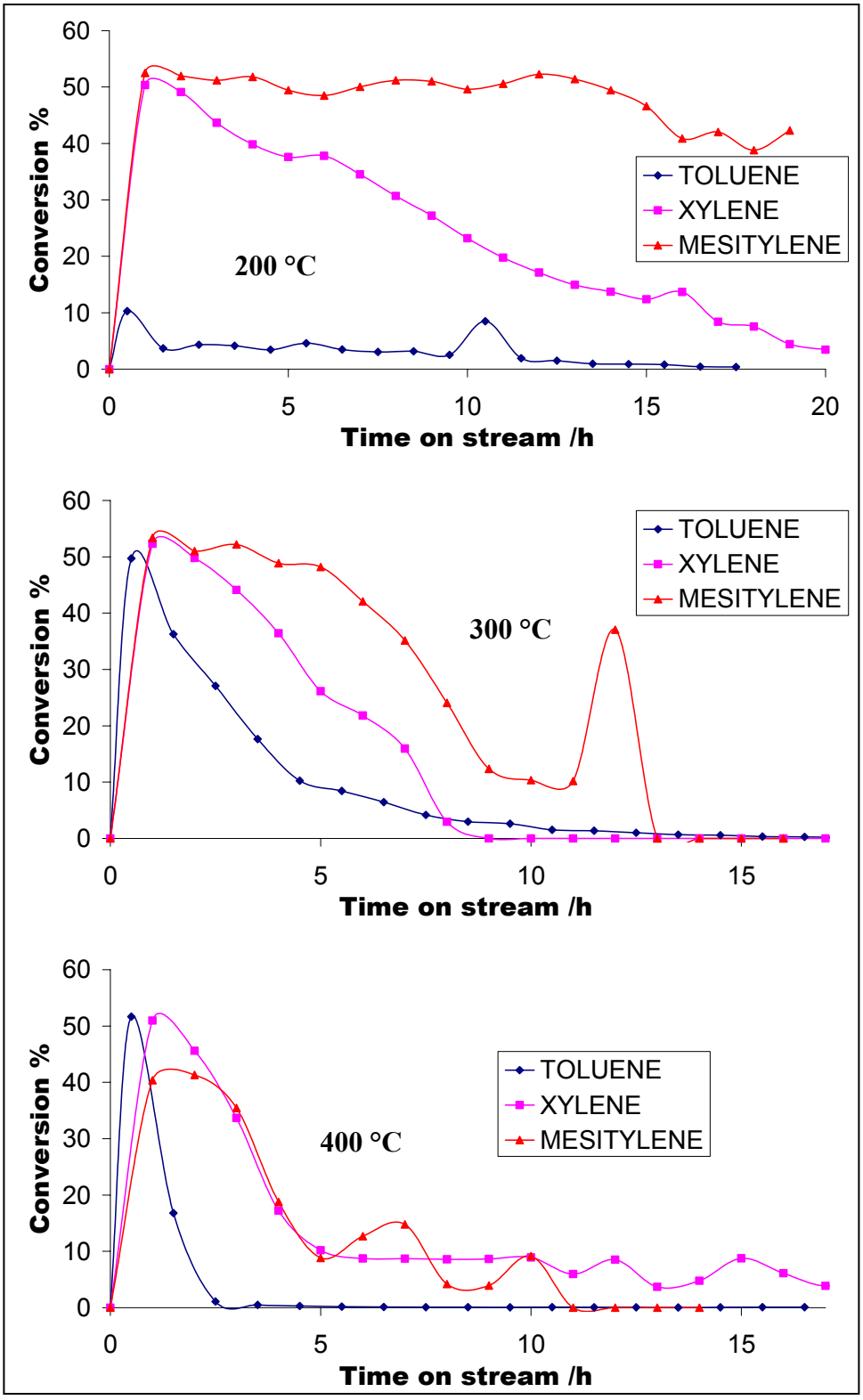

Figure 8.12: Alkyl-aromatic disproportionation (mol %) on mordenite

Further increase in the number of alkyl groups in mesitylene rendered it the most reactive of the three with less discrimination on the strength of the active sites. But, an increase in temperature which also results in an increase in acidic strengths of the sites resulted in an increase in the rate of deactivation for these molecules because of the poisoning of these sites by carbonaceous material depositions.

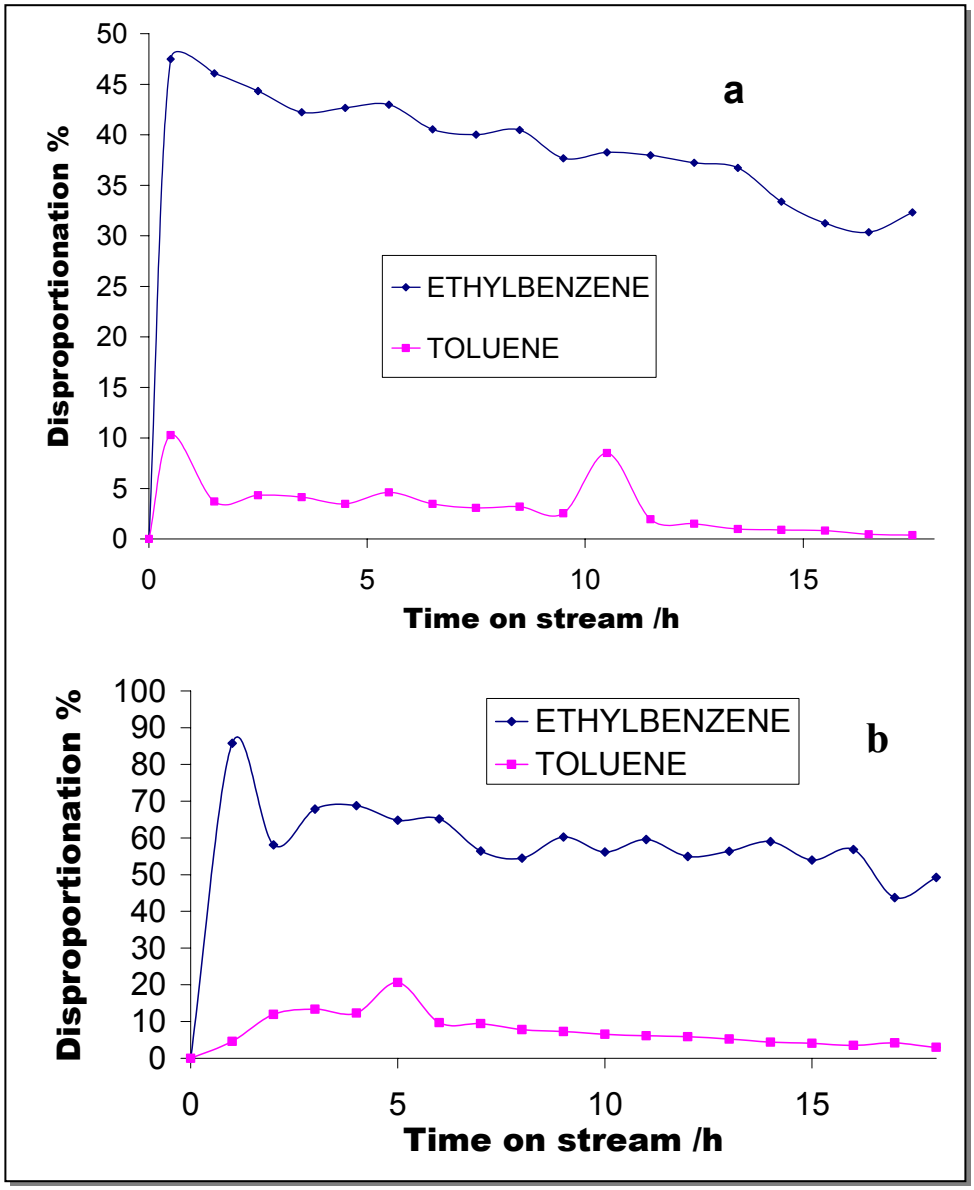

Figure 8.13: The effect of the alkyl group size (type) on the activity of the molecules (Ethylbenzene at 180 °C, Toluene at 200 °C); a) on H-mordenite, b) on H-LZY-82 (mol %)

Figure 8.13 also shows that relative reactivity is not governed only by the number of alkyl groups on the ring. The number of carbon atoms on the alkyl group (and probably the type of an alkyl group) had an effect on conversion and obviously on the deactivation of the catalyst. The higher the number of carbon atoms on the alkyl substituent the easier the conversion of the alkylaromatic.

8.4 Conclusion

In conclusion, both zeolites showed some reasonable activity for the disproportionation of mesitylene, and also proved to be ideal catalysts for studying the transalkylation reactions between mesitylene and benzene since very little benzene and toluene were formed during the disproportionation reactions; this may be due to the relatively long pathways to their formation which would require three sequential disproportionation steps from trimethylbenzene, xylenes, and then toluene (although the occurrence of some dealkylation/alkylation reactions could also lead to benzene and toluene, these reactions were less likely to be viable under the current conditions) but this was less likely to occur. The subsequent steps needed would require the accompanying subsequent increase in acid site strengths as the number of alkyl groups decreased.

The study has shown that there is a relation between the ease with which the molecule is converted and the rate of deactivation, and that higher temperatures also favoured high rates of deactivation especially through carbon depositions. It was also shown to some extent that deactivation by polymerization and molecular trapping in the zeolite had a smaller effect on the deactivation of the zeolite as compared to the actual site poisoning by carbon deposition.

Overall, it has been shown that the presence of alkyl groups on the ring and the type of alkyl groups present have significant influence on the reactivity of the alkylaromatics. The higher the number of alkyl-groups and the higher the number of carbons on the alkyl

9 BENZENE-MESITYLENE TRANSALKYLATION

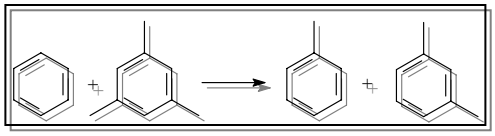

9.1 Introduction

Previous studies (chapter 5) have shown that benzene on H-mordenite only gets converted to about 7 % at high temperatures (400 °C) and this was accompanied by a strong decrease in activity due to carbonaceous material deposition on strong sites (figure 5.2). There was no conversion on HLZY-82 below 350 °C but considerable activities for benzene conversion were observed at 400 °C (figure 5.4); and this somehow rendered benzene as an almost inert compound below 400 °C on both catalysts. On the other hand the disproportionation of mesitylene on zeolites produced a maximum of 10 % toluene in the product stream at 400 °C which was the highest reaction temperature; this was observed only during the first 2 hours of the reaction. From the above it was considered reasonably practical to study transalkylation reactions between benzene (an almost inert compound) and mesitylene; any toluene significantly formed would be more likely to arise from transalkylation reactions to benzene from mesitylene and unlikely from disproportionation of the latter. Addition of benzene to the mesitylene feed will cause a dilution and hence this will result in lesser production (<10%) of toluene through disproportionation.

9.2 Experimental

Two feed compositions were prepared; one was studied on mordenite (24 % benzene and 75 % mesitylene) and the other on HLZY-82 (46 % benzene and 53 %

mesitylene). Analysis of these mixtures was carried out by running a blank at a selected high temperature, i.e. a run without a catalyst as shown in figure 9.1.

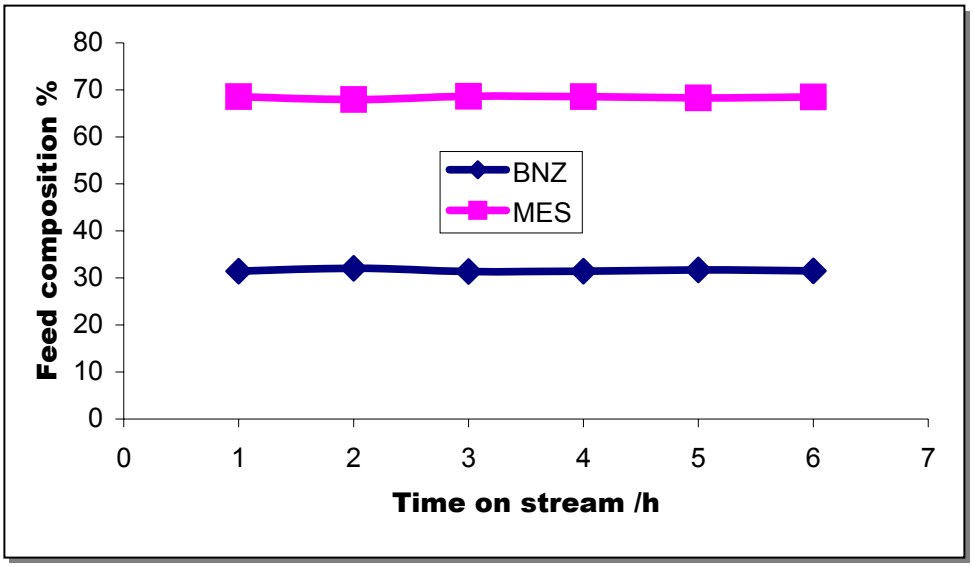

Figure 9.1: Feed composition (mol %) of a blank run at 400 °C (benzene/mesitylene)

9.3 Results and Discussions

9.3.1 Benzene–mesitylene transalkylation on H-mordenite

Due to complexities brought about by the adsorption/absorption and molecular diffusion problems of molecules in the zeolite, presenting transalkylation results as either conversion of benzene or mesitylene (starting materials) was impossible since this did not comply with the observations from the blank runs; i.e. the outlet showed benzene amounts higher than that of the feed as if there was production of benzene in the reaction. This phenomenon is better manifested and explained in the next chapter. Nevertheless, since the purpose of this study was to look at transalkylation, and from the fact that benzene was almost inert and mesitylene disproportionation did (almost) not produce toluene in the earlier studies, it was found safe to present the transalkylation results as percentage production of toluene:

$$\% \text{ Transalkylation} = \left(\frac{n_{Toluene}}{\sum n_{products}} \right) \times 100$$

Using the above equation which also indicated the transalkylation selectivity towards toluene, about 50 % transalkylation (amounts of toluene in the product stream) was achieved on H-mordenite (figure 9.2) at temperatures in the range of 250-400 °C during the early stages of the reaction. As expected from this uni-dimensionally structured catalyst the activity decreased significantly with increase in time on stream. The transalkylation behaviour of the catalyst was not very different from the mesitylene disproportionation behaviour (figure 8.1); which showed some degree of stability at low temperatures (200 °C), a heavy deactivation at 250 °C and an increase in activity and stability with increase in temperature to 350 °C, then a strong deactivation again at 400 °C.

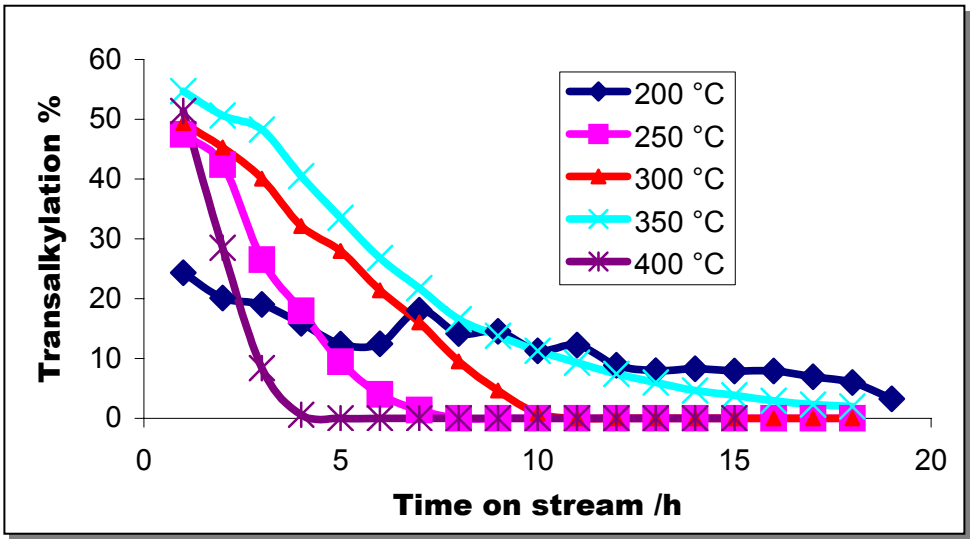

Figure 9.2: Benzene-mesitylene (24/75 mol %) transalkylation on H-mordenite

From the remarkable observations above it could be concluded that the activities were mesitylene rather than benzene dependent. The fact that the amounts of toluene produced by mostly transalkylation in the reactions followed the same trend as that of mesitylene disproportionation suggested that the bulky trimethylbenzenes were the dominant competitors for the acid sites (active sites). Steric effects did not play any

significant role in these large pore zeolites and the fact that methyl groups on the ring had an electron donor ability which increased the basicity of the molecule supported the suggestion that trimethylbenzenes were interacting preferably with the acid sites. The proposed transalkylation mechanism is thus shown in scheme 9.1. The trimethylbenzene molecule first adsorbs on the active site, an intermediate is then formed with either benzene (transalkylation) or with another trimethylbenzene molecule (disproportionation) which attacks the adsorbed species; the reaction is then completed by the formation of the appropriate products. With the mechanism below followed, it is apparent that manipulation of the feed composition will result in different extents of conversions, and this will be shown later in the chapter.

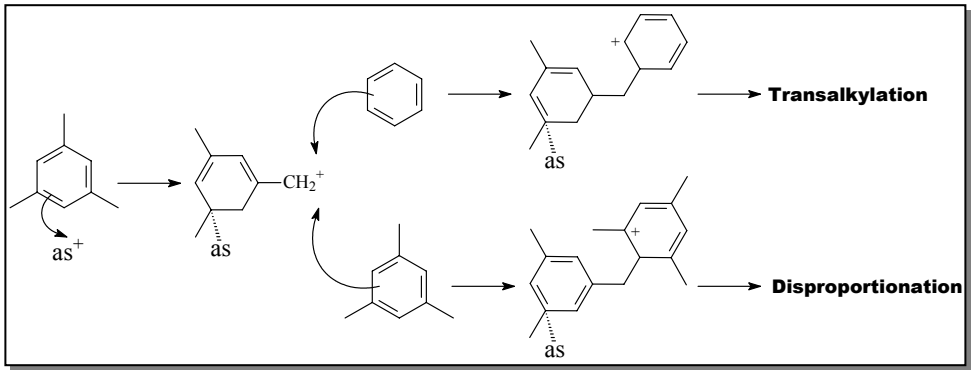

Scheme 9.1: Proposed transalkylation mechanism; **as** = active site

The mechanism was strongly supported by considering other alternatives, i.e. benzene becomes the molecule adsorbed on the active site (scheme 9.2). The activated benzene molecule on the active site would be very difficult to attack by the mesitylene molecule due to the steric effects posed by methyl groups, and if a bimolecular intermediate is formed then the alkyl-transfer reaction would not be possible unless otherwise.

From the product distribution on H-mordenite, the production of toluene during the initial stages of the reaction seemed to increase with increase in temperature and decreased with increase in time on stream due to deactivation of the catalyst (figure 9.3).

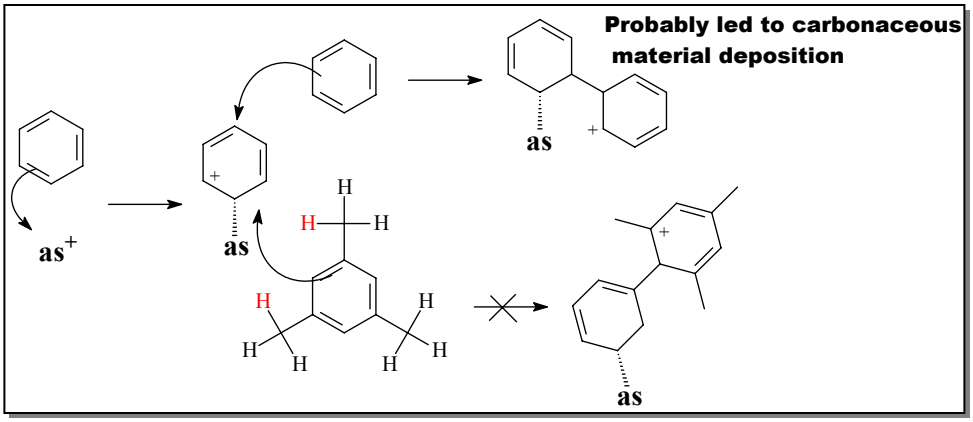

Scheme 9.2: An alternative to the proposed transalkylation mechanism; **as** = active site

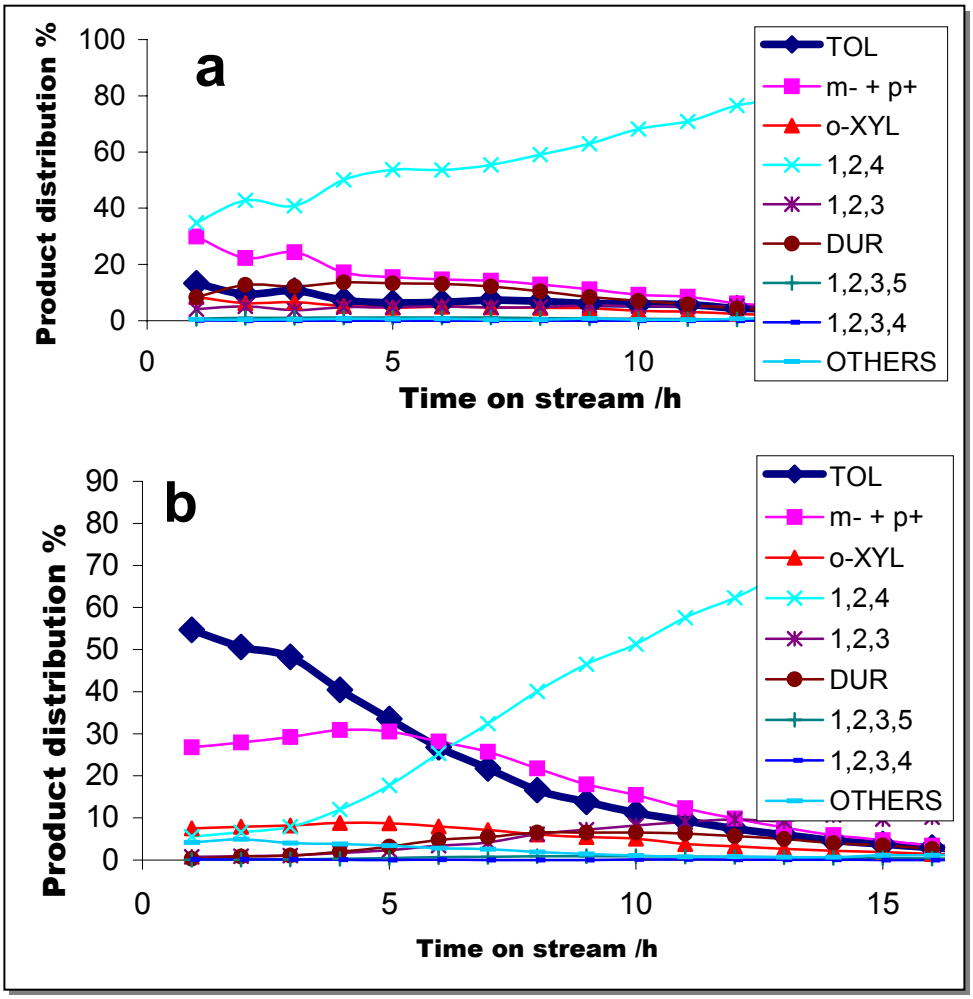

Figure 9.3: Benzene-mesitylene (24/75 mol %) transalkylation on H-mordenite; Product distribution at a) 200 °C, b) 350 °C [m- + p+ = meta and para-xylene]

From the figure it is observed that the dominant reaction at high temperatures was transalkylation followed by isomerization to 1,2,4-trimethylbenzene rather than disproportionation with increase in time on stream as the pores narrowed due to carbon deposition. Mesitylene disproportionation is a very facile reaction but the presence of benzene in the feed and an increase in temperature favoured transalkylation to a very great extent. This is further supported by the fact that during the early stages of the reaction at 350 °C only toluene and xylene dominated (figure 9.3) and with increasing time on stream isomerization was favoured while the formation of tetramethylbenzene (disproportionation) was hardly observed.

9.3.2 Benzene-mesitylene transalkylation on HLZY-82

The mixture used for transalkylation reactions on LZY-82 was different in composition percentages from that used on mordenite; the mixture was made up of 46 % benzene and 53 % mesitylene while on mordenite a 24/75 mol % mixture was used. An increase in temperature resulted in an increase in activity and catalyst lifetime as expected on LZY-82 (figure 9.4). Unlike the H-mordenite, the zeolite-Y did not show any resemblance in its activity to that of the mesitylene disproportionation (figure 8.8). This catalyst seemed to achieve its maximum transalkylation activity at 350-400 °C.

Since the transalkylation reaction was represented by the availability and the amounts in the product stream of toluene, the fact that an increase in temperature resulted in increased amounts of toluene produced suggested that transalkylation reaction was selectively favoured at higher temperatures. The above observations suggested strongly that transalkylation reactions would require high temperatures (or stronger sites) if effective alkyl-transfer is desired. This was a setback because it was concluded earlier that higher temperatures (or stronger sites) also favoured rapid deactivations.

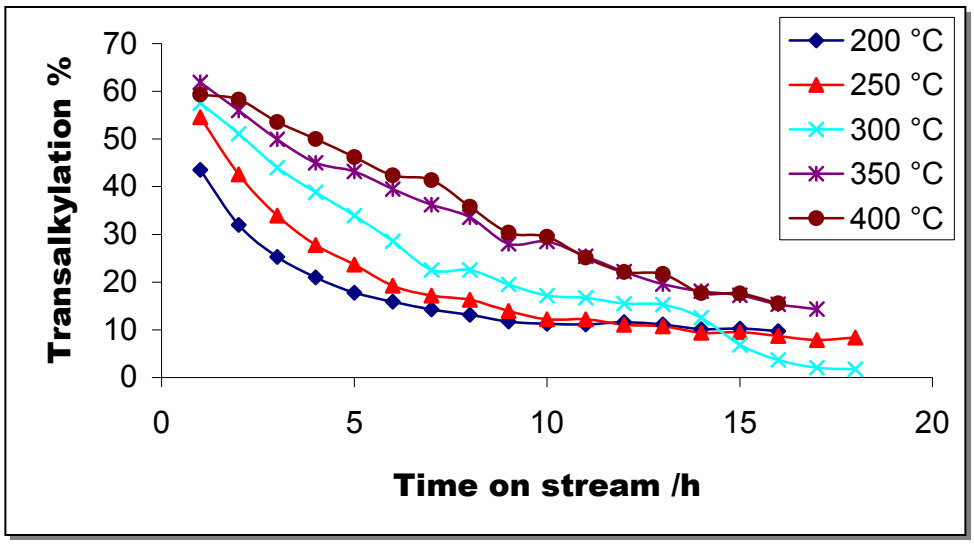

Figure 9.4: Benzene-mesitylene (46/53 mol %) transalkylation on HLZY-82

The product stream of the reactions on HLZY-82 was expectedly similar to that on H-mordenite. An interesting feature was observed when looking at the tetramethylbenzene isomer distribution in the product stream. On H-mordenite (24/75 mol % mixture) there was about a constant average of 90 % durene (DURENE), 9 % 1,2,3,5-tetramethylbenzene (1,2,3,5) and 1 % of 1,2,3,4-tetramethylbenzene (1,2,3,4) in the product stream (figure 9.5(a)), this was observed at the temperature range of 200-300 °C. At higher temperatures (350-400 °C) there was an increase in the product stream of the bulky and more sterically hindered 1,2,3,5- and 1,2,3,4-tetramethylbenzene by 15% and 30% (not shown) respectively (figure 9.5(b)); at the expense of mainly the less sterically hindered durene.

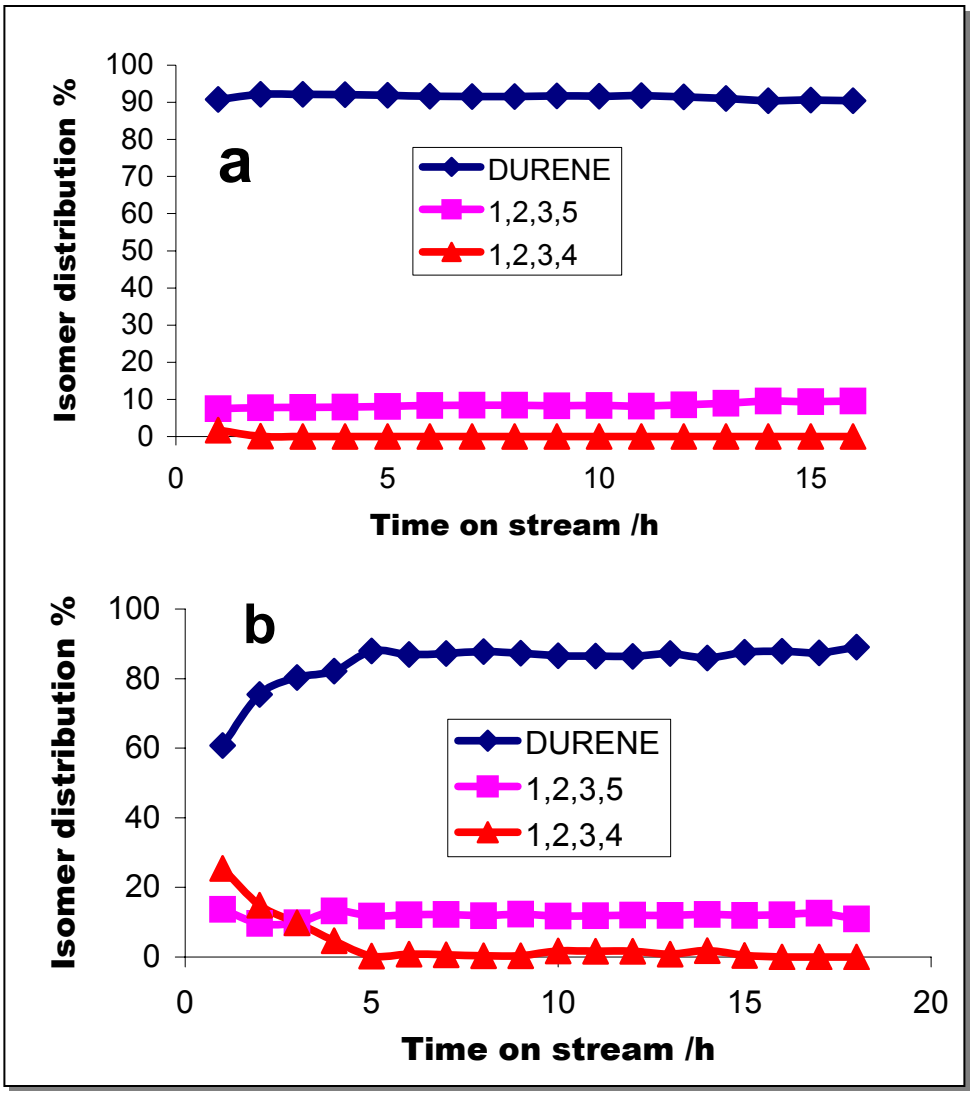

Figure 9.5: Benzene-mesitylene (24/75 mol %) transalkylation on H-mordenite at 300 °C; Tetramethylbenzene isomer distribution at a) 200 °C and b) 350 °C

The same 90:9:1 ratio was observed on the zeolite-Y (figure 9.6(a)) with the 46/53 % mol mixture, but only at low temperatures as mordenite (200-250 °C). About 50/50 % durene:1,2,3,4-tetramethylbenzene ratio was observed at 300 °C (figure 9.6(b)) only for the first 2 hours of the reaction, then the 1,2,3,4-tetramethlbenzene concentration decreased while the durene and the 1,2,3,5-tetramethylbenzene approached the 90:9:1 ratio.

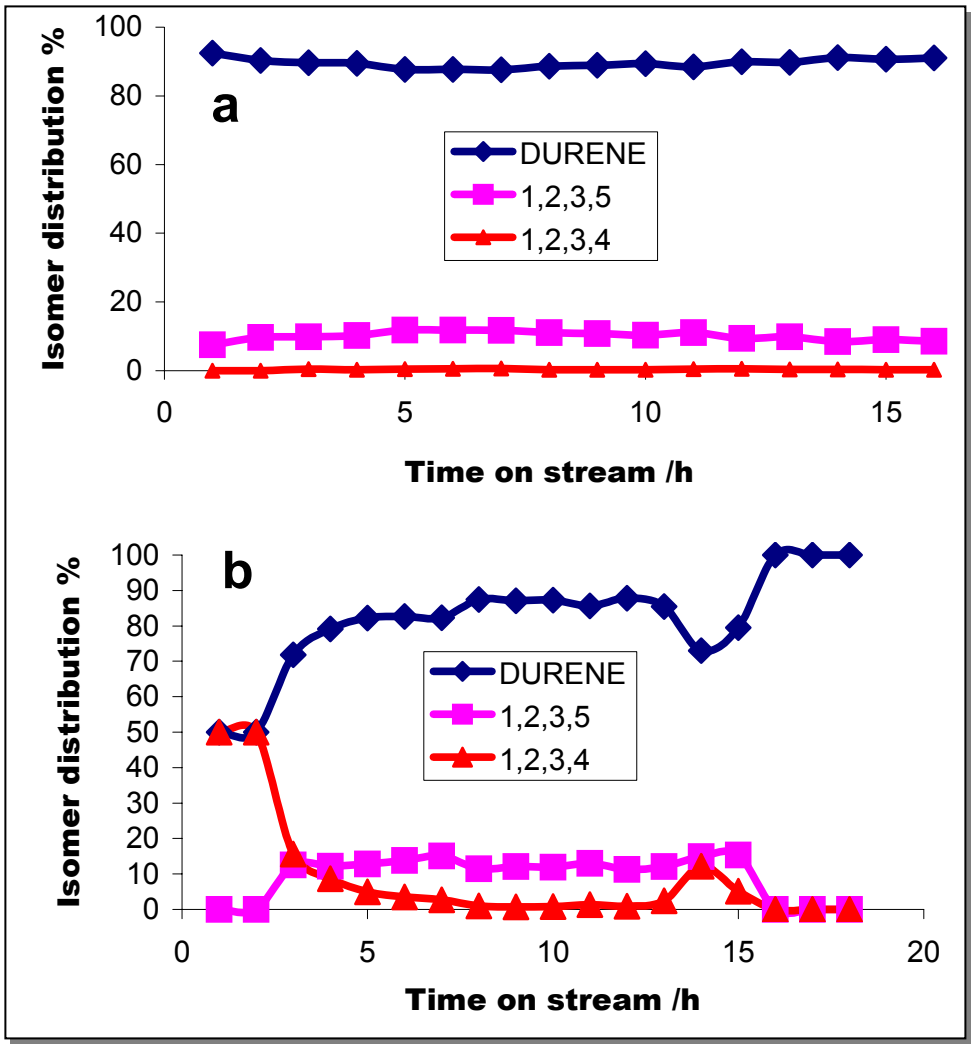

Figure 9.6: Benzene-mesitylene (46/53 mol %) transalkylation on HLZY-82; Tetramethylbenzene isomer distribution at a) 200 °C and b) 300 °C

The increase in the concentration of the 1,2,3,4-tetramethylbenzene in the product stream was very significant at 350 °C (> 75%, not shown) and at 400 °C (~ 85%), but the amount decreased with increase in time on stream to approach the 90:9:1 ratio; this is illustrated in figure 9.7.

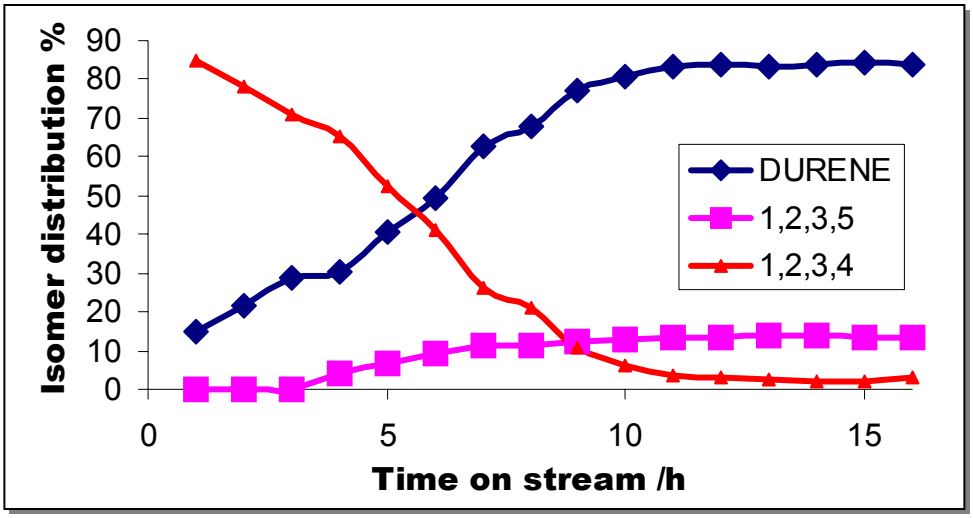

Figure 9.7: Benzene-mesitylene (46/53 mol %) transalkylation on HLZY-82; Tetramethylbenzene isomer distribution at 400 °C

From these unusual observations, it was suggested that the manner in which molecular interaction occur during transalkylation was strongly affected by temperature, and this strictly followed the biphenylmethane intermediate mechanism rather than the dealkylation-realkylation mechanism, which would not favour the formation of the sterically hindered 1,2,3,4-tetramethylbenzene observed here in high amounts.

The possible explanation may be that, at low temperatures, the reactions proceeded through all intermediates in scheme 9.3, and an increase in temperature led to the preferential formation of the intermediate 3, 6 and 8 consuming the durene and the 1,2,3,5-tetramethylbenzene, but transition state 4, 7, 9 and 10 were probably not involved in the reaction because they would consume the bulkier 1,2,3,4-tetramethylbenzene. These intermediates mostly led to the formation of the smaller alkylbenzenes, thus somehow favouring transalkylation. Intermediate 11 resulted in the formation of the tetramethylbenzene by disproportionation. This explanation is also supported by the fact that with increase in time on stream the 1,2,3,4-tetramethylbenzene concentration decreased as carbon formed in the catalyst narrowed the pores and cavities (reaction space); this slowly restricted the formation of the bulky intermediates and prevented the consumption of bulky molecules

(DURENE and 1,2,3,5). The above observations strongly and completely supported the suggestion that higher temperatures favoured transalkylation.

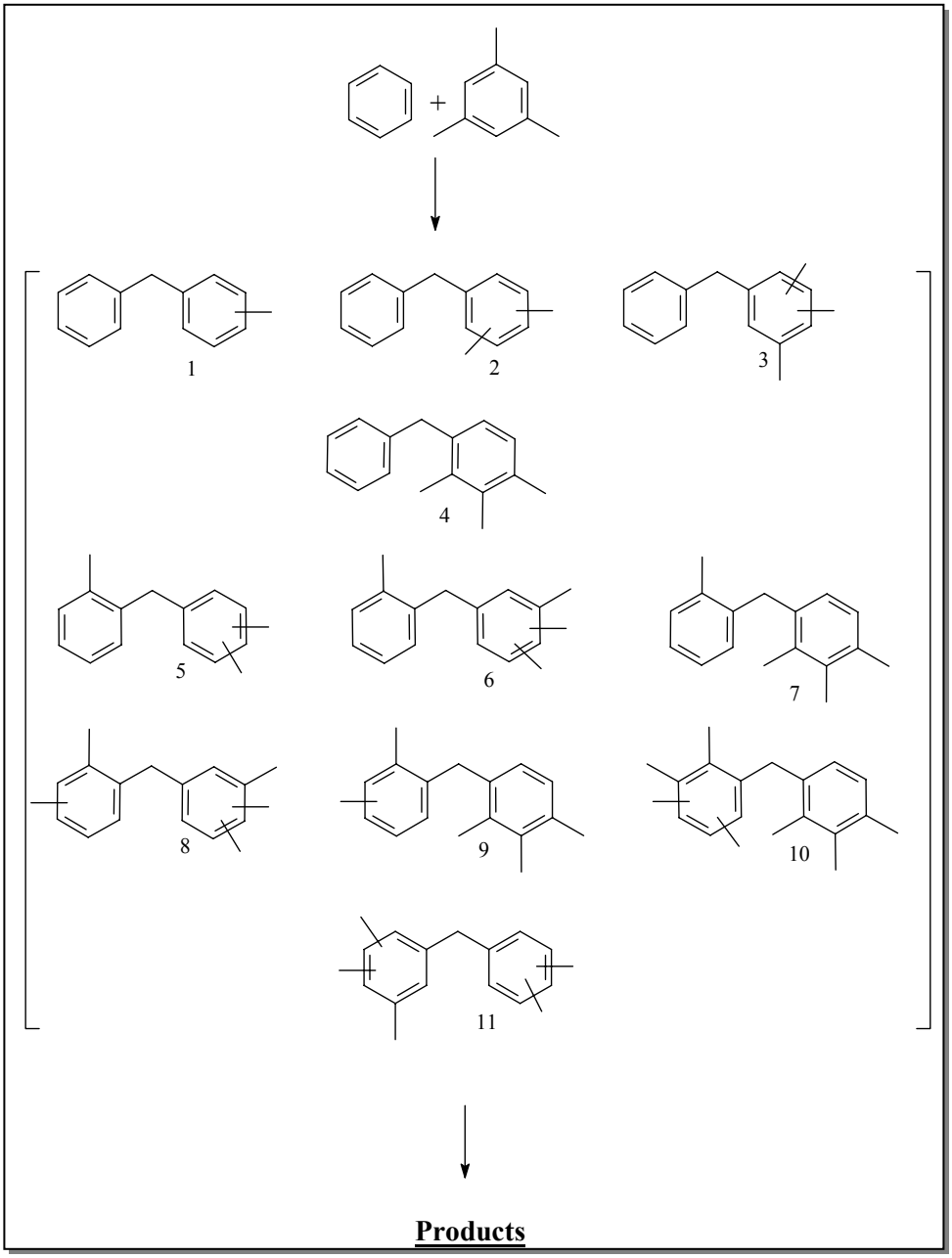

Scheme 9.3: Alkyl-transfer intermediates during benzene-mesitylene transalkylation reactions

The other possibility which may lead to a similar situation was that of isomerization of durene and the 1,2,3,5-*tetra*methylbenzene, but isomerization , like the dealkylation/realkylation type of alkyl-transfer, will almost always favour the lower energy structural conformations. In this case the lowest energy molecule (due to the steric repulsions between the methyl groups) would be durene, followed by the 1,2,3,5-*tetra*methylbenzene while the 1,2,3,4-*tetra*methylbenznene will be the highest energy molecule. Thus isomerization was ruled out in this case. Another explanation is the one that supports the suggestion that the formation of the transition state was temperature dependent, i.e. at lower temperatures, intermediates that would lead to the consumption of bulky molecules either did not form or they could not proceed to form products; and somehow an increase in temperature promoted the formation of such intermediates and/or led to the formation of products from such intermediates. Lastly and not least, approaching the active site by the bulky 1,2,3,4-tetramethylbenzene could have been difficult and this would have led to the isomer being essentially inert in the system.

The fact that more of the 1,2,3,4-tetramethylbenzene was observed in the product stream of the reactions on HLZY-82, further emphasized the flexibility due to the presence of larger cavities in the catalyst as compared to mordenite, allowing the formation of bulky intermediates.

9.3.3 The effect of feed composition on transalkylation

It was suggested earlier during the transalkylation reaction on H-mordenite that the reaction behaviour was mesitylene dependent, and from the proposed mechanism it was further suggested that an increase in the benzene content of the reaction feed should result in the increase in the transalkylation reaction activity (production of toluene); i.e. increasing the amount of benzene molecules available for accepting the methyl groups of the adsorbed species, and that the higher benzene amounts will promote rapid deactivations. These aspects were examined on the zeolite-Y.

The 24/75 % mixture was then reacted on the zeolite-Y at 200 °C and compared to the reaction at the same temperature on mordenite (figure 9.8). The figure showed that, as with the ethylbenzene, xylene and mesitylene disproportionation reactions, both catalysts had almost the same catalytic behaviour at low temperatures since there were almost equal amounts of toluene produced in this case. The comparison was made only at low temperatures because of the observed rapid deactivation on H-mordenite with increase in temperature while LZY-82 would show better activities under same conditions.

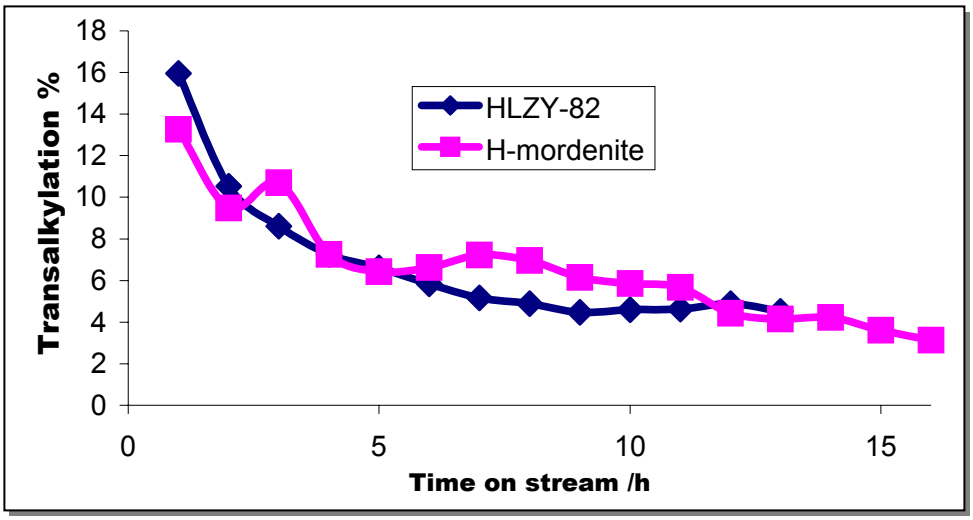

Figure 9.8: Benzene-mesitylene (24/75 % mol) transalkylation on zeolites at 200 °C

A higher benzene content mixture (46/53 % mol) was used on HLZY-82. As expected, the activity (toluene production) in the transalkylation reaction increased from 15 to 45 % during the initial stages of the reaction (figure 9.9). The increase was due to the increased chances of having a bimolecular intermediate consisting of benzene-mesitylene (transalkylation, scheme 9.1) instead of mesitylene-mesitylene (disproportionation, scheme 9.1), and thus hindering the disproportionation reaction to some extent while promoting transalkylation reactions. At this point it was apparent that mesitylene was a strong competitor for the active sites in the zeolite; and once it is adsorbed benzene gets a chance to scavenge for the methyl groups. This

was ironically also based on the fact that it was expected that a high amount of mesitylene in the feed will facilitate the alkylation of the minority benzene. But, the increase in the benzene concentration increased the amount of benzene available for the methyl groups of the adsorbed mesitylene molecules. The observations greatly supported the suggested transalkylation mechanism. It was also suggested that a further increase of benzene in the feed might result in a further removal of methyl groups from the mesitylene molecules. There was no observable evidence of rapid deactivations brought about by the higher benzene amounts in the feed.

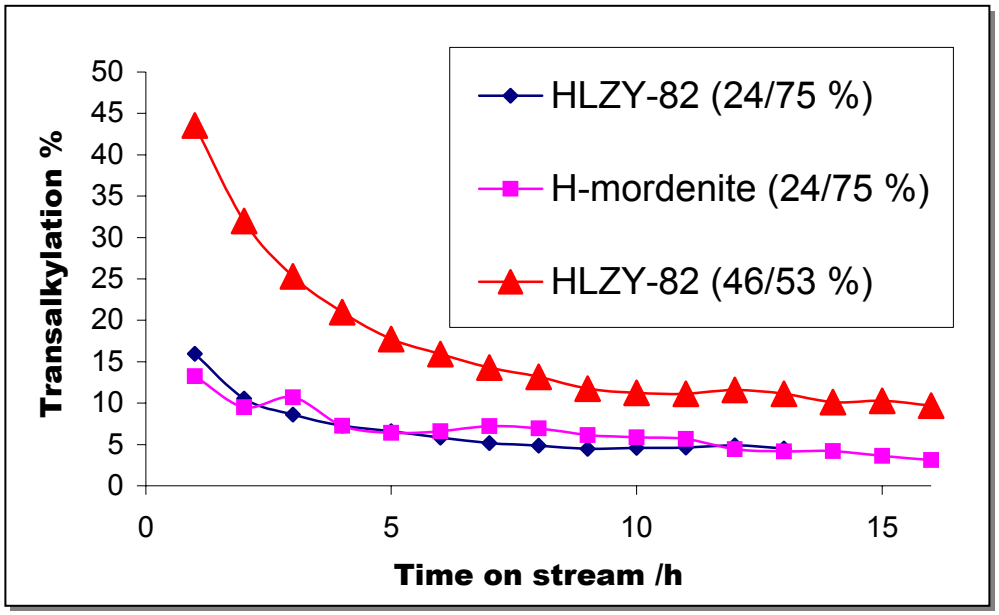

Figure 9.9: Benzene-mesitylene (mol %) transalkylation on zeolites at 200 °C

Comparison of the data in figure 9.10 obtained using two different (benzene/mesitylene ratio) mixtures at the same temperature (200 °C) on HLZY-82, showed a significant decrease in the 1,2,4-trimethylbenzne an isomerization product; and a decrease in the production of durene a disproportionation product almost to zero during the early stages of the reaction when benzene was increased in the feed. This proved that transalkylation was favoured on account of higher benzene amounts further supporting the proposed mechanism.

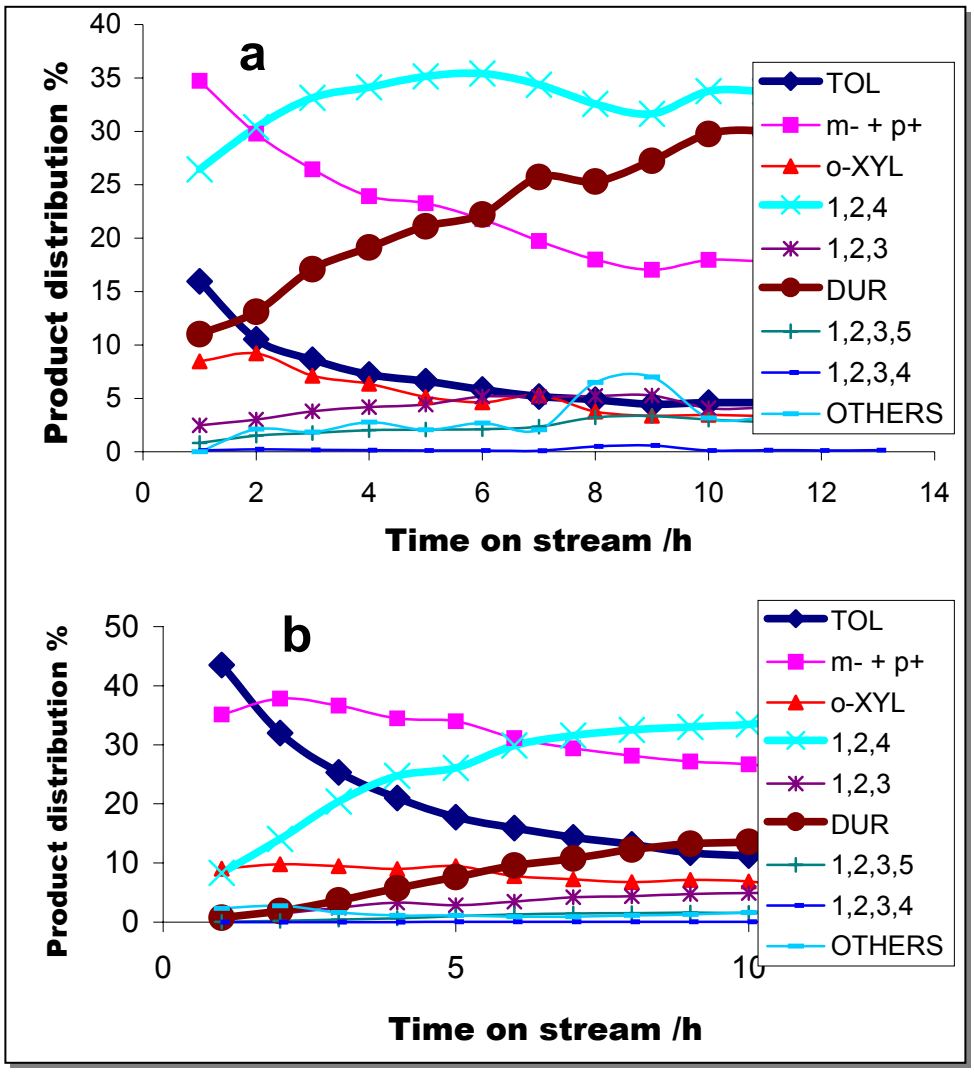

Figure 9.10: Benzene-mesitylene transalkylation on HLZY-82 at 200 °C; a = 24/75 mol %, b = 46/53 mol %

The comparison also suggested that the selectivity of the reaction depended to a great extent on the feed composition ratio. The formation or the concentration of the xylenes (m- + p+, o-XYL) was not significantly affected while toluene formation increased at the expense of large molecules which definitely suggested the occurrence of transalkylation reactions. It was expected that the formation of high concentrations of toluene in product stream would be accompanied by an increase in the concentration of the xylenes (due to toluene disproportionation). This was based on the fact that transalkylation between benzene and trimethylbenzene would result in

the formation of toluene and xylene, but that was not the case suggesting that transalkylation could have been from the bulky *tetra*methylbenzenes. The above observations strongly supported the suggestion that adsorption on the active site favoured the ring with the highest number of alkyl groups (mesitylene and to a lesser extent tetramethylbenzene).

The product stream of the reaction at 350 °C which was almost the same as that at 400 °C (figure 9.11), showed that effective transalkylation may be achieved by feed manipulations and to some extent higher temperature conditions. The product stream was dominated by transalkylation products, i.e. toluene and xylenes.

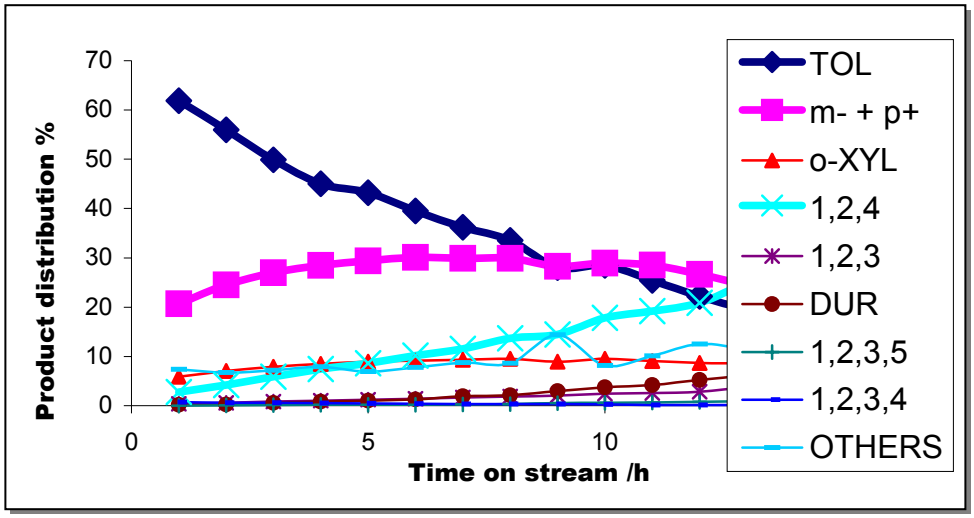

Figure 9.11: Benzene-mesitylene (46/53 mol %) transalkylation on HLZY-82 at 350 °C

9.4 Conclusion

The preferential adsorption on the active site of the alkyl group containing-aromatic molecule was very advantageous for transalkylation reactions since otherwise the smaller benzene would be the adsorbed molecule; it was also noted that the alkyl-acceptor was a small molecule, meaning that the transition state was favourable. The study has shown that transalkylation was favoured over disproportionation at higher

temperatures and this was in line with the earlier conclusion that disproportionation would only be effective at low temperatures compared to transalkylation. It also supported the fact that temperature influences the selectivity of alkyl-transfer reactions. The feed composition seemed to play a significant role in transalkylation and its manipulation may result in effective removal of alkyl groups from the alkyl-containing molecule.

Though the use of high temperatures had some beneficial effects on transalkylation reactions, working at high temperatures is associated with higher deactivation rates which are not desirable for any reaction.

The study was the first genuine confirmation of transalkylation reactions on both zeolites used.

10 BENZENE-METHYLNAPHTHALENE TRANSALKYLATION

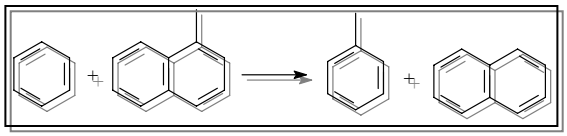

10.1 Introduction

Most alkyl-transfer studies on alkylnaphthalenes has been on alkylation towards naphthalene and almost none has been on transalkylation from alkylnaphthalenes; unless otherwise published in patented form. However, alkylation of naphthalene and alkylnaphthalenes has been greatly achieved on zeolites and it's a fairly researched topic. Alkyl derivatives of binuclear aromatic hydrocarbons containing from one to three carbon atoms in the alkyl substituents are applicable as intermediates in the preparation of aromatic *di*carbon acids to make thermotropic liquid crystal polymers.[36] 2-Methylnaphthalene is the raw material in vitamin-K synthesis and the 2,6-dimethylnaphthalene is obtainable from β-selective alkylation either as a secondary alkylation product of naphthalene or primary alkylation of 2-methylnaphthalene.[33; 54]

For this particular study interest was on transalkylation from alkylnaphthalene (α-methylnaphthalene) to a suitable alkyl-acceptor such as benzene. Conversions of up to 50 % at 400 °C during toluene disproportionation study were achieved on both zeolites and it was expected of methylnaphthalene to give similar behaviour, i.e. difficult conversions and rapid catalyst deactivation. Unlike toluene, methylnaphthalene was bulkier with two fused rings and accessing active sites might be a problem. Not only the critical sizes of aromatic derivatives but also their proton affinity (194.7 kcal/mol for naphthalene and 200.7 kcal/mol for mesitylene) are the reasons for different interaction and adsorption energies for aromatic hydrocarbon transformations.[76]

10.2 Experimental

Similar reaction conditions as for the benzene-mesitylene system in the previous chapter were employed. As discussed before, a flow type fixed-bed reactor system was used for benzene-α-methylnaphthalene; this arbitrarily prepared mixture was analyzed by running a blank and was found to be 62/37 % mol (benzene/methylnaphthalene) as shown in figure 10.1.

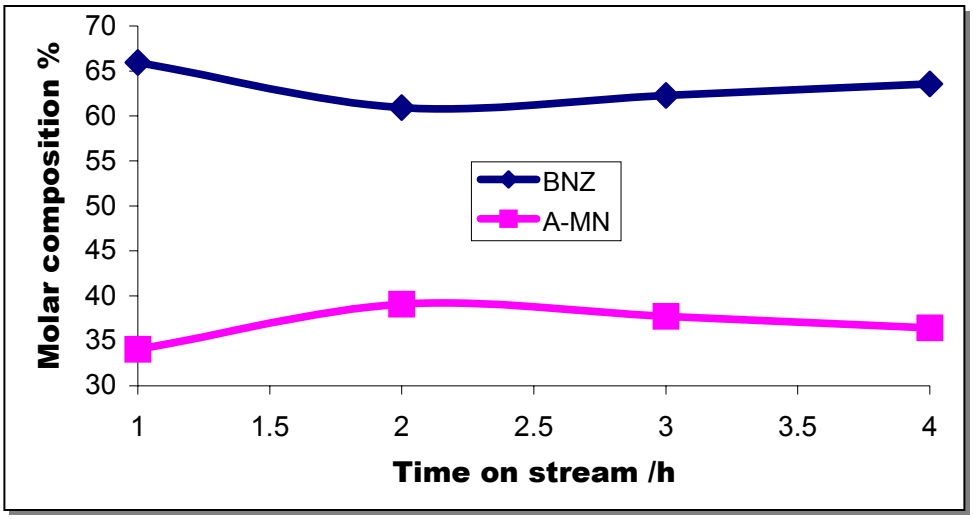

Figure 10.1: Blank run (mol %) of the benzene (BNZ) and methylnaphthalene (MN) system at 400 °C

The α-methylnaphthalene was a liquid at room temperature and so benzene was not necessarily acting as a solvent but simply as a reactant.

10.3 Results and Discussions

10.3.1 Conversion calculation problems

It was observed earlier during alkyl-transfer reactions of simpler alkylaromatics that the bulky molecules tend to diffuse slowly through the catalyst, allowing smaller molecules to diffuse quickly and thus concentrate themselves in the product stream;

and this complicated conversion calculations. This resulted in conversions being represented as toluene amounts in the product stream during transalkylation studies in the previous chapter since the intention of the study was to look at transalkylation reactions. The situation was even worse in the reaction between benzene and methylnaphthalene as shown in figure 10.2 below.

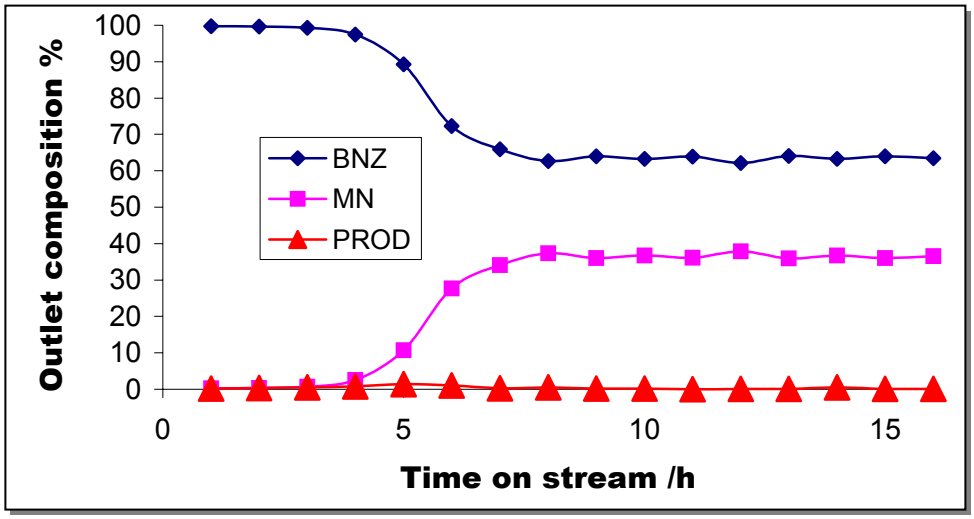

Figure 10.2: Outlet stream (mol %) of the reaction between benzene (BNZ) and α-methylnaphthalene (MN) (62/37 mol %) on H-mordenite at 200 °C; PROD = products

The outlet stream was mainly composed of benzene (~ 100 %) during the first 5 hours of the reaction and there was no sign of methylnaphthalene. Conversions could not be based on benzene since initially there was 62 % in the inlet stream and then there was almost 100 % in the product stream as if there was benzene production in the system. Methylnaphthalene was hardly observed in the outlet stream which implied consumption but there were no/or little of products observed. Like in the case of benzene-mesitylene transalkylation, toluene formation was to be used as an indication of transalkylation reactions; this was based on the fact that toluene was a transalkylation product and the advantage was that it was small enough to diffuse through the catalyst with great ease. The use of toluene to follow the transalkylation reaction had a very good advantage because its presence in the product stream also

indicated the catalyst's lifetime with respect to the desired reaction (transalkylation) and this was based on the fact that the transalkylation intermediate was the smallest (scheme 10.1) in the system. Though the disproportionation of toluene itself had an even smaller intermediate, its formation would not have any effect on transalkylation calculations.

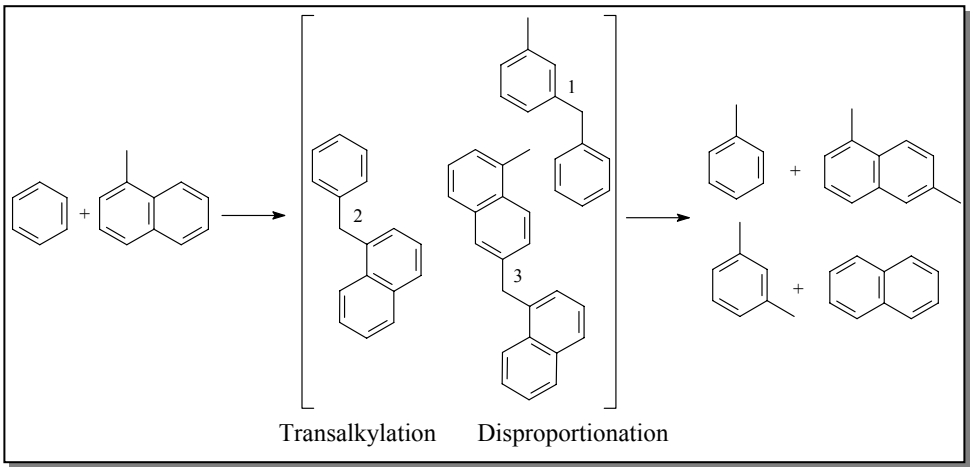

Scheme 10.1: Alkyl-transfer intermediates during benzene-methylnaphthalene transalkylation

The absence of toluene in the product stream should signify the absence or the inhibition of a transalkylation route in the zeolite. During hydrocarbon conversion in zeolites deactivation was mainly due to carbonaceous material deposition which blocked and narrowed the zeolite pores especially at higher temperatures, and thus alkyl-transfer intermediate inhibition should start with the disproportionation intermediate because of its bigger molecular size; and thus the absence of toluene in the stream signified the total catalyst deactivation point. The only major setback with using toluene as a measure of transalkylation reactions was that its amounts in the product stream did not really show levels of conversion since transalkylation to smaller molecules was not the only reaction route in the system.

These conversion calculation problems could be circumvented by using an inert substance that cannot 1) undergo any transformation in the zeolite under any conditions to avoid competing for active sites, 2) be preferentially adsorbed or

trapped within the catalysts, 3) be bulky such that it interferes with the formation of the transition state (intermediates). Such a compound was going to be useful in the mass-balance calculations but it was not sorted out; the substance had to be flammable so to be detected by the FID detector. A TCD (thermal conductivity detector) would have been able to detect even nitrogen but was not available for immediate use.

10.3.2 Benzene-Methylnaphthalene transalkylation on H-mordenite

There were very little amounts of products (figure 10.2) in the outlet stream suggesting that conversions were too low or products could not diffuse out of the catalyst; this was further supported by the fact that a lot of methylnaphthalene was somehow consumed but the expected significant amounts of toluene and naphthalene were not observed, implying that transalkylation was not the only reaction route. Figure 10.2 showed considerable molecular retention by the zeolite and this was mainly attributed to the sizes of molecules involved and reaction temperatures which were lower than the boiling temperature of some bulky molecules that might have formed in the zeolite.

The appearance of methylnaphthalene after 5 hours of time on stream in figure 10.2 was most probably due to filling up of pores and cavities of the zeolite which led to it not being able to adsorb/absorb and retain more molecules. Though there were almost no products in the outlet stream the little that got out of the catalyst were analyzed and plotted against time on stream and this is shown in figure 10.3. The good thing was that even though there were low conversions there were transalkylation reactions in the zeolite producing toluene (TOL).

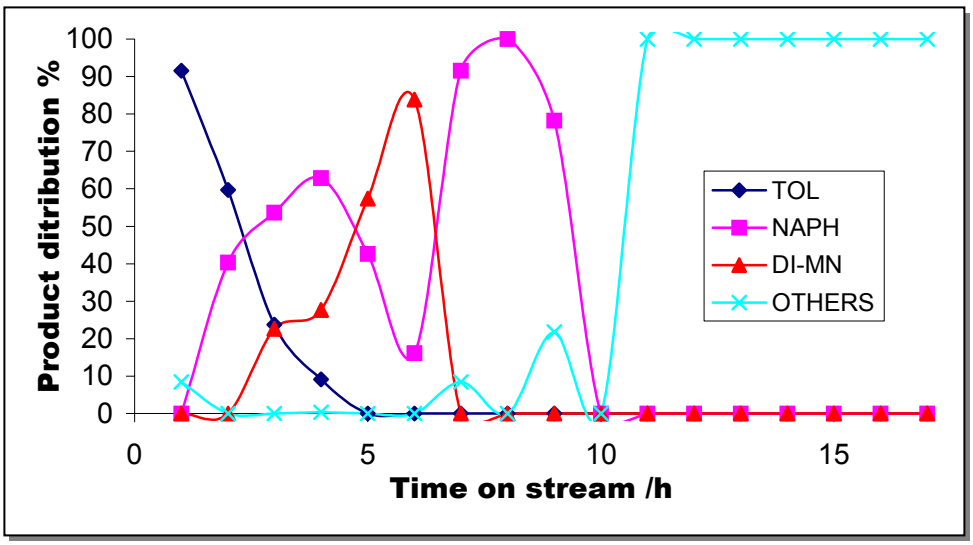

Figure 10.3: Benzene-methylnaphthalene transalkylation (mol %) on H-mordenite at 200 °C; Product distribution

Toluene, as expected, diffused out of the zeolite with great ease and concentrated itself in the product stream and thus being shown as the major product during the early stages; similar behaviour was observed during ethylbenzene disproportionation reactions on zeolite-Y.

It was no coincidence that toluene disappeared in the product stream after 5 hours which was exactly the same time at which methylnaphthalene showed up in the outlet stream (see figure 10.2). Considering catalyst deactivation either by site blocking or by site poisoning and molecular retention, there was unquestionably molecular build-up in the catalyst. This will consume the reaction space where bulky intermediates form, inhibiting firstly disproportionation then transalkylation. Thus the disappearance of toluene marked the catalyst death point (deactivation).

The slow diffusion of bulky molecules was shown by the appearance of naphthalene (NAPH) after 2 hours of the reaction since the production of toluene meant simultaneous formation of naphthalene. After 3 hours, the bulkier dimethylnaphthalene (DI-MN) showed up in the product stream and its formation was probably through both routes; i.e. disproportionation between two

methylnaphthalene molecules and transalkylation between toluene formed in the zeolite and methylnaphthalene. Considering deactivations being due to molecular build up in the zeolite at these low temperatures, it was apparent that the bulky molecules must have formed during the very early stages of the reaction while the catalyst was still having enough room for bulky intermediates to form. With growth of carbonaceous material in the zeolite, disproportionation got inhibited and the only route towards the formation of dimethylnaphthalene was now through transalkylation between toluene and methylnaphthalene; this was so because toluene was small enough to access the active sites even though there was steric stress. Further growth of carbonaceous material presumably pushed out retained (bulky molecules, 'OTHERS') molecules and since the growth was irregular the product stream also showed some chaotic behaviour.

Toluene formation resulted from transalkylation reaction through mainly the bimolecular phenyl-methyl-naphthalene (scheme 10.2(1)) rather than the dealkylation-realkylation mechanism, because of the instability of the methane radical. The transalkylation reaction went through the smallest bimolecular intermediate in this system.

The dimethylnaphthalenes resulted from the disproportionation reaction which proceeded through the bulky dinaphthylmethane intermediate (scheme 10.2(2)) but most probably through transalkylation between toluene and methylnaphthalene. GCMS showed that some of the species presented as 'others' were the phenylnaphthalene (3), anthracene (4) and phenanthracene (scheme 10.2(5)).

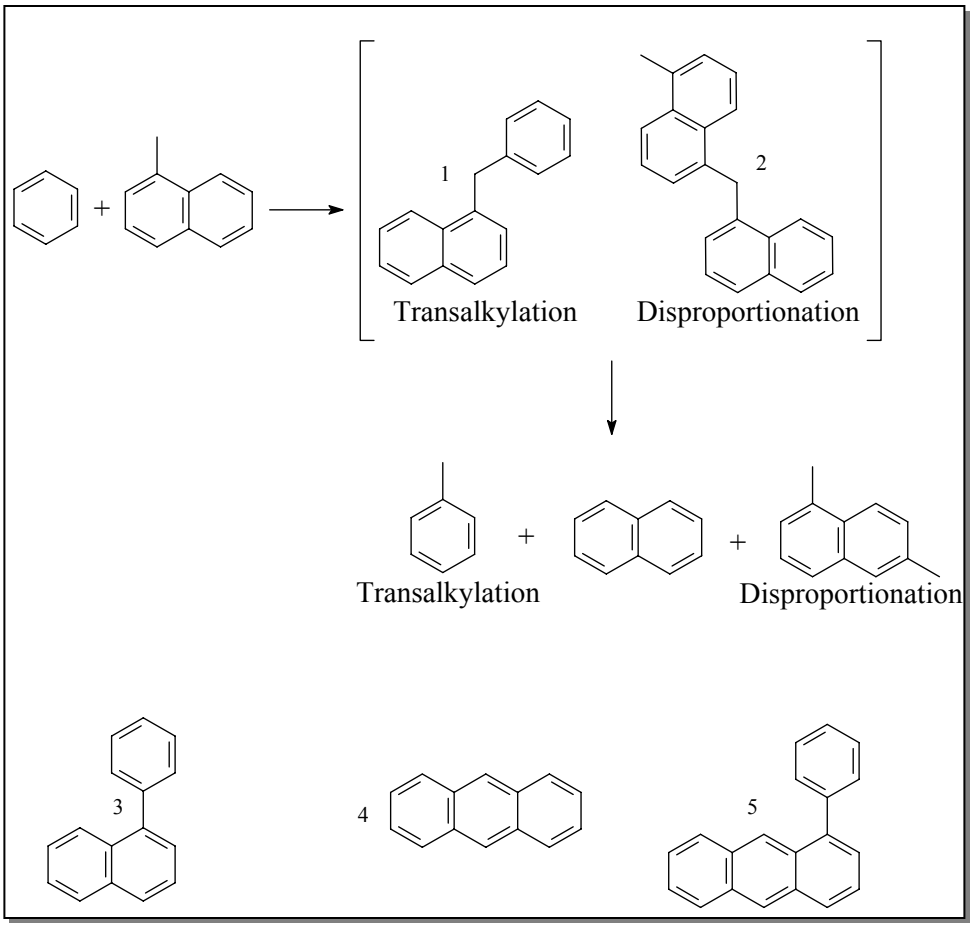

Scheme 10.2: Primary reactions of benzene-methylnaphthalene transalkylation reactions on zeolites

These bulky molecules most probably resulted from the adsorption of benzene and/or naphthalene (alkyl-free molecules) on the active sites, which does not favour transalkylation. Such adsorption blocks access of the bulky alkyl-containing molecules, which should be the adsorbed species for alkyl-transfer to occur. The formation of the bulky 'others' showed that the reaction feed should not consist of too much of the alkyl-acceptor so as to avoid side reactions, and again the alkyl-containing molecule should not be much either to avoid disproportionation. In a nutshell, the above suggested that the feed composition was a very important parameter to be considered and as concluded earlier during transalkylation reactions between benzene and mesitylene, the manipulation of the feed should result in a very effective transalkylation system.

Considering the fact that in zeolite catalysts deactivation was mainly due to carbon deposition which blocked the active sites and narrowed the pores, one should expect the disproportionation reaction which goes through the bulkier intermediate to occur during the early stages of the reaction while the catalyst is free of coke and still has enough space. With this being so, one should expect the dimethylnaphthalene to appear at least at the same time as naphthalene in the product stream (scheme 10.3); but that was not the case due to molecular retention and diffusion problems. Another reason for the retention of the bulky molecules in the zeolite might be that of low temperatures (200 °C) at which the reaction was run.

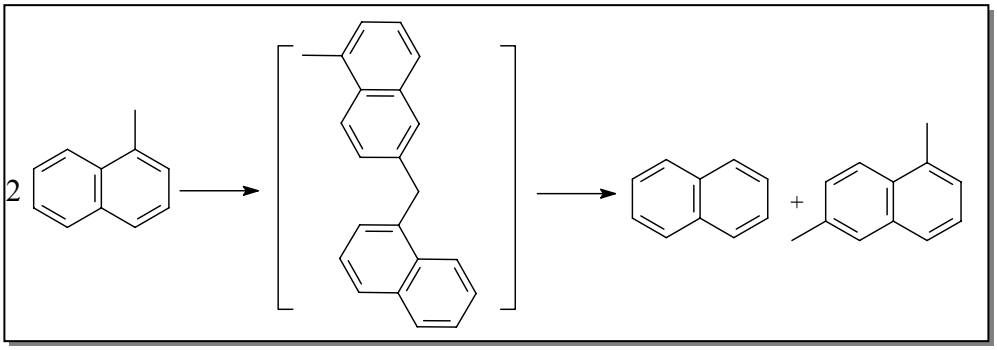

Scheme 10.3: Disproportionation of methylnaphthalene

From the proposed transalkylation mechanism with the benzene-mesitylene system (scheme 9.1), it was suggested that the benzene-α-methylnaphthalene would follow the same route with α-methylnaphthalene being the adsorbed species on the active site (scheme 10.4).

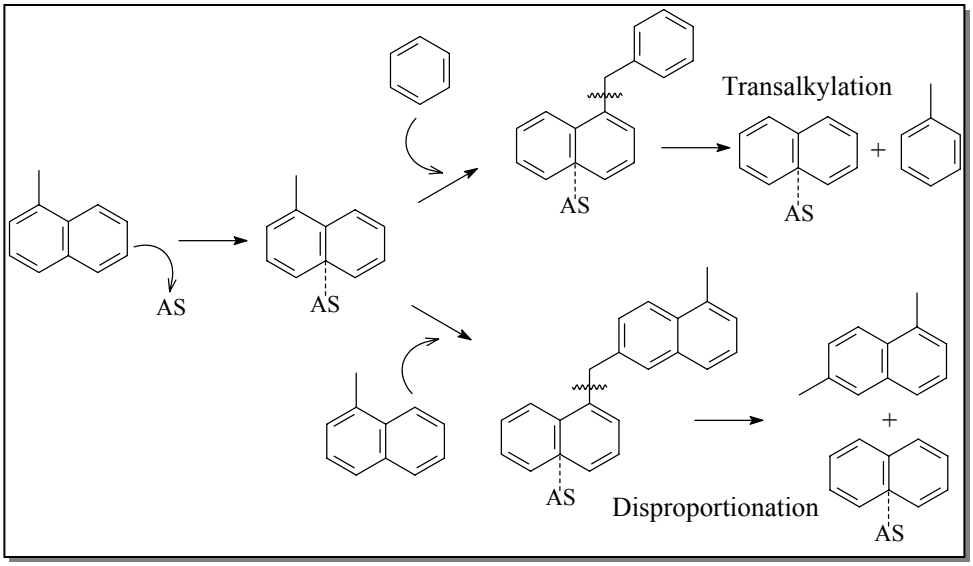

Scheme 10.4: Proposed alkyl-transfer mechanism; **AS** = active site

Two types of competition between the reactant molecules and products existed in the zeolite catalyst. The first one was the rate of diffusion through the pores of a zeolite which would obviously favour the diffusion of the smaller benzene and toluene molecules; the second type was the affinity for the active sites in the zeolite which favoured the more basic α-methylnaphthalene but there was some selectivity which was induced by carbon deposition and pore narrowing. This showed that with time on stream, toluene was preferentially adsorbed instead of the alkylnaphthalene, and this probably led to back transalkylation from toluene to naphthalene and methylnaphthalene forming alkyl-naphthalenes. Unfortunately the above was very difficult to observe in the product stream but the reaction will be proved in the following chapter.

The total deactivation by carbon deposition preventing transalkylation was observed after 5 hours (disappearance of toluene in the product stream, figure 10.3) at 200 °C.

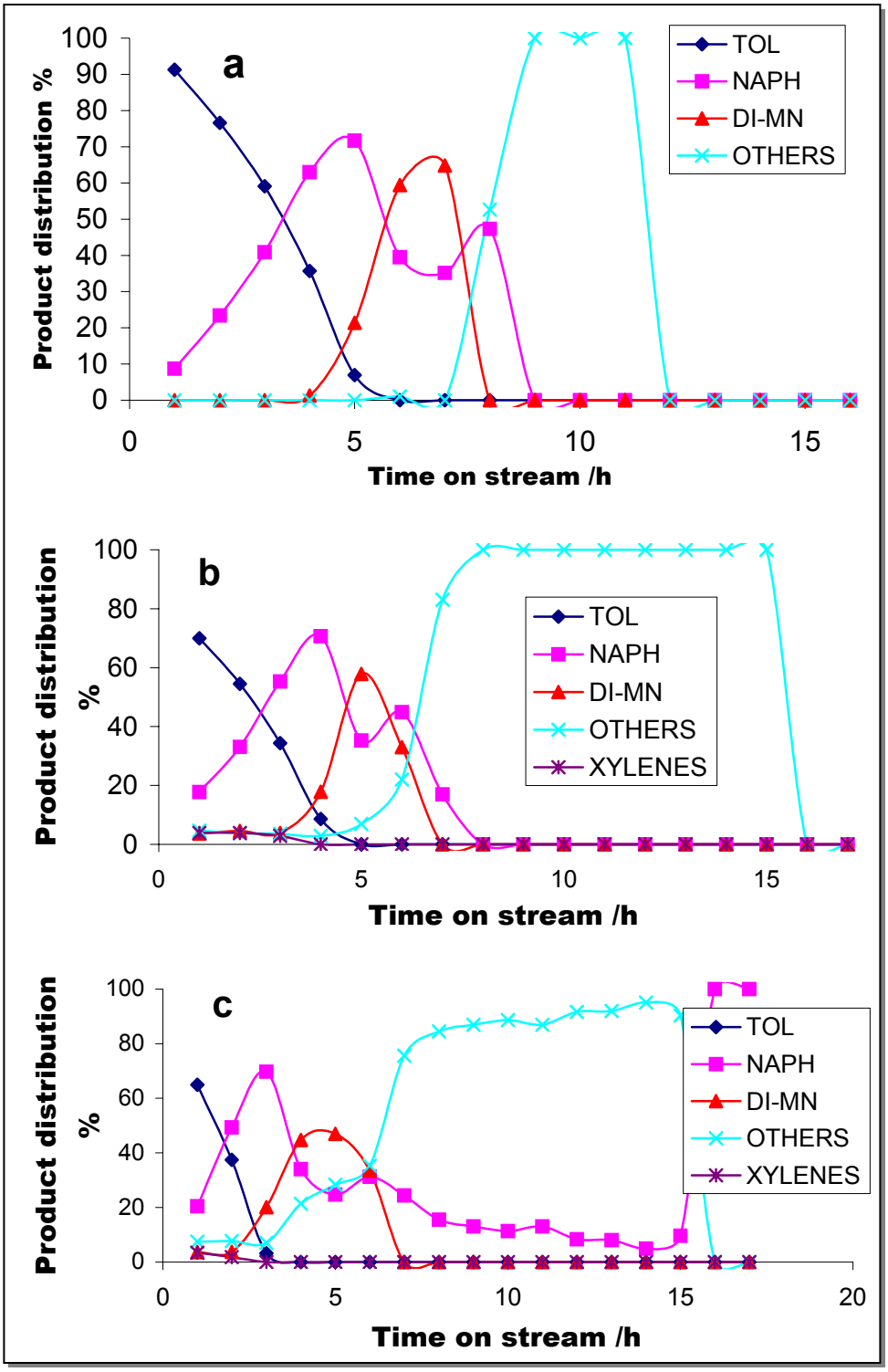

Figure 10.4: The effect of temperature on the product stream of the benzene-methylnaphthalene transalkylation reaction (mol %); a = 250 °C, b = 350 °C and c = 400 °C

The increase in the reaction temperature resulted in an increase in deactivation rates as expected. Figure 10.4 shows the same trend in the product streams at 250, 350 and 400 °C respectively, showing a decrease in the initial concentration of toluene in the product stream which might be mistakenly viewed as a decrease in transalkylation activity.

In fact the retention of bulky molecules was inhibited to some extent by higher temperatures causing a dilution of toluene in the product stream and not that little of it was produced. This was based on the fact that in the previous chapters it has been showed and concluded that higher temperatures favoured transalkylation. Thus the decrease was caused by desorption/diffusion of other molecules altering the outlet composition.

This led to the conclusion that toluene concentrations and patterns could not be used to show the activities of the catalyst but was very reliable in showing the catalyst lifetime. This was based on the fact that an increase in temperature almost always leads to an increase in conversion and the figure shows otherwise if toluene traces are followed. It was earlier concluded that transalkylation for these binary systems is favoured at high temperatures, and it was expected of figure 10.4 to show increase in the amounts of toluene in the product stream with temperature. Considering the fact that the rate of carbonaceous material deposition increases with increase in temperature, then this should also mean that there was an increase in the rate of pore narrowing, and this will favour the smaller transition states and diffusions of the smaller molecules. The figure shows the early appearances of the bigger molecules in the product stream and this surely meant improvement in diffusion rates, but the shortened time at which toluene disappear in the stream supported the fact that deactivation rate increased. The early appearance of the bulky molecules was then attributed to enhanced diffusion/desorption rates due to increased kinetic motions of molecules. If the suggestion of carbon growth in the catalyst, pushing and squeezing retained molecules out of the zeolite is true, then it would also comply with the

observations since increase in temperature would also result in increase in carbon growth rates leading to earlier appearances of retained bulky molecules.

The increase in conversion that accompanied an increase in temperature was shown by plotting the amounts of products (extent of conversion) that diffused out in the outlet stream against time on stream in figure 10.5 below; the figure also shows the increase in deactivation rates (catalyst lifetime).

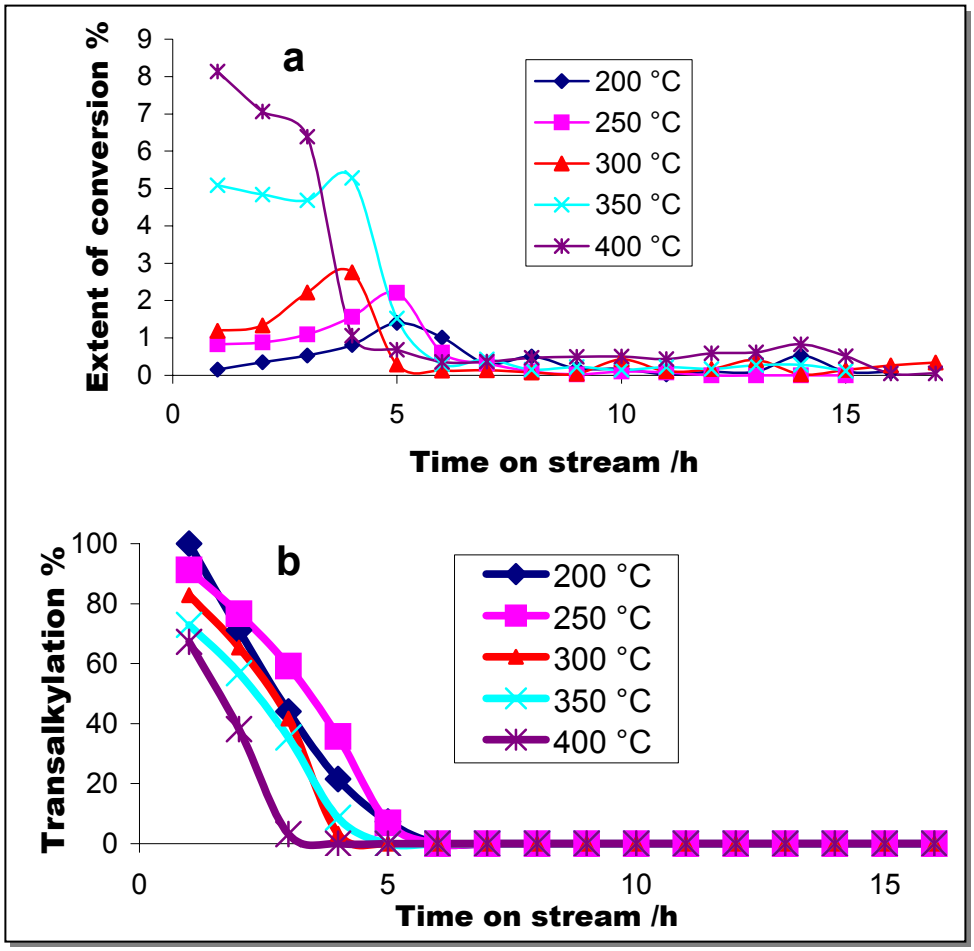

Figure 10.5: Benzene-methylnaphthalene transalkylation (mol %) on H-mordenite; a) extent of conversion, b) catalyst lifetime with temperature.

The figure shows that there was a very short lifetime on mordenite as shown also by the toluene disproportionation study. The lifetime lasted for at least 5 hours at low temperatures and this shortened with increase in temperature.

10.3.3 Benzene-methylnaphthalene transalkylation on HLZY-82

The presentation of the transalkylation reaction as the amount of toluene produced like it was done for the reactions on H-mordenite was also adopted here. The depiction in figure 10.6 showed (not obviously so) that there was an increase in deactivation rates with increase in temperature and with time on stream.

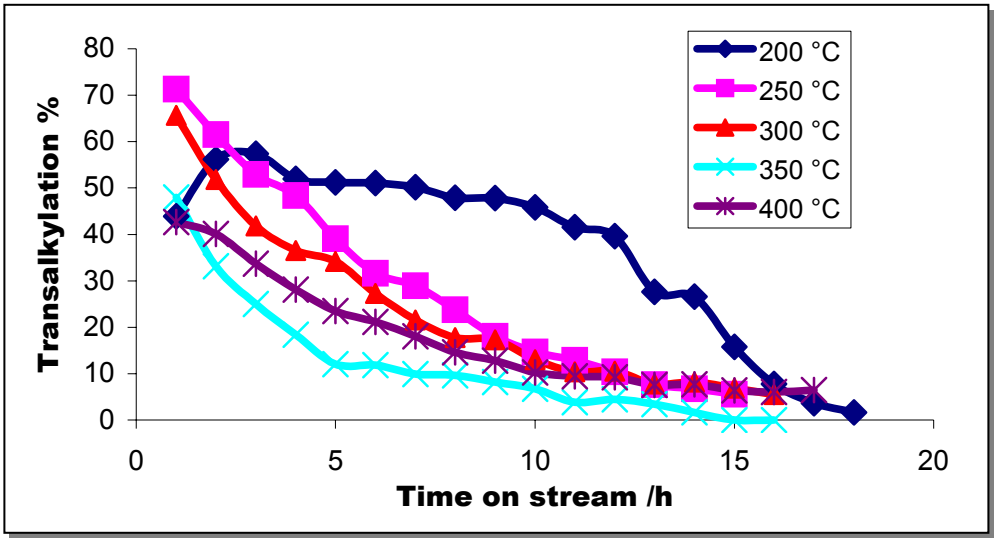

Figure 10.6: Benzene-methylnaphthalene transalkylation (mol %) on HLZY-82

Figure 10.6 also showed that the larger 3-D cavities of the zeolite-Y improved the lifetime of the catalyst. This further supported the fact that the reactions occurred in the pores of the zeolite not on the external surface, and deactivation was due to carbon deposition and retention of bulky molecules by the zeolite. Figure 10.6 also suggested that total deactivation occurred after 18 hours depending on the reaction temperature on this catalyst. Again the observed decrease in the amount of toluene in the product stream with increase in temperature was not due to the reason that less of

it was being produced but due to the enhanced diffusion rates of other (bulkier) molecules as also observed on mordenite (figure 10.5). Retention of molecules was also observed on the more open zeolite-Y and this is shown in figure 10.7 below. The figure also shows why zeolites (porous material) are sometimes used to separate gaseous and liquid mixtures.

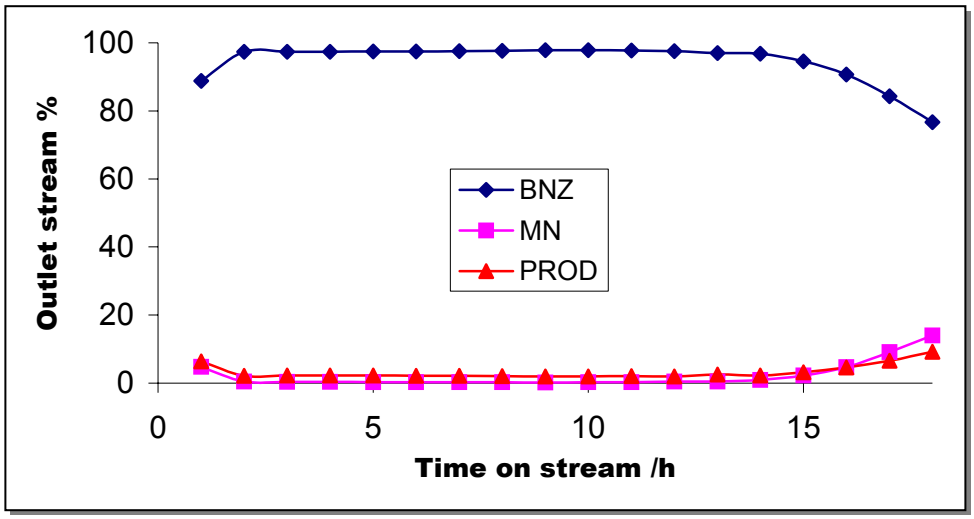

Figure 10.7: Benzene-methylnaphthalene transalkylation (mol %) on HLZY-82; Molecular retention

As expected, there was an increase in the overall conversion with temperature as shown by figure 10.8; the figure only shows the total amount of products in the outlet stream.

The figure shows what looks like a very long induction period, and the traces which were almost opposite traces shown in figure 10.5(a), which showed the amounts of products in the outlet stream. Figure 10.8 somehow supported the suggestion that carbon growth in the zeolite pushes out trapped molecules, but the most probable explanation was that of the slow diffusion of bulky molecules in this open structured zeolite.

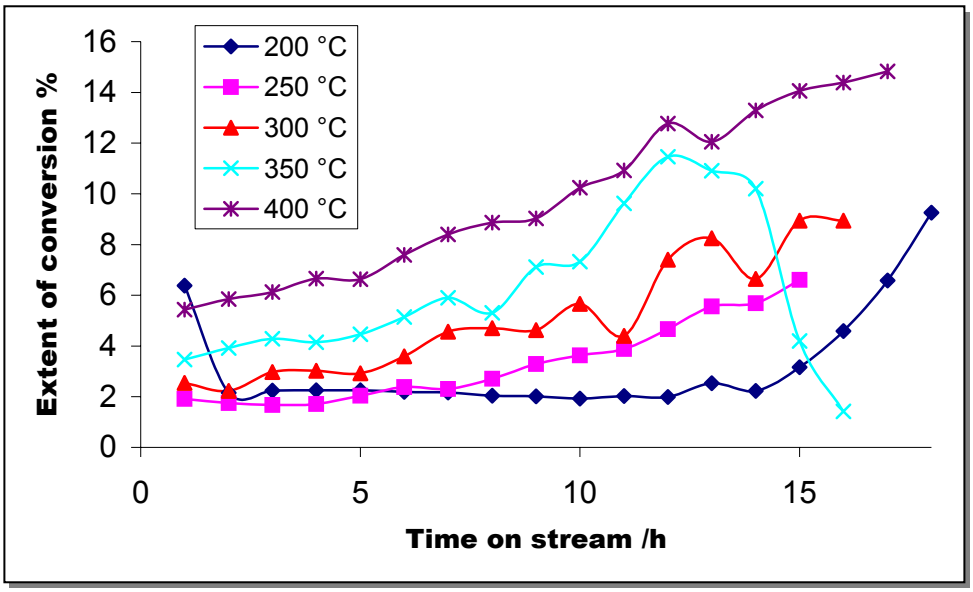

Figure 10.8: Benzene-methylnaphthalene transalkylation (mol %) on HLZY-82; the extent of conversion

The product stream of the reaction at 200 °C showed amazing results and the great potential of the zeolite-Y in transalkylation reactions of bulky molecules as compared to mordenite; showing the advantages of a three-dimensional structure as there was production of the xylenes (figure 10.9). There were two reaction routes which may have led to the production of xylene in the system which were somehow related to the catalyst structure since this was not observed on H-mordenite. Xylene could have been formed through the disproportionation reactions of toluene, or through secondary transalkylation between toluene formed in the zeolite (primary reaction) and alkyl-naphthalenes. Toluene disproportionation in this case would interfere with the desired reaction because a toluene molecule would be required to adsorb on the active site then another toluene molecule would come for the methyl group; thus the site would be used for a side reaction rather than transalkylation. On the other hand the formation of xylene through a secondary transalkylation from alkyl-naphthalenes to toluene would actually be favourable because the presence of a methyl group on the benzene ring (toluene) facilitates the addition of another alkyl group and this does not interfere with the intended transalkylation reactions. The only advantage the former route has over the later is that the toluene molecule is small enough to access

sites with less constrains and the transition state formed will be favoured due to smaller sizes.

The amount of toluene in the product stream on mordenite disappeared after 5 hours (figure 10.3) on stream and at the same time the naphthalene-dimethylnaphthalene lines crossed. The same behaviour was shown by the zeolite-Y (figure 10.9) where toluene disappeared after 18 hours and at the same time the naphthalene-dimethylnaphthalene lines crossed. If the observations on both figure 10.3 and 10.9 were solely related to diffusion rates then figure 10.9 should show the crossing point of naphthalene/dimethylnaphthalene earlier than it's shown in figure 10.3 since the zeolite-Y had a 3-D structure and thus enhanced diffusions. This somehow supports the suggestion that carbon growth in the zeolite ultimately pushes trapped molecules out of the zeolite.

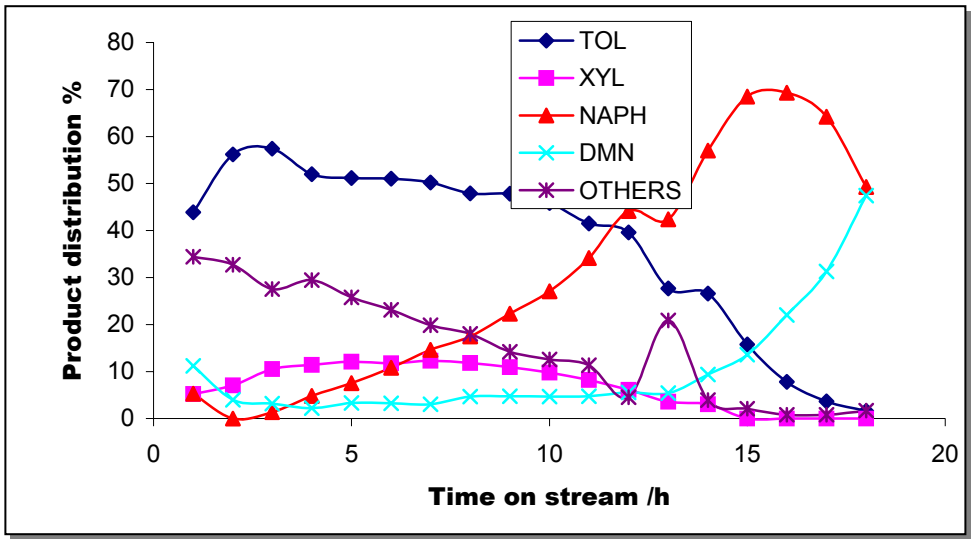

Figure 10.9: Benzene-methylnaphthalene transalkylation (mol %) on HLZY-82 at 200 °C; product distribution

Figure 10.9 can somehow be viewed as a magnification of the mordenite product stream during the first 5 hours. This suggested that, if the reaction had been allowed to go on for more than 18 hours, then the same behaviour in the product stream as

that on mordenite was going to be observed. If the above is true, then figure 10.9 showed the remarkable stability of the zeolite-Y.

At 250 °C (figure 10.10), there was more than 10 % of xylene during the initial stages of the reaction, 70 % of toluene and more than 10 % of naphthalene was observed and all other products were in very small quantities (> 3 %). This observation was not expected because higher temperatures should have meant enhanced diffusion rates and thus bulky molecules were expected to show up early in the product stream, their absence implied that they did not form though there was available reaction space. The only logical explanation for the observation was that there was selectivity in the system induced by higher temperatures. This is something that was observed earlier in the study that higher temperatures seemed to favour transalkylation. Judging by the presence of only toluene, xylene and naphthalene in the product stream, it was obvious that there was no methylnaphthalene disproportionation but transalkylation was dominant. The question is, why is this observed on the zeolite-Y and not on mordenite?

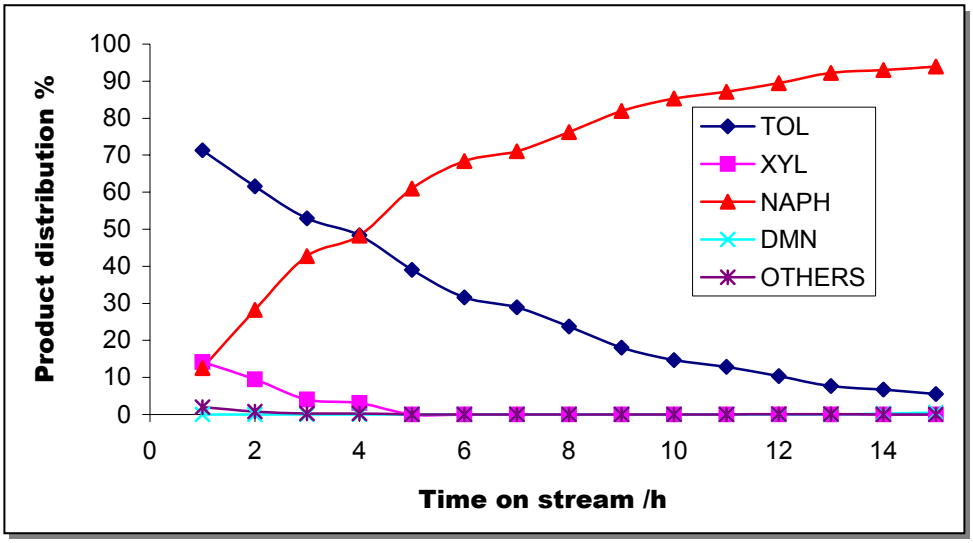

Figure 10.10: Benzene-methylnaphthalene transalkylation (mol %) on HLZY-82 at 250 °C; product distribution

The dominance of toluene and xylenes in product stream during the early stages of the reaction supported the fact that they diffused quickly out of the zeolite pores and the bulky naphthalene was retained for some time. With the decrease of toluene in the product stream caused by catalyst deactivation, naphthalene concentration increased as more of it desorbed and diffused out. The observations at longer time on stream may not be because more of the naphthalene desorbed, but that it was becoming the only product in the product stream.

Increasing the reaction temperature to 350 °C resulted in an almost complete disappearance of xylene and dimethylnaphthalene in the product stream (figure 10.11). The product stream showed the coming together of the naphthalene-dimethylnaphthalene lines which did not cross perhaps due to the higher rate of deactivation induced by higher temperatures, i.e. more carbon formed rapidly trapping molecules. The fact that the two lines did not cross showed that there was probably less methylnaphthalene disproportionation to form dimethylnaphthalene with increase in temperature, this further suggested that with a further increase in temperature the methylnaphthalene disproportionation could be inhibited. On the other hand, disproportionation may not be the only route to the dimethylnaphthalene formation; it could be resulting from transalkylation between toluene and methylnaphthalene (back transalkylation). The observed coming together of the two lines in figure 10.11 was much related to the fact that the same temperature showed the worst deactivation rate (figure 10.6) and thus the resulting behaviour should be from the same line of reasoning.

Further increase in temperature to 400 °C resulted in only toluene and naphthalene (transalkylation products) in the product stream (figure 10.12). The fact that increase in temperature resulted in increased molecular motions and enhanced diffusions was supported here by looking at figures 10.9, 10.10 and 10.11; focusing on the naphthalene traces, it is apparent that more molecules started showing up earlier in the product stream with increase in temperature. The same temperature effect should

have been shown by the dimethylnaphthalene in figure 10.12 but its absence suggested that it did not form.

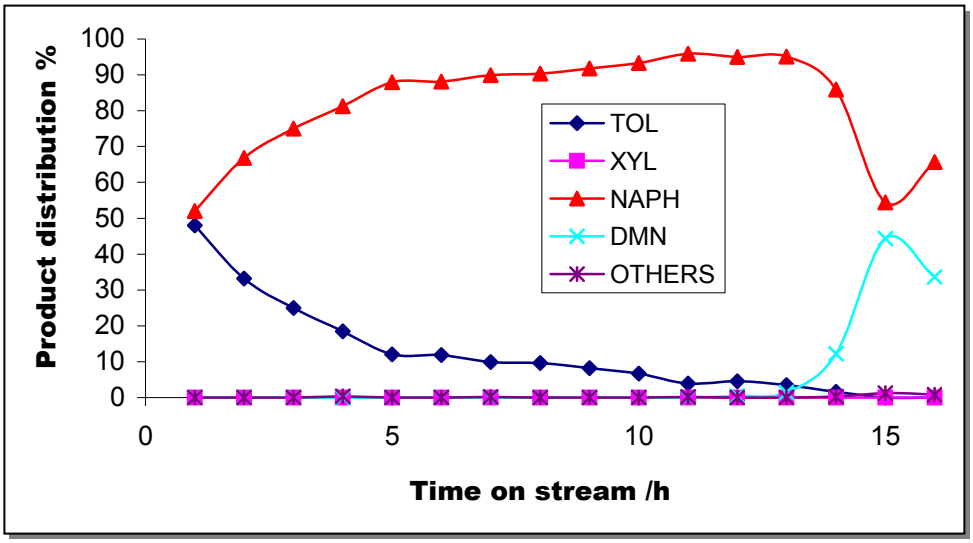

Figure 10.11: Benzene-methylnaphthalene transalkylation (mol %) on HLZY-82 at 350 °C; product distribution

The above suggested that there was preferential adsorption of methylnaphthalene on the active site and that toluene despite its smaller size was discriminated against. This was based on that fact that xylene was not observed in the product stream; but again the possibility that the adsorption of toluene could have resulted in back transalkylation to naphthalene (reverse reaction) cannot be rule out.

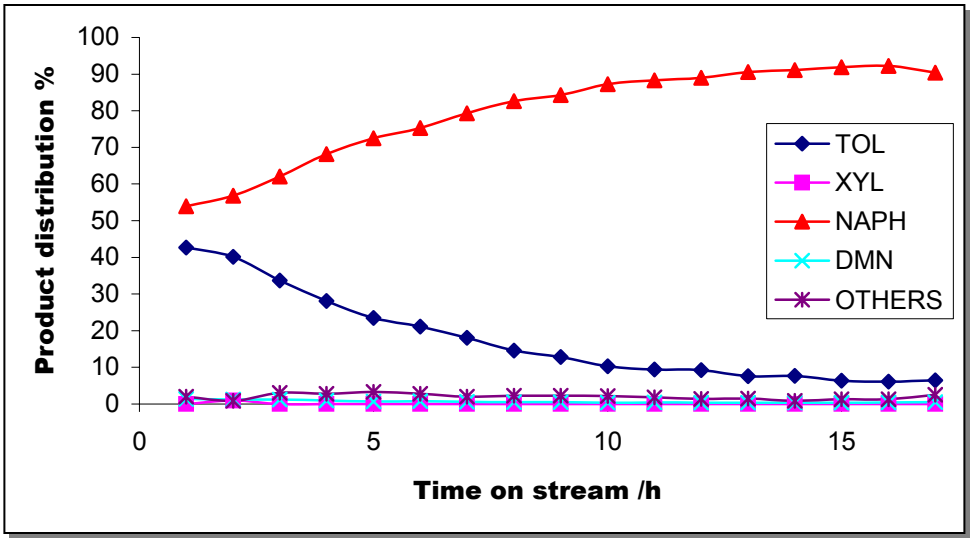

Figure 10.12: Benzene-methylnaphthalene transalkylation (mol %) on HLZY-82 at 400 °C; product distribution

10.4 High temperature reactions

It was observed earlier that there was some selectivity which was temperature induced on the zeolite-Y with the Benzene-methylnaphthalene transalkylation system, and this was observed at temperatures ranging from 200 to 400 °C. To confirm the observed selectivity, a 75/24 % mol benzene-methylnaphthalene mixture was prepared and studied at temperatures ranging from 400 to 600 °C on both catalysts; other reaction conditions remained unchanged.

Figure 10.13 below shows the percentage amount of transalkylation products (sum of toluene, xylene and trimethylbenzene) in the product stream on H-mordenite. During the first few hours of the reaction at 400 °C, of the 7 % of the total products about 4.4 % was the alkyl-benzenes (smaller molecules) and the amount decreased sharply with time on stream. Increase in temperature resulted in the decrease in amount of transalkylation products in the product stream. This was mainly attributed to the higher rate of carbonaceous material deposition which favoured consumption of smaller molecules as well as strong sites responsible for their transformations. It

would be demonstrated in the following chapters that at high temperatures deposition occurs immediately when an alkylaromatic contacts the catalyst, and thus covering it with carbonaceous materials and rendering it ineffective.

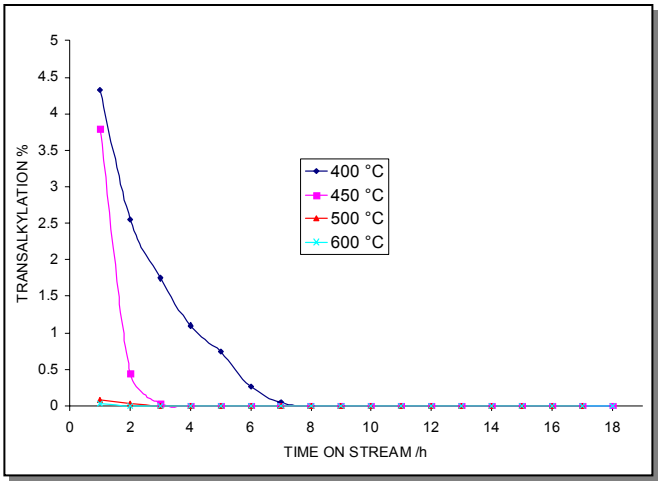

Figure 10.13: Benzene-methylnaphthalene (75/24 % mol) transalkylation on H-mordenite

Figure 10.14 below shows the effects of high temperatures on the zeolite-Y. The transalkylation activity increased with increase in temperature from 400 to 450 °C but decreased at 500 °C and higher temperatures due to carbon formation. Figure 10.13 and 10.14 showed expected behaviour but the rapid deactivations of the mordenite and the fact that higher temperature favoured deactivation is greatly highlighted.

The effects then of temperature in the product stream on H-mordenite are shown in figure 10.15. The figure also shows the disappearance of toluene in the product stream with increase in temperature, showing probably its participation in carbonaceous material deposition; this was accompanied by the crossing over of the naphthalene/dimethylnaphthalene traces as expected on mordenite.

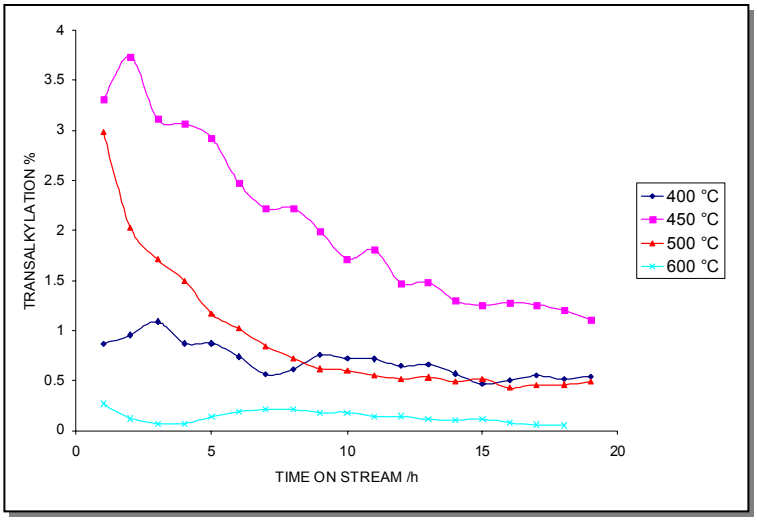

Figure 10.14: Benzene-methylnaphthalene (75/24 % mol) transalkylation on HLZY-82

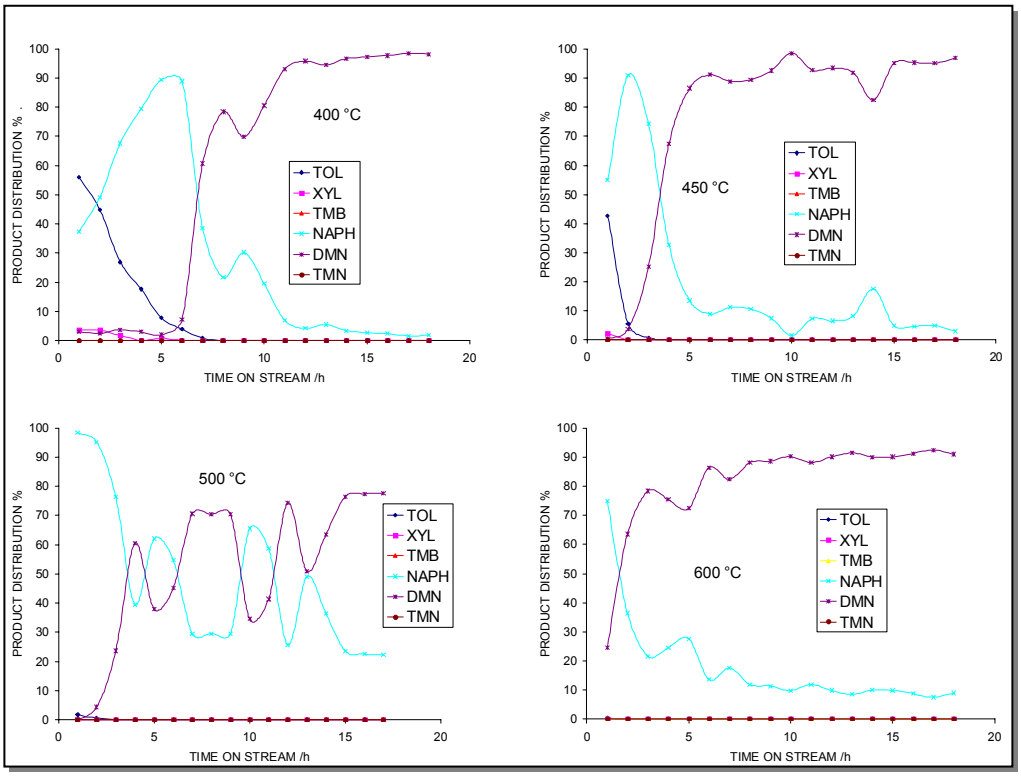

Figure 10.15: Benzene-methylnaphthalene (75/24 % mol) transalkylation on H-mordenite

The first point of the crossing of these lines shortened (with time on stream) with increase in temperature further supporting the dependence of deactivation rate on

temperature. Though there was disappearance of toluene with temperature in the product stream, it was not attributed to the absence of alkyl-transfer but to its contribution to carbonaceous material deposition. The observed increase/formation of dimethylnaphthalene was then associated with the dealkylation/realkylation mechanism at these high temperatures.

The presence of mainly toluene and naphthalene in the product stream of the reaction on the zeolite-Y was shown at temperatures ranging from 400 to 500 °C (figure 10.16). At 600 °C dimethylnaphthalene was observed during the first 2 hours then again after 16 hours of time on stream.

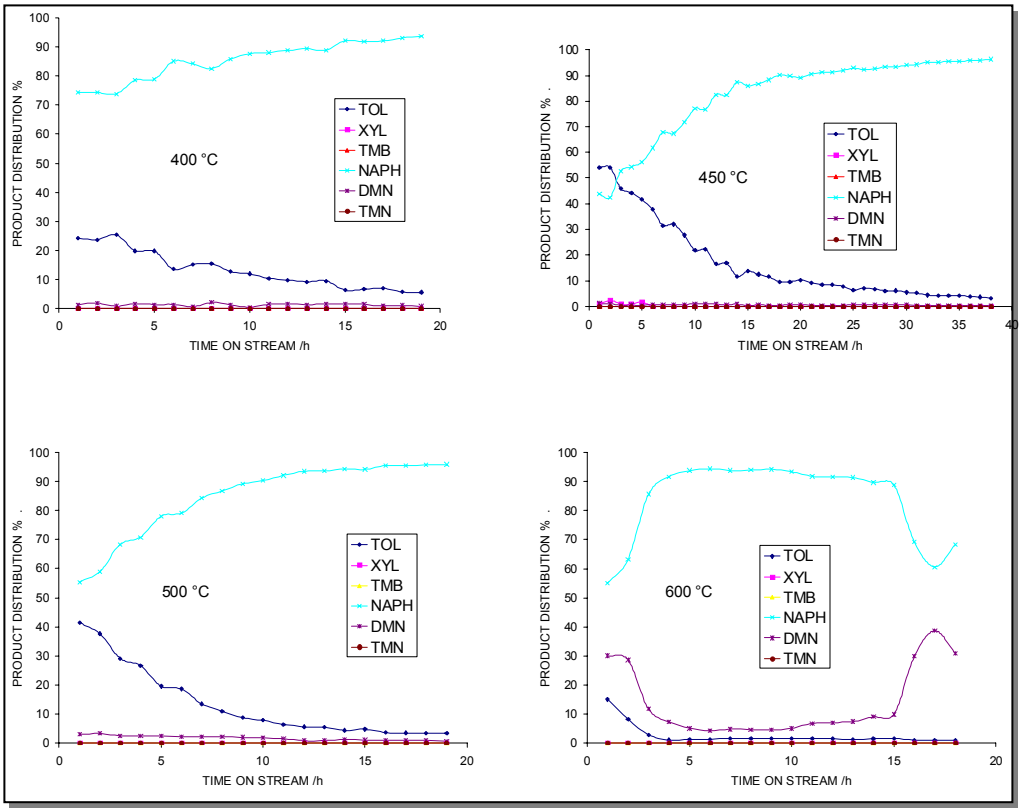

Figure 10.16: Benzene-methylnaphthalene (75/24 % mol) transalkylation on HLZY-82

Higher amounts of toluene were observed at 450 °C and dimethylnaphthalene did not show up even when the reaction was allowed for 38 hours in this case. The unusual

selectivity was somehow disturbed by higher temperatures. Still, the observed selectivity (absence of dimethylnaphthalene, ≤ 450 °C) was not understood. Nevertheless, this selective characteristic of the zeolite-Y will be very useful if conversions can be improved and an important reaction identified.

10.5 Conclusion

The very low conversions on this system as compared to the disproportionation system with smaller molecules further supported what was suggested during the transalkylation between benzene and mesitylene, that the alkyl-containing molecule must be the one adsorbed on the active site for any alkyl transfer reaction to occur. Since benzene was the smallest in the system, the possibility was that it blocked access to active sites for the methylnaphthalene since it was also in larger quantities. And again, access to active sites by bulkier methylnaphthalene was somehow affected by steric effects and hence the observed low conversions.

The observed selectivity on the zeolite-Y was inexplicable. Important results were that transalkylation from bulky molecules was a very possible reaction; though molecular diffusions for such bulky molecules might be problematic and this would lead to working at higher temperatures which are not good for catalyst's lifetime.

Overall the 3-D structure of LZY-82 proved to be the better way to go since it has shown resistance towards deactivation as compared to the uni-dimensional mordenite, this includes improved molecular diffusions and most of all selectivity towards the reaction of interest (transalkylation) with increase in temperature.

11 BENZENE-POLYMETHYLNAPHTHALENE TRANSALKYLATIONS

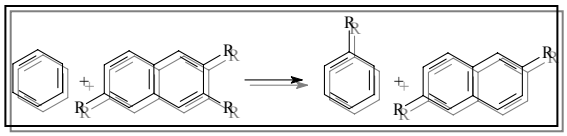

11.1 Introduction

Up to now alkyl-transfer (disproportionation) studies have shown that conversions increased with increase in number of alkyl groups on the aromatic ring. It has been shown also in the previous chapter that transalkylation between benzene and methylnaphthalene (mono-alkyl) gave low conversions and this was attributed to the lesser number of alkyl groups on the rings (naphthalene), and this was much expected since toluene (mono-alkyl) disproportionation has also shown almost similar observations. The observed low conversion on the transalkylation system (benzene-methylnaphthalene) was also attributed to the bulkiness of the methylnaphthalene which might have been a problem in accessing active sites. This however was not confirmed and thus the current study was to basically confirm the above by using even bulkier molecules; though the fact that there will be higher number of alkyl groups (higher conversions) might cause problems for the objectives of the study. The bulkier alkyl-aromatics used here were the di- and tri-methylnaphthalenes and transalkylation to benzene (which was a solvent and an alkyl-acceptor) was attempted on zeolites.

11.2 Experimental

Binary mixtures were prepared by dissolving alkyl-naphthalenes in benzene and the resulting mixture compositions were 50/49 mol % of benzene-(2,7-dimethylnaphthalene) and 79/21 mol % of benzene-(2,3,6-trimethylnaphthalene). The transalkylation study was carried out at 200 and 350 °C on both catalysts.

11.3 Results and Discussions

11.3.1 Benzene-dimethylnaphthalene transalkylation on H-mordenite

The outlet composition of the benzene-dimethylnaphthalene system at 200 and 350 °C is shown in figure 11.1, and it can be seen from the figure that there were very low conversions at both temperatures as observed with the methylnaphthalene system, and this was contrary to the xylene conversions which showed great differences (in terms of conversion) to that of toluene conversions. The figure also shows the retention of the bulky dimethylnaphthalene for at least 6 hours at 200 °C and about 9 hours at 350 °C. The differences brought about by the change in temperature on the retention of molecules despite the fact that conversions increased as well, were due to enhanced molecular diffusions since at 200 °C less of the products (PROD) was observed. With the possibility of disproportionation/transalkylation in the system for example, the 200 °C temperature was lower than the boiling temperatures (240-243 °C for methylnaphthalene) of some bulky molecules which in turn condensed in the catalyst, blocking the pores and filling up the zeolite and the appearance of dimethylnaphthalene after 6 hours was also due to the 'room-less' catalyst. Another view on this is that, the heat of physisorption of molecules increases as their size increase, and thus large (bulky) molecules will always be preferentially retained in the zeolite pores. Increase in temperature to 350 °C surely enhanced diffusions and thus better conversions and longer lifetime than at 200 °C; gas phase reactions were promoted as well.

It was expected that with the introduction of the second methyl group on the naphthalene ring the methyl group transfer to benzene (scheme 11.1) would be facilitated and a better conversion would be observed compared to the mono-alkyl methylnaphthalene (as was the case with toluene and xylene disproportionation). This was not really the case, and it was attributed mainly to the size of the transition state intermediate molecule. This intermediate was obviously bulkier than the benzene-methylnaphthalene intermediate and also to accessing of the active sites.

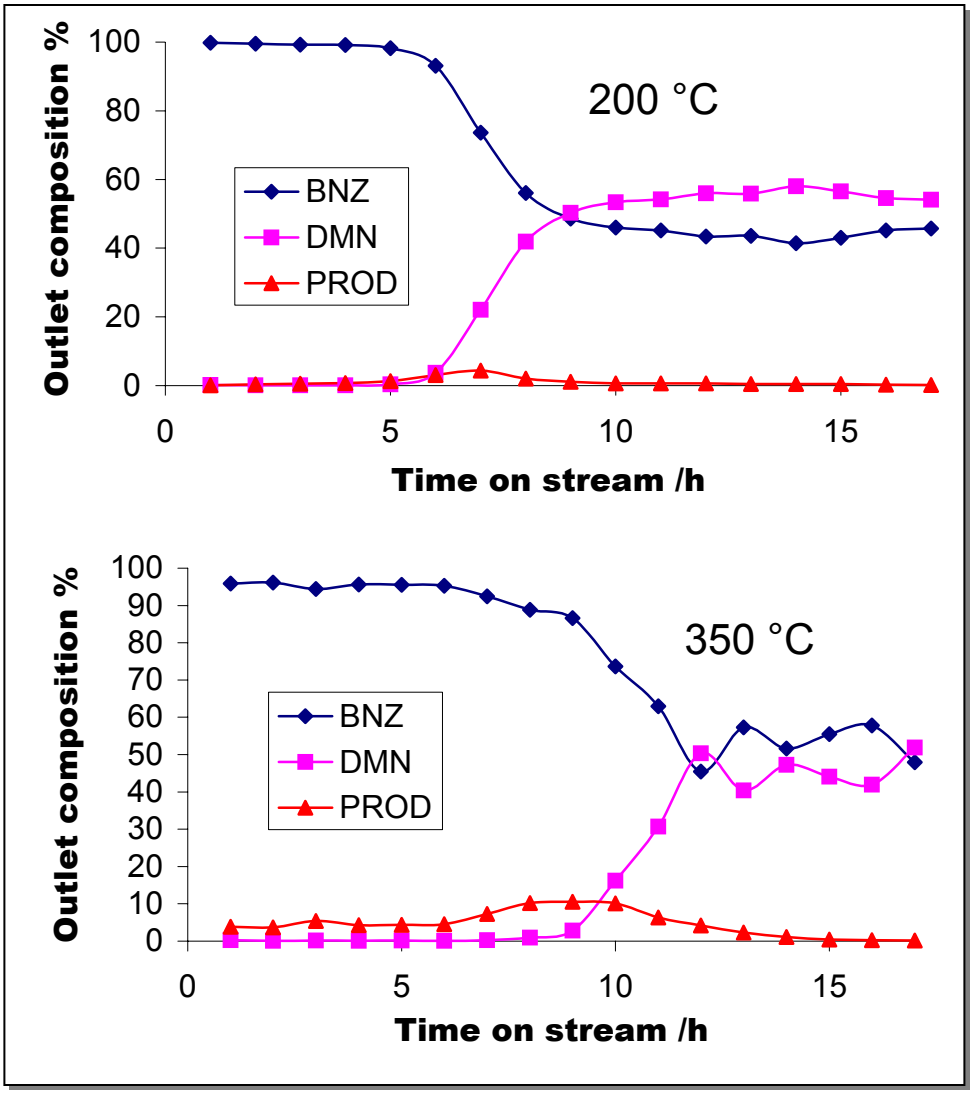

Figure 11.1: Benzene-dimethylnaphthalene transalkylation (mol %) on H-mordenite; outlet composition

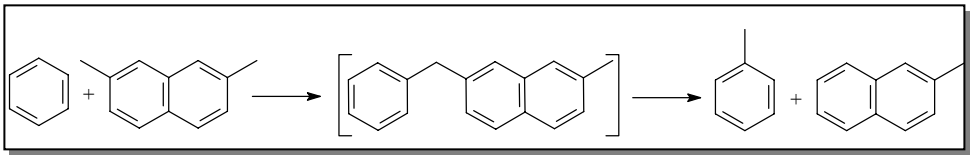

Scheme 11.1: Benzene-dimethylnaphthalene transalkylation

The product stream depicted in figure 11.2 showed that deactivation especially at 200 °C was mainly due to molecular retention than carbonaceous material deposition as earlier concluded. Toluene showed up quickly in the production stream and gradually its concentrations lowered until nothing was observed after 7 hours which marked the

lifetime of the catalyst. Bulky molecules only showed up after 3 hours and naphthalene which was not much, all diffused out after 8 hours. Methylnaphthalene which looked like the major bulky product kept on diffusing out even after 17 hours.

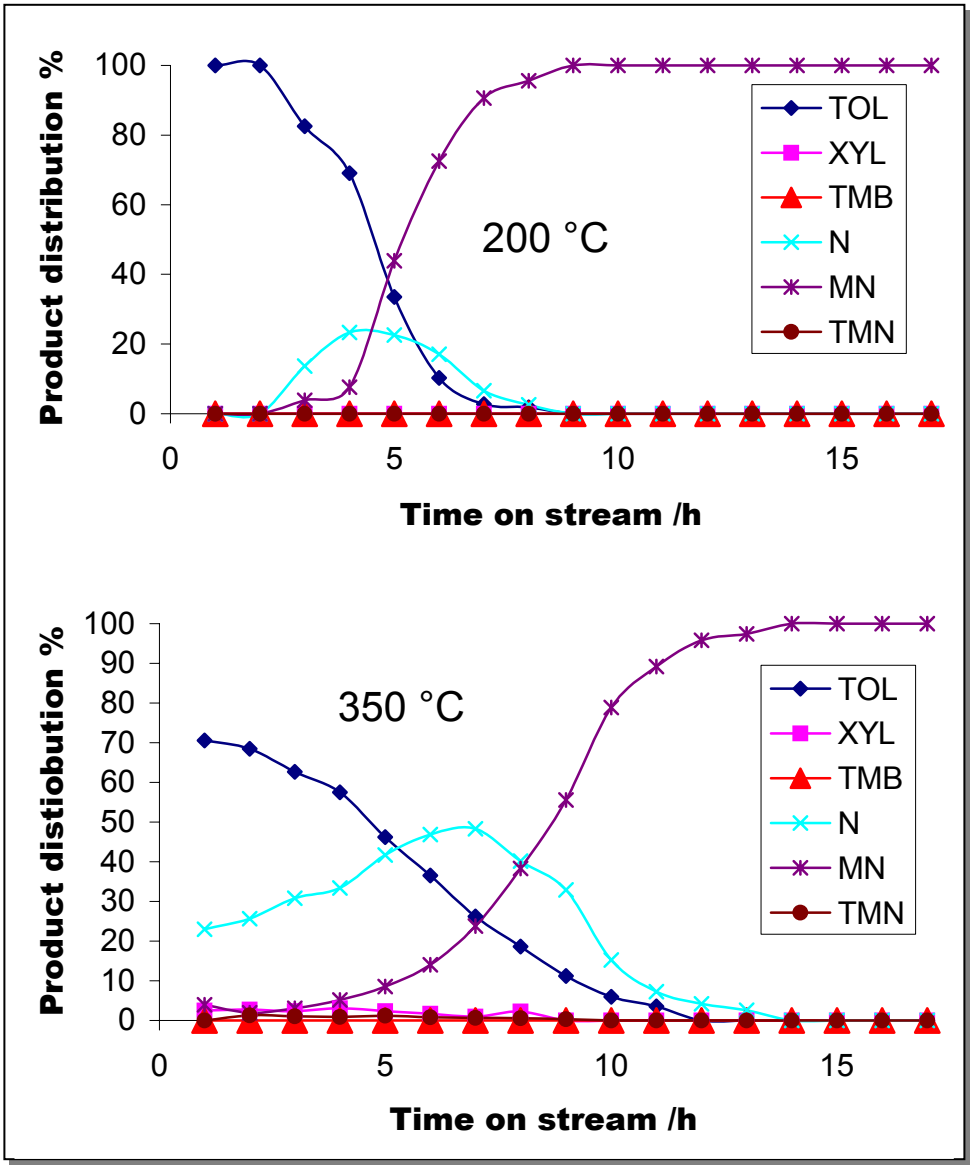

Figure 11.2: Benzene-methylnaphthalene transalkylation (mol %) on H-mordenite; product distribution

The fact that there was naphthalene in the product stream proved that the primary product (methylnaphthalene) reacted further to form naphthalene; and the fact that its disappearance in the product stream was almost exactly at the same time as that of

toluene showed that, pore narrowing in the catalyst inhibited the adsorption of the bulkier dimethylnaphthalene and the transalkylation observed at later stages was between benzene and the primary product, methylnaphthalene. This was due to 1) the favoured smaller transition state and 2) the ease with which the active site was accessed which favoured the smaller methylnaphthalene with time.

Carbon formation in the catalyst led to the inhibition of the formation of the transition states as follows:

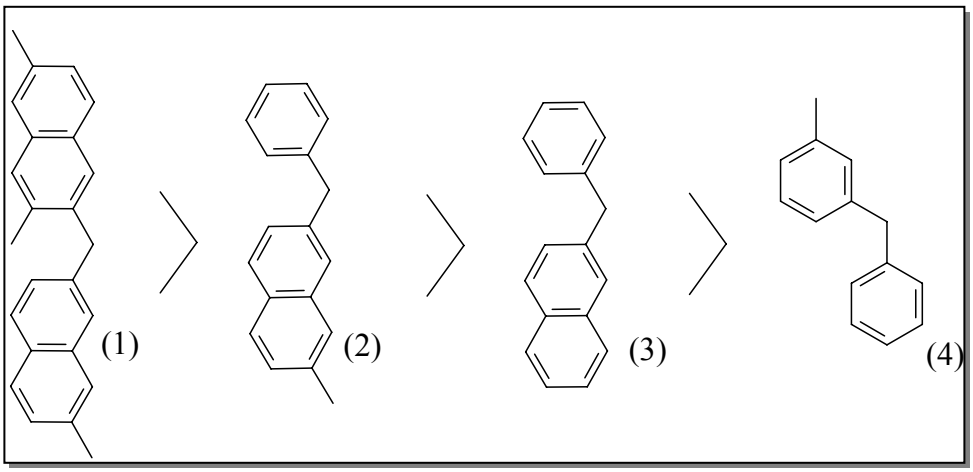

Figure 11.3: Transition state inhibition in the zeolite by narrowing of pores

Intermediate 1 was too bulky and probably did not occur in the catalyst, and if it did, it was going to produce methylnaphthalene and trimethylnaphthalene; at this stage there was no observable evidence of its occurrence. Higher temperatures (350 °C), as shown in figure 11.2, enhanced molecular diffusions and to support the fact that there were higher conversions there was a lot more of naphthalene in the product stream, and this showed up earlier in the product stream. The longer lifetime observed here was probably due to improved molecular desorption from active sites induced by high temperatures. The absence of trimethylnaphthalene in the system suggested that there was no primary disproportionation which could have led to the formation of the bulkiest transition state (figure 11.3(1)). This somehow showed selectivity induced by molecular size exclusion suggesting that transalkylation of even bulkier molecules might not be possible at all on mordenite.

Scheme 11.2 shows the most probable alkyl-transfer routes that have led to formation of products and reactions 4 and 5 probably did not occur; this was based on lack of evidence in the product stream of trimethylnaphthalene.

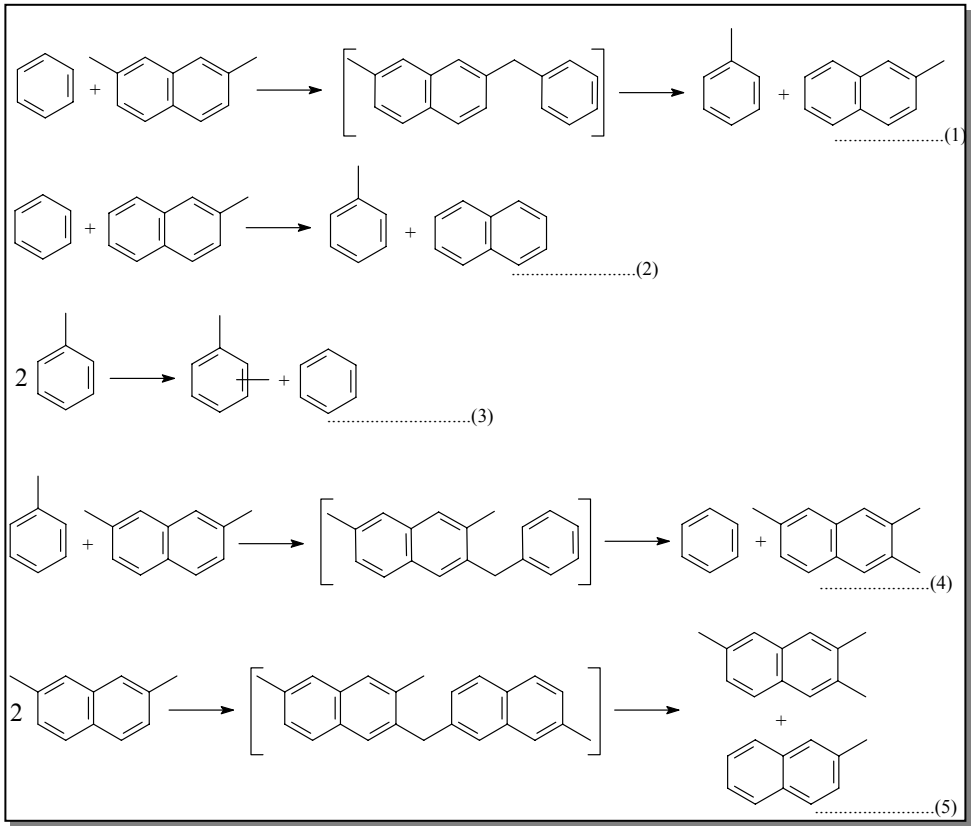

Scheme 11.2: Alkyl-transfer reactions of the benzene-dimethylnaphthalene system

11.3.2 Benzene-dimethylnaphthalene transalkylation on HLZY-82

Figure 11.4 below shows that there were also low conversions on the zeolite-Y with better activities at 350 °C. Unlike on mordenite (figure 11.1), there was no crossing over of the benzene/dimethylnaphthalene lines during a period of 18 hours (figure 11.4) at both temperatures due to the open and mainly the three-dimensional structure of this zeolite prolonging the catalyst's life.

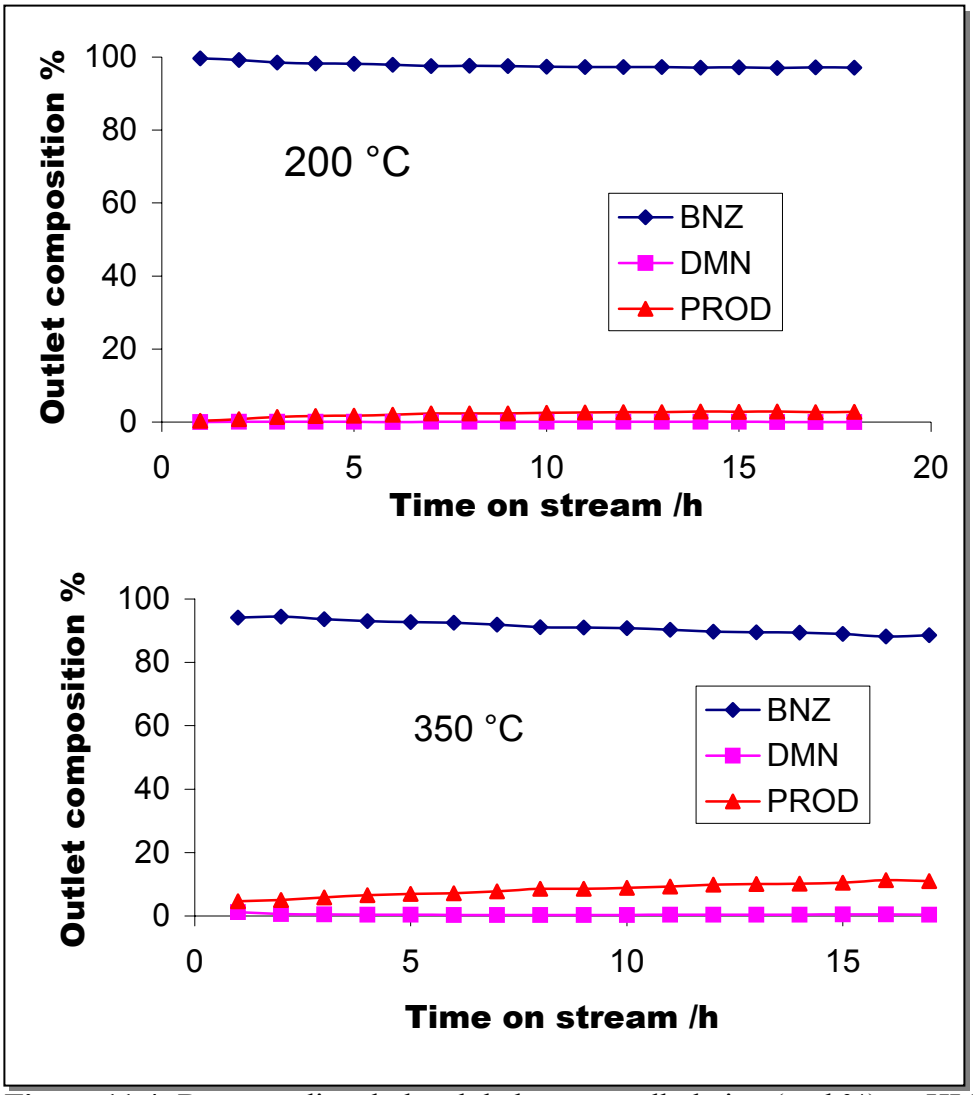

Figure 11.4: Benzene-dimethylnaphthalene transalkylation (mol %) on HLZY-82

Figure 11.5 shows product distribution of the reactions on zeolite-Y, and here trimethylnaphthalene was observed in the product stream at 200 °C. There are two routes to the formation of the trimethylnaphthalene in the zeolite; one is through disproportionation (scheme 11.2(5)), whereby, two dimethylnaphthalene molecules comes together to form a transition state, and since this was so bulky it was understood that it should have formed during the very early stages of the reaction, while it was still allowed (before inhibition by carbon). The second and the most probable one was the transalkylation from the primary product (toluene) to the dimethylnaphthalene (scheme 11.2(4)), and since it went through the smaller transition state intermediate it would keep forming trimethylnaphthalene even after

the dimethylnaphthalene disproportionation route has been inhibited. The second route (transalkylation reaction) was believed to be the major route towards the formation of the trimethylnaphthalene. This was based on the fact that, since the alkylating species must be the one adsorbed on the active site, toluene was small enough to gain access to the site as compared to the bulky dimethylnaphthalene. Trimethylnaphthalene was not observed on mordenite probably due to the transition state selectivity posed by the zeolite structure, diffusion/desorption problems and the rate of carbon deposition.

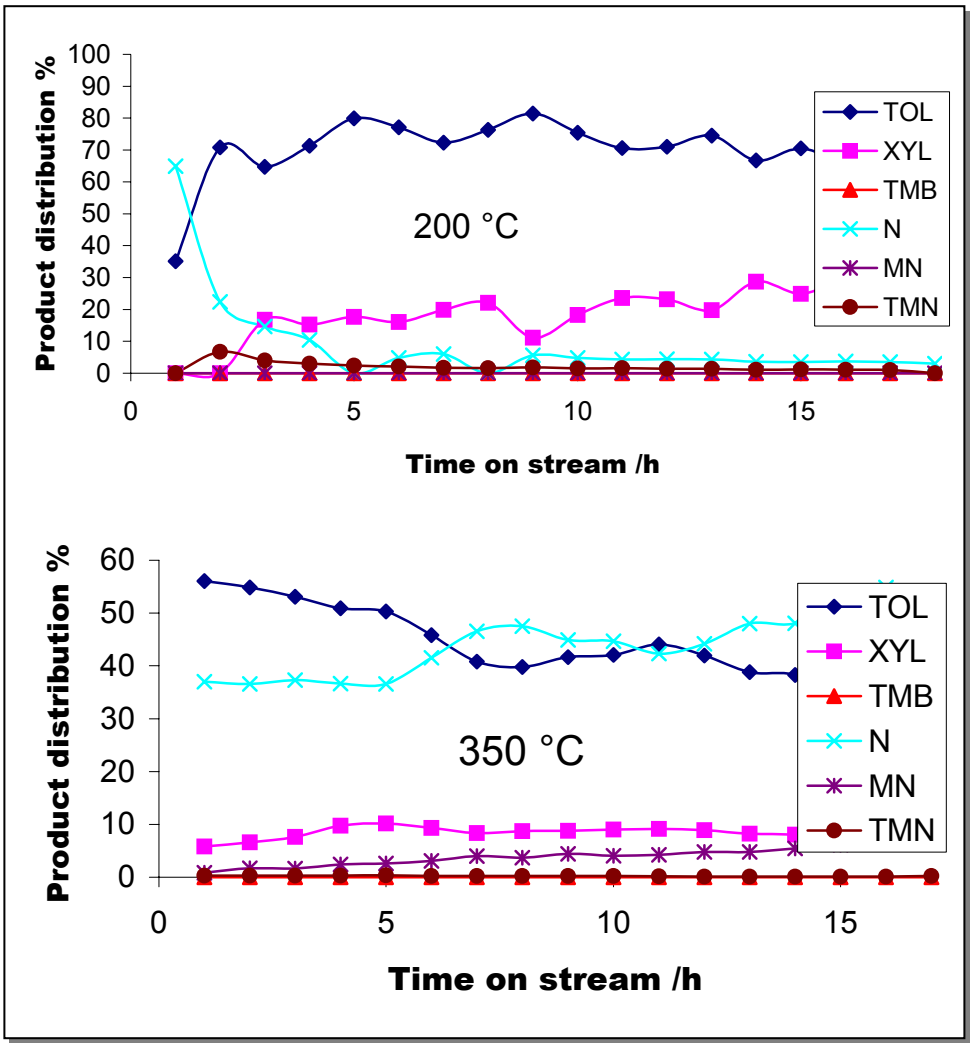

Figure 11.5: Benzene-dimethylnaphthalene transalkylation (mol %) on HLZY-82; Product distribution

The fact that there was appreciable amounts of toluene and xylene suggested that the adsorbed dimethylnaphthalene molecule may have suffered total alkyl-transfer before desorbing as naphthalene, and this could have been due to lower temperatures (200 °C) which did not promote desorption from the active site.

At 350 °C molecular retention was not significant, and methylnaphthalene was observed in the product stream. Trimethylnaphthalene was not observed at these high temperatures, this was attributed to the fact that the zeolite-Y showed earlier during the transalkylation between benzene and methylnaphthalene selectivity favouring transalkylation over disproportionation with increase in temperature. The zeolite-Y has shown this selectivity towards transalkylation during the benzene-mesitylene and benzene-methylnaphthalene transalkylation systems; and in this case it was also supported by naphthalene which did not have diffusion problems on this 3-D zeolite at 350 °C. During the early stages of the reaction there was complete alkyl-transfer to benzene which then disproportionated to xylene but with time on stream strong site deactivated and transalkylation stopped at methylnaphthalene (primary product), thus the observed slow increase of methylnaphthalene in the product stream.

11.3.3 Benzene-trimethylnaphthalene transalkylation on H-mordenite

Figure 11.6 shows that the conversions were even lesser than in the case of benzene-dimethylnaphthalene system, and this was obviously attributed to the bulkier starting material, and the conversion of which will go through a bulky intermediate. Due to the lower molar percentage (79/21 mol %) of the trimethylnaphthalene in the feed (dilute), molecular retention seemed prolonged as compared to the benzene-dimethylnaphthalene system where the alkylnaphthalene was in higher amounts.

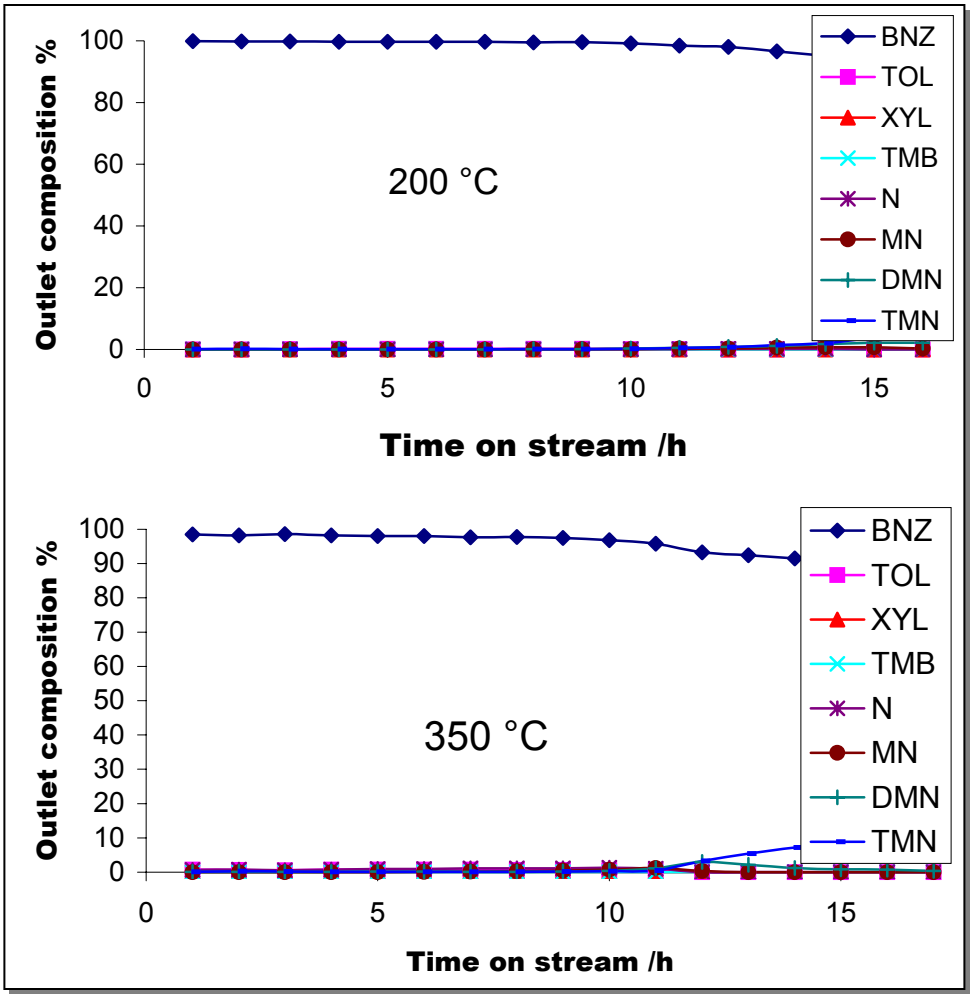

Figure 11.6: Benzene-trimethylnaphthalene transalkylation (mol %) on H-mordenite

A comparison of figure 11.7 with figure 11.2 showed that molecular retention was significant for the bulky reactants to such an extent that it even blocked the diffusion of the smaller toluene molecules. Toluene showed up after 2 hours and other products after 7 hours on stream at 200 °C.

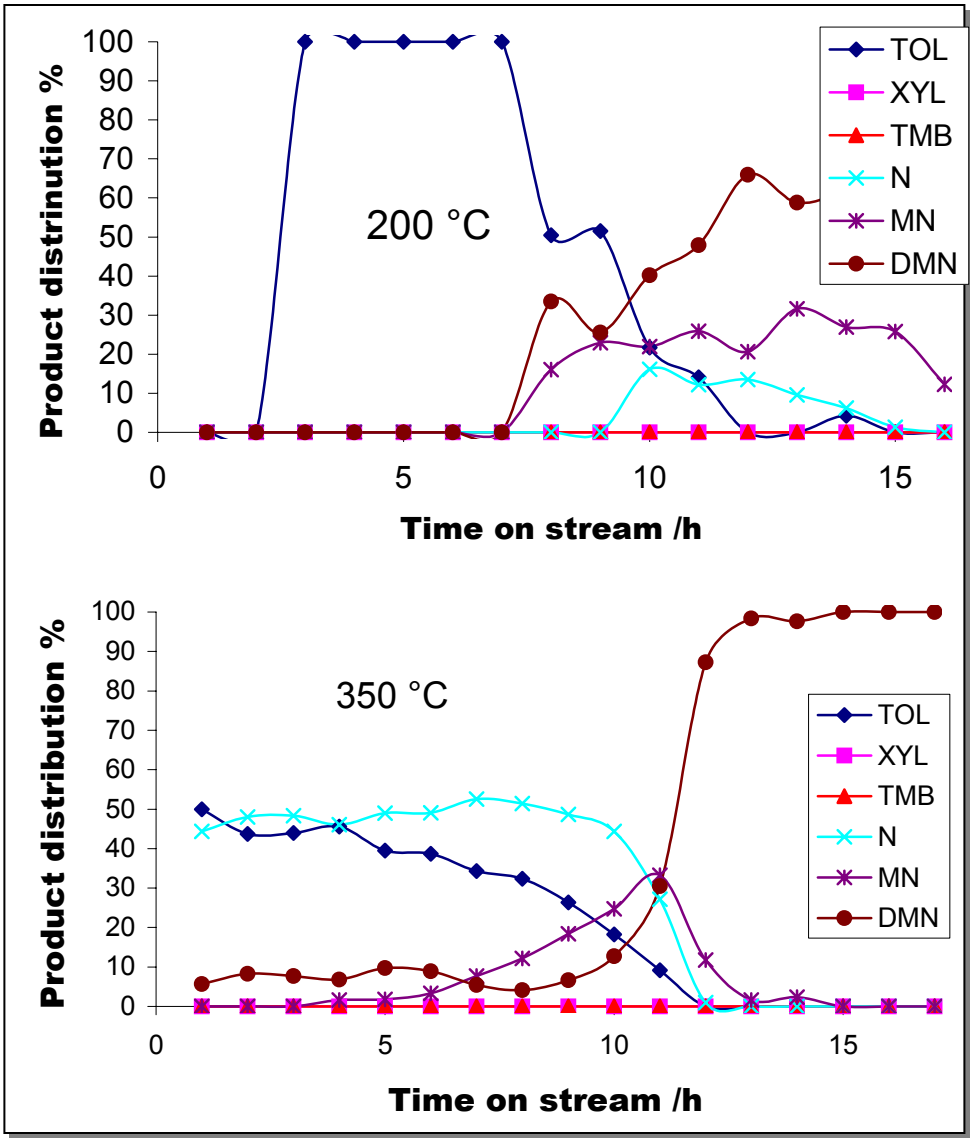

Figure 11.7: Benzene-trimethylnaphthalene transalkylation (mol %) on H-mordenite; product distribution

At higher temperatures (350 °C) molecular retention was inhibited and there was toluene, naphthalene and dimethylnaphthalene in the product stream during the early stages of the reaction. Here also, higher temperatures caused complete alkyl-transfer from the naphthalene derivatives and thus higher naphthalene concentrations. It is still not clear if the adsorbed alkylnaphthalene is stripped off of all its alkyl groups on the same catalytic site or the stripping occurs during its journey through the catalyst pores.

11.3.4 Benzene-trimethylnaphthalene transalkylation on HLZY-82

Like it was the case on mordenite, figure 11.8 shows that there were very little conversions on the zeolite-Y too. The only observable thing here was that of molecular retention at both temperatures.

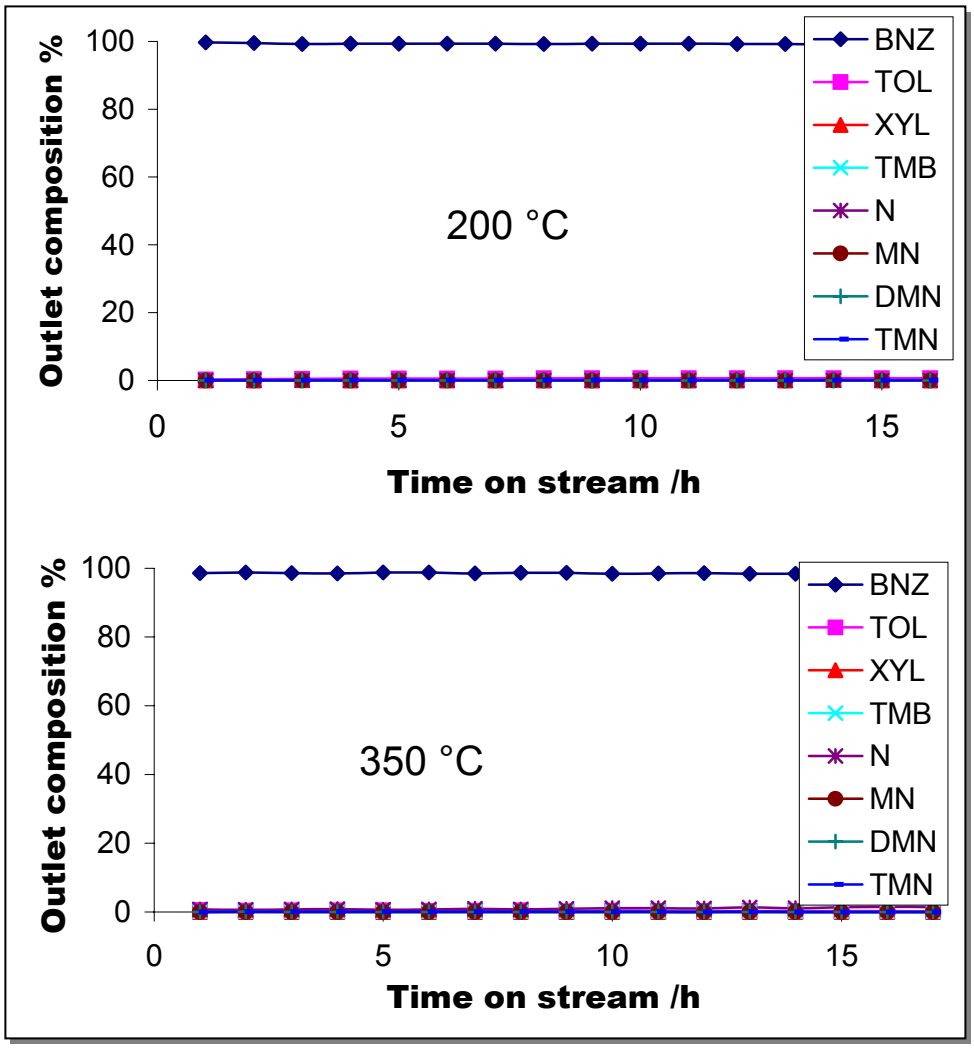

Figure 11.8: Benzene-trimethylnaphthalene transalkylation (mol %) on HLZY-82

The product distribution on the other hand (figure 11.9) showed that the major product was toluene at 200 °C followed by traces of xylene, and naphthalene started diffusing out after 15 hours of time on stream. At 350 °C the major product was

naphthalene followed by toluene and no xylene. Methylnaphthalene concentrations were very low in the product stream and dimethylnaphthalene was also present.

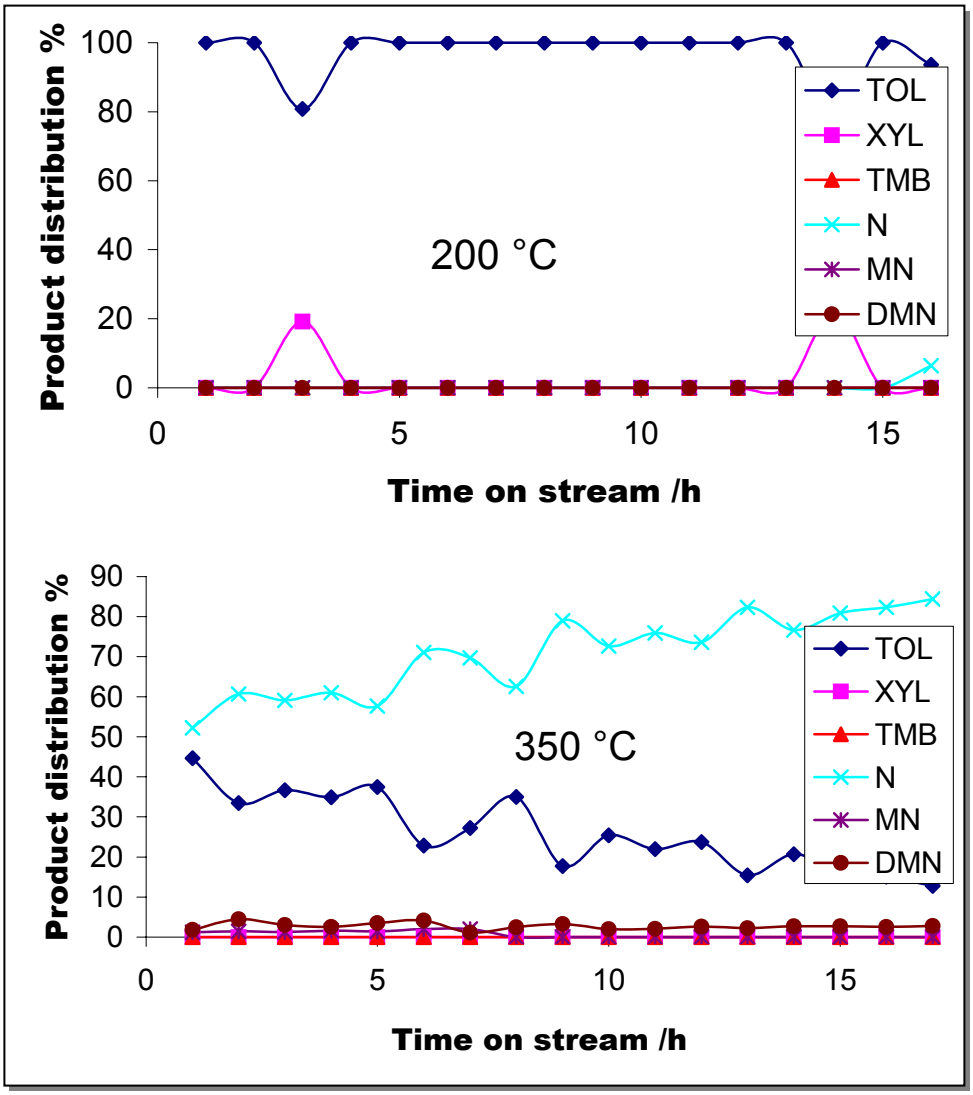

Figure 11.9: Benzene-trimethylnaphthalene transalkylation (mol %) on HLZY-82; Product distribution

11.4 Conclusion

The objectives of the study were successfully achieved and increasing the number of alkyl groups on the rings did not improve transalkylation conversions on these

catalysts, instead lower activities were observed; this supported greatly the suggestion that accessing active site by bulky molecules was a problem and that the alkyl-containing molecule should be the one adsorbed on the active site otherwise the opposite would have been observed since benzene did not have steric problems. Also observed was the selectivity towards transalkylation reactions at higher temperatures, a characteristic of the zeolite-Y in all systems studies so far. The study thus showed that if bulkier molecules are to be used in transalkylation reactions then bigger pore materials (catalysts) would be the way to go.

12 ALKYLBENZENE–[α-METHYLNAPHTHALENE] TRANSAKYLATION

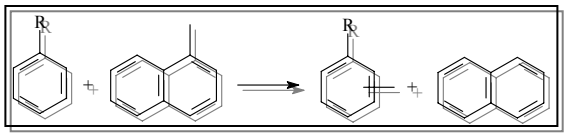

12.1 Introduction

Transalkylation reactions between benzene and alkyl-naphthalenes were shown to be possible in previous studies, but what also transpired was the fact that conversions were very low. The observed low conversions were mainly attributed to the size of pores and cavities of the zeolites which were small and thus hindered adsorption on the active site by the bulky alkyl-naphthalenes. The very well known organic chemistry factor is that addition of an alkyl group on the aromatic ring facilitates the addition of another group/s; and based on this factor the low conversions observed during transalkylation involving benzene might be due to the absence of alkyl groups on the aromatic ring and accepting alkyl groups might have been difficult. This will be supported if significant changes to the conversion levels are observed and this conversion should be through transalkylation to alkylbenzenes and not otherwise. Despite the conclusion that the observed low conversions were due to the restricting sizes of the zeolite pores and cavities, the main objective of this study was to evaluate the effect of an alkyl group on the alkyl-acceptor molecule on transalkylation reactions. Two alkyl-acceptor molecules chosen for this purpose were toluene and ethylbenzene (mono-alkylbenzenes) and transalkylation with methylnaphthalene was studied on both zeolites.

12.2 Experimental

The feed composition used here were 66/33 mol % toluene-[α-methylnaphthalene] and 66/33 mol % of ethylbenzene-[α-methylnaphthalene]. Other reaction conditions remained unchanged.

12.3 Results and Discussions

With the presence of the methyl group on the benzene ring, it was expected that transalkylation to toluene would be facilitated as compared to the transalkylation to benzene. During transalkylation to benzene, the existence of the reaction (transalkylation) was shown by the production of toluene (scheme 12.1(1)). Transalkylation to toluene (2) was somehow complicated by the toluene disproportionation reaction (3) forming benzene and xylene; and the production of the trimethylbenzenes resulting from xylene disproportionation reactions (4). Unlike in the transalkylation reactions to benzene where the catalyst lifetime was shown by the presence of toluene, in this system, the smallest intermediate (scheme 12.1(3)) was that of toluene disproportionation and not transalkylation. The formation of benzene and the xylenes will show only the activity and lifetime of the catalysts.

Matters were worsened by the fact that transalkylation to benzene (formed by toluene disproportionation (3)) will produce toluene which is one of the reactants, and transalkylation to toluene will result in the formation of the xylenes which are also produced by toluene disproportionation; transalkylation to xylenes (5) will produce trimethylbenzenes which are also produce by xylene disproportionation reactions. Thus the presence of both benzene and xylene may be used to show catalytic activity and not necessarily transalkylation.

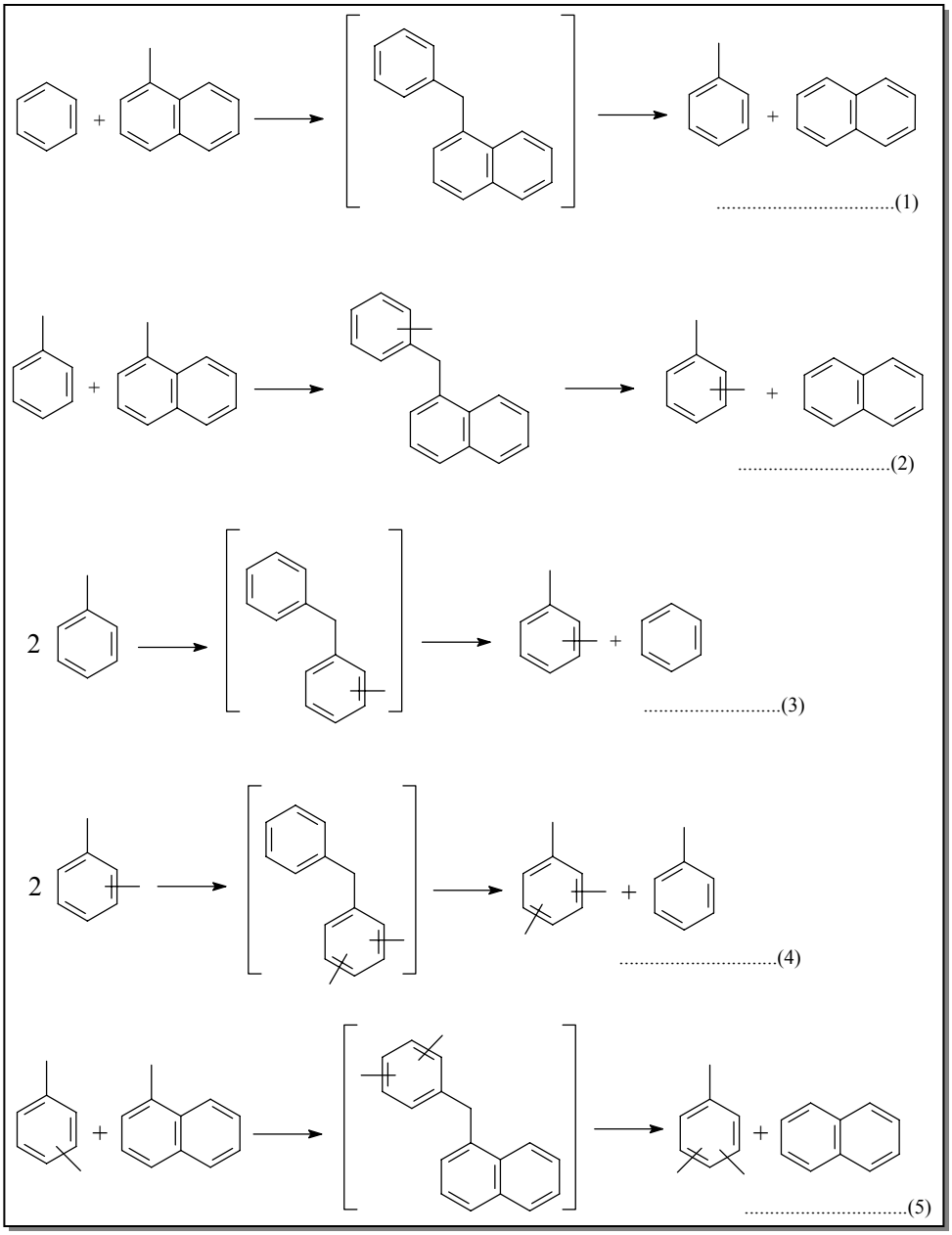

Scheme 12.1: Alkyl-transfer reactions

12.3.1 Toluene-methylnaphthalene transalkylation on H-mordenite

Figure 12.1 shows a plot of the outlet composition and the product distribution against time on stream on H-mordenite at 200 °C. The outlet stream was mainly

composed of the reactants (toluene and α-methylnaphthalene) as was shown also by the binary systems containing alkyl-naphthalenes studied previously.

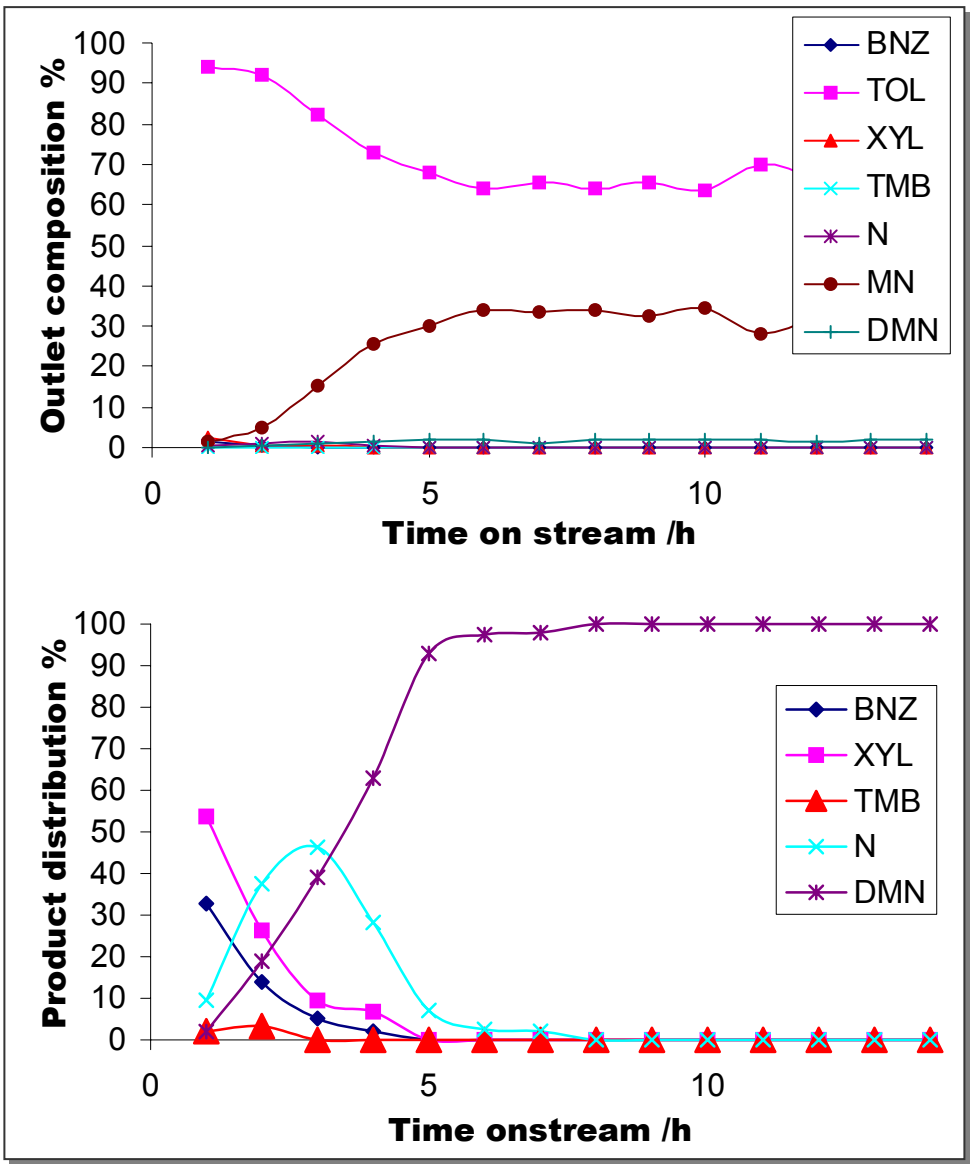

Figure 12.1: Toluene-methylnaphthalene transalkylation (mol %) on H-mordenite at 200 °C

There were very little conversions as shown by the outlet composition and there was also retention of the bulky molecules as shown by the product distribution, and this was partly attributed to the low reaction temperatures (200 °C) used. This

temperature was at least higher than the boiling temperature of toluene which should have shown a reasonable reactivity (disproportionation). The fact that the reaction temperature was lower than 240-243 °C (the boiling temperature of methylnaphthalene) somehow hindered the feasibility of the gas phase reactions. Thus supporting the suggestion that methylnaphthalene blocked access to the active sites and diffusion through the pores.

The product distribution showed a deviation from 1:1 of the benzene and the xylenes whereby there was about 30 % benzene and 50 % of the xylenes. Based on this observation it was apparent that the higher amounts of the xylenes in the product stream should be from transalkylation reaction between toluene and methylnaphthalene, but it also might be because of secondary transalkylation between benzene and methylnaphthalene producing toluene and thus consuming benzene (2, scheme 12.1); but then again, benzene deficit resulting from its contribution to carbon formation could not be ruled out as was observed with simpler aromatics.

Increase in temperature to 250 °C resulted in an increase in conversion as shown by the outlet composition in figure 12.2. The increase was about 40 % if one does not consider the retention of molecules by the zeolite. The increase in conversion was also attributed to the fact that 250 °C was higher than the boiling temperature (240 – 243 °C) of the bulky methylnaphthalene and thus promoted gas phase reactions. The higher temperatures should have induced the reaction between the adsorbed molecule and any other molecule; and also desorption of such molecules from the active sites and the diffusions through the catalyst pores.

The product distribution showed an increase in the production of the trimethylbenzenes which were presumably formed by xylene disproportionation (scheme 12.1(4)) and/or transalkylation from the methylnaphthalene to xylene (scheme 12.1(5)) since addition of an alkyl group facilitated the addition of more. Due to the bulkiness of the transalkylation intermediate, the formation of the trimethylbenzenes was much attributed to xylene disproportionation.

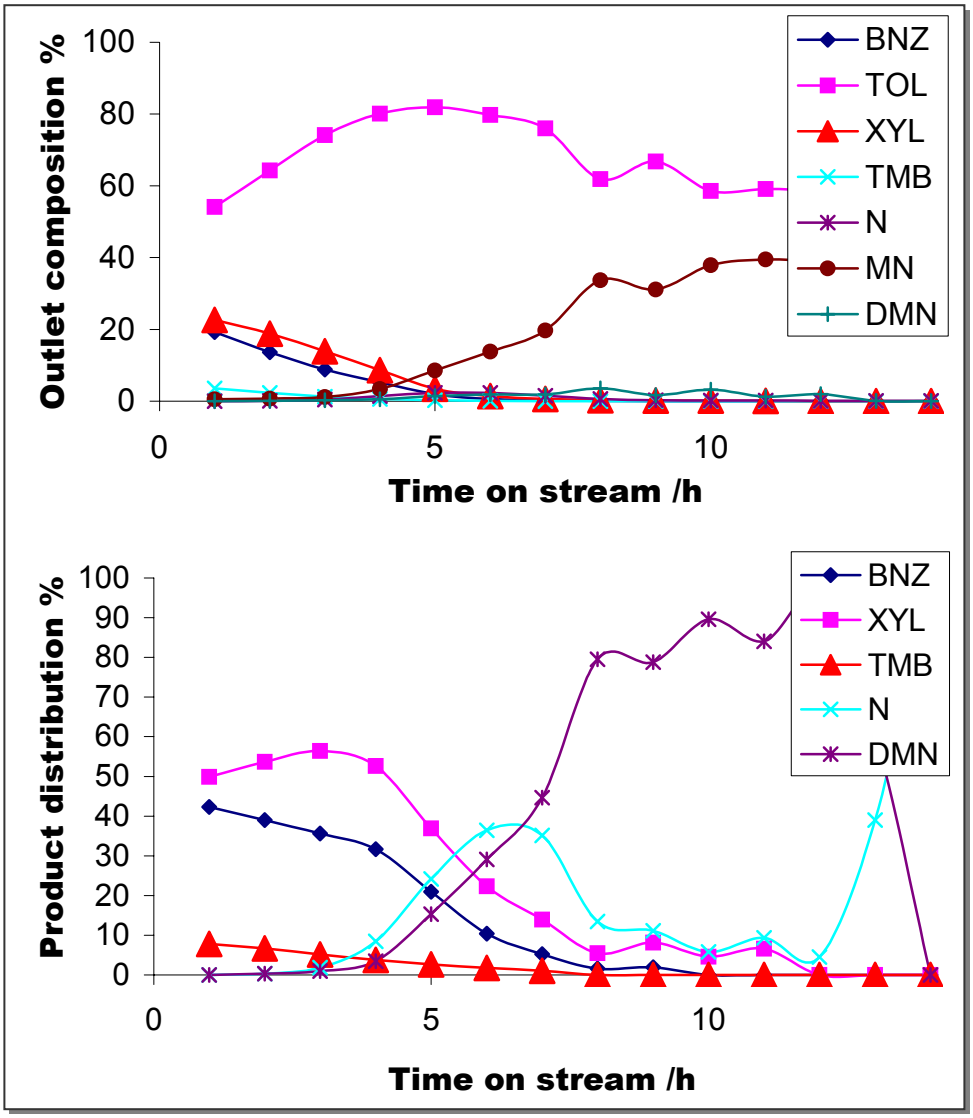

Figure 12.2: Toluene-methylnaphthalene transalkylation (mol %) on H-mordenite at 250 °C

The product distribution also shows that there was an increase in the catalyst lifetime with increase in temperature which was shown by the production of both benzene and the xylenes. Activity lasted for 5 hours at 200 °C and for about 11 hours at 250 °C. Deactivation at 200 °C was thus attributed mainly to molecular retention and filling up of pores than to carbon deposition.

The outlet composition showed a slight increase in conversion at 300 °C (figure 12.3) and the product distribution showed that there was an increase especially in the trimethylbenzenes concentration (more than 10 %). This was mainly attributed to the increased transalkylation activity with increase in temperature. The increased transalkylation would produce more xylenes, and the greater their production the better the chances of its disproportionation to form the trimethylbenzenes and toluene; hence the increase in the trimethylbenzene concentrations. The distribution also showed a decrease in the catalyst lifetime to about 8 hours which was mainly caused by an increase in the rate of carbon deposition with increase in temperature and also formation of bulkier and stable intermediates.

The reaction at 350 °C (figure 12.4) showed an almost 1:1 relation between benzene and the xylenes. The fact that figure 12.4 also showed a reasonable amount of the trimethylbenzene in the product stream proved again that there was in fact a transalkylation activity, but the uncertainty with concluding was that benzene consumption as concluded earlier was also due to carbonaceous material deposition.

The sudden increase in the benzene concentration at high temperatures (figure 12.5) was tentatively attributed to the suspected change in selectivity whereby alkylbenzenes were transalkylating back to the bulky molecules. This was based on the fact that the product stream showed an increase in the dimethylnaphthalene concentrations with increase in temperature from 200 to 400 °C. The increase in the dimethylnaphthalene concentrations led to a 1:1 relation between naphthalene and itself which was never observed with other systems.

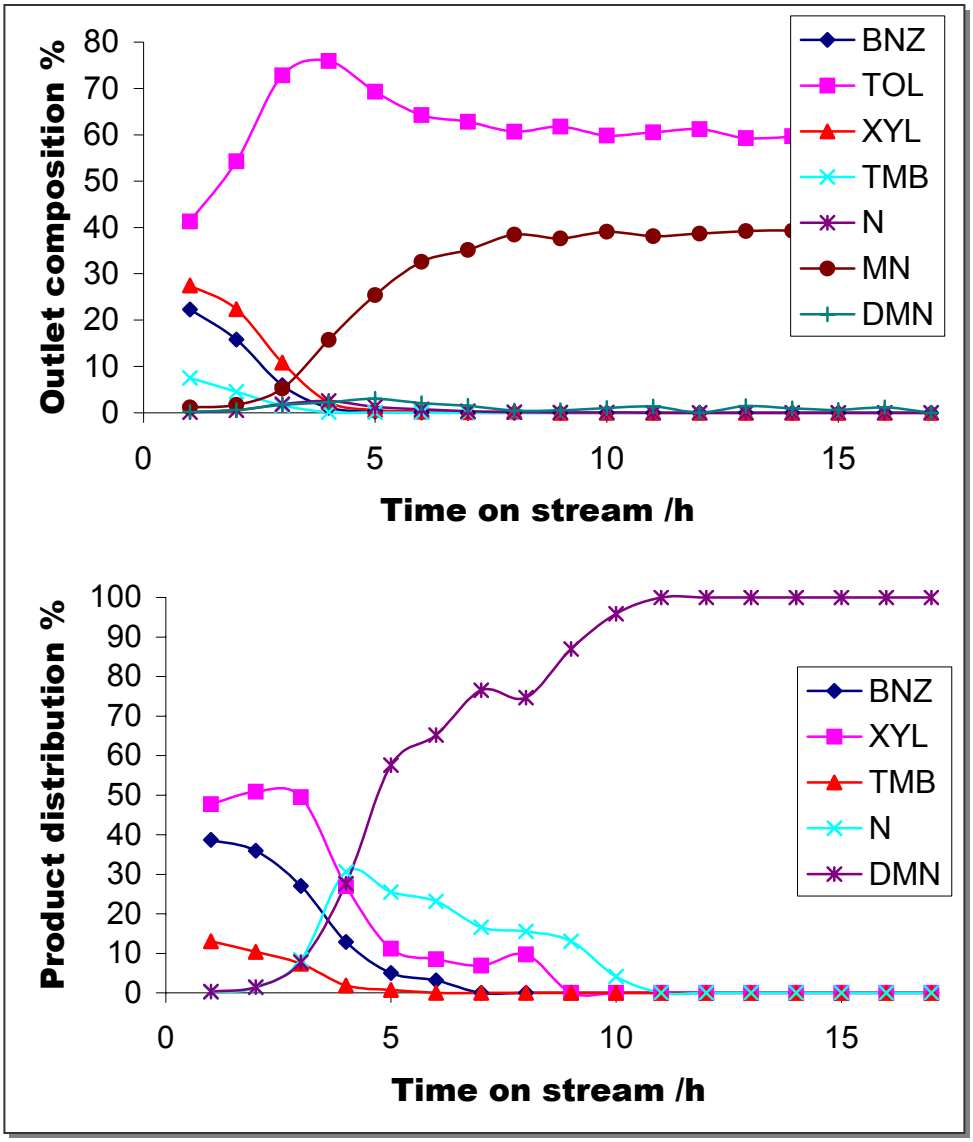

Figure 12.3: Toluene-methylnaphthalene transalkylation (mol %) on H-mordenite at 300 °C

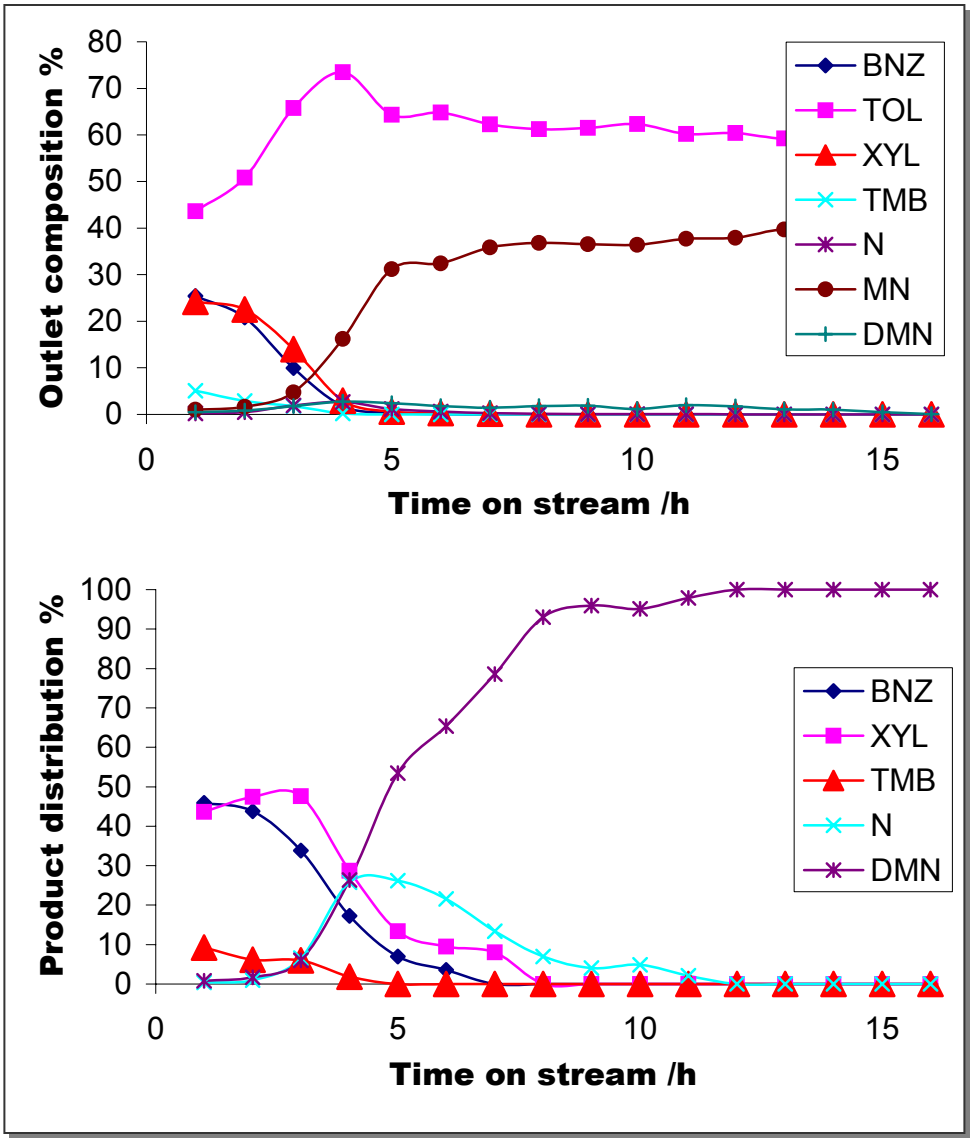

Figure 12.4: Toluene-methylnaphthalene transalkylation (mol %) on H-mordenite at 350 °C

During the earlier transalkylation reactions between benzene and methylnaphthalene there was a significant retention of the bulkier dimethylnaphthalene even at temperatures as high as 400 °C. The increased diffusion rate shown here was much attributed to the greater amounts formed rather than the desorption/diffusion phenomenon. Molecular size restrictions favoured toluene adsorption and most probably led to back transalkylation to the bulkier methylnaphthalene forming dimethylnaphthalene and benzene but this was yet to be confirmed.

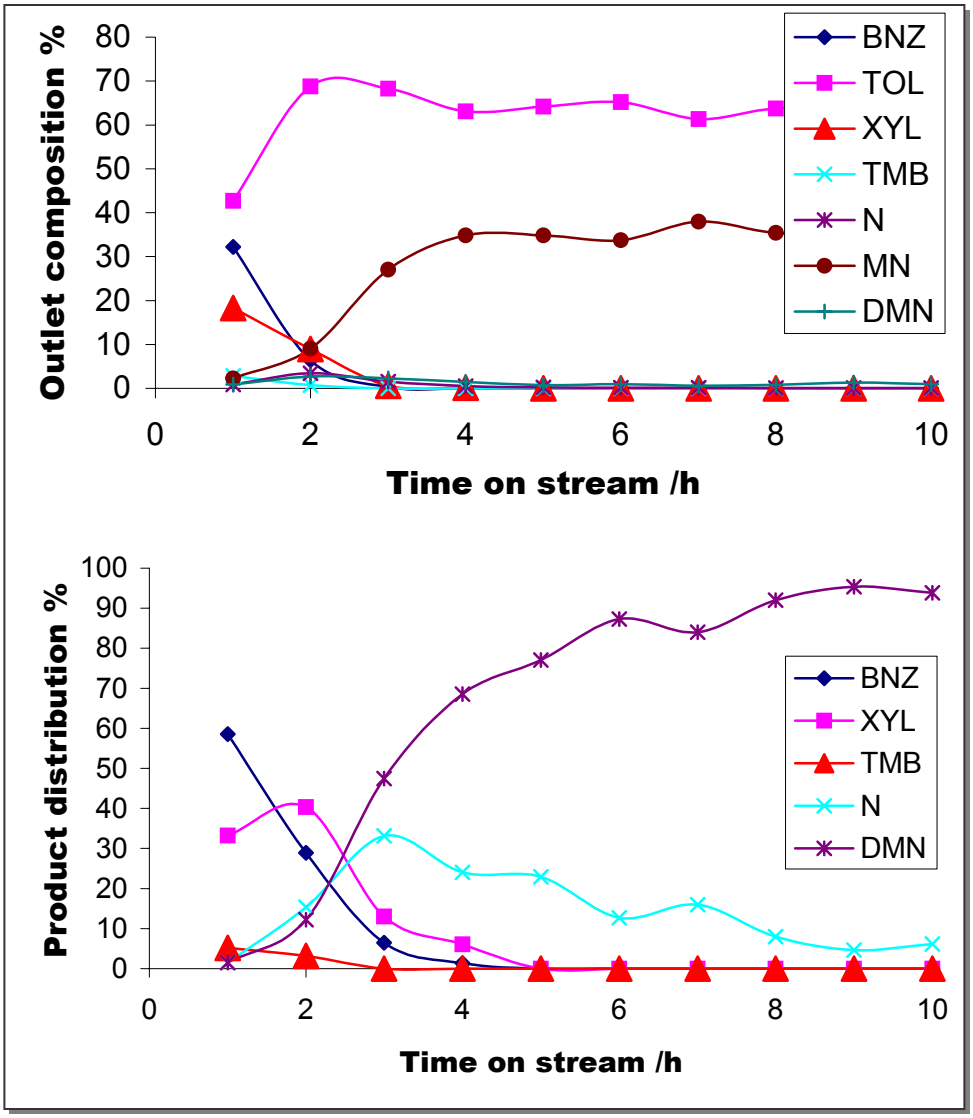

Figure 12.5: Toluene-methylnaphthalene transalkylation (mol %) on H-mordenite at 400 °C

12.3.2 Toluene-methylnaphthalene transalkylation on HLZY-82

On zeolite-Y at 200 °C (figure 12.6) there was a significant amount of the products in the outlet stream compared to mordenite. There was also prolonged reactant retention due to the bigger size and the dimensions of the catalyst pores and cavities. The product stream showed a significant deviation from a 1:1 ratio between benzene and

xylene (~ 3:6). Unlike on the mordenite, benzene was the major product during the very early stages of the reaction. This was mainly attributed to the differences in the catalyst structure and acidity which influenced adsorption/desorption and mostly diffusion of the molecules. Anyway, the quick diffusion of benzene out of the zeolite pores was characteristic of the 3-D structure in all systems studied so far.

The higher activity shown by this zeolite as compared to mordenite at the same temperature was mainly attributed to the fact that HLZY-82 contained a larger number of acid sites and larger cavities. The catalyst also showed a much better lifetime (more than 20 hours) than mordenite (5 hours) at 200 °C. If one considers the fact that the trimethylbenzenes were formed by xylene disproportionation (consumption of the xylenes) then figure 12.6 shows that there was in fact a significant transalkylation activity from the bulky methylnaphthalene. Actually this figure showed very large amounts of xylenes compared to benzene and on top of that there were undoubtedly significant amount of trimethylbenzene in the stream the formation of which would consume xylene. This proved beyond reasonable doubt that there was transalkylation from methylnaphthalene to toluene. Transalkylation from methylnaphthalene to xylene would also consume the xylenes if one considers the ease of accepting the methyl group due to the methyl groups already on the benzene ring, but this was not as feasible as xylene disproportionation (transition state selectivity).

The results also emphasized on the fact that transalkylation favoured larger cavities and a three dimensional structure, and not forgetting that accessing site by bulky molecules was more feasible on the zeolite-Y than on mordenite.

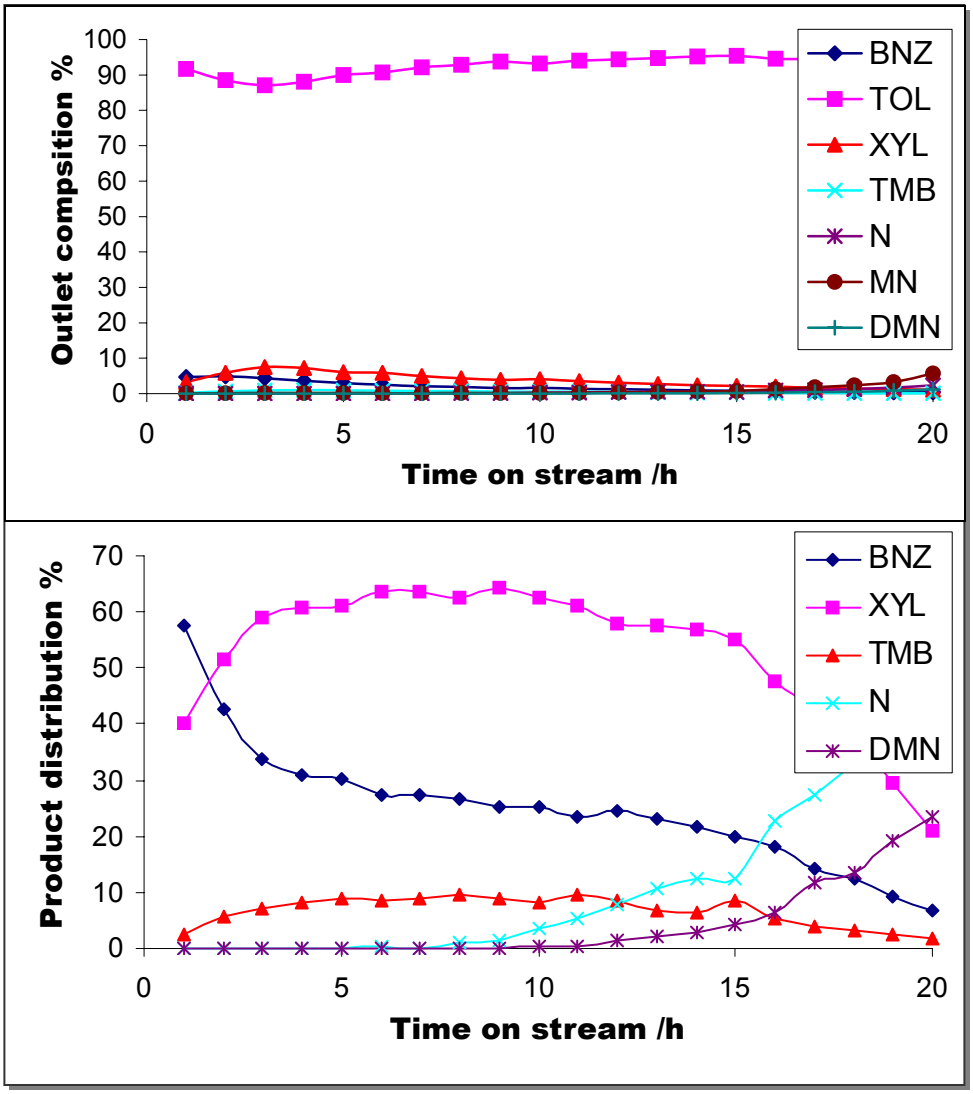

Figure 12.6: Toluene-methylnaphthalene transalkylation (mol %) on HLZY-82 at 200 °C

The observed benzene and alkylbenzenes (xylene and trimethylbenzenes) in the product stream could have been produced by toluene disproportionation; but the toluene disproportionation reaction studied earlier in chapter 6 showed almost a 1:1 relation between benzene and xylene (figure 6.5). The different situation observed in this case could be due to the presence of methylnaphthalene in the system but again the significant amount of alkylbenzenes clearly supports the transalkylation reactions towards mainly toluene. It might also be that after toluene disproportionation to form

benzene which was then transalkylated to by methylnaphthalene, decreasing its amount in the product stream while simultaneously producing toluene, further disproportionation to produce more alkylbenzenes from toluene occurred.

An increase in temperature to 250 °C (figure 12.7) was accompanied by an increase in conversion and mainly transalkylation. This was shown by an increase in the naphthalene concentrations in the product stream. The increase in conversion was shown by the increase in amounts of products in the outlet stream, but the increase or showing up earlier of the naphthalene in the product stream may be attributed to the increased temperatures and hence better diffusions.

The fact that the increase in naphthalene could have been due to the increased kinetic motions due to increase in temperature resulting in the increased diffusion rates was ruled out by the observation that almost the same percentage (~ 12 %) of the dimethylnaphthalene was observed after 18 hours at both 200 and 250 °C; i.e. there must have been some temperature effects on the dimethylnaphthalene as well. Therefore the observations on figure 12.7 were mostly attributed to increase in transalkylation.

The rapid decrease in the amount of the products formed was much attributed to the increase in carbonaceous material deposition with increase in temperature and also formation of bulkier transition states. If consideration is given to increase in carbon deposition with temperature, then the slow diffusion of the bulkier dimethylnaphthalene could be accounted for.

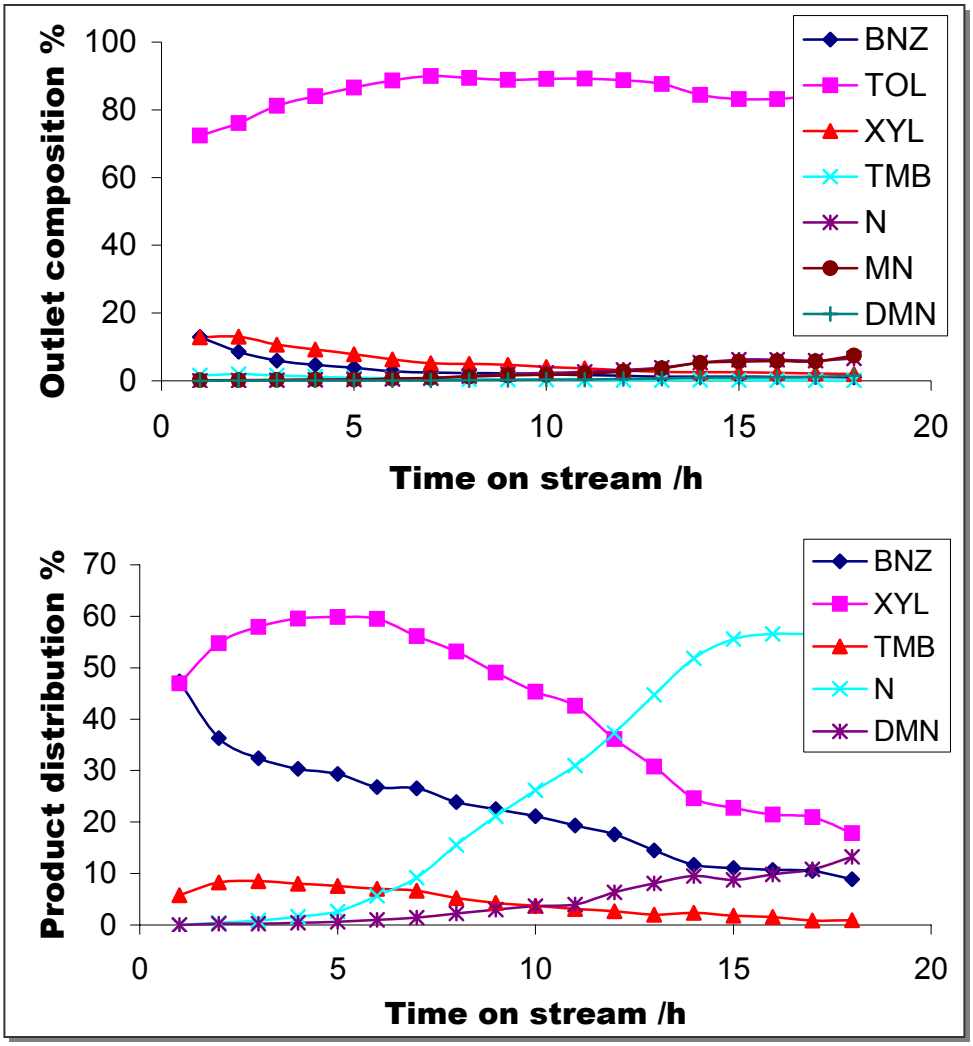

Figure 12.7: Toluene-methylnaphthalene transalkylation (mol %) on HLZY-82 at 250 °C

The outlet composition of the reaction at 300 °C (figure 12.8) showed an increase in conversion and an increase in deactivation with increase in temperature, as there was a significant increase in methylnaphthalene with time in the outlet stream. The main differences from that of the previous temperature were that of the increase in the dimethylnaphthalene concentrations with time on stream, and that of the naphthalene trace going through some sort of a maximum after 16 hours. This was mainly attributed to catalyst deactivation, carbon growth and late diffusions.

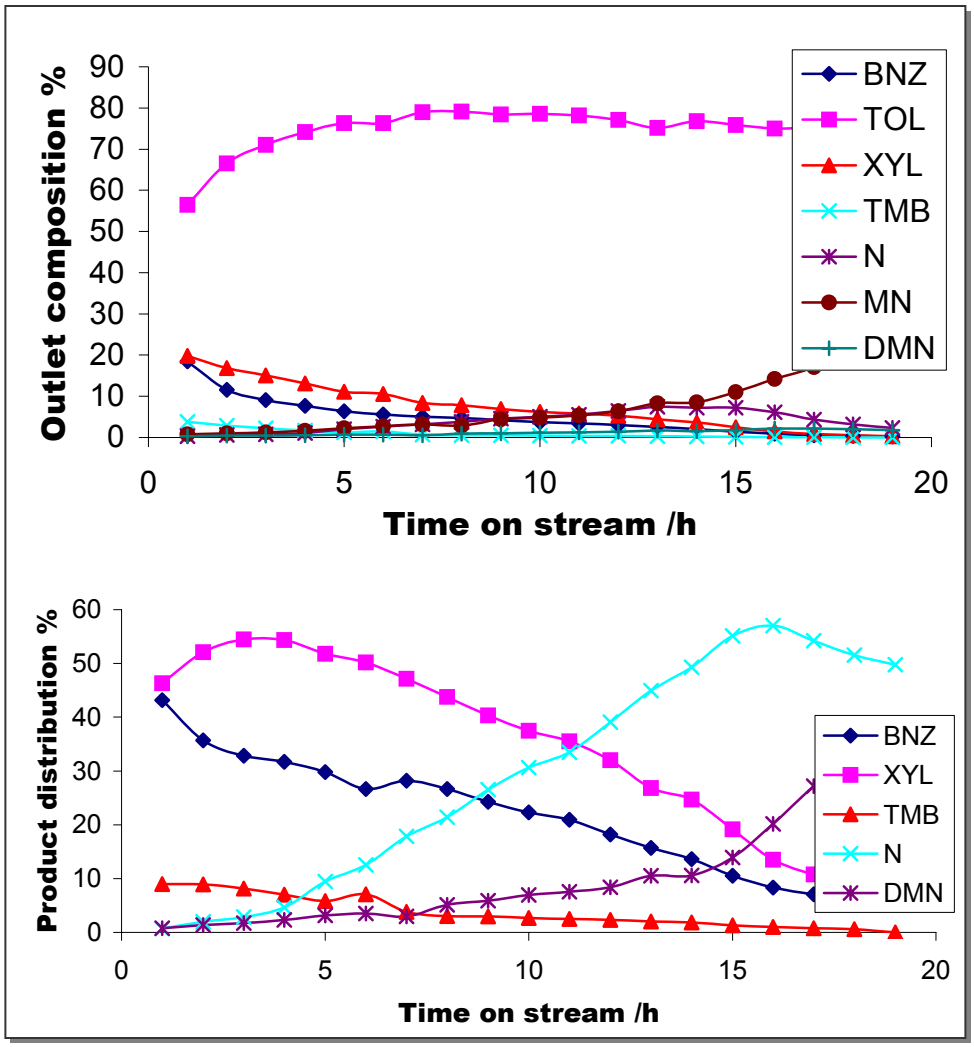

Figure 12.8: Toluene-methylnaphthalene transalkylation (mol %) on HLZY-82 at 300 °C

The behaviour was also observed at 350 °C (figure 12.9) and it was attributed to the effects of temperature on the mechanisms (alkyl-transfer and deactivations) involved.

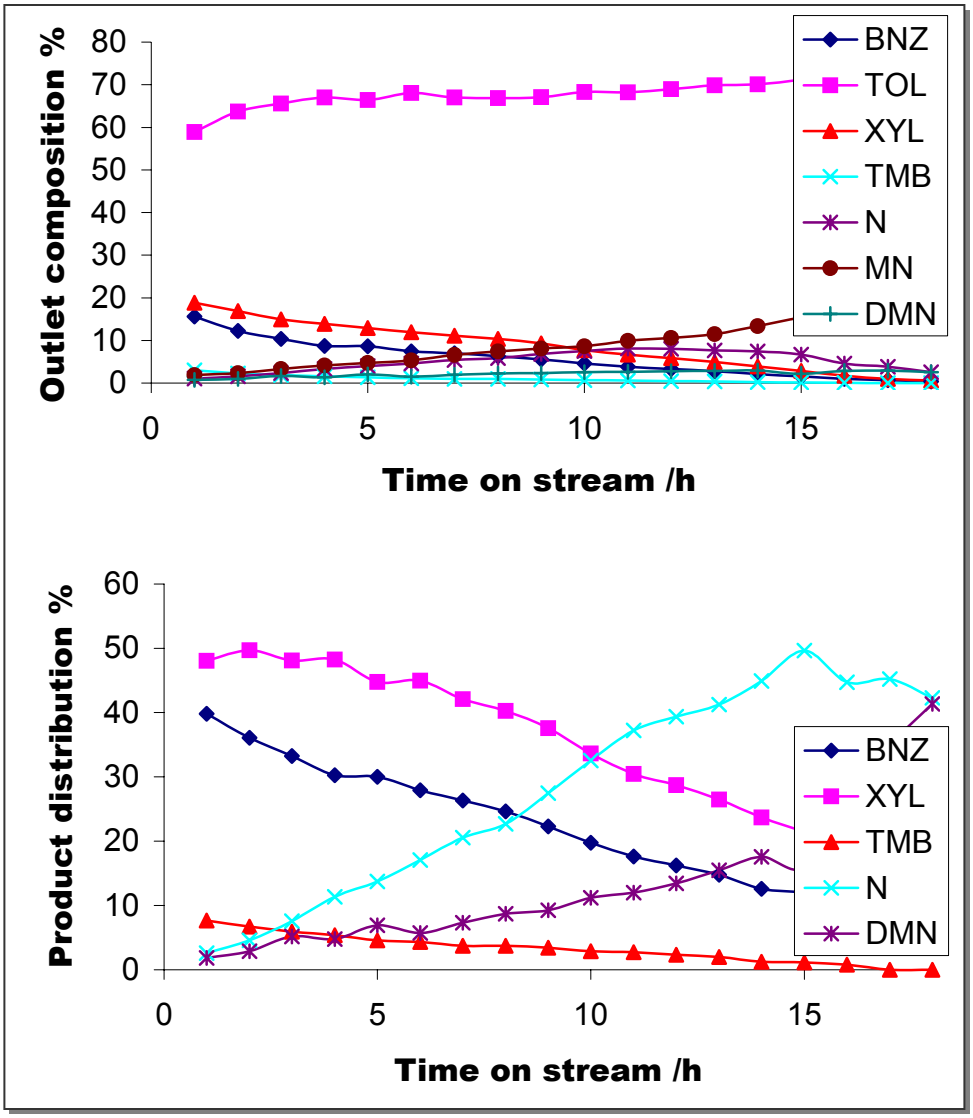

Figure 12.9: Toluene-methylnaphthalene transalkylation (mol %) on HLZY-82 at 350 °C

Different results were observed at 400 °C (figure 12.10) where the outlet composition showed the quick diffusion of benzene out of the zeolite pores and importantly the steady decreased in the formation of products (benzene and xylene) by which the catalyst lifetime was determined. Compared to the previous temperature where there was very little of benzene and xylene formed after 18 hours, reasonable mounts were still observed at 400 °C after the same time. The observations at 400 °C showed an unexpected increase in mainly the catalyst lifetime.

This led to the suggestion that deactivation on the zeolite-Y should have been mainly due to the trapped transition states in the catalyst, and not completely ruling out carbonaceous material deposition.

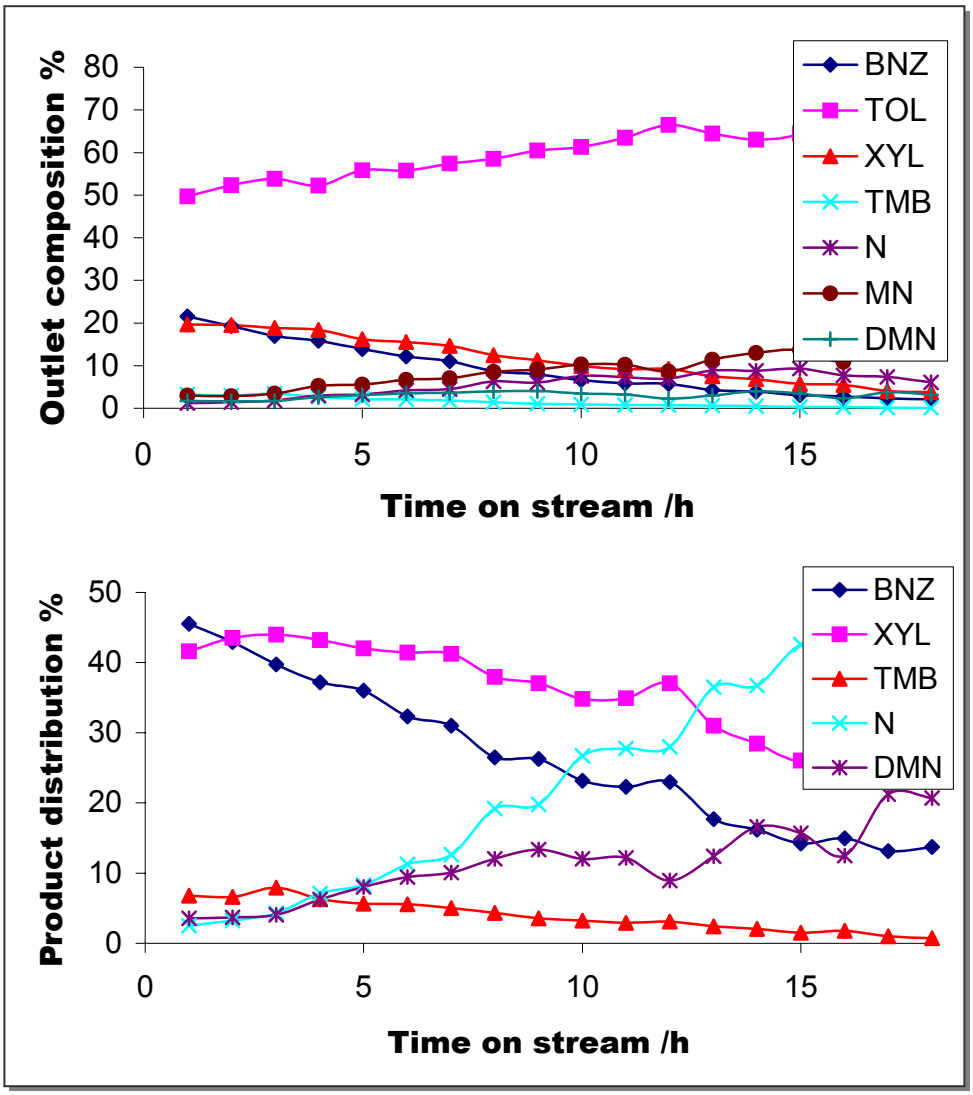

Figure 12.10: Toluene-methylnaphthalene transalkylation (mol %) on HLZY-82 at 400 °C

Thus an increase in temperature might have resulted in an increase in the formation of these transition states which couldn't go to completion due to the lower strength of the acid sites as compared to mordenite. And somehow higher temperatures helped in the completion of the reaction, or high temperatures resulted in the inhibition of the

retention of molecules in the pores, or high temperature increased the rate of molecular desorption from the active sites.

Like on mordenite, the increase in the initial benzene concentration was attributed to the suspected back transalkylation by toluene. The zeolite-Y had earlier shown some selectivity with increase in temperature during the transalkylation between benzene and methylnaphthalene; hence the observed behaviour was somehow related to the temperature induced selectivity of this catalyst, but it was still not clear.

12.3.3 Ethylbenzene–methylnaphthalene transalkylation on zeolites

The study was carried out at 200 and 350 °C. The two temperatures were chosen on the basis that ethylbenzene transformation is known to be sensitive to temperature, while both H-mordenite and HLZY-82 proved to be most active at 350 °C.

It was expected from the reaction that the presence of a longer alkyl group on the ring would further facilitate the introduction of another alkyl group on the ring. Significant amounts of ethyltoluene were expected but very little was produced and it was mostly produced during the very early stages of the reaction. This could be due to the bulkier molecular size of the transition state intermediate (scheme 12.2(1)) through which the reaction took place. Interpretation of the results was complicated by poor separation of the diethylbenzene and ethyltoluene. Failure to identify products and the amounts of ethyltoluene produced also contributed to the problem.

Figure 12.11 shows results of the reaction on H-mordenite at 200 °C which are shown as percentage distribution between benzene, toluene and the diethylbenzene (which contained ethyltoluene). This representation was based on the fact that toluene was expected to be formed by secondary reactions of the benzene from ethylbenzene

disproportionation and methylnaphthalene. Certainly, benzene and diethylbenzene were products of the ethylbenzene disproportionation reactions.

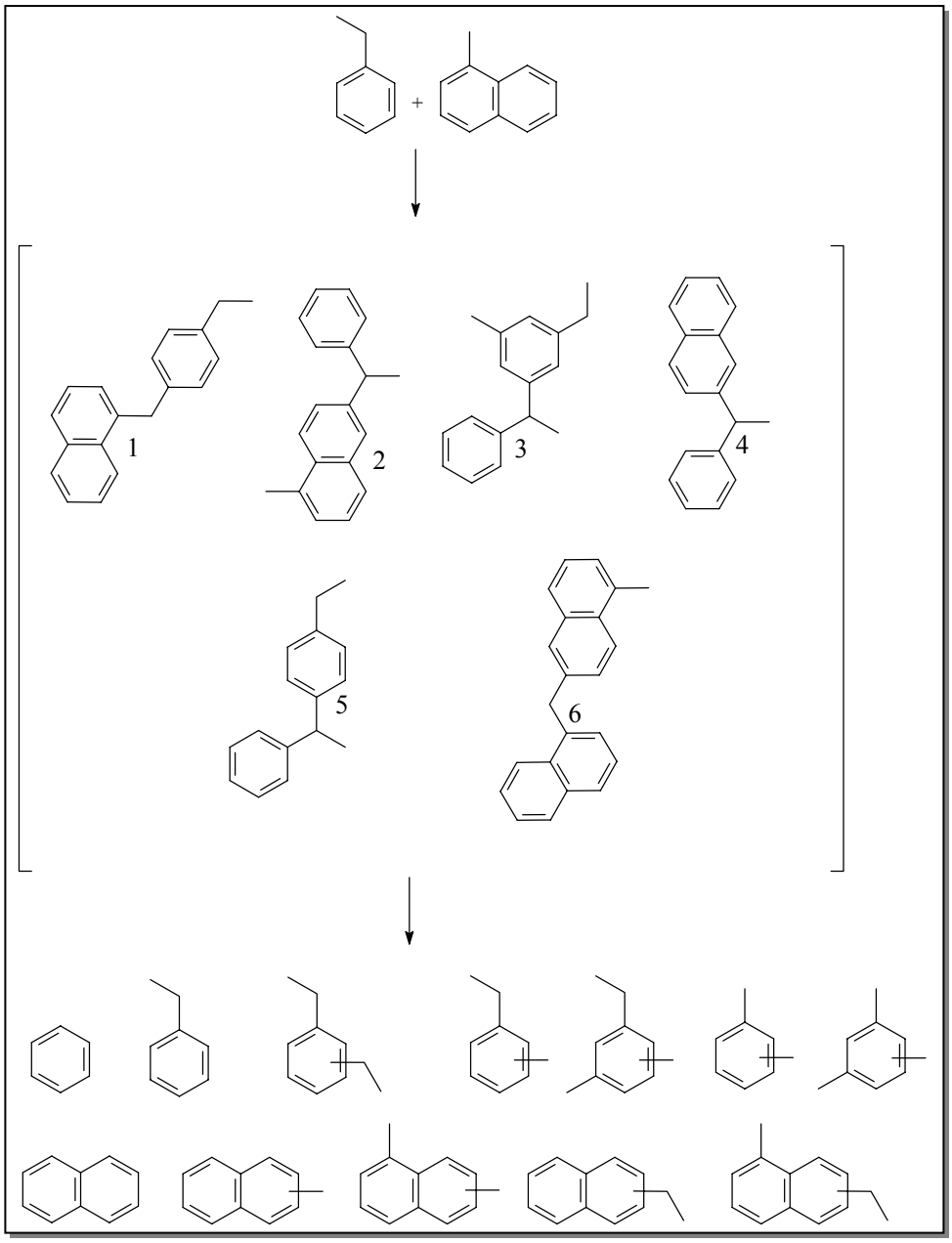

Scheme 12.2: Ethylbenzene–methylnaphthalene transalkylation reactions

Figure 12.11 show that toluene was formed in very small quantities. The higher amounts of diethylbenzene were most probably due to poor separation of ethyltoluene and diethylbenzene in the product stream. Benzene deficit was observed during

ethylbenzene disproportion (chapter 4) reactions but in this case the deficit was significant.

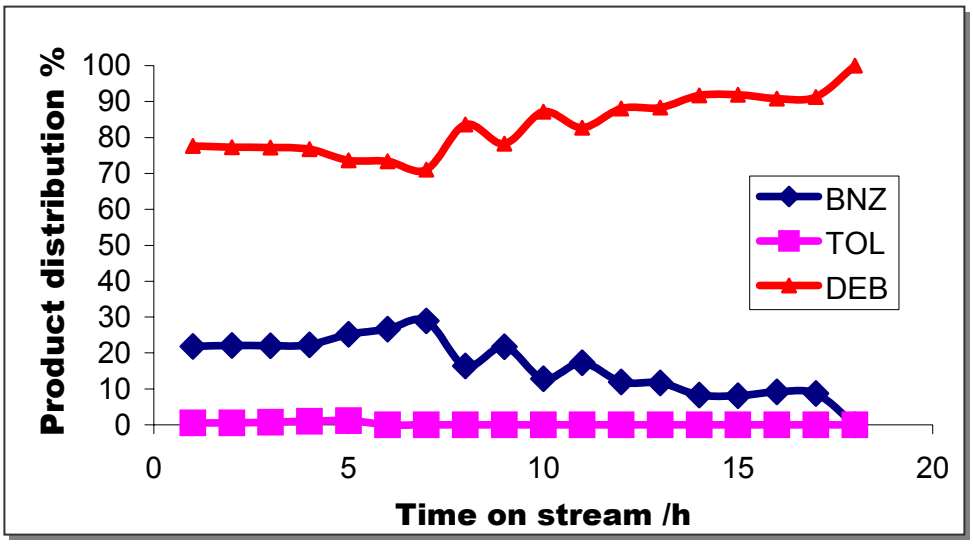

Figure 12.11: Ethylbenzene–[α-methylnaphthalene] transalkylation (mol %) on H-mordenite at 200 °C; Product distribution

The reaction on HLZY-82 produced about 8 % (figure 12.12) of toluene during the early stages.

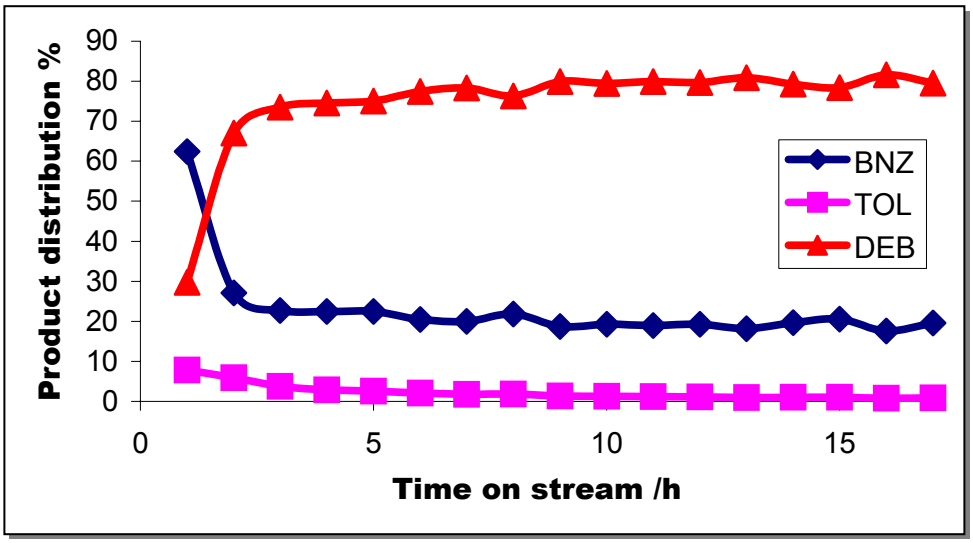

Figure 12.12: Ethylbenzene–[α-methylnaphthalene] transalkylation (mol %) on HLZY-82 at 200 °C; Product distribution

The higher number of active sites and slowed deactivation rates due to larger cavities allowed for the formation of toluene through secondary reactions. Like the ethylbenzene disproportionation reactions, the system showed that the smaller benzene would diffuse quickly through the pores with much ease and concentrate itself in the product stream (characteristic of the 3-D structure).

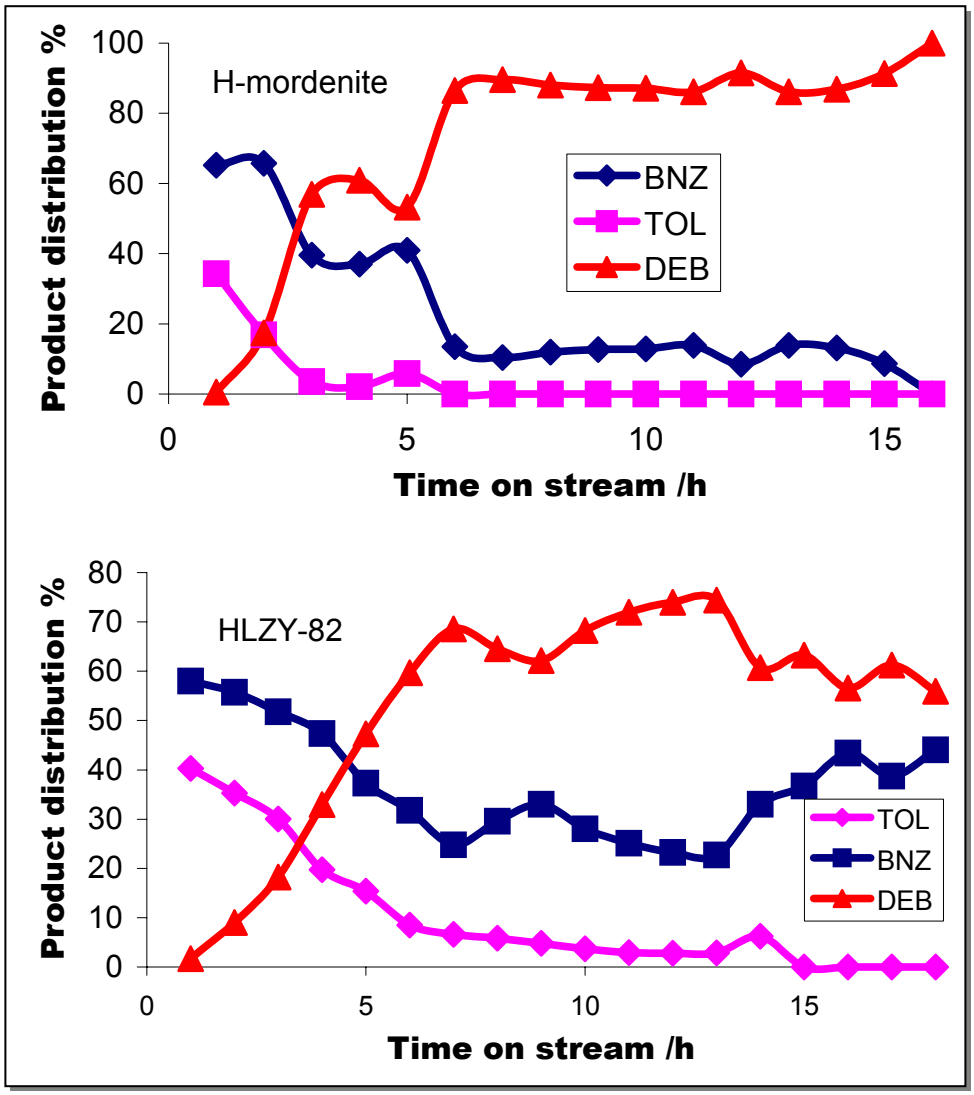

Figure 12.13: Ethylbenzene–methylnaphthalene transalkylation (mol %) on zeolites at 350 °C; Product distribution

At high temperatures (350 °C) some similarities between reactions on mordenite and zeolite-Y were shown during the early stages of the reaction, showing what looked like the retention of bulky molecules (figure 12.13).

Significant amounts of toluene (~ 30%) and about 60 % of benzene were observed in the product stream during the early stages while the bulky diethylbenzene showed up after 2 hours of time on stream. With time on stream there was rapid deactivation on mordenite with toluene production lasting for at least 6 hours, compared to the 15 hours of the zeolite-Y.

Due to separation problems during analysis valuable concrete information could not be extracted from this system but that of secondary reactions was evident to a great extent.

12.4 Conclusions

The study has showed that, working with bulky molecules will surely lead to high reaction temperatures if good conversions are to be achieved since gas phase reactions proved to be more feasible in zeolites; otherwise low temperatures will result in the catalyst deactivation. The deviation of the benzene-xylene ratio from 1:1 during toluene-methylnaphthalene transalkylation proved that there was transalkylation from methylnaphthalene to toluene. Supporting this was the fact that this deviation was not observed during the toluene disproportionation studies. Though the aim of the study was to improve transalkylation reactions, the observed high activities were also due to the disproportionation reactions of toluene and due to this reaction the extent of transalkylation could not be determined and thus comparison to the benzene-methylnaphthalene system could not be carried out.

With the ethylbenzene-methylnaphthalene system, the fact that about 30 % of toluene was observed in the product stream, despite the fact that its formation was through a

secondary reaction on both catalysts, showed that the catalyst pore/cavities are very important in the transalkylation reactions which proceeded through a bimolecular type of mechanism; i.e. smaller transition states are always favoured. Thus an increase in the pore/cavity size of the zeolite may result in the formation of the expected considerable amounts of ethyltoluene through primary reactions.

Though the transition state by ethylbenzene and methylnaphthalene was very bulky, ethyl-methylnaphthalene was also formed in the system probably through the other type of transalkylation mechanism, i.e. the dealkylation/realkylation mechanism.

Overall, the use of an alkyl-containing alkyl acceptor molecule led also to the suspected back transalkylation which was not desirable. This however can be circumvented by using less acidic catalysts because mono-alkylbenzenes, especially toluene, are stubborn molecules to transform, and their conversion requires strong sites. Due to undesirable reactions (disproportionation) in these binary systems the objectives of the study were not fully achieved. The highlighted point here was of the problem associated with using alkyl-containing aromatics as acceptor molecules in transalkylation reactions. But, for systems with interest in ethylbenzene disproportionation, the introduction of alkylnaphthalenes may help in the reduction of the unwanted carcinogenic benzene by forming toluene through transalkylation.

13 BACK-TRANSALKYLATION

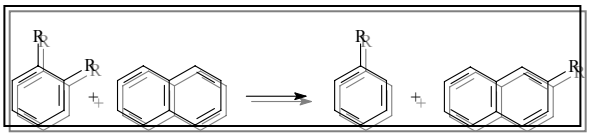

13.1 Introduction

During transalkylation reactions between benzene and alkyl-naphthalenes low conversions were observed and this was attributed to the difficulty in accessing active sites by the bulky alkyl-naphthalenes. An attempt to promote conversions by using alkyl-benzenes as alkyl-acceptors showed that alkylaromatics were competing for active sites and smaller molecules seemed to be favoured; this then resulted in the suggestion that there was transalkylation towards naphthalenes (back-transalkylation) and there was no evidence enough to support that. Since toluene was intended to be used as one of the alkyl-acceptors and alkylaromatics are products of transalkylation reactions, it was found necessary to look at how back-transalkylation would affect transalkylation in general. For this particular study toluene-naphthalene and *o*-xylene-naphthalene systems and the effect of feed composition were evaluated.

13.2 Experimental

The feed compositions used here were 67/32 mol % toluene-naphthalene on mordenite and 59/40 mol % on HLZY-82; and 87/13 mol % of *o*-xylene-naphthalene on both zeolites.

13.3 Results and discussions

Again, due to molecular retention by the zeolite there were difficulties in representing the catalytic activities as either conversion of the reactants or the formation of products. For analysis sake, an example of the used representation is shown in figure 13.1 and it shows the outlet composition in molar percentage of reactants (toluene (TOL), naphthalene (NAPH)) and products (PROD) at 400 °C in the outlet stream for the toluene-naphthalene system. This kind of representation showed only the activity of the catalyst and its lifetime; and it did not show whether the activity was due to transalkylation or disproportionation.

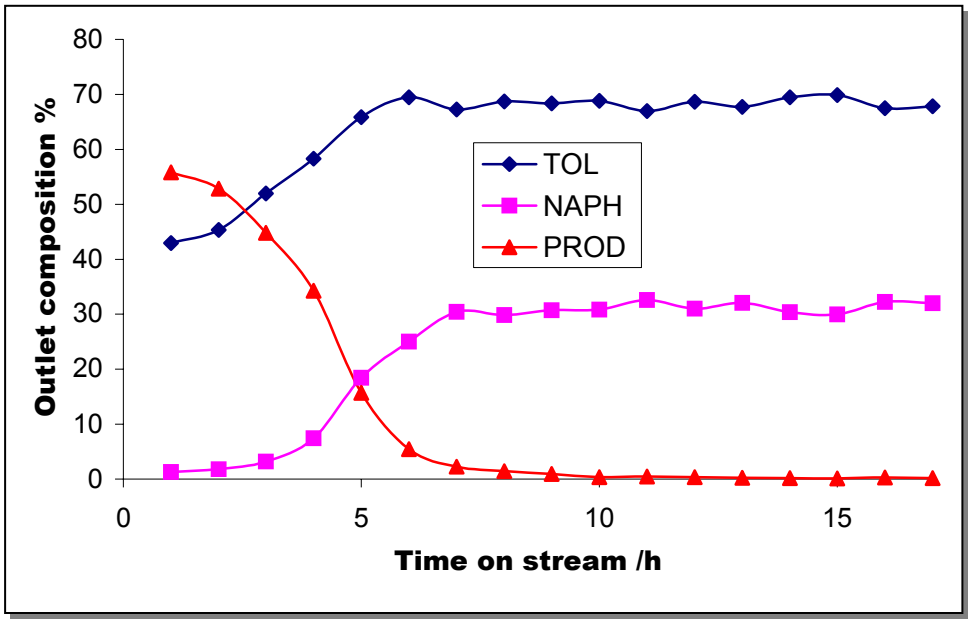

Figure 13.1: Toluene–naphthalene transalkylation (mol %) on H-mordenite at 400 °C: Outlet composition

13.3.1 Toluene-naphthalene transalkylation on H-mordenite

Figure 13.2 shows the amount in percentages of the products in the outlet stream at different temperatures. The figure clearly shows the increase in conversion with increase in temperature. If one considers the fact that at lower temperatures deactivation was dominantly by molecular retention and at higher temperatures by mostly carbon formation, then the figure suggests that with bulkier molecules deactivation will be much faster at lower temperatures; and thus higher temperatures would be ideal for such systems since gas phase reactions would also be favoured.

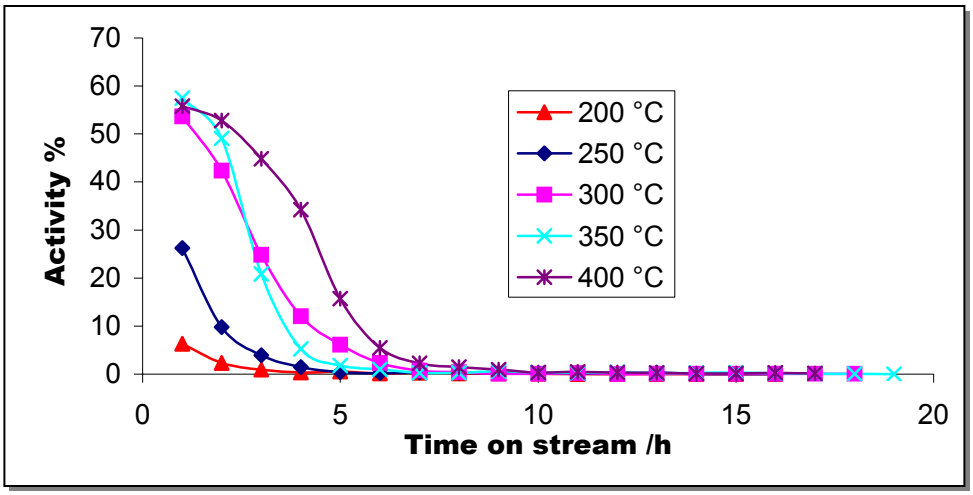

Figure 13.2: Toluene–naphthalene transalkylation (mol %) on H-mordenite

Since almost similar patterns were also observed with the toluene disproportionation reactions (figure 6.1), this suggested that disproportionation was the main reaction, or toluene preferentially adsorbed on the active sites. The catalyst deactivation was not as severe as that of toluene disproportionation (chapter 6) because of the presence on naphthalene in the current system which diluted the toluene feed. This explanation somehow supports the fact that smaller molecules are most actively involved in carbonaceous material deposition in the zeolites.

Looking at the product distribution of the reaction at 200 °C (figure 13.3) it is apparent that there was both disproportionation of toluene and transalkylation reactions between toluene and naphthalene. Disproportionation produced benzene, xylene and a very small amount of trimethylbenzene during the early stages of the reaction while transalkylation led to methylnaphthalene formation. A careful look at both figure 13.2 and 13.3 showed that the main reaction route was in fact disproportionation of toluene and not transalkylation. Figure 13.3 shows the appearance of methylnaphthalene in the product stream after 2 hours at 200 °C while figure 13.2 shows that at the same time and temperature the total amount of products diffusing out of the catalyst decreased, and as the methylnaphthalene becomes the major (more like the only product in the product stream) product after 3 hours in figure 13.3, there was very little of products diffusing out of the reactor (about 1 %). Nevertheless, the presence of methylnaphthalene showed that there were transalkylation reactions. The low transalkylation reactions activity could be due to 1) the stability of the toluene molecule and 2) its high amounts in the feed which will obviously favoured disproportionation.

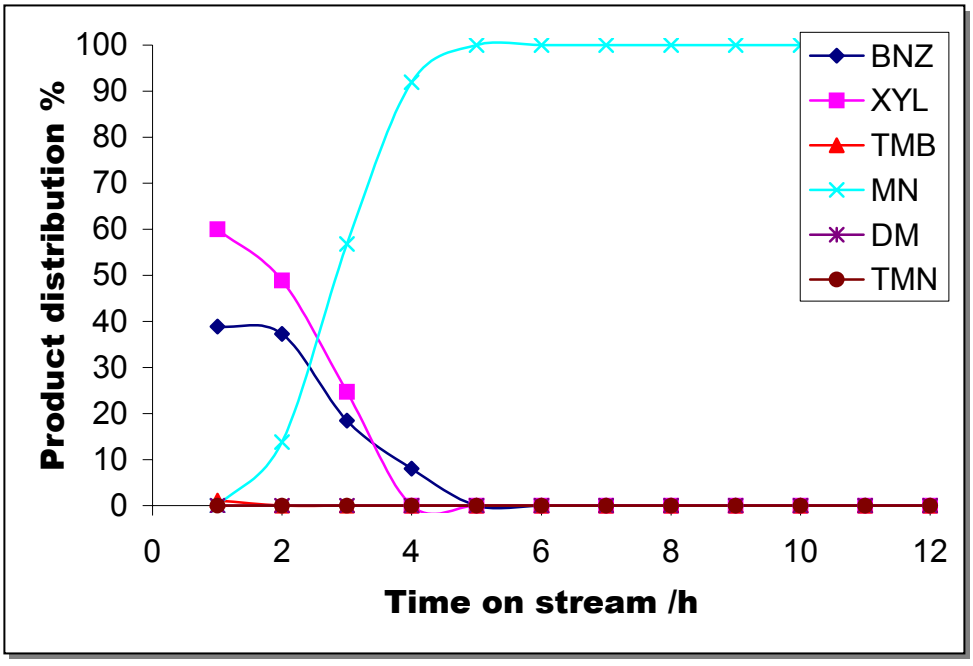

Figure 13.3: Toluene-naphthalene transalkylation (mol %) on H-mordenite at 200 °C; Product distribution.

The toluene disproportionation products alone from this reaction (figure 13.4) showed a deficit in benzene, which also supported the participation of smaller molecules in carbon deposition. After 4 hours on stream benzene became the major product (the only product) due to the formed carbon (carbonaceous material deposition) in the catalyst and diffusion of the bulky product was severely affected. Also in support of the observations in figure 13.2, figure 13.4 also showed that the total catalyst deactivation occurred after 4 hours at 200 °C (absence of products forming through smaller transition state molecules).

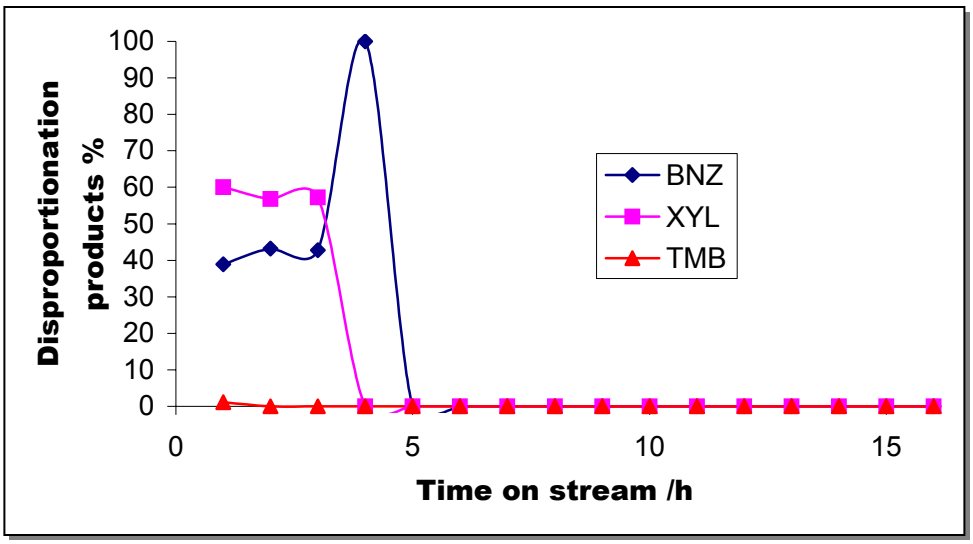

Figure 13.4: Toluene-Naphthalene transalkylation (mol %) on H-mordenite at 200 °C; Toluene disproportionation product distribution

An increase in temperature to 250 °C resulted not only in the increase in conversion and catalyst lifetime but in the increase in number of products formed (figure 13.5), i.e. dimethylnaphthalene showed up in the product stream. This meant that there was an increase in the transalkylation activity and similar behaviour was also observed at 300 °C.

Figure 13.6 shows the disproportionation product distribution of toluene at high temperatures and it can be seen that at 350 °C the pattern was still almost similar to that shown by the reactions at lower temperatures (figure 13.4); but at 400 °C there was a 1:1 relation between benzene and the alkylbenzenes formed despite the transalkylation reactions.

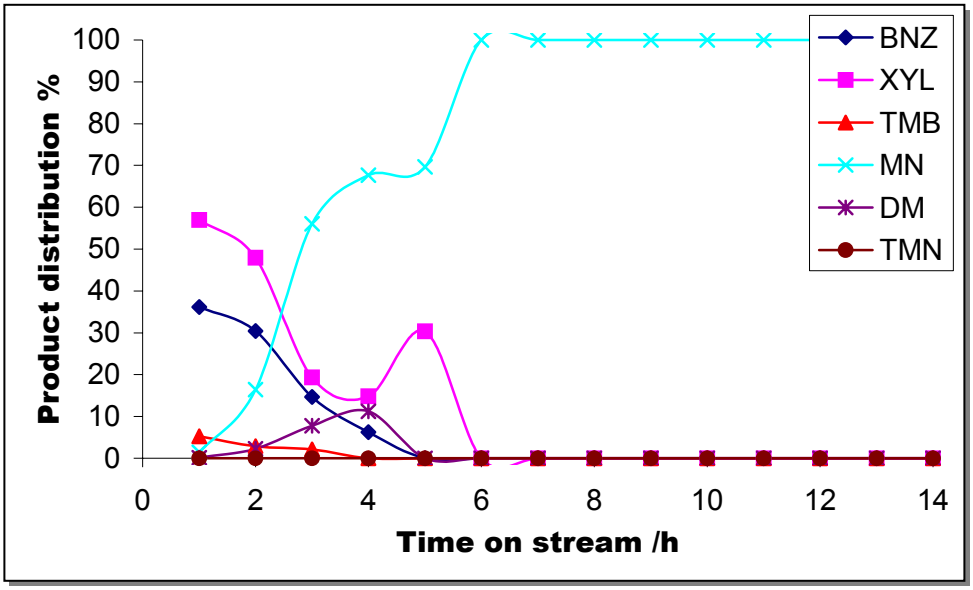

Figure 13.5: Toluene-naphthalene transalkylation (mol %) on H-mordenite at 250 °C; Product distribution

Figure 13.7 shows that the lower amounts of xylene in the product stream compared to benzene shown by figure 13.6 (at 400 °C) was also due to transalkylation to naphthalene forming methylnaphthalene, dimethylnaphthalene and trimethylnaphthalene.

Figure 13.2 depicted the amount of products formed and thus from the product distributions a very rough estimation of the extent of transalkylation could be achieved. The product distribution shows relative amounts of products formed (i.e. diffusing out) by both disproportionation and transalkylation, thus subtracting the disproportionation products from the conversion levels in figure 13.2 would give only

transalkylation products (alkylnaphthalenes). Figure 13.8 shows the transalkylation estimate since it does not account for the retained species and diffusion problems.

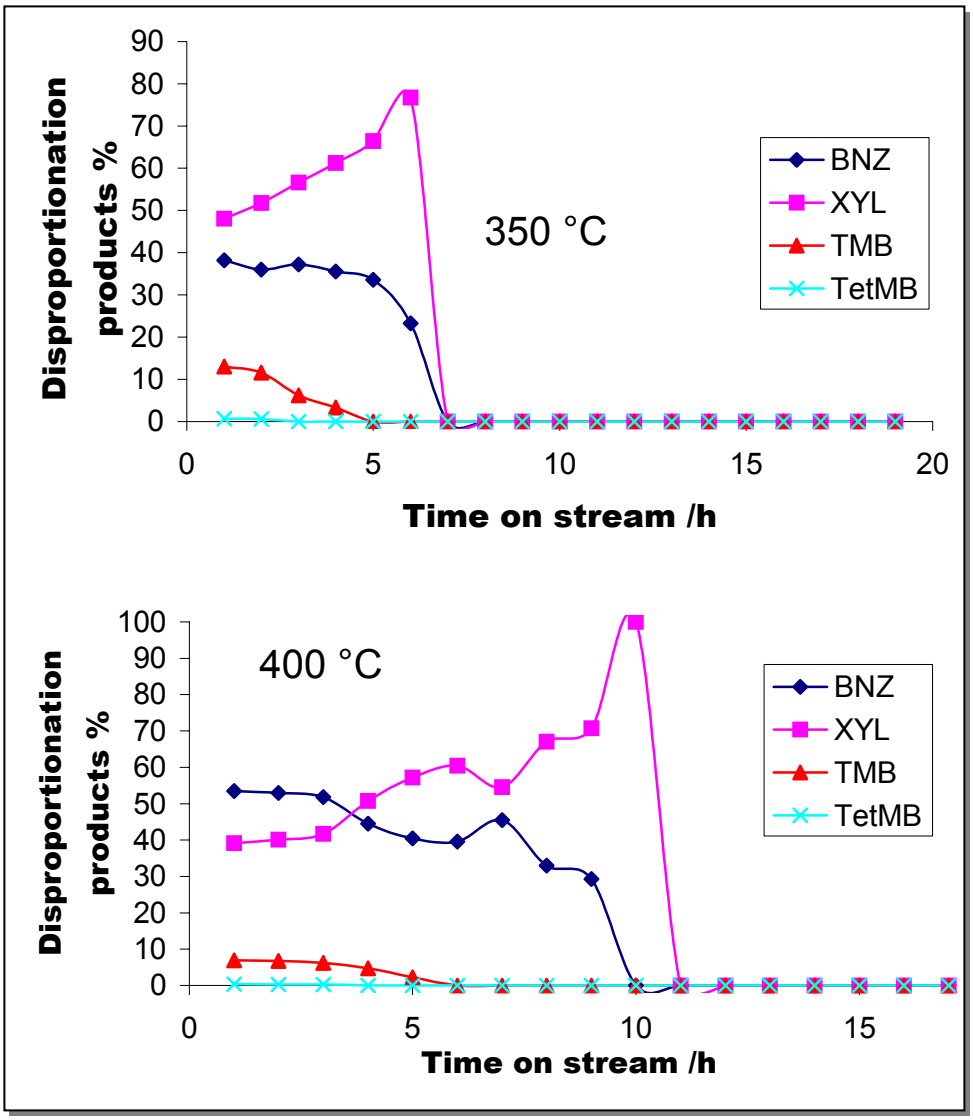

Figure 13.6: Toluene-naphthalene transalkylation (mol %) on H-mordenite; Toluene disproportionation products

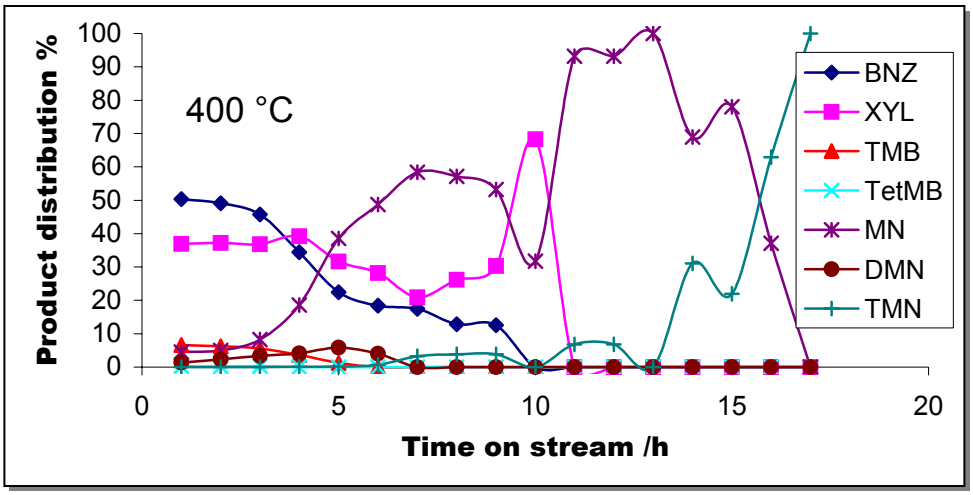

Figure 13.7: Toluene-naphthalene transalkylation (mol %) on H-mordenite; Product distribution

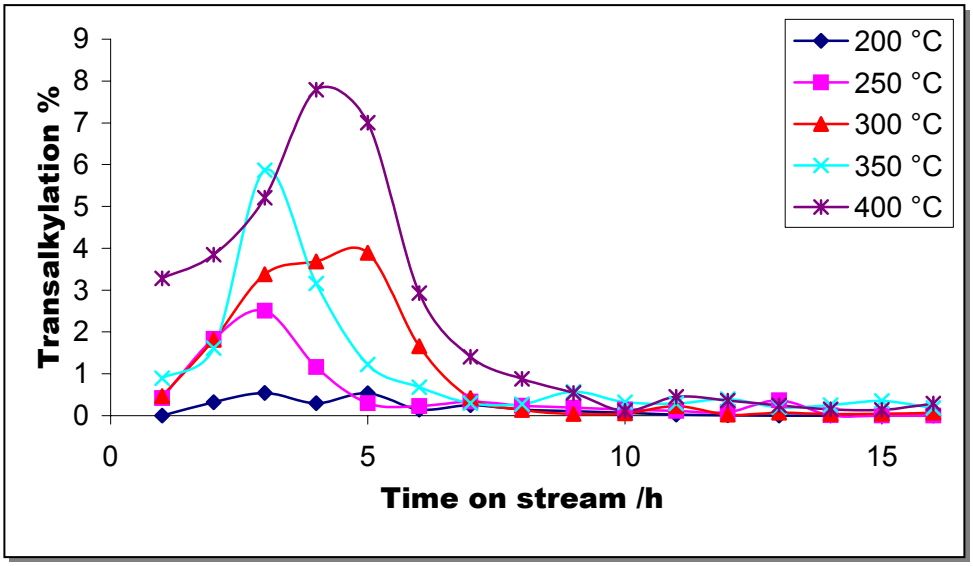

Figure 13.8: Toluene-naphthalene transalkylation (rough estimation) (mol %) on H-mordenite

The transalkylation estimate supported the suggestion that there was an increase in transalkylation activity with temperature. The figure also shows that the transalkylation products went through a maximum which might be mistakenly viewed as some kind of an induction period; in fact these products were produced during the very early stages of the reaction but due to the smaller molecules diffusing out

quickly and that the bulkiness hindered their diffusion they appeared much later in the product stream.

13.3.2 Toluene-naphthalene transalkylation on HLZY-82

On the zeolite-Y a different feed composition was used, i.e. 59/40 mol % toluene-naphthalene, and figure 13.9 shows an increase in conversion and lifetime with temperature which was characteristic of this zeolite in all systems studied.

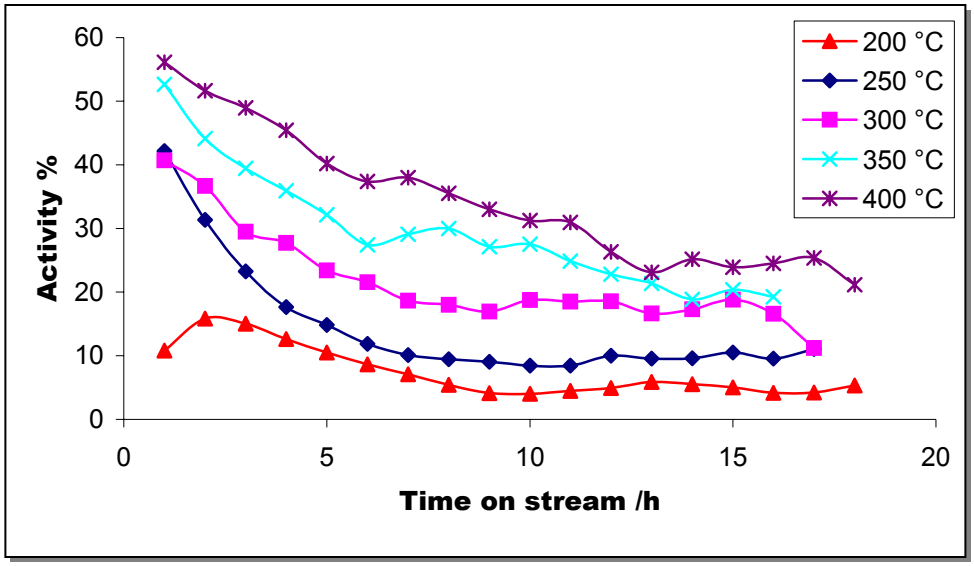

Figure 13.9: Toluene-naphthalene transalkylation (mol %) on HLZY-82

The product stream on the other hand (figure 13.10) showed molecular retention and a diffusion pattern that reflected on the structure of the zeolite, i.e. benzene was normally in high concentration during the initial stages of the reaction. Due to the uni-dimensional structure of mordenite catalyst, all molecules had to go through the same channel they came in, and so they somehow showed up at the same time in the product stream. On the zeolite-Y with its three-dimensional structure, the smaller

benzene molecule can just diffuse quickly through the catalyst in any direction and concentrates itself in the product stream, but ultimately every thing diffused through and relative amount were observed.

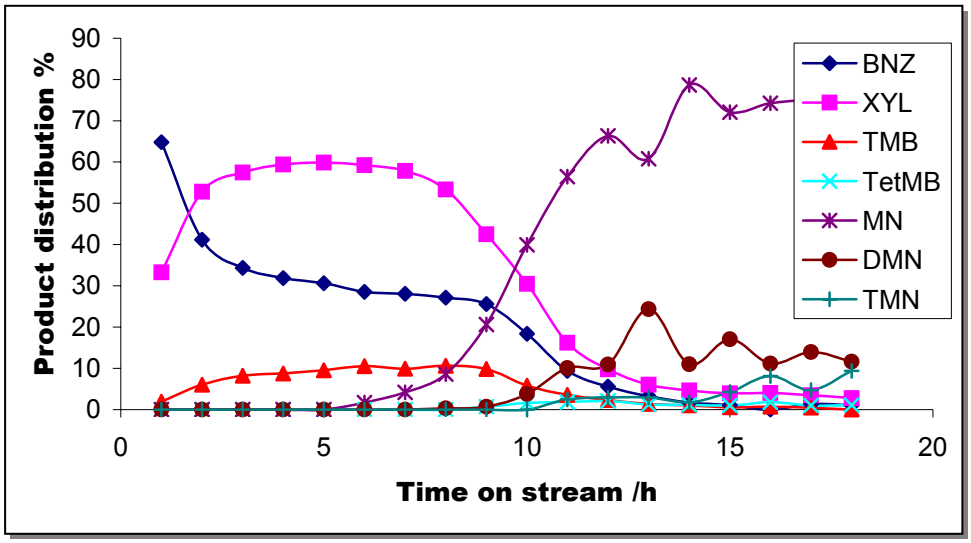

Figure 13.10: Toluene-naphthalene transalkylation (mol %) on HLZY-82 at 200 °C; product distribution

This figure shows the product distribution of the reaction at 200 °C. It has to be emphasized that the late appearance of bulky transalkylation products does not reflect their time of formation in the catalyst but mostly the rate at which they diffused through. Methylnaphthalene showed up first as expected and this was after 6 hours, then *tetra*-methylbenzene (TetMB) and dimethylnaphthalene (DMN) after 9 hours respectively and on the 11th hour came up the *tri*-methylnaphthalene (TMN).

An increase in temperature resulted in an increase in the kinetic motion of molecules and diffusion became less of a problem. Figure 13.11 shows the product distribution of the reactions at higher temperatures (350 - 400 °C). Bulky products showed up earlier in the product stream with temperature.

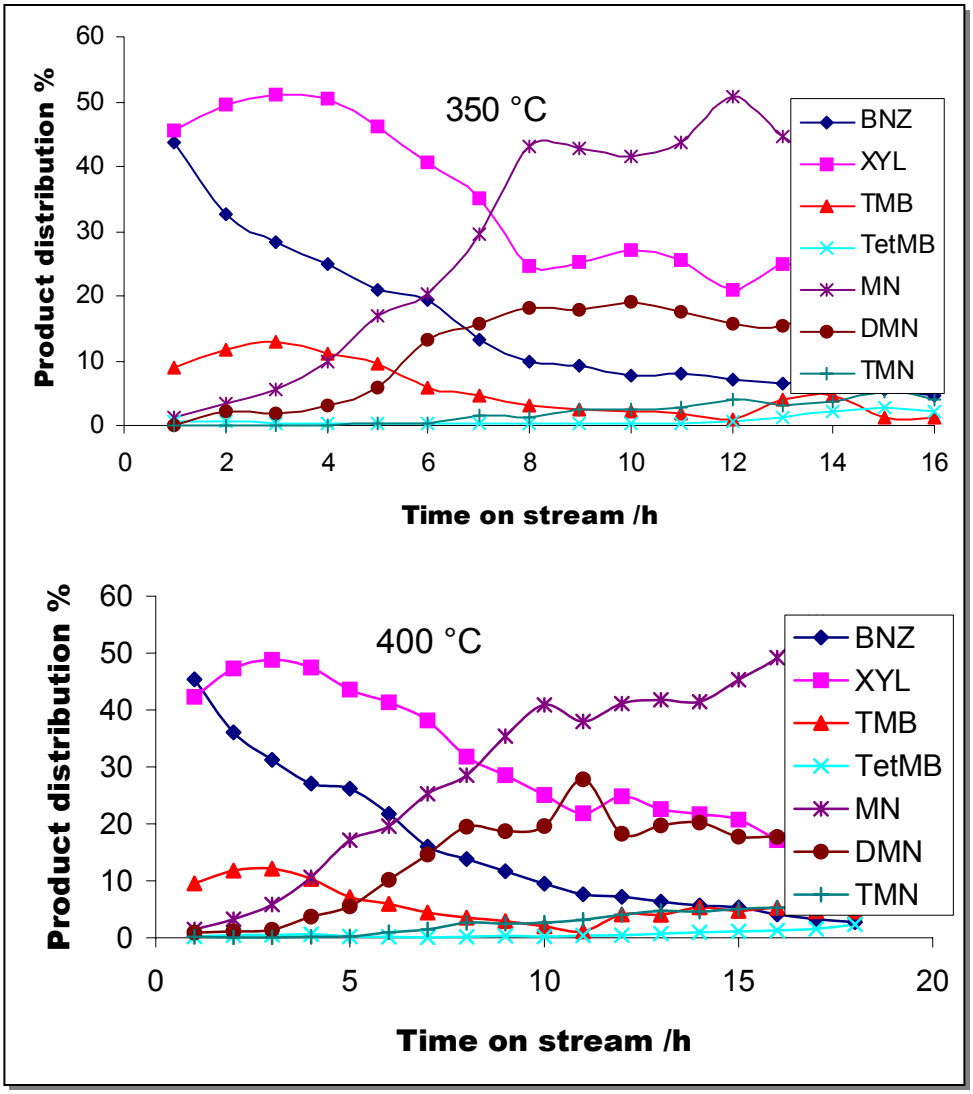

Figure 13.11: Toluene-naphthalene transalkylation (mol %) on HLZY-82; Product distribution

The effects of temperature were also shown by the changes in the diffusion patterns in figure 13.12 which shows the disproportionation products. This is shown clearly during the very early stages of the reaction.

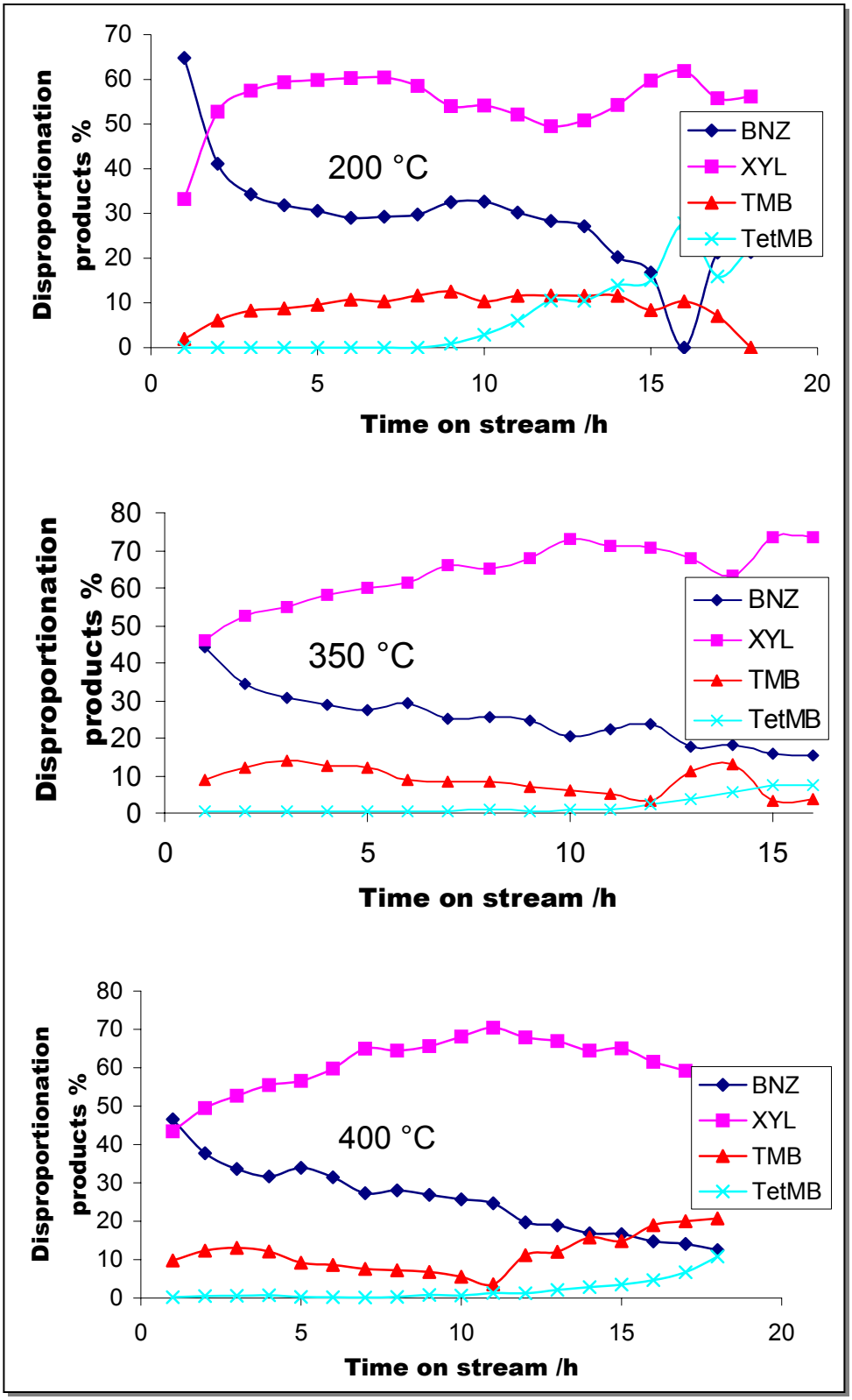

Figure 13.12: Toluene-naphthalene transalkylation (mol %) on HLZY-82; Toluene disproportionation

Transalkylation estimate on the zeolite-Y supported the fact that the transalkylation products were retained by the catalyst due to their bulky sizes. Figure 13.13 below also supported the fact that transalkylation favoured the open three-dimensional structure of the zeolite judging by the large amount of products, proving again that transalkylation required bigger zeolite pores and cavities. Both zeolites showed that there was an increase in transalkylation with increase in temperature, and the maximum achieved on mordenite was ~ 8 % and on the zeolite-Y ~ 20 % (estimates) at the same temperature. The figure (13.13) can also be viewed as a magnification of the first few hours of what was observed on H-mordenite (figure 13.8), which shows again the advantages of a three dimensional structure. Similar behaviour was observed in the product distribution of the benzene-methylnaphthalene system.

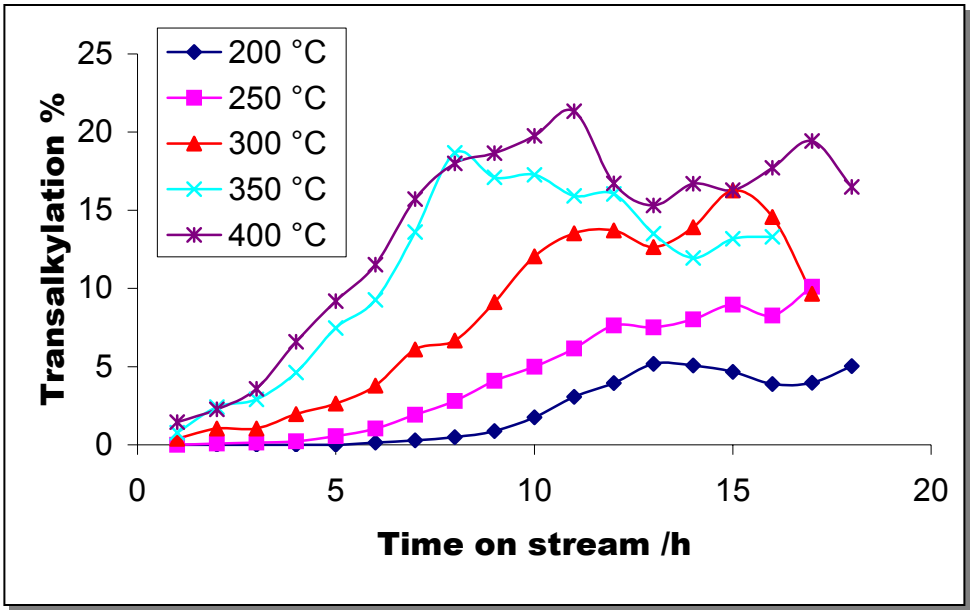

Figure 13.13: Toluene-naphthalene transalkylation (mol %) on HLZY-82; Transalkylation products

13.3.3 The effect of feed composition on back-transalkylation

Different toluene-naphthalene feed compositions were prepared and transalkylation reactions were studied at 200 and 350 °C on both zeolites under similar conditions.

The compositions were 67/32, 72/27, 87/12 % mol (toluene/naphthalene) on mordenite and 59/40, 72/27, 87/12 % mol on the zeolite-Y respectively.

There seemed to be no significant effect on the total amount of products in the outlet stream on changing the feed composition. On mordenite (figure 13.14) there were about 10 % of the products in the outlet stream at 200 °C and the amounts increased to 60 % at 350 °C during the initial stages of the reaction. The figure also shows that at both temperatures, the mordenite catalyst totally deactivated after 5 hours. This was weird because deactivation was attributed to mainly molecular retention (trapping) at lower temperatures but carbonaceous material deposition at higher temperatures.

Better activities were shown by the zeolite-Y at 200 °C, showing some kind of an induction period which reached a maximum after 3 hours. At 350 °C there were about 50 % of the products in the outlet stream. The better catalysts behaviour shown by the zeolite-Y at lower temperatures was mostly due to the fact that the catalyst contained a higher number of active sites than the mordenite, and these sites were mostly accessed by the smaller toluene molecules and thus promoting alkyl transfer reactions. The “induction period” observed here was most probably due to diffusion problems rather than the acid strength of the catalyst.

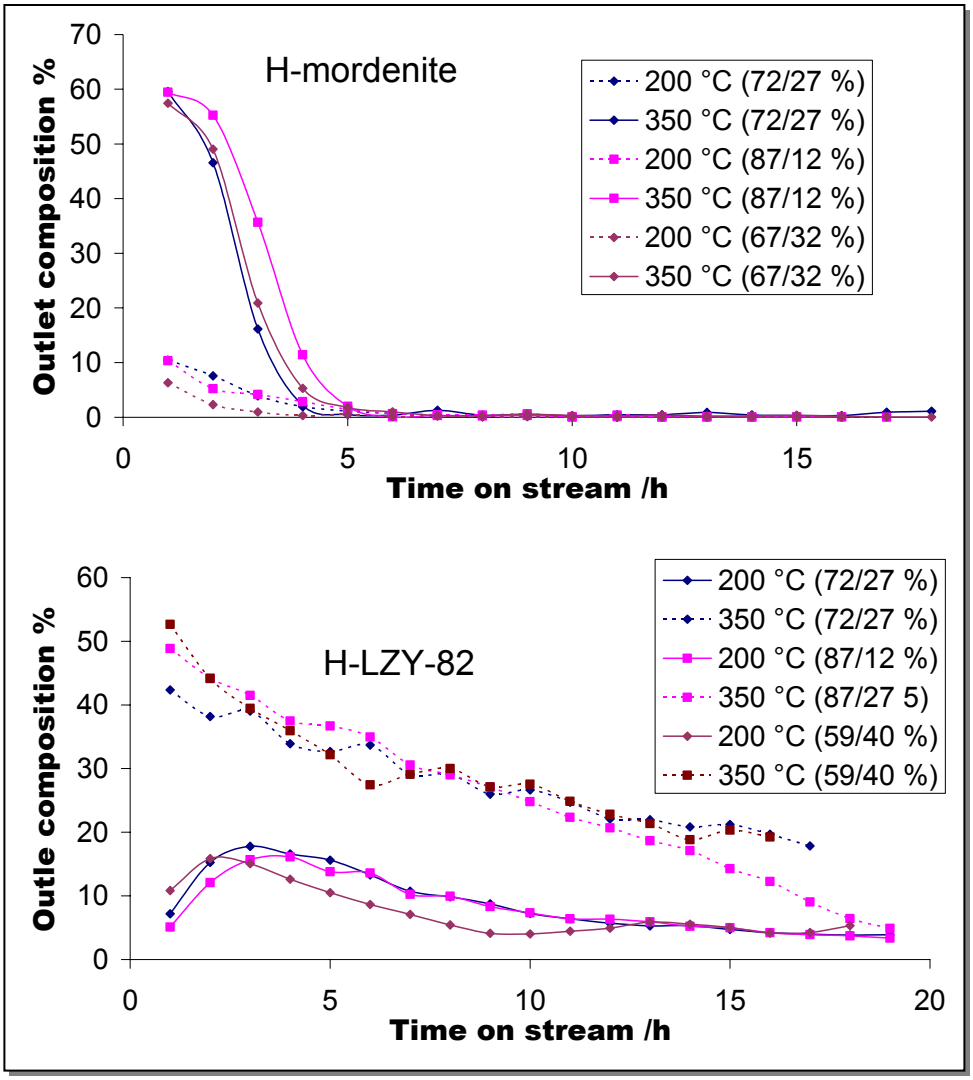

Figure 13.14: Toluene-naphthalene transalkylation (mol %) on zeolites; amounts of products in the outlet stream

The observed independency of the amount of products formed on the feed composition suggested that the rate of transalkylation was not that different from that of disproportionation. If the suggestion holds, then it would mean that it does not matter which molecule comes for the methyl group of the adsorbed toluene, the rate of the methyl group cleavage is the same. If toluene is the recipient of the methyl group then disproportionation occurs, but if it is naphthalene then transalkylation occurs.

The product distribution of the reactions on mordenite (figure 13.15) shows the deactivation rate to be dependant on the amount of the bulky naphthalene in the feed (diluting the toluene feed) at low temperatures. At 200 °C activity (presence of the smaller benzene and xylene) lasted for 5, 8 and 9 hours respectively with the decrease in naphthalene in the feed. This was mainly attributed to the fact that at low temperatures, the higher the amount of bulky molecules in the feed, the higher the amounts that would be retained by the catalyst and thus promoting deactivation.

At 200 °C trimethylnaphthalene was not observed in the product stream. An increase in temperature not only resulted in the formation of the trimethylnaphthalene but also showed that the rate of deactivation increased with the increase in the amounts of small molecules in the feed, i.e. the lifetime increased from 5 (at 200 °C) to 7 (at 350 °C) hours but decrease from 8 to 5 and from 9 to 6 respectively with increase in the amounts of toluene in the feed. This greatly supported the conclusions that deactivation by carbonaceous material deposition at higher temperatures favoured the consumption of smaller molecules; and catalyst deactivation by molecular retention at low temperatures was greatly affected by bulkier molecules.

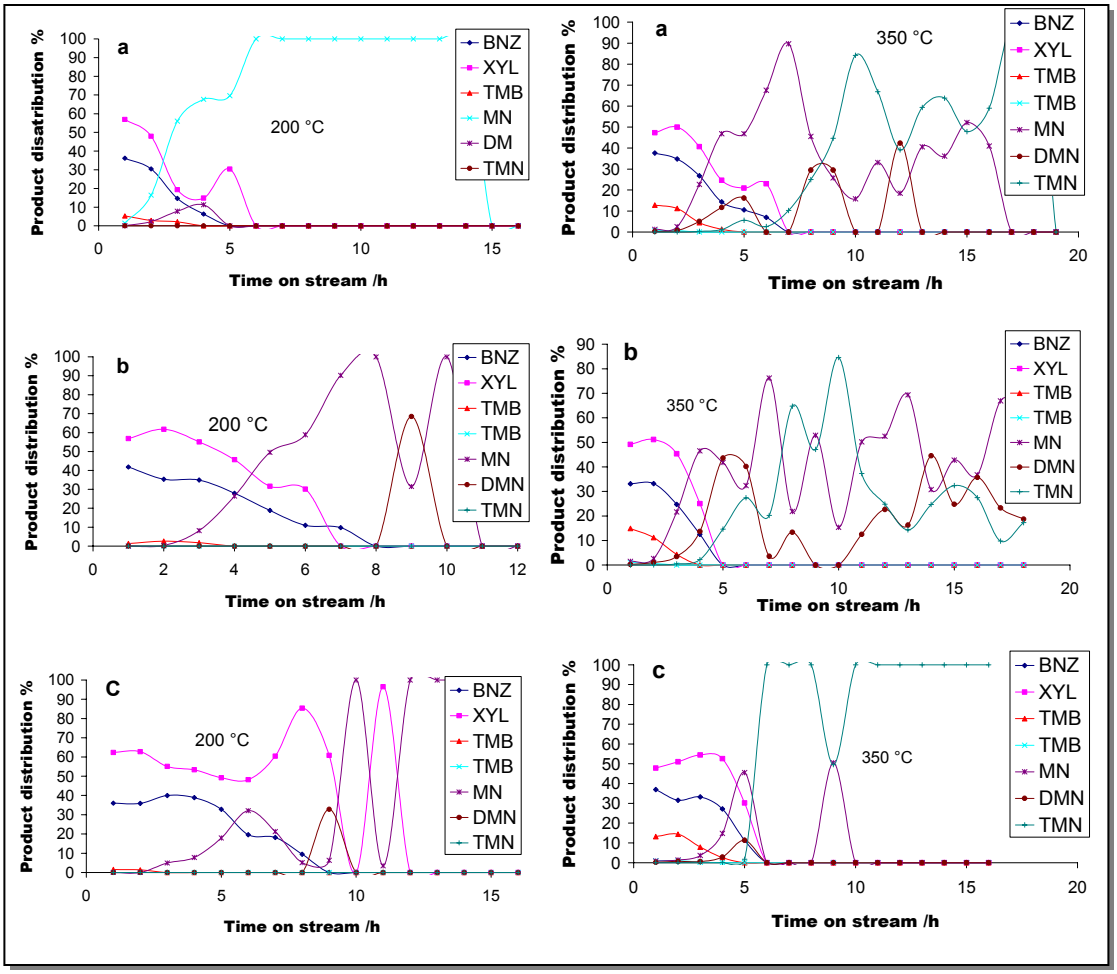

Figure 13.15: Toluene-naphthalene transalkylation (mol %) on H-mordenite; a = 67/32 %, b = 72/27 %, c = 87/12 % mol.

Figure 13.16 shows a dramatic increase in the catalyst lifetime with a decrease in the amounts of naphthalene in the feed on zeolite-Y. The lower the naphthalene content the lesser the amounts of bulky molecules that would be formed in the catalyst, and the longer the catalyst lifetime at lower temperatures. The formed bulky molecules were probably trapped in the catalyst by pore narrowing or retained by low temperatures. A decrease in naphthalene in the feed from 40 to 27 % improved the catalyst lifetime form 13 to more than 20 hours of time on stream; and a further decrease of naphthalene to 12 % most probably resulted in a further increase in the catalyst lifetime as suggested by the figure.

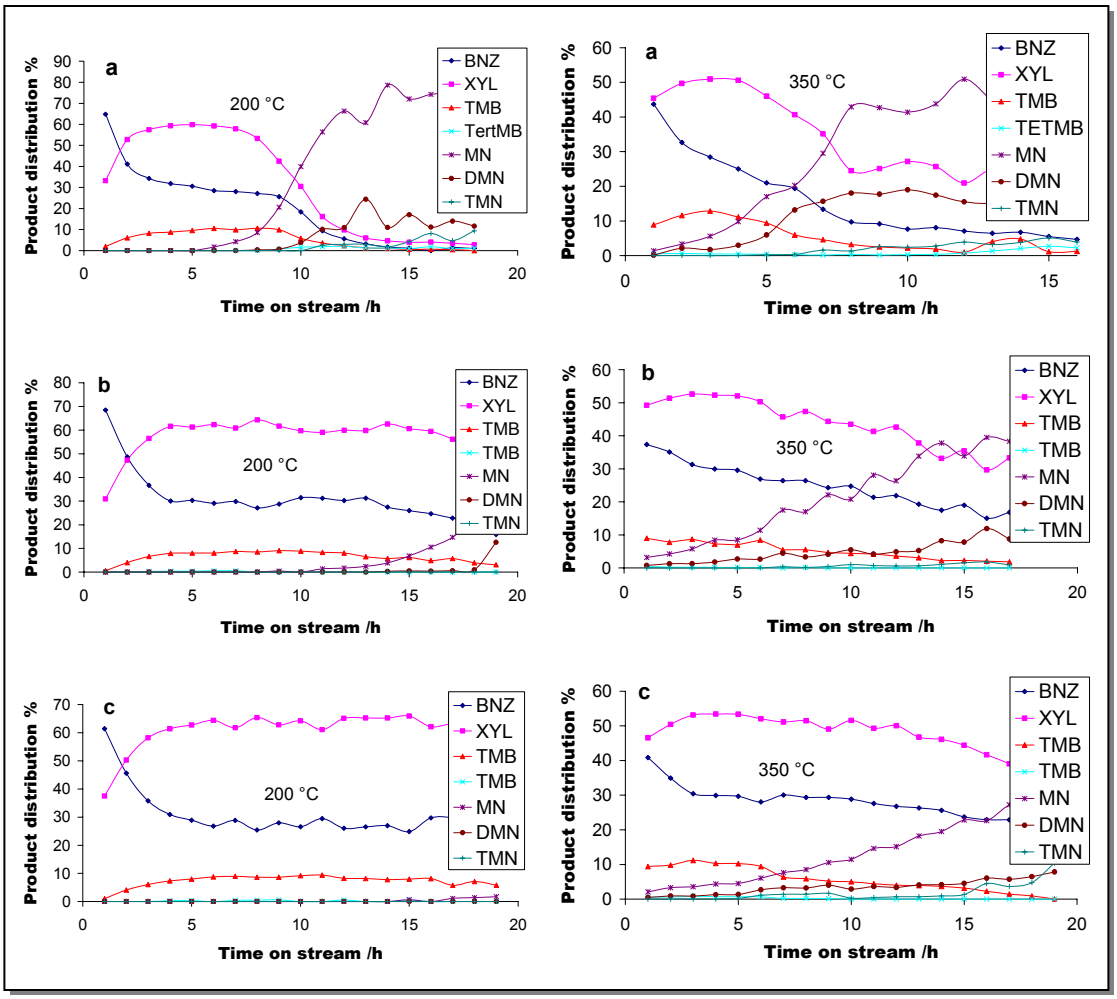

Figure 13.16: Toluene-naphthalene transalkylation (mol %) on HLZY-82; a = 59/40 %, b = 72/27 %, c = 87/12 % mol

Methylnaphthalene showed up in the product stream after 6 hours with the 59/40 % feed at 200 °C, and this was probably due to its higher amounts in the zeolite. The 72/27 % feed showed methylnaphthalene after 11 hours and the 87/12 % showed methylnaphthalene after 17 hours. The suggestion that the rate of alkyl-transfer was constant is supported here to a great extent since the product stream of this system showed great differences in reaction routes followed while the total amounts of products in the outlet showed none (figure 13.14).

The increase in temperature to 350 °C enhanced the diffusion of bulky molecules and cleared up the pores for new molecules to come and react, thus improved the catalyst lifetime from 13 hours to more than 16 hours with the 59/40 % feed. Though it was

not clear as to what happened with other feed compositions on increasing temperature, the observable thing was that methylnaphthalene, dimethylnaphthalene and trimethylnaphthalene showed up earlier in the product stream, supporting the fact that retention was inhibited by high temperatures; and thus tentatively concluded that temperature somehow improved the catalyst lifetime. The appearance of bulkier molecules early in the system might also be due to temperature induced selectivity towards transalkylation.

Since the decrease in the amounts of naphthalene in the feed resulted in the decrease in the amounts of formation of bulky molecules, this should also mean that there was a decrease in the transalkylation activity in favour of disproportionation. Figure 13.17 shows the amounts of bulky molecules (alkylnaphthalenes) that diffused out of the pores of both mordenite and LZY-82 respectively, these are represented as transalkylation products in percentages in the outlet stream. It was not very clear on whether composition had significant effects on transalkylation on mordenite only at low temperatures (200 °C); but on going to 350 °C, it could be seen that the amounts of transalkylation product decreased with a decrease in naphthalene amount in the feed. This was mostly attributed to the accompanying decrease in the competing number of naphthalene molecules against toluene for the alkyl group of the adsorbed species; the same were observed on HLZY-82. The differing diffusion patterns of the two zeolites were mainly due to different structural effects of the catalyst.

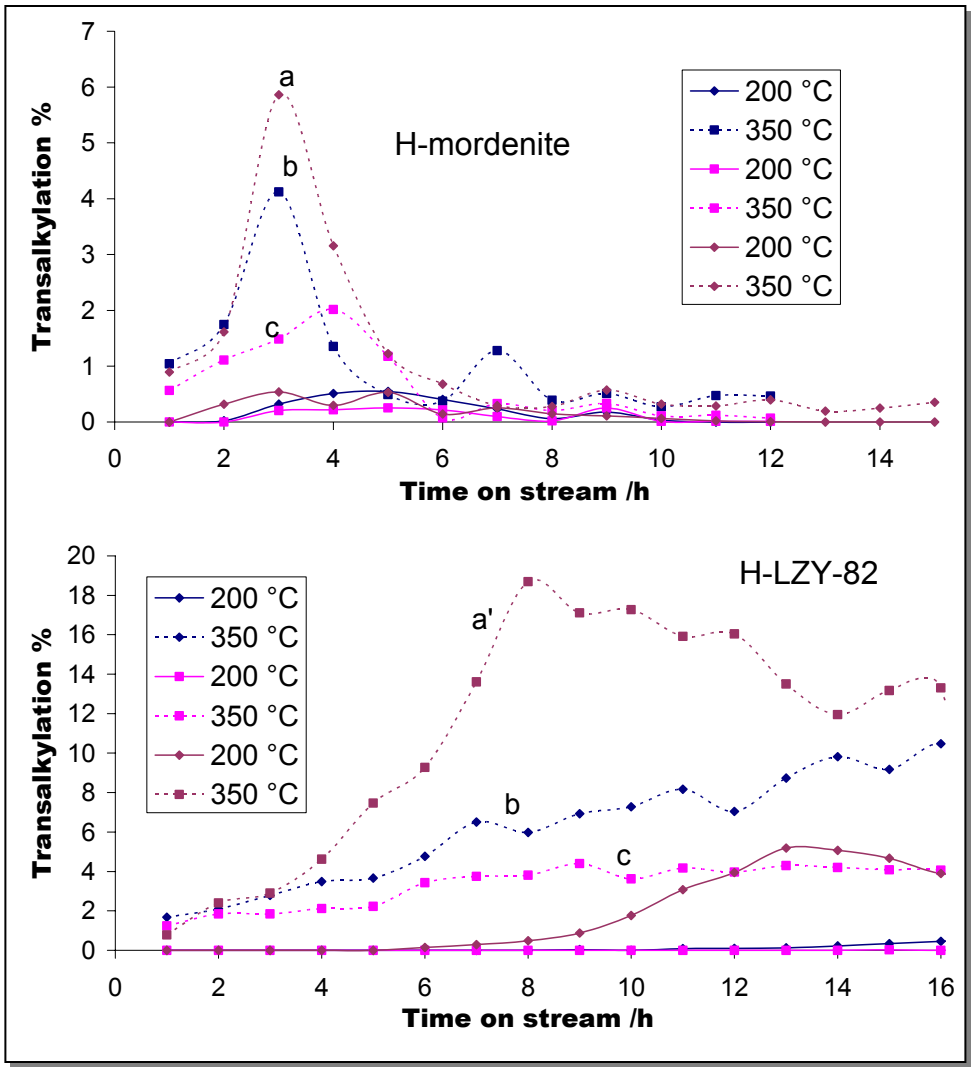

Figure 13.17: Toluene-Naphthalene transalkylation (mol %) on zeolites; a = 67/32 %, a' = 59/40 %, b = 72/27 %, c = 87/12 % mol

13.3.4 [*o*-Xylene]-naphthalene transalkylation on zeolites

Xylene and mesitylene disproportionation reactions have shown earlier that the ease of conversion increased with increasing number of alkyl groups on the benzene ring, even though some of the conversion was due to isomerization. It was then expected that back-transalkylation would be enhanced as compared to the toluene-naphthalene system. The only anticipated problem here was that of transition state selectivity, i.e.

the xylene-naphthalene bimolecular intermediate might be too big to form in the pores.

A feed of about 87/13 % (xylene: naphthalene) was prepared and alkyl transfer reactions were studied under same conditions as with the toluene-naphthalene system. The only difference was that, instead of 200 °C the reaction was studied at 400 °C. This was carried out to see if there would be any selectivity induced by temperature as it was shown by toluene-naphthalene system. The outlet composition of this reaction on both catalysts showed that a lot of products were produced during the very early stages of the reaction (figures 13.18 and 13.19). The figure shows that an increase in temperature resulted in a decrease in catalyst lifetime from 7 hours at 350 °C to 3 hours at 400 °C on mordenite. This was attributed to the increase in the rate of carbon formation with increase in temperature and the suspected temperature influence on the reaction mechanisms involved. The same behaviour was shown by the zeolite-Y.

The product stream (figure 13.20) of these reactions showed a toluene deficit on both zeolites. This was mainly attributed to 1) further toluene disproportionation to form benzene and xylene, 2) transalkylation to naphthalene since the transition state involved was smaller than the xylene-naphthalene intermediate, and 3) its participation in carbon deposition since all spent catalysts were black in colour. Nevertheless, the same toluene deficit was observed in the product stream of the *o*-xylene disproportionation system (chapter 7). Though toluene disproportionation was a sure thing in the catalyst, the product stream showed presence of methylnaphthalene, dimethylnaphthalene and trimethylnaphthalene to support transalkylation.

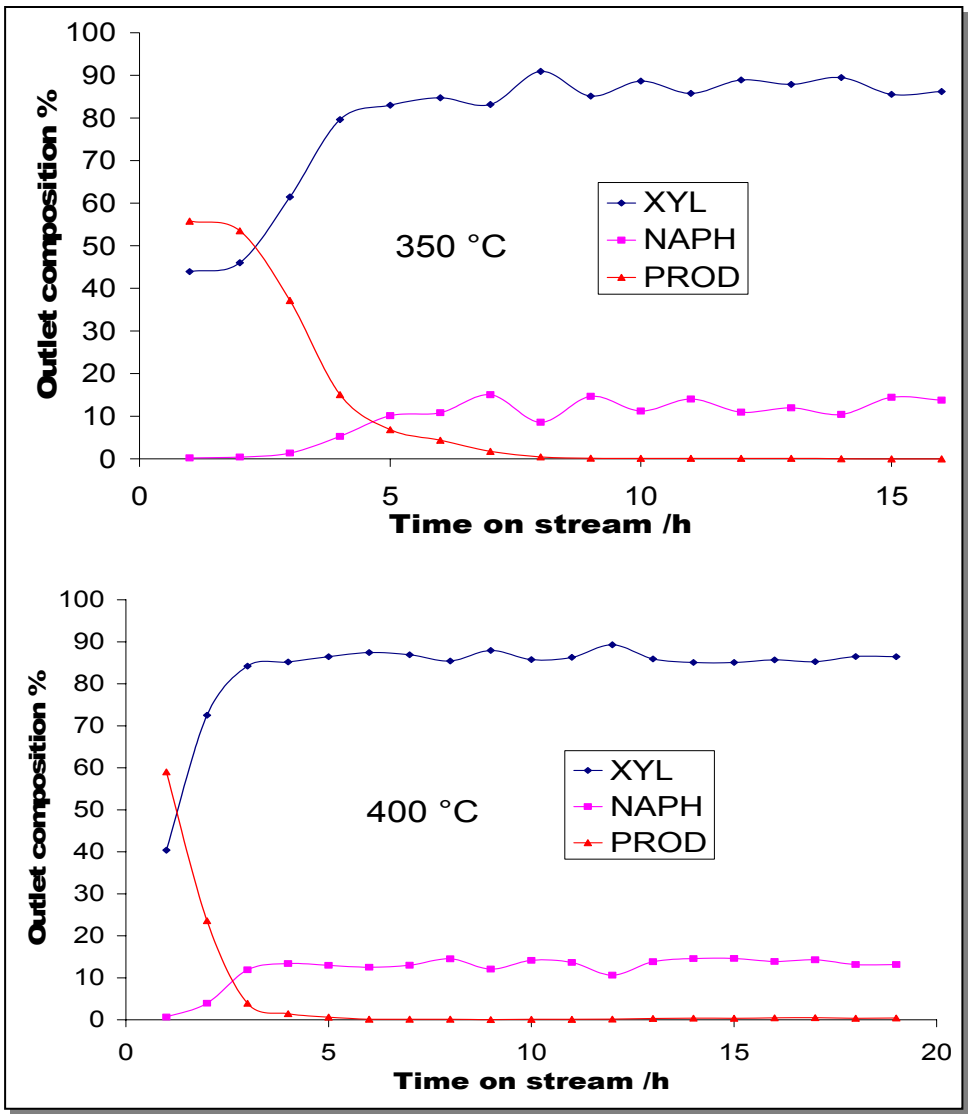

Figure 13.18: *o*-Xylene-Naphthalene transalkylation (mol %) on H-mordenite

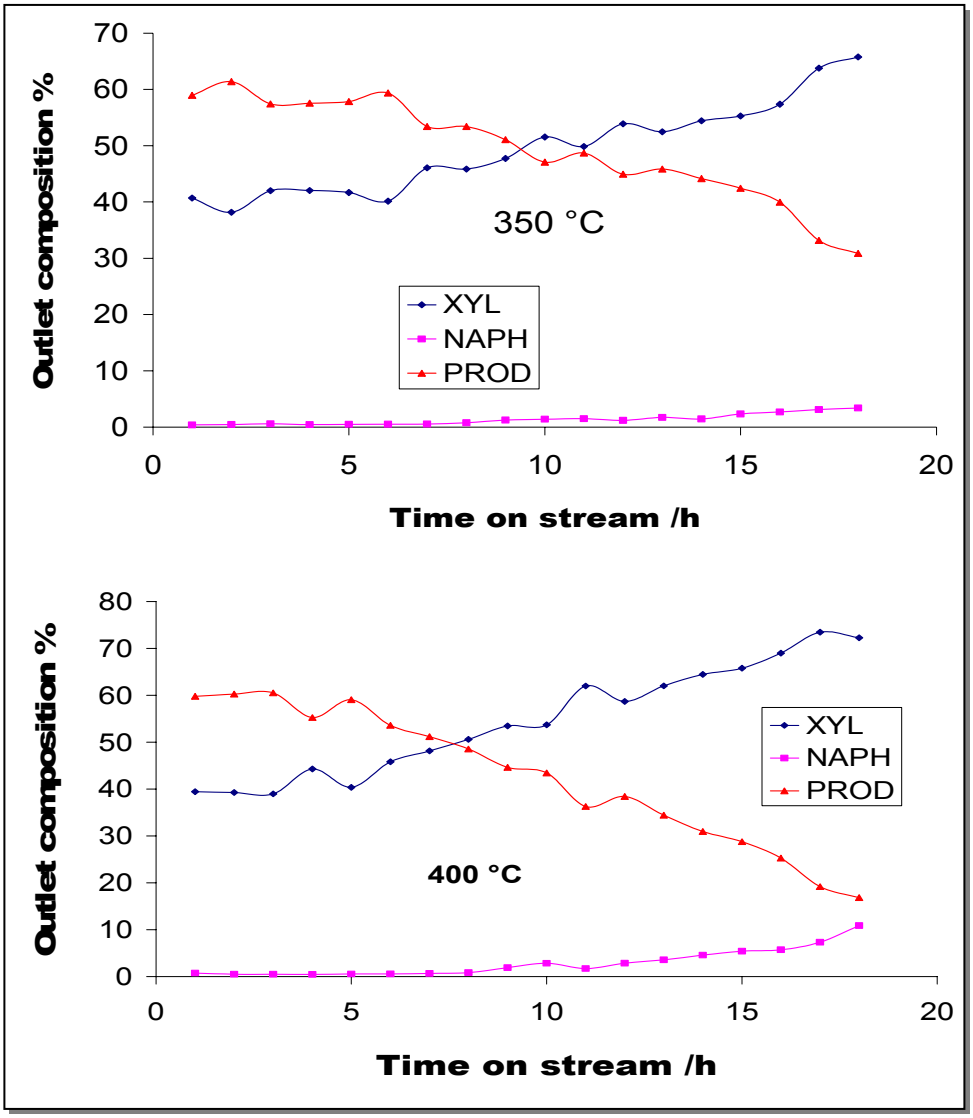

Figure 13.19: *o*-Xylene-naphthalene transalkylation (mol %) on HLZY-82

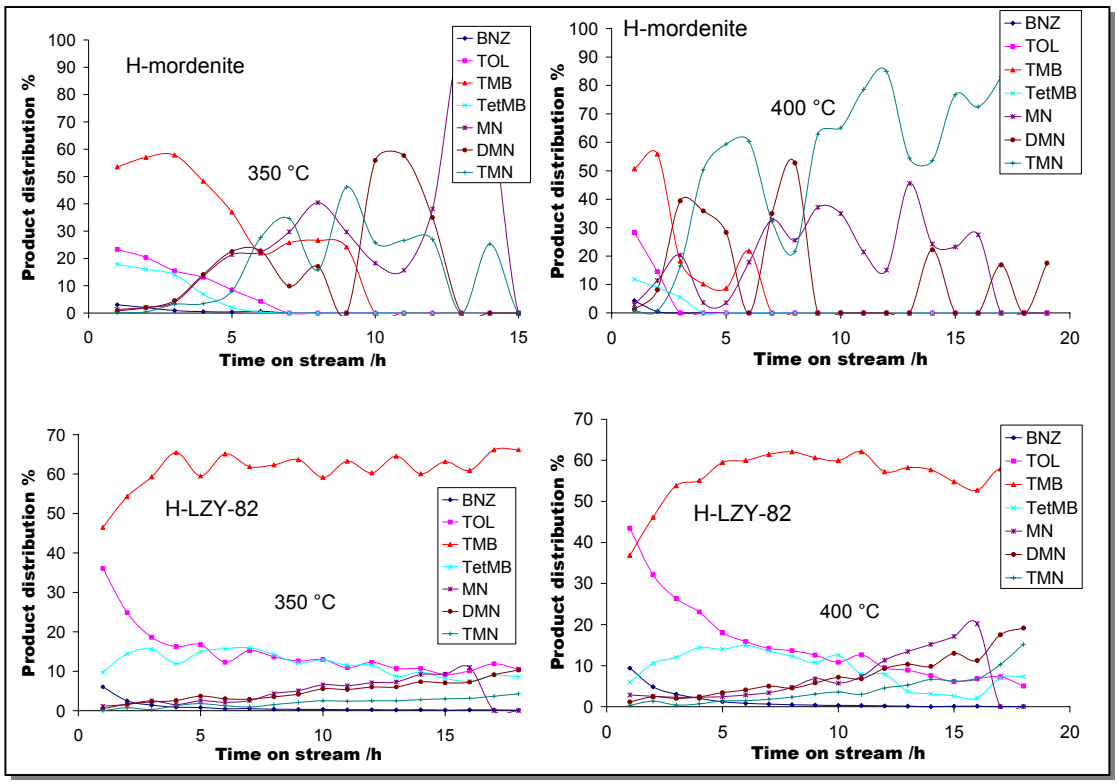

Figure 13.20: *o*-Xylene-naphthalene transalkylation (mol %) on zeolites; product distribution

The alkyl-benzene distribution which was mainly due to xylene disproportionation showed that trimethylbenzene was the dominant species in the product stream (figure 13.21). Mesitylene disproportionation studied earlier showed that bulky alkylbenzenes were dominant in the product stream, and this was attributed to the mere fact that once they are formed, bulky molecules are no more involved in any further alkyl-transfer reactions due to transition state selectivity and the difficulty of accessing active sites; and thus the presence of the bulkier *tetra*methylbenzene in higher amounts in the present study. An increase in temperature resulted in toluene diffusing quickly out of the zeolite-Y pores during the very early stages of the reaction; but a deficit was shown with time on stream.

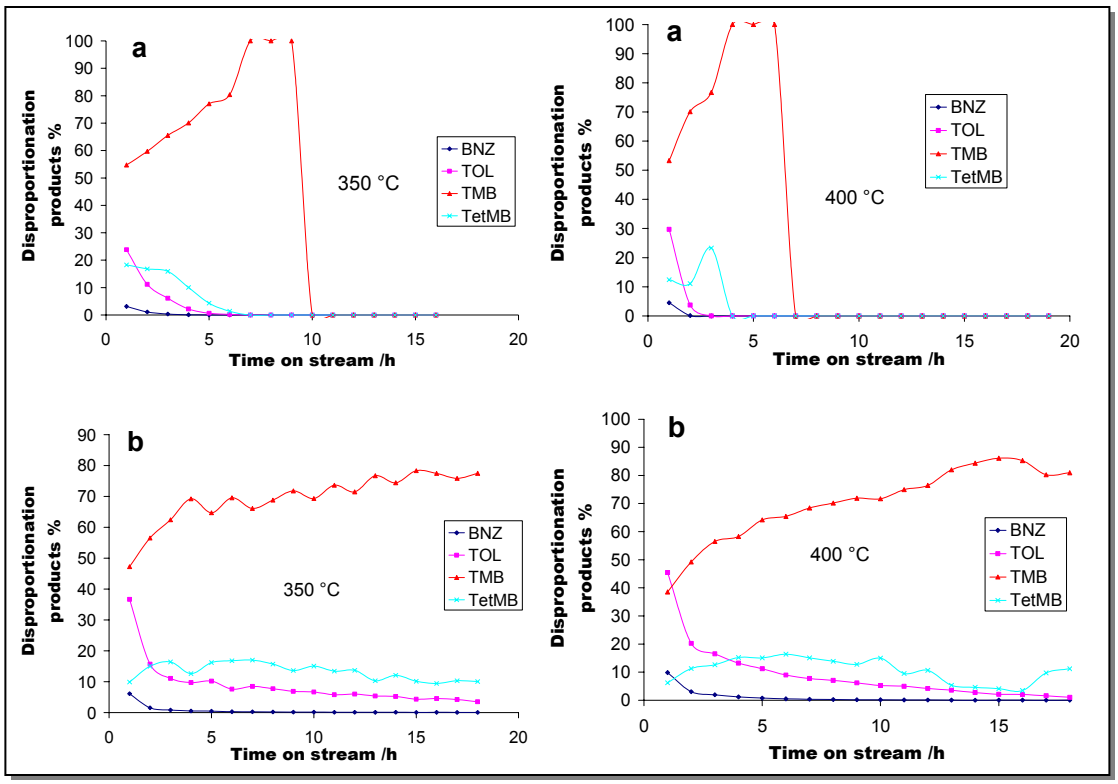

Figure 13.21: *o*-Xylene-naphthalene transalkylation (mol %); a = H-mordenite; b = HLZY-82

Since a similar toluene-naphthalene feed composition was prepared and studied earlier, a comparison was made at 350 °C. The fact that an extra methyl group on the xylene enhanced the stability of the carbenium ion that formed, and also increased the ease of the first methyl group removal, alkyl-transfer reactions were expected to be higher than in the case of the toluene system. It is shown in figure 13.22 that there were no significant changes or differences in the amount of products in the outlet stream on mordenite at 350 °C.

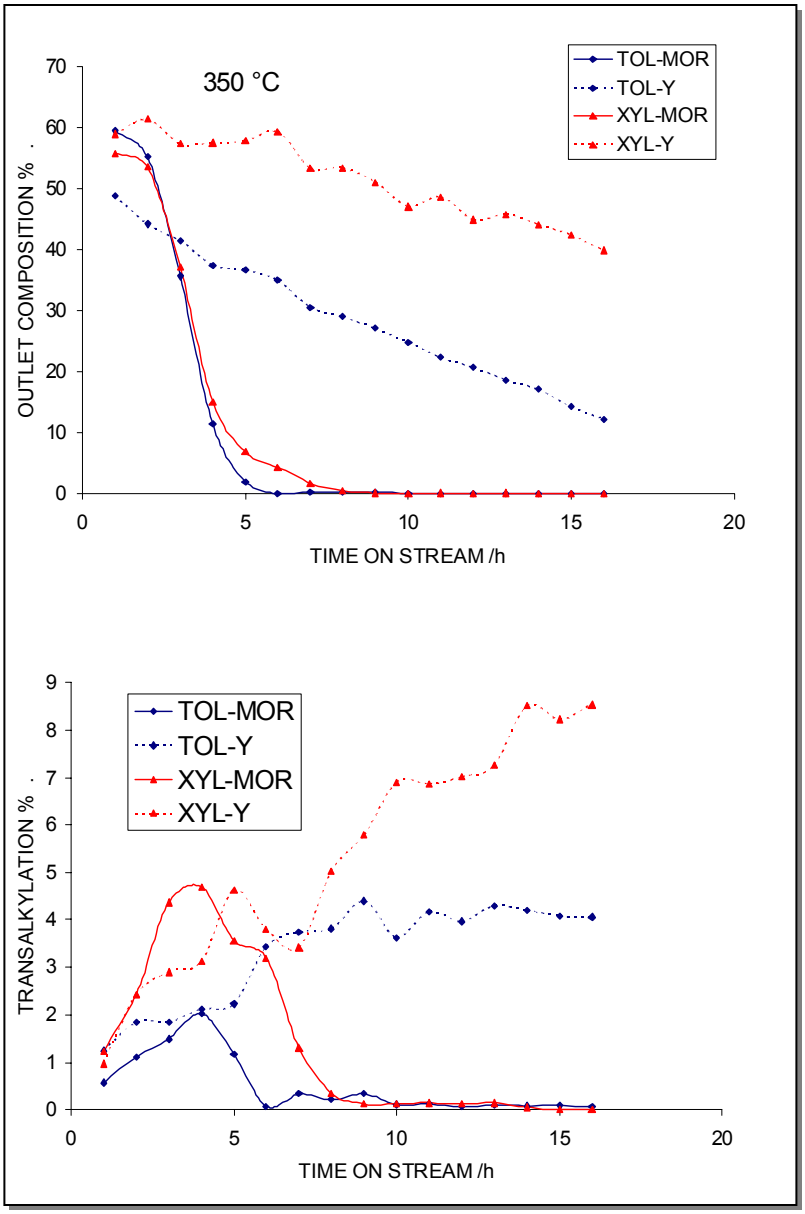

Figure 13.22: A comparison between toluene-naphthalene and xylene-naphthalene systems (mol %); TOL-MOR = Toluene system on mordenite, XYL-MOR = Xylene system on mordenite, etc.

This was believed to be due to 1) approaching of the active site by toluene was faster than that of xylene, but the stability of the latter carbenium ion was favoured, 2) the transition state with toluene was smaller than that formed by xylene, but the ease of removal of the methyl group favoured the latter, 3) the rate of deactivation seemed to be somehow constant since toluene can disproportionate to xylene, and xylene

formed toluene by similar mechanism, thus products produced were somehow similar, 4) the one-dimensional structure of the mordenite catalyst which did not give molecules much diffusion choices. On the zeolite-Y, approaching the active site by xylene and the transition state formed was less of a problem and thus the xylene-naphthalene system produced more products, and the three-dimensional structure allowed for molecular diffusions. The transalkylation graph showed that an extra methyl group indeed favoured transalkylation on both zeolites. The observed induction period here was not attributed to the catalyst behaviour but the diffusion/desorption rates displayed by these bulky molecules.

13.4 Conclusions

Transalkylation from toluene to naphthalene seemed more feasible than from methylnaphthalene to benzene. This was mostly attributed to the accessibility of the active sites where a carbenium ion has to be formed for any alkyl-transfer reactions to occur. The benzene-methylnaphthalene system showed very low conversions as compared to that of alkylbenzene-naphthalene systems, simply because the alkyl containing species must be the one adsorbed on the active site, and in the latter system alkylbenzenes were small enough to access the sites with less difficulties, and thus alkyl-transfer reactions were enhanced; but with the former system methylnaphthalene was bulky and approaching of the active site was somehow sterically retarded, and so were alkyl-transfer reactions.

Transalkylation reactions are reversible reactions and since back-transalkylation is favoured in zeolites the desired transalkylation reactions are expected to show low conversions due to competing reactions.

It has been shown also that with increase in the number of alkyl groups on the alkyl-acceptor favouring back-transalkylation and the suggestion that toluene is a better

alkyl-acceptor than benzene; it is not advisable to use alkylbenzenes in such reactions even though reaction conditions would have to be a little hash for appreciable conversions to be achieved with benzene.

It has been observed that systems with bulky molecules will suffer severe deactivations through molecular build-up (retention) if reactions are carried out at lower temperatures (<250 °C). On the other hand, reactions at higher temperatures will suffer rapid deactivation through carbonaceous deposits if the system contains smaller molecules.

14 DEACTIVATION AND REGENERATION OF SOLID ACID CATALYSTS

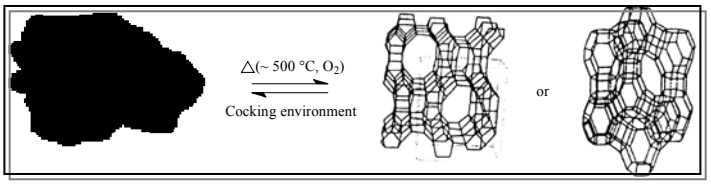

14.1 Introduction

Catalytic hydrocarbon conversion processes are of great industrial importance in the refinery and petrochemical industries. During these processes, the catalyst is deactivated by the formation of carbonaceous material on its surface; which denotes the carbonaceous residues formed from 'secondary' reactions within the catalysts. Deactivation of acid zeolites is caused mainly by the retention of these carbonaceous compounds (coke) inside the pores or on the outer surface of the crystallite.[77] This depends on the characteristics of the active sites and on the operating conditions: reaction time, temperature, pressure and the nature of the reactants. The coke formation is slow when transformation of an alkyl aromatic is by disproportionation and fast with dealkylation, and coking rate increases with the basicity of the aromatic ring. At low temperatures carbonaceous deposits are mainly consisting of unconverted reactants and at high temperatures one finds condensed ring aromatics; and the rate of coke formation increases with temperature, i.e. H/C ratio decreases.[77]

Products, even when they are not bulky, remain blocked in zeolite (not steric blockage), they are retained in the zeolite because of their low volatility (boiling points higher than the reaction temperature) and also because of their chemical or physical adsorption, when working at low temperatures.[40] At higher temperatures coke composition becomes that of condensed polynuclear aromatics. By burning-off the coke with oxygen mixtures the catalyst is regenerated.

High coke content leads to less efficient regeneration. It was found that, the physical structure of the catalyst cannot be fully regenerated[40] even if the coke has been fully removed. It was shown also that, the total elimination of carbonaceous residue by decoking induces changes in the pore size distribution and tortuosity of the catalyst. Scheme 14.1 outlines the effects of temperature on the type of carbonaceous material formed by secondary reactions during toluene conversion.

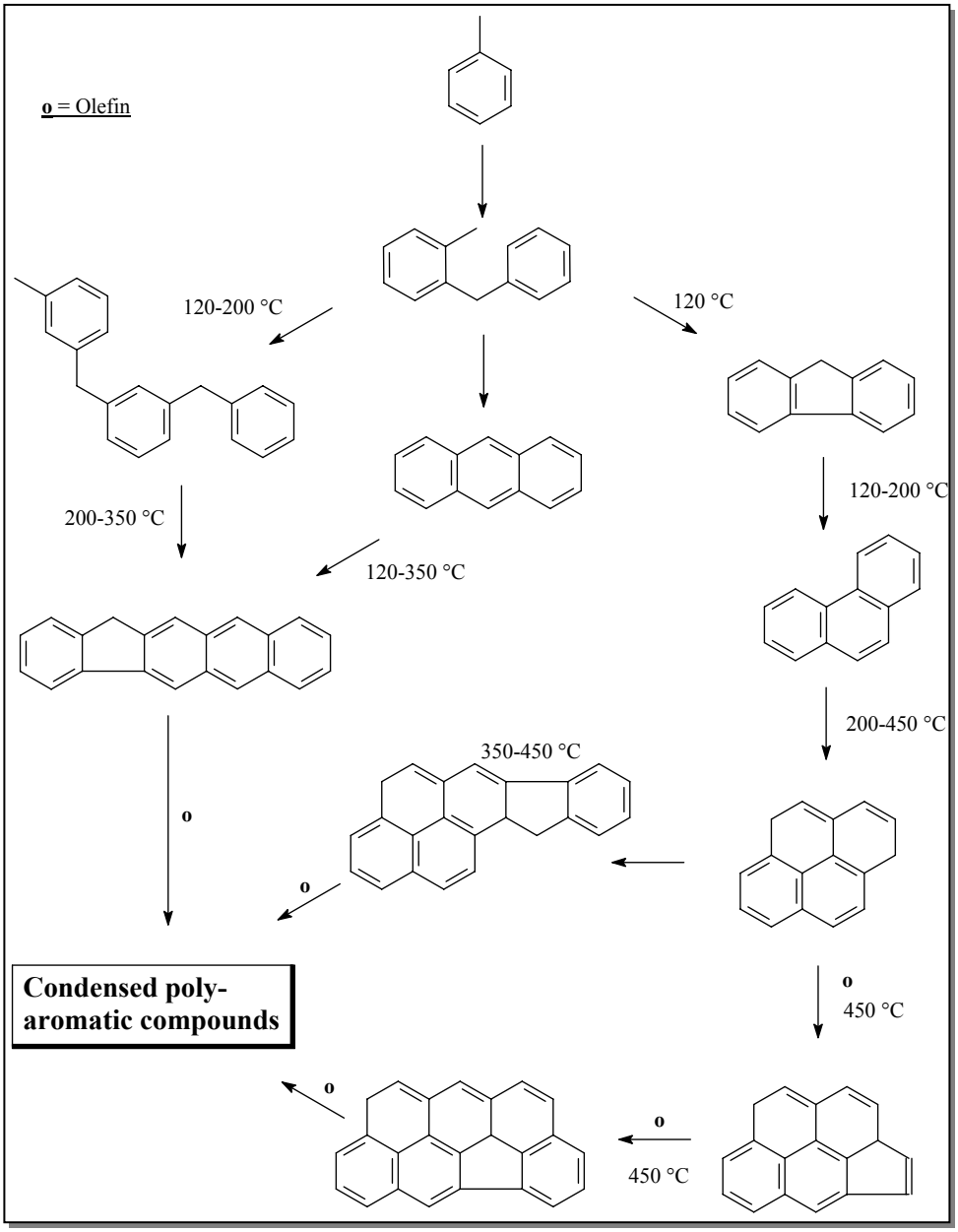

Scheme 14.1: The effects of reaction temperature on the type of carbonaceous materials formed in the catalyst during toluene conversion[40]

Magnoux *et al*.[78] carried out solid acid catalyst regeneration under air flow. They deposited coke on the USHY-zeolite by using model molecules like *m*-xylene (scheme 14.2), *n*-heptane and propane. After the reaction step, the coked catalyst was stripped under steam in order to eliminate the residual feed and to remove volatile hydrocarbons before regeneration. This was the process during which substantial modifications of coke composition took place. It has been shown also that if coked catalysts were maintained under nitrogen flow, at the same coking temperature, the aromaticity of coke molecules was enhanced. Their method of recovering coke from coked zeolite samples consisted of treating the zeolite with HF solution in order to dissolve the zeolite matrix and to liberate the inner coke material. They suggested that less bulky molecules were the most reactive to produce heavy poly-aromatic coke,[78] and that this result was related to the size and the location on the cavity of the bulky molecules. Bulky molecules with the sizes close to that of zeolite cavities were strongly blocked in the super-cages and did not easily react through a coupling reaction with other molecules located in the adjacent super-cages.

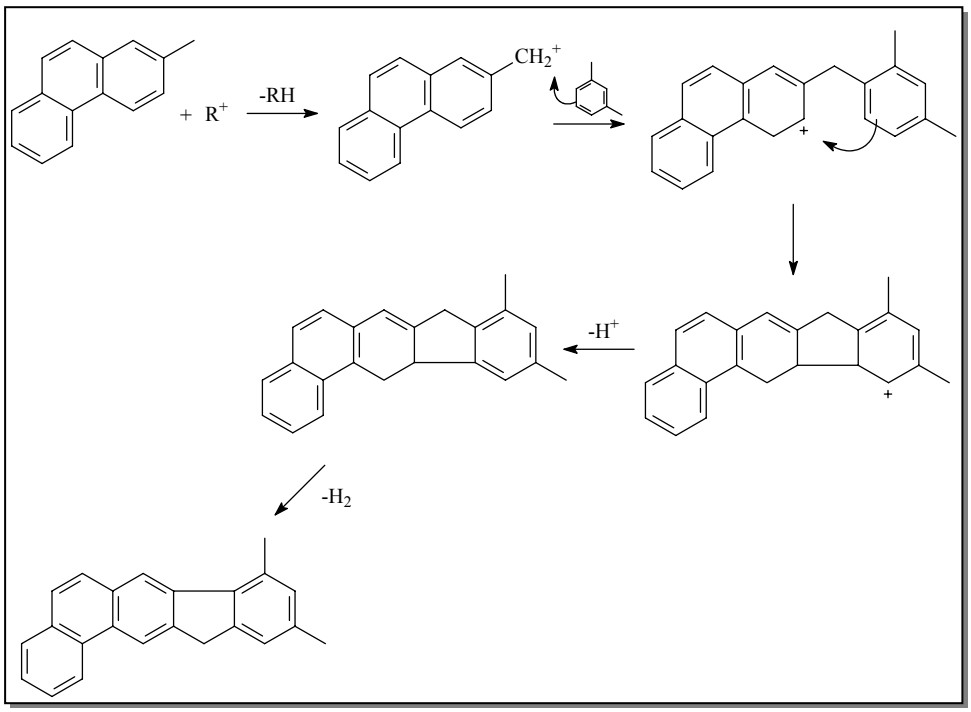

Scheme 14.2: Coke formation during Xylene conversion[78]

Coke formation is an intrinsic property of the zeolite pore structure; the spatial restrictions in the small-pore zeolite often severely inhibit formation of coke and of its precursors.[58] On HY-zeolite, the rate of coke formation (deactivation) is about 4 times slower than on H-mordenite and on HZSM-5 nearly 1000 times slower.[59]

The coke that forms in the zeolite pores/cavities may be effectively removed when H_2 is used as a carrier gas.[61] Coke that deposit on the external surface of the zeolite is mostly bulky hard coke. This coke is more difficult to remove by simple H_2 treatment. As a result, this external coke effectively modifies the surface acid properties of the zeolite.

Coke present in the inter-crystalline channels is removed preferentially to that present on the external surface during oxidation.[63] The activity of the catalyst can also be partly recovered while the coked catalyst is reactivated in the presence of H_2, although a lesser amount of coke is removed in this case.

The oxidative treatment of fouled zeolites depends on the characteristic of the coke and thermal stability of the zeolite catalyst. Moljord *et al.*[79] concluded that three types of reactions may take place during coke oxidation:

1) Condensation of poly-aromatic molecules
2) Oxidation of poly-aromatics into aldehydes, ketones, acids and anhydrides
3) Decarboxylation or decarbonylation of the oxygenated compounds

The zeolite pores (channels, cages, channel intersections) being of molecular size, the growth of carbonaceous material is limited, hence coke molecules are not very bulky in comparison to those found with conventional solid catalysts. Guisnet[80] was able to get high *para*-xylene selectivity by using MFI zeolite coked at high temperatures. At these high temperatures, a very poly-aromatic coke was formed covering part of the outer surface of the crystallite. The selectivity (*para*-xylene) increase had two origins:

1) The access to the non-shape selective acid sites of the outer surface was blocked
2) The sieving properties of the zeolite were improved

Transalkylation between the aromatic substrate and poly-alkylated compounds trapped in the zeolite nanopores was also shown to play a role.

Although the extent of carbon formation in catalytic cracking depends on the type of catalyst, the feed stock, and operating conditions; it has been found that there is an intrinsic uniformity in the way the carbon deposits on the catalyst increase with time.

The purpose of the present work was to study the influence of temperature and feed type on the deactivation (carbon deposition) of H-mordenite and HLZY-82 in their alkyl aromatic transalkylation/disproportionation reactions.

14.2 Carbon deposition

14.2.1 Experimental

Benzene conversion, toluene and mesitylene disproportionation/transalkylation reactions were used as model reactions for the study. The feeds were introduced into the reactor set at various temperatures ranging from 200 to 600 °C at 0.3 h^{-1} (WHSV) for four hours during which the results were analyzed by an online FID (G.C). After four hours, the flow of the feed was stopped and spent catalysts were flushed with N_2 (3ml/min) overnight to remove all the volatiles and loosely held molecules. Spent catalysts were then analyzed by the TGA for the total weight amount of molecules trapped in the pores and the carbon formed.

14.2.2 Results and discussion

Benzene conversion to simpler compounds seemed to be an impossible reaction in the present reaction conditions. This stemmed from the fact that the ring's aromaticity is very stable and that of the absence of a hydrogenating environment made it look like an impossible process, but previous studies (chapter 5) have shown that something does take place on zeolites. The darkening of the spent catalysts from white to grey at 200 °C and from white to black at 600 °C (on mordenite) proved that some carbonaceous materials were forming on the catalyst. On the zeolite-Y, considerable colour change was observed only at 400 °C and this intensified on increasing temperature. Since mordenite catalyst contained stronger sites than the zeolite-Y, colour change occurred at lower temperatures on the former; this also supported the fact that carbon formation was an acid catalyzed reaction. This was in line with the observations in chapter 5 during benzene conversions on zeolites, i.e. products were observed in the temperature range of 200-400 °C on mordenite but only at 400 °C on zeolite-Y. This suggested that carbon formation accompanied hydrocarbon transformation in zeolites, which might mean that, "no transformation then no carbonaceous material deposition (no supporting evidence)". Due to the blackening of the catalysts by benzene, three mechanisms for the formation of carbonaceous material were proposed (scheme 14.3).

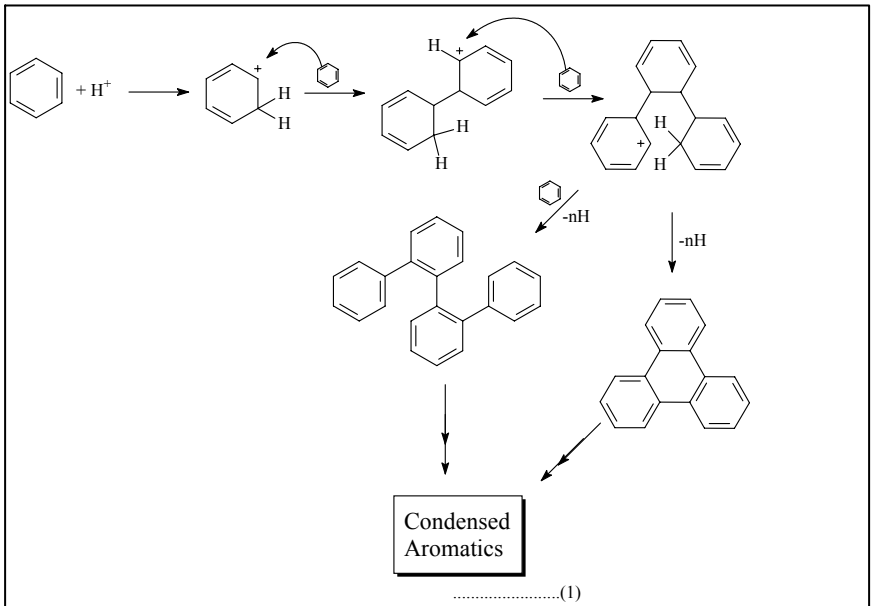
+ H+
H
H
H
H
H
H
H
-nH
-nH
Condensed Aromatics

.....(1)

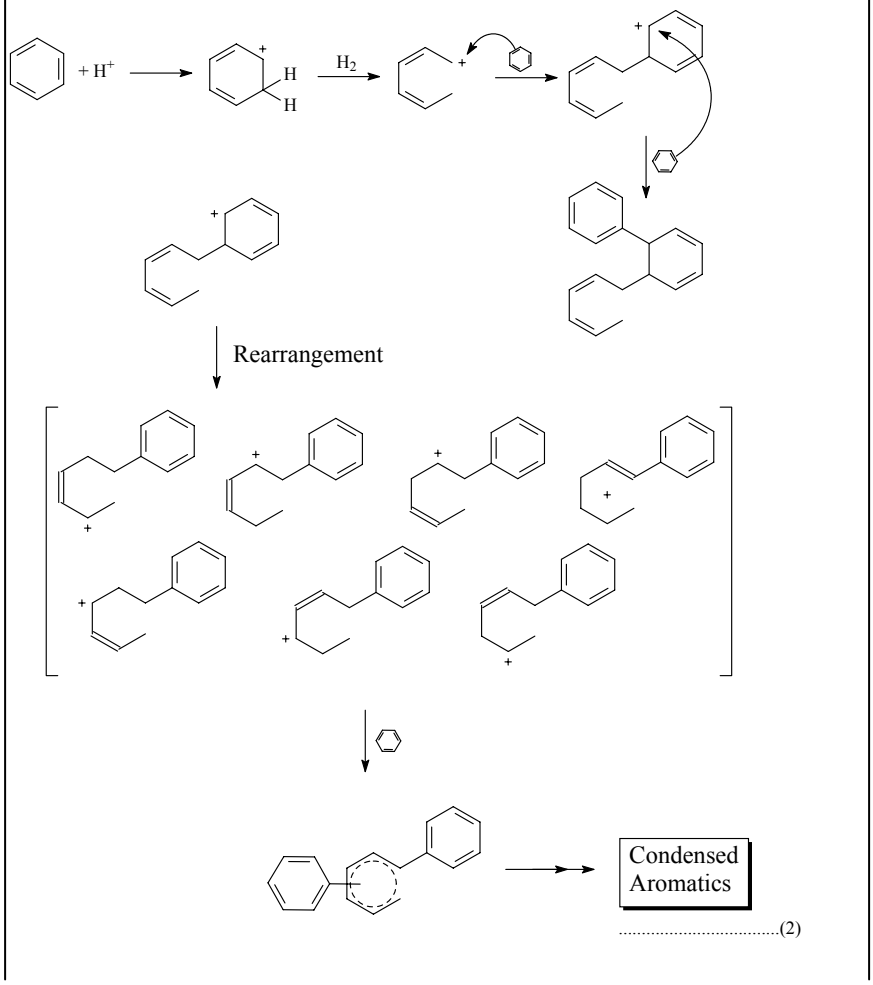
+ H+
H
H
H2
Rearrangement
Condensed Aromatics

.....(2)

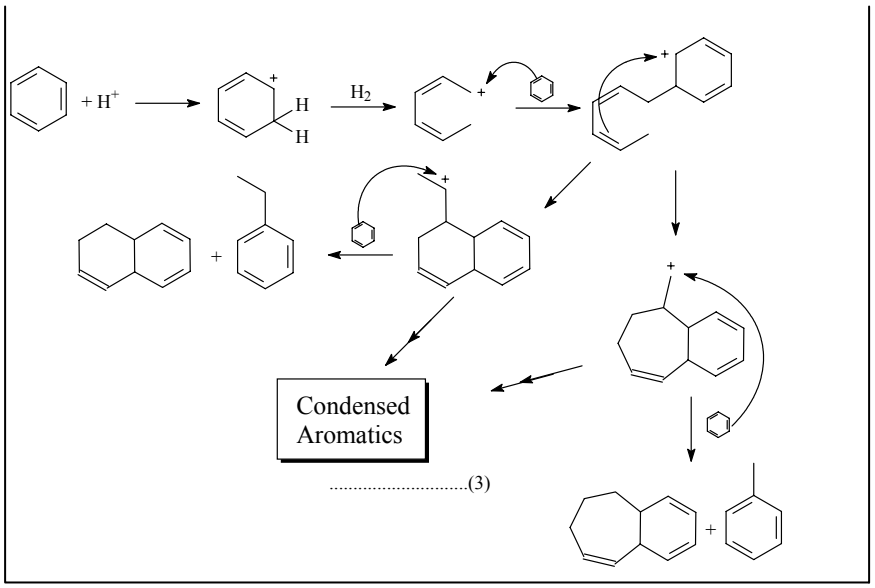

Scheme 14.3: Proposed mechanisms for the formation of carbonaceous material by benzene.

Route 1 on scheme 14.3 was the most probable one because it does not go through ring opening which would require a lot of energy and might also lead to cracking. This then was believed to be the dominant route especially at high temperatures. Bulky carbonaceous material could only form on the external surface of the catalyst depending on the strength of the acid sites and reaction conditions; but polymeric carbonaceous material (figure 14.1) were believed to be the dominant species in the zeolite pores. The second and the third routes (2, 3), though believed to be unlikely, might be occurring in the zeolite pores and/or on the external surface.

In addition to unknown products which were shown by the online G.C but could not be collected (by condensation) in an ice-bath while benzene was fed on both catalysts at elevated temperatures (chapter 5), both the online G.C and the G.C.M.S showed presence of toluene in the product stream. It was not clear whether other products resulted from benzene cracking or other reactions. The presence of toluene suggested that there were ring opening and probably cracking reactions in the catalysts. Since ring opening and cracking required at least H_2 in order to occur, the source might have been from the condensation of bulky carbonaceous products as shown on scheme 14.3(1); this in turn suggested that catalyst deactivation (fouling) triggered

these reactions. Due to the presences of other products in the product stream, and due to catalyst blackening during benzene conversion, it was concluded that benzene was converted probably to a less extent on zeolites and that carbonaceous material were formed in the catalyst.

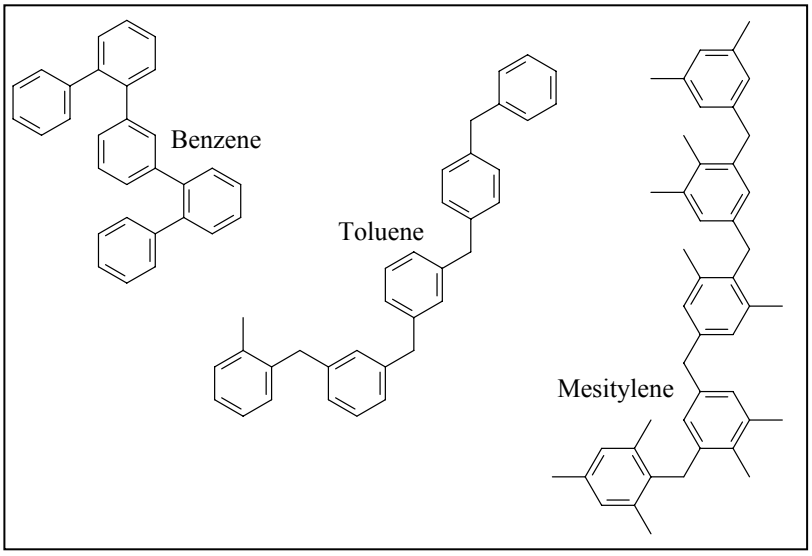

Figure 14.1: Polymeric carbonaceous species that formed in the zeolite

Toluene and mesitylene disproportionation/transalkylation reactions were more feasible than benzene conversion. An idea on the mechanism of coke formation by toluene (scheme 14.1) was outlined by Magnoux *et al*.[2] suggesting some sort of a chain reaction involving the formation of a carbenium ion on the acid site, and the consequent formation of biphenyl methane, followed by the formation of polymeric substances and finally condensation to coke material. The formation of carbonaceous material by mesitylene probably followed the same route with bulkier polymeric materials forming (figure 14.1).

As it was suggested earlier that there was some intrinsic uniformity in the way carbon deposited with time,[80] and suppose that the rate of deposition was independent of feed; if this was the case then the rate of deactivation of the catalyst should increase with increase in the size of the feed molecules, i.e. fewer molecules are needed to

completely block access to active sites with bulkier molecules. As it was shown before, deactivation was fast with benzene as the feed, and with toluene it was rapid but slower than benzene's; with ethylbenzene, xylene and mesitylene deactivation was much slower. Though this seemed to be in contrast to the above suggestion, considering the rates of molecular diffusion through the pores, the smaller benzene would be favoured and deactivation would be faster in this case (a lot would enter the zeolite pores and active site would be searched and reached quicker) and longer catalyst lifetime shown by the bulkier molecules might be due to slower molecular diffusions. This would be in agreement with what Magnoux *et al*.[78] earlier suggested that less bulky molecules were the most reactive in the production of heavy poly-aromatics. The most probable explanation was that of the required strength of the active sites for a particular reaction. Very strong acid sites were required to convert benzene and the required strength decreased with the number and chain length of the alkyl groups on the aromatic ring. Normally the strongest acid sites are the ones that are firstly deactivated, which might explain the high rate of deactivation shown by benzene and toluene as compared to ethylbenzene, xylene and mesitylene. The lifetime might also be prolonged by the weaker external acid sites in the case of poly-alkylated aromatics and those containing longer alkyl chains as they are easily converted.

The weight derivative against temperature for the spent catalysts after benzene deposition for four hours at different temperatures is shown in figure 14.2. The indicated temperatures are the deposition temperatures while feeding benzene through the catalysts. The 'PURE' means no deposition was carried out on the particular sample and the observed weight loss was mainly due to adsorbed water. This weight loss occurred around 50-120 °C implying that the water was both physisorbed and chemisorbed. Both mordenite and the zeolite-Y contained adsorbed water and that's why pre-treatment was very necessary before any reactions.

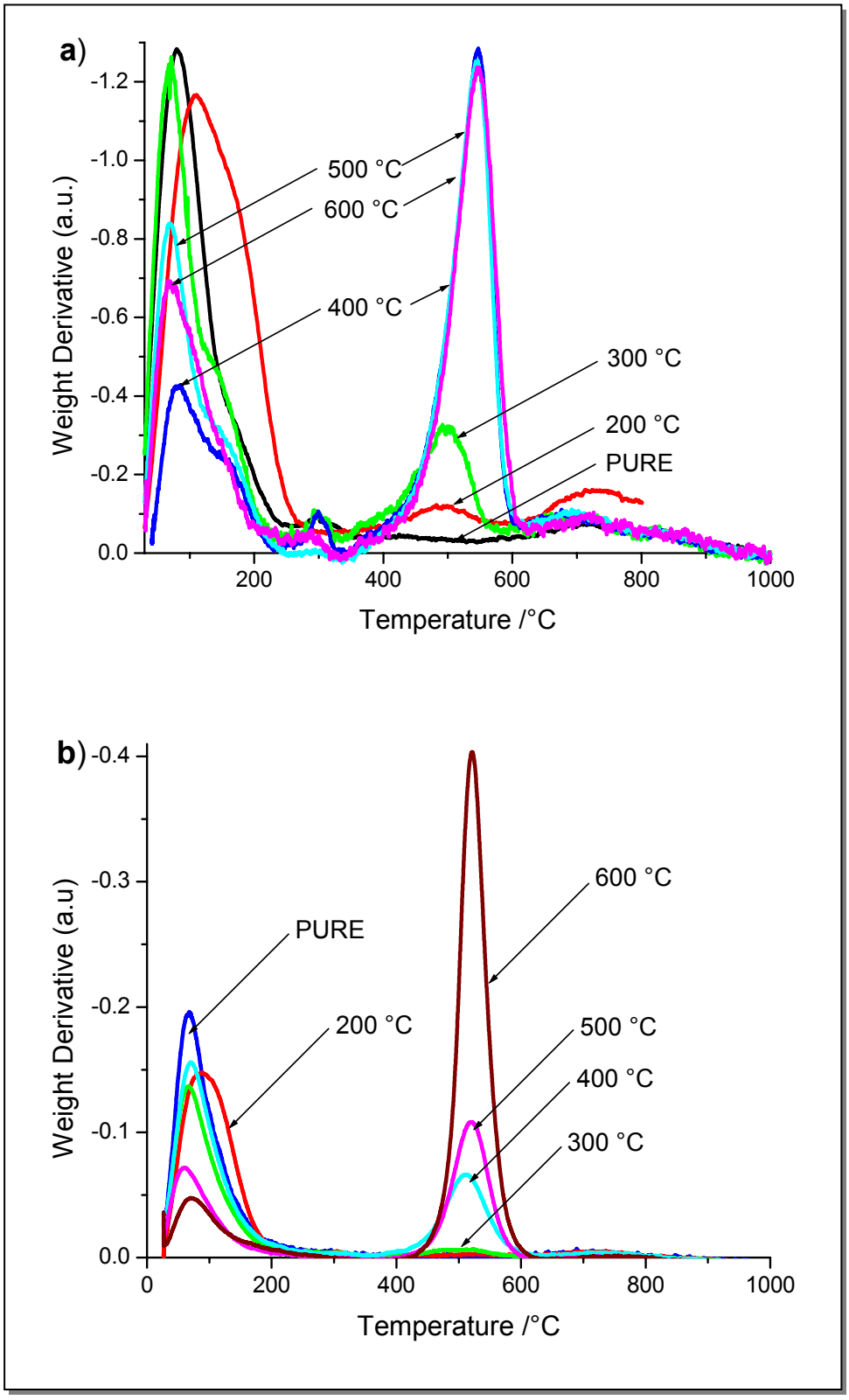

Figure 14.2: Weight derivative against temperature (benzene deposition); a) H-mordenite, b) HLZY-82.

Deposition of carbonaceous material on mordenite occurred at temperatures as low as 200 °C, the weight derivative showed loss of weight around 450-550 °C where carbon and carbonaceous material decomposed (gasified in an oxidizing atmosphere). This was not observed on the zeolite-Y at such temperatures supporting the fact that the strength of acid sites played a significant role in the formation of coke material. Keeping all other reaction conditions unchanged except the deposition temperature, showed that the amount of carbonaceous material increased with increase in temperature, and significant weight loss (carbon decomposition) on the zeolite-Y was shown by the sample on which deposition was carried out at 400 °C and high temperatures, and the amount lost increased with further increase in the deposition temperature. What was inferred by the above was that the acid strength was enhanced by the increase in temperature because:

1) the flow of reactants into the reactor was maintained constant on both zeolites at all temperatures,
2) at 200 °C on both catalysts there was no conversion but there was deposition on mordenite

This acid strength enhancement might be dependent on the type, position and strength of the active sites. Due to the mono-dimensional structure of the mordenite catalyst where entrapment of molecules was a more feasible process enhanced also by carbon deposition, the observed weight loss at 200 °C might be also due to the release of those trapped molecules, but the colour change observed on mordenite (from white to grey) as compare to the zeolite-Y favoured carbon deposition.

The presence of alkyl groups on toluene and mesitylene as feeds for carbon deposition seemed to influence the rate of pore occupation, and this was simply due to the bigger molecular sizes respectively. Figure 14.3 is a plot of weight lost at low temperatures (50-120 °C) against deposition temperature; this particular loss of

weight was due to the release of the chemisorbed/physisorbed water and other volatile molecules.

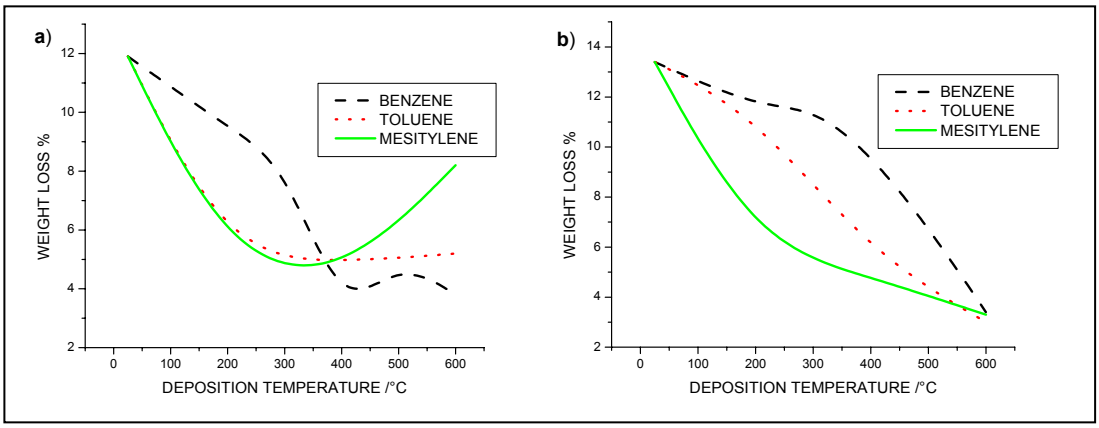

Figure 14.3: Weight loss at lower temperatures (50 – 120 °C) against deposition temperature; a) H-mordenite, b) HLZY-82.

The first point at 30 °C (deposition temperature) which represents the pure sample (no deposition) showed that almost more than 13 % of weight loss occurred on the zeolite-Y while less than 12 % was observed on mordenite, supporting the fact that, even though the pore diameters were almost similar, the three dimensional arrangement increased the pore volume of the catalyst.

With benzene as a feed, the consumption of the catalyst pore volume was much slower than with toluene and mesitylene. That is, the more carbonaceous material deposition there is in the zeolite the lesser the available space for water and other species to adsorb; and thus the high amounts lost on mordenite (figure 14.3) indicates the available space for adsorption. Since mordenite contained stronger sites, an almost similar behaviour between toluene and mesitylene was observed; i.e. no discrimination based on the ease of molecular transformation. This supported what was mentioned earlier from the literature that hydrocarbon conversion on zeolite depends on the type of the active site, the structure of the catalyst and feed type. On the zeolite-Y three distinct routes were followed showing exactly that there was an

increase in the ease of conversion and this observation was marked by strong sites on mordenite.

Murakami *et al*.[81] showed that temperature influences the mode and the position of carbon deposition. They showed that at higher temperatures deposition occurred mostly on the outer surface of the catalyst while at low temperatures deposition started at the centre of the pelleted catalyst, and this is shown in figure 14.4 below.

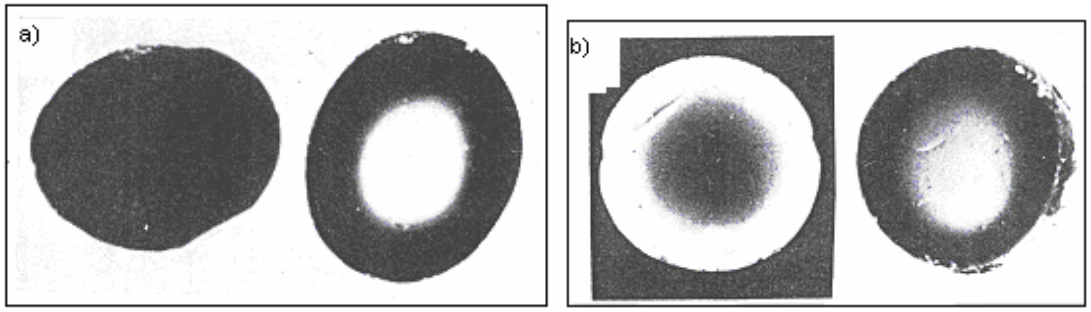

Figure 14.4: Cross section of catalyst pellet, a) after 10 minutes (toluene disproportionation), left = 440 °C, right = 530 °C; b) after 50 minutes (*n*-butyl alcohol), left = 400 °C, right = 480 °C. Black part represents carbonaceous material[81]

Thus in the present study the benzene trace showed a decrease in pore volume with deposition temperature on the zeolite-Y and from 30-400 °C on mordenite where it became almost constant from 400-600 °C. This suggested that increase in temperature had minimum influence on benzene compared to other feeds because of the difficulty in converting the stable ring, i.e. even at high temperatures benzene had to at least diffuse into the catalyst (occupying more space) to the stronger sites for conversion to occur. Though the zeolite-Y with its weaker site showed only the decrease in pore volume (for species (water) adsorption) with increase in deposition temperature and increase in the size of feed molecules (figure 14.3), the mordenite showed almost similar behaviour with the alkyl-benzenes showing that at high temperatures the toluene trace behaved more or less like the benzene trace, and only that with benzene there was more carbon deposition. The mesitylene trace strongly supported the fact that at higher temperatures carbon deposited on the external surface as less carbon

deposited (figure 14.3) at higher deposition temperatures. This was attributed to the influence of temperature on the active site, i.e. molecules are not necessarily required to diffuse into the zeolite pore to be converted because the external acid sites are activated; thus carbon is formed almost immediately when the molecules come into contact with the catalyst. Mesitylene was the simplest of all when it comes to conversion thus its trace showed a decrease in the amount of carbon formed on the catalyst at high temperatures, and thus carbon forming on the external surface blocked access to the active inner part of the catalyst crystallite. If carbon forms from the centre of the catalyst towards the surface then a lot carbon is formed (maximum deposition), but very little is deposited if carbon formation occurs on the external surface for the process is not as continuous as it is from the centre outwards.

The convergence of these lines on the zeolite-Y at 600 °C (figure 14.3) as was observed at lower temperatures (400 °C) on mordenite, suggested that a further increase in temperature might have resulted in a similar behaviour as shown by the mordenite at 600 °C, this also highlighted the fact that mordenite had stronger sites than the zeolite-Y and this meant that the stronger the sites the higher the rate of deactivation. This greatly supported the fact that stronger sites will always deactivate first and fast.

Looking at the total weight loss due to carbon decomposition (around 500 °C), figure 14.5 showed that in general there was a lot of carbon deposition when mesitylene was the feed.

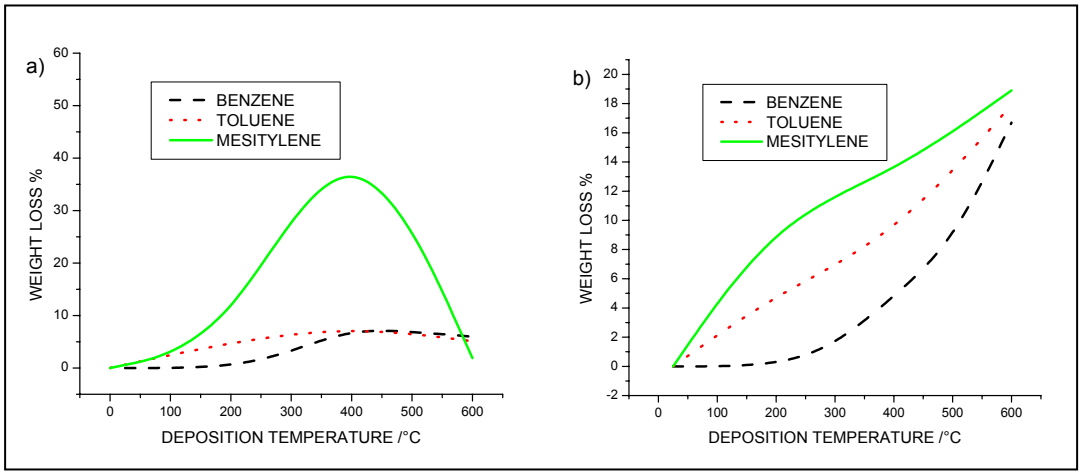

Figure 14.5: Weight loss at higher temperatures (~ 500 °C) against deposition temperature, a) H-mordenite, b) HLZY-82.

Benzene and toluene feeds prove yet that there were more active sites on the Y-zeolite than on mordenite, i.e. the maximum attainable mass loss on mordenite was only 7 % and about 16 % on zeolite-Y (by mass) showing that the very strong sites required to convert these stable molecules were quickly consumed and the catalyst would deactivate very fast. On the zeolite-Y increase in temperature would activate some of the inactive sites for the conversion of benzene and toluene, and thus conversion increased along with catalyst lifetime and temperature. The same was observed during disproportionation reactions.

At high temperatures (600 °C) the mesitylene trace showed that very little carbon would form on the external surface (outer most) and block the catalyst on mordenite, and on the zeolite-Y the traces seemed to converge as they show increase in weight loss. The graphs are almost opposite what has been observed at lower temperatures (figure 14.3).

14.3 Regeneration of the catalysts

14.3.1 Experimental

Toluene was used as a feed to foul the catalysts at 300 °C and WHSV of 0.3 h^{-1}. The fouling process was allowed for four hours after which both mordenite and the zeolite-Y were black in colour. The catalysts underwent the usual pre-treatment process before reactions and after four hours of fouling they were flushed with nitrogen for 16 hours at room temperature. The spent catalysts were then heated in a furnace to the desired temperature and gasification (regeneration) took place in air. After gasification the catalysts retained their white colour, and fouling was then conducted all over again on the same catalysts under similar reaction conditions. Activities were followed by the analysis of catalysis products by an online G.C.

14.3.2 Results and Discussion

After the first run, the catalysts were heated to 600 °C in air for 5 hours to regenerate them; and the second run showed that about 50 % of the activity was lost on the zeolite-Y while very little was lost on mordenite, this is shown in figure 14.6. After the second run the catalysts were regenerated at 500 °C and activity loss was at least brought to a minimum, this was then used as the regeneration temperature for the rest of the study. This then suggested that regeneration of the catalyst at reasonably low temperatures would probably result in minimum losses in the overall activity.

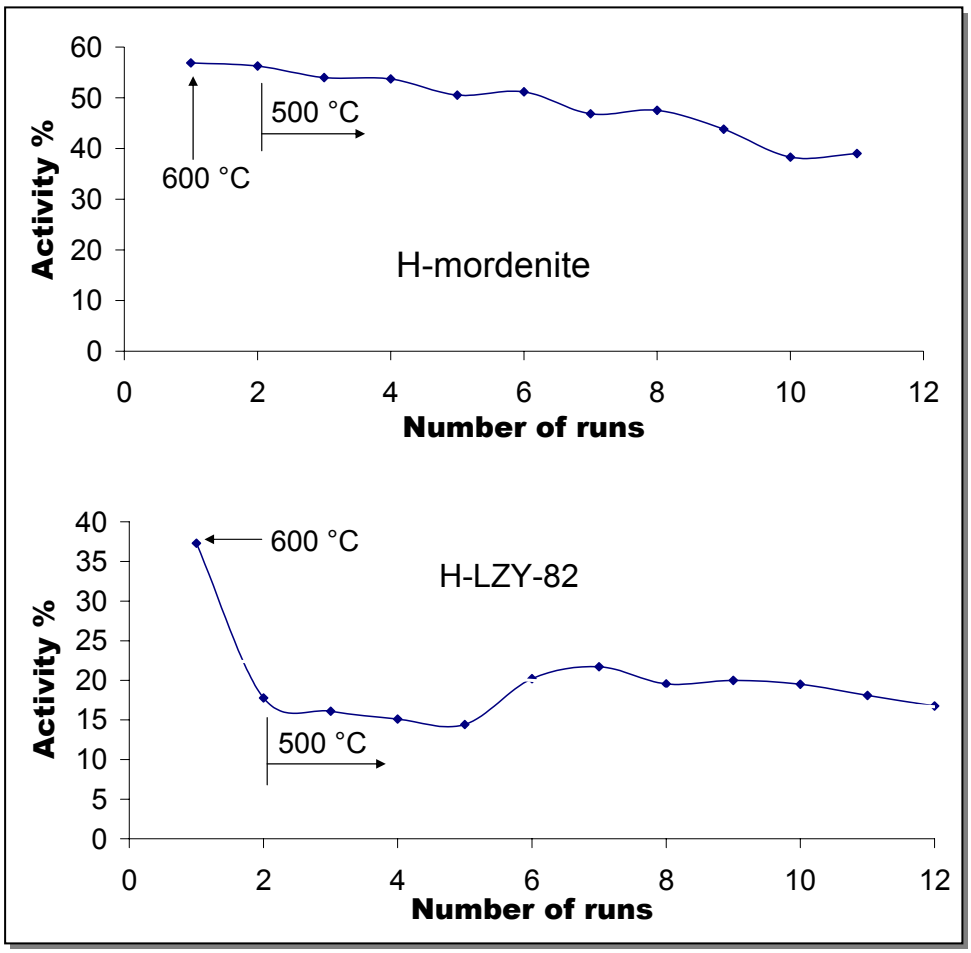

Figure 14.6: Regeneration in air as activity (mol %) against number of runs

This was in line with what was found by earlier authors[40] that the physical structure of the zeolite cannot be fully regenerated even though the carbon has been totally burnt off, and figure 14.6 showed a decrease in activity with number of runs (regeneration times). After a total of 5 runs there was an observed increase in activity on the Y-zeolite of about 50 %. This increase was attributed to the interactions of the framework sites with those of extra-framework species which were created by mostly exposure to high temperatures which led to the dealumination of the catalyst. The behaviour was then similar to that of the mordenite catalyst up until the 12th run. The almost constant behaviour shown by the mordenite catalyst was due to its robust mono-dimensional structure as compared to the more fragile three-dimensional structure of the zeolite-Y.

To evaluate the effect of regeneration temperature on zeolites, fresh samples were fouled at 300 °C and regenerated at 400 and 500 °C respectively. The results are depicted in figure 14.7 showing that the activity of both catalysts was recovered even at temperatures such as 400 °C. Though there was recovery in activity at 400 °C the catalysts samples did not completely turn white again, they were somehow brownish in colour but active. This somehow supported what was mentioned earlier that carbon/carbonaceous materials formed in the zeolite pores were preferentially gasified compared to the one on the external surface; and this further supported that these alkyl transfer reactions occurred in the zeolite pores where preferential regeneration occurred due to site strength and thus activity was recovered.

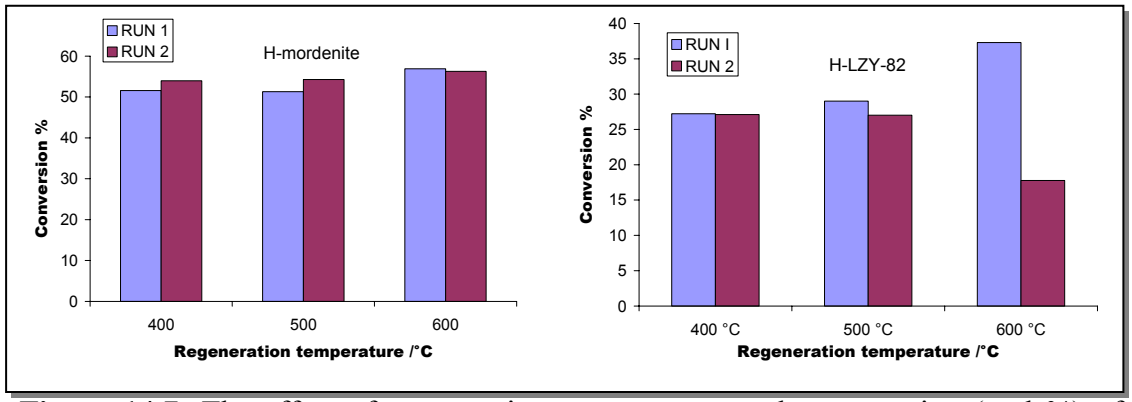

Figure 14.7: The effect of regeneration temperature on the conversion (mol %) of toluene; RUN 1 = fresh sample, RUN 2 = after regeneration

What was inferred here was that carbonaceous material, if ever formed on the pore mouths of the catalysts, even though these are close to the external surface are also gasified preferentially to the external surface carbon.

Very little of the initial conversion was lost on zeolite-Y after regeneration at 400 °C and on mordenite the process seemed to even increase the activity by about 4 %. Regeneration at 500 °C resulted in an increase of about 5 % on mordenite and an equivalent percentage decrease on the zeolite-Y. At high temperature (600 °C) the mordenite catalyst showed a loss in activity, even though that was very little (~ 1 %)

what it suggested was that regeneration temperature had an effect and that higher temperatures might result in catalyst's structural implications[40] (collapse or changes), this was better shown by the dramatic decrease observed on the zeolite-Y. The above observations are manifested in figure 14.8.

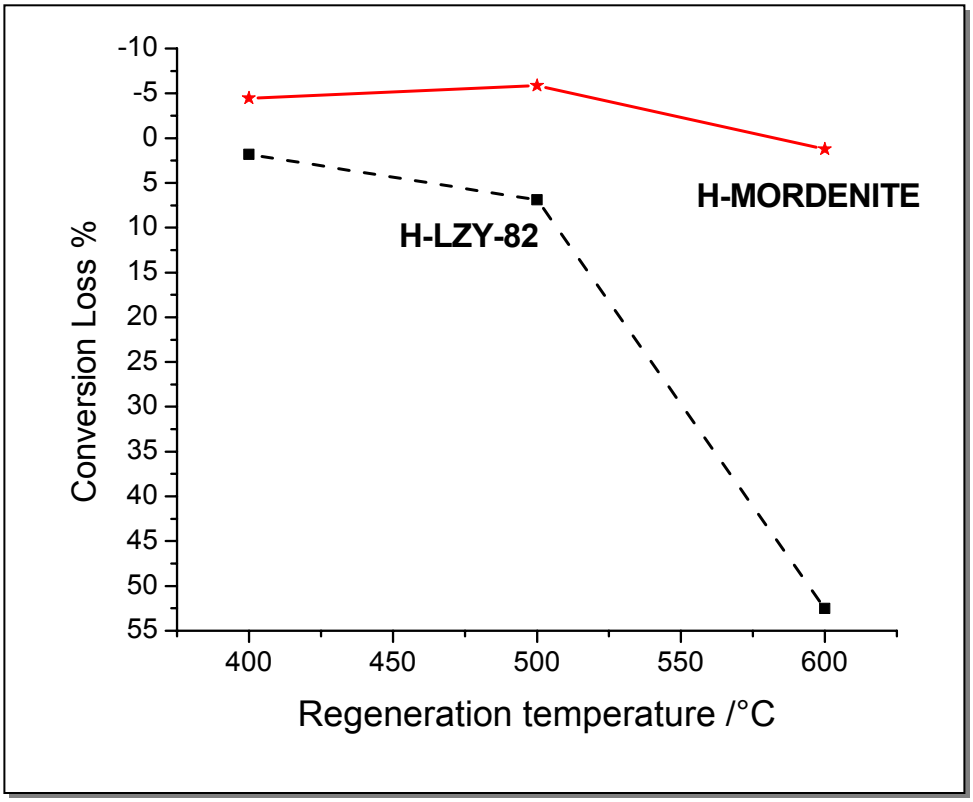

Figure 14.8: The effect of regeneration temperature on conversion (mol %)

14.4 Discrepancies

Earlier during the disproportionation of toluene on both catalysts the product stream showed a 1:1 relation between benzene and xylene at 300 °C. Though this was what was expected in the product stream, present studies showed great differences to the above. Figure 14.9 shows that there was a great benzene deficit in the product stream on both catalysts, and almost similar results were observed on both catalysts.

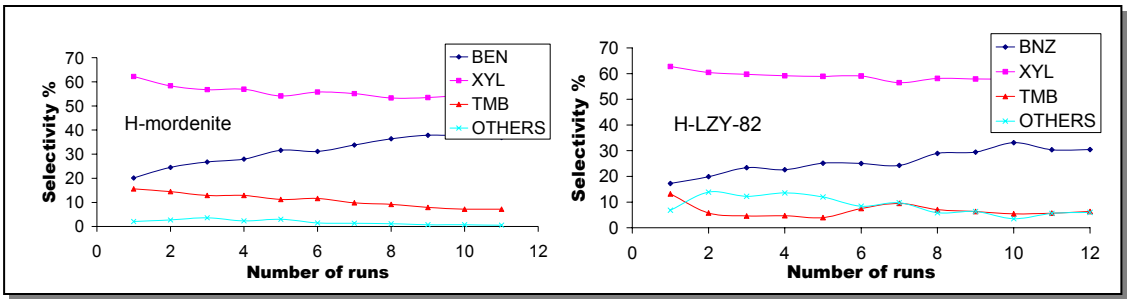

Figure 14.9: Catalyst behaviour as selectivity (mol %, product distribution); the effect of regeneration

It is shown in the figure that the probable cause of activity loss even though all the carbon has been burnt up after regeneration was structural collapse, which lead to the blockage and destruction of pores and degradation of the catalyst. Due to this structural collapse selectivity of the catalyst was affected gradually with regeneration processes. As expected the amount of benzene increased with number of runs in the expense of the bulkier trimethylbenzene and the 'OTHERS', this was because the presence of extra-framework species would reduce the pore volumes and thus restrict the formation of bulky products.

The observed discrepancies were probably brought about by the fact that the reaction conditions were different from the earlier study; i.e. the WHSV used here was 0.3 h^{-1} compared to the 1.0 h^{-1} of the earlier study, and the nitrogen flow rates were 3 folds higher which diluted the feed and thus impacted on the reaction routes of the disproportionation and deactivation processes.

14.5 Conclusion

Though benzene was believed to be a very stable compound, carbonaceous material were formed in the catalyst when it was fed. Carbon deposition increased with temperature because acid sites strength was consequently enhanced, and therefore the rate of deactivation and carbon deposition increases with the strength of active sites. The more difficult it is to convert molecules the faster is the deactivation, and this is

due to the fact that stronger sites are required for the process and they are normally consumed before weaker sites. Regeneration of the catalyst strongly influences the selectivity of the catalyst and this was related to structural collapse (degradation).

The study has shown that in fact smaller (more stubborn) molecules were the most actively involved species in carbonaceous material deposition process as compared to the bulkier counter parts.

It has been shown in the study that zeolites can be regenerated if they are to be used in transalkylation reactions.

15 THE EFFECT OF ALKYL GROUP/S AND THE TYPE OF AROMATIC CONJUGATION ON TRANSALKYLATION REACTIONS OF ALKYLAROMATICS

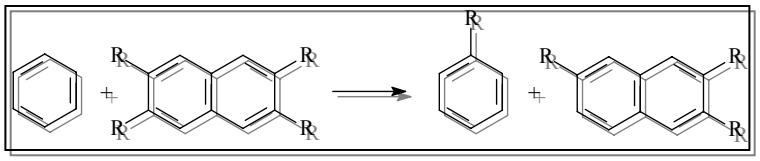

15.1 Introduction

The potential of Al-MCM-41 in catalyzing alkyl-transfer reactions of alkyl-aromatics will be dealt with in the following chapter where ethylbenzene and mesitylene disproportionation reactions were looked at. These mesoporous materials though showed very weak acid site strengths as compared to mordenite and LZY-82 are still catalysts of interest since it was also earlier concluded that the ease of alkyl-transfer reaction increases with the number, chain length and type of an alkyl group/s on the aromatic ring. This led to crowning of these catalytic materials as good candidates in reactions involving bulky molecules (poly-alkyl species) owing to their very large pores.

The alkyl-transfer study was greatly supplemented by the work which was carried out at SASOL by Pat Skhonde who calculated thermodynamic values of transalkylation reactions of alkyl-aromatics including polynuclear and heteroatomic aromatics. There were unexpected discrepancies between results of the current study and the calculated thermodynamic values mainly due to the fact that catalytic interactions were not taken into considerations during the calculations.

15.2 Experimental

Thermodynamic calculations of alkyl-transfer reactions were carried out at SASOL using the DMol^3 Density Functional Theory (DFT) code from Accelrys, Inc.
In evaluating at the effect of the type of an alkyl group on the aromatic ring on transalkylation reactions three alkyl-benzenes were used, all with the formula C_9H_{12} (scheme 15.1), i.e. mesitylene (1.1, 1.2), cumene (2.1, 2.2) and *n*-propylbenzene (3.1, 3.2). Other reaction conditions were kept constant.

15.3 Results and discussion

15.3.1 Alkyl-transfer reactions

Disproportionation of mesitylene was less than 75 % (figure 15.1), cumene reached 100 % during the initial stages of the reaction and propylbenzene reached 95 % on both mordenite and LZY-82; and lower conversion were observed on Al-MCM-41 (*4 and *5). The observed high conversions on acidic zeolites (mordenite and LZY-82) though very much attributed to stronger catalytic acid sites, were also due to:

1) more than one reaction path way (2.1, 2.2, 3.1 and 3.2 (scheme 15.1)),
2) the ease with which the alkyl-group is cleaved off from the ring and
3) the stability of the carbenium ion that formed.

The ease of alkyl group cleavage was much related to the stability of the carbenium ion. The carbenium ion CH_3-CH^+-CH_3 (scheme 15.1(2.2)) was the most stable one because it had two alkyl groups (CH_3) which better balanced out the positive charge on the middle carbon. The CH_2^+-CH_2-CH_3 (scheme 15.1(3.2)) ion was less stable since it had only one alkyl group (CH_2CH_3) stabilizing the charge while the CH_3^+ (scheme 15.1(1.2)) carbenium ion was the least stable and as a result there was

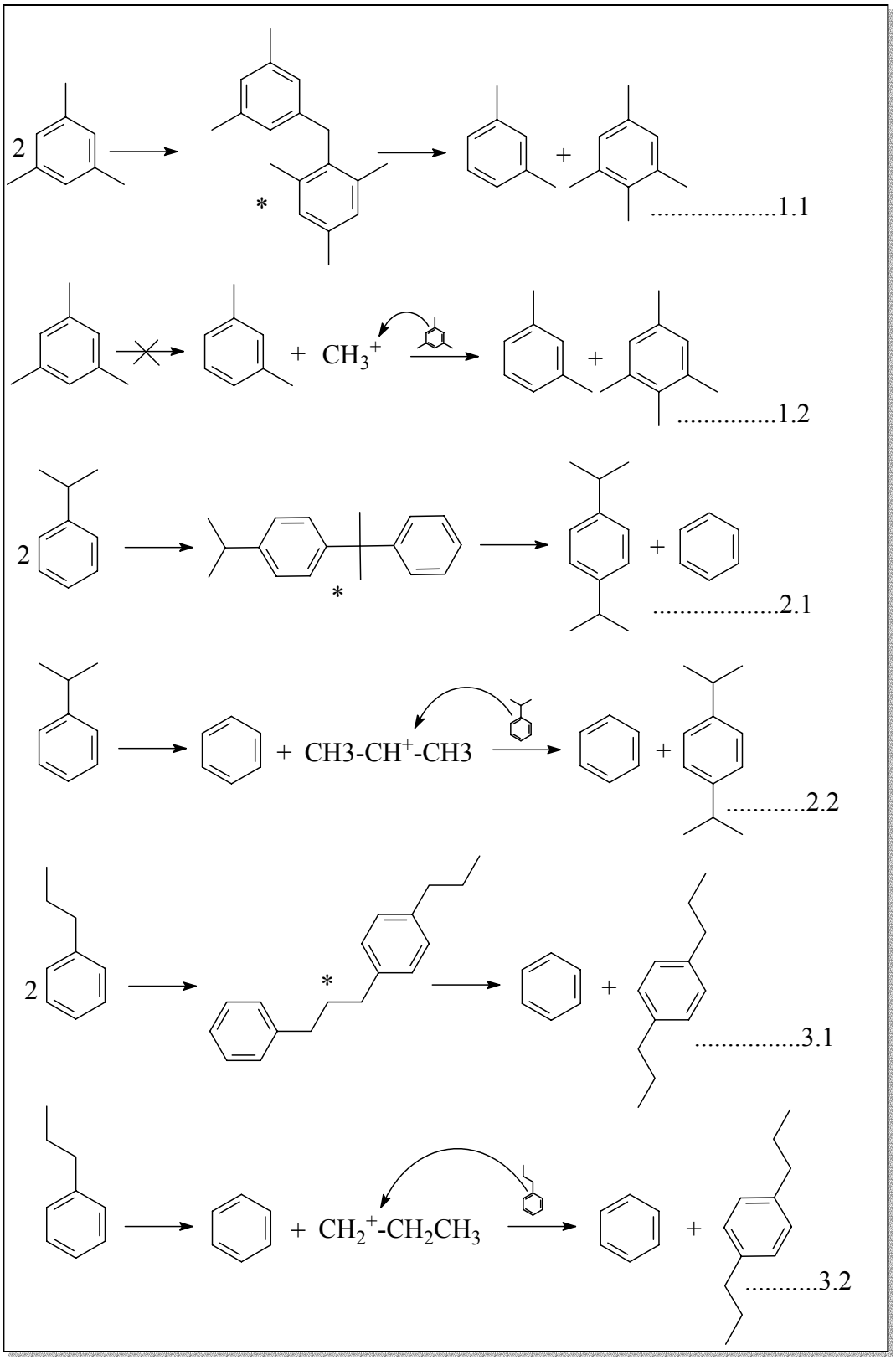

Scheme 15.1: Alkyl-benzenes (C_9H_{12}) and their possible reactions on zeolites:

* = Bimolecular intermediate

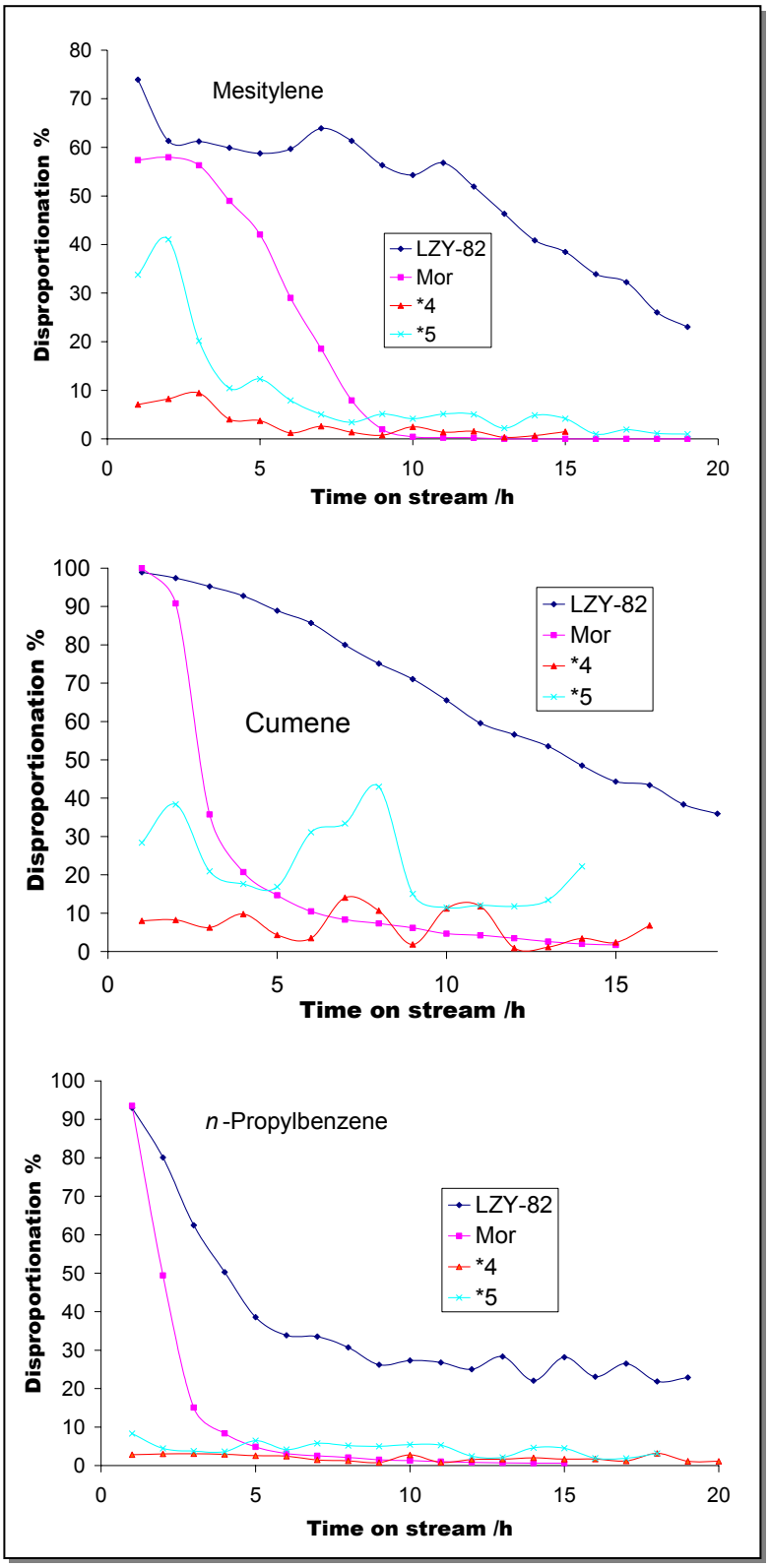

Figure 15.1: Alkyl-benzene disproportionation traces with time on stream (mol %) at 300 °C

probably one route towards alkyl-transfer reactions (scheme 15.1(1.1 not 1.2)), namely, the bimolecular intermediate system.

The other factor which might had favoured high conversions was probably the lack of a reverse reaction for cumene and propylbenzene, i.e. the products formed were mainly diisopropylbenzenes and di-*n*-propylbenzenes both of which were very bulky and as a result accessing active site became a problem as earlier concluded and consequently they were not involved in further reactions.

The simplest explanation for high conversions would be: for mesitylene to disproportionate, two molecules had to be involved while for cumene and propylbenzene one molecule was sufficient to contribute towards conversion (not necessarily disproportionation).

The fact that reversible reactions were responsible for lower disproportionations was supported by higher disproportionations for mesitylene than propylbenzene on the less acidic Al-MCM-41s and this is better depicted in figure 15.2.

This suggested that mesitylene was easily disproportionated than propylbenzene and that the dealkylation-realkylation route (scheme 15.1(3.2)) required strong acid sites (mainly for the dealkylation reaction). What seemed to be competing with mesitylene was cumene. Though dealkylation required strong sites; steric effects played an important role in the cleavage of the alkyl group. These steric effects were higher for cumene with two CH_3 groups closer to the aromatic ring and due to repulsion forces between the ring and the alkyl groups dealkylation was favoured. *n*-Propylbenzene had less steric effects to such an extant that dealkylation or alkyl group cleavage relied solely on the acid site strength of the catalyst.

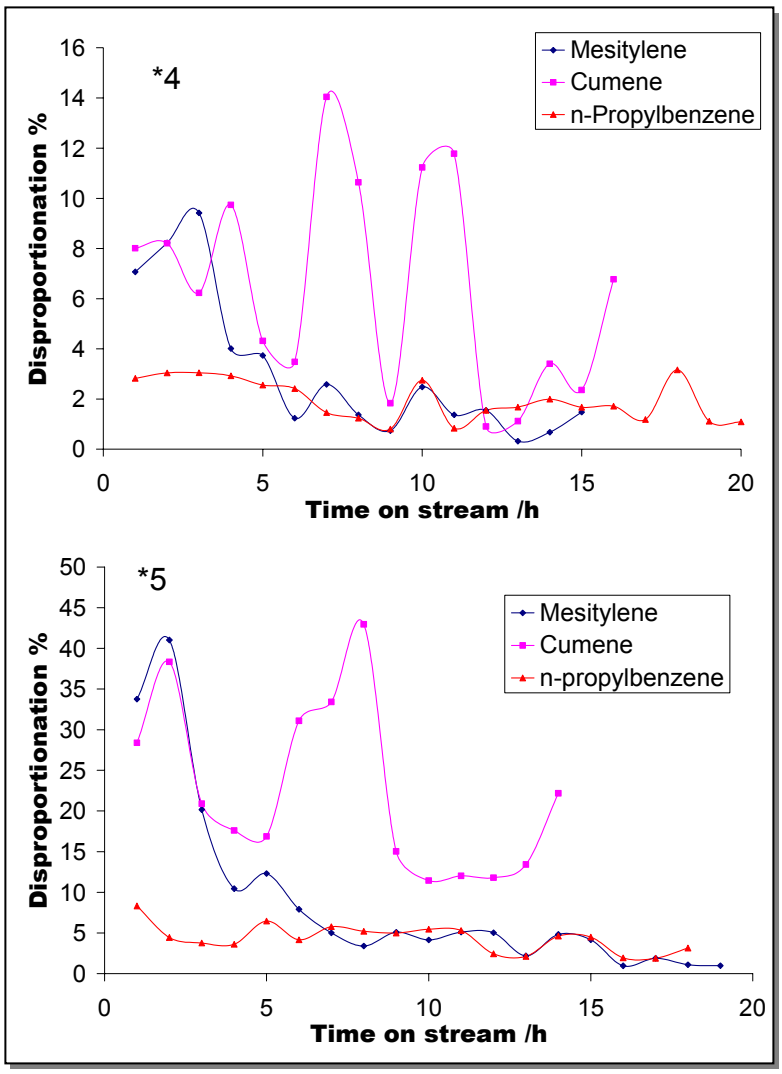

Figure 15.2: Alkyl-benzene disproportionation with time on stream (mol %) on Al-MCM-41 at 300 °C

The other noticeable feature of figure 15.2 was that the mesitylene trace showed strong catalytic deactivation than other molecules probably due to the fact that mesitylene disproportionation formed xylene and *tetra*-methylbenzene; hence with the decrease in the number of alkyl groups on the ring for xylene, disproportionation was difficult and most probably strong adsorption on the active sites was favoured resulting in blockage of active sites and deactivation. Due to this quick deactivation and the observed high disproportionations for cumene, mesitylene was ratted less reactive and the order of reactivity is shown in figure 15.3. This showed that the order

of reactivity favoured the sterically stressed molecules and for the less stressed molecules the number of alkyl groups on the ring was the determining factor compared to the alkyl group chain lengths.

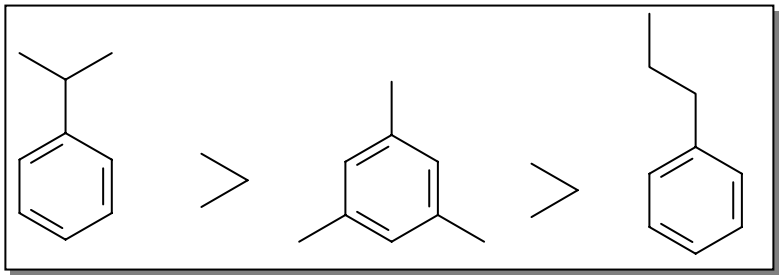

Figure 15.3: Effects of alkyl group/s on the reactivity of alkyl-aromatics.

The observed chaotic behaviour in figure 15.2 was attributed to polymerization and subsequent cracking reactions in the zeolite pores as explained in the previous chapter where mesitylene showed the same behaviour at higher temperatures (500 °C). As expected disproportionation depended on the amount of Al atoms in the framework structure of the zeolite, i.e. *5 (Si/Al = 9.9) showed better activities than *4 (Si/Al = 30).

15.3.2 Thermodynamic calculations

SASOL's results on thermodynamic calculations showed the following values for transalkylation between alkyl-naphthalenes and benzene:

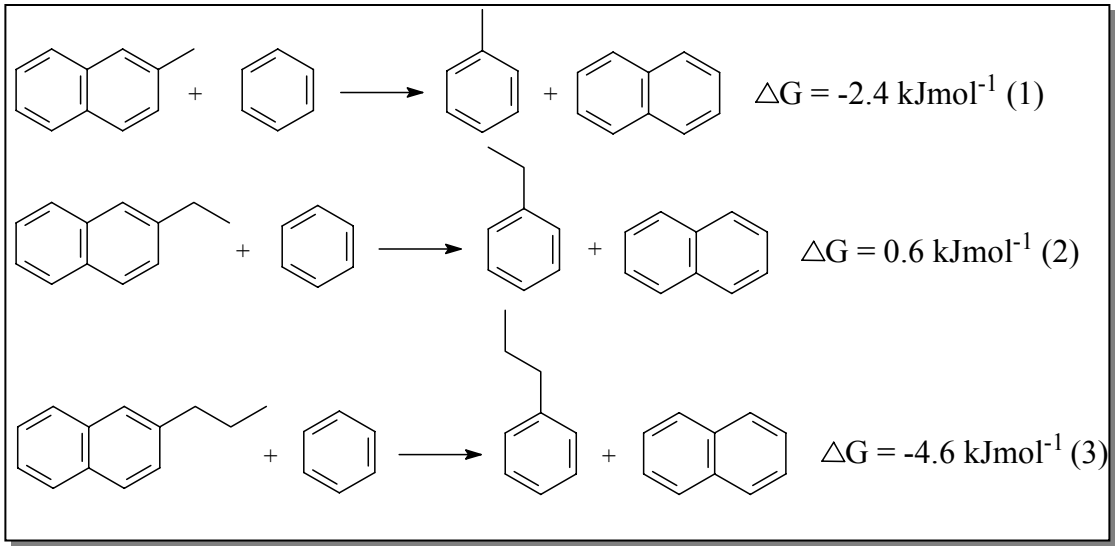

Scheme 15.2: Thermodynamic values of transalkylation reactions between alkyl-naphthalenes and benzene

There seems to be a brake in the trend of ΔG values from reaction 1 to 3 on scheme 15.2, since one would expect reaction 2 to have a value close to -3.5 kJmol^{-1} and not more than the value of reaction 1. If catalytic interactions (constraints) were taken into consideration the value for reaction 2 would be acceptable but then that of reaction 3 would be out of order if one considers molecular size restrictions. The above results did not agree well with the fact that the stability of the carbenium ion increases with the chain length of the alkyl group and that the ease of cleavage of such groups increases accordingly.

Similar reactions from alkyl-transfer studies were compared to the above results and scheme 15.3 shows typical reactions that were looked at. Though these reactions were catalysed by acidic mordenite and LZY-82, presumably, similar results should be observed on AL-MCM-41s since all three molecules were mono-alkyl-benzenes. The traces in figure 15.4 are surely from different temperatures but the very noticeable fact was that of toluene and ethylbenzene. Ethylbenzene with one extra carbon atom on the alkyl group showed much better reactivities than toluene even though its disproportionation was performed at lower temperatures than that of toluene.

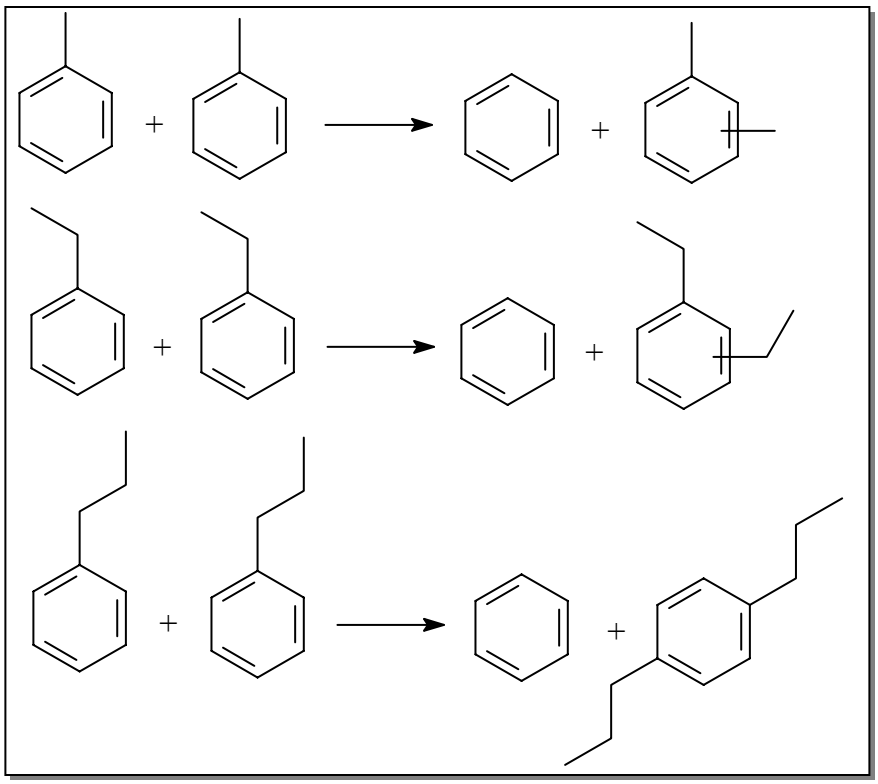

Scheme 15.3: Disproportionation reactions of alkyl-benzenes

Studies on alkyl-transfer reaction have shown an increase in disproportionation with temperature but ethylbenzene was certainly more reactive than toluene and this agrees well with previous conclusions on the type of alkyl groups in transalkylation reactions; and thus from the above discussions it became difficult to conceive the thermodynamic value presented here.

Very interesting and important results from SASOL's calculations are shown in scheme 15.4 and 15.5 respectively. The first set of values (1) on scheme 15.4 showed that with increase in conjugation (number of aromatic rings fused together) there was a corresponding increase in the ease of alkyl group removal (cleavage) from the rings. The indicated values are an average of the ΔG values for the removal of a methyl group from any position on a particular aromatic conjugation. These values increased from -14.6 $kJmol^{-1}$ for phenanthrene derivatives to -4.8 $kJmol^{-1}$ of the pirene derivatives indicating that even though there was an increase in conjugation, the type of conjugation also played a significant role, and the same was shown by the huge

gap between the ΔG values of anthracenic and phenanthrenic derivatives both of which consist of three rings.

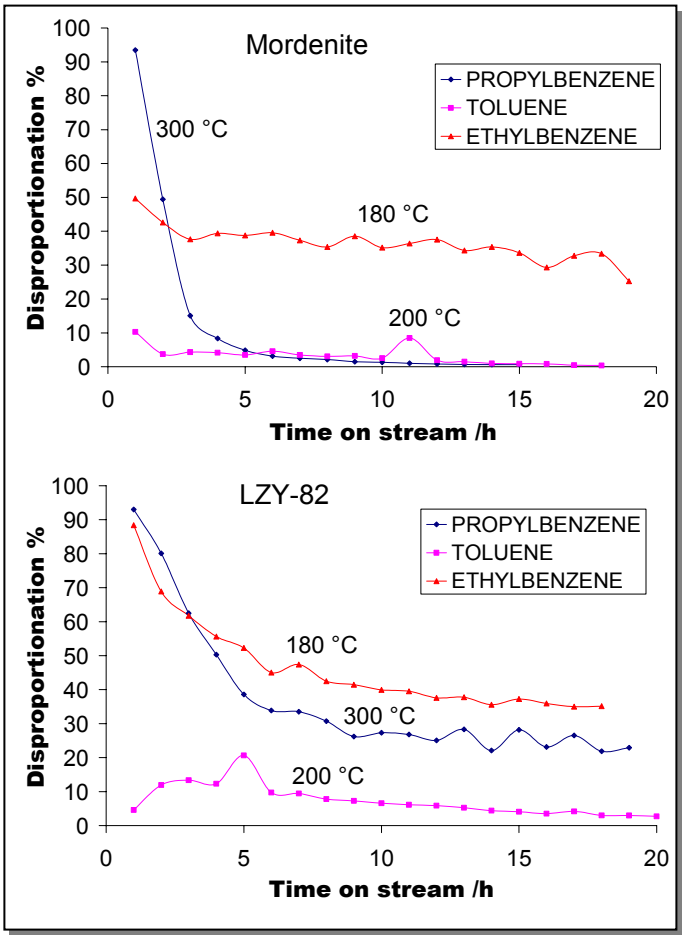

Figure 15.4: Disproportionation traces of alkyl-benzenes (mol %)

The second set of values (2) in scheme 15.4 showed again an unexpected brake in the decrease in ΔG values with respect to only one type of conjugation and similar methyl group position. The expected value would be close to -3.8 $kJmol^{-1}$ for anthracenic derivatives. The low value for tetracene suggested that there was some stability with increase in conjugation which resulted in the methyl group being less bound to the rings. From the values observed in scheme 15.4 it was concluded that the ease of alkyl group removal increased with the amount and type of conjugation of the alkyl-aromatic species even though the trend in thermodynamic values was not always as expected.

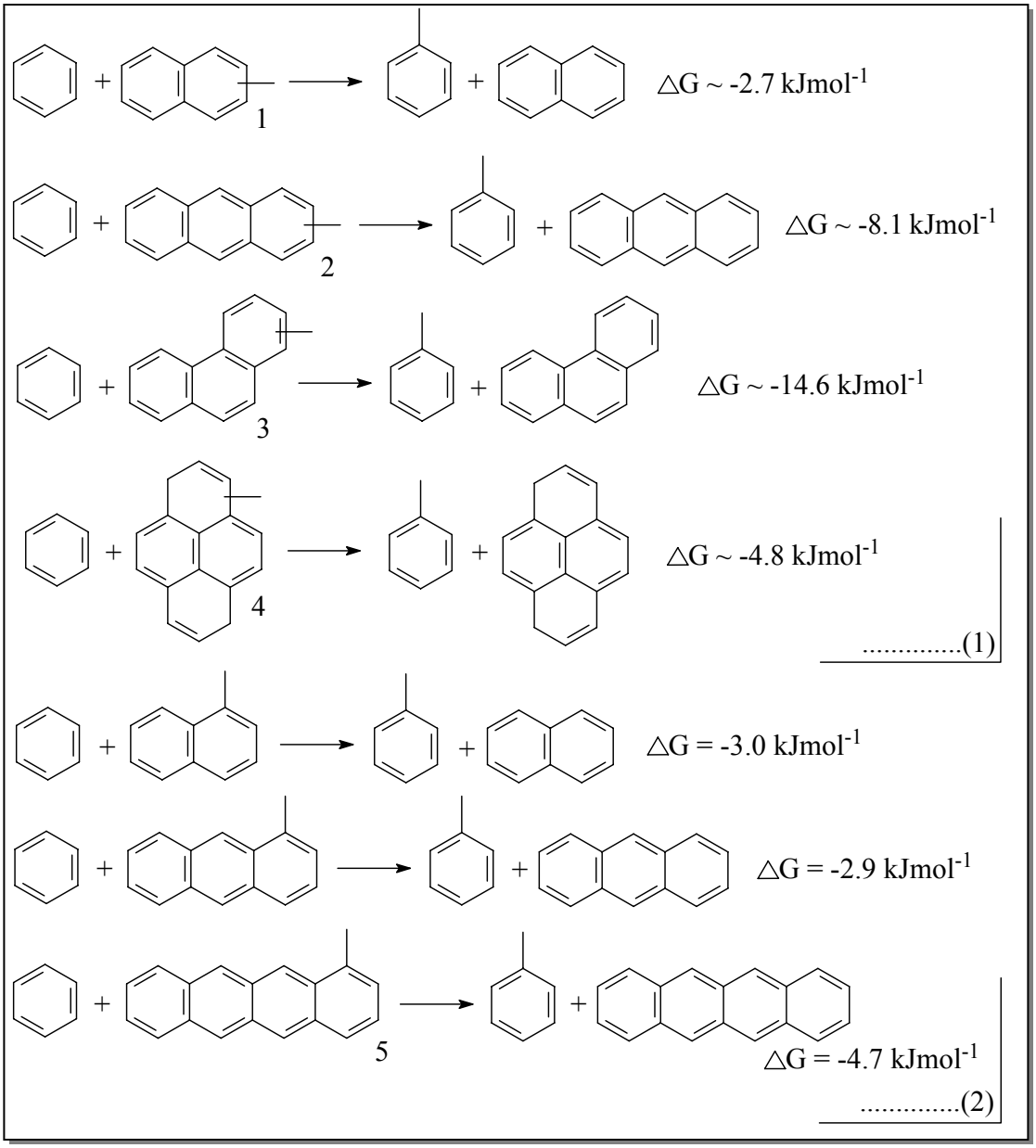

Scheme 15.4: Thermodynamic values showing the effect of conjugation on transalkylation to benzene: 1 = naphthalenic, 2 = anthracenic, 3 = phenanthrenic, 4 = pirenic, 5 = tetracenic derivatives

This was important since aromatic molecular sizes increases with conjugation and this would obviously lead to the need to use large pore zeolites for their transformations; and the larger the pores of these catalysts the less acidic are the active sites that catalyses transalkylation reactions. This would be supplemented by

the increase in the ease of alkyl group removal which accompanies increase in molecular size of alkyl-aromatics.

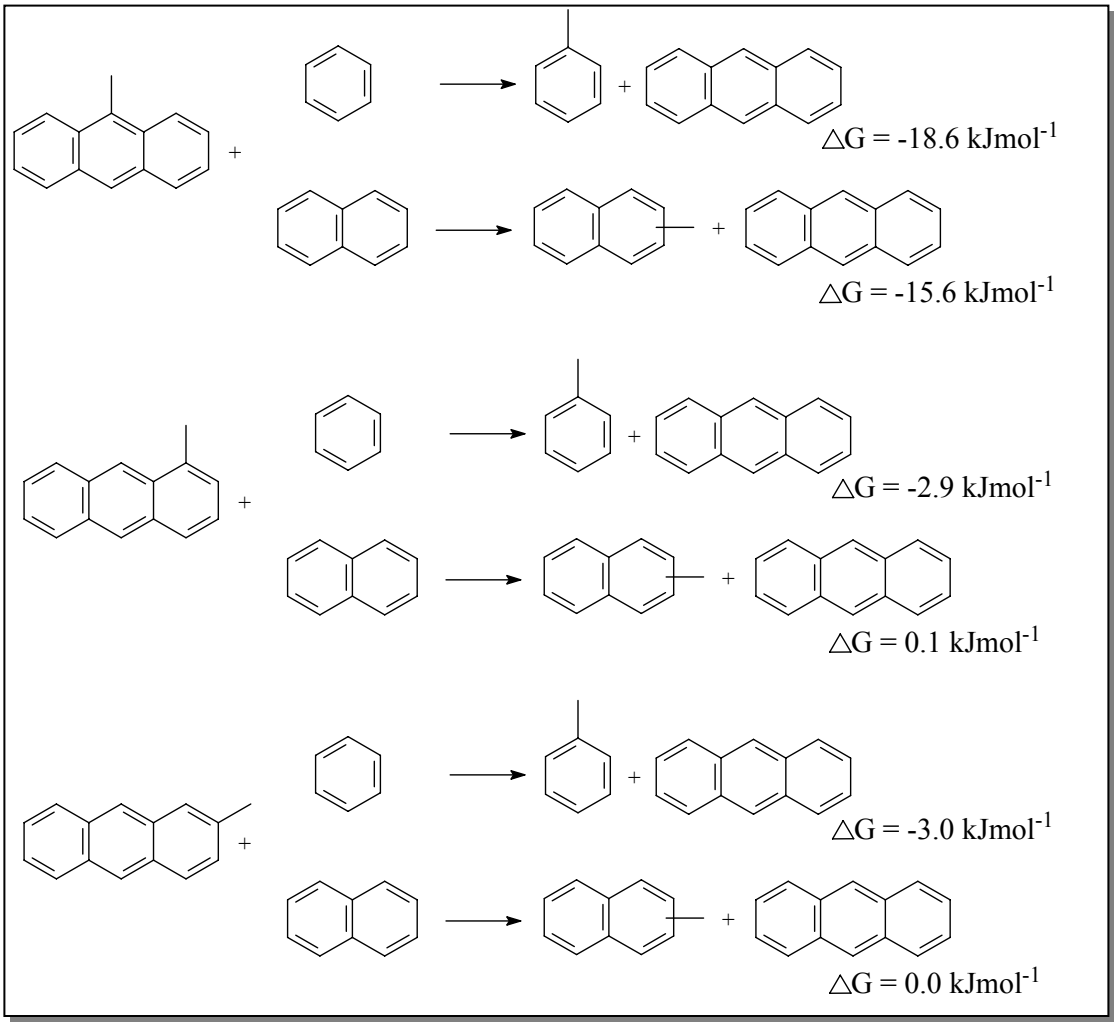

Scheme 15.5: Thermodynamic values showing the effect of an alkyl acceptor (in absence of catalytic interactions) on transalkylation reactions

Thermodynamic values on scheme 15.5 shows a comparison of the abilities or strengths with which the alkyl-acceptor accepts or removes (in case of a bimolecular system) the alkyl group from a conjugated system. In all cases shown in scheme 15.5, benzene certainly was a better acceptor than naphthalene; and since the ΔG value for transalkylation from methylnaphthalene to benzene is negative (scheme 15.4), presumably this could mean that transalkylation would prefer alkylation of smaller rings (with lesser conjugations). With the above being true, the question of whether

the alkyl group of an alkyl-naphthalene would go to benzene or anthracene in such a mixture (scheme 15.6) would be answered.

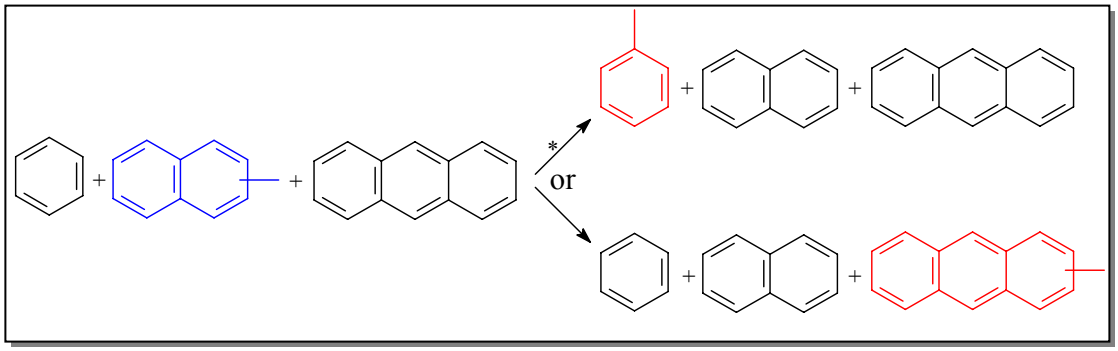

Scheme 15.6: Preference of transalkylation in aromatics: * = preferred route.

SASOL's study also included calculations involving bulky aromatics, non-alkyl substituents and heteroatomic aromatics (scheme 15.7 and 15.8).

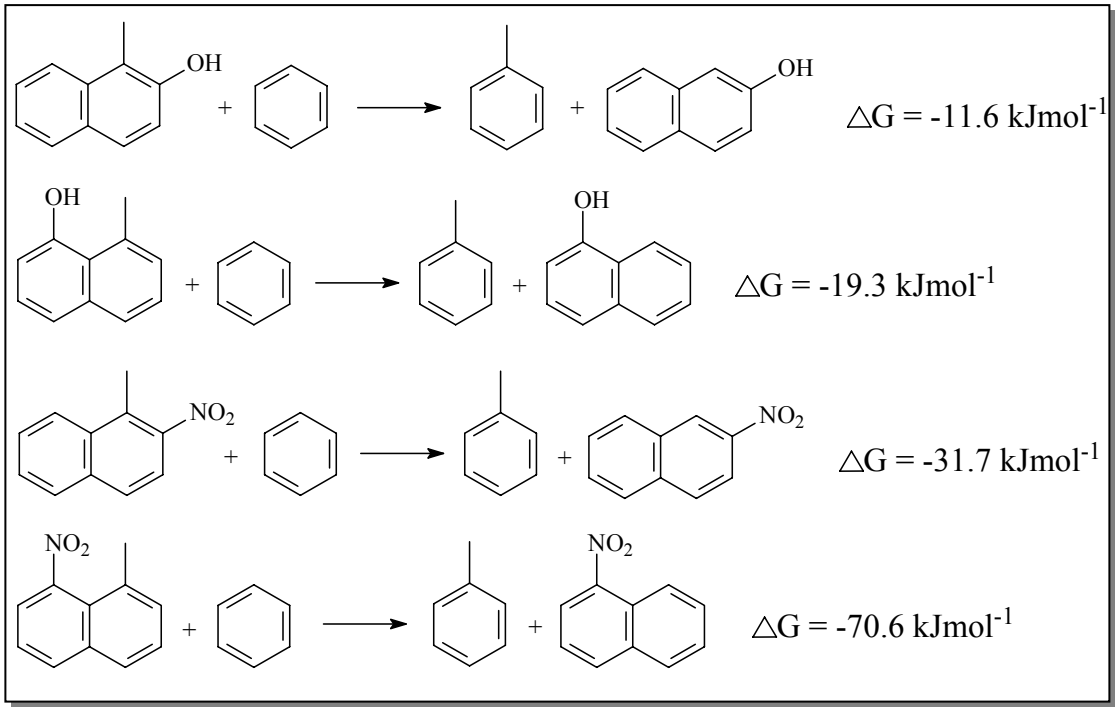

Scheme 15.7: Thermodynamic values indicating the effect of non-alkyl substituents on transalkylation

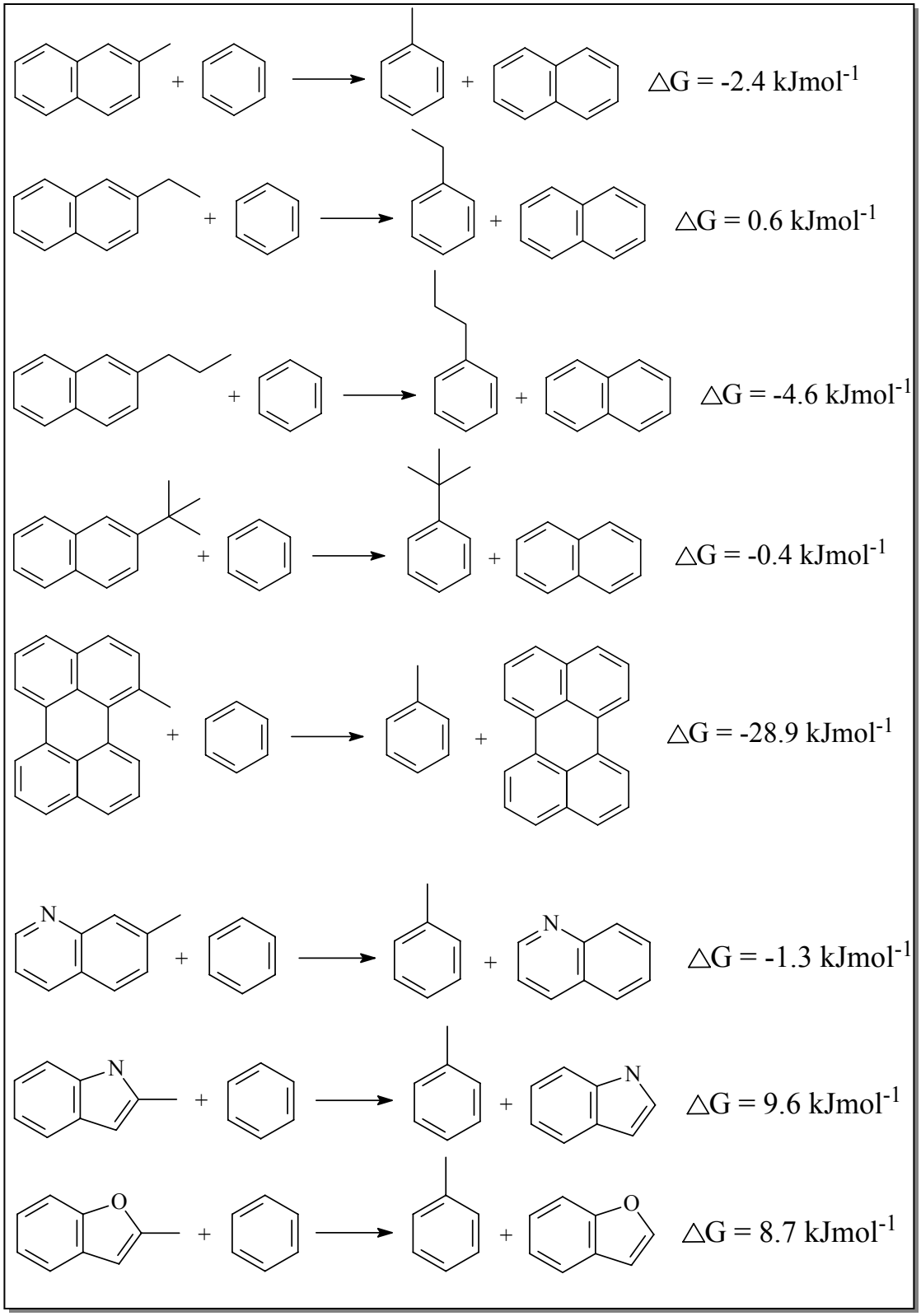

Scheme 15.8: Thermodynamic values for transalkylation between benzene and alkyl/alkyl-heteroatomic aromatics.

15.4 Conclusion

The study has shown that alkyl group removal (not necessarily transalkylation) from the aromatic ring favoured sterically stressed molecules, and if there is less stress then removal from the ring with the most alkyl groups is favoured over the alkyl group size.

It had been concluded earlier that the ease of alkyl group removal increased with the number, chain length and type of an alkyl group, to add on this, present work has shown that the amount and type of aromatic ring conjugation also played an important role in alkyl-transfer reactions of alkyl-aromatics. The position of the alkyl group on the aromatic moiety also affects alkyl-transfer due to both electronic effects and more importantly the steric factors. Contrary to the ease of dealkylation or alkyl group removal favouring conjugation, alkylation or alkyl group acceptance favoured smaller aromatics or lesser conjugation.

With the above observations and the fact that the ease of alkyl group removal increased with aromatic conjugation, and considering the fact that benzenic derivatives required stronger acid sites for activation, the use of less acidic large pore zeolites like the MCM-41 and MCM-48 might result in a selective one-way (no reverse reactions) alkyl-transfer from bulky molecules to smaller benzenic derivatives as shown also in chapter 16.

16 Al-MCM-41 MATERIALS FOR TRANSALKYLATION REACTIONS OF ALKYLAROMATICS

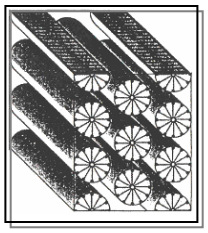

16.1 Introduction

Recently a new family of mesoporous molecular sieves denoted as M41S was invented by Mobil researchers. One member of this series, MCM-41, posses a regular array of uniform and one-dimensional mesopores that can be tuned to the desired pore diameter in a range of 15 to 100Å.[24] This narrow pore size distribution and extremely high surface area of ca. 1000 m^2g^{-1} makes these material promising candidates as catalysts or catalyst supports. However, it was apparent that these materials have a lower acidity and poorer thermal stabilities than the widely used catalysts such as the zeolite-Y and ZSM-5. Al-containing MCM-41 tends to dealuminate during the removal of the surfactant by calcinations during synthesis. This has been attributed to hydrolysis of the framework Al by steam generated from the combustion of the surfactants. The higher temperatures during calcinations or under process conditions leads to disruptions in the framework and to the subsequent collapse of pores or channels in the molecular sieve when too much alumina is incorporated.

With increase in the Al content the surface area and pore size decreases, and a further increase of Al in the synthesis gel results in materials which are no longer mesoporous and with surface areas of about 336 m^2g^{-1}. In contrast, materials prepared by post-alumination of Si-MCM-41 remains mesoporous even after the incorporation of a large amount of Al.

With increase in Al content of the samples, the amount of Brönsted and Lewis acid sites both increased while their acid strengths decreased[26] and cracking of cumene is often used as a test for strong acid sites of Al-MCM-41 materials.[29]

It was concluded earlier during the transalkylation reactions between toluene/benzene and alkyl-naphthalenes that, since the conversion decreased with increasing size of the aromatic molecule, the bulkier the alkylaromatic the more difficult it was to access the active sites. The present study was conducted on the basis that the MCM-41 contained larger pores which will have lesser effects on bulky molecules when it comes to accessing the active sites, and it was expected of the catalyst to give reasonable evidence to support these earlier conclusions. This chapter is reporting on the characterization of these potential catalysts in relation to their alkyl-transfer abilities.

16.2 Experimental

A total of 5 samples were prepared (see chapter 3 for the synthesis method) and they contained Al from Al $(NO_3)_3$ source, and these were designated as *1, *2, *3, *4 and *5 according to their synthesis methods. These samples had a Si/Al = 30 ratio except for *5 which was 9.9, and were all as-synthesized (Al incorporated during their synthesis) materials. Both Al and Si sources were introduced at the same time in the synthesis of *1, but $Al(NO_3)_3$ was introduced before acid treatment for *2 and after acid treatment for *3, *4 was prepared similarly to *1 but only aged for 2 days at room temperature. The last sample, *5 was synthesized in an oil-bath instead of an autoclave.

XRD was used to assess the crystallinity of the catalyst materials and to confirm the structure. Temperature Programmed Desorption (TPD) of ammonia was used to evaluate the acidities of the catalysts.

Ethylbenzene and mesitylene disproportionation test reactions were carried out in a flow-type fix-bed reactor system at varying temperatures.

16.3 Results and Discussions

16.3.1 X-Ray diffractions

What was inferred form the XRD results was that all samples were crystalline or had a reasonable degree of crystallinity as they all showed a similar peak pattern as shown in figure 16.1.

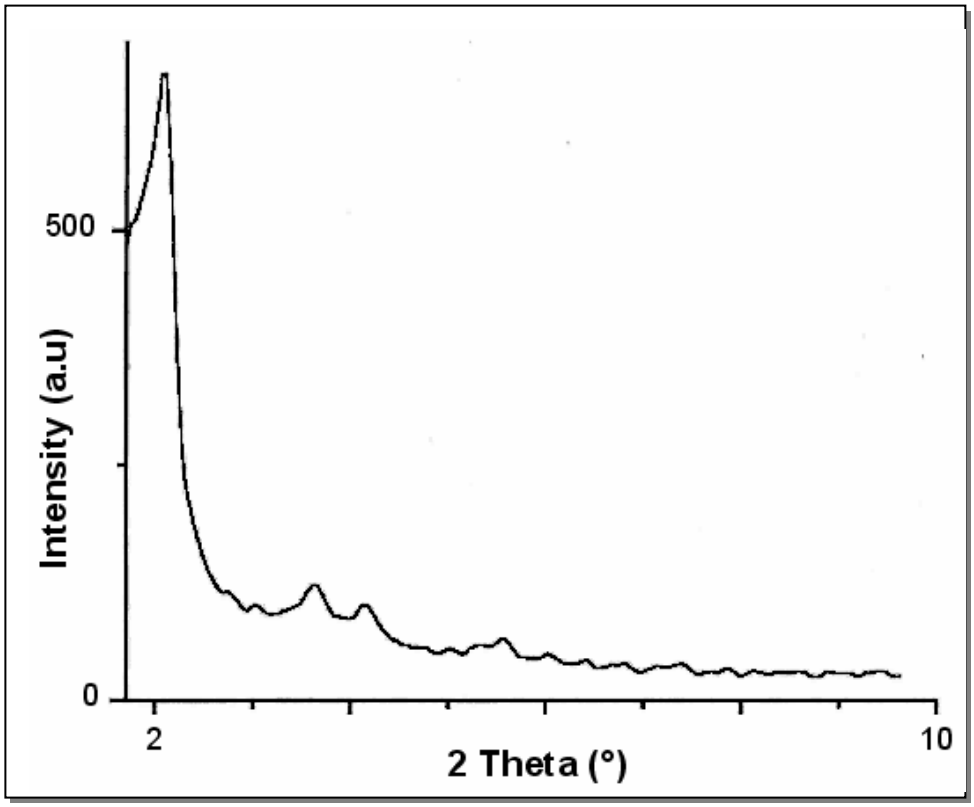

Figure 16.1: A characteristic XRD pattern shown by all Al-MCM-41 samples confirming the retention of the MCM-41 structure

Importantly the pattern was that of purely siliceous crystalline material. The pattern might imply that aluminium was incorporated into the framework of the MCM-41 structure. The pattern also confirms that correct synthesis conditions were adhered to as any change of conditions might result in an undesirable zeolitic structure.

16.3.2 Ammonia TPD analysis

It is normally assumed that acid-base interactions dominate the adsorption of ammonia on solid acid materials, and that the extent of the interaction is related to acid strength. A base catalyst, CaO, also showed two peaks both in the high temperature or strong acid region, and by conventional interpretation of the TPD results the calcium oxide would be classified as a stronger acid than either the zeolite-Y or the beta-zeolites.[82] This analytical technique may well be the most widely used method for characterization of site densities in solid acids due to the perceived simplicity of the technique; however, the actual interpretation of ammonia TPD results is far from simple and it has even been argued that the technique is not useful.[83] The major problem is that ammonia adsorption does not distinguish between Brönsted and Lewis sites.

Most zeolitic materials contain non-framework alumina and other species; this represents a very significant problem when it comes to TPD analysis. As shown by earlier authors,[82] adsorption on non-Brönsted sites may be stronger than on Brönsted sites, and the temperature at which desorption occurs from both sites depends strongly on conditions used for the experiment.[84] Camiloti *et al*.[67] concluded earlier in their work that ammonia desorbing between 380 and 600 °C was appropriate in quantifying the density of Brönsted acid sites in the zeolites since at lower temperatures part of ammonia desorbs not from Brönsted sites but form structural defects, Lewis sites and other non-framework species. Their work also showed that TPD peaks above 600 °C resulted from dehydroxylation of the zeolite.

A comparative study was carried out with the well know mordenite and LZY-82 zeolites from which a characteristic 3 peak pattern was shown (figure 16.2), and these traces were compared to one of the MCM-41's (*1) material. As discussed by earlier authors,[62] peaks below 250 °C were attributed to ammonia (and water molecules) desorbing from defects, Lewis sites and from extra-framework species. Logically the first peak around 150 °C might be assigned to desorption from mostly defects since these catalysts are highly crystalline. The fact that the particular peak is more intense for LZY-82 somehow supports the defect desorption phenomenon because it has a three-dimensional structure which must be having more defects than the uni-dimensional mordenite, or it could be simply that the 3-D zeolite had greater pore volumes. Lewis sites (and extraframework materials) might be responsible for the second peak around 200 to 300 °C. The high temperature peak (above 350 °C) was then attributed to Brönsted sites of the catalysts which were not observed for Al-MCM-41 material. Intense peaks may also support the fact that mordenite and LZY-82 had much stronger acid sites than the Al-MCM-41 materials.

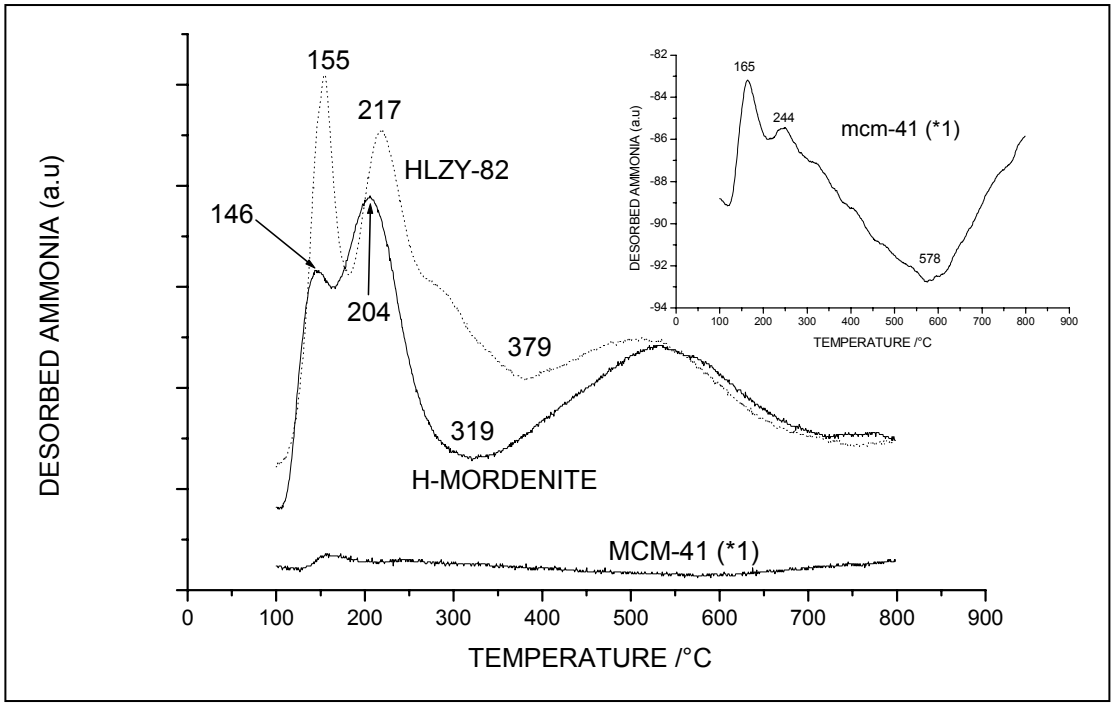

Figure 16.2: Ammonia TPD traces from mordenite, zeolite-Y and Al-MCM-41.

TPD results from Al-MCM-41 materials are shown in figure 16.3. Pure siliceous material represented as 0 % Al did not show any peaks which proved that the peaks resulted from the presence of Al in the zeolite structure, that's either from framework, non-framework or from both positions. All others samples containing Al showed presence of low temperature peaks but no significant high temperature peak due to Brönsted sites. The above suggested two things; 1) the aluminium was not incorporated into the framework structure but existed as extra-framework species, 2) if the aluminium was in the framework positions, then the resulting acidity was not strong enough to adsorb NH_3 or to keep it adsorbed at low temperatures. This led to the inferred conclusion that the Brönsted acid sites of Al-MCM-41 catalysts, if they exist, are very weak.

The only observed high temperature peak was above 600 °C for *5 and this was associated with dehydroxylation of the framework structure due to higher Al content causing thermal instabilities (Si/Al = 9.9), leading to its collapse and destruction at high temperatures.

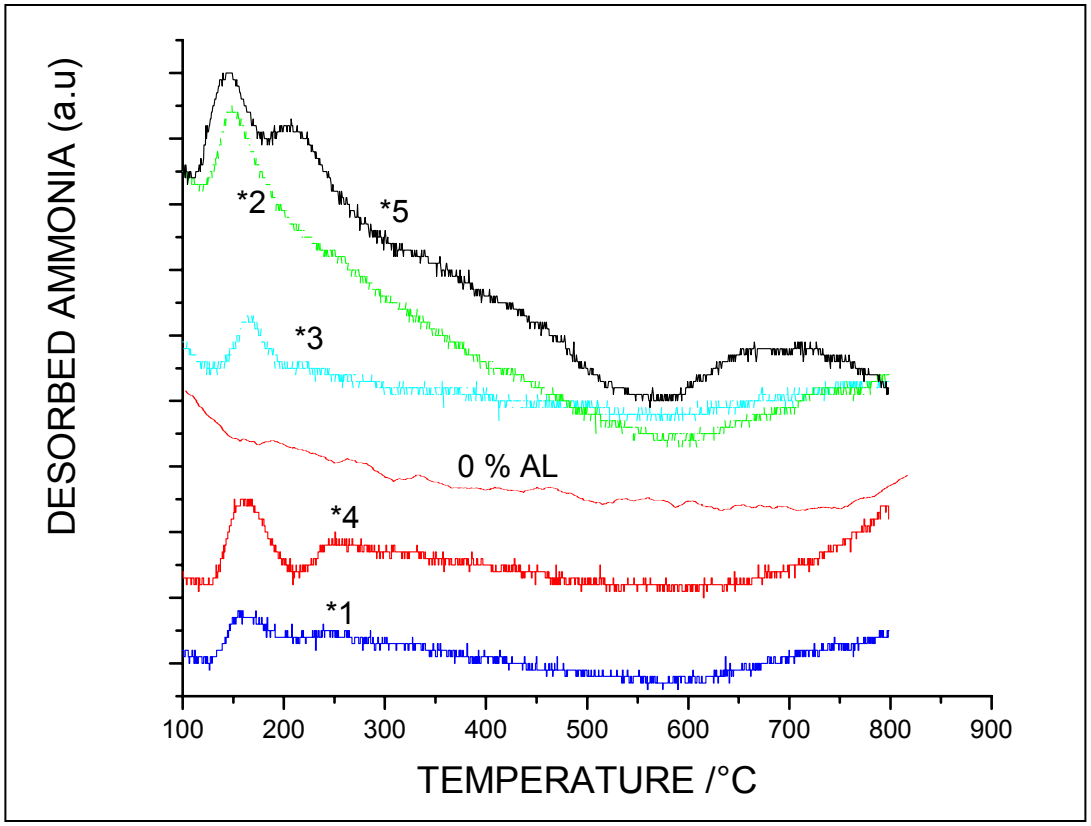

Figure 16.3: Ammonia TPD patterns of siliceous and Al-MCM-41 materials.

16.4 Catalytic test reactions

16.4.1 Ethylbenzene test reactions

The only simple and reliable method of assessing the catalyst's acid sites is by running catalytic tests, and since ethylbenzene disproportionation was used as a test reaction for mordenite and LZY-82, it was also used here to test these large pore materials. Three temperature conditions were used (180, 300 and 500 °C) and average conversions in percentage were calculated over a period of 4 hours for each catalyst and results are shown in figure 16.4.

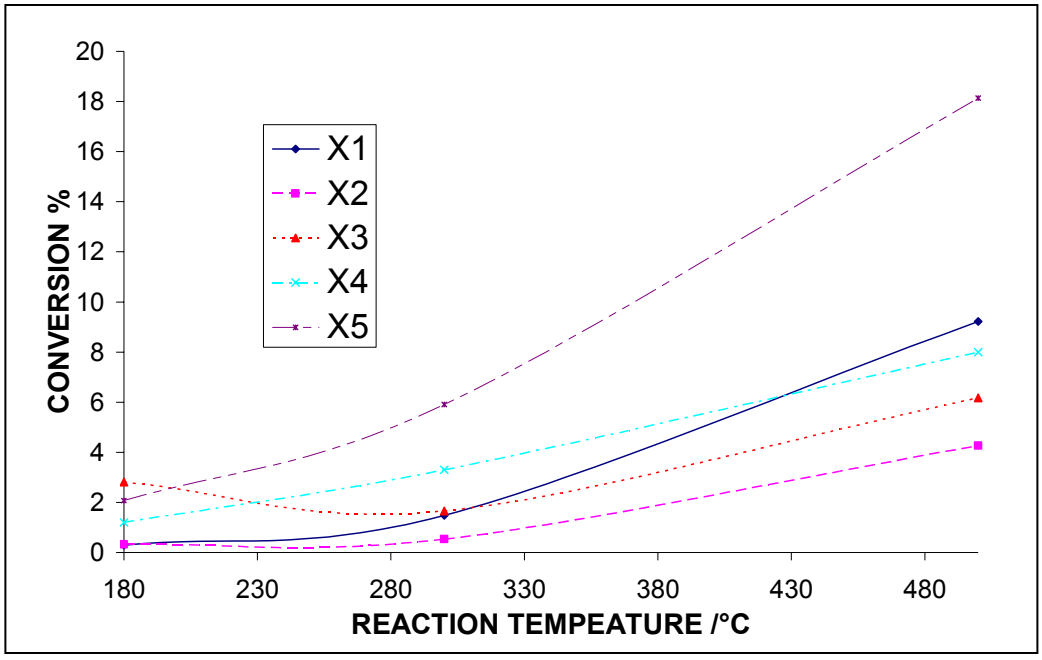

Figure 16.4: Ethylbenzene disproportionation (mol %) on Al-MCM-41, average conversions

The figure showed that there were very little conversions at 180 °C (less than 3 %) as compared to the ~ 50 % observed on the zeolite-Y and mordenite (chapter 4) at the same temperature respectively. This further supported the fact that these materials have very weak acid sites. As expected, the conversion increased with increase in reaction temperature to about 18 % on *5 (Si/Al = 9.9) and less than 8 % for samples with Si/Al = 30. Surprisingly, with current temperature conditions used the main reaction was not ethylbenzene disproportionation but isomerization to xylene.

The isomerization of ethylbenzene has been extensively studied in the past and the process goes through hydroisomerization. The standard catalyst for the isomerization is precious metals on solid acid support, and normally hydrogen is added to promote the isomerization and prevent coking on the catalyst.[85] But general consensus is that the metal site is used for hydrogenation/dehydrogenation and the solid acid support is served for skeletal rearrangement. Ethylbenzene isomerization can only take place in the presence of bifunctional catalysts,[86] presumable through a mechanism involving

particularly hydrogenated intermediates like alkylcyclohexanes.[87] Many bifunctional catalysts commercially used to isomerize the C_8 aromatic fractions contain a zeolitic component (either mordenite or ZSM-5), in combination with a noble metal (platinum) supported on alumina or silica-alumina, where the metal provides the hydrogenation/dehydrogenation function. Hydroisomerization requires an adequate balance between acidic and metallic sites. Fernandes *et al*.[87] suggested the following mechanism for isomerization reactions:

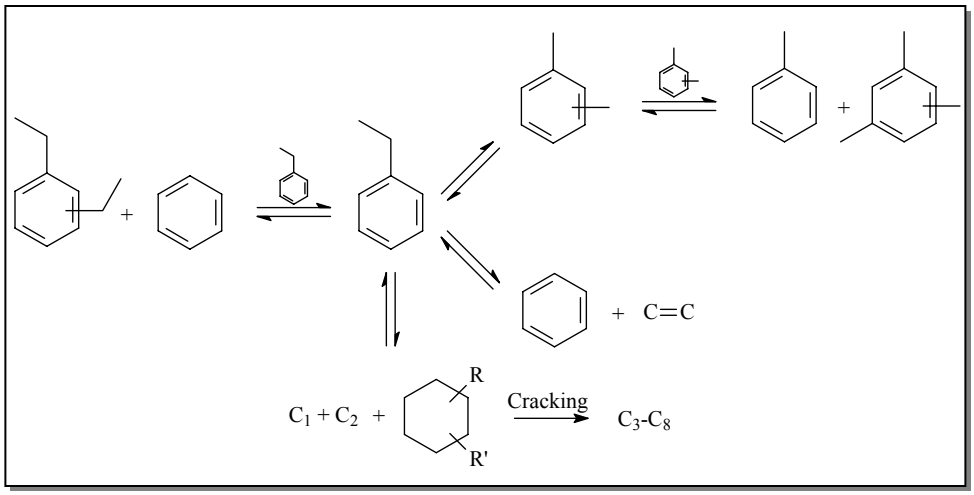

Scheme 16.1: Hydroisomerization reactions of ethylbenzene[87]

They found out that low Brönsted acidity and high mesopores volumes, gave the highest yield of xylenes within the beta series. Polinski *et al*.[88] on the other hand found that hydrogenation-dehydrogenation activity without the addition of the Pt on H-mordenite occurred when hydrogen was used as a carrier gas in the system.

The possibility of ethylbenzene isomerization to xylene on Al-MCM-41 might be due to the fact that low Brönsted acidity and high mesopores volumes favoured the reaction as showed by Fernandes *et al*.[87] on beta zeolites, and Polinski *et al*.[88] showed that hydrogenation-dehydrogenation activities without the addition of Pt occurred on mordenite. The Al-MCM-41 in the present study fits the above descriptions except that of hydrogen carrier gas and this required hydrogen might have been produced from coupling (polymerization) reactions and to a less extent from carbonaceous material deposition. The lack of disproportionation in this case was mainly due to the

weaker acid sites of this catalyst and to support this, an increase in Al amounts resulted in better conversion; even though it was isomerization dominant disproportionation also occurred to some extent.

Ethylbenzene disproportionation was introduced as a test reaction for Brönsted acidity and the estimation of the number of acid sites, but earlier during the disproportionation study it was concluded that even the structure (uni- or tri-dimensional) of the catalyst can be determined by following the benzene traces in the product stream; in the present study it seems like the reaction can also be used to characterize low acidic catalyst materials with respect to the isomerization reaction. Though the above sounded interesting, the fact that these materials were known to contain more of the extraframework species, the observed isomerization might have been made possible by their presence and thus the test might not show low acidities but the presence of such species. Unfortunately at the moment this was not the reaction of interest and it was not expected on these materials.

From TPD results and ethylbenzene disproportionation test reactions it can be concluded that an increase in the Al content leads both to increased acidity (activity) of the catalyst and to thermal instability of the framework structure. This was in agreement with what was found by earlier authors about the effect of aluminium content on MCM-41 materials.

16.4.2 Mesitylene test reactions

Although low conversions were observed on MCM-41 materials during ethylbenzene disproportionation, these materials were still considered as potential catalysts from the perspective that the ease of conversion for alkyl-aromatics increases with 1) the type of alkyl group/s on the ring/s, 2) the chain length of the alkyl group/s and 3) the number of alkyl groups on the ring/s. It was for this reason that mesitylene disproportionation reaction was used to further test these materials.

It was observed on mordenite and LZY-82 that mesitylene disproportionation did not depend much on the reaction temperature and this was mainly attributed to its high reactivity. Two different temperatures were adopted for this reaction and these were 300 and 500 °C. Only *4 (Si/Al = 30) and *5 (Si/Al = 9.9) which showed a closer resemblance of the TPD traces to that of the highly active zeolite-Y and mordenite catalysts, showing two clear low temperature (< 300 °C) peaks (figure 16.3). Results shown in figure 16.5 for reactions on *4 at low temperature (300 °C) showed some kind of an induction period which reached a maximum after 3 hours and then deactivated. During this particular disproportionation reaction no strange isomerization were observed but only the expected isomerization to 1,2,4- and 1,2,3-trimethylbenzenes. The figure then shows conversions only due to disproportionation (alkyl-transfer) and not isomerization.

At higher temperatures (500 °C) the behaviour was very chaotic and a straight line drawn through the points did not show any significant evidence for deactivation of the catalyst. Again the fact that 500 °C was much higher than 300 °C did no have any significant effect on conversion. Very similar results were observed on *5 (figure 16.6) but in this case conversions were much higher (about 40 %) at 300 °C and the induction period was observed but it was shorter than on *4. This was attributed to the fact that increasing aluminium content resulted in increase in the acid site density and thus also the higher conversions.

Again temperature did not have any significant effects on the conversion on this reaction and this was also attributed to the ease of conversion due to the increased number of alkyl groups on the ring. The only observable differences between the results of the two temperature conditions were that lower temperatures showed considerable catalytic deactivation and higher temperatures showed chaotic behaviour.

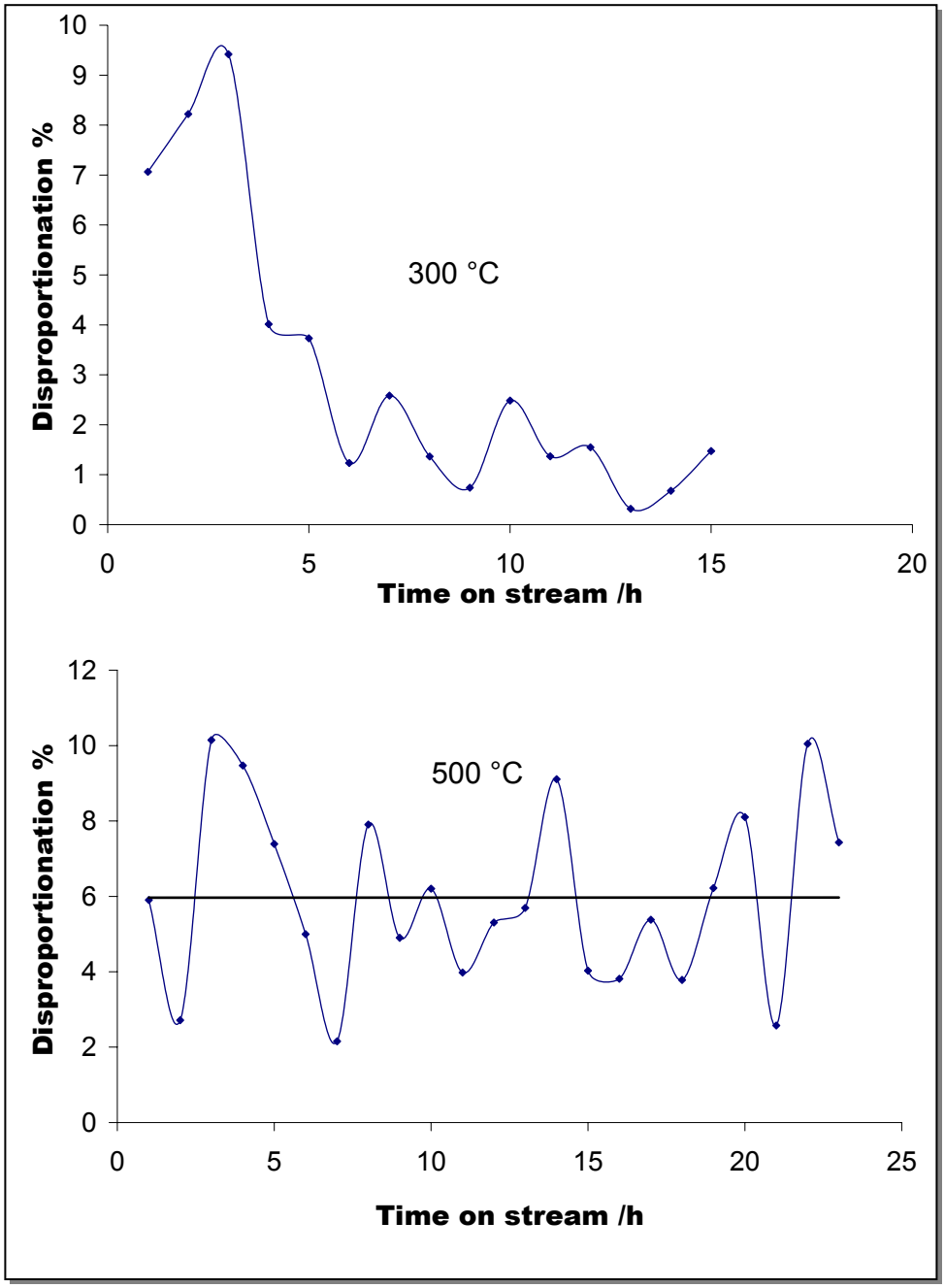

Figure 16.5: Mesitylene disproportionation (mol %) on Al-MCM-41 (*4)

At high temperatures strong adsorptions also occurred but later desorption occurred and unblocked the channels. The phenomenon is better represented in scheme 16.2. The same occurred during the earlier studied reactions with smaller molecules, but the existence of such activity is clearly manifested as molecular sizes of the reactants

increases. The catalyst pore-sizes also seemed to have a certain influence on this activity, but its all speculations at this stage.

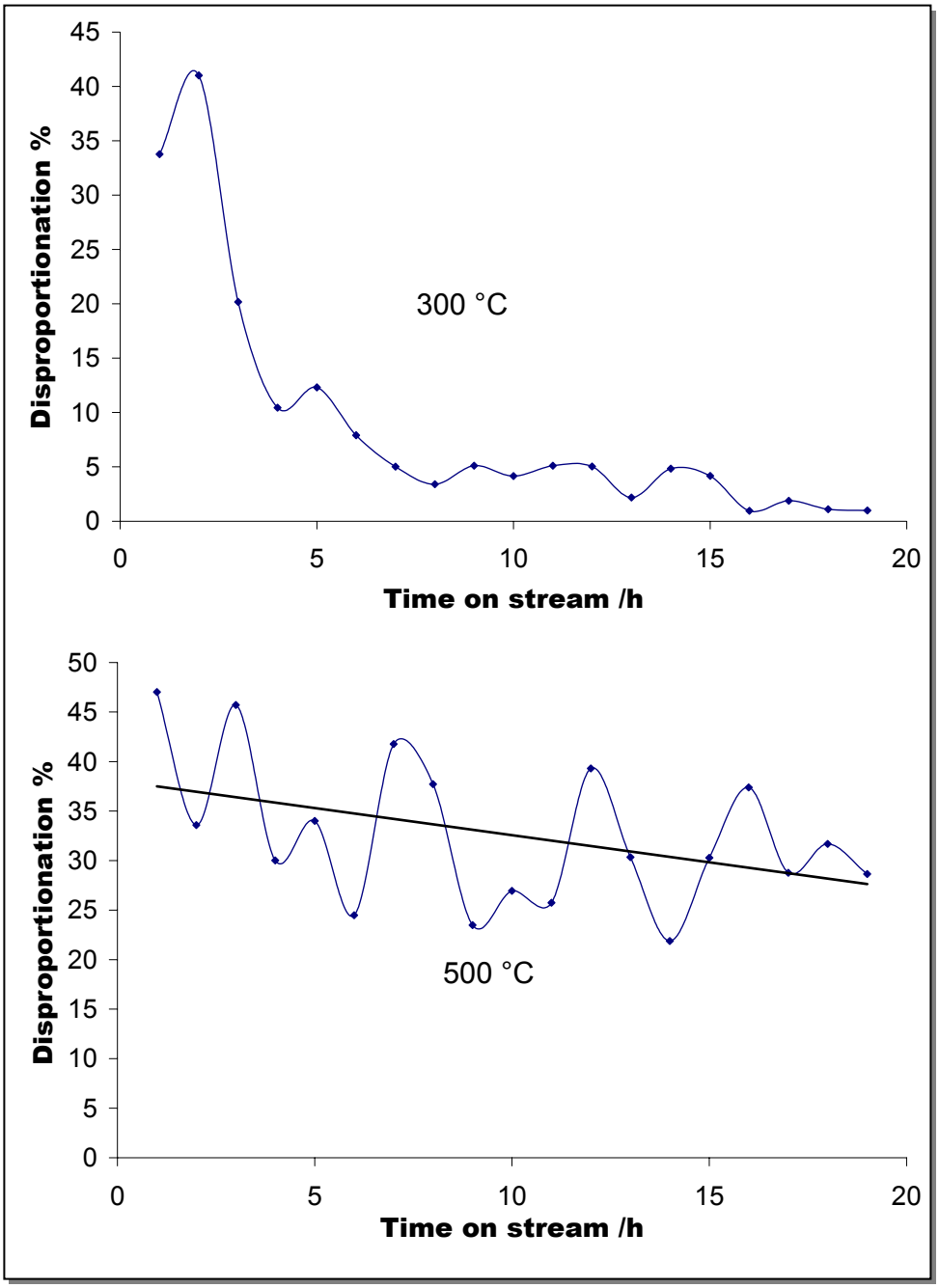

Figure 16.6: Mesitylene disproportionation (mol %) on Al-MCM-41 (*5)

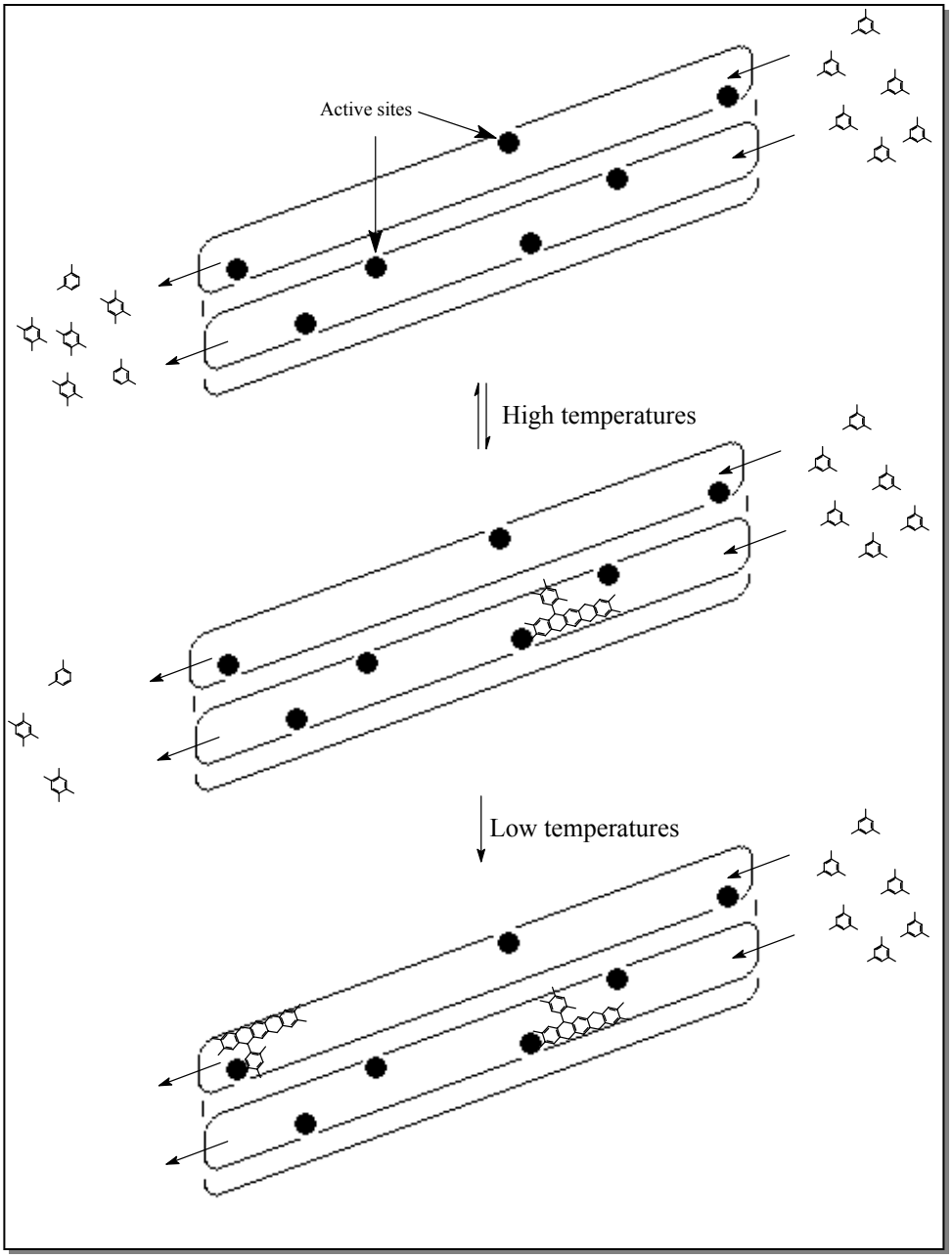

Scheme 16.2: Deactivation of MCM-41 by aromatic compounds and the effect of temperature

Mesitylene disproportionation on the highly active mordenite and LZY-82 catalysts resulted in the formation of benzene and toluene due to further disproportionation of the resulting smaller molecules, while the sterically hindered bulky *tetra*methylbenzene (TetMB) and the *penta*methylbenzene (PMB) did not react further and thus were major products in the outlet stream. The very interesting feature

of the Al-MCM-41 species understudy was the observed selectivity in a sense that the first disproportionation product xylene did not disproportionate further to form toluene or further to benzene. The above observations supported the fact that the ease of conversion increased with the number of alkyl groups on the aromatic ring, and thus the decreased alkyl group number on xylene needed stronger acid sites to pursue further reactions, and this was in close agreement with what was observed during ethylbenzene disproportionation on the catalysts.

The product stream (figure 16.7) from this reaction also showed what was observed on mordenite and LZY-82; that is, the deficit of smaller molecules (xylene) and again this was attributed to their active involvement in deactivating the catalyst by forming carbonaceous materials. For both MCM-41 catalysts at any temperature conditions studied, the absence of toluene or benzene in the product stream showed that these materials can be used in selective disproportionation reactions and even more importantly in this case the selective transalkylation. Bulkier (solid) alkyl group/s containing aromatics (naphthalenic, anthrancenic, etc) can be dissolved in benzene and/or toluene and alkyl-transfer reactions be conducted without the solvent taking part in the reactions (disproportionation), or the alkyl-acceptor molecule back transalkylating (toluene and benzene were intended to be used as solvents and alkyl-acceptor molecules).

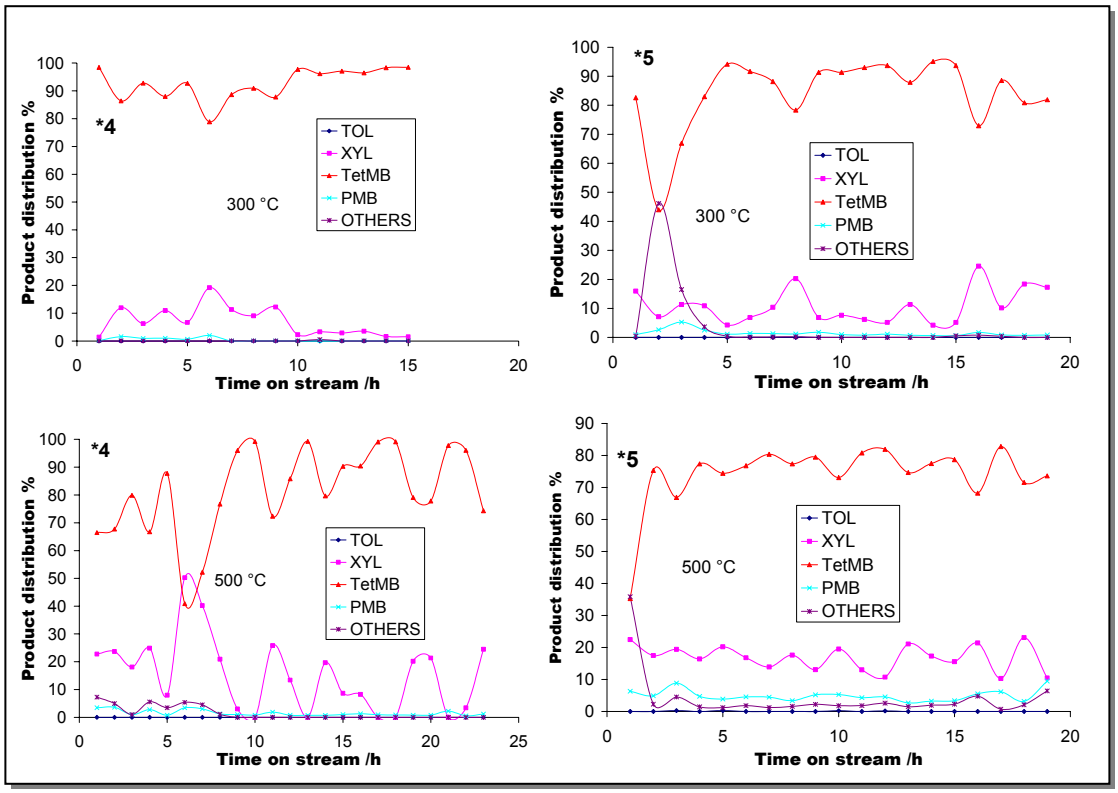

Figure 16.7: Product distribution (mol %) of mesitylene disproportionation reactions on MCM-41

16.5 Conclusion

Al-MCM-41 materials have proved to be potential catalysts for alkyl-transfer reactions. Their low acid strengths can be used advantageously to selectively transalkylate complex alkyl aromatics without the risk of further converting initial products formed as shown by the mesitylene disproportionation reaction. The advantage of using these materials, though not confirmed, is that deactivation either by carbon deposition or polymerization is prolonged by the absence of strong acid sites and by the more open larger cavities respectively and thus better catalyst lifetime than the mordenite and zeolite-Y. The only problem encountered with these materials was the lower acidity and the difficulty of incorporating Al into the framework structure which is the source of these active Brönsted sites in this case. The fact that

incorporation of Al results in thermal instabilities showed that regenerating spent catalysts at high temperatures will definitely destroy the structure and the catalyst's low acidity will most probably require even higher temperatures for the combustion of carbonaceous material since acidity also plays a role in catalyst regeneration.

17 Al-MCM-48; POTENTIAL MATERIAL FOR ALKYL-TRANSFER REACTIONS OF ALKYLAROMATICS: A COMPARISON STUDY

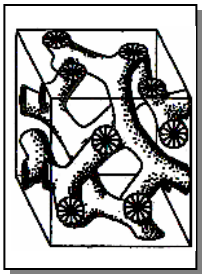

17.1 Introduction

Alkyl-transfer reaction studies on the uni-dimensional mordenite and the tri-dimensional LZY-82 has shown that the latter was a preferential catalyst because of its resistance to deactivation compared to the former. The resistance was mainly attributed to the 3-D structure of the catalyst material offering more entrance/exit alternatives and thus enhanced molecular diffusion. It was discovered later that both catalysts contained small/narrow pores and cavities which could not accommodate larger bimolecular intermediates formed during alkyl-transfer reactions of alkyl-aromatics; and so the use of larger pore materials was the only logical option from the above.

Alkyl-transfer studies on Al-MCM-41 which contained larger pores proved that such reactions were possible on these materials, but an increase in the amount of Al in the bulk composition in an attempt to increase the number of Brönsted sites resulted in a more fragile MCM-41 material (thermally unstable). An ideal solution was to synthesize purely siliceous material without Al (scheme 17.1(b)) and post-alumination would only graft the Al atoms on the surface of the framework structure (c). This would not affect the stability as it would if Al was in the framework structure (a) where it could start interfering directly with the stability of the material. To supplement on the above a 3-D material would be preferred in order to have a catalyst with a reasonable life-time. MCM-41, as mentioned by Schumacher *et al.*[64] consists of a hexagonal array of uni-dimensional, hexagonally shaped pores. MCM-48 (a member of the family) has a three-dimensional, cubic ordered cylindrical pore

system (figure 17.1) and feature pore sizes similar to those of MCM-41 when the same template is used during synthesis, but has a smaller synthesis regime than MCM-41.

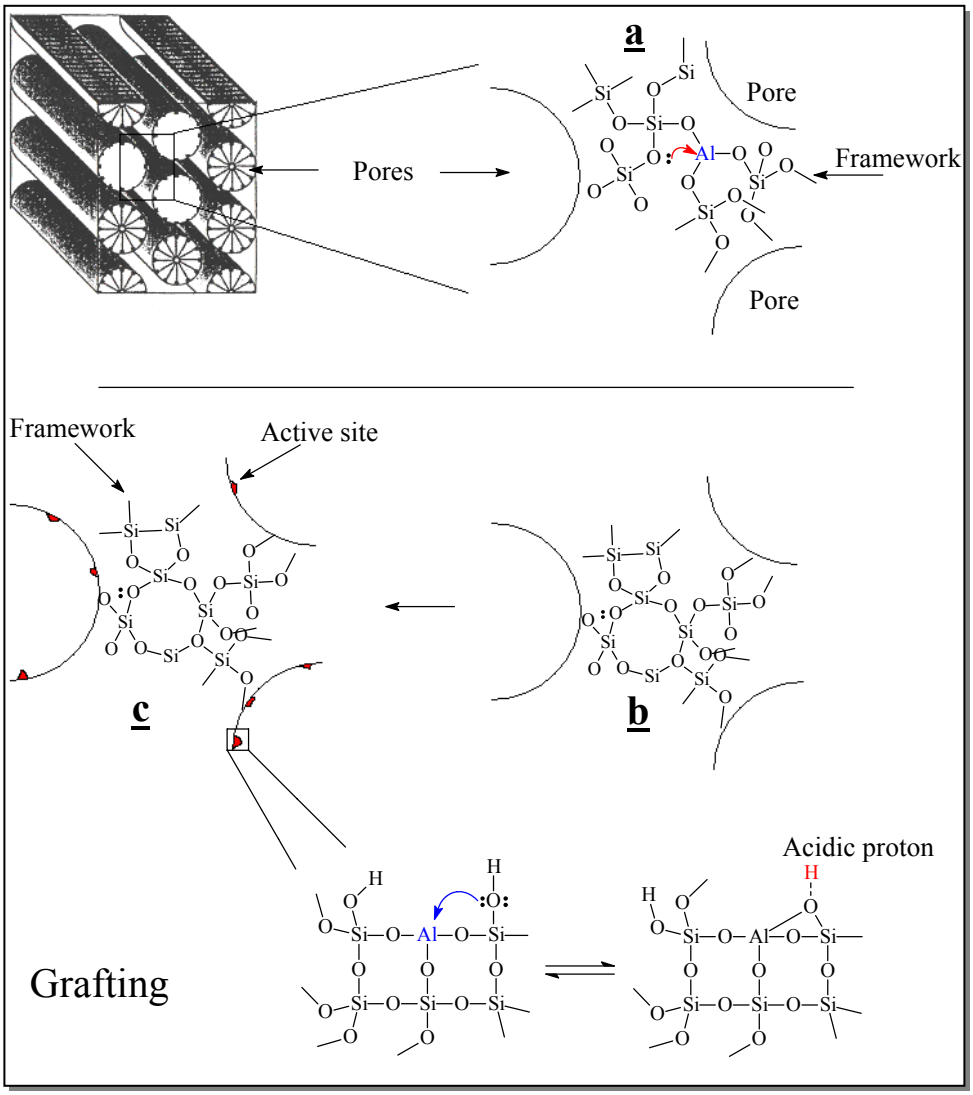

Scheme 17.1: Grafting process on mesoporous materials; a = as-synthesized material, b = siliceous material and c = grafted material

Other interesting physical properties of these materials include a highly specified surface area of up to 1000 m^2/g, a specified pore volume of up to 13 ml/g and a reasonable thermal stability, all of which make them suitable for many catalytic

applications. Therefore, this type of materials has potential application as acid catalysts for petrochemical processes in the refining industry in processes requiring moderate acidity and involving bulky molecules.[89]

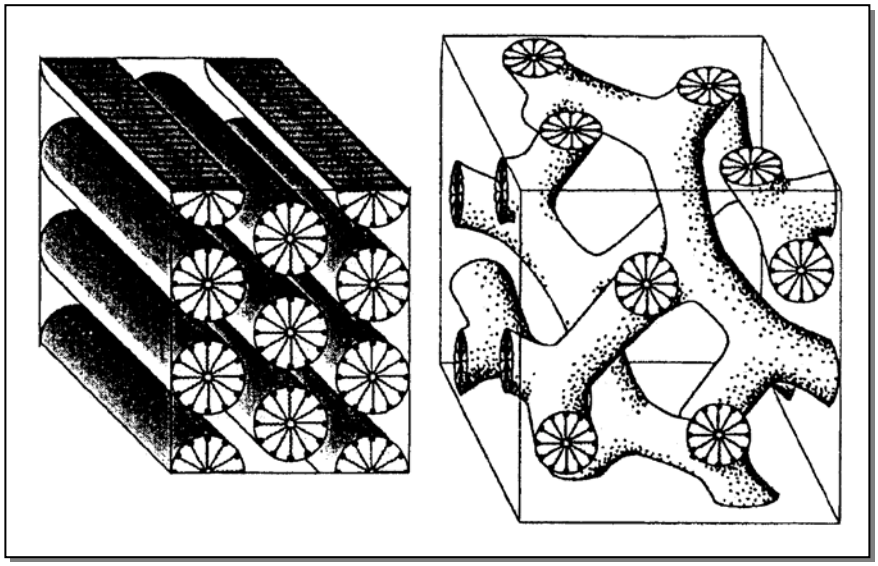

Figure 17.1: Large pore materials[64], Left = MCM-41, Right = MCM-48

Schumacher *et al*.[64] had reported on the room temperature synthesis of MCM-48 which was adopted in this study. A post-alumination method which entails slurring for 1 hour the siliceous material in absolute ethanol solution containing an anhydrous salt forms of various metal compounds like $AlCl_3$, $Al(NO_3)_3$, $SnCl_2$, $Zn(O_2CMe)_2$ and $Mn(O_2CMe)_2$ was reported by Ryong Ryoo *et al*.[90] The resulting material is filtered, washed with ethanol, dried and calcined at 550 °C for 6 hours.

Current study focused on the room temperature synthesis of siliceous MCM-48 and its post-alumination via incipient wetness method with distilled water or ethanol $Al(NO_3)_3$ solutions. Catalytic reactions of the resulting material using compounds of the formula C_9H_{12} were compared to those of Al-MCM-41 material studied earlier.

17.2 Experimental

The synthesis and Al-grafting of MCM-48 materials is outlined in the experimental section (chapter 3) as well as the characterization methods. C_9H_{12} hydrocarbon compounds were used for catalytic tests at 300 and 500 °C; other reaction conditions remained unchanged.

17.3 Results and Discussions

17.3.1 X-RD results

Eimer *et al*.[89] mentioned in one of their recent work that high quality MCM-48 could only be obtained in autoclaves (hydrothermally), and an X-ray diffraction pattern of their Al-MCM-48 synthesized with HTMABr as a template hydrothermally is shown in figure 17.2. The patterns consists of the main peak around 2 (MCM-41) and 2.5 (MCM-48) 2θ (211) with a small shoulder peak around 3 (2θ) (220) similar to characteristic diffraction pattern of the cubic member of the M41S family, MCM-48, reported by other authors.

The structure is further confirmed by a cluster of peaks between 4 and 6 (2θ) degrees which are characteristic of the MCM materials.

The X-ray diffraction pattern of the room temperature synthesis (figure 17.3) closely resembled Eimer's autoclave synthesis results. Two siliceous materials were synthesized for 6 hours (A) and for 3 days (B) respectively. Both samples showed the main peak around 2.5-3.0 (2θ) with no observable (220) shoulder peak (probably due to poor resolutions), but they both showed something around 4 – 6 (2θ) to somehow confirm that an MCM-48 related structure was formed, and since this was better shown on sample A (6 hours) most of the work focused on it. There was a shift in peak position towards higher 2θ values with increase in synthesis time; this was also

observed by Schumacher *et al*.[64] who suggested the room temperature synthesis method adopted here.

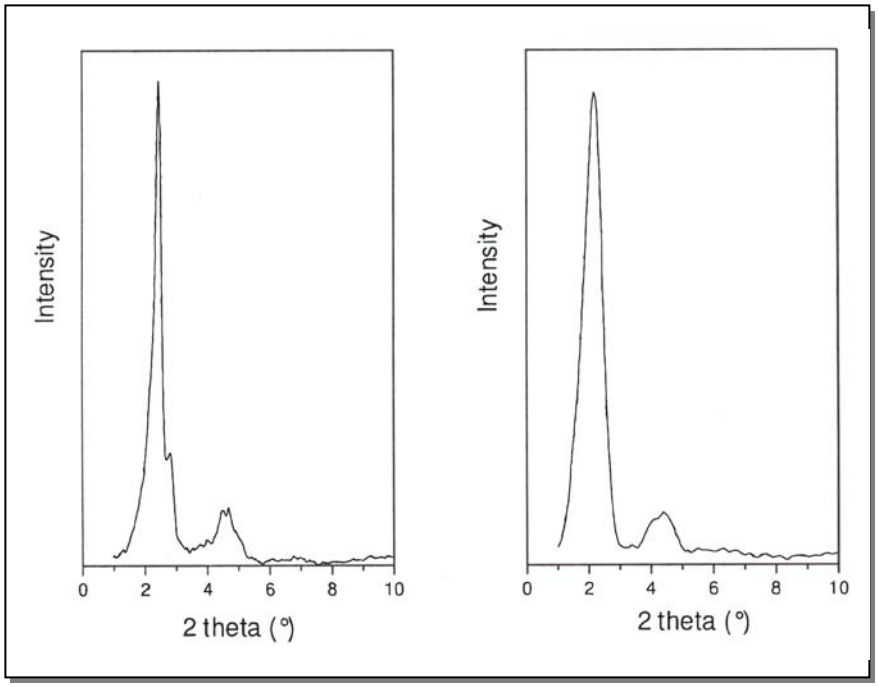

Figure 17.2: X-ray diffraction pattern characteristic of MCM-48 (left) and MCM-41 (right)[89]

MCM-48 material designated as A (6 hours synthesis) was post-aluminated with $Al(NO_3)_3$ aqueous solution and designated as (A-H_2O) and ethanol solution which was designated as (A-OH). There seemed to be a decrease in the X-ray diffraction peak intensities accompanying alumination (figure 17.4), and there seemed also to be a disappearance of the 4 – 6 (2θ) peaks.

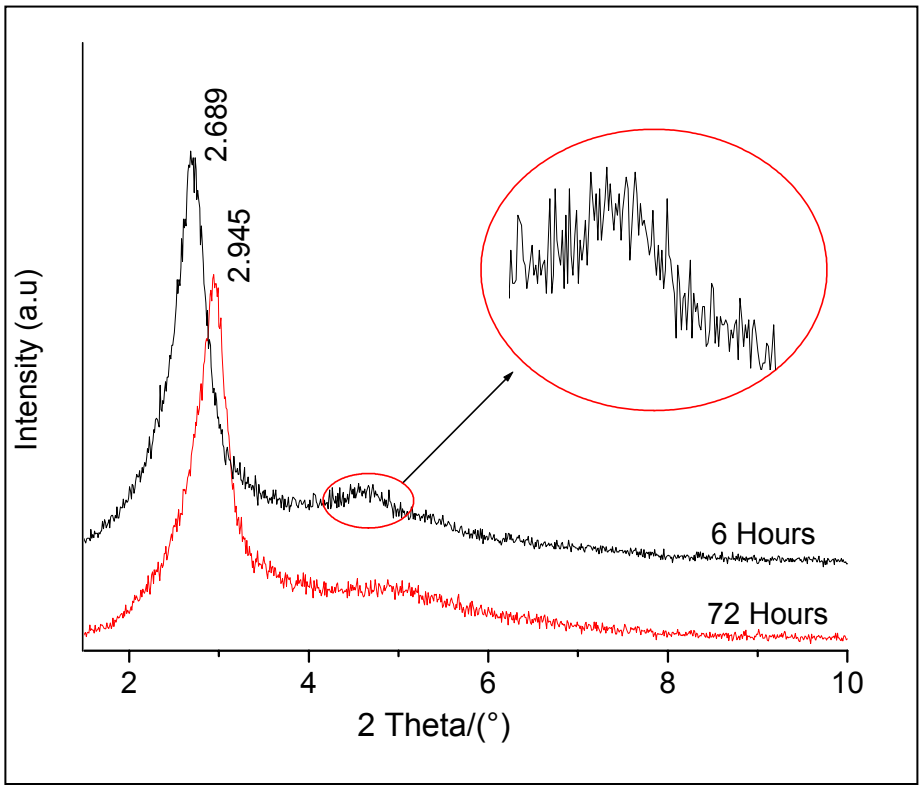

Figure 17.3: X-ray diffraction pattern of the room temperature synthesized material A = 6 hours, B = 72 hours

Figure 17.4 showed that there was a greater difference with alcohol than with water and this was probably due to grafting of Al on the surface of the framework structure and thus altering to some extent the shape of the material. The greater differences with the alcohol grafting suggested that i) different amounts of Al were grafted on the surface and or ii) there were some directing properties as to where the Al (active sites) was grafted on the material which was solvent induced. This type of Al-introduction led to extra-framework species with less crystallinity and hence the observed peak intensity decrease.

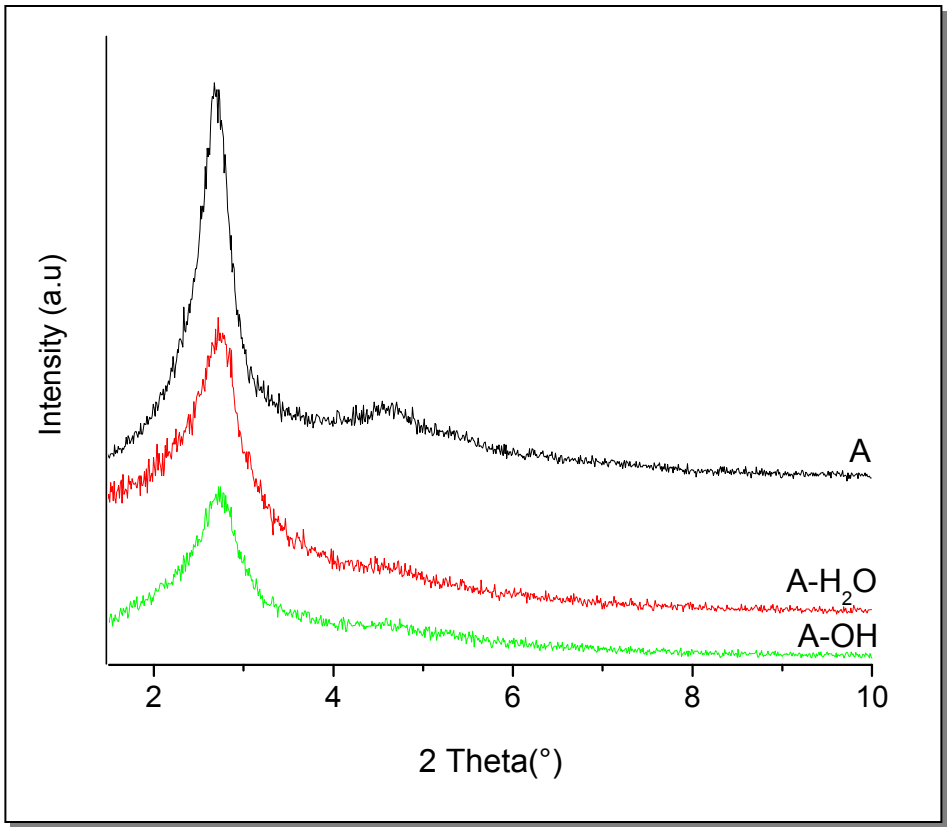

Figure 17.4: X-ray diffraction patterns of MCM-48 (A) and grafted materials, A-H_2O = aqueous solution and A-OH = alcohol solution grafting

Overall, the X-ray analyses showed that the main structure was retained after alumination and that Al grafted MCM-48 material were successfully synthesized.

17.3.2 Catalytic reactions

i) Propylbenzene disproportionation

Although the anticipation was that the acid strengths of these materials would be lesser than those on Al-MCM-41 and it was also concluded earlier that propylbenzene disproportionation required strong sites to undergo any alkyl-transfer reactions, both methods of grafting proved to produce reasonable acid strengths on the MCM-48

materials. Propylbenzene was actually converted on these grafted materials as shown in figure 17.5. The aqueous solution grafting showed an upper hand over the alcohol grafting, probably due to the solubility of the $Al(NO_3)_3$ in the respective solvents favouring the aqueous solution (NB: these grafting solutions were not standard, almost saturates of each were arbitrarily prepared). In all cases there was a gradual decrease in activity with time on stream.

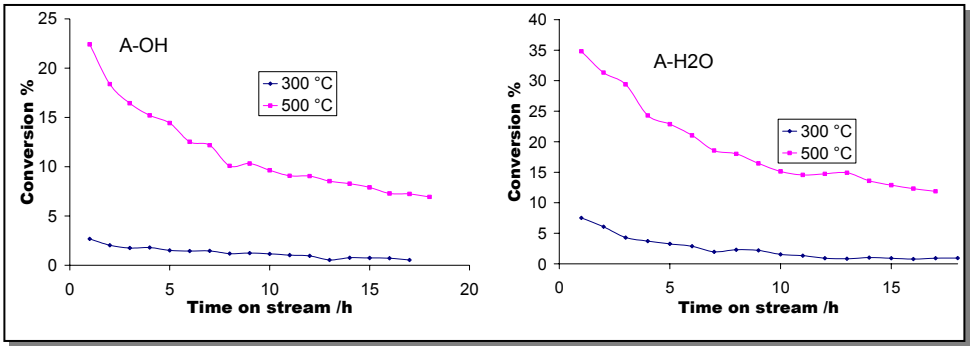

Figure 17.5: Propylbenzene disproportionation (mol %) on Al-MCM-48 material

Increasing the temperature resulted in an increase in conversion as expected, i.e. less than 3 % at 300 °C increased to less than 25 at 500 °C on A-OH and less than 8 % at 300 °C increased to almost 35 % at 500 °C (initial conversions) on A-H_2O. These were very good results as they showed that Al-MCM-48 was also a candidate for alkyl-aromatic conversions. This also proved that Al atoms were actually grafted as Brönsted sites on the MCM-48 surface.

The product distribution on both materials at 300 °C shown in figure 17.6 suggested that there was almost the same catalytic behaviour on both A-OH and A-H_2O. As shown earlier with other disproportionation systems that bulky molecules always dominated the outlet stream, similar observations were also encountered here.

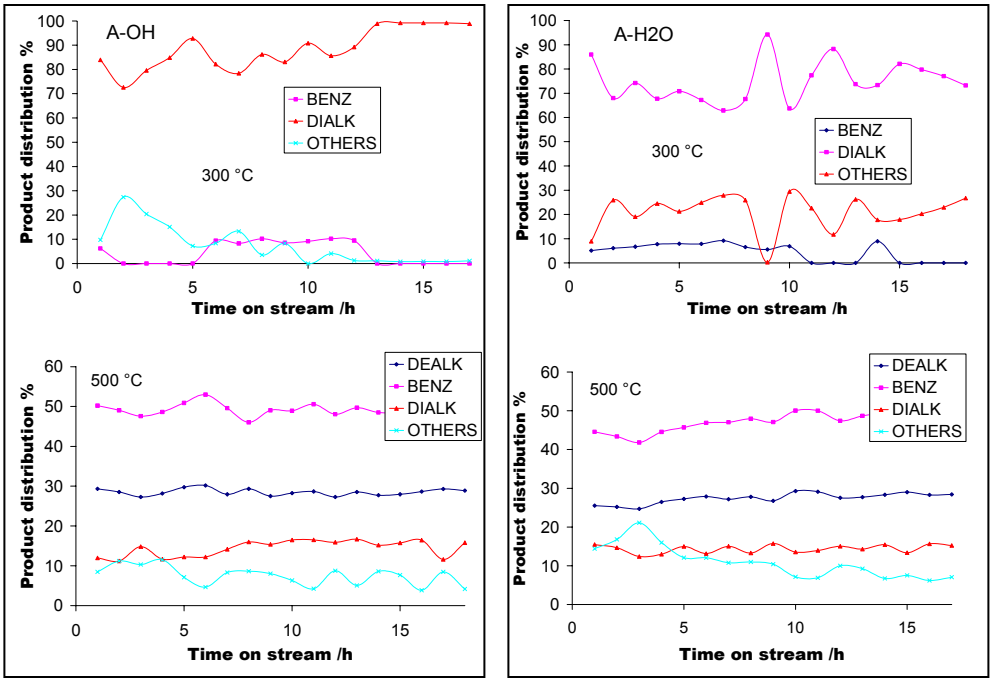

Figure 17.6: Product distribution of propylbenzene disproportionation (DEALK = dealkylation products (mol %), DIALK = dialkylbenzenes, OTHERS = unknowns)

The major product was the dialkylated benzene species (DIALK) followed by the heavy unknowns (OTHERS) while benzene was hardly showing up. It was concluded earlier that benzene (or rather smaller molecules) were actively involved in catalyst deactivation through poisoning of the active sites by strong adsorption and through molecular build-up by polymerization reactions, the same was probably the case in this regard.

The behaviour was still similar at 500 °C (figure 17.6) but the reaction route had changed. The dominant reaction at high temperatures was dealkylation rather than disproportionation. Unlike the reaction at 300 °C high temperatures produced a lot of benzene (BENZ) and less of the dialkylated benzenes (DIALK); there was also appreciable amounts of dealkylation products ((DEALK), propane and/or propene)). The dealkylation reaction was not so pronounced on smaller pore zeolites, but then with these large pore materials there were less constraints and thus high diffusion rates; which meant that smaller products diffused out of the zeolite quicker than the

diffusion in and out of the catalyst by the starting material. The logical explanation of the sudden switch of the reaction routes was probably that there was an activation of acid sites with increase in temperature resulting in sites which were strong enough to cleave off the alkyl group from the ring. The actual and known fact is that, acid site strength does not change but activity does as even expected from the Arhenius's law.

The above observations suggested that the Al grafted MCM-48 material might posses some temperature induced selectivity as it was shown by the 3-Dzeolite-Y.

ii) Cumene disproportionation

Cumene with high steric effects (on the alkyl group) showed the expected high conversions on both materials, less than 30 % on the A-OH and almost 50 % on A-H_2O at 300 °C (figure 17.7). Again in both cases there was a gradual deactivation with time on stream as shown earlier by the propylbenzene disproportionation reaction. The instability of the reaction on A-H_2O was attributed to constant blocking and unblocking of the zeolite pores through polymerization and subsequent cracking. Though the unstable behaviour was earlier observed on Al-MCM-41 the product stream of the reaction on A-H_2O greatly supported the polymerization/cracking activities (figure 17.8).

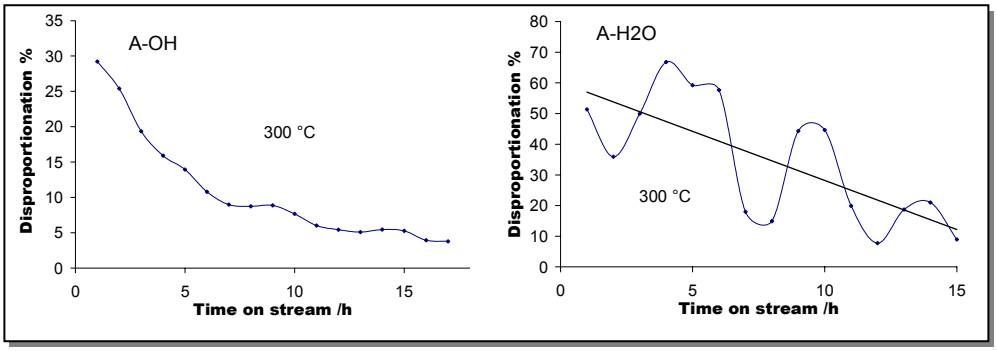

Figure 17.7: Cumene disproportionation (mol %) on Al-MCM-48 at 300 °C

A stable behaviour was shown by the A-OH catalyst which exhibited a lot of dealkylation producing benzene and the alkene/alkane. The fact that there was no 1:1 relation between benzene and the dealkylation products showed that even though steric effects enhanced and preferentially favoured the cleavage of the alkyl groups, realkylation to another cumene molecule was inevitable.

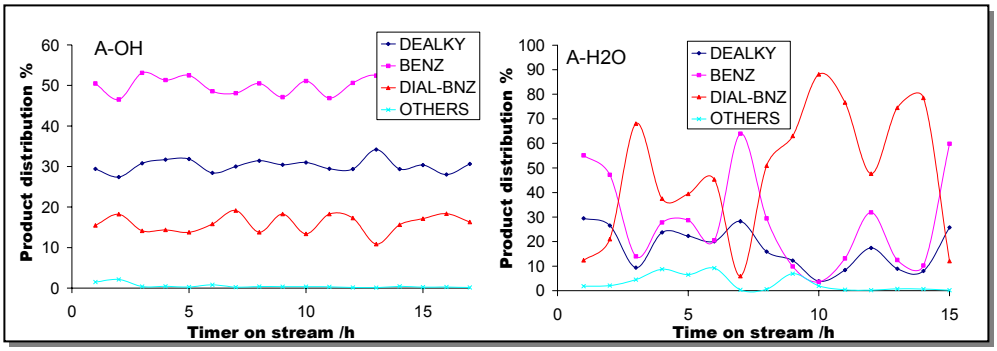

Figure 17.8: Product distribution of cumene disproportionation reaction (mol %) on Al-MCM-48 at 300 °C

The realkylation reaction consumed both the staring material and the dealkylation products and thus the resulting lower amounts of dealkylation products. A-H_2O showed a decrease in the smaller molecules (benzene and dealkylation products) in figure 17.8 between 1 and 3 hours which accompanied a decrease in conversion between 1 and 2 hours in figure 17.7, and at the very same time there was an increase in the amounts of the dialkylbenzenes in the product stream in figure 17.8. An increase in conversion between 2 and 4 hours in figure 17.7 that followed resulted in an increase in the smaller molecules in the product stream while there was also a decrease in the amount of bulkier molecules (figure 17.8). The increase in the amounts of the bulkier (dialkylbenzenes) molecules in the product stream suggested that this was a result of cracking reactions in the zeolite producing bulky molecules which had earlier blocked the pores leading to low conversions. The increase in conversion after 2 - 4 hours accompanied by smaller molecules suggested that polymerization reaction had started mostly consuming bulky molecules and thus beginning to clog the pores and only smaller molecules could diffuse out. The

product stream showed that these activities kept occurring as shown also by the conversion trace on figure 17.7 through out the reactions.

There were very interesting observations on figure 17.8 which showed the product distribution of cumene disproportionation reaction on grafted catalysts at 300 °C. The main products on A-OH were benzene and dealkylation products suggesting that dealkylation dominated, and disproportionation products (dialkylbenzenes) were only minor in the outlet stream. Looking into the product stream of the A-H_2O reactions, though the traces were very chaotic, it looked like disproportionation products (dialkylbenzenes) were the major products and this somehow suggested disproportionation as the dominant route. Since these reactions were performed under same conditions the observed selectivities could only be attributed to the catalysts themselves with peculiar sites respectively. The comprehensive and logical explanation for the above observations was that as concluded earlier during the disproportionation reactions of propylbenzene on the same catalyst that A-H_2O contained stronger sites than the A-OH, deactivation by site poisoning was higher than on A-OH and this kind of deactivation consumed smaller molecules. Though deactivation through pore blockage occurred, it was continuously counteracted by the subsequent cracking induced by acid sites themselves. The product distribution of the reaction on A-OH showed some extent of stability but this did not mean that there were no pore blockages through polymerization, it was probably occurring but to a very less extent due to the kind of acid sites that existed, and the fact that there was less of the bulky disproportionation products was probably suggesting that polymerization occurred consuming bulky molecules and that there was no subsequent cracking due to acid site characteristics.

Interesting and undesirable results were observed at elevated temperatures (500 °C) on both catalysts which showed almost the same behaviour. Figure 17.9 showed that almost 100 % conversions were achieved on both materials under similar reaction conditions. Focusing closer on the traces showed that the A-OH exhibited rapid deactivation as compared to A-H_2O and this was attributed to thermally activated acid

sites which initiated deactivation processes and thus increased the rate of deactivation. The nature of these active sites was unknown but what was observed was that A-H_2O and A-OH contained different acid sites and they most probably had different characteristics.

The interesting feature was that of the mere fact that conversions were so high meaning that the pores, channels and cavities were so open that molecules diffused freely into the material, reaction intermediates formed without any constraints, adsorption/desorption of reactants and products respectively occurred at reasonable rates and lastly, products diffused out of the catalyst with much ease.

There were no appreciable differences in the product distribution of these materials (figure 17.10) at these high temperatures; both showed a very strong dealkylation activity rather than the desired alkyl-transfer reaction.

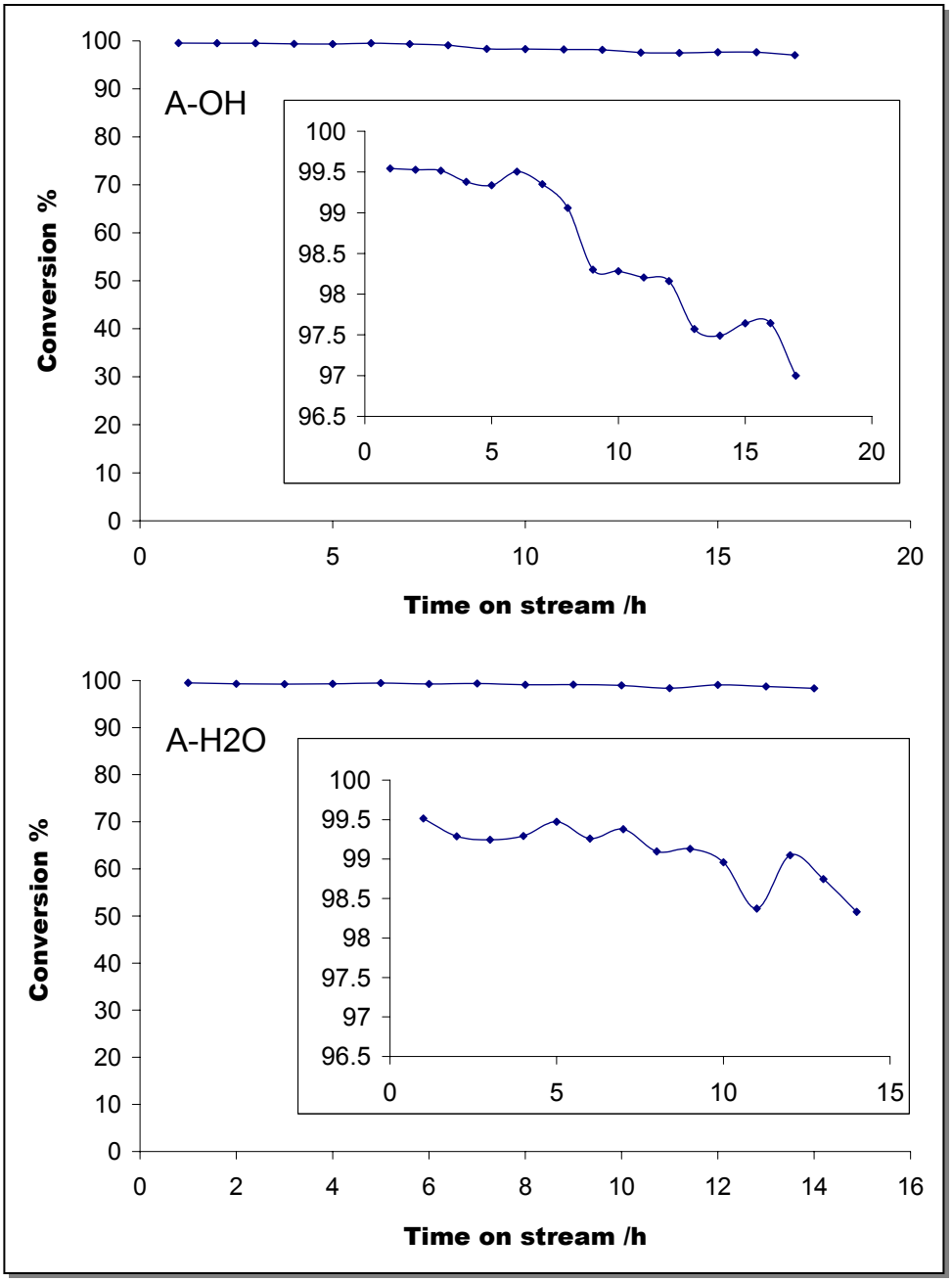

Figure 17.9: Cumene conversion (mol %) on Al-MCM-48 at 500 °C

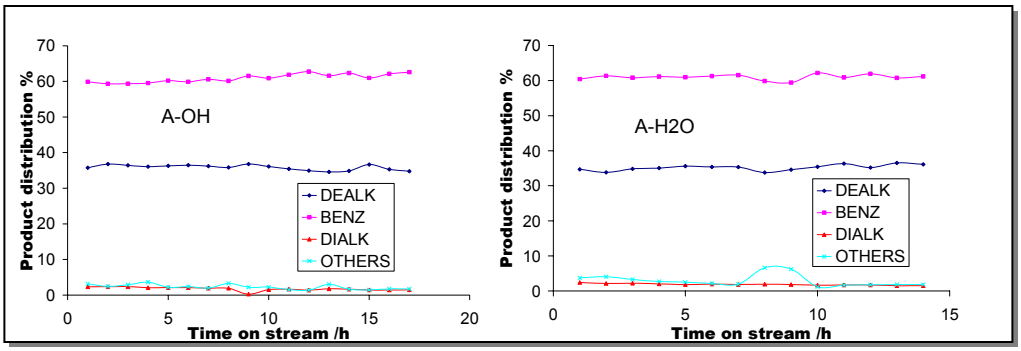

Figure 17.10: Product distribution (mol %) of the cumene reaction on Al-MCM-48 material At 500 °C

The figure also showed that there was no 1:1 relation between benzene (BENZ) and the dealkylation products (DEALK). While the formation of dialkylbenzenes consumed some of the dealkylation products there was still catalyst blackening even though the conversion traces did not show much of the deactivation evidence. Benzene was earlier confirmed as one of the actively involved molecules in carbonaceous material deposition during alkyl-transfer reactions but in this case the dealkylation products surpasses benzene in the formation of carbonaceous materials, thus the consumption of dealkylation products (DEALK) was attributed to the formation of dialkylated products and carbon deposition. The above observations suggested that these materials were ideal cracking catalysts with reasonable lifetime but the idea of working at high temperatures seemed to be their setback.

iii) Mesitylene disproportionation

Mesitylene was also converted to around 30 % on A-H_2O and just above 25 % on A-OH at 300 °C (figure 17.11). The trace on A-H_2O though showed signs of deactivation did not show any evidence of polymerization/cracking reactions as did the cumene reaction. This might be due to the absence of the dealkylation route which would produce alkenes/alkanes that also take part in polymerization reactions themselves; the only possible reactions were monomolecular isomerization and the bimolecular alkyl-transfer reactions.

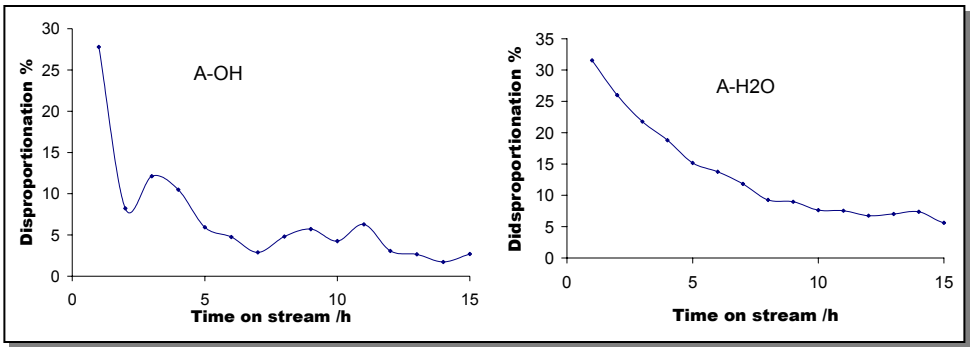

Figure 17.11: Mesitylene disproportionation (mol %) on Al-MCM-48 at 300 °C

Reactions on A-OH revealed what seemed to be an interesting characteristic about the particular materials. There was a high conversion during the very first hour of the reaction then the conversion went down from 25 to around 10 % just after 2 hours (figure 17.11(A-OH)), and then there was a familiar oscillation in conversion for the next 14 hours. The unusual behaviour suggested that the material had two types of active sites and a few of them were strong acid sites. These sites deactivated very rapidly supporting the suggestion that they were few or they were considerably strong.

As expected from the smooth conversion curve shown by the reaction on A-H_2O the product stream did not show any signs of chaotic behaviour. On A-H_2O the product traces behaved more like reactions on mordenite, LZY-82 and Al-MCM-41, i.e. there was a deficit in the amounts of smaller molecules while the bulkier *tetra*methylbenzene (TetMB) dominated the product stream; *penta*methylbenzene (PentMB) was also produced but in very small quantities. There was no sign of toluene or the smaller benzene suggesting that the smallest molecules in the zeolite were of xylene and its deficit should be due to its involvement in carbonaceous material deposition which deactivated the catalyst. The observed behaviour on the particular material also suggested that water grafting produced active sites similar to those found on the as-synthesized materials and unfortunately there was no enough evidence to support this.

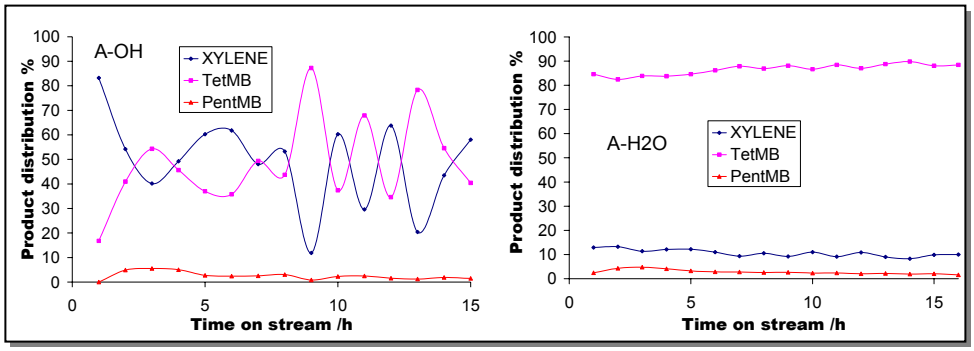

Figure 17.12: Product distribution (mol %) of the mesitylene disproportionation reaction on Al-MCM-48 at 300 °C

On A-OH xylene dominated the product stream only for the first 2 hours probably due to the 3-D structure of the catalyst with weaker acid sites (minimum strong adsorption) which allowed smaller molecules to diffuse quickly out of the zeolite pores. But a comparison of the two graphs in figure 17.12 shows that the quick diffusion of smaller molecules observed on A-OH was not actually due to the tri-dimensional structure, this is because both A-OH and A-H_2O are tri-dimensional; the only possible explanation is that there was polymerization reactions in A-OH which reduced the pore volumes and thus allowed smaller molecules to diffuse preferentially. The chaotic behaviour that followed further supported the polymerization/cracking reactions; when the xylenes trace goes up then the *tetra*methylbenzene (TetMB) trace goes down and visa versa, i.e. when polymerization blocked the pores only smaller molecules could diffuse out and when cracking cleared up the pores then bulky molecules dominated the stream and the circle continued over and over again.

Higher temperatures (500 °C) did not show a significant effect on the catalyst behaviour on both catalytic materials (figure 17.13) which is what was observed with the mordenite, LZY-82 and Al-MCM-41 catalysts. The only noticeable change was on A-OH where temperature seemed to prolong the lifetime of stronger acid sites and increased the conversion form less than 30 to more than 70 % during the first three hours of the reaction. With time on stream the strong sites deactivated and the expected low conversion polymerization/cracking reactions commenced. The nature

of these sites was not understood but it was expected of them to show some effects on transalkylation reactions.

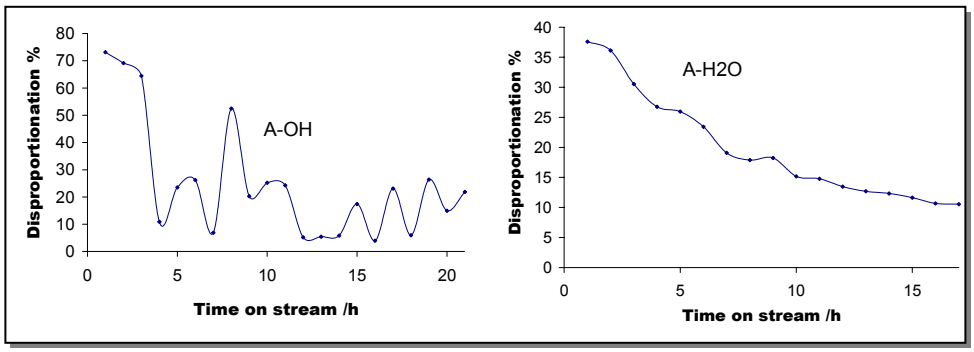

Figure 17.13: Mesitylene disproportionation (mol %) on Al-MCM-48 at 500 °C

The product stream of the reaction on A-H_2O did not show much change from that at 300 °C further supporting the earlier conclusion that mesitylene disproportionation reaction does not depend munch on the reaction temperature (figure 17.14). High temperature reactions on A-OH seemed to shift the deactivation route towards carbonaceous material deposition rather than adsorption as it was expected. There was a deficit in xylene to support the above but the chaotic behaviour suggested that there were still some polymerization/cracking reactions which somehow contributed to deactivation.

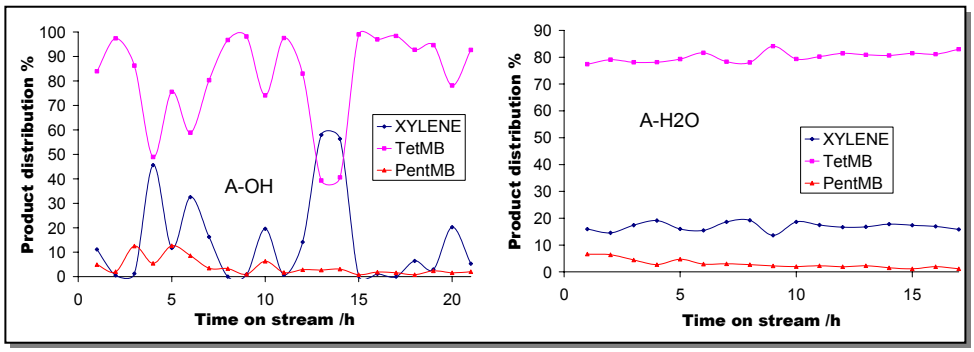

Figure 17.14: Product distribution (mol %) of the mesitylene disproportionation on Al-MCM-48

Overall, Al grafted MCM-48 materials showed or proved to be strong candidates for more complex alkyl-aromatic alkyl-transfer reactions.

17.4 A comparison between Al-MCM-41 and Al-MCM-48 materials

Al-MCM-41's prepared earlier by Peter Mokhonoana were hydrothermally as-synthesized materials and they were designated as *4 (Si/Al = 30) and *5 (Si/Al = 9.9) respectively. MCM-48's (siliceous material) were synthesized at room temperature then post-aluminated through an aqueous and ethanol solutions with $Al(NO_3)_3$ as a source of Al. It was noticed earlier that the as-synthesized Al-MCM-41 lost its structure around 600 °C and higher temperatures and this was mainly attributed to the aluminum atoms in the framework structure which affected the stability. Purely siliceous MCM-48 materials were prepared in order to improve on the thermal stability of these large pore materials, and thereafter post-alumination was carried out. The 3-D structure of the MCM-48 material was expected to improve on the lifetime observed on the uni-dimensional Al-MCM-41 material. A-H_2O was believed to contain more sites than the A-OH and this is also shown in figure 17.15 below showing initial conversions on A-H_2O to be comparable to those of *5 (Si/Al = 9.9) while the A-OH was comparable to that of *4 (Si/Al = 30).

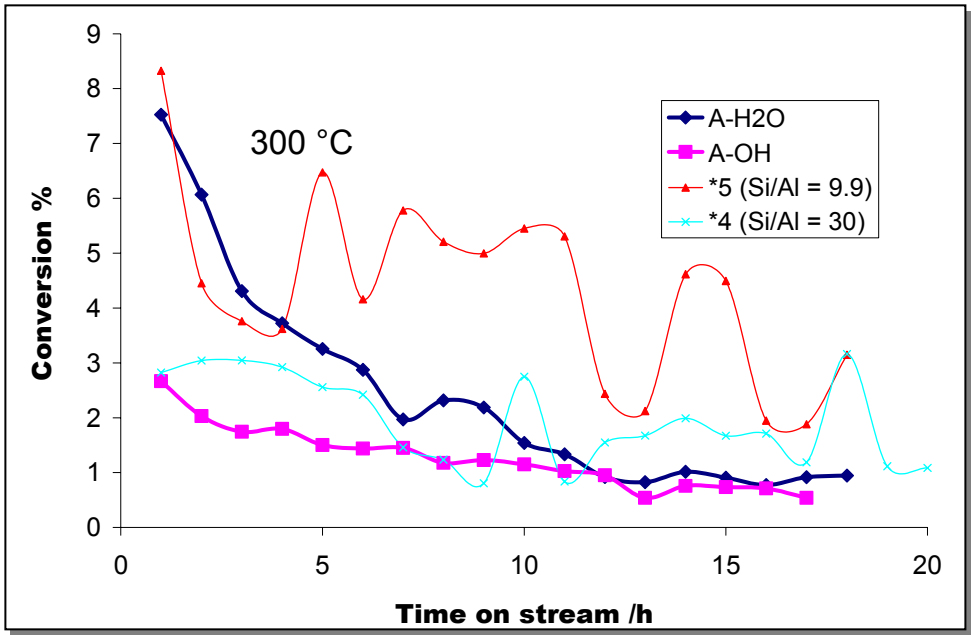

Figure 17.15: Propylbenzene disproportionation (mol %) on large pore zeolite at 300 °C

A closer look at figure 17.15 for the first four hours focusing on the *5 and the A-H_2O traces, the former deeps sharply as it deactivates/blocked while on the later deactivation was not as quick. Al-MCM-41's exhibited cracking activities making it look a better catalyst than Al-MCM-48.

On the other hand A-H_2O and A-OH showed an upper hand (figure 17.16) on their Al-MCM-41 counter parts respectively when cumene was used as a feed. Both Al-MCM-48 materials showed better activities but only A-H_2O exhibited cracking abilities shown by Al-MCM-41 materials. The better activities shown by Al-MCM-48 material on cumene conversion was brought about by the fact that cumene cracking is a very facile reaction but the real advantage was that of a 3-D structure which provided more room for the reaction, even though there was more than enough on these mesoporous materials.

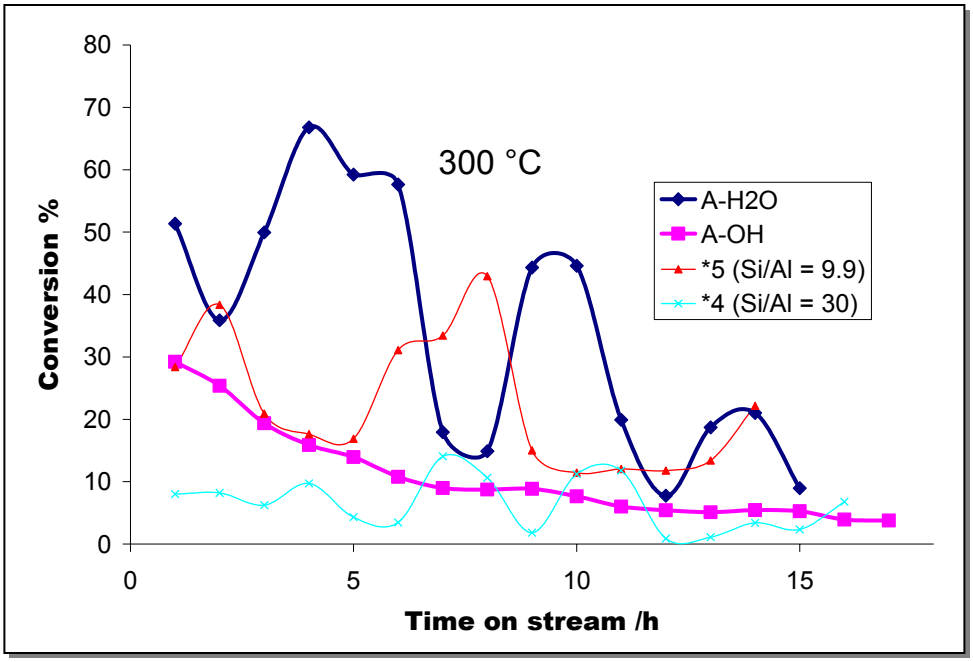

Figure 17.16: Cumene disproportionation (mol %) on large pore zeolites at 300 °C

The mesitylene disproportionation reaction showed that Al-MCM-48 materials had lower acid strengths but better catalyst lifetime and this was better shown by A-H_2O traces (figure 17.17). A very short induction period was shown by *5 and it was followed by a rapid deactivation which was mainly attributed to stronger sites and the one-dimensional structure of the material, on the other hand A-H_2O though showed lower activities it exhibited a longer lifetime. A-OH showed cracking activities during this reaction and better conversions than *4.

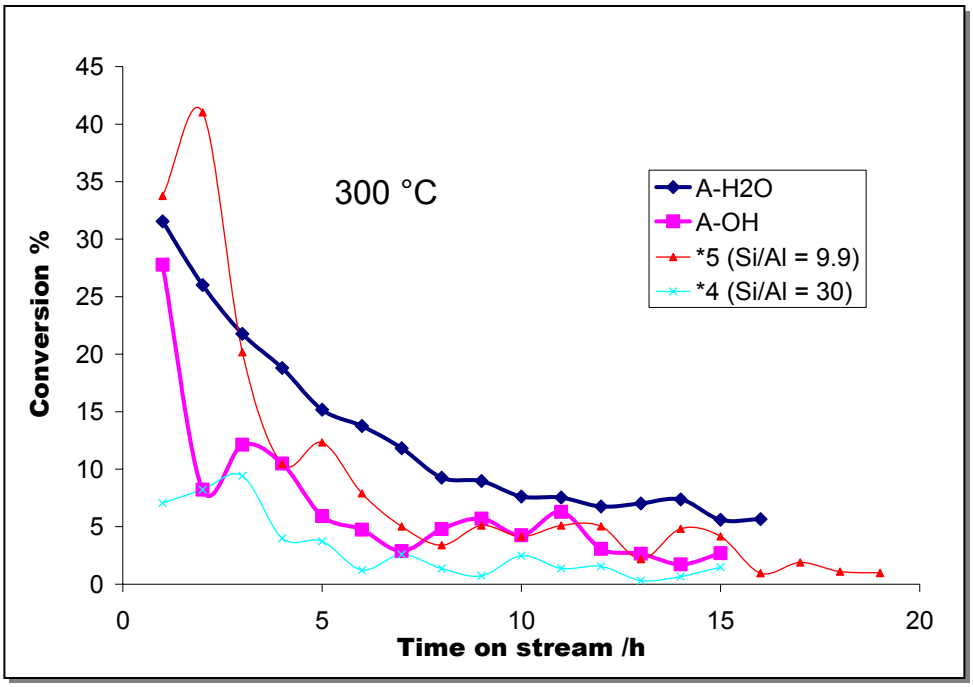

Figure 17.17: Mesitylene disproportionation (mol %) on large pore zeolites at 300 °C

Al-MCM-41 material exhibited polymerization/cracking reactions on all the C_9H_{14} feeds, but this was not the case with the Al-MCM-48. Both A-H_2O and A-OH showed smooth traces for the propylbenzene conversion, for cumene 'cracking' only A-H_2O exhibited the polymerization/cracking reaction and A-OH showed this kind of behaviour during mesitylene disproportionation while A-H_2O did not. The above observations suggested that the Al-MCM-48 materials had some different hidden selectivities associated with the feed and this was expected to be also revealed on binary mixtures during transalkylation reactions. The determining factor on whether the catalyst will exhibit polymerization/cracking reactions (and why?) were not understood.

17.5 Conclusion

The synthesis at room temperature of MCM-48 was achieved even though X-ray diffraction did not show good quality peaks; nevertheless, the synthetic route was much simpler and less time consuming. Al grafting by either the aqueous or the

alcohol solution produced Brönsted acid sites which were required for alkyl-transfer reactions. These were presumably on the surface of the siliceous MCM-48 material. The successfully synthesized Al-MCM-48 material showed preferential cracking activities on propylbenzene and cumene rather than the desired alkyl-transfer reactions. Aqueous solution grafting produced acid sites with characteristics comparable to those of as-synthesized materials while the alcohol solution grafting produced acid sites of unknown nature.

In comparison to Al-MCM-41 (as-synthesized material), Al-MCM-48 (grafted material) showed that if similar Si/Al ratio and similar type of acid sites between the two were achieved it would be a much better catalyst than Al-MCM-41 because of 1) the three-dimensional structure providing more room for the reactions and molecular diffusion alternatives, 2) with the same Si/Al ratio the grafted Al-MCM-48 would have more site exposed to reactants than the as-synthesized materials (higher surface area), and 3) deactivation on Al-MCM-48 material by pore blocking would have minimal effect due to the 3-D structure and so would deactivation by site poisoning due to the weaker acid sites. Their disadvantage was that of weaker sites and the fact that maximum performances can be achieved at high temperatures (at increased activity, not increased acid strength), not overlooking the issue of unknown acid site properties.

18 THE EFFECT OF Al GRAFTING ON ALKYL-TRANSFER REACTIONS ON MCM-48 MATERIALS: THERMAL STABILITY

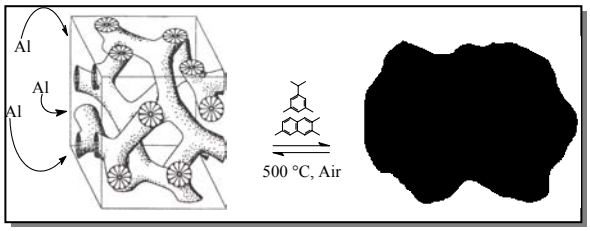

18.1 Introduction

In the previous chapter, arbitrary amounts of $Al(NO_3)_3$ (close to saturation) in both water and alcohol solutions were used to graft Al atoms on the siliceous framework structure of MCM-48. Not only did grafting occur but also active sites capable of initializing alkyl-transfer reactions of alkyl-aromatics were created. Grafted catalysts proved to be potential catalysts in alkylaromatic transformations and thus this study focused on further exploring this type of catalysts. Standard solutions of $Al(NO_3)_3$ in water and alcohol respectively were prepared and grafting was carried out on siliceous MCM-48 materials. This was carried out with the intention of looking at the effect of Al atom concentration in the framework structure on alkyl-transfer reactions. Test reactions for these materials included transformation of binary mixtures of benzene and alkylaromatics where transalkylation was evaluated. Since the idea of grafting Al atoms on the siliceous framework was to improve on the stability of mesoporous materials, their thermal stability was studied via regeneration methods at 500 °C using a suitable alkylaromatic, i.e. the easily converted compound so as to effectively monitor catalytic behaviour of these grafted materials.

18.2 Experimental

18.2.1 Room temperature synthesis of MCM-48

The synthesis procedure followed in the previous chapter was adopted here and the final mixture was stirred overnight during the synthesis and the solid crystalline particles were recovered by filtration. The full synthesis method and characterization is outlined in chapter 3. The resulting zeolitic materials were designated as A-H_2O (grafted by the aqueous solution, 0.5 M) and A-OH (grafted by the ethanol solution, 0.5 M) and A'-H_2O (grafted by the water solution, 1.0 M) and A'-OH (grafted by the alcohol solution, 1.0 M).

For regeneration studies, cumene was used as the feed at WHSV = 2.0 h^{-1} to foul the catalysts at 500 °C and under nitrogen flowing at 5 ml/min. Spent catalysts were regenerated in the calcination ovens at 500 °C in air for 8 hours.

18.3 Results and Discussion

18.3.1 XRD Analysis

The XRD pattern for the room temperature synthesis of MCM-48 material had a main peak around 2.5-3.0 2θ (211) degrees with a suspected small shoulder peak around 3.0 2θ (220) degrees (figure 18.1). The pattern also showed a cluster of peaks between 4 and 6 2θ degrees characteristic of the MCM-48 material. This XRD pattern was similar to that of high quality MCM-48 which was obtained by Eimer *et al*.[89] which had a main peak around 2.5 2θ (211) degrees and a small shoulder peak around 3.0 2θ (220) degrees as shown in figure 18.2.

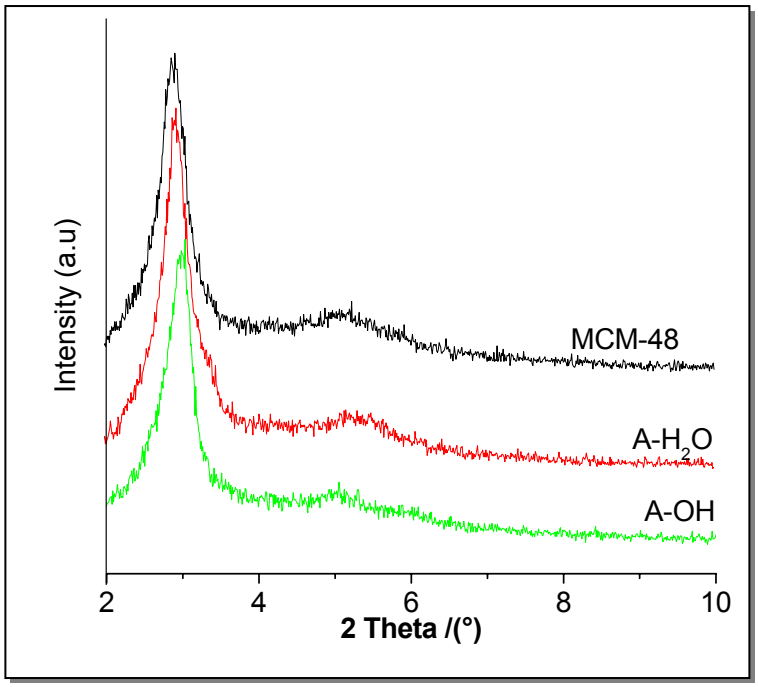

Figure 18.1: XRD patterns of MCM-48, A-H_2O and A-OH.

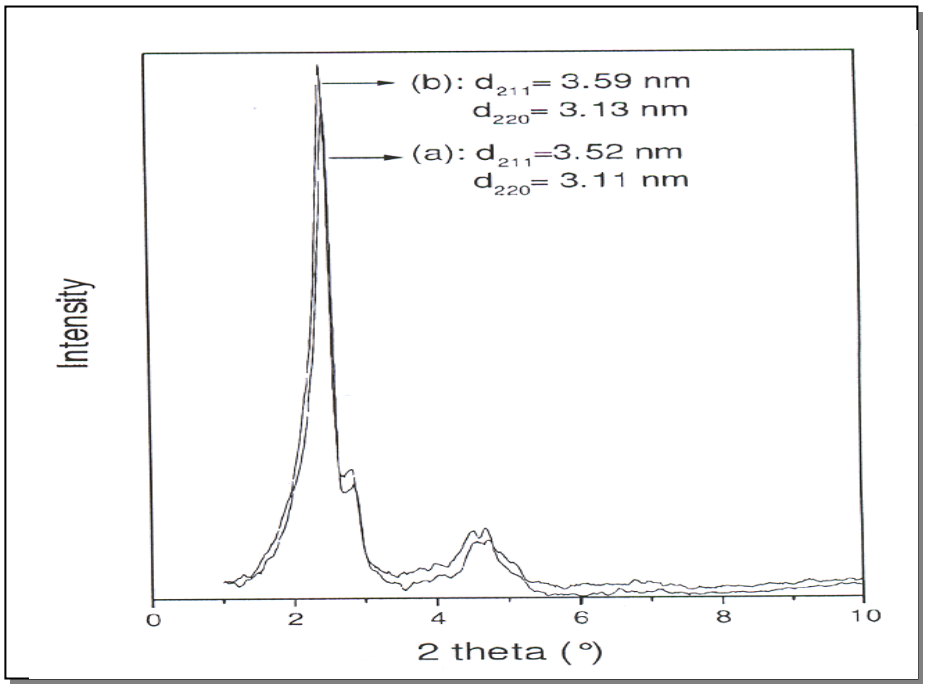

Figure 18.2: XRD pattern of MCM-48 obtained by G. Eimer et al[89].

Figure 18.1 showed that the MCM-48 characteristic structure was successfully synthesized at room temperature though the quality of the materials was not as good as those which were hydrothermally synthesized (figure 18.2). Unlike in the previous chapter, grafting Al atoms did not have any significant effects on the resulting Al-MCM-48 structure as shown in figure 18.1. This was due to the lesser concentrations of $Al(NO_3)_3$ in the grafting solutions this case.

18.3.2 Catalytic test reactions

It has been shown earlier that mesoporous materials are less acidic than microporous and large pore solid acid catalysts, and reports from the literature[23] stated that grafted mesoporous materials are even weaker in acidity compared to hydrothermally (as-synthesized) synthesized mesoporous materials; this was also shown in the previous chapter. Very low conversions were also earlier observed in the study on hydrothermally synthesized Al-MCM-41 materials. Thus, it was suggested that cumene (easily converted) was a good probe material for the characterization of mesoporous catalyst's Brönsted acidities.[91] In this case cumene and mesitylene were used to characterize grafted materials.

i) Cumene disproportionation

Cumene transformation on grafted materials at 300 °C showed reasonable initial conversions on both materials, 16 % on the A-H_2O and just above 20 % on the A-OH catalysts (figure 18.3). Comparatively, the A-OH catalyst showed higher conversions than the A-H_2O catalyst, this could be due to the nature of the active sites formed and these might have been brought about by the effect of the solvent used on the way in which grafting occurred on siliceous materials. On the contrary, using almost saturated solutions resulted in higher activities being observed with the water

grafting, this was highlighted in the previous chapter but in this case the opposite was observed.

In both cases, gradual deactivation was observed with time on stream and this was attributable to the blocking of the zeolitic pores through polymerization and carbonaceous material deposition. The observed conversions proved that these materials contained Brönsted sites which were responsible for molecular transformations.

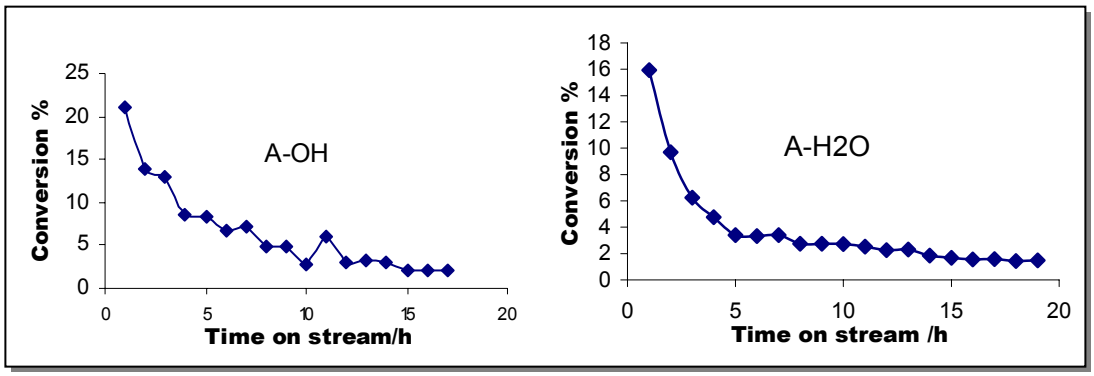

Figure 18.3: Cumene conversion (mol %) on Al-MCM-48 at 300 °C

The product stream (figure 18.4) of the reactions on both materials showed that the main reaction was not disproportionation (alkyl-transfer) as intended but dealkylation to benzene (BENZ) and alkanes/enes (DEALK). The ratio between these products was not 1:1 as should be expected. This was due to the fact that the dealkylation products (DEALK) were re-alkylating on cumene molecules. The re-alkylation reactions consumed both the dealkylation products and the starting material; this resulted in lower amounts of the dealkylation products and the formation of disproportionation products (DIALK, dialkylbenzenes). Conversion decreased gradually (figure 18.3) with time on stream showing a deactivation curve similar to the one shown by the uni-dimensional large pore catalyst (H-mordenite), i.e. there was a very sharp decline in activity in a short space of time which was characteristic of uni-dimensional microporous material with strong acid sites. The

expected behaviour was that of slowed deactivation characteristic of the tri-dimensional catalytic materials (LZY-82). The behaviour could mainly be attributed to rapid carbon formation by cracking products (DEALK). Benzene has shown earlier to also contribute significantly towards carbonaceous material deposition but with less acidic material like the MCM-48 the rapid carbon formation by benzene was possible but unlikely considering its inertness (stability).

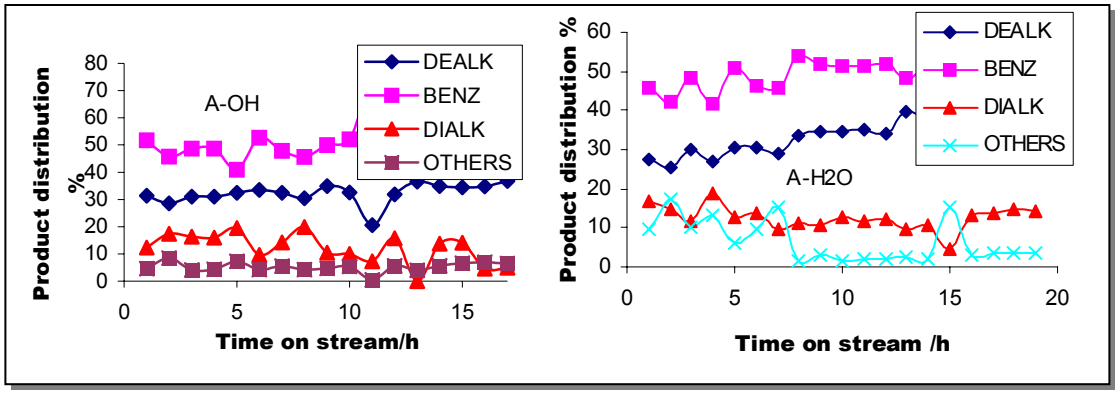

Figure 18.4: Cumene conversion (mol %) on Al-MCM-48 at 300 ° C, product distribution (DEALK = dealkylation products, BENZ = benzene and DIALK = dialkylbenzenes)

Transformation (since the main reaction was not disproportionation) of cumene increased with increase in temperature (500 °C) to almost 100 % conversions (figure 18.5). The A-H_2O catalyst showed a more rapid deactivation relative to the A-OH catalyst and this might be attributable to the strong sites on the A-H_2O since strong sites deactivate more rapidly;[59] or the higher number of Al atoms effectively grafted by the alcohol solution offered prolonged activities for A-OH materials.

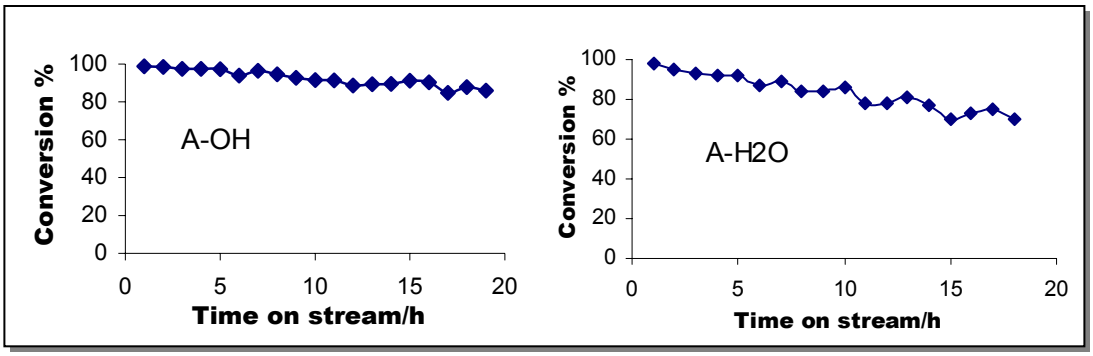

Figure 18.5: Cumene conversion (mol %) on Al-MCM-48 at 500 °C

The improved lifetimes at high temperatures showed that deactivation at low temperature was mainly due to molecular retention which was greatly inhibited at high temperatures where activity had been thermally enhanced. The product stream (figure 18.6) of the high temperature reactions (500 °C) showed benzenes (BENZ) and alkanes/alkenes (dealkylation products, DEALK) as the major products. The lesser amounts of dialkylbenzenes (DIALK) in the product stream at 500 °C compared to 300 °C supported the suggestion that at lower temperatures deactivation was mainly due to molecular retention of bulkier products since larger amounts of the bulky molecules were produced at lower temperatures, i.e. at high temperatures the bulkier molecules are cracked down to smaller molecules. Deactivation by pore blockage (large molecules involved) will indeed show higher rates of deactivation than deactivation by site poisoning (carbon deposition). The observations also suggested that disproportionation (via dealkylation/realkylation mechanism) was better favoured at low temperatures (300 °C) while higher temperatures strictly favoured dealkylation (cracking). Nevertheless, both A-H_2O and A-OH showed very similar catalytic behavior.

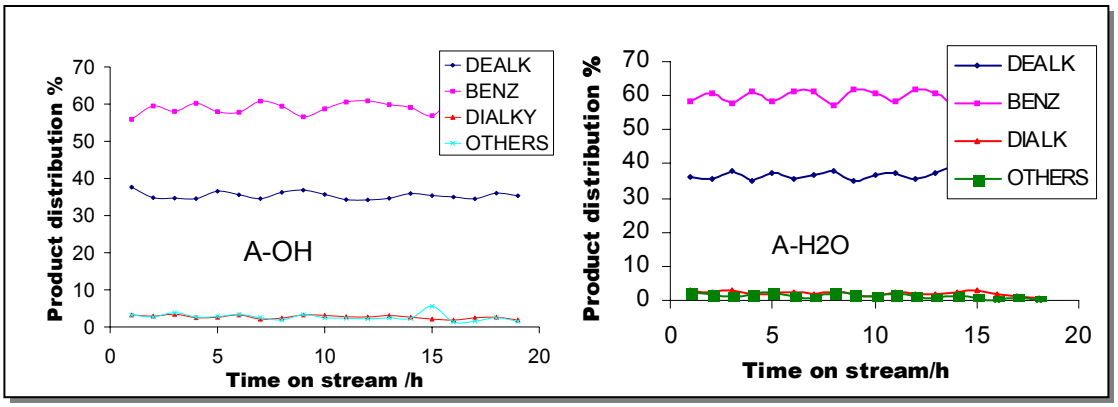

Figure 18.6: Cumene conversion (mol %) on Al-MCM-48 at 500 ° C, product distribution (DEALK = dealkylation products, BENZ = benzene and DIALK = dialkylbenzenes)

From these observations it can be concluded that these catalysts became selective as the temperature was increased, whereby dealkylation was greatly favoured over the desired disproportionation.

To ensure that these changes in conversions and the observed product distributions were due to the catalytic interactions, a run was carried out at 500 °C with cumene in the feed stream but without the catalyst in the reactor bed (blank run). For this run no conversion was observed and only cumene (starting material) was detected (figure 18.7) in the outlet stream.

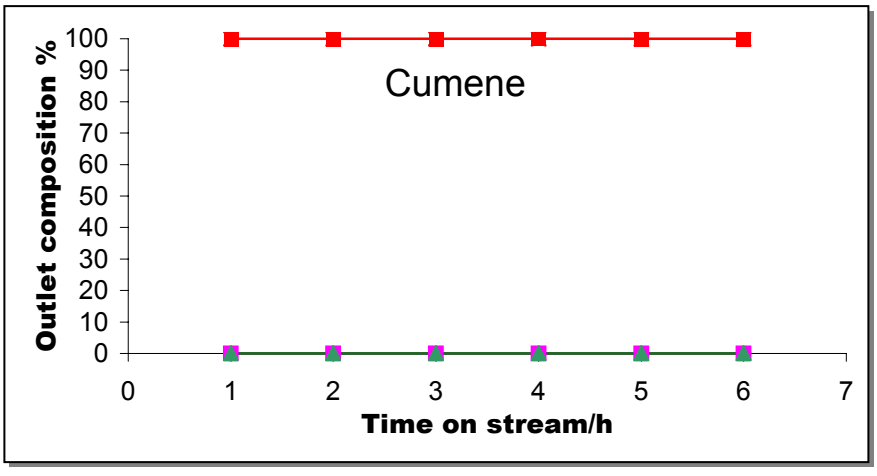

Figure 18.7: A blank run at 500 °C (mol %) with Cumene as the feed

An increase in the amount of Al atoms grafted on the MCM-48 surface by a factor of 2 on A-H_2O and A-OH (0.5M $Al(NO_3)_3$ solution) respectively resulted in double the conversion on the resulting A'-H_2O and a four fold increase on A'-OH (1.0M $Al(NO_3)_3$ solution) respectively (figure 18.8). The logical explanation was that of increased number of active sites with increase in the amount of Al in the grafting solutions. The observed deactivation rates did not give a clear indication of whether there was a change in active site strengths on increasing the amount of Al in the zeolites or not. The remarkable increase in conversions on A'-OH somehow suggested that Al atoms were more effectively grafted by the alcohol solution as also suggested by Ryoo *et al*.[90] or stronger sites were somehow created.

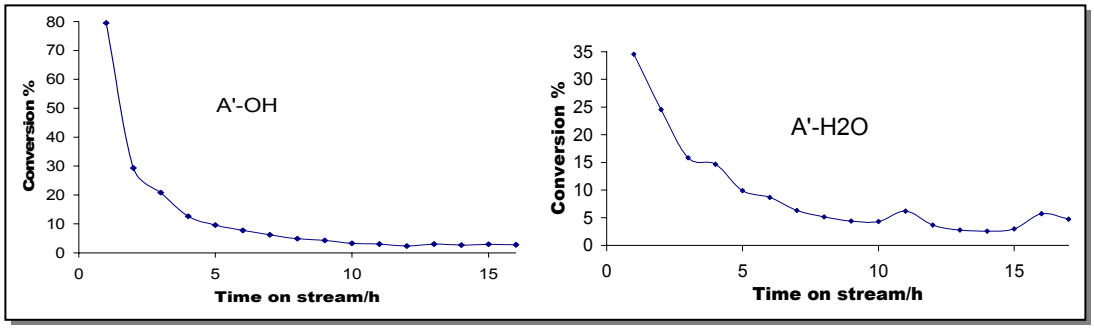

Figure 18.8: Cumene conversion (mol %) on Al-MCM-48 (1M loading) at 300 °C

The product stream of these reactions showed similar behaviour to that of low Al content catalysts (figure 18.9). The only observable difference was that of A'-OH material at the very early stages of the reaction where disproportionation (DIALK) products appeared after 2 hours of time on stream, suggesting that the observed four fold increase in conversion was mainly through dealkylation reactions and somehow supporting the creation of stronger sites.

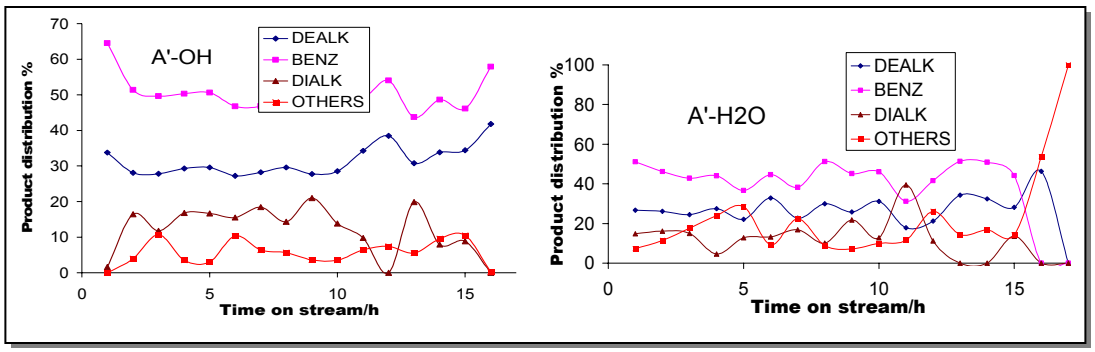

Figure 18.9: Cumene conversion (mol %) on Al-MCM-48 at 300 °C, product distribution (DEALK = dealkylation products, BENZ = benzene and DIALK = dialkylbenzenes)

An increase in the reaction temperature to 500 °C also resulted in almost 100 % conversions as observed on the 0.5M aluminium catalysts (A-H_2O and A-OH), but a closer look at the traces (figure 18.10) showed that the rapid deactivation was now on the A'-OH catalyst, further supporting that stronger sites were created there compared to A'-H_2O.

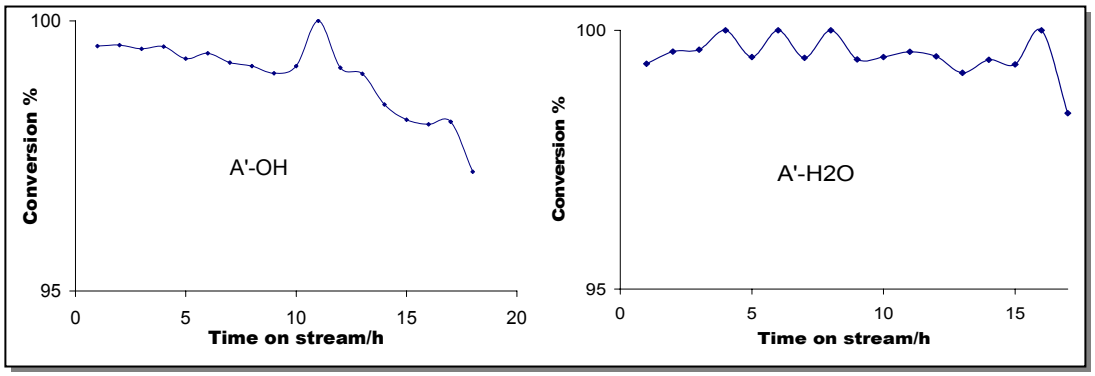

Figure 18.10: Cumene conversion (mol %) on Al-MCM-48 at 500 °C

The product stream on the other hand did not show any differences between the water and the alcohol catalytic samples or between the amounts of Al in the catalysts if one compares figure 18.6 and figure 18.11 and also the results of the previous chapter (figure 17.10). As shown earlier, the catalyst lifetime were also greatly enhanced by an increase in the reaction temperature.

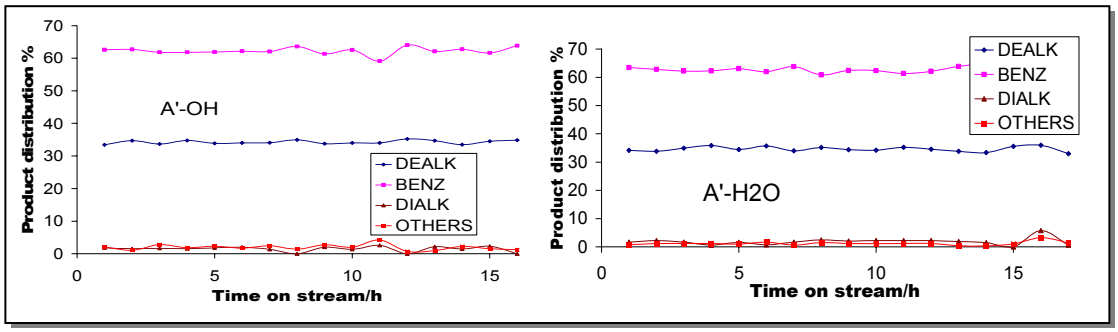

Figure 18.11: Cumene conversion (mol %) on Al-MCM-48 at 500 °C, product distribution: (DEALK = dealkylation, BENZ = benzene and DIALK = dialkylation)

It was then presumed on the basis of the observations that a further increase in the amounts of Al would result in better conversions especially at low reaction temperatures, where disproportionation reactions were observed.

ii) Mesitylene disproportionation

On the contrary, mesitylene disproportionation on the 0.5M Al loaded samples (A-H_2O and A-OH) showed that at low loadings the water sample contained stronger sites and this was shown by higher conversions on A-H_2O catalyst compared to A-OH catalyst (figure 18.12). A short induction period was observed on the A-H_2O and this reached a maximum of 20 % conversion before showing a rapid deactivation. This was further supplemented by the better lifetime shown by the A-OH catalyst confirming the existence of less acidic sites on the latter. This really seemed to be in direct contradiction to the observations made earlier on these grafted materials during cumene conversion. The explanation for this might be that, like in the case of catalytic enzyme reactions, different solvents used in grafting solutions produced catalytic sites with different abilities (characteristics) in pursuing and inducing certain catalytic routes. This might be resulting from the position (environment) in the framework structure where sites were created, the number of such sites in the environment and their strengths. This then led to the conclusion that different sites (or different catalysts) were created using different solvents in the grafting processes.

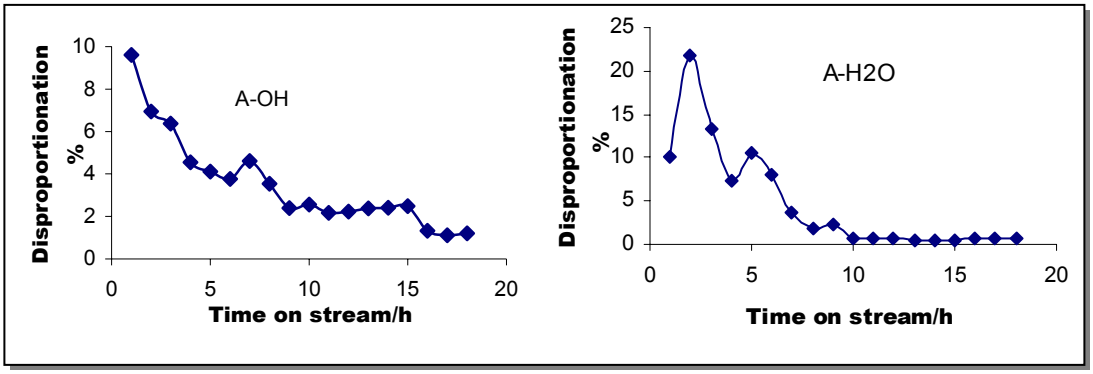

Figure 18.12: Mesitylene disproportionation (mol %) on Al-MCM-48 at 300 °C

The product stream on the other hand has shown a characteristic deficit in smaller molecules (xylene, figure 18.13). The deficit was mainly attributed to the active involvement of smaller molecules in carbonaceous material deposition which deactivated the catalyst. The product stream did not show secondary reaction products (toluene and benzene) further proving that these materials contained weaker sites, and since the ease of conversion increases with increase in number of alkyl groups on the ring and visa versa, the lesser the alkyl groups the more stubborn is the molecule.

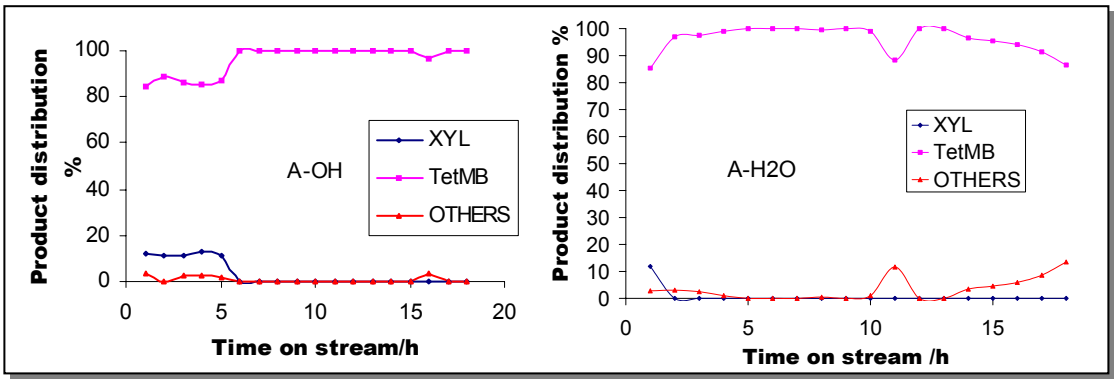

Figure 18.13: Mesitylene disproportionation (mol %) on Al-MCM-48 at 300 °C, product distribution, (XYL = xylene, TetMB = tetramethylbenzene)

Unlike the cumene reaction, mesitylene showed only alkyl-transfer (isomerization not considered) reactions (disproportionation) rather than the undesired dealkylations (cracking).

Figure 18.14 shows that higher reaction temperatures (500 °C) resulted in increased disproportionation reactions as expected and an even stronger deactivation on A-H_2O. In addition, there was some polymerization/cracking activity as shown by the disproportionation traces on A-H_2O.

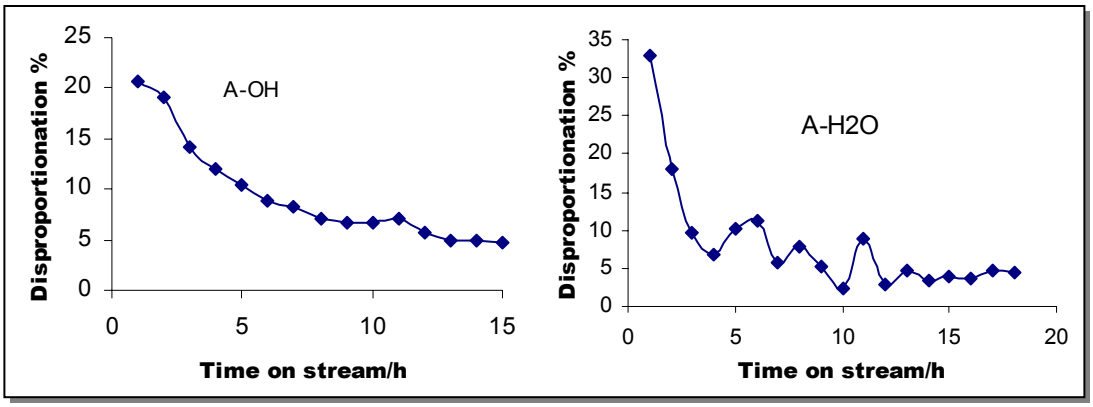

Figure 18.14: Mesitylene disproportionation (mol %) on Al-MCM-48 at 500 °C

The product distribution was not that different from that of low temperature reactions (fig 18.15), the observation on the A-H_2O confirmed polymerization/cracking activities. In addition to the observed xylene deficit the product stream of the A-H_2O catalyst showed that an increase in xylene concentration was always accompanied by a decrease in the bulky tetramethylbenzenes and visa versa. This means bulky products were mostly involved in polymerization which blocked the pores and allowed smaller molecules to diffuse and thus the observed decrease of bulky molecules and an increase in smaller ones in the product stream. At a particular instance cracking of the polymerized species occurred releasing bulky molecules in large amounts which over shadowed smaller molecules and this cycle continued over and over again.

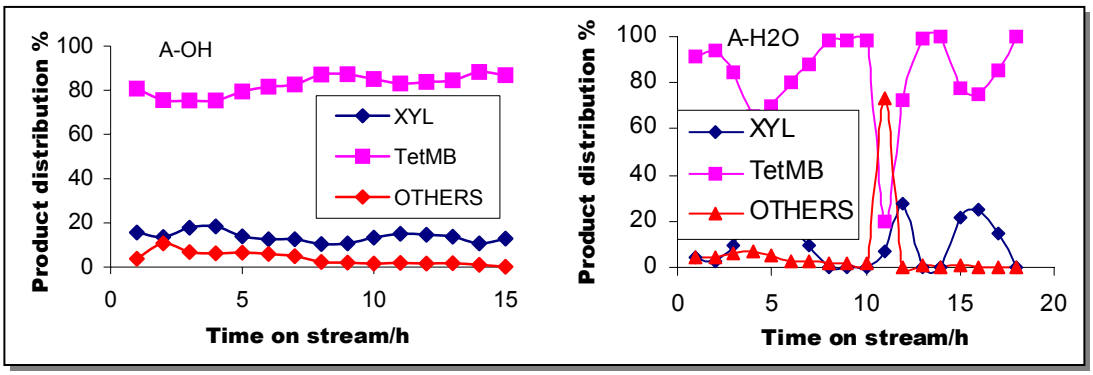

Figure 18.15: Mesitylene disproportionation (mol %) on Al-MCM-48 at 500 °C, product distribution (XYL = xylene and TetMB = tetramethylbenzene)

It was presumed that increasing the Al content (A'-H_2O and A'-OH) will show similar behaviour as shown by the cumene reactions earlier and thus the reactions on such catalysts were omitted.

18.3.3 Benzene-mesitylene transalkylation

Mesitylene disproportionation reactions studied on grafted zeolites earlier showed that water grafting gave better initial conversions but also rapid deactivations which were characteristic of strong sites, maximum conversion reached a high of about 20 %. With the introduction of benzene in the feed this conversion was obviously expected to decrease. Three compositions comprising of benzene and mesitylene were prepared for transalkylation studies on grafted catalysts and the intension was obviously to look at the effect of feed composition on transalkylation. These compositions were 16/83, 23/75 and 65/34 mol % benzene/mesitylene respectively. Determination of these compositions was carried out by running a blank (without catalyst) on the arbitrarily prepared mixtures and an example is shown in figure 18.16 below for the 65/34 mol % mixture at 500 °C.

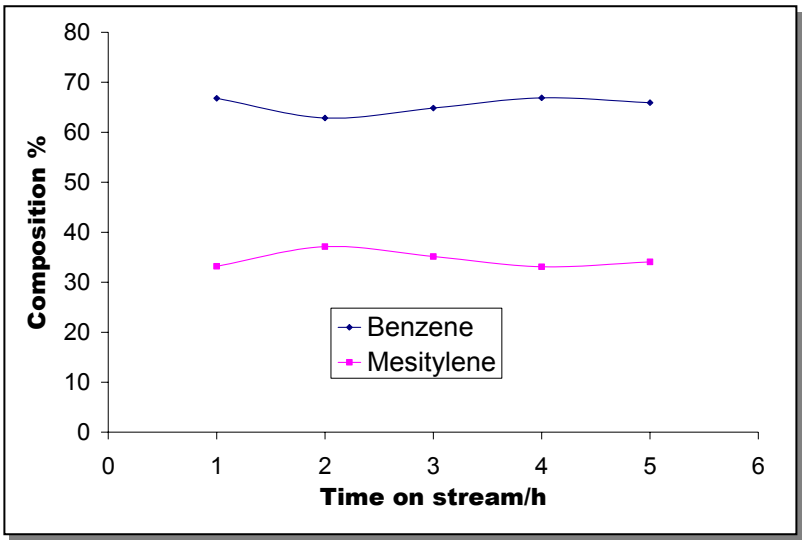

Figure 18.16: Blank run (mol %) of the benzene-mesitylene system

As it was observed before with binary mixtures that smaller molecules would diffuse out of the catalyst with much ease and concentrate themselves in the product stream while bulky molecules had difficulties in diffusing and were consequently retained in the catalyst; this created complications for conversion calculations and it led to the representation of conversion as the "extent of conversion" by looking at the total amounts of products diffusing out of the catalyst. An example of such representation is shown in figure 18.17 showing amounts of reactants and products diffusing out of the catalyst (outlet stream) against time on stream. Since isomerization of mesitylene was not considered the graph below shows trimethylbenzene (TMB) as one of the reactants.

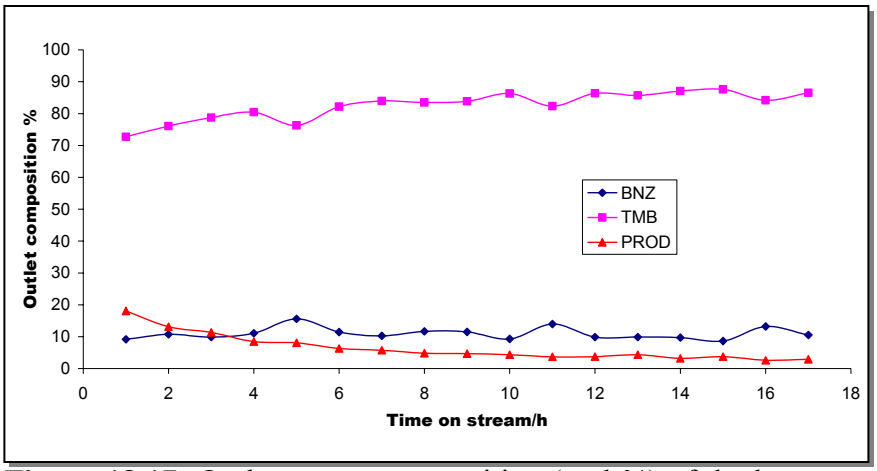

Figure 18.17: Outlet stream composition (mol %) of the benzene-mesitylene system at 500 °C, (BNZ = benzene, TMB = trimethylbenzene and PROD = products)

The total amounts of products diffusing out which represented the extent of conversion (alkyl-transfer) at 300 and 500 °C for grafted catalysts are shown in figure 18.18 for the three different compositions stated above. It was apparent from this figure that conversions around 20 % were achieved at high temperatures (500 °C) with the mixture that contained a lot of mesitylene (16/83 mol %).

Unlike the mesitylene disproportionation reactions, better conversions were shown by the alcohol grafted catalyst (A-OH) and this was almost inexplicable. Increasing the amount of benzene in the feed saw the expected decrease in the amount of products formed. This was due to the fact that transalkylating to benzene required stronger sites which were not much in these grafted catalysts.

The presence of benzene in the feed also diluted the mesitylene concentrations on the active sites meaning that fewer mesitylene molecules would be around for methyl groups of the adsorbed species and this is highlighted in figure 18.19; and/or there were fewer mesitylene molecules which saw active sites.

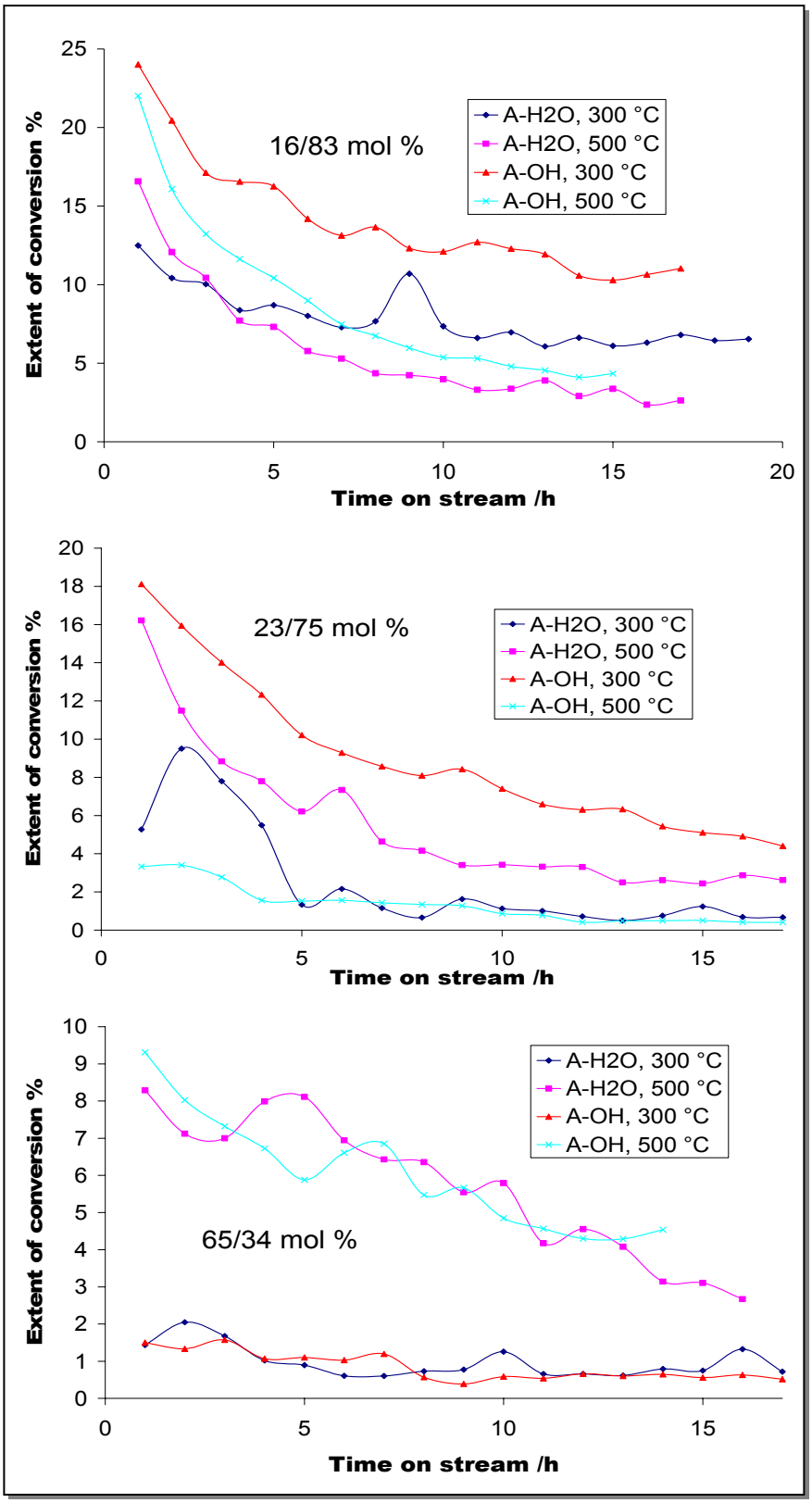

Figure 18.18: Benzene-mesitylene transalkylation (mol %) on grafted catalysts; the extent of conversion

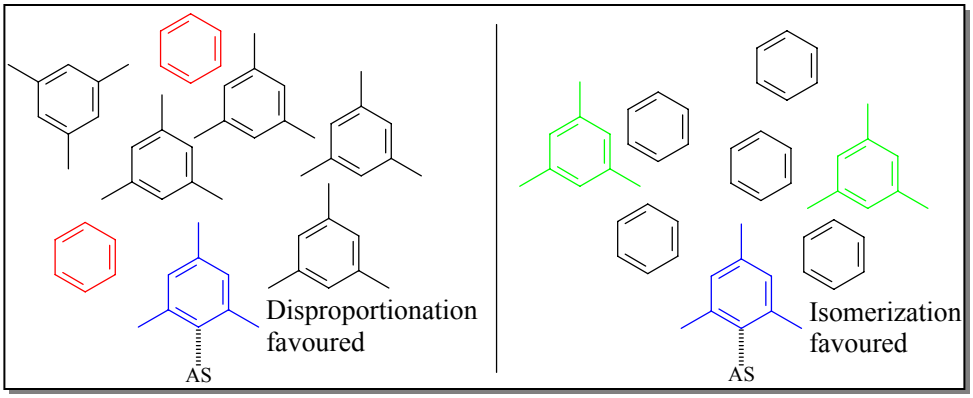

Figure 18.19: The effect of benzene concentrations in the binary feed, AS = active site

The above suggestion was greatly supplemented by the low conversions observed with the 65/34 mol % mixture where the two catalysts behaved more similarly and lowest conversions were observed.

The product stream on the other hand agreed well with the above suggestion that an increase in benzene amounts resulted in decreased activities (alkyl-transfer activities and not isomerization). Figure 18.20 shows that there was no/or very little of toluene (transalkylation product) formed at 300 °C for the three mixtures used, and so the catalyst lifetime would better be viewed by looking at the smallest disproportionation product, xylene in the outlet stream (transalkylation required stronger sites which deactivated first).

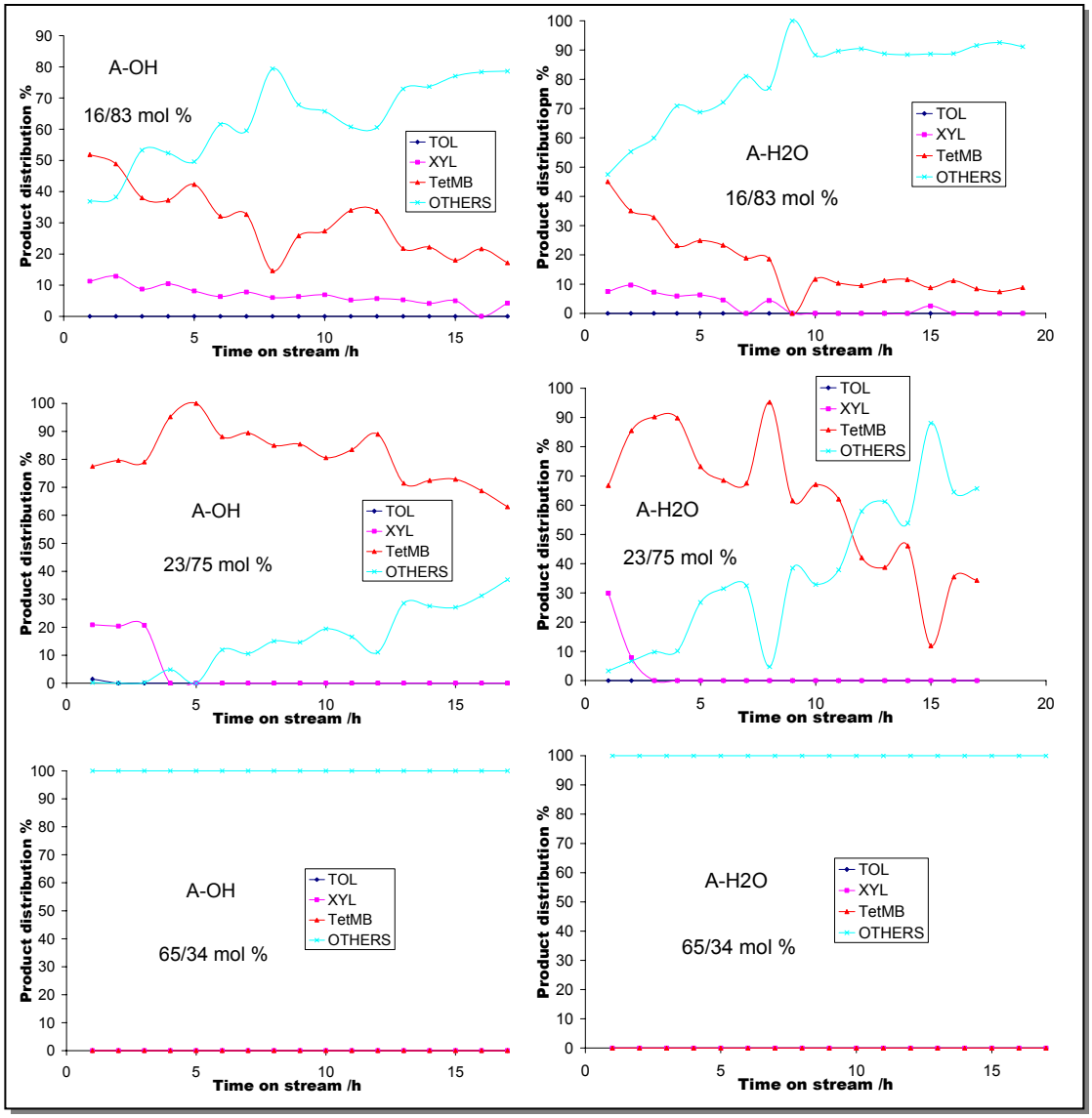

Figure 18.20: Benzene-mesitylene transalkylation (mol %) on grafted catalysts at 300 °C; Product distribution (TOL = toluene, XYL = xylene and TetMB = tetramethylbenzene)

By following xylene (XYL) traces it was apparent that activities decreased with increase in benzene amounts, the alcohol grafted catalyst showed an upper hand by having a lifetime of about 16-17 hours while the water grafted catalyst lasted for 9 hours for the 16/83 mol % mixture; with increase in benzene amount (23/75 mol %) lifetimes went down to 4 hours for both catalysts and the 65/43 mol % mixture saw the disappearance of disproportionation products. Since the isomerization activities

were not shown by the graphs, it looked like there was no activity at all while in fact there was monomolecular isomerization.

This is better understood by considering the previous figure 18.19 which depicts the effect of benzene dilution in the feed; i.e. the more benzene there is, the lesser the chances of having a mesitylene-mesitylene kind of intermediate and so the preferentially adsorbed mesitylene molecule would have only benzene to transalkylate to, but due to the weak sites and low temperatures this was not possible and hence the observations and isomerization reactions.

Poly-alkyl and bulky molecules were represented as 'OTHERS' and their amounts in the product stream decreased with the decrease in mesitylene amounts in the feed proving that they were mostly formed from the bulky mesitylene, and with the 65/34 mol % mixture they were major products mainly due to the fact that stronger sites were required to initiate alkyl-transfer reactions and thus transition states formed desorbed without forming products and thus the observed concentrations of bulky unknown products (not disproportionation products).

Increase in temperature to 500 °C resulted in the increase in activity and toluene was observed in the product stream (figure 18.21) meaning that transalkylation occurred. Increase in benzene amounts resulted in increased amounts of toluene formed as the chances of having benzene as the alkyl-acceptor increased and active sites were strong enough then to initiate transalkylation. To supplement the above, the product stream of the highest benzene composition mixture (65/34 mol %) showed higher amounts of xylene (XYL) compared to the bulkier tetramethylbenzenes (TetMB) which was opposite what was observed with other reaction mixtures and the observations during mesitylene disproportionation reactions on the same catalysts, suggesting that significant transalkylation reactions occurred forming toluene (TOL)

and xylene. This also supported the conclusion made in earlier chapters that high temperatures favoured transalkylation over disproportionation in binary mixtures.

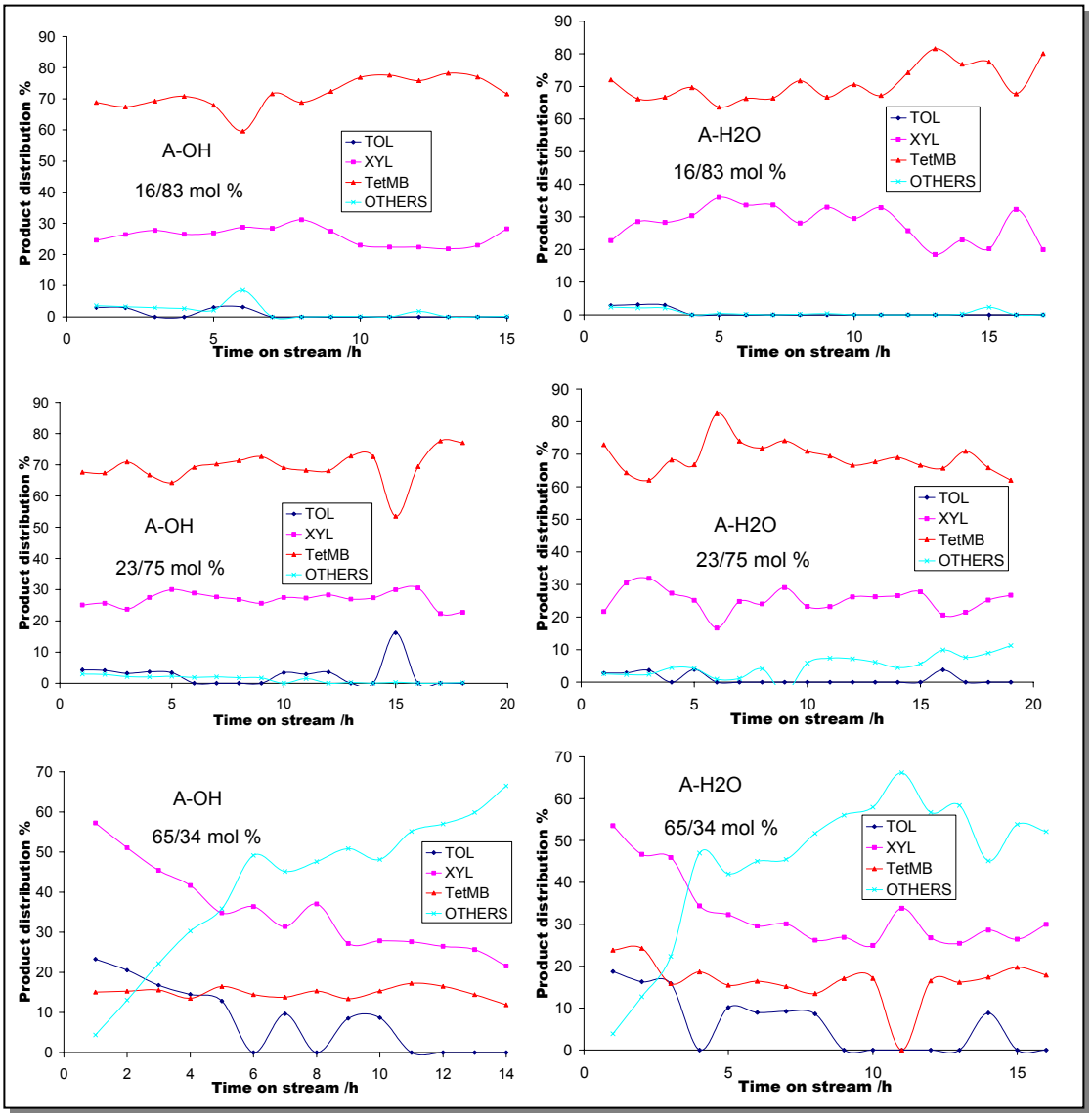

Figure 18.21: Benzene-mesitylene transalkylation (mol %) on grafted catalysts at 500 °C; Product distribution (TOL = toluene, XYL = xylene and TetMB = tetramethylbenzene)

These grafted materials though capable of alkyl-transfer reactions as shown above proved that they can be used to selectively isomerizes alkyl aromatics without

initiating alkyl-transfer reactions by either using less acidities (at low temperatures) or by feed dilution with an almost inert solvent like benzene.

18.3.4 Benzene-trimethylnaphthalene transalkylation

An arbitrary mixture between benzene and trimethylnaphthalene was prepared and a blank run composition determination showed that it was 81/18 mol % benzene-trimethylnaphthalene. Transalkylation was studied on the 0.5M grafted catalysts (A-H_2O and A-OH) at 300 and 500 °C. This reaction was similar to the benzene-mesitylene reaction and was expected to at least show some familiar behaviour with low conversions since there was a lot of benzene in the feed. The difference was that of the extra-ring conjugation on the naphthalene moiety and consequently the bulkier molecular sizes (scheme 18.1). The higher amounts of benzene in the feed was expected to direct the reaction route towards transalkylation but since the acid sites of the catalysts were not strong enough disproportionation was also expected to be a competing reaction.

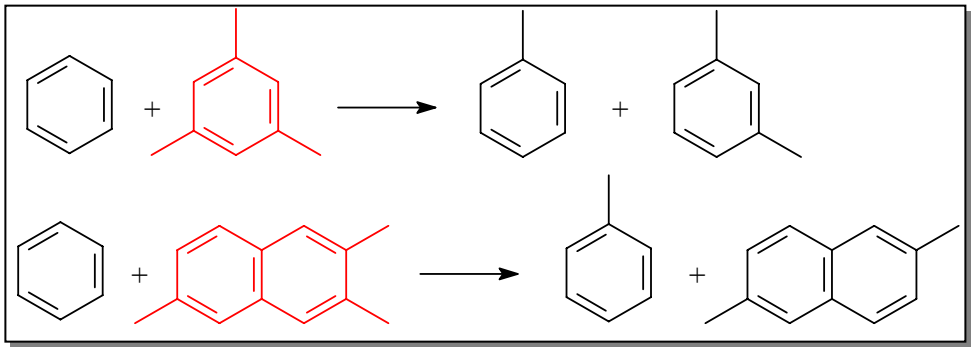

Scheme 18.1: Alkyl-transfer reactions

The method of representation used for the benzene-mesitylene system was also adopted here for same reasons as mentioned earlier. The extent of conversion for the

benzene-trimethylnaphthalene system at 300 and 500 °C on grafted catalysts is shown in figure 18.22. The observed reaction patterns showed similar behavior for these grafted materials at both temperatures except during the very first hour of the reaction on A-H_2O catalyst at 300 °C which showed higher activities than the rest.

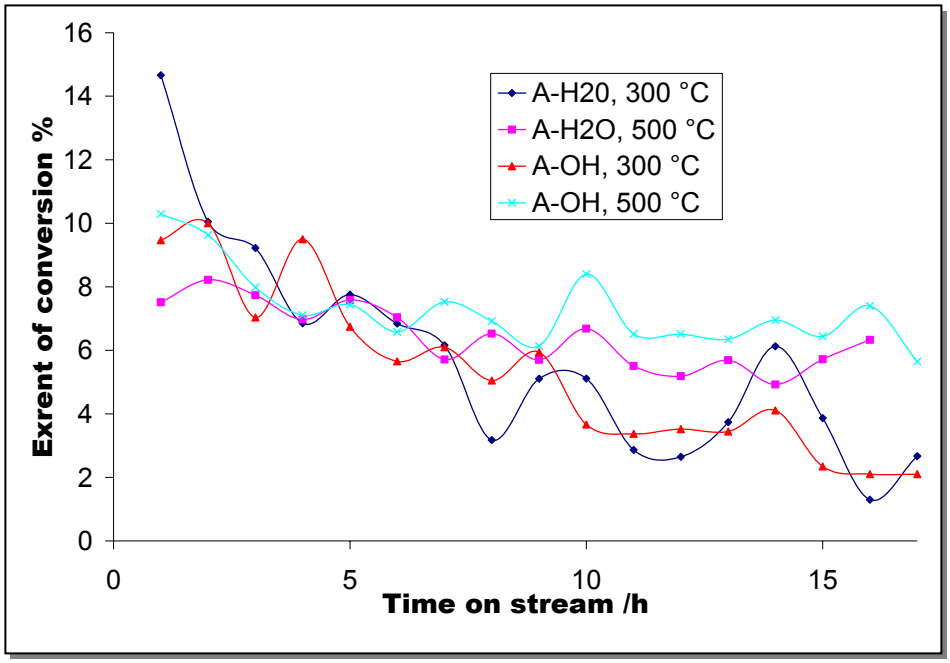

Figure 18.22: Benzene-trimethylnaphthalene transalkylation (mol %) on grafted catalysts; the extent of conversion

The overall low conversions observed here were obviously attributed to the low acidities of the catalysts but mainly to the low concentrations of the alkyl-aromatics in the feed (18 mol %). The conversions can be presumably improved by manipulating the feed composition as shown by the benzene-mesitylene systems studied earlier, though decreasing the amount of benzene in the feed will probably lead to higher methylnaphthalene disproportionation reactions.

The product distribution of this system at 300 °C on both catalysts is shown in figure 18.23, the figure shows that toluene (TOL) was not produced in the system at

these temperatures (similar to the benzene-mesitylene system) meaning that the observed high activities on A-H_2O were in fact due to trimethylnaphthalene disproportionation with the major product being dimethylnaphthalene (DMN) and tetramethylnaphthalene (OTHERS) and bulkier molecules. The existence of secondary disproportionation reactions was observed on the A-H_2O catalyst which had earlier showed higher conversions during the very early stages the reaction, thus the acid sites were strong enough to initiate secondary disproportionations but not transalkylation reaction. This also highlighted the inertness of benzene on these low acidic mesoporous materials, though it is known that alkyl-acceptance will favour the ring with alkyl-group/s already on it (alkylnaphthalene in this case). Anyway the behavior was similar for both grafted materials at 300 °C.

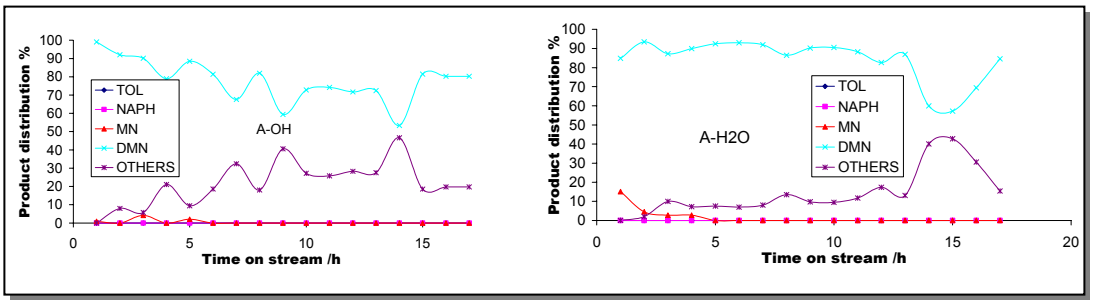

Figure 18.23: Benzene-trimethylnaphthalene transalkylation (mol %) on grafted catalysts at 300 °C; Product distribution (TOL = toluene, NAPH = naphthalene, MN = methylnaphthalene, DMN = dimethylnaphthalene)

The figure clearly showed that the main reaction was disproportionation and obviously the isomerization reactions which are not shown in this study.

Increase in reaction temperature to 500 °C led to the formation of toluene (TOL) but this was only for a short time, i.e. transalkylation occurred for at least 2 hours before strong sites deactivated (figure 18.24). Transalkylation occurred to a very less extent but disproportionation went to the extent of forming naphthalene (NAPH), and as

expected its formation did not last long since stronger sites were responsible for the reaction and deactivation is normally rapid for such sites. Dimethylnaphthalene (DMN) and methylnaphthalene (MN) were the major products in the product stream while the bulky others were not as much as during the reactions at 300 °C, this was attributed to the observed transalkylation reactions induced by high temperatures.

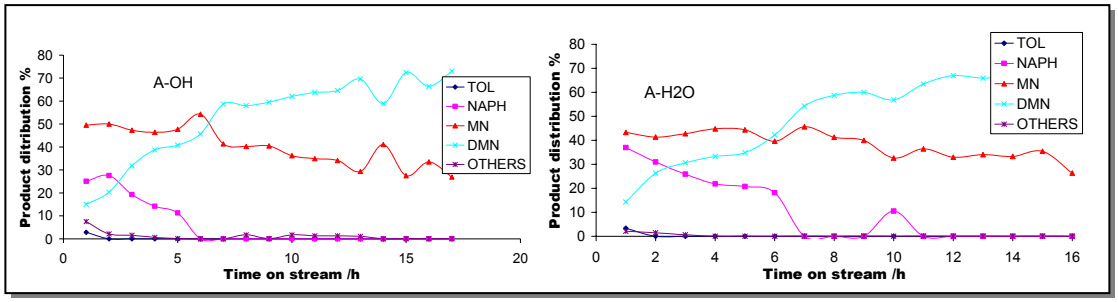

Figure 18.24: Benzene-trimethylnaphthalene transalkylation (mol %) on grafted catalysts at 500 °C; Product distribution (TOL = toluene, NAPH = naphthalene, MN = methylnaphthalene and DMN = dimethylnaphthalene)

The system has shown again that benzene can be used as an inert solvent for even bulkier molecules depending on the reaction conditions used. It was shown in chapter 16 that the ease of alkyl group removal from the alkylaromatic increases with 1) the increase in number of alkyl groups on the aromatic ring, 2) the chain length of the alky group and 3) the type of alkyl group and aromatic conjugation. The above implies that the bigger the alkylaromatic, whether it being due to the size/number of alkyl group/s or it being due to the higher aromatic conjugation will always result in increased ease of conversion. Consequently it can be assumed that these mesoporous catalytic materials are potential catalysts for even bulkier molecular transformations even though they have lesser acidic strengths; this will no more be a disadvantage in future developments.

18.4 Thermal stability of Al grafted MCM-48

During the catalyst thermal stability study of the grafted MCM-48 materials, the catalyst samples were fouled with cumene at 500 °C for 4 hours at WHSV = 2.0 h^{-1} for significant carbonaceous material deposition to occur. Spent catalysts (black in colour) were then regenerated at 500 °C in calcination ovens for 8 hours in air; and regenerated catalysts (white in colour) were fouled again under same reaction conditions. This was carried out on both A'-H_2O and A'-OH with 1M $Al(NO_3)_3$ loading. During these processes the conversions and selectivities were monitored. Figure 18.25 below shows the loss of activity with consecutive runs from over 90 % to below 70 %. The unsteady behaviour in the activity traces was mainly caused by dealumination (hydroxylation) of the framework structure of the catalyst instead of the possible incomplete regeneration. This was based on the fact that after the 7^{th} run A'-H_2O catalyst showed sings of significant dealumination which resulted in considerable loss in activity but this picked up with the following runs as interaction between extraframework aluminium (EFA) species and the remaining acid site intensified and enhanced the acidic strengths of the acid sites, i.e. the above was not going to be observed if the behaviour in figure 18.25 was due to incomplete regenerations (or varying degrees of regeneration) since regenerations were carried out at the same temperature and the same regeneration time. The traces also shows the varying degrees of the dealumination on both catalytic materials further supporting the fact that Al atoms were grafted differently on the framework structure with different solvents.

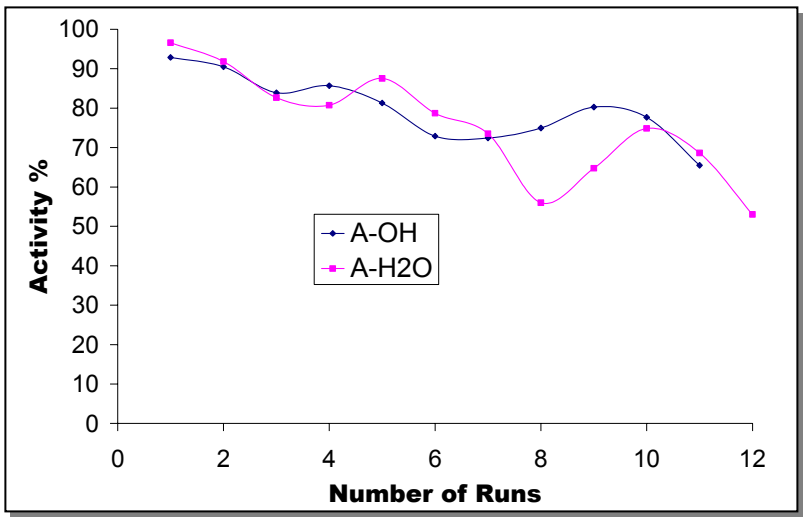

Figure 18.25: Activity of the catalyst (mol %) with number of regenerations

The effect of regeneration on the selectivity of the catalysts is shown in figure 18.26. The figure showed considerable effects being on the A'-H_2O catalyst where the amounts of benzene produced increased from around 60 % during the first run to above 70 % after 12th run, and there was a corresponding decrease in the amounts of dealkylation products (Dealk) and dialkylbenzenes (Others) which also supported that the acid site strengths increased with dealumination and this favoured dealkylation and increased deactivation rates (consumption of dealkylation products) due to increased strengths, decreased number of sites and high amounts of alkane/alkene produced by dealkylation. This was not that obvious with the A'-OH which showed steady dealumination.

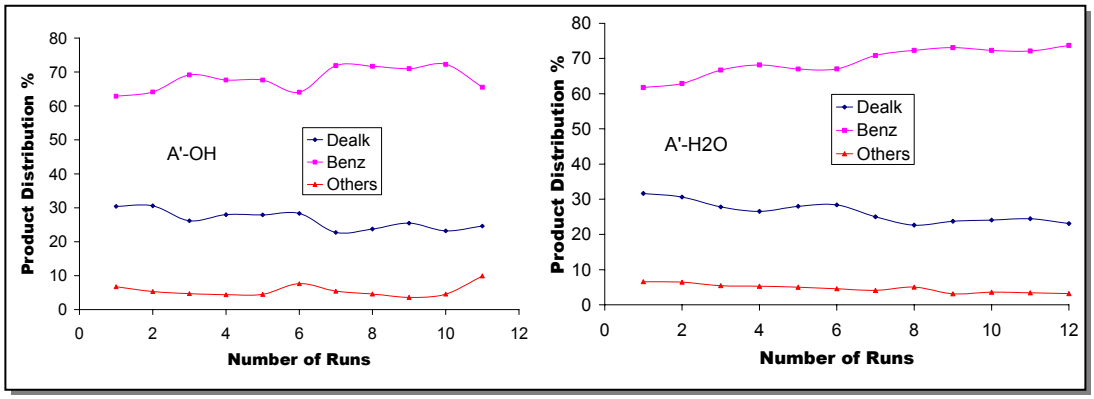

Figure 18.26: The effect of regeneration (mol %) on product stream selectivities

Catalyst regeneration was studied earlier on mordenite and LZY-82 and steady deactivations with increase in the number of runs was observed (figure 14.6) showing some remarkable resistance towards dealumination compared to grafted MCM-48's. The resistance was due to 1) the narrow pore sizes which made the framework structure robust and 2) these materials were as-synthesized and so Al atoms were not only on the 'extreme' surface but also in the bulk of the framework microporous materials; grafted catalysts were more susceptible to dealumination since Al was mainly on the 'extreme' surface of the framework structure and the materials are 'known to be' thermally unstable and their structure collapses at high temperatures. The only advantage with the more open structure of MCM-48 is that after dealumination, extraframework species have little effect on the selectivity of the catalysts unlike narrow pore size materials.

Looking at the catalyst behaviour on the first and the 11th runs, it could be noticed that indeed the loss of initial activity attributed to dealumination also resulted in increased rates of deactivation attributed to less number of active sites and their increased strengths. This is shown in figure 18.27 and similar behaviour for both catalysts was observed. The product streams of these reactions are shown in figure 18.28 and very slight differences were observed. This highly suggested that there was no structural collapse and that the framework was in fact thermally stable to some considerable extents.

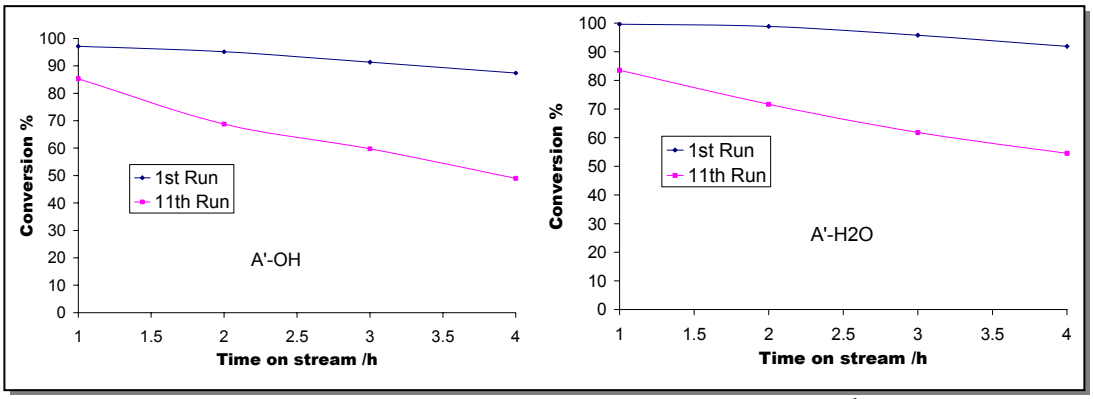

Figure 18.27: Catalytic behaviour (mol %) on the first and the 11th runs

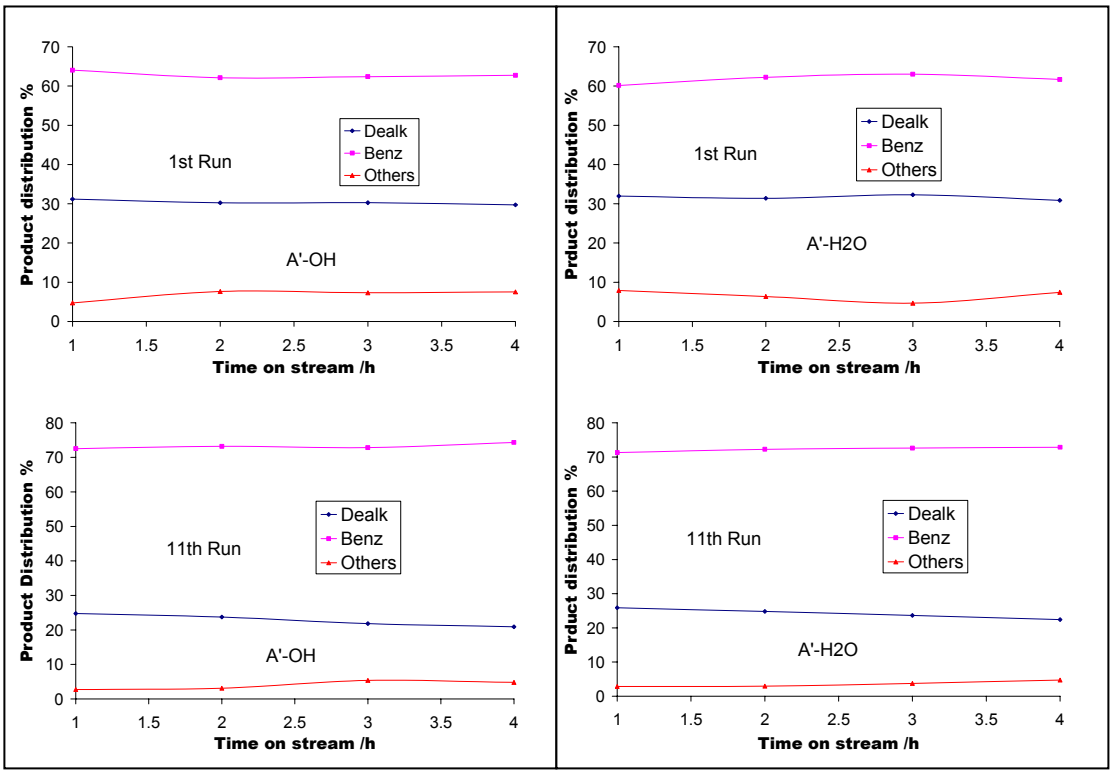

Figure 18.28: The effect of regeneration (mol %) on the product stream composition

18.5 Conclusion

Siliceous MCM-48 materials were again successfully synthesized by the room temperature synthesis method as confirmed by the X-RD analysis which gave similar results as found in the literature. Cumene and mesitylene disproportionation test reactions proved that Al atoms were grafted on the MCM-48 surfaces and Brönsted acid sites were created. Tentatively, water grafting produced stronger sites as compared to the alcohol grafting which proved to effectively graft Al atoms but lesser acidic site strengths were formed. It has been showed that acid site strengths of these materials can be controlled by varying the amount of Al grafted on the surfaces bearing in mind that high amounts of Al in the grafting solution is bound to lead to creation of considerable amounts of extra framework species.

Overall, low acidities were characteristic of these mesoporous materials as shown by alkyl-transfer reactions and better activities could only be achieved at elevated temperatures. Observed disproportionation reactions of the bulky alkylnaphthalene proved that these catalysts had large reaction spaces (pores and cavities) with minimum diffusion problems and most probably improved catalyst lifetime, this greatly showed that accessing active sites on mesoporous materials by bulky molecules was not a problem as compared to large pore materials. It has been showed also that, due to low acidities exhibited by these materials, binary mixtures involving benzene (inert on mesoporous materials) can be used to direct reaction routes of alkyl aromatic interconversions in the desired direction by manipulation of the feed composition and the use of suitable reaction conditions.

Grafted materials were thermally stable to a great extent as they showed behaviour similar to thermally stable large pore materials (mordenite and LZY-82). The disadvantage with grafting methods was that of lower acid site strengths otherwise the method would be most preferred if regenerations are of prime importance as it is normally the case when transforming very bulky molecules.

18.6 Acknowledgements

Most of the work in this chapter, except thermal stability studies, was carried out by Mr. Philemon P. Magampa in fulfillment of his Honors degree at Wits University. Thanks for the hard work and determination he displayed during the study.

19 CONCLUSION

During the conversion of hydrocarbons on solid acid catalysts (zeolites) deactivation, mainly by carbonaceous material deposition was severe on uni-dimensionally structured materials, and better lifetimes (resistance) were exhibited by *tri*-dimensionally structured materials. Since benzene and toluene were chosen as solvents and alkyl-acceptor molecules in binary systems (alkyl-transfer reactions), it has been shown that on strong catalysts (Brönsted acidity) they will almost always participate considerably in carbonaceous material deposition (catalyst deactivation). While benzene forms coke in large-pore and microporous catalytic materials, toluene is actually converted (disproportionation) to a great extent which in turn will almost probably interfere with the intended transalkylation reactions; on the hand toluene is a better alkyl-acceptor than benzene which is much more stable (inert) than the former.

Alkylbenzenes with the number of alkyl groups more than 1, or the chain length of more than 1 carbon and sterically stressed alkyl substituent cannot be used as alkyl-acceptors or as solvents in binary mixtures because they are easily converted on acidic zeolites even though they do not foul the catalyst as severely as toluene and benzene does; they also tend to transalkylate to bulkier molecules instead of themselves being alkyl-acceptors. In large pore (and microporous) materials with narrower pores and channels where access to active sites favours the smaller molecules, back-transalkylation in binary systems is favoured. Thus benzene and toluene are the favourable candidates as solvents and alkyl-acceptors in alkyl-transfer reactions of binary systems because of their stabilities.

In hydrocarbon conversions especially those involving binary systems, temperatures lower than 300 °C favoured the disproportionation reactions while higher temperatures favoured transalkylation. The feed composition in binary mixtures can also be manipulated to positively affect alkyl-transfer routes, transalkylation or disproportionation, while a 50/50 mixture would have the two routes competing with each other especially if the two molecules involved are of similar sizes. It was constantly observed during the study that transalkylation was preferentially favoured on the 3-D catalyst at high temperatures, most probably due to the more open structure allowing for the formation of the required intermediates.

It was suggested earlier that during transalkylation between aromatics, the alkyl containing aromatic somehow preferentially adsorbs on the active sites of the zeolite catalyst, and this was based on the observations from different transalkylation systems. The actual transalkylation mechanism was outlined in the Handbook of Heterogeneous Catalysis by Weitkamp *et al*.[92] (Eds), they showed that carbenium ions like those shown in figure 19.1 formed on contact with the active site, and that their stability was dependent on the inductive effects of their substituents.[93] Since alkyl groups have electron donating properties, the stability of the alkyl aromatic carbenium ions increases primarily with the number, type and the chain length of alkyl substituents.

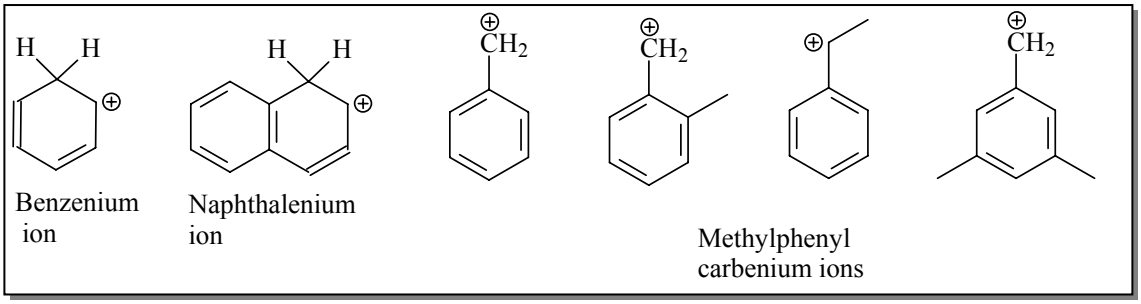

Figure 19.1: Carbenium ions[92]

Basically, the π-electron cloud of the hydrocarbon interacts with the catalyst's proton-donor groups, and the proton on the catalytic surface forms a bond to one carbon atom in the C=C moiety. The surface O-H bond (scheme 19.1) is broken, and

another oxygen atom of the surface forms a bond with the other carbon atom of the C=C moiety. Regardless of how this actually occurs, the result is a covalently bonded surface alkoxy species, which is regarded as an intermediate in these kinds of reactions.

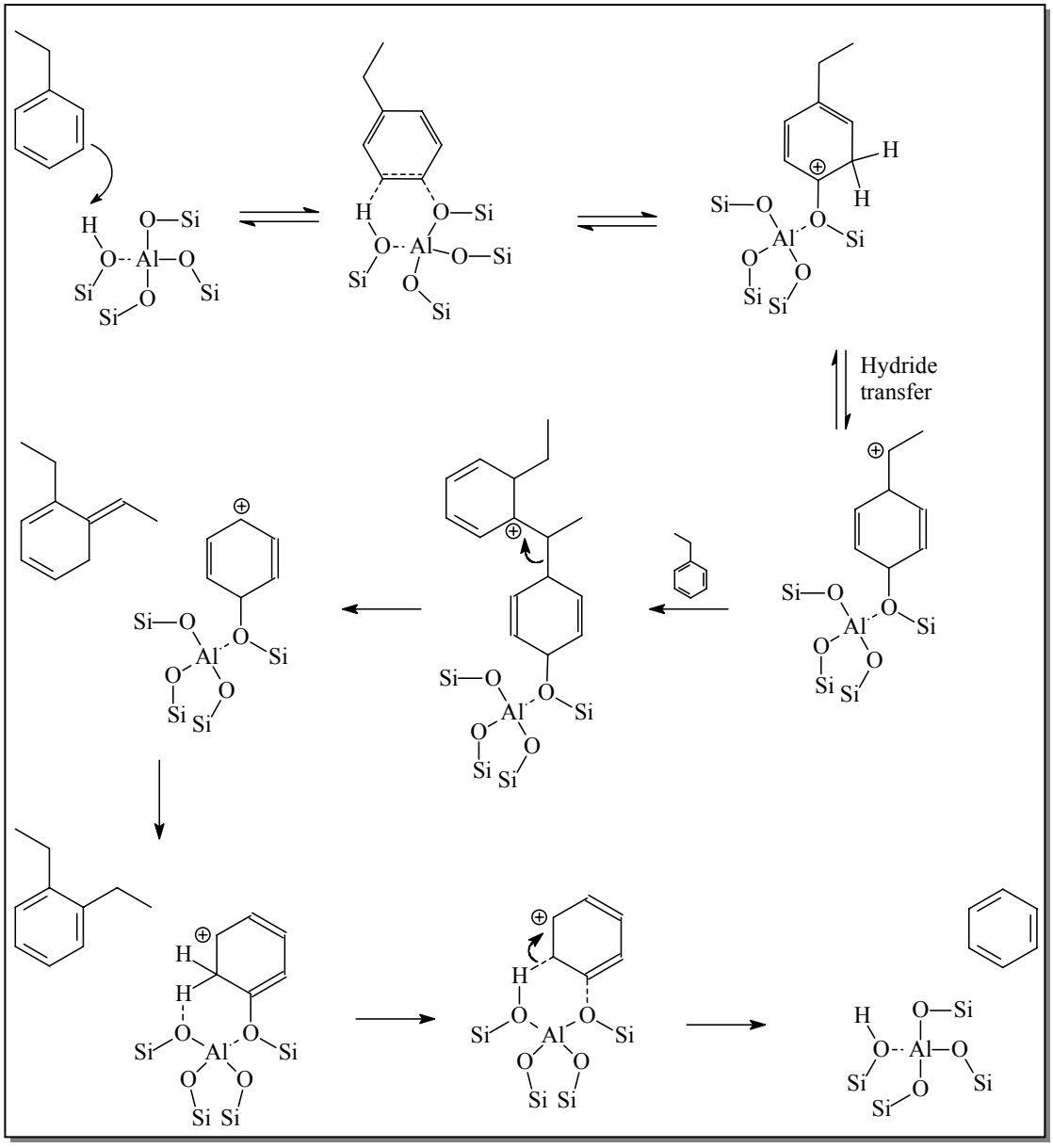

Scheme 19.1: Transalkylation mechanism; Modified from the Handbook of Heterogeneous Catalysis[92]

It was then realized from the scheme that for alkyl transfer to occur in binary systems, the alkyl containing species must actually be the one adsorbed on the active site so that an alkyl carbenium ion is formed; if the situation is the other way round, then some kind of a benzenium ion would form and an undesired intermediate would be formed (scheme 19.2).

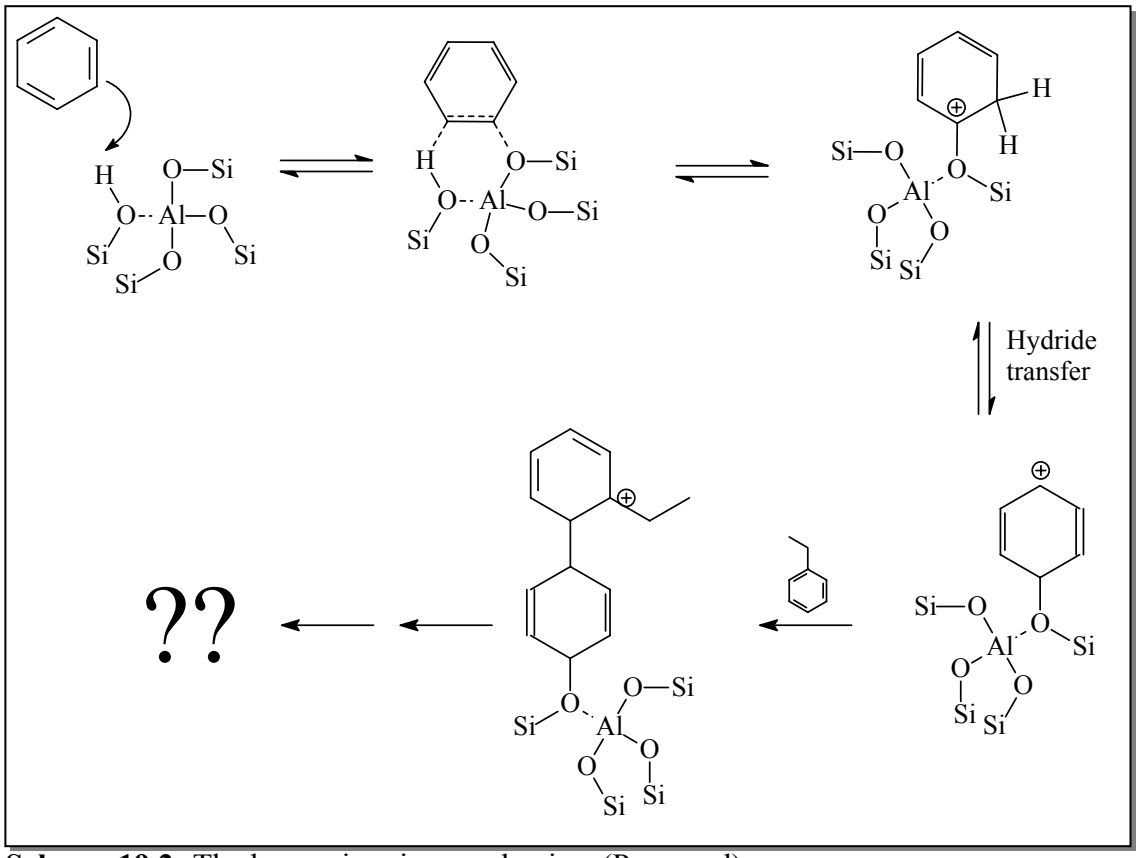

Scheme 19.2: The benzenium ion mechanism (Proposed)

The situation (scheme 19.2) was unlikely to result in transalkylation (alkyl transfer) reactions but was believed to be initial stages of carbon deposition (formation).

The above accounts for the observed lower conversions during toluene disproportionation as compared to ethylbenzene, mesitylene and xylene (stability of the carbenium ion); this in turn attributes the lower transalkylation activity observed between benzene and alkylnaphthalenes primarily to catalyst pore dimensions, i.e. limited access to the active sites of the bulky alkylnaphthalenes and restricted

transalkylation intermediate formation. The above restrictions on transalkylation can be alleviated by the use of acidic (Brönsted) mesoporous materials.

Studies on mesoporous materials (Al-MCM-41/48) have shown that the problem of accessing active sites by bulkier molecules can be solved and this in turn will favour transalkylation from bulkier molecules to smaller ones since the former preferentially adsorb on the active sites, thus back-transalkylation possibilities are minimized due to the stability of smaller molecules and the weaker acid sites of these materials. The disadvantage of using these materials is that they are less acidic (Brönsted), it is also difficult to create such sites by incorporation of Al in the framework (as-synthesized or post-alumination) and the structure of these materials is thermally unstable.

It has also been shown that these materials can be advantageously used to transalkylate from easily converted bulky molecules to more stable smaller molecules, and thus effectively inducing a one-way alkyl-transfer selectively without any secondary reactions of the products formed. Grafting Al atoms on siliceous mesoporous materials has shown that 1) the acid strength of these materials can be improved by either using different amounts of Al (presumably also from different sources) and different solvents and, 2) thermal stability of such material is significantly improved, making the regeneration at elevated temperatures possible without the risk of losing the structure. These mesoporous materials have proved anyway to be potential catalysts in alkyl-transfer reactions.

Overall, it has been apparent from the study that for effective alkyl-transfer reactions between alkylaromatics few conditions have to be satisfied:

1) For Disproportionation systems:

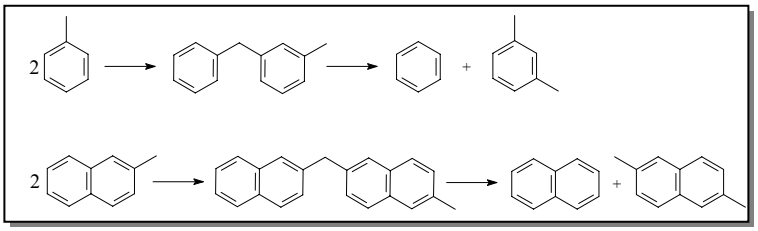

i) An acid catalyst will initialize the reaction (zeolites, for environmental reasons)

ii) In case of zeolites (or porous materials), the cavities and pore channels must be big enough to accommodated the required transition state especially for alkylaromatics with stubborn alkyl groups (bimolecular intermediate), otherwise the formation of the relevant di- or poly-alkylaromatic should be accommodated (dealkylation/realkylation mechanism)

iii) Reaction temperatures below 350 °C will selectively favour coupling of alkylaromatics and consequently disproportionation, very low temperatures will lead to rapid deactivations by molecular retention and might not favour formation of products

2) For Transalkylation systems:

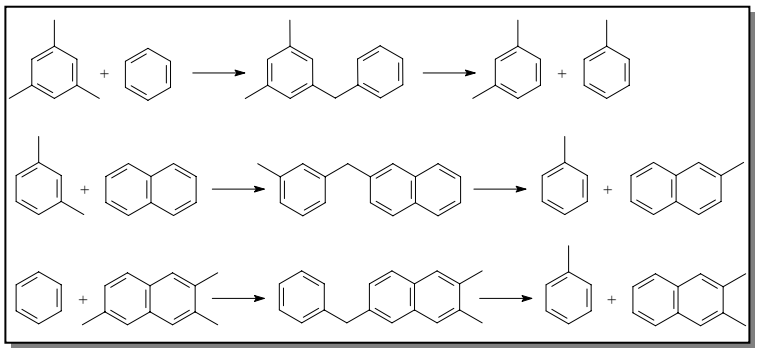

i) An acid catalyst will initialize the reaction (zeolites, for environmental reasons)

ii) In case of zeolites (or porous materials), the cavities and pore channels must be big enough to accommodated the required transition state especially for alkylaromatics with stubborn alkyl groups (bimolecular intermediate), otherwise the formation of the relevant di- or poly-alkylaromatic should be accommodated (dealkylation/realkylation mechanism)

iii) Reaction temperature higher than 300 °C will favour transalkylation but very high temperatures will lead to dealkylation and consequently rapid deactivations by carbonaceous material deposition

iv) The alkyl containing aromatic molecule (the one that has to loose the alkyl group) must have unlimited access to the active sites (steric constrains, catalyst choice) for effective transalkylation reactions

Similar conclusions made earlier by Mobil researchers[94] (Development corporation, central research laboratories) are outlined below:

1) The normal alkyl substituents are transferred without isomerization
2) The normal alkyl substituents of various lengths (C_2 – C_{10}) are all transferred from polyaromatic to monoaromatic rings at the same rate
3) The rate of transalkylation is strongly influenced by the degree of aromatic ring condensation of the donor; it increases with the size of the aromatic system
4) The rate of transalkylation is dependent in a surprising way on acid concentration and on chemical structures of the donor and acceptor.

These were made during the characterization of coal and coal liquids via transalkylation to simpler molecules that can be easily characterized. The extractable information from such analysis was that of the functional groups on coal particles/bulky molecules. The transalkylation in this case was initiated by liquid super-acids as catalysts like the sulfonic acid, $HF\text{-}BF_3$ and CF_3SO_3H.

20 REFERENCES

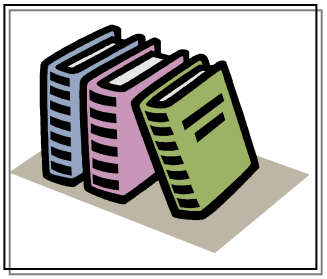

1. Tseng-Chang Tsai, Shang-Bin Liu, Ikai Wang., *Applied Catalysis A: General*, **181**, (1999), 355-398
2. Lubango L. M., *Dissertation submitted to the faculty of science, University of the Witwatersrand, Johannesburg, in fulfillment of the requirements for the degree of masters of Science*, December 2002
3. Kingzett's Chemical Encyclopedia [More details]
4. http://www.cancer.ie/information/carcinogen/#B
5. Kirk-Othmer, *Encyclopedia of Chemical Technology,* 3rd edition, ***vol 6,*** (1978), 224-376
6. Kirk-Othmer, *Encyclopedia of Chemical Technology,* 3rd edition, ***vol 22,*** (1978), 564-600
7. H. G. Karge, S. Ernst, M. Weihe, U. Weiβ, and J. Weitkamp, *Zeolites and related Microporous Materials: State of the Art 1994, Studies in Surface Science and Catalysis*, **84**, (1994), 1805-1812
8. http://www.iza-catalysis.org/EB_Disproportionation.html
9. J.M. Thomas, R.G. Bell and C.R.A. Catlow (Aut), G.Ertl, H. Knözinger, J. Weitkamp (Eds), *Handbook of Heterogeneous Catalysis*, **1**, (1997), 287-310
10. E.J.P. Feijen, J.A. Martens and P.A. Jacobs, (Aut), G.Ertl, H. Knözinger, J. Weitkamp (Eds), *Handbook of Heterogeneous Catalysis*, **1**, (1997), 311-323

11. J.A. Martens, W. Souverijns, W. Van Rhijn and P.A. Jacobs (Aut), G.Ertl, H. Knözinger, J. Weitkamp (Eds), *Handbook of Heterogeneous Catalysis*, **1**, (1997), 324-362
12. J.E. Naber, K.P. de Jong, W.H.J. Stork, H.P.C.E. Kuipers and M.F.M. Post (Aut), J. Weitkamp, H.G. Karge, H. Pfeifer and W. Holderich (Eds) *Zeolites and relate Microporous Materials: State of the Art 194. Studies in Surface Science and Catalysis,* **84**. © 1994 Elsevier Science B.V. All rights reserved. Pp 2197.
13. M. Crocker, R.H.M. Herold, M.H.W Sonnemans, C.A. Emeis, A.E Wilson and J.N. van der Molen, *J. Phys. Chem.* **97**, (1993) 432
14. A. van dijk, A.F. de Vries, J.A.R. van Veen, W.H.J Stork and P.M.M. Blauwhoff, *Catalysis Today,* **11**, (1991), 129
15. J.M. Thomas, R.G. Bell and C.R.A. Catlow, (Aut), G.Ertl, H. Knözinger, J. Weitkamp (Eds), *Handbook of Heterogeneous Catalysis*, 1, (1997), 286-364.
16. Eric G. Derouane (Ed.), *A Molecular View of Heterogeneous Catalysis*, Proceedings of the First Francqui Colloquium, 19 -20 February 1996, Brussels.
17. H.A. Benesi, *J. Catal*, **8**, (1967), 368-374
18. Patrick J O'Malley (Aut), J. Weitkamp, H.G. Karge, H. Pfeifer and W. Holderich (Eds) *Zeolites and relate Microporous Materials: State of the Art 194. Studies in Surface Science and Catalysis,* **84**. © 1994 Elsevier Science B.V. All rights reserved. Part C, Pp 2163-2170.
19. M.H.W Sonnemans, C. den Heijer and M. Croker. *J. Phys. Chem.* **97** (1993) 440
20. A.I. Biaglow, D.J. Parrillo, G.T. Kokotailo, R.J. Gorte, *J. Catal*, **148**, (1994), 213-223
21. G.J. Hutchings, A. Burrows, C. Rhodes, C.J. Kiely and R. McClung, *J. Chem. Soc. Faraday. Trans,* **93**, (1997), 3593
22. Peng Wu, Takayuki Komatsu and Tatsuaki Yashima, *J. Chem. Soc, Faraday Trans,* **92**, (1996) 861-869

23. L.Y. Chen, Z Ping, G.K. Chuah, S Jaenicke, G. Simon, *Microporous and Mesoporous Materials,* **27**, (1999), 231-242
24. Kondam Madhusudan Reddy and Chunshan Song, *Catalysis letters*, **36**, (1996), 103-109
25. Zhaohua Luan, Heyong He, Wuzong Zhou, Chi-Feng Cheng and Jacek Klinowski, *J. Chem. Soc. Faraday. Trans,* **91**, (1995), 2955-2959
26. Xiaoyin Chen, Limin Huang, Guozhong Ding and Quanzhi Li, *Catalysis Letters*, **44**, (1999), 123-128
27. A. Corma, V. Fornés, M.T. Navarro, J. Pérez-Pariente, *J. Catal,* **148**, (1994), 569-574
28. M.L. Occelli, S. Biz, A. Auroux, G.J. Ray, *Microporous and Mesoporous Materials*, **26,** (1998), 193-213
29. M. Ziolek, I Nowak, *Catalysis Letters*, **45**, (1997), 259-265
30. J.S. Beck and W.O. Haag, (Aut), G. Ertl, H. Knözinger, J. Weitkamp (Eds), *Handbook of Heterogeneous Catalysis*, **5**, (1997), 2123-2135
31. K. Tanabe, M. Misono, Y. Ono, H. Hattori, *Studies in Surface Science and Catalysis*, **51**, (1989), 160-247
32. Kutz W.M and Corson B.B, *J. Amer. Chem. Soc,* **67**, (1945), 1312
33. Z. Popova, M. Yankov, L. Dimitrov (Aut), J. Weitkamp, H.G. Karge, H. Pfeifer and W. Holderich (Eds) *Zeolites and relate Microporous Materials: State of the Art 194. Studies in Surface Science and Catalysis,* **84**. © 1994 Elsevier Science B.V. All rights reserved. Pp 1829-1835
34. D. Fraenkel, M. Zhirinovsky, B. Utah, M. Levy, *J. Catal,* **101**, (1986), 273
35. T. Matsuda, K. Yigo, Y. Mogi, E. Kikuchi, C*hemistry letters*, (1990), 1085-1088
36. A.S. Loktev, P.S. Chekriy, (Aut), J. Weitkamp, H.G. Karge, H. Pfeifer and W. Holderich (Eds) *Zeolites and relate Microporous Materials: State of the Art 194. Studies in Surface Science and Catalysis,* **84**. © 1994 Elsevier Science B.V. All rights reserved. Pp 1845-1851
37. T. Matsuzaki, T. Hanaoka, Y. Kubota, X. Tu, M. Matsumoto, (Aut), J. Weitkamp, H.G. Karge, H. Pfeifer and W. Holderich (Eds) *Zeolites and*

relate Microporous Materials: State of the Art 194. Studies in Surface Science and Catalysis, **84**. © 1994 Elsevier Science B.V. All rights reserved. Pp 1837-1844

38. J.A. Horsley, J.D. Fellmann, E.G. Derouane, C.M. Freeman, *J. Catal,* **147**, (1994) 231-240
39. J.S. Beck and W.O. Haag (Aut), G.Ertl, H. Knözinger, J. Weitkamp (Eds), *Handbook of Heterogeneous Catalysis*, **5**, (1997), 2136-2139
40. P. Magnoux, C. Canaff, F. Machado, M. Guisnet, *J. Catal*, **134**, (1992) 286-289
41. M.A. Lanewala and A.P. Bolton, *Journal of Organic Chemistry*, **34**, (1969), 3107
42. Sigmund M. Csicsery and Donald A. Hickson, *J. Catal*, **19**, (1970), 386-393
43. L.B. Young, S.A. Butter and W.M. Kaeding, *J. Catal*, **76**, (1982), 418-432
44. Ikai Wang, Tseng-Chang Tsai, and Sheng-Tai Huang, *Ind. Eng. Chem, Res,* **29**, (1990), 2005-2012
45. G.V. Bhaskar, D.D. Do, *Ind. Eng. Chem. Res,* **29**, (1990), 355-361
46. H.G. Karge, Z. Sarbak, K. Hatuda, J. Weitkamp and P.A. Jacobs, *J. Catal.,* **82**, (1983), 236-239
47. Ajit R. Pradhan, Tien-Sung Lin, Wen-Hua Chen, Sung-Jeng Jong, Jin-Fu Wu, Kuei-Jung Chao, Shang-Bin Liu, *J. Catal*, **184**, (1999), 29-38
48. Sabine Melson and Ferdi Schiith, *J. Catal*, **170**, (1997), 46-53
49. Z. Popova, M. Yankov, L. Dimitrov, I. Chervenkov, *Reaction Kinetics, Catalysis Letters*, **52**, (1994), 1
50. Sigmund M. Csicsery, *J, Catal*, **23**, (1971), 124-130
51. L. Forni, G. Cremona, F. Missineo, G Bellussi, C. Perego, G. Pazzuconi, *Applied Catalysis A: General*, **121**, (1995), 261-272
52. Tseng-Chang Tsai, Wen-Hua Chen, Shang-Bin Liu, Cheng-Hsien Tsai, Ikai Wang, *Catalysis Today*, **73**, (2002), 39-47

53. Katsutoshi Nakajima, Shogo Tawada, Yoshihiro Sugi, Yoshihiro Kubota, Taka-aki Hanaoka, Takehiko Matsuzaki, Kimio Kunimori, *Chemistry Letters*, iss 3, (1999), 215-216
54. T. Komatsu, Y. Araki, S. Namba, T. Yashima, (Aut), J. Weitkamp, H.G. Karge, H. Pfeifer and W. Holderich (Eds) *Zeolites and relate Microporous Materials: State of the Art 194. Studies in Surface Science and Catalysis,* **84**. © 1994 Elsevier Science B.V. All rights reserved. Pp 1821-1828
55. D.E. Walsh, L.D. Rollmann, *J. Catal*, **56**, (1979), 195-197
56. J.P. Lange, A. Gutsze, H.G. Karge, *J. Catal*, **114**, (1988), 136-143
57. P. Gallezot, C. Leclercq, M. Guisnet, P. Magnoux, *J. Catal*, **114**, (1988), 100-111
58. D.E. Walsh, L.D. Rollmann, *J. Catal*, **49**, (1977), 369-375
59. P. Magnoux, P. Cartraud, S. Mignard and M. Guisnet, *J. Catal*, **106**, (1987) 242-250
60. D. Eisenbach and E. Gallei, *J. Catal*, **56**, (1979) 377-389
61. Liang-Yuan Fang, Shang-Bin Liu and Ikai Wang, *J. Catal*, **185**, (1999), 33-42
62. G. Colón, I. Ferino, E. Rombi, E. Selli, L. Forni, P. Magnoux, M. Guisnet, *Applied Catalysis A: General*, **168**, (1998), 81-92
63. Sung-Jeng Jong, Ajit R. Pradhan, Jin-fu Wu, Tseng-Chang Tsai, Shang-Bin Liu, *J. Catal*, **174**, (1998), 210-218
64. K. Schumacher, P.I. Ravikovitch, A. DuChesne, A.V. Niemark, and K.K. Unger, *Langmuir,* **16**, (2000), 4648-4654
65. D. Cardoso, N. D. Velasco, M. da, S. Machado, *Brazilian Journal of Chemical Engeneering,* **15**, (1998), 225-230
66. http://www.iza-catalysis.org/EB_Disproportionation.html
67. A. M. Camiloti, S. L. John, N.D. Velasco, L. F. Moura, D. Cardoso, *Appl. Catal. A:Gen,* **182**, (1999), 107-113
68. N. Arsenova-Hartel, H. Bludau, R. Schumacher, W.O Haag, H.G Karge, E. Brunner, U. Wild, *Journal of Catalysis,* **151**, (2000), 326-331

69. Nigel P. Rhodes and Robert Rudham, *J. Chem. Soc. Far. Trans*. **89**, (1993), 2551-2557
70. W.W. Kaeding, C. Chu, L.B. Young and S.A Butter, *J. Catal,* **69**, (1986), 327-334
71. Jagannath Das, Yajnavalkya S. Bhat and Anand B. Haalgeri, *Catal. Lett*, **23**, (1994), 161-168
72. Don S. Santilli, *J, Catal*, **99**, (1986), 327-334
73. Yusheng Xiong, Paul G. Rodewald and Clarence D. Cheng, *J. Am. Chem. Soc*, **117**, (1995), 9427-9431
74. S. Morin, N.S. Gnep, and M. Guisnet, *J. Catal*, **159**, (1996), 296-3043
75. F. Moreau, N.S. Gnep, S. Lacombe, E. Merlene, M. Guisnet, *Appl. Catal. A: Gen,* **230**, (2002), 253-262
76. Oscar A. Anunziata and Liliana B. Pierella, *Catal Lett*, **44**, (1997), 259-263
77. X. H. Ren, M. Bertmer, S. Stapf, D.E. Demco, B. Blümich, C. Kern, A. Jess, *Appl. Catal., A: Gen.,* **228,** (2002), 39-52
78. P. Magnoux, H. S. Cerqueira, M. Guisnet, *Appl. Catal., A: Gen,* **235** (2002), 93-99
79. K. Moljord, P. Magnoux, M. Guisnet, Catal. Lett. **28**, (1994), 53
80. M.Guisnet, *J. Mol. Catal. A: Chem.,* **182-183**, (2002), 367-382
81. Yuichi Murakami, Takeshi Kobayashi, Tadashi Hattori, Moriyoshi Masuda, *Ind. and Eng. Chem: Fund,* **7**, (1968), 599-605
82. M.V. Juskelis, T.P. Slanga, T.G. Roberie, A.W. Peters, *J. Catal*, **138**, (1992), 391-394
83. http://www.seas.upenn.edu/~oferi/GCaminetrapping.htm
84. R.J. Gorte, *Catalysis Letters*, **62**, (1999), 1-13
85. Y. S. Hsu, T. Y. Lee and H. C. Hu, *Industrial and engineering chemical research*, **27**, (1988) 942-947
86. Karl-H. Röbschlager and Erhard G. Christoffel, *Ind. Eng. Chem. Prod. Res. Dev*, 18, no 4, (1979), 347 – 352

87. L. D. Fernandes, J. L. F. Monteiro, E. F. Sousa-Aguiar, A. Martinez and A. Corma, Journal of Catalysis, **177**, (1998), 363 – 377

88. Leon M. Polinski, Michael J. Baird, *Ind. Eng. Chem. Prod. Res. Dev*, **24**, (1985), 540 – 544

89. G.A. Eimer, L.B. Pierella, G.A. Monti, nad O.A. Anunziata, *Catl. Lett,* **78**, (2002), nos. 1-4, 65-75

90. Ryong Ryoo, Shinae Jun, Ji Man Kim and Mi Jeong kim, *Chem. Commun,* (1997), 2225-2226

91. Tseng-Chang Tsai, Chin-Lan Ay and Ikai Wang, *Applied Catalysis*, **77**, (1991), 199-207

92. D.S. Santilli and B.C. Gates (Aut), G.Ertl, H. Knözinger, J. Weitkamp (Eds), *Handbook of Heterogeneous Catalysis*, **3**, (1997), 1123-1136

93. J.A. Martens and P.A. Jacobs (Aut), G.Ertl, H. Knözinger, J. Weitkamp (Eds), *Handbook of Heterogeneous Catalysis*, **3**, (1997), 1137-1148

94. Malvina Farcusiu, *Symposium on Chemistry of Coal Liquefaction and Catalysis*, Sponsored by Hokkaido University, March 17-20, 1985, at Hokkaido University (Hokkaido University, Sapporo 060, Japan)

LIST OF SCHEMES **PAGE**